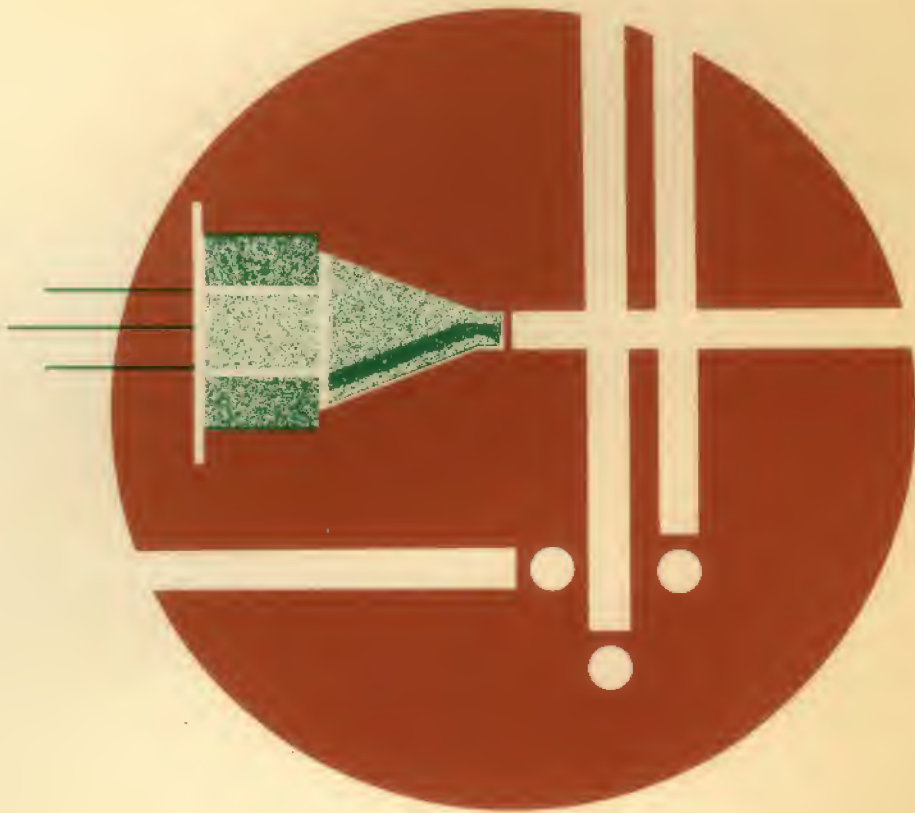


OPTOELECTRONIC 81-82

81-82
OPTOELECTRONIC
DATA BOOK



MOTOROLA Semiconductors

OPTOELECTRONICS

General Information

1

Selector Guide and Cross-Reference

2

Data Sheets

3

Applications Information

4

FIBER OPTICS

General Information

5

Selector Guide

6

Data Sheets

7

Applications Information

8



MOTOROLA

OPTOELECTRONIC DEVICE DATA

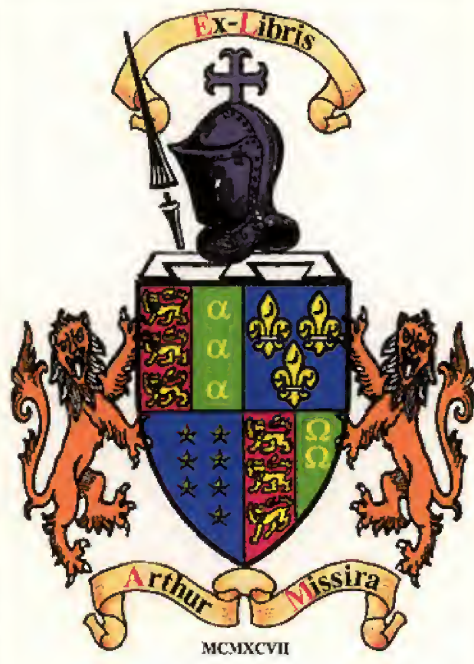
Prepared by
Technical Information Center

Motorola has concentrated on infrared, GaAs emitters, silicon detectors, high-technology opto coupler/isolators and an innovative approach to Fiber Optic components, modules and links. This Optoelectronic Data Book contains up-to-date specifications on the complete product line.

The catalog is divided into the two major sections of Opto and Fiber Optics. The Table of Contents and Alphanumeric Index cover all products. Each section has its own General Information, Selector Guide, and Data Sheets.

All devices listed are available direct from Motorola and from Motorola's Authorized Distributors. Applications assistance and information on pricing and delivery are available from the nearest Motorola sales office.

Motorola reserves the right to make changes to any product herein to improve reliability, function or design. Motorola does not assume any liability arising out of the application or use of any product or circuit described herein; neither does it convey any license under its present patent rights nor the rights of others.



Annular, Straight Shooter and Unibloc are trademarks of Motorola Inc.

CONTENTS

| | Page |
|--------------------------|------|
| ALPHANUMERIC INDEX | iii |

OPTOELECTRONICS

| | |
|--|------------|
| CHAPTER 1 — GENERAL INFORMATION | 1-1 |
| The Motorola Spectrum of Optoelectronics | 1-2 |
| Optical Isolators/Couplers | 1-3 |
| Optoelectronic Definitions | 1-5 |
| CHAPTER 2 — SELECTOR GUIDE AND CROSS-REFERENCE | 2-1 |
| Opto Couplers/Isolators | 2-2 |
| Transistor Output | 2-2 |
| Darlington Output | 2-2 |
| Triac Driver Output | 2-3 |
| Digital IC Output | 2-3 |
| Linear Amplifier Output | 2-3 |
| SCR Output | 2-4 |
| SCR Cross-Reference | 2-4 |
| Infrared-Emitting Diodes | 2-5 |
| Silicon Photo Detectors | 2-5 |
| Photodiodes | 2-5 |
| Phototransistors | 2-6 |
| Photodarlingtons | 2-6 |
| Photo Triac Drivers | 2-6 |
| Cross-Reference | 2-7 |
| CHAPTER 3 — DATA SHEETS | 3-1 |
| Data Sheet Listing (See Page 3-2) | |
| CHAPTER 4 — APPLICATIONS INFORMATION | 4-1 |
| AN-440 — Theory and Characteristics of Phototransistors | 4-2 |
| AN-508 — Applications of Phototransistors in Electro-Optic Systems | 4-13 |
| AN-571A — Isolation Techniques Using Optical Couplers | 4-27 |
| AN-780A — Applications of the MOC3011 Triac Driver | 4-35 |

FIBER OPTICS

| | |
|---|------------|
| CHAPTER 5 — GENERAL INFORMATION | 5-1 |
| Fiber Optics | 5-2 |
| Basic Concepts of Fiber Optics and Fiber Optic Communications | 5-3 |
| Basic Fiber Optic Terminology | 5-23 |
| CHAPTER 6 — SELECTOR GUIDE | 6-1 |
| Infrared Emitters | 6-2 |
| Photo Detectors | 6-2 |
| Transmitters | 6-3 |
| Receivers | 6-3 |
| Links | 6-4 |
| Accessories | 6-4 |

CONTENTS (continued)

| | Page |
|--|------------|
| CHAPTER 7 — DATA SHEETS | 7-1 |
| Data Sheet Listing (See Page 7-2) | |
| CHAPTER 8 — APPLICATIONS INFORMATION | 8-1 |
| AN-794 — A 20-Mbaud Full Duplex Fiber Optic Data Link Using Fiber Optic Active Components | 8-2 |
| AN-804 — Applications of Ferruled Components to Fiber Optic System | 8-30 |
| MFOL02 — Theory of Operation | 8-38 |
| Fiber Optic Circuit Ideas | |
| 20-Megabaud Data Link | 8-43 |
| 10-Megabaud Data Link | 8-44 |
| 2.0-Megabaud Data Link | 8-45 |
| 1.0-Megabit System | 8-46 |
| 100-Kilobit Receiver | 8-48 |
| 1/10/100 Kilobit Receiver | 8-49 |
| Darlington Receiver | 8-50 |
| Phototransistor Receiver | 8-50 |
| A Microcomputer Data Link Using Fiber Optics | 8-51 |

ALPHANUMERIC INDEX

| Device | Page | Device | Page | Device | Page |
|----------|------|----------|------|---------|------|
| 2N5777 | 3-3 | MCT274 | 3-90 | MRD150 | 3-63 |
| 2N5778 | 3-3 | MCT275 | 3-90 | MRD160 | 3-66 |
| 2N5779 | 3-3 | MCT277 | 3-90 | MRD300 | 3-69 |
| 2N5780 | 3-3 | MFOD100 | 7-3 | MRD310 | 3-69 |
| 4N25 | 3-5 | MFOD102F | 7-5 | MRD360 | 3-73 |
| 4N25A | 3-5 | MFOD104F | 7-7 | MRD370 | 3-73 |
| 4N26 | 3-5 | MFOD200 | 7-9 | MRD450 | 3-77 |
| 4N27 | 3-5 | MFOD202F | 7-11 | MRD500 | 3-80 |
| 4N28 | 3-5 | MFOD300 | 7-13 | MRD510 | 3-80 |
| 4N29 | 3-9 | MFOD302F | 7-15 | MRD3010 | 3-83 |
| 4N29A | 3-9 | MFOD402F | 7-17 | MRD3011 | 3-83 |
| 4N30 | 3-9 | MFOD404F | 7-21 | MRD3050 | 3-86 |
| 4N31 | 3-9 | MFOD405F | 7-25 | MRD3051 | 3-86 |
| 4N32 | 3-9 | MFOE100 | 7-29 | MRD3054 | 3-86 |
| 4N32A | 3-9 | MFOE102F | 7-31 | MRD3055 | 3-86 |
| 4N33 | 3-9 | MFOE103F | 7-33 | MRD3056 | 3-86 |
| 4N35 | 3-13 | MFOE106F | 7-35 | TIL111 | 3-90 |
| 4N36 | 3-13 | MFOE200 | 7-37 | TIL112 | 3-90 |
| 4N37 | 3-13 | MFOL01 | 7-39 | TIL113 | 3-90 |
| 4N38 | 3-17 | MFOL02 | 7-41 | TIL114 | 3-90 |
| 4N38A | 3-17 | MLED60 | 3-23 | TIL115 | 3-90 |
| H11A1 | 3-90 | MLED90 | 3-23 | TIL116 | 3-90 |
| H11A2 | 3-90 | MLED92 | 3-25 | TIL117 | 3-90 |
| H11A3 | 3-90 | MLED93 | 3-27 | TIL119 | 3-90 |
| H11A4 | 3-90 | MLED94 | 3-27 | TIL124 | 3-90 |
| H11A5 | 3-90 | MLED95 | 3-27 | TIL125 | 3-90 |
| H11A520 | 3-90 | MLED900 | 3-29 | TIL126 | 3-90 |
| H11A550 | 3-90 | MLED930 | 3-31 | TIL127 | 3-90 |
| H11A5100 | 3-90 | MOC119 | 3-33 | TIL128 | 3-90 |
| H11B1 | 3-90 | MOC1005 | 3-37 | TIL153 | 3-90 |
| H11B2 | 3-90 | MOC1006 | 3-37 | TIL154 | 3-90 |
| H11B3 | 3-90 | MOC3000 | 3-41 | TIL155 | 3-90 |
| H11B255 | 3-90 | MOC3001 | 3-41 | TIL156 | 3-90 |
| IL1 | 3-90 | MOC3002 | 3-41 | TIL157 | 3-90 |
| IL12 | 3-90 | MOC3003 | 3-41 | | |
| IL15 | 3-90 | MOC3009 | 3-44 | | |
| IL74 | 3-90 | MOC3010 | 3-44 | | |
| L14H1 | 3-21 | MOC3011 | 3-44 | | |
| L14H2 | 3-21 | MOC3020 | 3-48 | | |
| L14H3 | 3-21 | MOC3021 | 3-48 | | |
| L14H4 | 3-21 | MOC3030 | 3-50 | | |
| MCA230 | 3-90 | MOC3031 | 3-50 | | |
| MCA231 | 3-90 | MOC5005 | 3-53 | | |
| MCA255 | 3-90 | MOC5006 | 3-53 | | |
| MCT2 | 3-90 | MOC5010 | 3-55 | | |
| MCT2E | 3-90 | MOC8020 | 3-57 | | |
| MCT26 | 3-90 | MOC8021 | 3-57 | | |
| MCT271 | 3-90 | MOC8030 | 3-59 | | |
| MCT272 | 3-90 | MOC8050 | 3-59 | | |
| MCT273 | 3-90 | MRD14B | 3-3 | | |

OPTOELECTRONICS

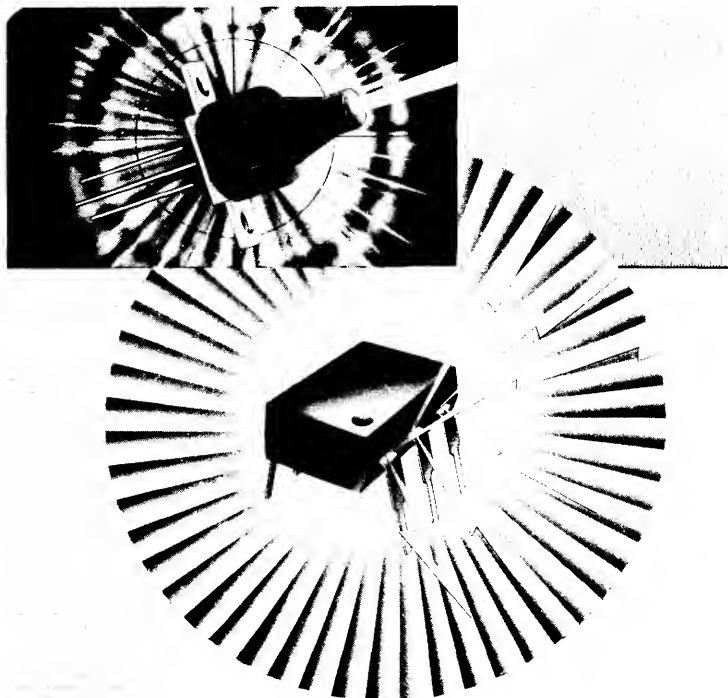
General Information

Motorola Optoelectronic products include infrared-emitting diodes, silicon photo detectors and opto-couplers/isolators.

Motorola is the leader in high technology opto-couplers. For control of 110 and 220 Vac lines, the triac drivers (MOC3010, MOC3020, MOC3030) are unequaled.

All Motorola opto-couplers have a minimum isolation voltage of 7500 Vac peak, the highest available. The broad opto-coupler line includes nearly all the transistor, Darlington, SCR, and Triac output devices now available in the industry.

Each device is presented in the easy-to-use Selector Guide and is included in a detailed data sheet in a succeeding section.



The Motorola Spectrum of

OPTOELECTRONICS

INFRARED-LIGHT-EMITTING DIODES

The infrared-light-emitting diode emits radiation in the near infrared region when forward bias current (I_F) flows through the PN junction. The light output power (P_O) is a function of the drive current (I_F) and is measured in milliwatts.

Infrared-light-emitting diodes are used together with photosensors.

FIGURE 1

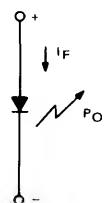
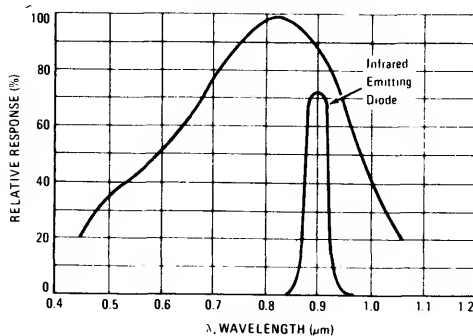


FIGURE 2 – Constant Energy Spectral Response



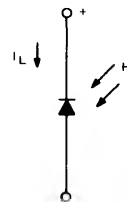
PHOTOSENSORS

Silicon photosensors respond to the entire visible radiation range as well as to the near infrared radiation range. The radiation response of a photosensor is a function of the material and the diffusion depth of the light-sensitive PN junction. All silicon photosensors (diodes, transistors, darlington, triacs) show the same basic radiation frequency response which peaks in the near infrared radiation range. Therefore, the sensitivity range of Motorola silicon sensors is ideally suited to Motorola infrared-emitting diodes.

Photodiodes

Radiation falling at the PN junction will generate hole electron pairs which cause the carriers to move, thus causing a current flow (I_L). The power density of the radiation H (measured in mW/cm^2) determines the current flow, I_L . At zero radiation, a small leakage current, called dark current (I_D) will remain.

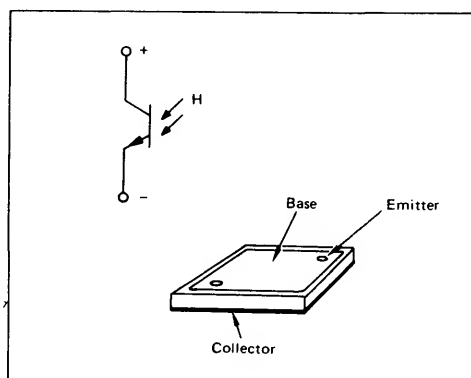
FIGURE 3



Phototransistors

The phototransistor is a light radiation controlled transistor. The collector base junction is enlarged and works as a reversed biased photodiode controlling the transistor. The collector current, I_L , depends on the radiation density (H) and the dc current gain of the transistor. Under dark condition, the transistor is switched off; the remaining leakage current, I_{CEO} , is called collector dark current.

FIGURE 4



Photodarlingtons

The photodarlington works on the same principle as a phototransistor. The collector base junction of the driver transistor is radiation sensitive and controls the driver transistor. The driver transistor controls the following transistor. The darlington configuration yields a high current gain which results in a photodetector with very high light sensitivity.

Phototriacs

The gate of the phototriac is radiation sensitive and triggers the triac at a certain specified radiation density (H). At dark condition, the triac is not triggered. The remaining leakage current is called peak blocking current (I_{DRM}). The device is bilateral and designed to switch ac signals.



Optical Isolators/Couplers

ISOLATORS

An optoelectronic isolator contains both an IRED and a photodetector in the same package, arranged so that energy radiated from the IRED is efficiently coupled to the detector through a clear, isolating dielectric. An opaque material surrounds the dielectric and provides ambient light protection.

Since there is no electrical connection between input and output, and since gallium-arsenide emitters and silicon detectors cannot reverse their roles, a signal is able to pass through the isolator in one direction only. To a degree determined by the package input-output capacitance and dielectric characteristics, the device is unresponsive to common mode input signals and provides input circuitry protection from the output circuit environment. Ground loop prevention, dc level shifting, and logic control of high voltage power circuitry are therefore typical areas where isolators are very useful.

The measure of an isolator's ability to efficiently pass a desired signal is most commonly referred to as Current Transfer Ratio (CTR). It is dependent upon the radiative efficiency of the IRED, the spacing between the IRED and the detector, the area and sensitivity of the detector, and the amplifying gain of the detector. It is subject to the nonlinearities (current, voltage, temperature) of both chips, causing a rather complex transfer function which should be evaluated closely when used at non-specified conditions.

The ability of an isolator to provide standoff protection is usually expressed as an Isolation Surge Voltage and is essentially a measure of the integrity of the package and the dielectric strength of the insulating materials.

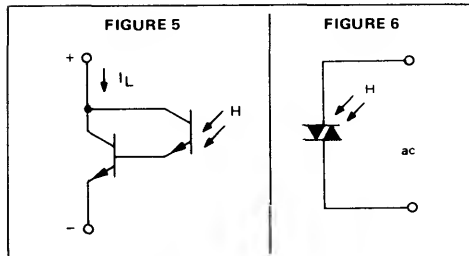
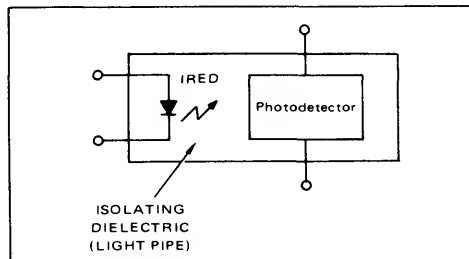


FIGURE 7 – BASIC OPTO ISOLATOR (COUPLER)



ISOLATION VOLTAGE

The primary function of an optoelectronic isolator is to provide electrical separation between input and output, especially in the presence of high voltages. The amount of stress that an isolator can safely withstand and the stability of this protection varies considerably with package construction techniques used.

Figure 8 shows an older isolation technique, where the light transmission medium is a small amount of a clear, silicone-rubber type of material. Surrounding it is usually a black epoxy or phenolic compound. It has been found that the weakest point in this approach is the interface between the "light-pipe" and the overmold. It is a relatively short path between lead frames along this interface, and the two materials are dissimilar enough that the integrity of the interface is usually poor. This technique initially gives marginal standoff protection and stability

ISOLATION VOLTAGE

FIGURE 8 – Standard

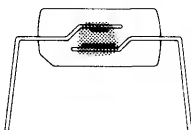
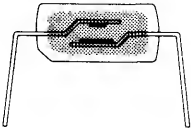


FIGURE 9 – Motorola



under voltage stress is very poor.

Figure 9 shows Motorola's improved construction technique. The clear dielectric used here is a transfer-molded epoxy that encompasses a large volume of the interior of the package. The overmold is a transfer-molded opaque epoxy. The result is a much longer interface (typically ten times longer) between two very similar, electrically stable compounds. Minimum specified isolation voltage capability is 7500 volts ac peak on all Motorola isolators, and typical units provide in excess of 12,000 volts ac peak protection on a reliable, repeatable basis (in a clean and low humidity environment). External ambient conditions (humidity, cleanliness, etc.) tend to be the limiting factors when using Motorola isolators. Representative test data at typical applied voltages are shown below:

| Test | No. of Units | Applied Voltage | Failure @ 1000 Hrs |
|------|--------------|-----------------|--------------------|
| A | 100 | 1500 V ac peak | 0 |
| B | 100 | 5000 V dc peak | 0 |

Isolation voltage has been specified in terms of both dc and ac conditions, sometimes with no associated test duration. In general, ac conditions are more severe than dc. Any imperfections or discontinuities in the isolating dielectric tend to have a lower dielectric constant than the surrounding areas and assume a disproportionate share of the total ac applied field, in the same manner that the smallest capacitance in a series string assumes the highest voltage drop under ac conditions. Microscopic ruptures can occur at these points, causing localized degradation and propagation of the weakened areas until large-scale puncture occurs. Dc fields tend to distribute more linearly. Additionally, ac fields are more effective in causing mobile impurities to align themselves and produce leakage paths.

Continuous ratings are therefore difficult to guarantee reliably as the result of individual unit testing or sorting. Instead, surge isolation voltage ratings should be specified

with an associated test duration, while continuous ratings must be the result of a well-controlled, well-characterized assembly technique and realistic generic data. Since ac conditions are usually the most severe, it has become common to give them the most attention.

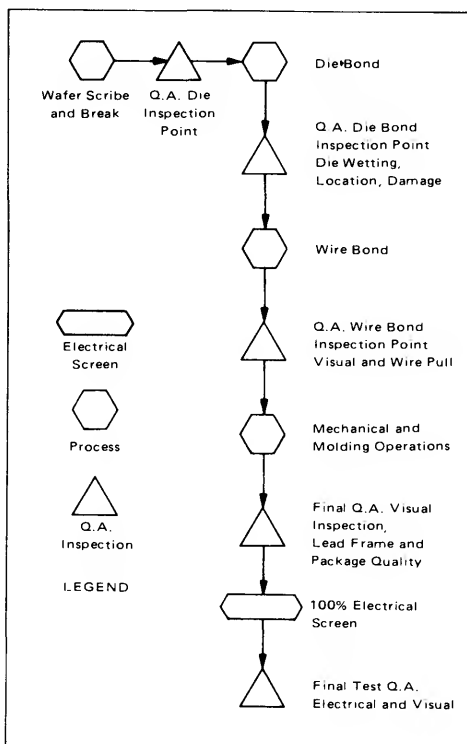
UNDERWRITERS' LABORATORIES RECOGNIZED

Most Motorola isolators are available under the Underwriters' Laboratories Component Recognition Program. It should be noted that applicable Motorola isolators are recognized for use in applications up to 240 Vac. Under the U.L. criteria, these devices must have passed isolation voltage tests at approximately 5000 volts ac peak for one second. In addition, Motorola tests every coupler to 7500 V ac peak for 5 seconds.

COUPLER PROCESS FLOW/QUALITY CHECK POINTS

Every optocoupler manufactured by Motorola undergoes extensive in-process checks for quality. After each process step (for example, die bond, encapsulation, electrical test, etc.) the product is randomly sampled. If the sample does not pass high-quality standards, the product flow is halted and corrective action is taken. In this manner, quality is built in at Motorola.

FIGURE 10 – Coupler Process Flow/Quality Check Points

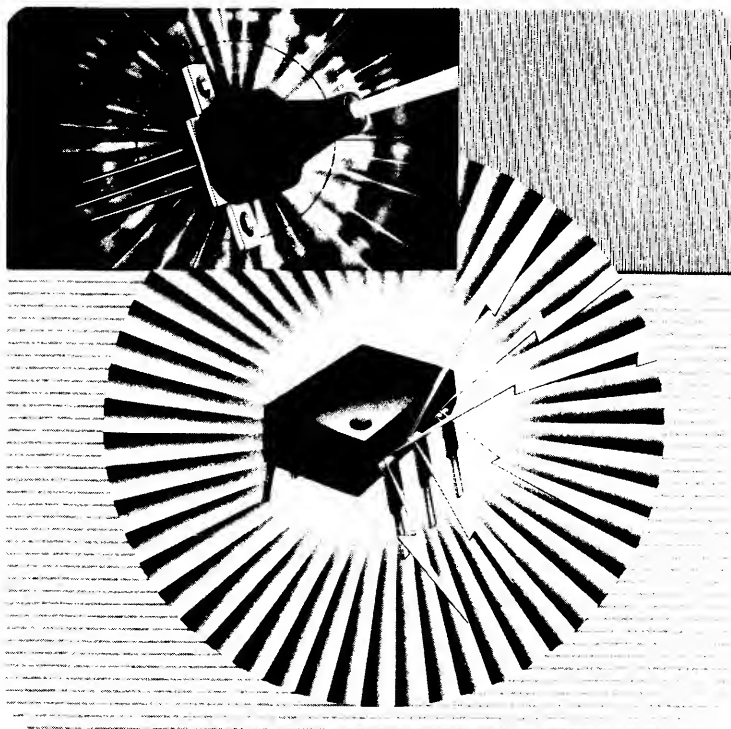


OPTOELECTRONIC DEFINITIONS, CHARACTERISTICS, AND RATINGS

| | | |
|------------------------|---|---|
| CTR | Current Transfer Ratio — The ratio of output current to input current, at a specified bias, of an opto coupler. | from the 10% point to the 90% point when pulsed with the stated GaAs (gallium-arsenide) source under stated conditions of collector voltage, load resistance, and ambient temperature. |
| dv/dt | Commutating dv/dt — A measure of the ability of a triac to block a rapidly rising voltage immediately after conduction of the opposite polarity. Coupled dv/dt — A measure of the ability of an opto thyristor coupler to block when the coupler is subjected to rapidly changing isolation voltage. | Triac A thyristor which can block or conduct in either polarity. Conduction is initiated by forward bias of a gate-MTI junction. |
| E | Luminous Flux Density (Illuminance) [lumens/ft. ² = ft. candles] — The radiation flux density of wavelength within the band of visible light. | T_{STG} V_{(BR)R} Storage Temperature Reverse Breakdown Voltage — The minimum dc reverse breakdown voltage at stated diode current and ambient temperature. |
| H | Radiation Flux Density (Irradiance) [mW/cm ²] — The total incident radiation energy measured in power per unit area. | V_{(BR)CBO} Collector-Base Breakdown Voltage — The minimum dc breakdown voltage, collector to base, at stated collector current and ambient temperature. (Emitter open and H ≈ 0) |
| I_{CEO} | Collector Dark Current — The maximum current through the collector terminal of the device measured under dark conditions, (H ≈ 0), with a stated collector voltage, load resistance, and ambient temperature. (Base open) | V_{(BR)CEO} Collector-Emitter Breakdown Voltage — The minimum dc breakdown voltage, collector to emitter, at stated collector current and ambient temperature. (Base open and H ≈ 0) |
| I_D | Dark Current — The maximum reverse leakage current through the device measured under dark conditions, (H ≈ 0), with a stated reverse voltage, load resistance, and ambient temperature. | V_{(BR)ECO} Emitter-Collector Breakdown Voltage — The minimum dc breakdown voltage, emitter to collector, at stated emitter current and ambient temperature. (Base open and H ≈ 0) |
| I_{FT} | Input Trigger Current — Emitter current necessary to trigger the coupled thyristor. | V_{CBO} Collector-Base Voltage — The maximum allowable value of the collector-base voltage which can be applied to the device at the rated temperature. (Base open) |
| I_L | Collector Light Current — The device collector current measured under defined conditions of irradiance, collector voltage, load resistance, and ambient temperature. | V_{CEO} Collector-Emitter Voltage — The maximum allowable value of collector-emitter voltage which can be applied to the device at the rated temperature. (Base open) |
| R_s | Series Resistance — The maximum dynamic series resistance measured at stated forward current and ambient temperature. | V_{ECO} Emitter-Collector Voltage — The maximum allowable value of emitter-collector voltage which can be applied to the device at the rated temperature. (Base open) |
| SCR | Silicon Controlled Rectifier — A reverse blocking thyristor which can block or conduct in forward bias, conduction between the anode and cathode being initiated by forward bias of the gate cathode junction. | V_F Forward Voltage — The maximum forward voltage drop across the diode at stated diode current and ambient temperature. |
| t_f | Photo Current Fall Time — The response time for the photo-induced current to fall from the 90% point to the 10% point after removal of the GaAs (gallium-arsenide) source pulse under stated conditions of collector voltage, load resistance and ambient temperature. | V_{ISO} Isolation Surge Voltage — The dielectric withstanding voltage capability of an optocoupler under defined conditions and time. |
| t_r | Photo Current Rise Time — The response time for the photo-induced current to rise | V_R Reverse Voltage — The maximum allowable value of dc reverse voltage which can be applied to the device at the rated temperature. λ_{s(μm)} Wavelength of maximum sensitivity in micrometers. |

OPTOELECTRONICS

Selector Guide and Cross-Reference



OPTICAL COUPLERS/ISOLATORS

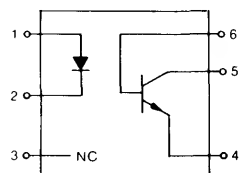
Couplers are designed to provide isolation protection from high-voltage transients, surge voltage, or low-level noise that would otherwise damage the input or generate erroneous information. They allow interfacing systems of different logic levels, different grounds, etc., that would otherwise be incompatible. Motorola couplers are tested and specified to an isolation voltage of 7500 Vac peak.

Motorola offers a wide array of standard devices with a wide range of specifications (including the first series of DIP transistors and Darlington couplers to achieve JEDEC registration: transistors — 4N25 thru 4N38, and Darlintons — 4N29 thru 4N33). All Motorola couplers are UL Recognized with File Number E54915.

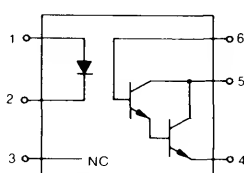
CASE 730A



The Transistor Coupler is probably the most popular form of isolator since it offers moderate speed (approximately 300 kHz), sensitivity and economy. In addition, the collector-base junction can be used as a photodiode to achieve higher speeds. The output in the diode mode is lower, requiring amplification for more usable output levels.



The Darlington Transistor Coupler is used when high transfer ratios and increased output current capability are needed. The speed, approximately 30 kHz, is slower than the transistor type but the transfer ratio can be as much as ten times as high as the single transistor type.



Transistor Output
Isolation Voltage is 7500 V (Min)
on all devices. See notes

| Device Type | DC Current Transfer Ratio % Min | V _{(BR)CEO} Volts Min |
|-------------|---------------------------------|--------------------------------|
| TIL112 | 2.0 | 20 |
| TIL115 | 2.0 | 20 |
| IL15 | 6.0 | 30 |
| MCT26 | 6.0 | 30 |
| TIL111 | 8.0 | 30 |
| TIL114 | 8.0 | 30 |
| IL12 | 10 | 20 |
| 4N27 | 10 | 30 |
| 4N28 | 10 | 30 |
| H11A4 | 10 | 30 |
| TIL124 | 10 | 30 |
| TIL153 | 10 | 30 |
| IL74 | 12.5 | 20 |
| TIL125 | 20 | 30 |
| TIL154 | 20 | 30 |
| 4N25 | 20 | 30 |
| 4N26 | 20 | 30 |
| H11A2 | 20 | 30 |
| H11A3 | 20 | 30 |
| H11A520 | 20 | 30 |
| IL1 | 20 | 30 |
| MCT2 | 20 | 30 |
| TIL116 | 20 | 30 |
| 4N38 | 20 | 80 |
| H11A5 | 30 | 30 |
| MCT271 | 45 | 30 |
| H11A1 | 50 | 30 |
| H11A550 | 50 | 30 |
| TIL117 | 50 | 30 |
| TIL126 | 50 | 30 |
| TIL155 | 50 | 30 |
| CNY17 | 62 | 70 |
| MCT275 | 70 | 80 |
| MCT272 | 75 | 30 |
| MCT277 | 100 | 30 |
| 4N35 | 100 | 30 |
| 4N36 | 100 | 30 |
| 4N37 | 100 | 30 |
| H11A5100 | 100 | 30 |
| MCT273 | 125 | 30 |
| MCT274 | 225 | 30 |

Darlington Output
Isolation Voltage is 7500 V (Min)
on all devices. See notes

| Device Type | DC Current Transfer Ratio % Min | V _{(BR)CEO} Volts Min |
|-------------|---------------------------------|--------------------------------|
| 4N31 | 50 | 30 |
| H11B3 | 100 | 25 |
| 4N29 | 100 | 30 |
| 4N30 | 100 | 30 |
| MCA230 | 100 | 30 |
| H11B25 | 100 | 55 |
| MCA255 | 100 | 55 |
| H11B2 | 200 | 25 |
| MCA231 | 200 | 30 |
| MOC119' | 300 | 30 |
| TIL119' | 300 | 30 |
| TIL113' | 300 | 30 |
| MOC8030' | 300 | 80 |
| TIL127' | 300 | 30 |
| TIL128' | 300 | 30 |
| TIL156' | 300 | 30 |
| TIL157' | 300 | 30 |
| H11B1 | 500 | 25 |
| 4N32 | 500 | 30 |
| 4N33 | 500 | 30 |
| MOC8020' | 500 | 50 |
| MOC8050' | 500 | 80 |
| MOC8021' | 1000 | 50 |

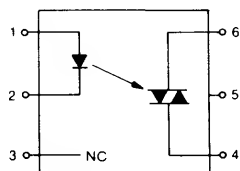
*Pin 3 and Pin 6 are not connected

Notes:

- 1 Isolation Surge Voltage, V_{ISO} , is an internal device dielectric breakdown rating. For this test LED pins 1 and 2 are common and phototransistor pins 4, 5 and 6 are common.
- 2 All Motorola couplers are specified at 7500 Vac peak (5 seconds). This usually exceeds the originator's specification and JEDEC registered values.
- 3 See Case 730A 01 Style 3

OPTICAL COUPLERS/ISOLATORS (continued)

The Triac Driver Output Coupler is a gallium-arsenide IRED, optically coupled to a silicon bilateral switch designed for applications requiring isolated triac triggering such as interface from logic to 110/220 V RMS line voltage. These devices offer low current, isolated ac switching, high output blocking voltage, small size, and low cost.



Triac Driver Output

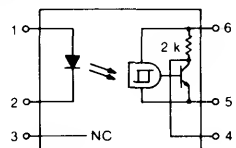
Isolation Voltage is 7500 V (min)
on all devices. See notes.

| Device Type | LED Trigger Current mA Max | Peak Blocking Voltage Volts Max |
|-------------|----------------------------------|--|
| MOC3009 | 30 | 250 |
| MOC3010 | 15 | 250 |
| MOC3011 | 10 | 250 |
| MOC3020 | 30 | 400 |
| MOC3021 | 15 | 400 |
| MOC3030** | 30 | 250 |
| MOC3031** | 15 | 250 |

**With Zero-Crossing Detector

The Digital Logic Coupler is a gallium-arsenide IRED optically coupled to a high-speed integrated detector. Designed for applications requiring electrical isolation, fast response time, and digital logic compatibility such as interfacing computer terminals to peripheral equipment, digital control of power supplies, motors, and other servo machine applications.

Intended for use as a digital inverter, the application of a current to the IRED input results in a LOW voltage, with the IRED off the output voltage is HIGH.

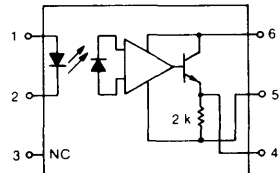


Digital IC Output

Isolation Voltage is 7500 V (min)
on all devices. See notes.

| Device Type | Output Voltage | | ton/toff ns Max |
|-------------|---|--------------------------------------|-----------------------|
| | @ IF = 16 mA VCC = 5.0 V I _{sink} = 10 mA Volts Max | @ IF = 0 VCC = 5.0 V Volts Min | |
| MOC5005 | 0.6 | 4.0 | 700 |
| MOC5006 | 0.6 | 4.0 | 350 |

The Optically-Isolated AC Linear Coupler is a gallium-arsenide IRED optically coupled to a bipolar monolithic amplifier. Converts an input current variation to an output voltage variation while providing a high degree of electrical isolation between input and output. Can be used for telephone line coupling, peripheral equipment isolation, audio and other applications.



Linear Amplifier Output

Isolation Voltage is 7500 V (min).

See notes.

| Device Type | Transfer Gain @ VCC = 12 V, mV/mA Typ | Single Ended Distortion @ VCC = 12 V, I _{sig} = 1.0 mA % Typ |
|-------------|--|---|
| MOC5010 | 200 | 0.2 |

OPTICAL COUPLERS/ISOLATORS (continued)

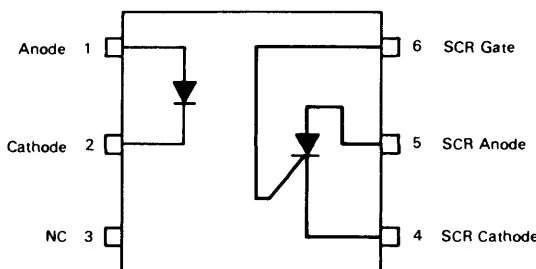
SCR Couplers

The **SCR Output Coupler** is a gallium-arsenide IRED optically coupled to a photo sensitive silicon controlled rectifier (SCR). It is designed for applications requiring high electrical isolation between low voltage circuitry like integrated circuits, and the ac line.

SCR Output

Isolation Voltage is 7500 V (min) on all devices.

| Device Type | LED Trigger Current mA Max | | Peak Blocking Voltage Volts Max |
|-------------|--|---|--|
| | V _{AK} = 50 V R _{GK} = 10 k _{!!} | V _{AK} = 100 V R _{GK} = 27 k _{!!} | |
| MOC3000 | 30 | 14 | 400 |
| MOC3001 | 20 | 11 | 400 |
| MOC3002 | 30 | 14 | 250 |
| MOC3003 | 20 | 11 | 250 |



These SCR Couplers are interchangeable with many devices available in the industry

| Device | Manufacturer | Motorola Equivalent |
|---------|--------------|------------------------|
| H11C1 | GE | MOC3003 |
| H11C2 | GE | MOC3003 |
| H11C3 | GE | MOC3002 |
| H11C4 | GE | MOC3001 |
| H11C5 | GE | MOC3001 |
| H11C6 | GE | MOC3000 |
| MCS2 | GI | MOC3002* |
| MCS2400 | GI | MOC3000* |
| OPI4201 | Optron | MOC3003 |
| OPI4202 | Optron | MOC3002 |
| OPI4401 | Optron | MOC3001 |
| OPI4402 | Optron | MOC3000 |
| SCS11C1 | Spectronics | MOC3003 |
| SCS11C3 | Spectronics | MOC3002 |
| SCS11C4 | Spectronics | MOC3001 |
| SCS11C6 | Spectronics | MOC3000 |

*Minor electrical difference

INFRARED-EMITTING DIODES

Infrared (900 nm) gallium-arsenide emitters are available from Motorola for use in light modulators, shaft or position encoders, punched card and tape readers, optical switching and logic circuits. They are spectrally matched for use with silicon detectors.

Peak Emission Wavelength = 900 nm (Typ)
Forward Voltage @ 50 mA = 1.2 (Typ).

Emission Angle — Angle at which IR emission is 15% of maximum intensity.

| Package | Device Type | Emission Angle α | Instantaneous Power Output Typ |
|--|--------------------------------------|-------------------------|---|
|  Case 209-02 Metal  | MLED930 | 30° | 650 μ W @ 100 mA |
|  Case 29-02 Plastic  | MLED92 MLED93 MLED94 MLED95 | 110° | 650 μ W @ 100 mA 3.0 mW @ 100 mA 5.0 mW @ 100 mA 8.0 mW @ 100 mA |

SILICON PHOTO DETECTORS

A variety of silicon photo detectors are available for a wide range of light detecting applications. Devices are available in packages offering choices of viewing angle and size in either low-cost, economical, plastic cases or rugged, hermetic, metal cans. Advantages over photo tubes are high sensitivity, good temperature stability, and proven silicon reliability. Applications include card and tape readers, pattern and character recognition, shaft encoders, position sensors, counters, and others. Maximum sensitivity occurs at approximately 800 nm.

Photodiodes

Photodiodes are used where high speed is required (1.0 ns).

| Package | Type Number | Light Current μ A Typ @ H mW/cm ² | | $V_{(BR)R}$ Volts Min | Dark Current nA Max @ Volts | |
|--|-------------|--|-----|--------------------------|--------------------------------|----|
|  Case 209-02 Metal Convex Lens  | MRD500 | 9.0 | 5.0 | 100 | 2.0 | 20 |
|  Case 210-01 Metal Flat Lens  | MRD510 | 2.0 | 5.0 | 100 | 2.0 | 20 |

SILICON PHOTO DETECTORS (continued)

Phototransistors

Phototransistors are used where moderate sensitivity and medium speed ($2.0 \mu\text{s}$) are required.

| Package | Type Number | Light Current mA Typ @ H mW/cm ² | | V _{(BR)CEO} Volts Min | Dark Current nA Max @ V _{CE} Volts | |
|---|---|--|---------------------------------|--------------------------------------|--|----------------------------|
|  Actual Size Case 82-05 Metal | MRD310 MRD300 | 2.5 7.5 | 5.0 5.0 | 50 50 | 25 25 | 20 20 |
|  Actual Size Case 29-02 | L14H4 L14H1 L14H2 L14H3 | 0.5 0.5 2.0 2.0 | 10 10 10 10 | 30 60 30 60 | 100 100 100 100 | 10 10 10 10 |
|  Actual Size Case 82-05 Metal | MRD3050 MRD3051 MRD3054 MRD3055 MRD3056 | 0.2 0.2 1.2 1.8 2.5 | 5.0 5.0 5.0 5.0 5.0 | 30 30 30 30 30 | 100 100 100 100 100 | 20 20 20 20 20 |

Photodarlingtions

Photodarlingtions are used where maximum sensitivitiy is required with typical rise and fall times of $50 \mu\text{s}$.

| Package | Type Number | Light Current μA Typ @ H mW/cm ² | | V _{(BR)CEO} Volts Min | Dark Current nA Max @ Volts | |
|---|--|--|---------------------------------|--------------------------------------|-----------------------------------|----------------------------|
|  Actual Size Case 82-05 Metal | MRD370 MRD360 | 10 20 | 0.5 0.5 | 40 40 | 100 100 | 10 10 |
|  Actual Size Case 29-02 Plastic | MRD14B 2N5777 2N5778 2N5779 2N5780 | 2.0 4.0 4.0 8.0 8.0 | 2.0 2.0 2.0 2.0 2.0 | 12 25 40 25 40 | 100 100 100 100 100 | 12 12 10 12 12 |

Photo Triac Drivers

Photo triac drivers contain a light sensitive IC acting as a trigger device for direct interface with a triac.

| Package | Type Number | Trigger* Sensitivity H mW/cm ² Typ | On-State RMS Current mA Max | Off-State Output Terminal Voltage Volts Peak Min | Peak Blocking Current nA Typ |
|---|--------------------|---|--------------------------------------|---|--|
|  Actual Size Case 82-05 | MRD3010 MRD3011 | 1.0 0.5 | 100 100 | 250 250 | 10 10 |

*Irradiance level to Latch Output

CROSS-REFERENCE

The following is a cross-reference of all known optoelectronic devices at the time of printing. This list is meant to serve as a substitution guide for existing competitive devices to Motorola's optoelectronic product line.

Motorola's nearest equivalent devices are selected on the basis of general similarity of electrical characteristics. Interchangeability in particular applications is not guaranteed. Before using a substitute, please compare the detailed specifications of the substitute device to the data sheet of the original device.

In the event the device we recommend does not exactly meet your needs, we encourage you to look for another device from the same line source which will have similar characteristics, or contact your nearest distributor or Motorola sales office for further information.

CODE

- A = Direct Replacement
- B = Minor Electrical Difference
- C = Minor Mechanical Difference
- D = Significant Electrical Difference
- E = Significant Mechanical Difference

CROSS-REFERENCE

| Device | Manufacturer | Description | Motorola Equivalent | Code |
|----------------|--------------|---|---------------------|------|
| BP101 | Siemens | TO-1B Lensed Phototransistor | MRD3050 | C |
| BP102 | Siemens | TO-18 Lensed Phototransistor | MRD3050 | C |
| BPW14 | Telefunken | TO-18 Lensed Phototransistor | MRD300 | A |
| BPW15 | Pro Electron | PILL Lensed Phototransistor | MRD602 | A |
| BPW16 | Telefunken | Plastic Lensed Phototransistor | MRD160 | A |
| BPW17 | Telefunken | Plastic Lensed Phototransistor | MRD160 | A |
| BPW24 | Telefunken | TO-92 Lensed Phototransistor | L14H1 | C |
| BPW30 | Telefunken | TO-18 Lensed Photodarlington | MRD360 | A |
| BPX25A | Philips | TO-1B Lensed Photodarlington | MRD370 | A |
| BPX25 | Philips | TO-1B Lensed Phototransistor | MRD300 | A |
| BPX29A | Philips | TO-18 Lensed Photodarlington | MRD370 | A |
| BPX29 | Philips | TO-18 Lensed Phototransistor | MRD310 | A |
| BPX37 | Philips | TO-18 Lensed Phototransistor | MRD300 | A |
| BPX38 | Philips | TO-18 Lensed Phototransistor | MRD3055 | A |
| BPX43 | Siemens | TO-18 Lensed Phototransistor | MRD300 | A |
| BPX58 | Siemens | TO-18 Lensed Phototransistor | MRD300 | A |
| BPX59 | Siemens | TO-18 Lensed Photodarlington | MRD360 | A |
| BPX62-1 | Siemens | PILL Lensed Phototransistor | MRD601 | A |
| BPX62-2 | Siemens | PILL Lensed Phototransistor | MRD602 | A |
| BPX62-3 | Siemens | PILL Lensed Phototransistor | MRD603 | A |
| BPX62-4 | Siemens | PILL Lensed Phototransistor | MRD604 | A |
| BPX70, C, D, E | Philips | Plastic Lensed Phototransistor | MRD450 | BE |
| BPX72, C, D, E | Philips | Plastic Lensed Phototransistor | MRD450 | BE |
| BPX81 | Siemens | Plastic Lensed Phototransistor | MRD160 | A |
| BPY62 | Siemens | TO-18 Lensed Phototransistor | MRD3050 | A |
| CL100 | Centralab | TO-18 Lensed I.R. LED | MLED930 | B |
| CL110 | Centralab | TO-18 Lensed I.R. LED | MLED930 | A |
| CL110A | Centralab | TO-18 Lensed I.R. LED | MLED930 | A |
| CL110B | Centralab | TO-18 Lensed I.R. LED | MLED930 | B |
| CLI-2 | Clairex | 6-Pin DIP, Coupler, Transistor Output | 4N38 | B |
| CLI-3 | Clairex | 6-Pin DIP, Coupler, Transistor Output | 4N35 | B |
| CLI-5 | Clairex | 6-Pin DIP, Coupler, Transistor Output | 4N26 | A |
| CLI-10 | Clairex | 6-Pin DIP, Coupler, Transistor Output | 4N33 | B |
| CLR2050 | Clairex | TO-18 Lensed Photodarlington | MRD3050 | A |
| CLR2060 | Clairex | TO-18 Lensed Photodarlington | MRD360 | A |
| CLR2110 | Clairex | TO-18 Lensed Phototransistor | MRD310 | A |
| CLR2140 | Clairex | TO-18 Lensed Phototransistor | MRD310 | A |
| CLR2150 | Clairex | TO-18 Lensed Phototransistor | MRD300 | A |
| CLR2160 | Clairex | TO-18 Lensed Phototransistor | MRD300 | A |
| CLR2170 | Clairex | TO-18 Lensed Photodarlington | MRD370 | A |
| CLR2180 | Clairex | TO-18 Lensed Photodarlington | MRD360 | A |
| CLT3020 | Clairex | PILL Lensed Phototransistor | MRD601 | A |
| CLT3030 | Clairex | PILL Lensed Phototransistor | MRD602 | A |
| CLT3160 | Clairex | PILL Lensed Phototransistor | MRD603 | A |
| CLT3170 | Clairex | PILL Lensed Phototransistor | MRD604 | A |
| CLT4020 | Clairex | PILL Lensed Phototransistor | MRD601 | E |
| CLT4030 | Clairex | PILL Lensed Phototransistor | MRD602 | E |
| CLT4060 | Clairex | PILL Lensed Phototransistor | MRD603 | E |
| CLT4070 | Clairex | PILL Lensed Phototransistor | MRD604 | E |
| CNY17 | Siemens | 6-Pin DIP Coupler Transistor Output | CNY17 | A |
| CNY1B | Siemens | 6-Pin DIP Coupler Transistor Output | 4N25 | A |
| CNY21 | Telefunken | Long DIP Coupler Transistor Output | 4N25 | E |
| COY10 | Pro Electron | TO-18 Lensed I.R. LED | MLED930 | B |
| COY11, B, C | Philips | TO-18 Lensed I.R. LED | MLED930 | B |
| COY12, B | Philips | TO-18 Lensed I.R. LED | MLED930 | B |
| COY13 | Pro Electron | 6-Pin DIP, Coupler, Transistor Output | 4N26 | B |
| COY14 | Pro Electron | 6-Pin DIP, Coupler, Transistor Output | 4N26 | B |
| COY15 | Pro Electron | 6-Pin DIP, Coupler, Transistor Output | 4N26 | B |
| COY31 | Pro Electron | 6-Pin DIP, Coupler, Transistor Output | MLED930 | B |
| COY32 | Pro Electron | 6-Pin DIP, Coupler, Transistor Output | MLED930 | B |
| COY36 | Pro Electron | Plastic DIP, Coupler, Transistor Output | MLED60 | B |

CROSS-REFERENCE (continued)

| Device | Manufacturer | Description | Motorola Equivalent | Code |
|-----------------|---------------------|---------------------------------------|----------------------------|-------------|
| COY40, 41 | ITT | 6-Pin DIP, Coupler, Transistor Output | 4N26 | A |
| CQY80 | Telefunken | 6-Pin DIP, Coupler, Transistor Output | MOC1005 | B |
| EE60 | EEP | Plastic, Lensed I.R. LED | MLED60 | C |
| EE100 | EEP | Plastic, Lensed I.R. LED | MLED60 | E |
| EP2 | EEP | 6-Pin DIP, Coupler, Transistor Output | 4N26 | B |
| EPY62-1 | EEP | TO-18 Lensed Phototransistor | MRD3055 | A |
| EPY62-2 | EEP | TO-18 Lensed Phototransistor | MRD3056 | A |
| EPY62-3 | EEP | TO-18 Lensed Phototransistor | MRD310 | A |
| FCD810, A | Fairchild | 6-Pin DIP, Coupler, Transistor Output | 4N27 | A |
| FCD810, B, C, D | Fairchild | 6-Pin DIP, Coupler, Transistor Output | 4N27 | A |
| FCD820, A | Fairchild | 6-Pin DIP, Coupler, Transistor Output | 4N26 | A |
| FCD820, B | Fairchild | 6-Pin DIP, Coupler, Transistor Output | 4N25 | A |
| FCD820, C, D | Fairchild | 6-Pin DIP, Coupler, Transistor Output | MOC1005 | B |
| FCD825, A | Fairchild | 6-Pin DIP, Coupler, Transistor Output | 4N35 | A |
| FCD825, B | Fairchild | 6-Pin DIP, Coupler, Transistor Output | 4N35 | A |
| FCD825C, D | Fairchild | 6-Pin DIP, Coupler, Transistor Output | 4N35 | A |
| FCD830, A | Fairchild | 6-Pin DIP, Coupler, Transistor Output | 4N26 | A |
| FCD830, B | Fairchild | 6-Pin DIP, Coupler, Transistor Output | 4N25 | A |
| FCD830, C, D | Fairchild | 6-Pin DIP, Coupler, Transistor Output | 4N26 | A |
| FCD831, A | Fairchild | 6-Pin DIP, Coupler, Transistor Output | 4N27 | A |
| FCD831, B | Fairchild | 6-Pin DIP, Coupler, Transistor Output | 4N25 | A |
| FCD831, C, D | Fairchild | 6-Pin DIP, Coupler, Transistor Output | MOC1006 | A |
| FCD836 | Fairchild | 6-Pin DIP, Coupler, Transistor Output | 4N27 | A |
| FCD836C, D | Fairchild | 6-Pin DIP, Coupler, Transistor Output | MOC1006 | A |
| FCD850C, D | Fairchild | 6-Pin DIP, Coupler, Darlington Output | 4N29 | A |
| FCD855C, D | Fairchild | 6-Pin DIP, Coupler, Darlington Output | 4N29 | A |
| FCD860C, D | Fairchild | 6-Pin DIP, Coupler, Darlington Output | 4N32 | A |
| FCD865C, D | Fairchild | 6-Pin DIP, Coupler, Darlington Output | 4N32 | B |
| FPE100 | Fairchild | TO-18, Lensed, I.R. LED | MLED930 | A |
| FPE410 | Fairchild | TO-18, Lensed, I.R. LED | MLED930 | B |
| FPE500 | Fairchild | TO-18, Lensed, I.R. LED | MLED930 | B |
| FPE520 | Fairchild | Metal, FO, IRED | MFOE200 | D |
| FPT100 | Fairchild | Plastic, Lensed Phototransistor | MRD160 | E |
| FPT100, A | Fairchild | Plastic, Lensed Phototransistor | MRD160 | E |
| FPT100, B | Fairchild | Plastic, Lensed Phototransistor | MRD160 | E |
| FPT120, A | Fairchild | Plastic, Lensed Phototransistor | MRD450 | E |
| FPT120, B | Fairchild | Plastic, Lensed Phototransistor | MRD450 | E |
| FPT120, C | Fairchild | Plastic, Lensed Phototransistor | MRD300 | B |
| FPT131 | Fairchild | Plastic, Lensed Phototransistor | MRD160 | E |
| FPT132 | Fairchild | Plastic, Lensed Phototransistor | MRD160 | E |
| FPT220 | Fairchild | Plastic, Lensed Phototransistor | MRD160 | E |
| FPT400 | Fairchild | Plastic, Lensed Darlington Transistor | MRD360 | A |
| FPT500, A | Fairchild | TO-18, Lensed, Transistor | MRD300 | A |
| FPT510 | Fairchild | TO-18, Lensed, Transistor | MRD3054 | A |
| FPT510, A | Fairchild | TO-18, Lensed, Transistor | MRD3055 | A |
| FPT520 | Fairchild | TO-18, Lensed, Transistor | MRD300 | A |
| FPT520A | Fairchild | TO-18, Lensed, Transistor | MRD300 | B |
| FPT530A | Fairchild | TO-18, Lensed, Transistor | MRD300 | A |
| FPT450A | Fairchild | TO-18, Lensed, Transistor | MRD300 | B |
| FPT550A | Fairchild | TO-18, Lensed, Transistor | MRD300 | B |
| FPT560 | Fairchild | TO-18, Lensed, Phototransistor | MRD300 | B |
| FPT570 | Fairchild | TO-18, Lensed, Phototransistor | MRD360 | A |
| GG686 | Fairchild | TO-18, Lensed, Phototransistor | MRD300 | B |
| GS101 | Gen'l Sensors | PILL, Lensed, Phototransistor | MRD601 | A |
| GS103 | Gen'l Sensors | PILL, Lensed, Phototransistor | MRD601 | A |
| GS161 | Gen'l Sensors | PILL, Lensed, Phototransistor | MRD601 | A |
| GS163 | Gen'l Sensors | PILL, Lensed, Phototransistor | MRD601 | A |
| GS165 | Gen'l Sensors | PILL, Lensed, Phototransistor | MRD604 | A |
| GS167 | Gen'l Sensors | PILL, Lensed, Phototransistor | MRD604 | A |
| GS201 | Gen'l Sensors | PILL, Lensed, Phototransistor | MRD601 | E |
| GS203 | Gen'l Sensors | PILL, Lensed, Phototransistor | MRD601 | E |
| GS261 | Gen'l Sensors | PILL, Lensed, Phototransistor | MRD601 | E |

CROSS-REFERENCE (continued)

| Device | Manufacturer | Description | Motorola Equivalent | Code |
|--------------------|---------------------|-------------------------------------|----------------------------|-------------|
| GS263 | Gen'l Sensors | PILL, Lensed, Phototransistor | MRD601 | E |
| GS265 | Gen'l Sensors | PILL, Lensed, Phototransistor | MRD604 | E |
| GS267 | Gen'l Sensors | PILL, Lensed, Phototransistor | MRD604 | E |
| GS501 | Gen'l Sensors | PILL, Lensed, Phototransistor | MRD604 | E |
| GS503 | Gen'l Sensors | PILL, Lensed, Phototransistor | MRD601 | E |
| GS561 | Gen'l Sensors | PILL, Lensed, Phototransistor | MRD601 | E |
| GS567 | Gen'l Sensors | PILL, Lensed, Phototransistor | MRD604 | E |
| GS600, 3, 6, 9, 10 | Gen'l Sensors | TO-18, Lensed, Phototransistor | MRD300 | A |
| GS612 | Gen'l Sensors | TO-18, Lensed, Phototransistor | MRD3050 | A |
| GS670 | Gen'l Sensors | TO-18, Lensed, Phototransistor | MRD3050 | A |
| GS680 | Gen'l Sensors | TO-18, Lensed, Phototransistor | MRD300 | A |
| GS683 | Gen'l Sensors | TO-18, Lensed, Phototransistor | MRD300 | A |
| GS686 | Gen'l Sensors | TO-18, Lensed, Phototransistor | MRD300 | A |
| H11A1 | GE | 6-Pin DIP Coupler Transistor Output | H11A1 | A |
| H11A2 | GE | 6-Pin DIP Coupler Transistor Output | H11A2 | A |
| H11A3 | GE | 6-Pin DIP Coupler Transistor Output | H11A3 | A |
| H11A4 | GE | 6-Pin DIP Coupler Transistor Output | H11A4 | A |
| H11A5 | GE | 6-Pin DIP Coupler Transistor Output | H11A5 | A |
| H11A520 | GE | 6-Pin DIP Coupler Transistor Output | H11A520 | A |
| H11A550 | GE | 6-Pin DIP Coupler Transistor Output | H11A550 | A |
| H11A5100 | GE | 6-Pin DIP Coupler Transistor Output | H11A5100 | A |
| H74A1 | GE | 6-Pin DIP Coupler Transistor Output | 4N26 | B |
| H11AA1 | GE | 6-Pin DIP Coupler Transistor Output | 4N26 | D |
| H11AA2 | GE | 6-Pin DIP Coupler Transistor Output | 4N27 | D |
| H11B1 | GE | 6-Pin DIP Coupler Darlington Output | H11B1 | A |
| H11B2 | GE | 6-Pin DIP Coupler Darlington Output | H11B2 | A |
| H11B3 | GE | 6-Pin DIP Coupler Darlington Output | H11B3 | A |
| H11B255 | GE | 6-Pin DIP Coupler Darlington Output | H11B255 | A |
| H11C1, 2, 3 | GE | 6-Pin DIP Coupler SCR Output | MOC3003 | A |
| H11C4, 5, 6 | GE | 6-Pin DIP Coupler SCR Output | MOC3001 | A |
| H1174C1, 2 | GE | 6-Pin DIP Coupler SCR Output | MOC3001 | A |
| H11D1, 2, 3, 4 | GE | 6-Pin DIP Coupler Hi V. Transistor | MOC3001 | DE |
| IL 1 | Litronix | 6-Pin DIP Coupler Transistor Output | IL1 | A |
| IL 5 | Litronix | 6-Pin DIP Coupler Transistor Output | 4N25 | B |
| IL 12 | Litronix | 6-Pin DIP Coupler Transistor Output | IL12 | A |
| IL 15 | Litronix | 6-Pin DIP Coupler Transistor Output | IL15 | A |
| IL 16 | Litronix | 6-Pin DIP Coupler Transistor Output | IL16 | A |
| IL 74 | Litronix | 6-Pin DIP Coupler Transistor Output | IL74 | A |
| ILA 30 | Litronix | 6-Pin DIP Coupler Darlington Output | 4N33 | B |
| ILA 55 | Litronix | 6-Pin DIP Coupler Darlington Output | 4N33 | B |
| ILCA2-30 | Litronix | 6-Pin DIP Coupler Darlington Output | 4N33 | B |
| ILCA2-55 | Litronix | 6-Pin DIP Coupler Darlington Output | 4N33 | B |
| IRL40 | Litronix | TO-18 Lensed I.R. LED | MLED930 | B |
| IRL60 | Litronix | Plastic, Lensed I.R. LED | MLED60 | A |
| L8, L9 | GE | TO-18 Lensed Phototriac | MRD3011 | D |
| L14F1 | GE | TO-18 Lensed Photodarlington | MRD360 | A |
| L14F2 | GE | TO-18 Lensed Photodarlington | MRD370 | A |
| L14G1 | GE | TO-18 Lensed Phototransistor | MRD300 | A |
| L14G2 | GE | TO-18 Lensed Phototransistor | MRD310 | A |
| L14G3 | GE | TO-18 Lensed Phototransistor | MRD310 | A |
| L14H1 | GE | TO-92 Phototransistors | L14H1 | A |
| L14H2 | GE | TO-92 Phototransistors | L14H2 | A |
| L14H3 | GE | TO-92 Phototransistors | L14H3 | A |
| L14H4 | GE | TO-92 Phototransistors | L14H4 | A |
| L15E | GE | PILL, Lensed, Phototransistor | MRD603 | A |
| L15A | GE | PILL, Lensed, Phototransistor | MRD602 | A |
| L15AX601 | GE | PILL, Lensed, Phototransistor | MRD601 | A |
| L15AX602 | GE | PILL, Lensed, Phototransistor | MRD602 | A |
| L15AX603 | GE | PILL, Lensed, Phototransistor | MRD603 | A |
| L15AX604 | GE | PILL, Lensed, Phototransistor | MRD604 | A |

CROSS-REFERENCE (continued)

| Device | Manufacturer | Description | Motorola Equivalent | Code |
|-------------------|---------------------|---------------------------------------|----------------------------|-------------|
| LD261 | Siemens | Plastic, I.R. LED | MLED60 | C |
| LED 56, F | GE | TO-18, Lensed, I.R. LED | MLED930 | A |
| LPT | Litronix | Plastic, Lensed, Phototransistor | MRD450 | E |
| LPT100A | Litronix | Plastic, Lensed, Phototransistor | MRD450 | E |
| LPT100B | Litronix | Plastic, Lensed, Phototransistor | MRD450 | E |
| M-161 | GI | Plastic, Lensed, Phototransistor | MRD160 | C |
| M-162 | GI | Plastic, Lensed, Phototransistor | MRD160 | C |
| M-163 | GI | Plastic, Lensed, Phototransistor | MRD450 | E |
| M-164 | GI | Plastic, Lensed, Phototransistor | MRD450 | E |
| M-165 | GI | Plastic, Lensed, Phototransistor | MRD450 | E |
| ME60 | GI | Plastic, Lensed, I.R. LED | MLED60 | C |
| ME61 | GI | Plastic, Lensed, I.R. LED | MLED60 | C |
| ME702 | GI | Plastic, Lensed, I.R. LED | MLED900 | E |
| MCA230 | GI | 6-Pin, DIP, Coupler Darlington Output | MCA230 | A |
| MCA231 | GI | 6-Pin, DIP, Coupler Darlington Output | MCA231 | A |
| MCA255 | GI | 6-Pin, DIP, Coupler Darlington Output | MCA255 | A |
| MCS2 | GI | 6-Pin, DIP, Coupler SCR Output | MOC3011 | DE |
| MCS2400 | GI | 6-Pin, DIP, Coupler SCR Output | MOC3011 | DE |
| MCT2 | GI | 6-Pin, DIP, Coupler Transistor Output | MCT2 | A |
| MC2E | GI | 6-Pin, DIP, Coupler Transistor Output | MCT2E | A |
| MCT26 | GI | 6-Pin, DIP, Coupler Transistor Output | 4N27 | B |
| OP123 | Optron | PILL, Lensed, I.R. LED | MLED910 | A |
| OP124 | Optron | PILL, Lensed, I.R. LED | MLED910 | A |
| OP130 | Optron | TO-18, Lensed, I.R. LED | MLED930 | A |
| OP131 | Optron | TO-18, Lensed, I.R. LED | MLED930 | A |
| OP160 | Optron | Plastic, Lensed, I.R. LED | MLED900 | E |
| OP500 | Optron | Plastic, Lensed, Phototransistor | MRD450 | E |
| OP600 | Optron | PILL, Lensed Phototransistor | MRD601 | A |
| OP601 | Optron | PILL, Lensed Phototransistor | MRD601 | A |
| OP602 | Optron | PILL, Lensed Phototransistor | MRD602 | A |
| OP603 | Optron | PILL, Lensed Phototransistor | MRD603 | A |
| OP604 | Optron | PILL, Lensed Phototransistor | MRD604 | A |
| OP640 | Optron | PILL, Lensed Phototransistor | MRD601 | A |
| OP641 | Optron | PILL, Lensed Phototransistor | MRD601 | A |
| OP642 | Optron | PILL, Lensed Phototransistor | MRD602 | A |
| OP643 | Optron | PILL, Lensed Phototransistor | MRD602 | A |
| OP644 | Optron | PILL, Lensed Phototransistor | MRD603 | A |
| OP800 | Optron | TO-18 Lensed Phototransistor | MRD3055 | A |
| OP801 | Optron | TO-18 Lensed Phototransistor | MRD3050 | A |
| OP802 | Optron | TO-18 Lensed Phototransistor | MRD310 | A |
| OP803 | Optron | TO-18 Lensed Phototransistor | MRD300 | A |
| OP804 | Optron | TO-18 Lensed Phototransistor | MRD300 | A |
| OP805 | Optron | TO-18 Lensed Phototransistor | MRD300 | A |
| OP830 | Optron | TO-18 Lensed Phototransistor | MRD300 | A |
| OPI110 | Optron | 6-Pin, DIP, Coupler Transistor Output | MOC1005 | DE |
| OPI2150 | Optron | 6-Pin, DIP, Coupler Transistor Output | MOC1006 | A |
| OPI2151 | Optron | 6-Pin, DIP, Coupler Transistor Output | 4N27 | A |
| OPI2152 | Optron | 6-Pin, DIP, Coupler Transistor Output | 4N26 | A |
| OPI2153 | Optron | 6-Pin, DIP, Coupler Transistor Output | 4N26 | D |
| OPI2250 | Optron | 6-Pin, DIP, Coupler Transistor Output | MOC1006 | A |
| OPI2251 | Optron | 6-Pin, DIP, Coupler Transistor Output | MOC1006 | A |
| OPI2252 | Optron | 6-Pin, DIP, Coupler Transistor Output | 4N25 | A |
| OPI2253 | Optron | 6-Pin, DIP, Coupler Transistor Output | 4N25 | D |
| PC503 | Sharp | 6-Pin, DIP, Coupler Transistor Output | 4N26 | A |
| SD1440-1,-2,-3,-4 | Spectronics | PILL, Lensed Phototransistor | MRD3050 | DE |
| SD2440-1 | Spectronics | PILL, Lensed Phototransistor | MRD601 | A |
| SD2440-2 | Spectronics | PILL, Lensed Phototransistor | MRD602 | A |
| SD2440-3 | Spectronics | PILL, Lensed Phototransistor | MRD603 | A |
| SD2440-4 | Spectronics | PILL, Lensed Phototransistor | MRD604 | A |
| SD2441-1 | Spectronics | PILL, Lensed Phototransistor | MRD602 | A |

CROSS-REFERENCE (continued)

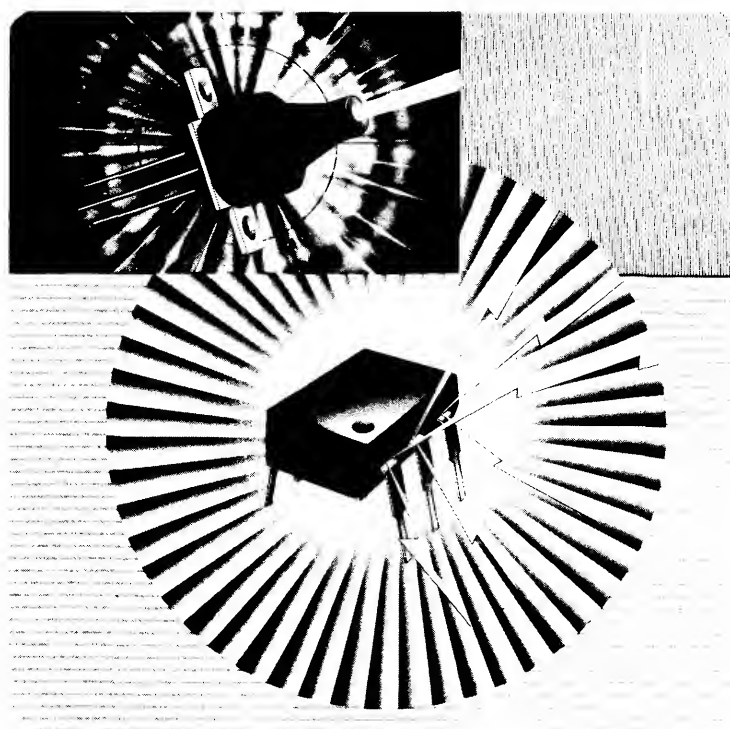
| Device | Manufacturer | Description | Motorola Equivalent | Code |
|----------------|---------------------|---|----------------------------|-------------|
| SD2441-2 | Spectronics | PILL, Lensed Phototransistor | MRD603 | A |
| SD2441-3 | Spectronics | PILL, Lensed Phototransistor | MRD604 | A |
| SD2441-4 | Spectronics | PILL, Lensed Phototransistor | MRD604 | B |
| SD3420-1,-2 | Spectronics | TO-18, Flat Window Pin, Photodarlington | MRD510 | A |
| SD5400-1 | Spectronics | TO-18, Lensed Photodarlington | MRD370 | A |
| SD5400-2 | Spectronics | TO-18, Lensed Photodarlington | MRD360 | A |
| SD5400-3 | Spectronics | TO-18, Lensed Photodarlington | MRD360 | A |
| SD5420-1 | Spectronics | TO-18, Lensed Photodarlington | MRD500 | A |
| SD5440-1 | Spectronics | TO-18, Lensed Phototransistor | MRD3052 | A |
| SD5440-2 | Spectronics | TO-18, Lensed Phototransistor | MRD3056 | A |
| SD5440-3 | Spectronics | TO-18, Lensed Phototransistor | MRD300 | A |
| SD5440-4 | Spectronics | TO-18, Lensed Phototransistor | MRD300 | B |
| SD5442-1,-2,-3 | Spectronics | TO-18, Lensed Phototransistor | MRD300 | B |
| SE1450 series | Spectronics | TO-18, Lensed Phototransistor | MLED930 | E |
| SE2450 series | Spectronics | PILL, Lensed I.R. LED | MLED910 | 8 |
| SE2460 series | Spectronics | PILL, Lensed I.R. LED | MLED910 | 8 |
| SE5450 series | Spectronics | TO-18, Lensed I.R. LED | MLED930 | A |
| SE5451 series | Spectronics | TO-18, Lensed I.R. LED | MLED930 | B |
| SG1001 series | RCA | PILL, Lensed I.R. LED | MLED910 | B |
| SPX2 | Spectronics | 6-Pin DIP, Coupler Transistor Output | 4N35 | A |
| SPX2E | Spectronics | 6-Pin DIP, Coupler Transistor Output | 4N35 | A |
| SPX4 | Spectronics | 6-Pin DIP, Coupler Transistor Output | 4N35 | A |
| SPX5 | Spectronics | 6-Pin DIP, Coupler Transistor Output | 4N35 | A |
| SPX6 | Spectronics | 6-Pin DIP, Coupler Transistor Output | 4N35 | A |
| SPX26 | Spectronics | 6-Pin DIP, Coupler Transistor Output | 4N27 | A |
| SPX28 | Spectronics | 6-Pin DIP, Coupler Transistor Output | 4N27 | A |
| SPX35 | Spectronics | 6-Pin DIP, Coupler Transistor Output | 4N35 | A |
| SPX36 | Spectronics | 6-Pin DIP, Coupler Transistor Output | 4N35 | A |
| SPX37 | Spectronics | 6-Pin DIP, Coupler Transistor Output | 4N35 | A |
| SSL4, F | Solar Systems | TO-18, Lensed I.R. LED | MLED930 | B |
| SSL34, 54 | Solar Systems | TO-18, Lensed I.R. LED | MLED930 | B |
| STPT10 | Sensor Tech | Plastic Lensed Phototransistor | MRD160 | C |
| STPT15 | Sensor Tech | Plastic Lensed Phototransistor | MRD160 | C |
| STPT20 | Sensor Tech | PILL, Lensed Phototransistor | MRD604 | A |
| STPT21 | Sensor Tech | PILL, Lensed Phototransistor | MRD601 | A |
| STPT25 | Sensor Tech | PILL, Lensed Phototransistor | MRD603 | A |
| STPT45 | Sensor Tech | Plastic Lensed Phototransistor | MRD450 | A |
| STPT51 | Sensor Tech | TO-18, Lensed Phototransistor | MRD3050 | A |
| STPT53 | Sensor Tech | TO-18, Lensed Phototransistor | MRD3056 | A |
| STPT60 series | Sensor Tech | PILL, Lensed Phototransistor | MRD601 series | A |
| STPT80 | Sensor Tech | TO-18, Lensed Phototransistor | MRD3056 | A |
| STPT80 | Sensor Tech | TO-18, Lensed Phototransistor | MRD3056 | A |
| STPT81 | Sensor Tech | TO-18, Lensed Phototransistor | MRD3052 | A |
| STPT82 | Sensor Tech | TO-18, Lensed Phototransistor | MRD3053 | A |
| STPT83 | Sensor Tech | TO-18, Lensed Phototransistor | MRD3054 | A |
| STPT84 | Sensor Tech | TO-18, Lensed Phototransistor | MRD3056 | A |
| STPT260 | Sensor Tech | TO-18, Lensed Darlington Transistor | MRD360 | A |
| STPT300 | Sensor Tech | TO-18, Lensed Phototransistor | MRD300 | A |
| STPT310 | Sensor Tech | TO-5, Lensed Photodarlington | MRD360 | C |
| TIL23 | Texas Instr. | PILL, Lensed Phototransistor | MLED910 | A |
| TIL24 | Texas Instr. | PILL, Lensed Phototransistor | MLED910 | B |
| TIL26 | Texas Instr. | Plastic, Lensed I.R. LED | MLED60 | E |
| TIL31 | Texas Instr. | TO-18, Lensed Phototransistor | MLED930 | 8 |
| TIL33 | Texas Instr. | TO-18, Lensed Phototransistor | MLED930 | B |
| TIL34 | Texas Instr. | TO-18, Lensed Phototransistor | MLED930 | A |
| TIL63 | Texas Instr. | TO-18, Lensed Phototransistor | MRD3050 | A |
| TIL64 | Texas Instr. | TO-18, Lensed Phototransistor | MRD3050 | A |
| TIL65 | Texas Instr. | TO-18, Lensed Phototransistor | MRD3052 | A |
| TIL66 | Texas Instr. | TO-18, Lensed Phototransistor | MRD3054 | A |
| TIL67 | Texas Instr. | TO-18, Lensed Phototransistor | MRD3056 | A |
| TIL78 | Texas Instr. | Plastic, Lensed Phototransistor | MRD450 | C |

CROSS-REFERENCE (continued)

| Device | Manufacturer | Description | Motorola Equivalent | Code |
|---------------|---------------------|--------------------------------------|----------------------------|-------------|
| TIL81 | Texas Instr. | TO-18, Lensed Phototransistor | MRD300 | A |
| TIL111 | Texas Instr. | 6-Pin DIP, Coupler Transistor Output | TIL111 | A |
| TIL112 | Texas Instr. | 6-Pin DIP, Coupler Transistor Output | TIL112 | A |
| TIL113 | Texas Instr. | 6-Pin DIP, Coupler Transistor Output | TIL113 | A |
| TIL114 | Texas Instr. | 6-Pin DIP, Coupler Transistor Output | TIL114 | A |
| TIL115 | Texas Instr. | 6-Pin DIP, Coupler Transistor Output | TIL115 | A |
| TIL116 | Texas Instr. | 6-Pin DIP, Coupler Transistor Output | TIL116 | A |
| TIL117 | Texas Instr. | 6-Pin DIP, Coupler Transistor Output | TIL117 | A |
| TIL118 | Texas Instr. | 6-Pin DIP, Coupler Transistor Output | MOC1006 | C |
| TIL119 | Texas Instr. | 6-Pin DIP, Coupler Transistor Output | TIL119 | A |
| TIL601 | Texas Instr. | PILL, Lensed Phototransistor | MRD601 | A |
| TIL602 | Texas Instr. | PILL, Lensed Phototransistor | MRD602 | A |
| TIL603 | Texas Instr. | PILL, Lensed Phototransistor | MRD603 | A |
| TIL604 | Texas Instr. | PILL, Lensed Phototransistor | MRD604 | A |
| TLP501 | Toshiba | 6-Pin DIP, Coupler Transistor Output | 4N27 | B |
| TLP503 | Toshiba | 6-Pin DIP, Coupler Transistor Output | 4N25 | B |
| TLP504 | Toshiba | 6-Pin DIP, Coupler Transistor Output | 4N25 | B |
| 1N5722 | Industry | PILL, Lensed Phototransistor | MRD601 | A |
| 1N5723 | Industry | PILL, Lensed Phototransistor | MRD602 | A |
| 1N5724 | Industry | PILL, Lensed Phototransistor | MRD603 | A |
| 1N5725 | Industry | PILL, Lensed Phototransistor | MRD604 | A |
| 2N5777 | Industry | TO-92, Plastic Photodarlington | 2N5777 | A |
| 2N5778 | Industry | TO-92, Plastic Photodarlington | 2N5778 | A |
| 2N5779 | Industry | TO-92, Plastic Photodarlington | 2N5779 | A |
| 2N5780 | Industry | TO-92, Plastic Photodarlington | 2N5780 | D |
| 4N25 | Industry | 6-Pin DIP, Coupler Transistor Output | 4N25 | A |
| 4N26 | Industry | 6-Pin DIP, Coupler Transistor Output | 4N26 | A |
| 4N27 | Industry | 6-Pin DIP, Coupler Transistor Output | 4N27 | A |
| 4N28 | Industry | 6-Pin DIP, Coupler Transistor Output | 4N28 | A |
| 4N29 | Industry | 6-Pin DIP, Coupler Darlington Output | 4N29 | A |
| 4N30 | Industry | 6-Pin DIP, Coupler Darlington Output | 4N30 | A |
| 4N31 | Industry | 6-Pin DIP, Coupler Darlington Output | 4N31 | A |
| 4N32 | Industry | 6-Pin DIP, Coupler Darlington Output | 4N32 | A |
| 4N33 | Industry | 6-Pin DIP, Coupler Darlington Output | 4N33 | A |
| 4N35 | Industry | 6-Pin DIP, Coupler Transistor Output | 4N35 | A |
| 4N36 | Industry | 6-Pin DIP, Coupler Transistor Output | 4N37 | A |
| 4N37 | Industry | 6-Pin DIP, Coupler Transistor Output | 4N37 | A |
| 4N38 | Industry | 6-Pin DIP, Coupler Transistor Output | 4N38 | A |
| 4N39 | Industry | 6-Pin DIP, Coupler SCR Output | MOC3011 | DE |
| 4N40 | Industry | 6-Pin DIP, Coupler SCR Output | MOC3011 | DE |
| 4N45 | Industry | 6-Pin DIP, Coupler Darlington Output | 4N32 | DE |
| 4N46 | Industry | 6-Pin DIP, Coupler Darlington Output | 4N32 | DE |
| 6N135 | Industry | 8-Pin DIP, Coupler Transistor Output | MOC1006 | DE |
| 6N136 | Industry | 8-Pin DIP, Coupler Transistor Output | MOC1005 | DE |
| 6N138 | Industry | 8-Pin DIP, Coupler Darlington Output | 4N32 | DE |
| 6N139 | Industry | 8-Pin DIP, Coupler Darlington Output | 4N32 | DE |
| 5082-4203 | Hewlett-Packard | TO-18, Lensed Photo PIN Diode | MRD500 | A |
| 5082-4204 | Hewlett-Packard | TO-18, Lensed Photo PIN Diode | MRD500 | A |
| 5082-4207 | Hewlett-Packard | TO-18, Lensed Photo PIN Diode | MRD500 | A |
| 5082-4220 | Hewlett-Packard | TO-18, Lensed Photo PIN Diode | MRD500 | A |
| 5082-4350 | Hewlett Packard | 8-Pin DIP, Coupler Transistor Output | MOC1006 | DE |
| 5082-4351 | Hewlett Packard | 8-Pin DIP, Coupler Transistor Output | MOC1005 | DE |
| 5082-4352 | Hewlett Packard | 8-Pin DIP, Coupler Transistor Output | MOC1005 | DE |
| 5082-4370 | Hewlett Packard | 8-Pin DIP, Coupler Darlington Output | 4N32 | DE |
| 5081-4371 | Hewlett Packard | 8-Pin DIP, Coupler Darlington Output | 4N32 | DE |

OPTOELECTRONICS

Data Sheets



OPTOELECTRONICS DATA SHEETS

| | Page |
|--|-------|
| 2N5777 thru 2N5780, MRD14B | 3-3 |
| 4N25, A; 4N26, 4N27, 4N28 | 3-5 |
| 4N29, A; 4N30, 4N31, 4N32, A; 4N33 | |
| 4N35, 4N36, 4N37 | 3-9 |
| 4N38, A | 3-13 |
| L14H1 thru L14H4 | 3-17 |
| MLED60, MLED90 | 3-21 |
| MLED92 | 3-23 |
| MLED93 thru MLED95 | 3-25 |
| MLED900 | 3-27 |
| MLED930 | 3-29 |
| MOC119 | 3-31 |
| MOC1005, MOC1006 | 3-33 |
| MOC3000 thru MOC3003 | 3-37 |
| MOC3009 thru MOC3011 | 3-41 |
| MOC3020, MOC3021 | 3-44 |
| MOC3030, MOC3031 | 3-48 |
| MOC5005, MOC5006 | 3-50 |
| MOC5010 | 3-53 |
| MOC8020, MOC8021 | 3-55 |
| MOC8030, MOC8050 | 3-57 |
| MRD150 | 3-59 |
| MRD160 | 3-63 |
| MRD300, MRD310 | 3-66 |
| MRD360, MRD370 | 3-69 |
| MRD450 | 3-73 |
| MRD500, MRD510 | 3-77 |
| MRD3010, MRD3011 | 3-80 |
| MRD3050, MRD3051, MRD3054, MRD3055, MRD3056 | 3-83 |
| Opto Couplers/Isolators (Industry) | 3-86 |
| Plastic NPN Silicon Photo Darlington Amplifiers | 3-89 |
| NPN Phototransistor and PN Infrared-Emitting Diode | 3-90 |
| NPN Photodarlington and PN Infrared-Emitting Diode | 3-91 |
| NPN Phototransistor and PN Infrared-Emitting Diode | 3-92 |
| Optical Coupler with NPN Transistor Output | 3-93 |
| Plastic NPN Silicon Photo Transistors | 3-94 |
| Infrared-Emitting Diodes | 3-95 |
| Infrared-Emitting Diode | 3-96 |
| Infrared-Emitting Diodes | 3-97 |
| Infrared-Emitting Diode | 3-98 |
| Infrared-Emitting Diode | 3-99 |
| Opto Coupler with Darlington Output | 3-100 |
| Opto Coupler with Transistor Output | 3-101 |
| Opto SCR Coupler | 3-102 |
| Optically-Isolated Triac Driver, 250 V | 3-103 |
| Optically-Isolated Triac Driver, 400 V | 3-104 |
| Zero Voltage Crossing Optically-Isolated Triac Driver, 250 V | 3-105 |
| Digital Logic Coupler | 3-106 |
| Optically-Isolated AC Linear Coupler | 3-107 |
| High CTR Darlington Coupler | 3-108 |
| 80-Volt Darlington Coupler | 3-109 |
| Plastic NPN Silicon Photo Transistor | 3-110 |
| Plastic NPN Silicon Photo Transistor | 3-111 |
| NPN Silicon High Sensitivity Photo Transistor | 3-112 |
| NPN Silicon High Sensitivity Photo Darlington Transistor | 3-113 |
| Plastic NPN Photo Transistor | 3-114 |
| PIN Silicon Photo Diode | 3-115 |
| 250-V NPN Silicon Photo Triac Driver | 3-116 |
| NPN Silicon Photo Transistors | 3-117 |
| Phototransistor and Photodarlington Opto Couplers | 3-118 |



MOTOROLA

**2N5777 thru
2N5780
MRD14B**

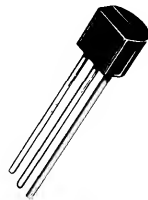
**PLASTIC NPN SILICON PHOTO
DARLINGTON AMPLIFIERS**

. . . designed for applications in industrial inspection, processing and control, counters, sorters, switching and logic circuits or any design requiring extremely high radiation sensitivity, and stable characteristics.

- Economical Plastic Package
- Sensitive Throughout Visible and Near Infrared Spectral Range for Wide Application
- Range of Radiation Sensitivities and Voltages for Design Flexibility
- TO-92 Clear Plastic Package for Standard Mounting
- Annular Passivated Structure for Stability and Reliability
- Precision Die Placement

**12, 25, 40 VOLT
PHOTO DARLINGTON
AMPLIFIERS
NPN SILICON**

200 MILLIWATTS



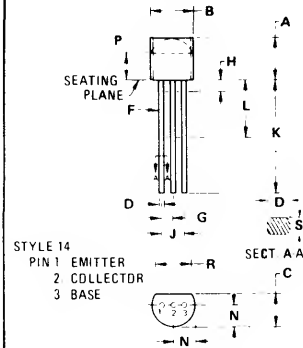
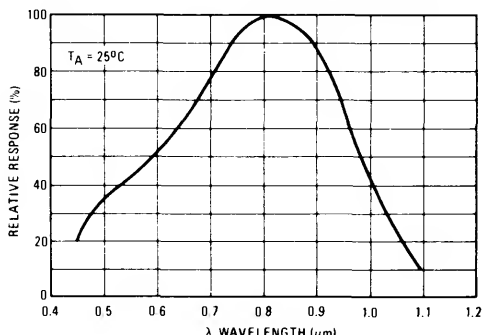
MAXIMUM RATINGS

| Rating | Symbol | MRD14B | 2N5777* | 2N5779 | 2N5778* | Unit |
|---|--|--------|-------------|--------|---------|------|
| Collector-Emitter Voltage | V _{CEO} | 12 | 25 | 40 | Volts | |
| Collector-Base Voltage | V _{CBO} | 18 | 25 | 40 | Volts | |
| Emitter-Base Voltage | V _{EBO} | 8.0 | 8.0 | 12 | Volts | |
| Light Current | I _L | — | 250 | — | mA | |
| Total Device Dissipation @ T _A = 25°C Derate above 25°C | P _D | — | 200 | — | mW | |
| | | — | 2.67 | — | mW/°C | |
| Operating and Storage Junction Temperature Range | T _J , T _{Stg} ⁽¹⁾ | — | -65 to +100 | — | °C | |

*Indicates JEDEC Registered Data.

(1) Heat Sink should be applied to leads during soldering to prevent case temperature from exceeding 100°C.

FIGURE 1 – CONSTANT ENERGY SPECTRAL RESPONSE



NOTES

1. CONTOUR OF PACKAGE BEYOND ZONE P
2. IS UNCONTROLLED
- DIM "F" APPLIES BETWEEN "H" AND "L". DIM "D" & "S" APPLIES BETWEEN "L" & 12.70 mm (0.5") FROM SEATING PLANE. LEAD DIM IS UNCONTROLLED IN "H" & BEYOND 12.70 mm (0.5") FROM SEATING PLANE

| DIM | MILLIMETERS | | INCHES | |
|-----|-------------|------|--------|-------|
| | MIN | MAX | MIN | MAX |
| A | 4.32 | 5.33 | 0.170 | 0.210 |
| B | 4.44 | 5.21 | 0.175 | 0.205 |
| C | 3.18 | 4.19 | 0.125 | 0.165 |
| D | 0.41 | 0.56 | 0.016 | 0.022 |
| F | 0.41 | 0.48 | 0.016 | 0.019 |
| G | 1.14 | 1.40 | 0.045 | 0.055 |
| H | — | 2.54 | — | 0.100 |
| J | 2.41 | 2.67 | 0.095 | 0.105 |
| K | 12.70 | — | 0.500 | — |
| L | 6.35 | — | 0.250 | — |
| N | 2.03 | 2.92 | 0.080 | 0.115 |
| P | 2.92 | — | 0.115 | — |
| R | 3.43 | — | 0.135 | — |
| S | 0.36 | 0.41 | 0.014 | 0.016 |

All JEDEC dimensions and notes apply
CASE 29 02
TO-92

2N5777 THRU 2N5780 , MRD14B

* STATIC ELECTRICAL CHARACTERISTICS ($T_A = 25^\circ\text{C}$ unless otherwise noted)

| Characteristic | Symbol | Min | Typ | Max | Unit |
|---|---------------|------------------|-------------|-----|---------------|
| Collector Dark Current (Note 2) ($V_{CE} = 12 \text{ V}$) | I_{CEO} | — | — | 0.1 | μA |
| Collector-Emitter Breakdown Voltage (Note 2) ($I_C = 10 \text{ mA}$) | $V_{(BR)CEO}$ | 12 25 40 | — — — | — | Volts |
| Collector-Base Breakdown Voltage (Note 2) ($I_C = 100 \mu\text{A}$) | $V_{(BR)CBO}$ | 18 25 40 | — — — | — | Volts |
| Emitter-Base Breakdown Voltage (Note 2) ($I_E = 100 \mu\text{A}$) | $V_{(BR)EBO}$ | 8.0 8.0 12 | — — — | — | Volts |

* OPTICAL CHARACTERISTICS ($T_A = 25^\circ\text{C}$ unless otherwise noted)

| Characteristic | Fig. No. | Symbol | Min | Typ | Max | Unit |
|---|----------|-------------|-------------------|-------------------|-------------|---------------|
| Collector Light Current (Notes 1,4,5) ($V_{CE} = 5.0 \text{ V}$) | — | I_L | 0.5 0.5 2.0 | 2.0 4.0 8.0 | — — — | mA |
| DC Current Gain (Note 2) ($V_{CE} = 5.0 \text{ V}$, $I_C = 0.5 \text{ mA}$) | — | h_{FE} | 2.5 k 5.0 k | — — | — — | — |
| Wave Length of Maximum Sensitivity | 1 | λ_s | 0.7 | 0.8 | 1.0 | μm |
| Turn-On Delay Time (Notes 3, 4) | 2,3 | t_{d1} | — | — | 100 | μs |
| Rise Time (Notes 3, 4) | 2,3 | t_r | — | — | 250 | μs |
| Turn-Off Delay Time (Notes 3, 4) | 2,3 | t_{d2} | — | — | 5.0 | μs |
| Fall Time (Notes 3, 4) | 2,3 | t_f | — | — | 150 | μs |
| Collector-Base Capacitance ($V_{CB} = 10 \text{ V}$, $f = 1.0 \text{ MHz}$, $I_E = 0$) | — | C_{cb} | — | — | 10 | pF |

* Indicates JEDEC Registered Data.

NOTES:

1. Radiation Flux Density (H) equal to 2.0 mW/cm^2 emitted from a tungsten source at a color temperature of 2870°K .
2. Measured under dark conditions. ($H \approx 0$).
3. For unsaturated rise time measurements, radiation is provided by a pulsed GaAs (gallium-arsenide) light-emitting diode ($\lambda \approx 0.9$

μm) with a pulse width equal to or greater than 500 microseconds (see Figures 2 and 3).

4. Measurement mode with no electrical connection to the base lead.
5. Die faces curved side of package.

FIGURE 2 – PULSE RESPONSE TEST CIRCUIT

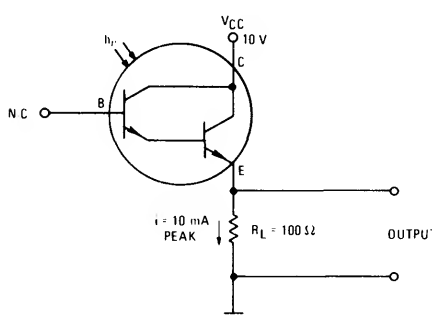
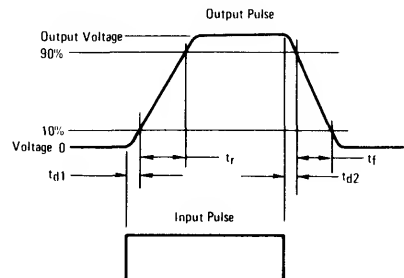


FIGURE 3 – PULSE RESPONSE TEST WAVEFORM





MOTOROLA

4N25, 4N25A

4N26

4N27

4N28

**NPN PHOTOTRANSISTOR AND
PN INFRARED EMITTING DIODE**

... Gallium Arsenide LED optically coupled to a Silicon Photo Transistor designed for applications requiring electrical isolation, high-current transfer ratios, small package size and low cost; such as interfacing and coupling systems, phase and feedback controls, solid-state relays and general-purpose switching circuits.

- High Isolation Voltage — $V_{ISO} = 7500$ V (Min)
- High Collector Output Current @ $I_F = 10$ mA — $I_C = 5.0$ mA (Typ) — 4N25,A,4N26
 2.0 mA (Typ) — 4N27,4N28
- Economical, Compact, Dual-In-Line Package
- Excellent Frequency Response — 300 kHz (Typ)
- Fast Switching Times @ $I_C = 10$ mA
 $t_{on} = 0.87 \mu s$ (Typ) — 4N25,A,4N26
 $2.1 \mu s$ (Typ) — 4N27,4N28
 $t_{off} = 11 \mu s$ (Typ) — 4N25,A,4N26
 $5.0 \mu s$ (Typ) — 4N27,4N28
- 4N25A is UL Recognized File Number E54915

*MAXIMUM RATINGS ($T_A = 25^\circ C$ unless otherwise noted).

| Rating | Symbol | Value | Unit |
|--------|--------|-------|------|
|--------|--------|-------|------|

INFRARED-EMITTING DIODE MAXIMUM RATINGS

| | | | |
|---|-------|-----|----------------|
| Reverse Voltage | V_R | 3.0 | Volts |
| Forward Current — Continuous | I_F | 80 | mA |
| Forward Current — Peak Pulse Width = 300 μs , 2.0% Duty Cycle | I_F | 3.0 | Amp |
| Total Power Dissipation @ $T_A = 25^\circ C$ Negligible Power in Transistor Derate above 25°C | P_D | 150 | mW |
| | | 2.0 | mW/ $^\circ C$ |

PHOTOTRANSISTOR MAXIMUM RATINGS

| | | | |
|---|-----------|-----|----------------|
| Collector-Emitter Voltage | V_{CEO} | 30 | Volts |
| Emitter-Collector Voltage | V_{ECO} | 7.0 | Volts |
| Collector-Base Voltage | V_{CBO} | 70 | Volts |
| Total Device Dissipation @ $T_A = 25^\circ C$ Negligible Power in Diode Derate above 25°C | P_D | 150 | mW |
| | | 2.0 | mW/ $^\circ C$ |

TOTAL DEVICE RATINGS

| | | | |
|--|-----------|-------------|----------------|
| Total Device Dissipation @ $T_A = 25^\circ C$ | P_D | 250 | mW |
| Equal Power Dissipation in Each Element Derate above 25°C | | 3.3 | mW/ $^\circ C$ |
| Junction Temperature Range | T_J | -55 to +100 | $^\circ C$ |
| Storage Temperature Range | T_{stg} | -55 to +150 | $^\circ C$ |
| Soldering Temperature (10 s) | | 260 | $^\circ C$ |

*Indicates JEDEC Registered Data.

FIGURE 1 — MAXIMUM POWER DISSIPATION

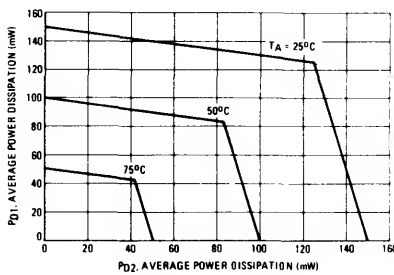
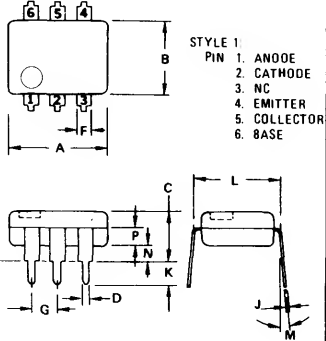
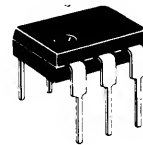


Figure 1 is based upon using limit values in the equation
 $T_{J1} - T_A = R_{\theta JA}(P_{D1} + K_\theta P_{D2})$ where
 T_{J1} Junction Temperature (100°C)
 T_A Ambient Temperature
 $R_{\theta JA}$ Junction to Ambient Thermal Resistance (500°C/W)
 P_{D1} Power Dissipation in One Chip
 P_{D2} Power Dissipation in Other Chip
 K_θ Thermal Coupling Coefficient (20%)
Example
With $P_{D1} = 90$ mW in the LED
@ $T_A = 50^\circ C$, the transistor
 $P_D (P_{D2})$ must be less than 50 mW

OPTO COUPLER/ISOLATOR

TRANSISTOR OUTPUT



NOTES.

1. DIMENSIONS A AND B ARE DATUMS.
2. T IS SEATING PLANE.
3. POSITIONAL TOLERANCES FOR LEADS: Ø 0.013 (0.009) T AWB(M)
4. DIMENSION L TO CENTER OF LEADS WHEN FORMED PARALLEL.
5. DIMENSIONING AND TOLERANCING PER ANSI Y14.5, 1973.

| DIM | MILLIMETERS | | INCHES | |
|-----|-------------|------|--------|-------|
| | MIN | MAX | MIN | MAX |
| A | 8.13 | 8.89 | 0.320 | 0.350 |
| B | 6.16 | 6.60 | 0.240 | 0.260 |
| C | 2.92 | 5.08 | 0.115 | 0.200 |
| D | 0.41 | 0.51 | 0.016 | 0.020 |
| F | 1.02 | 1.78 | 0.040 | 0.070 |
| G | 2.54 | 8.56 | 0.100 | 0.330 |
| J | 0.20 | 0.30 | 0.008 | 0.012 |
| K | 2.54 | 3.81 | 0.100 | 0.150 |
| L | 7.62 | 8.56 | 0.300 | 0.330 |
| M | 0.00 | 1.50 | 0.00 | 0.150 |
| N | 0.36 | 2.54 | 0.015 | 0.100 |
| P | 1.27 | 2.03 | 0.050 | 0.080 |

CASE 730A-01

4N25, 4N25A, 4N26, 4N27, 4N28

LED CHARACTERISTICS ($T_A = 25^\circ\text{C}$ unless otherwise noted)

| Characteristic | Symbol | Min | Typ | Max | Unit |
|--|--------|-----|-------|-----|---------------|
| *Reverse Leakage Current ($V_R = 3.0 \text{ V}$, $R_L = 1.0 \text{ M ohms}$) | I_R | — | 0.005 | 100 | μA |
| *Forward Voltage ($I_F = 10 \text{ mA}$) | V_F | — | 1.2 | 1.5 | Volts |
| Capacitance ($V_R = 0 \text{ V}$, $f = 1.0 \text{ MHz}$) | C | — | 150 | — | pF |

PHOTOTRANSISTOR CHARACTERISTICS ($T_A = 25^\circ\text{C}$ and $I_F = 0$ unless otherwise noted)

| | | | | | | |
|---|-----------------------------|---------------|-----|----------|-----------|-------|
| *Collector-Emitter Dark Current ($V_{CE} = 10 \text{ V}$, Base Open) | 4N25, A, 4N26, 4N27 4N28 | I_{CEO} | — | 3.5 — | 50 100 | nA |
| *Collector-Base Dark Current ($V_{CB} = 10 \text{ V}$, Emitter Open) | | I_{CBO} | — | — | 20 | nA |
| *Collector-Base Breakdown Voltage ($I_C = 100 \mu\text{A}$, $I_E = 0$) | | $V_{(BR)CBO}$ | 70 | — | — | Volts |
| *Collector-Emitter Breakdown Voltage ($I_C = 1.0 \text{ mA}$, $I_B = 0$) | | $V_{(BR)CEO}$ | 30 | — | — | Volts |
| *Emitter-Collector Breakdown Voltage ($I_E = 100 \mu\text{A}$, $I_B = 0$) | | $V_{(BR)ECO}$ | 7.0 | 8.0 | — | Volts |
| DC Current Gain ($V_{CE} = 5.0 \text{ V}$, $I_C = 500 \mu\text{A}$) | | h_{FE} | — | 325 | — | — |

COUPLED CHARACTERISTICS ($T_A = 25^\circ\text{C}$ unless otherwise noted)

| | | | | | | |
|--|--|----------------------|-------------------------------------|-----------------------|-----------------------|-------|
| *Collector Output Current (1) ($V_{CE} = 10 \text{ V}$, $I_F = 10 \text{ mA}$, $I_B = 0$) | 4N25, A, 4N26 4N27, 4N28 | I_C | 2.0 1.0 | 5.0 2.0 | — | mA |
| Isolation Surge Voltage (2, 5) (60 Hz Peak ac, 5 Seconds) (60 Hz Peak) | *4N25, A *4N26, 4N27 *4N28 *4N25A | V_{ISO} | 7500 2500 1500 500 1775 | — — — — — | — — — — — | Volts |
| (60 Hz RMS for 1 Second) (3) | | | | | | |
| Isolation Resistance (2) ($V = 500 \text{ V}$) | | — | — | 10^{11} | — | Ohms |
| *Collector-Emitter Saturation ($I_C = 2.0 \text{ mA}$, $I_F = 50 \text{ mA}$) | | $V_{CE(\text{sat})}$ | — | 0.2 | 0.5 | Volts |
| Isolation Capacitance (2) ($V = 0$, $f = 1.0 \text{ MHz}$) | | — | — | 1.3 | — | pF |
| Bandwidth (4) ($I_C = 2.0 \text{ mA}$, $R_L = 100 \text{ ohms}$, Figure 11 (2)) | | — | — | 300 | — | kHz |

SWITCHING CHARACTERISTICS

| | | | | | | |
|--------------|---|-------|---|--------------|---|---------------|
| Delay Time | (4N25, A, 4N26 2N27, 4N28) Figures 6 and 8) | t_d | — | 0.07 0.10 | — | μs |
| Rise Time | | t_r | — | 0.8 2.0 | — | μs |
| Storage Time | (4N25, A, 4N26 4N27, 4N28) Figures 7 and 8) | t_s | — | 4.0 2.0 | — | μs |
| Fall Time | | t_f | — | 8.0 8.0 | — | μs |

*Indicates JEDEC Registered Data

(1) Pulse Test: Pulse Width = 300 μs , Duty Cycle $\leq 2.0\%$.

(2) For this test LED pins 1 and 2 are common and phototransistor pins 4, 5, and 6 are common.

(3) RMS Volts, 60 Hz. For this test, pins 1, 2, and 3 are common and pins 4, 5, and 6 are common.

(4) I_F adjusted to yield $I_C = 2.0 \text{ mA}$ and $i_c = 2.0 \text{ mA}$ p-p at 10 kHz.

(5) Isolation Surge Voltage, V_{ISO} , is an internal device dielectric breakdown rating.

DC CURRENT TRANSFER CHARACTERISTICS

FIGURE 2 - 4N25,A,4N26

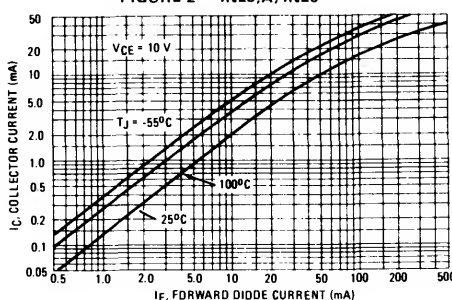
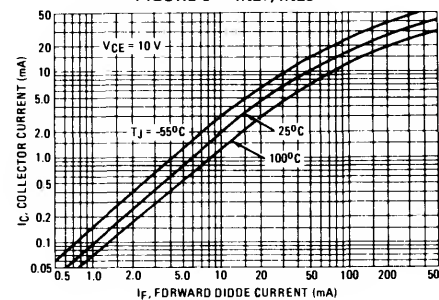


FIGURE 3 - 4N27,4N28



4N25, 4N25A, 4N26, 4N27, 4N28

TYPICAL ELECTRICAL CHARACTERISTICS

FIGURE 4 – FORWARD CHARACTERISTICS

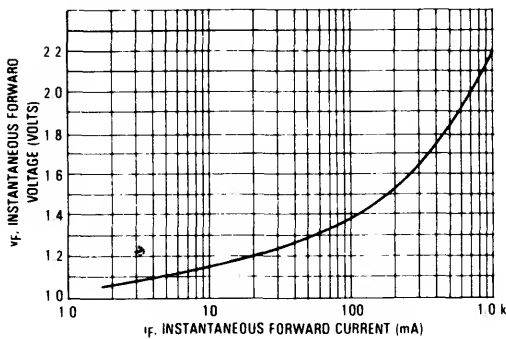


FIGURE 5 – COLLECTOR SATURATION VOLTAGE

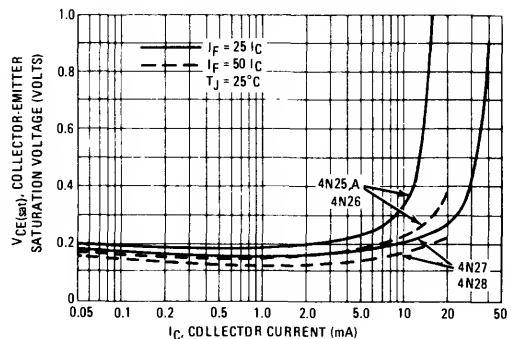


FIGURE 6 – TURN-ON TIME

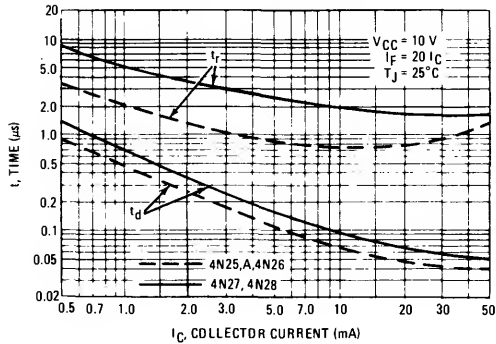


FIGURE 7 – TURN-OFF TIME

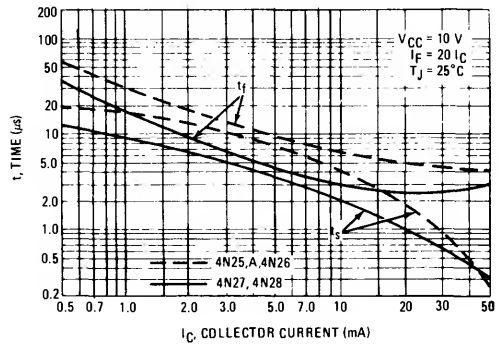


FIGURE 8 – SATURATED SWITCHING TIME TEST CIRCUIT

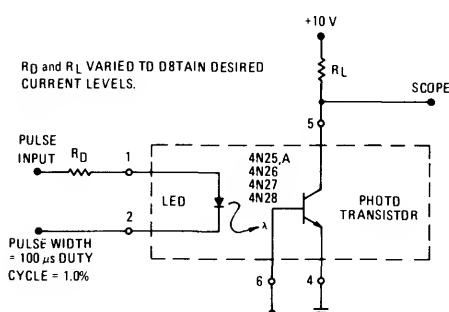
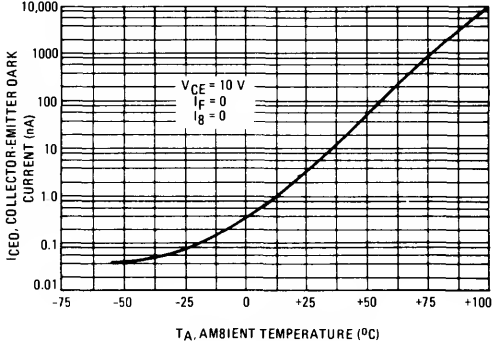
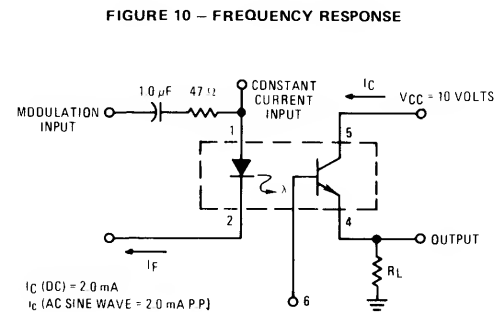
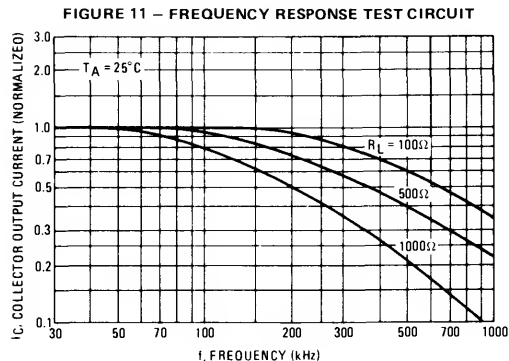


FIGURE 9 – DARK CURRENT versus AMBIENT TEMPERATURE



4N25, 4N25A, 4N26, 4N27, 4N28



TYPICAL APPLICATIONS

FIGURE 12 – ISOLATED TTL TO MOS (P-CHANNEL) LEVEL TRANSLATOR

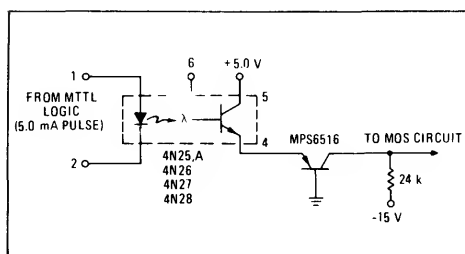


FIGURE 13 – COMPUTER/PERIPHERAL INTERCONNECT

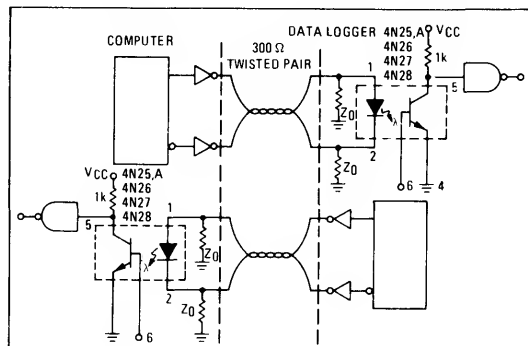


FIGURE 14 – POWER AMPLIFIER

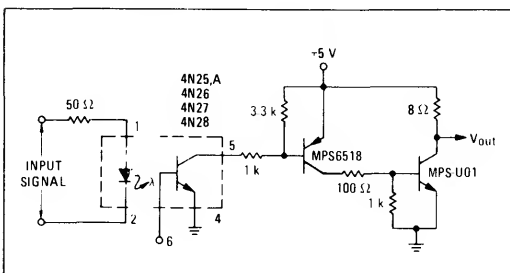
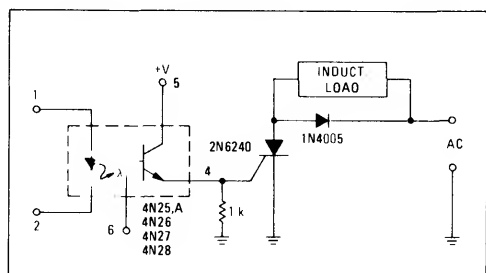


FIGURE 15 – INTERFACE BETWEEN LOGIC AND LOAD





MOTOROLA

NPN PHOTO DARLINGTON AND PN INFRARED EMITTING DIODE

... Gallium Arsenide LED optically coupled to a Silicon Photo Darlington Transistor designed for applications requiring electrical isolation, high-current transfer ratios, small package size and low cost; such as interfacing and coupling systems, phase and feedback controls, solid-state relays and general-purpose switching circuits.

- High Isolation Voltage
 $V_{ISO} = 7500$ V (Min)
 - High Collector Output Current
@ $I_F = 10$ mA –
 $I_C = 50$ mA (Min) – 4N32,33
10 mA (Min) – 4N29,30
5.0 mA (Min) – 4N31
 - Economical, Compact,
Dual-In-Line Package
 - Excellent Frequency Response –
30 kHz (Typ)
 - Fast Switching Times @ $I_C = 50$ mA
 $t_{on} = 2.0\ \mu s$ (Typ)
 $t_{off} = 25\ \mu s$ (Typ) – 4N29,30,31
60 μs (Typ) – 4N32,33
 - 4N29A, 4N32A are UL Recognized
File Number E54915

MAXIMUM RATINGS (TA = 25°C unless otherwise noted)

| Rating | Symbol | Value | Unit |
|--------|--------|-------|------|
|--------|--------|-------|------|

INFRARED-EMITTING DIODE MAXIMUM RATINGS

| | | | |
|--|-------|-----|---------------|
| Reverse Voltage | V_R | 3.0 | Volts |
| Forward Current Continuous | I_F | 80 | mA |
| Forward Current - Peak <i>(Pulse Width = 300 μs, 2.0% Duty Cycle)</i> | I_F | 3.0 | Amp |
| Total Power Dissipation @ $T_A = 25^\circ C$ | P_D | 150 | mW |
| Negligible Power in Transistor | | | |
| Derate above $25^\circ C$ | | 2.0 | $mW/^\circ C$ |

PHOTOTRANSISTOR MAXIMUM RATINGS

| | | | |
|--|-----------|-----|---------------|
| Collector-Emitter Voltage | V_{CEO} | 30 | Volts |
| Emitter-Collector Voltage | V_{ECO} | 5.0 | Volts |
| Collector-Base Voltage | V_{CBO} | 30 | Volts |
| Total Power Dissipation @ $T_A = 25^\circ C$ | P_D | 150 | mW |
| Negligible Power in Diode | | | |
| Derate above $25^\circ C$ | | 2.0 | $mW/^\circ C$ |

TOTAL DEVICE RATINGS

| Total Device Dissipation @ $T_A = 25^\circ\text{C}$ Equal Power Dissipation in Each Element Derate above 25°C | P_D | 250 | mW |
|---|-----------|-------------|----------------------------|
| | | 3.3 | $\text{mW}/^\circ\text{C}$ |
| Operating Junction Temperature Range | T_J | -55 to +100 | $^\circ\text{C}$ |
| Storage Temperature Range | T_{stg} | -55 to +150 | $^\circ\text{C}$ |
| Soldering Temperature (10 s) | — | 260 | $^\circ\text{C}$ |

FIGURE 1 – MAXIMUM POWER DISSIPATION

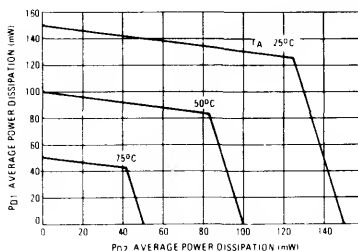


Figure 1 is based upon using limit values in the equation

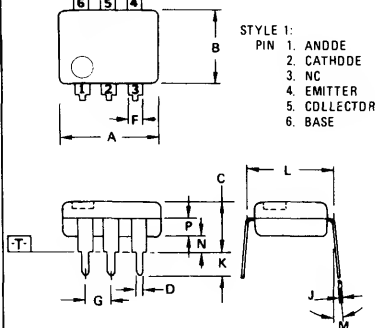
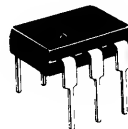
where
 T_{J1} Junction Temperature (100°C)
 T_A Ambient Temperature
 R_{HJA} Junction to Ambient Thermal Resistance

P_{D1} Resistance (500°C/W)
 P_{D2} Power Dissipation in One Chip
 P_{D3} Power Dissipation in Other Chip

K_B Thermal Coupling Coefficient
(20%)
Example
With $P_{D1} = 90 \text{ mW}$ in the LED
@ $T_A = 50^\circ\text{C}$, the Darlington
 $P_B = (P_{D1}) = \text{mW}$ be less than 50 mW

**4N29, 4N29A
4N30
4N31
4N32, 4N32A
4N33**

**OPTO
COUPLER/ISOLATOR
DARLINGTON OUTPUT**



NDTES

1. DIMENSIONS A AND B ARE DATUMS.
 2. -T- IS SEATING PLANE.
 3. POSITIONAL TOLERANCES FOR LEADS:

 4. DIMENSION L TD CENTER OF LEADS
WHEN FORMED PARALLEL.
 5. DIMENSIONING AND TOLERANCING PER
ANSI Y14.5 1973.

| DIM | MILLIMETERS | | INCHES | |
|-----|-------------|------|--------|-------|
| | MIN | MAX | MIN | MAX |
| A | 8.13 | 8.89 | 0.320 | 0.350 |
| B | 6.10 | 6.60 | 0.240 | 0.260 |
| C | 2.92 | 5.08 | 0.115 | 0.200 |
| D | 0.41 | 0.51 | 0.016 | 0.020 |
| F | 1.02 | 1.78 | 0.040 | 0.070 |
| G | 2.54 | BSC | 0.100 | BSC |
| J | 0.20 | 0.30 | 0.008 | 0.012 |
| K | 2.54 | 3.81 | 0.100 | 0.150 |
| L | 7.62 | BSC | 0.300 | BSC |
| M | 0° | 150 | 0° | 150 |
| N | 0.38 | 2.54 | 0.015 | 0.100 |

CASE 730A-01

4N29, 4N29A, 4N30, 4N31, 4N32, 4N32A, 4N33

LED CHARACTERISTICS ($T_A = 25^\circ\text{C}$ unless otherwise noted)

| Characteristic | Symbol | Min | Typ | Max | Unit |
|--|--------|-----|-------|-----|---------------|
| *Reverse Leakage Current ($V_R = 3.0 \text{ V}$, $R_L = 1.0 \text{ M ohms}$) | I_R | — | 0.005 | 100 | μA |
| *Forward Voltage ($I_F = 50 \text{ mA}$) | V_F | — | 1.2 | 1.5 | Volts |
| Capacitance ($V_R = 0 \text{ V}$, $f = 1.0 \text{ MHz}$) | C | — | 150 | — | pF |

PHOTOTRANSISTOR CHARACTERISTICS ($T_A = 25^\circ\text{C}$ and $I_F = 0$ unless otherwise noted)

| Characteristic | Symbol | Min | Typ | Max | Unit |
|---|---------------|-----|------|-----|-------------|
| *Collector-Emitter Dark Current ($V_{CE} = 10 \text{ V}$, Base Open) | I_{CEO} | — | 8.0 | 100 | nA |
| *Collector-Base Breakdown Voltage ($I_C = 100 \mu\text{A}$, $I_E = 0$) | $V_{(BR)CBO}$ | 30 | 110 | — | Volts |
| *Collector-Emitter Breakdown Voltage ($I_C = 100 \mu\text{A}$, $I_B = 0$) | $V_{(BR)CEO}$ | 30 | 75 | — | Volts |
| *Emitter-Collector Breakdown Voltage ($I_E = 100 \mu\text{A}$, $I_B = 0$) | $V_{(BR)ECO}$ | 5.0 | 8.0 | — | Volts |
| DC Current Gain ($V_{CE} = 5.0 \text{ V}$, $I_C = 500 \mu\text{A}$) | h_{FE} | — | 15 K | — | — |

COUPLED CHARACTERISTICS ($T_A = 25^\circ\text{C}$ unless otherwise noted)

| Characteristic | Symbol | Min | Typ | Max | Unit |
|--|----------------------|------|-----------|-----|--------------|
| *Collector Output Current (1) ($V_{CE} = 10 \text{ V}$, $I_F = \text{mA}$, $I_B = 0$) | I_C | 50 | 80 | — | mA |
| 4N32, 4N33 | | 10 | 40 | — | |
| 4N29, 4N30 | | 5.0 | — | — | |
| 4N31 | | | | | |
| Isolation Surge Voltage (2, 5) (60 Hz ac Peak, 5 Seconds) | V_{ISO} | 7500 | — | — | Volts |
| *4N29, 4N32 | | 2500 | — | — | |
| *4N30, 4N31, 4N33 | | 1500 | — | — | |
| Isolation Resistance (2) ($V = 500 \text{ V}$) | — | — | 10^{11} | — | Ohms |
| *Collector-Emitter Saturation Voltage (1) | $V_{CE(\text{sat})}$ | — | 0.8 | 1.2 | Volts |
| 4N31 | | — | 0.8 | 1.0 | |
| 4N29, 4N39, 4N32, 4N33 | | | | | |
| Isolation Capacitance (2) ($V = 0$, $f = 1.0 \text{ MHz}$) | — | — | 0.8 | — | pF |
| Bandwidth (3) ($I_C = 2.0 \text{ mA}$, $R_L = 100 \text{ ohms}$, Figures 6 and 8) | — | — | 30 | — | kHz |

SWITCHING CHARACTERISTICS (Figures 7 and 9), (4)

| | | | | | |
|---|-----------|---|-----|-----|---------------|
| Turn-On Time ($I_C = 50 \text{ mA}$, $I_F = 200 \text{ mA}$, $V_{CC} = 10 \text{ V}$) | t_{on} | — | 2.0 | 5.0 | μs |
| Turn-Off Time ($I_C = 50 \text{ mA}$, $I_F = 200 \text{ mA}$, $V_{CC} = 10 \text{ V}$) | t_{off} | — | 25 | 40 | μs |
| 4N29, 30, 31 | | — | 60 | 100 | |
| 4N32, 33 | | | | | |

*Indicates JEDEC Registered Data.

(1) Pulse Test: Pulse Width = 300 μs , Duty Cycle $\leq 2.0\%$.

(2) For this test, LED pins 1 and 2 are common and phototransistor pins 4, 5, and 6 are common.

(3) I_F adjusted to yield $I_C = 2.0 \text{ mA}$ and $i_c = 2.0 \text{ mA P-P}$ at 10 kHz.

(4) t_d and t_f are inversely proportional to the amplitude of I_F ; t_d and t_f are not significantly affected by I_F .

(5) Isolation Surge Voltage, V_{ISO} , is an internal device dielectric breakdown rating.

FIGURE 2 – 4N29, 4N30, 4N31 DC CURRENT TRANSFER CHARACTERISTICS

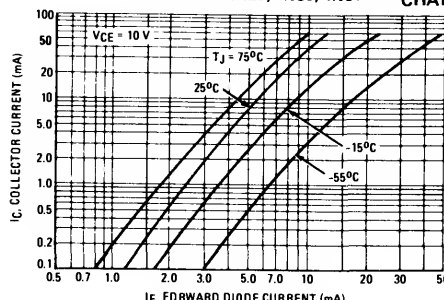
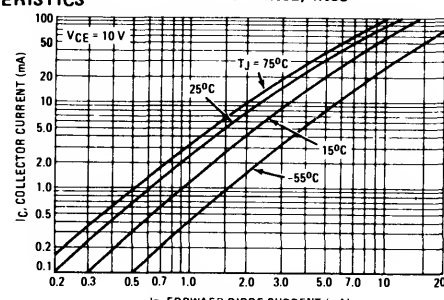


FIGURE 3 – 4N32, 4N33



4N29, 4N29A, 4N30, 4N31, 4N32, 4N32A, 4N33

TYPICAL ELECTRICAL CHARACTERISTICS (Printed Circuit Board Mounting)

FIGURE 4 – FORWARD CHARACTERISTIC

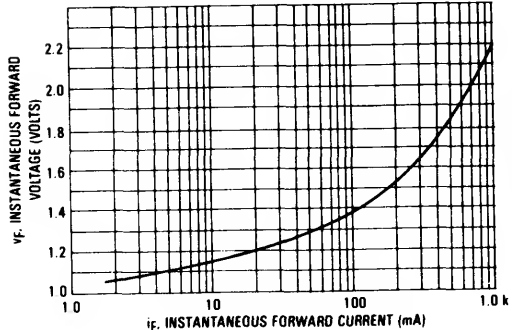


FIGURE 5 – COLLECTOR-EMITTER CUTOFF CURRENT

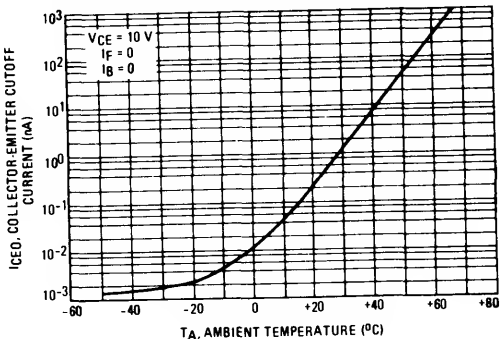


FIGURE 6 – FREQUENCY RESPONSE

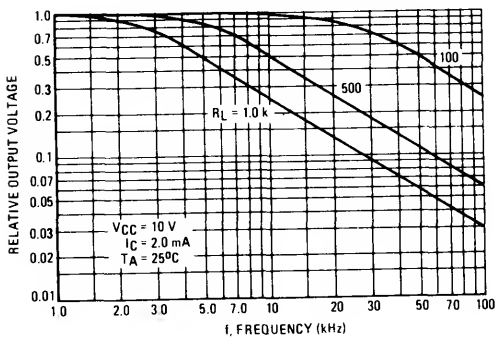


FIGURE 7 – SWITCHING TIMES

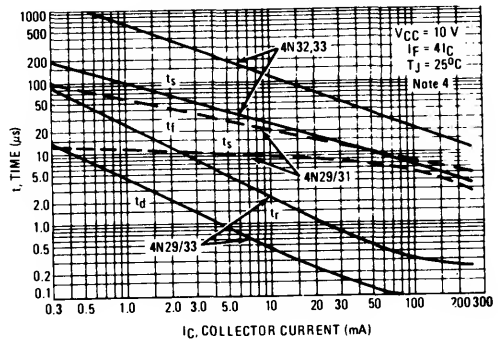


FIGURE 8 – FREQUENCY RESPONSE TEST CIRCUIT

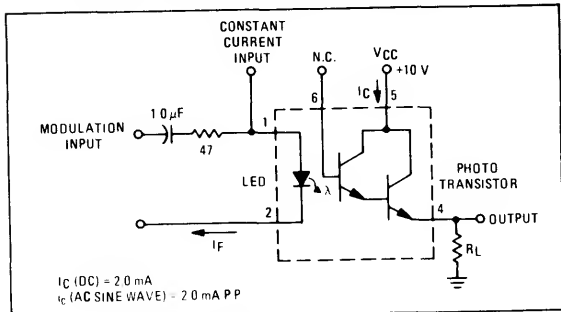
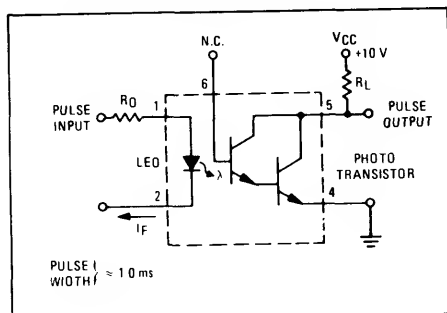


FIGURE 9 – SWITCHING TIME TEST CIRCUIT



4N29, 4N29A, 4N30, 4N31, 4N32, 4N32A, 4N33

TYPICAL APPLICATIONS

FIGURE 10 – VOLTAGE CONTROLLED TRIAC

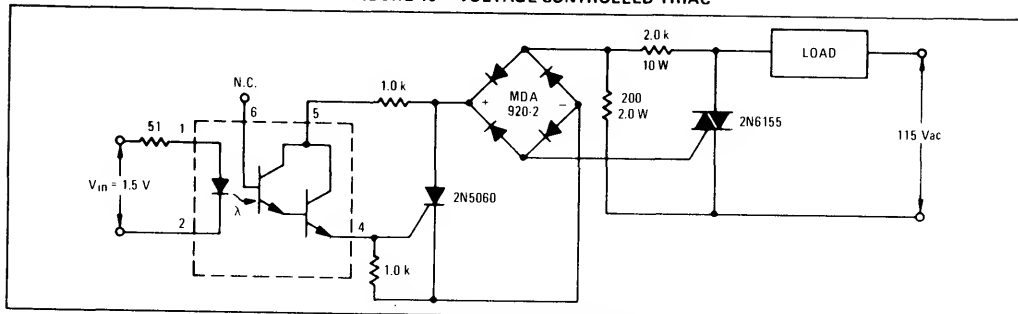


FIGURE 11 – AC SOLID STATE RELAY

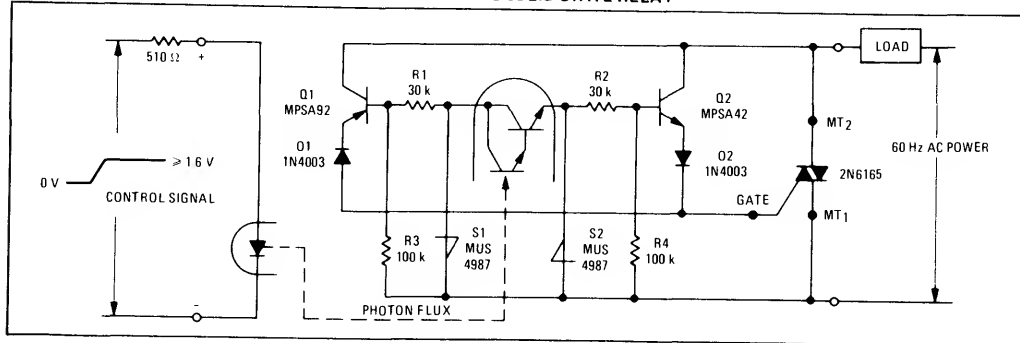


FIGURE 12 – OPTICALLY COUPLED ONE SHOT

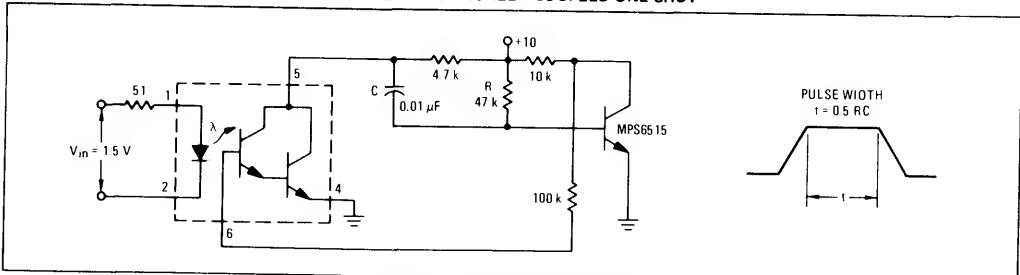
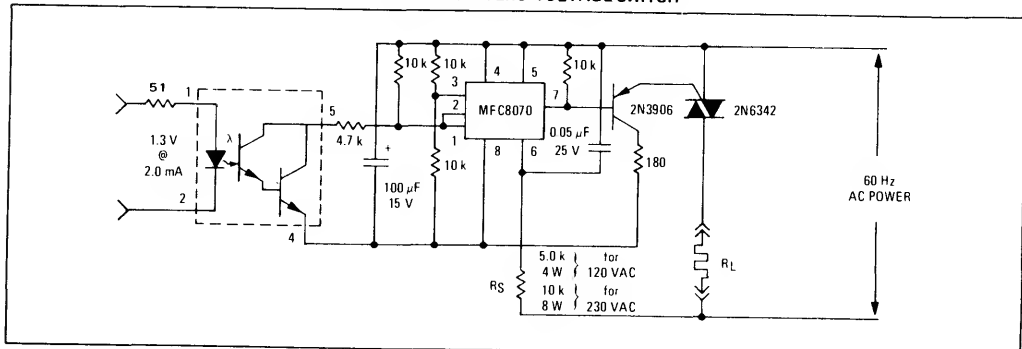


FIGURE 13 – ZERO VOLTAGE SWITCH





MOTOROLA

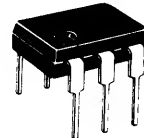
**4N35
4N36
4N37**

**NPN PHOTOTRANSISTOR AND
PN INFRARED EMITTING DIODE**

. . . gallium-arsenide LED optically coupled to a silicon phototransistor designed for applications requiring electrical isolation, high-current transfer ratios, small package size and low cost such as interfacing and coupling systems, phase and feedback controls, solid-state relays and general-purpose switching circuits.

- High Electrical Isolation $V_{ISO} = 7500$ V (Min)
- High Transfer Ratio –
100% (min) @ $I_F = 10$ mA, $V_{CE} = 10$ V
- Low Collector-Emitter Saturation Voltage –
 $V_{CE(sat)} = 0.3$ Vdc (max) @ $I_F = 10$ mA, $I_C = 0.5$ mA
- UL Recognized File Number E54915

**OPTO
COUPLER/ISOLATOR
TRANSISTOR OUTPUT**



MAXIMUM RATINGS ($T_A = 25^\circ\text{C}$ unless otherwise noted)

| Rating | Symbol | Value | Unit |
|---|----------|------------|----------------------------------|
| *INFRARED-EMITTER DIODE MAXIMUM RATINGS | | | |
| Reverse Voltage | V_{RB} | 6.0 | Volts |
| Forward Current – Continuous | I_F | 60 | mA |
| Forward Current – Peak Pulse Width = 1.0 μs , 2.0% Duty Cycle | I_F | 3.0 | Amp |
| Total Power Dissipation @ $T_A = 25^\circ\text{C}$ Negligible Power in Transistor Derate above 25°C | P_D | 100 1.3 | mW $\text{mW}/^\circ\text{C}$ |
| Total Power Dissipation @ $T_C = 25^\circ\text{C}$ Derate above 25°C | P_D | 100 1.3 | mW $\text{mW}/^\circ\text{C}$ |

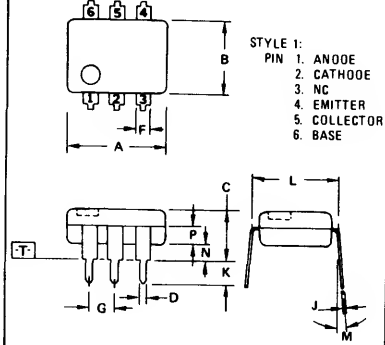
***PHOTOTRANSISTOR MAXIMUM RATINGS**

| | | | |
|--|-----------|------------|----------------------------------|
| Collector-Emitter Voltage | V_{CEO} | 30 | Volts |
| Emitter-Base Voltage | V_{EBO} | 7.0 | Volts |
| Collector-Base Voltage | V_{CBO} | 70 | Volts |
| Output Current – Continuous | I_C | 100 | mA |
| Total Power Dissipation @ $T_A = 25^\circ\text{C}$ Negligible Power in Diode Derate above 25°C | P_D | 300 4.0 | mW $\text{mW}/^\circ\text{C}$ |
| Total Power Dissipation @ $T_C = 25^\circ\text{C}$ Derate above 25°C | P_D | 500 6.7 | mW $\text{mW}/^\circ\text{C}$ |

TOTAL DEVICE RATINGS

| | | | |
|--|---|-------------|----------------------------------|
| *Total Power Dissipation @ $T_A = 25^\circ\text{C}$ Derate above 25°C | P_D | 300 3.3 | mW $\text{mW}/^\circ\text{C}$ |
| Input to Output Isolation Voltage, Surge 60 Hz Peak ac, 5 seconds | V_{ISO} | 7500 | Volts V_{pk} |
| JEDEC Registered Data @ 8 ms | 4N35 = 3500 V 4N36 = 2500 V 4N37 = 1500 V | | |
| *Junction Temperature Range | T_J | -55 to +100 | $^\circ\text{C}$ |
| *Storage Temperature Range | T_{stg} | -55 to +150 | $^\circ\text{C}$ |
| *Soldering Temperature (10 s) | — | 260 | $^\circ\text{C}$ |

* Indicates JEDEC Registered Data



NOTES:

1. DIMENSIONS A AND B ARE DATUMS.
2. T IS SEATING PLANE.
3. POSITIONAL TOLERANCES FOR LEADS: ± 0.013 (0.005) T A (W) B (H)
4. DIMENSION L TO CENTER OF LEADS WHEN FORMED PARALLEL.
5. DIMENSIONING AND TOLERANCING PER ANSI Y14.5, 1973.

| DIM | MILLIMETERS | | INCHES | |
|-----|-------------|------|-----------|-------|
| | MIN | MAX | MIN | MAX |
| A | 8.13 | 8.89 | 0.320 | 0.350 |
| B | 6.10 | 6.60 | 0.240 | 0.260 |
| C | 2.92 | 5.08 | 0.115 | 0.200 |
| D | 0.41 | 0.51 | 0.016 | 0.020 |
| F | 1.02 | 1.78 | 0.040 | 0.070 |
| G | 2.54 BSC | | 0.100 BSC | |
| J | 0.20 | 0.30 | 0.008 | 0.012 |
| K | 2.54 | 3.81 | 0.100 | 0.150 |
| L | 7.62 BSC | | 0.300 BSC | |
| M | 0.09 | 150 | 0.005 | 150 |
| N | 0.38 | 2.54 | 0.015 | 0.100 |
| P | 1.27 | 2.03 | 0.050 | 0.080 |

CASE 730A-01

4N35, 4N36, 4N37

ELECTRICAL CHARACTERISTICS

| Characteristic | Symbol | Min | Typ | Max | Unit |
|--|----------------------------------|-------------------|---------------|-------------------|------------------------------|
| LED CHARACTERISTICS ($T_A = 25^\circ\text{C}$ unless otherwise noted) | | | | | |
| *Reverse Leakage Current ($V_R = 6.0 \text{ V}$) | I_R | — | 0.005 | 10 | μA |
| *Forward Voltage ($I_F = 10 \text{ mA}$) ($I_F = 10 \text{ mA}, T_A = -55^\circ\text{C}$) ($I_F = 10 \text{ mA}, T_A = 100^\circ\text{C}$) | V_F | 0.8 0.9 0.7 | 1.2 — — | 1.5 1.7 1.4 | Volts |
| Capacitance ($V_R = 0 \text{ V}, f = 1.0 \text{ MHz}$) | C | — | 150 | — | pF |
| PHOTOTRANSISTOR CHARACTERISTICS ($T_A = 25^\circ\text{C}$ and $I_F = 0$ unless otherwise noted) | | | | | |
| Collector-Emitter Dark Current ($V_{CE} = 10 \text{ V}$, Base Open) ($V_{CE} = 30 \text{ V}$, Base Open, $T_A = 100^\circ\text{C}$) | I_{CEO} | — — | 3.5 | 50 500 | nA μA |
| Collector-Base Dark Current ($V_{CB} = 10 \text{ V}$, Emitter Open) | I_{CBO} | — | — | 20 | nA |
| Collector-Base Breakdown Voltage ($I_C = 100 \mu\text{A}, I_E = 0$) | $V_{(BR)CBO}$ | 70 | — | — | Volts |
| Collector-Emitter Breakdown Voltage ($I_C = 1.0 \text{ mA}, I_B = 0$) | $V_{(BR)CEO}$ | 30 | — | — | Volts |
| Emitter-Base Breakdown Voltage ($I_E = 100 \mu\text{A}, I_B = 0$) | $V_{(BR)EBO}$ | 7.0 | 8.0 | — | Volts |
| COUPLED CHARACTERISTICS ($T_A = 25^\circ\text{C}$ unless otherwise noted) | | | | | |
| Current Transfer Ratio ($V_{CE} = 10 \text{ V}, I_F = 10 \text{ mA}$) ($V_{CE} = 10 \text{ V}, I_F = 10 \text{ mA}, T_A = -55^\circ\text{C}$) ($V_{CE} = 10 \text{ V}, I_F = 10 \text{ mA}, T_A = 100^\circ\text{C}$) | I_C/I_F | 1.0 0.4 0.4 | 1.2 | — — — | — |
| Input to Output Isolation Current (2) (3) ($V_{IO} = 3550 \text{ V}_{pk}$) ($V_{IO} = 2500 \text{ V}_{pk}$) ($V_{IO} = 1500 \text{ V}_{pk}$) | I_{IO} 4N35 4N36 4N37 | — — — | — — — | 100 100 100 | μA |
| Isolation Resistance (2) ($V = 500 \text{ V}$) | R_{IO} | 10^{11} | — | — | Ohms |
| Collector-Emitter Saturation Voltage ($I_C = 0.5 \text{ mA}, I_F = 10 \text{ mA}$) | $V_{CE(sat)}$ | — | 0.14 | 0.3 | Volts |
| Isolation Capacitance (2) ($V = 0, f = 1.0 \text{ MHz}$) | — | — | 1.3 | 2.5 | pF |
| SWITCHING CHARACTERISTICS (Figure 1) | | | | | |
| Turn-On Time ($V_{CC} = 10 \text{ V}, I_C = 2.0 \text{ mA}, R_L = 100 \Omega$) | t_{on} | — | 4.0 | 10 | μs |
| Turn-Off Time ($V_{CC} = 10 \text{ V}, I_C = 2.0 \text{ mA}, R_L = 100 \Omega$) | t_{off} | — | 4.0 | 10 | μs |

* Indicates JEDEC Registered Data.

NOTES: 1. Pulse Test: Pulse Width = 300 μs , Duty Cycle $\leq 2.0\%$.

2. For this test LED pins 1 and 2 are common and phototransistor pins 4, 5, and 6 are common.

3. Pulse Width $\leq 8.0 \text{ ms}$.

4N35, 4N36, 4N37

TYPICAL ELECTRICAL CHARACTERISTICS

FIGURE 1 – SWITCHING TIMES TEST CIRCUIT

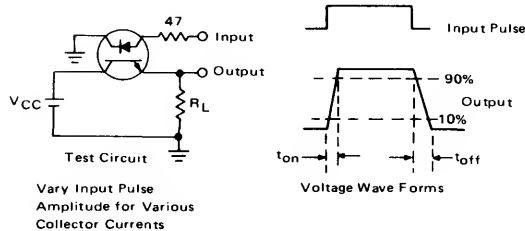


FIGURE 2 – FORWARD CHARACTERISTICS

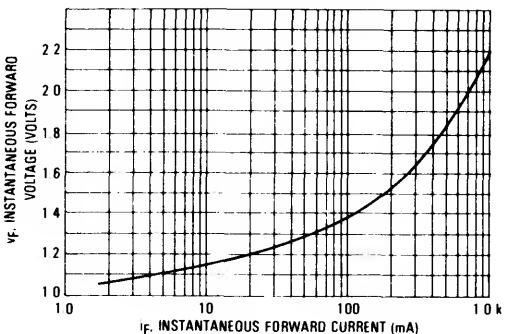


FIGURE 3 – COLLECTOR SATURATION REGION

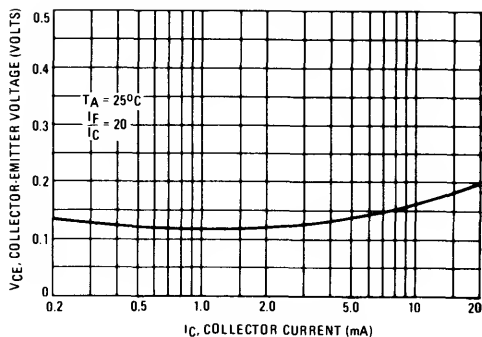


FIGURE 4 – COLLECTOR BASE CURRENT versus INPUT CURRENT

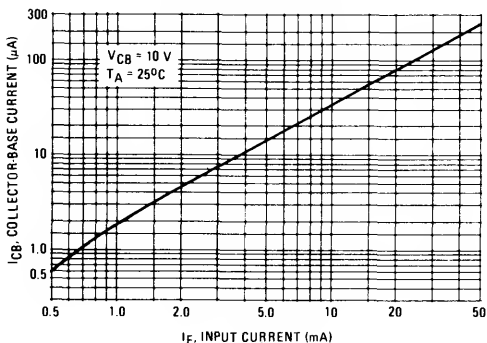


FIGURE 5 – COLLECTOR LEAKAGE CURRENT versus TEMPERATURE

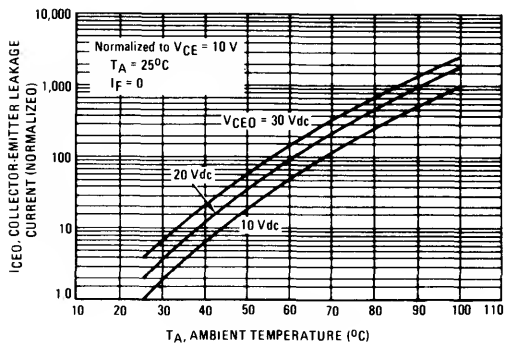
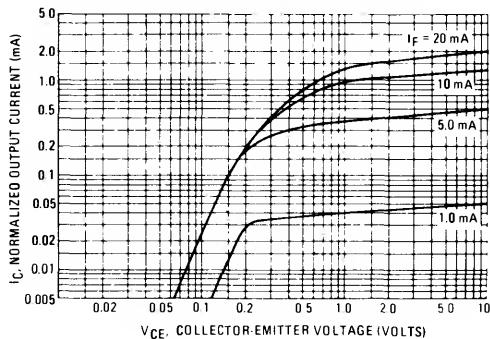


FIGURE 6 – COLLECTOR CHARACTERISTICS



4N35, 4N36, 4N37

TYPICAL APPLICATIONS

**FIGURE 7 – ISOLATED MTTL TO MOS
(P-CHANNEL) LEVEL TRANSLATOR**

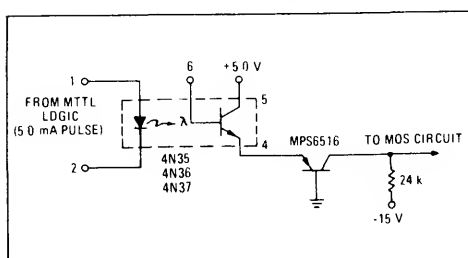


FIGURE 8 – COMPUTER/PERIPHERAL INTERCONNECT

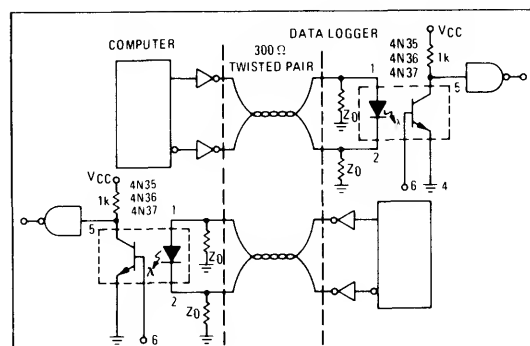


FIGURE 9 – POWER AMPLIFIER

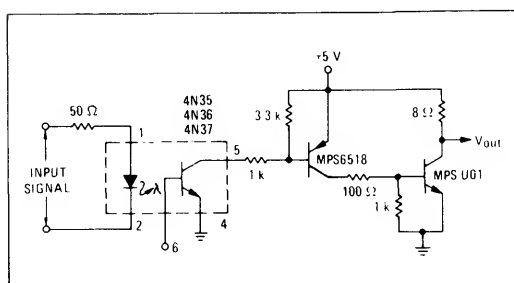
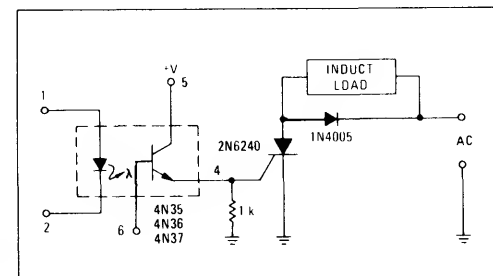


FIGURE 10 – INTERFACE BETWEEN LOGIC AND LOAD





MOTOROLA

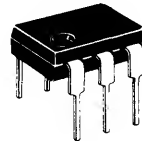
**4N38
4N38A**

**OPTICAL COUPLER WITH NPN
TRANSISTOR OUTPUT**

... gallium-arsenide LED optically coupled to a silicon phototransistor. Designed for applications requiring electrical isolation, high breakdown voltage and low leakage such as teletypewriter interfacing, telephone line pulsing and driving high-voltage relays.

- High Isolation Voltage –
 $V_{ISO} = 7500$ V (Min)
- High Collector Emitter Breakdown Voltage –
 $V_{(BR)CEO} = 80$ V (Min)
- Economical Dual-in-Line Package
- 4N38A UL Recognized, File Number E54915

**OPTO
COUPLER/ISOLATOR
TRANSISTOR OUTPUT**



*MAXIMUM RATINGS ($T_A = 25^\circ\text{C}$ unless otherwise noted)

| Rating | Symbol | Value | Unit |
|--|--------|-------|----------------------------|
| INFRARED EMITTING DIODE MAXIMUM RATINGS | | | |
| Reverse Voltage | V_R | 3.0 | Volts |
| Forward Current – Continuous | I_F | 80 | mA |
| Forward Current – Peak Pulse Width = 300 μs , 2.0% Duty Cycle | I_F | 3.0 | Amp |
| Total Device Dissipation @ $T_A = 25^\circ\text{C}$ Negligible Power in Transistor Derate above 25°C | P_D | 150 | mW |
| | | 2.0 | $\text{mW}/^\circ\text{C}$ |

PHOTOTRANSISTOR MAXIMUM RATINGS

| | | | |
|---|-----------|-----|----------------------------|
| Collector-Emitter Voltage | V_{CEO} | 80 | Volts |
| Emitter-Collector Voltage | V_{ECO} | 7.0 | Volts |
| Collector-Base Voltage | V_{CBD} | 80 | Volts |
| Total Device Dissipation @ $T_A = 25^\circ\text{C}$ Negligible Power in Diode Derate above 25°C | P_D | 150 | mW |
| | | 2.0 | $\text{mW}/^\circ\text{C}$ |

TOTAL DEVICE RATINGS

| | | | |
|---|-----------|-------------|----------------------------|
| Total Device Dissipation @ $T_A = 25^\circ\text{C}$ Equal Power Dissipation in Each Element Derate above 25°C | P_D | 250 | mW |
| | | 3.3 | $\text{mW}/^\circ\text{C}$ |
| Junction Temperature Range | T_J | -55 to +100 | $^\circ\text{C}$ |
| Storage Temperature Range | T_{stg} | -55 to +150 | $^\circ\text{C}$ |
| Soldering Temperature (10 s) | | 260 | $^\circ\text{C}$ |

* Indicates JEDEC Registered Data.

FIGURE 1 – MAXIMUM POWER DISSIPATION

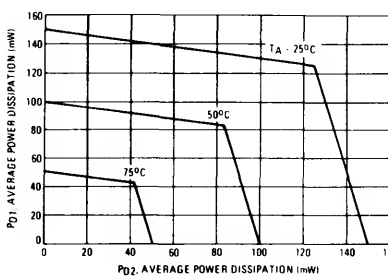


Figure 1 is based upon using limit values in the equation

$$T_J1 - T_A = R_{\theta JA}(P_{D1} + K_{\theta} P_{D2}) \text{ where}$$

T_{J1} Junction Temperature (100°C)

T_A Ambient Temperature

$R_{\theta JA}$ Junction to Ambient Thermal Resistance (500°C/W)

P_{D1} Power Dissipation in One Chip

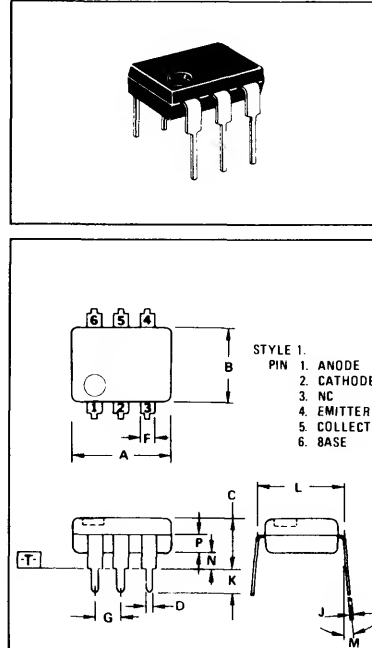
P_{D2} Power Dissipation in Other Chip

K_{θ} Thermal Coupling Coefficient (20%)

Example

With $P_{D1} = 90$ mW in the LED
@ $T_A = 50^\circ\text{C}$, the transistor
 $P_D (P_{D2})$ must be less than 50 mW

**OPTO
COUPLER/ISOLATOR
TRANSISTOR OUTPUT**



NOTES

1. DIMENSIONS A AND B ARE DATUMS
2. T IS SEATING PLANE
3. POSITIONAL TOLERANCES FOR LEADS $\pm 0.13 (0.005)$
4. DIMENSION L TO CENTER OF LEADS WHEN FORMED PARALLEL
5. DIMENSIONING AND TOLERANCING PER ANSI Y14.5, 1973

| DIM. | MILLIMETERS | | INCHES | |
|------|-------------|------|--------|-------|
| | MIN | MAX | MIN | MAX |
| A | 8.13 | 8.89 | 0.320 | 0.350 |
| B | 6.10 | 6.60 | 0.240 | 0.260 |
| C | 2.92 | 5.08 | 0.115 | 0.200 |
| D | 0.41 | 0.51 | 0.016 | 0.020 |
| F | 1.02 | 1.78 | 0.040 | 0.070 |
| G | 2.54 | 2.54 | 0.100 | 0.100 |
| J | 0.20 | 0.30 | 0.008 | 0.012 |
| K | 2.54 | 3.81 | 0.100 | 0.150 |
| L | 7.62 | 7.62 | 0.300 | 0.350 |
| M | 0.00 | 150 | 0.00 | 150 |
| N | 0.38 | 2.54 | 0.015 | 0.100 |
| P | 1.27 | 2.03 | 0.050 | 0.080 |

CASE 730A-01

4N38, 4N38A

LED CHARACTERISTICS ($T_A = 25^\circ\text{C}$ unless otherwise noted.)

| Characteristic | Symbol | Min | Typ | Max | Unit |
|--|--------|-----|-------|-----|---------------|
| *Reverse Leakage Current ($V_R = 3.0 \text{ V}$) | I_R | — | 0.005 | 100 | μA |
| *Forward Voltage ($I_F = 10 \text{ mA}$) | V_F | — | 1.2 | 1.5 | Volts |
| Capacitance ($V_R = 0 \text{ V}$, $f = 1.0 \text{ MHz}$) | C | — | 150 | — | pF |

PHOTOTRANSISTOR CHARACTERISTICS ($T_A = 25^\circ\text{C}$ and $I_F = 0$ unless otherwise noted.)

| Characteristic | Symbol | Min | Typ | Max | Unit |
|---|---------------|-----|-----|-----|-------------|
| *Collector-Emitter Dark Current ($V_{CE} = 60 \text{ V}$, Base Open) | I_{CEO} | — | 3.5 | 50 | nA |
| *Collector-Base Dark Current ($V_{CB} = 60 \text{ V}$, Emitter Open) | I_{CBO} | — | — | — | nA |
| *Collector-Base Breakdown Voltage ($I_C = 100 \mu\text{A}$, $I_E = 0$) | $V_{(BR)CBO}$ | 80 | 120 | — | Volts |
| *Collector-Emitter Breakdown Voltage ($I_C = 1.0 \text{ mA}$, $I_B = 0$) | $V_{(BR)CEO}$ | 80 | 90 | — | Volts |
| *Emitter-Collector Breakdown Voltage ($I_E = 100 \mu\text{A}$, $I_B = 0$) | $V_{(BR)ECO}$ | 7.0 | 8.0 | — | Volts |
| DC Current Gain ($V_{CE} = 5.0 \text{ V}$, $I_C = 500 \mu\text{A}$) | h_{FE} | — | 250 | — | — |

COUPLED CHARACTERISTICS ($T_A = 25^\circ\text{C}$ unless otherwise noted.)

| Characteristic | Symbol | Min | Typ | Max | Unit |
|---|----------------------|------|-----------|-----|-------------|
| Isolation Surge Voltage (2, 3) (60 Hz Peak ac, 5 Seconds) (3) | V_{ISO} | 7500 | — | — | Volts |
| *(60 Hz Peak ac) | | 1500 | — | — | |
| *(60 Hz RMS for 1 second) | | 2500 | — | — | |
| | | 1775 | — | — | |
| Isolation Resistance (2) ($V = 500 \text{ V}$) | | — | 10^{11} | — | Ohms |
| *Collector-Emitter Saturation ($I_C = 4.0 \text{ mA}$, $I_F = 20 \text{ mA}$) | $V_{CE(\text{sat})}$ | — | — | 1.0 | Volts |
| Isolation Capacitance (2) ($V = 0$, $f = 1.0 \text{ MHz}$) | | — | 1.3 | — | pF |

SWITCHING CHARACTERISTICS

| | | | | | | |
|--------------|--|-------|---|------|---|---------------|
| Delay Time | ($I_C = 10 \text{ mA}$, $V_{CC} = 10 \text{ V}$) Figures 6 and 8 | t_d | — | 0.07 | — | μs |
| Rise Time | | t_r | — | 0.8 | — | μs |
| Storage Time | ($I_C = 10 \text{ mA}$, $V_{CC} = 10 \text{ V}$) Figures 7 and 8 | t_s | — | 4.0 | — | μs |
| Fall Time | | t_f | — | 7.0 | — | μs |

* Indicates JEDEC Registered Data. (1) Pulse Test; Pulse Width = 300 μs , Duty Cycle $\leq 2.0\%$.

(2) For this test LED pins 1 and 2 are common and Photo Transistor pins 4, 5 and 6 are common.

(3) Isolation Surge Voltage, V_{ISO} , is an internal device dielectric breakdown rating.

TYPICAL TRANSFER CHARACTERISTICS

FIGURE 2 – COLLECTOR-CURRENT versus
DIODE FORWARD CURRENT

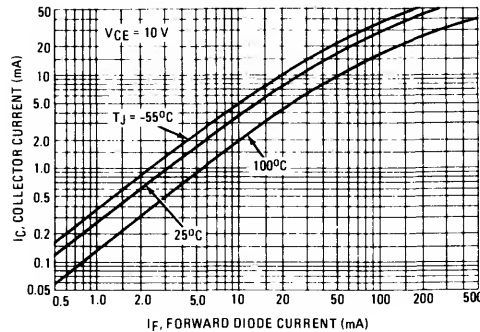
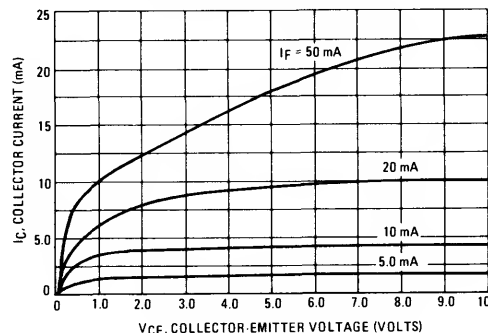


FIGURE 3 – COLLECTOR-CURRENT versus
COLLECTOR-EMITTER VOLTAGE



TYPICAL ELECTRICAL CHARACTERISTICS

FIGURE 4 – FORWARD CHARACTERISTICS

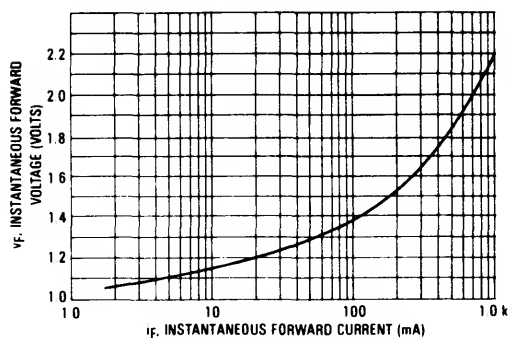


FIGURE 5 – COLLECTOR SATURATION VOLTAGE

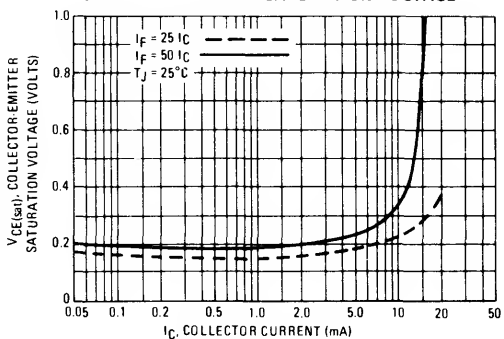


FIGURE 6 – TURN-ON TIME

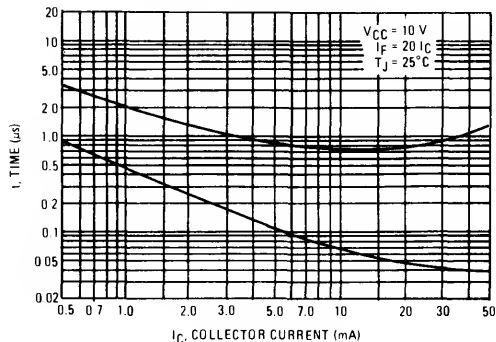


FIGURE 7 – TURN-OFF TIME

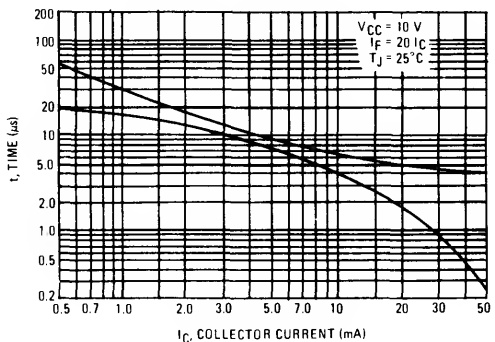


FIGURE 8 – SATURATED SWITCHING TIME TEST CIRCUIT

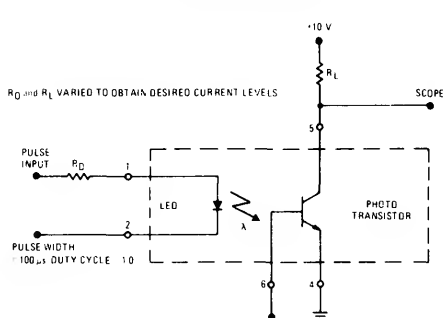
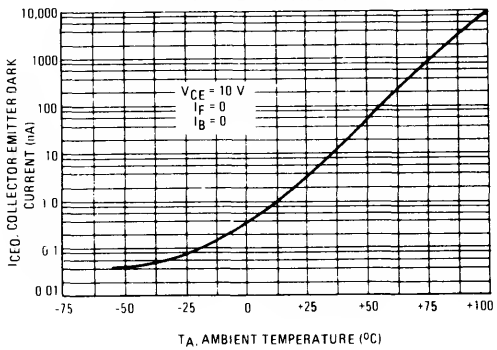


FIGURE 9 – DARK CURRENT versus AMBIENT TEMPERATURE



4N38, 4N38A

TYPICAL APPLICATIONS

The applications below utilize the 80 volt breakdown capability of the 4N38 and 4N38A eliminating the need for divider networks, zener diodes and the associated assembly costs.

FIGURE 10 – TYPICAL TELETYPE INTERFACE

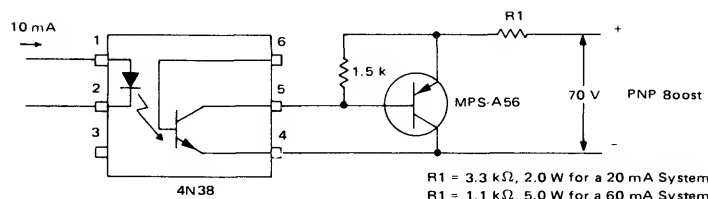
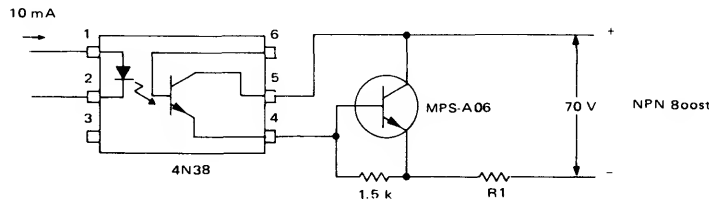


FIGURE 11 – TELEPHONE LINE PULSE CIRCUIT

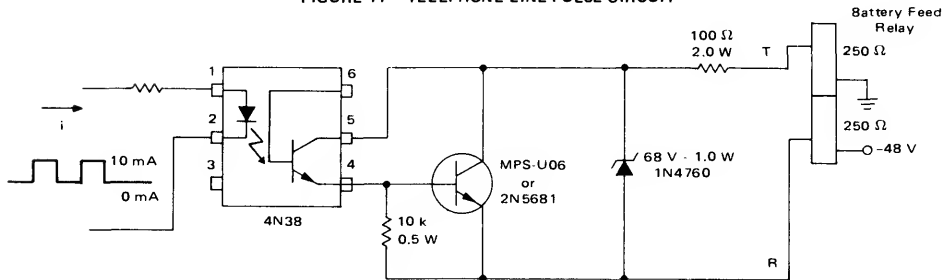
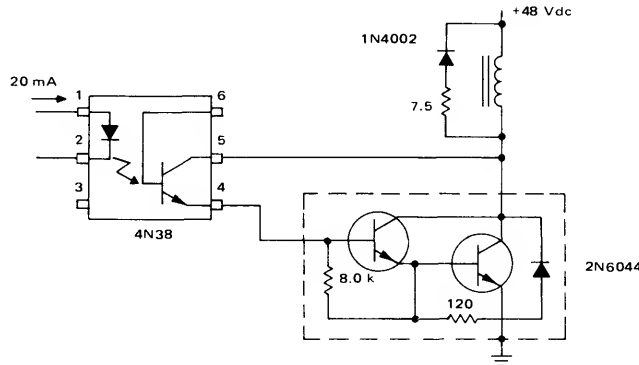


FIGURE 12 – 4-AMPERE SOLENOID DRIVER





MOTOROLA

**L14H1
thru
L14H4**

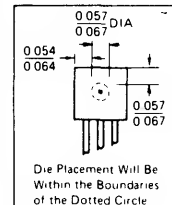
PLASTIC NPN SILICON PHOTO TRANSISTORS

. . . designed for applications in industrial inspection, processing and control, counters, sorters, switching and logic circuits or any design requiring extremely high radiation sensitivity, and stable characteristics.

- Economical Plastic Package
- Sensitive Throughout Visible and Near Infrared Spectral Range for Wide Application
- Range of Radiation Sensitivities and Voltages for Design Flexibility
- TO-92 Clear Plastic Package for Standard Mounting
- Annular Passivated Structure for Stability and Reliability
- Ideal Companion to the MLED92, 93, 94, and 95 IR Emitter

TO-92 PHOTO TRANSISTORS

NPN SILICON



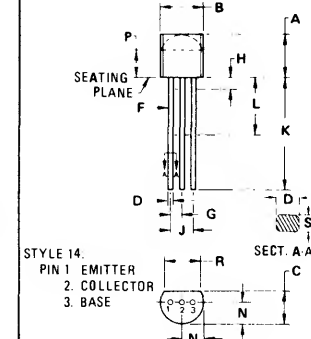
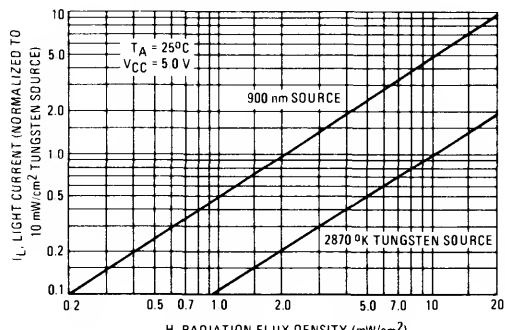
MAXIMUM RATINGS

| Rating | Symbol | L14H1,3 | L14H2,4 | Unit |
|--|--------------------|-------------|---------|----------------------------------|
| Collector-Emitter Voltage | V_{CEO} | 60 | 30 | Volts |
| Collector-Base Voltage | V_{CBO} | 60 | 30 | Volts |
| Emitter-Base Voltage | V_{EBO} | 5.0 | 5.0 | Volts |
| Light Current | I_L | 100 | | mA |
| Total Device Dissipation @ $T_A = 25^\circ\text{C}$ Derate above 25°C | P_D | 200 | 2.67 | mW $\text{mW}/^\circ\text{C}$ |
| Operating and Storage Junction Temperature Range | T_J, T_{stg} (1) | -65 to +100 | | °C |

(1) Indicates JEDEC Registered Data.

(1) Heat Sink should be applied to leads during soldering to prevent case temperature from exceeding 100°C .

FIGURE 1 – NORMALIZED LIGHT CURRENT versus RADIATION FLUX DENSITY



NOTES.

1. CONTOUR OF PACKAGE BEYOND ZONE "P"
2. UNCONTROLLED
DIM "F" APPLIES BETWEEN "H" AND "L". DIM "O" & "S" APPLIES BETWEEN "L" & 12.70 mm (0.5") FROM SEATING PLANE. LEAD DIM IS UNCONTROLLED IN "H" & BEYOND 12.70 mm (0.5") FROM SEATING PLANE

| DIM | MILLIMETERS | | INCHES | |
|-----|-------------|------|--------|-------|
| | MIN | MAX | MIN | MAX |
| A | 4.32 | 5.33 | 0.170 | 0.210 |
| B | 4.44 | 5.21 | 0.175 | 0.205 |
| C | 3.18 | 4.19 | 0.125 | 0.165 |
| D | 0.41 | 0.56 | 0.016 | 0.022 |
| F | 0.41 | 0.48 | 0.016 | 0.019 |
| G | 1.14 | 1.40 | 0.045 | 0.055 |
| H | — | 2.54 | — | 0.100 |
| J | 2.41 | 2.67 | 0.095 | 0.105 |
| K | 12.70 | — | 0.500 | — |
| L | 6.35 | — | 0.250 | — |
| N | 2.03 | 2.92 | 0.080 | 0.115 |
| P | 2.92 | — | 0.115 | — |
| R | 3.43 | — | 0.135 | — |
| S | 0.36 | 0.41 | 0.014 | 0.016 |

All JEDEC dimensions and notes apply.
CASE 29-02
TO-92

L14H1 THRU L14H4

STATIC ELECTRICAL CHARACTERISTICS ($T_A = 25^\circ\text{C}$ unless otherwise noted.)

| Characteristic | Symbol | Min | Typ | Max | Unit |
|---|----------------------|----------|--------|--------|-------|
| Collector Dark Current (Note 2) ($V_{CE} = 10 \text{ V}$) | I_D | — | — | 100 | nA |
| Collector-Emitter Breakdown Voltage (Note 2) ($I_C = 10 \text{ mA}$) L14H2, 4 L14H1, 3 | $V_{(BR)CEO}$ | 30 60 | — — | — — | Volts |
| Collector-Base Breakdown Voltage (Note 2) ($I_C = 100 \mu\text{A}$) ($I_F = 0$) L14H2, 4 L14H1, 3 | $V_{(BR)CBO}$ | 30 60 | — — | — — | Volts |
| Emitter-Base Breakdown Voltage (Note 2) ($I_E = 100 \mu\text{A}$, $I_C = 0$) | $V_{(BR)EBO}$ | 5.0 | — | — | Volts |
| Saturation Voltage ($I_C = 10 \text{ mA}$, $I_B = 1.0 \text{ mA}$) | $V_{CE(\text{sat})}$ | — | — | 0.4 | Volts |

OPTICAL CHARACTERISTICS ($T_A = 25^\circ\text{C}$ unless otherwise noted.)

| Characteristic | Symbol | Min | Typ | Max | Unit |
|--|-----------|------------|--------|--------|---------------|
| Collector Light Current (Notes 1, 4, 5) ($V_{CE} = 5.0 \text{ V}$, $R_L = 100 \Omega$) L14H1, 4 L14H2, 3 | I_L | 0.5 2.0 | — — | — — | mA |
| Turn-On Time (Note 3) | t_{on} | — | — | 8.0 | μs |
| Turn-Off Time (Note 3) | t_{off} | — | — | 7.0 | μs |

NOTES

- 1 Radiation Flux Density (H) equal to 10 mW/cm^2 emitted from a tungsten source at a color temperature of 2870°K .
2. Measured under dark conditions. ($H \approx 0$).
3. For unsaturated rise time measurements, radiation is provided by a pulsed GaAs (gallium-arsenide) light-emitting diode ($\lambda \approx 0.9$

μm) with a pulse width equal to or greater than 500 microseconds

- 4 Measurement mode with no electrical connection to the base lead
- 5 Die faces curved side of package

FIGURE 2 – CONTINUOUS LIGHT CURRENT versus DISTANCE

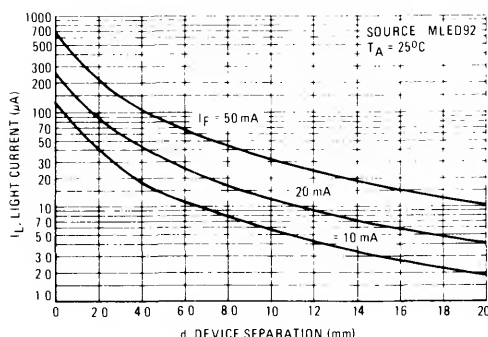
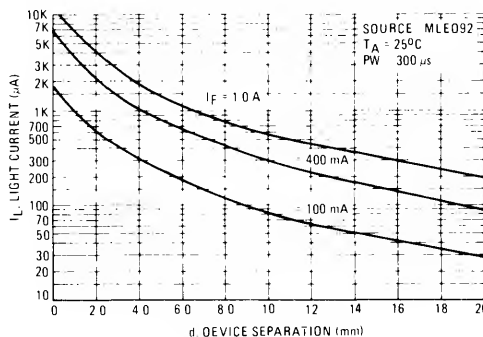


FIGURE 3 – PULSED LIGHT CURRENT versus DISTANCE





MOTOROLA

**MLED60
MLED90**

INFRARED-EMITTING DIODES

... designed for applications requiring high power output, low drive power and very fast response time. This device is used in industrial processing and control, light modulators, shaft or position encoders, punched card and tape readers, optical switching, and logic circuits. It is spectrally matched for use with silicon detectors.

- High Intensity — 550 $\mu\text{W}/\text{str}$ (Typ) @ $I_F = 50 \text{ mA}$ — MLED60
350 $\mu\text{W}/\text{str}$ (Typ) @ $I_F = 50 \text{ mA}$ — MLED90
- Infrared Emission — 930 nm (Typ)
- Low Drive Current — Compatible with Integrated Circuits
- Unique Molded Lens for Durability and Long Life
- Economical Plastic Package
- Small Size for High Density Mounting
- Easy Cathode Identification — Wider Lead

MAXIMUM RATINGS

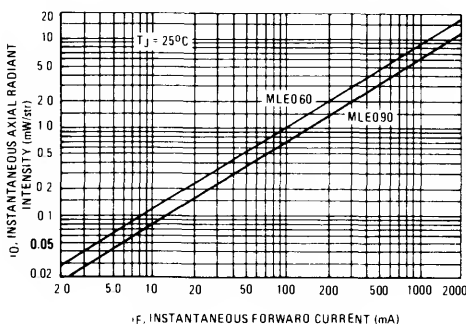
| Rating | Symbol | Value | Unit |
|---|----------------|-------------|----------------------------------|
| Reverse Voltage | V_R | 3.0 | Volts |
| Forward Current-Continuous | I_F | 80 | mA |
| Total Power Dissipation @ $T_A = 25^\circ\text{C}$ Derate above 25°C | $P_D(1)$ | 1.20 2.0 | mW $\text{mW}/^\circ\text{C}$ |
| Operating and Storage Junction Temperature Range | T_J, T_{Stg} | 40 to +85 | °C |

THERMAL CHARACTERISTICS

| Characteristic | Symbol | Max | Unit |
|---|--------------|---------------------------------|------|
| Thermal Resistance, Junction to Ambient | $R_{JJA}(1)$ | 500 | °C/W |
| Solder Temperature | | 260°C for 3 sec 1/16" from case | |

(1)Printed Circuit Board Mounting

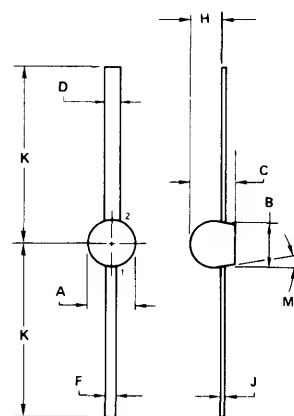
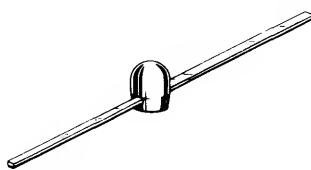
FIGURE 1 — INSTANTANEOUS RADIANT INTENSITY versus FORWARD CURRENT



INFRARED-EMITTING DIODES

**930 nm
PN GALLIUM ARSENIDE**

120 MILLIWATTS



STYLE 2
PIN 1 ANODE
2 CATHODE

| DIM | MILLIMETERS | | INCHES | |
|-----|-------------|------|--------|-------|
| | MIN | MAX | MIN | MAX |
| A | 2.34 | 2.59 | 0.092 | 0.102 |
| B | 2.11 | 2.36 | 0.083 | 0.093 |
| C | 2.39 | 2.64 | 0.094 | 0.104 |
| D | 0.64 | 0.74 | 0.025 | 0.029 |
| F | 0.46 | 0.56 | 0.018 | 0.022 |
| H | 1.57 | 1.83 | 0.062 | 0.072 |
| J | 0.20 | 0.30 | 0.008 | 0.012 |
| K | 9.65 | — | 0.380 | — |
| M | 9° | 11° | 9° | 11° |

CASE 234-04

MLED60, MLED90

ELECTRICAL CHARACTERISTICS ($T_A = 25^\circ\text{C}$ unless otherwise noted)

| Characteristic | Fig. No. | Symbol | Min | Typ | Max | Unit |
|--|----------|-------------|-----|-----|-----|-------|
| Reverse Leakage Current ($V_R = 30 \text{ V}$, $R_L = 1 \text{ Megohm}$) | — | I_R | — | 50 | — | nA |
| Reverse Breakdown Voltage ($I_R = 100 \mu\text{A}$) | — | $V_{(BR)R}$ | 3.0 | — | — | Volts |
| Forward Voltage ($I_F = 50 \text{ mA}$) | 2 | V_F | — | 1.2 | 1.5 | Volts |
| Total Capacitance ($V_R = 0 \text{ V}$, $f = 1.0 \text{ MHz}$) | — | C_T | — | 50 | — | pF |

OPTICAL CHARACTERISTICS ($T_A = 25^\circ\text{C}$ unless otherwise noted)

| Characteristics | Fig. No. | Symbol | Min | Typ | Max | Unit |
|--|----------|-----------------|------------|------------|-----|--------------------------------|
| Axial Radiant Intensity ($I_F = 50 \text{ mA}$) | 1 | P_O | 400 200 | 550 350 | — | $\mu\text{W}/\text{Steradian}$ |
| Peak Emission Wavelength | — | λ_P | — | 930 | — | nm |
| Spectral Line Half Width | — | $\Delta\lambda$ | — | 48 | — | nm |

FIGURE 2 – FORWARD CHARACTERISTICS

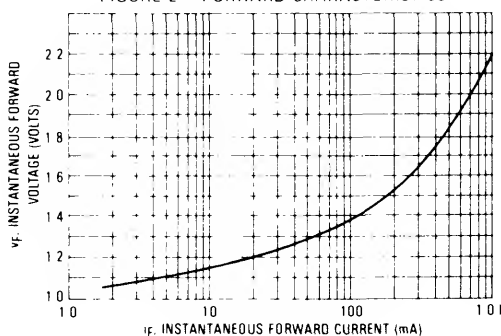


FIGURE 4 – CONTINUOUS RADIANT INTENSITY versus FORWARD CURRENT

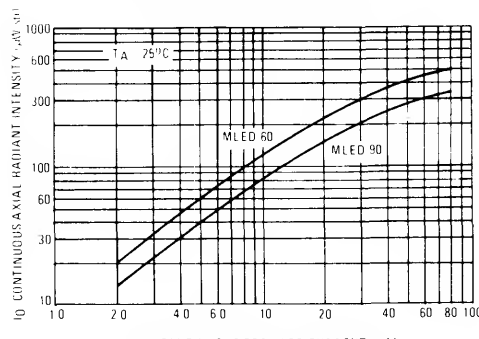


FIGURE 3 – RADIANT INTENSITY versus JUNCTION TEMPERATURE

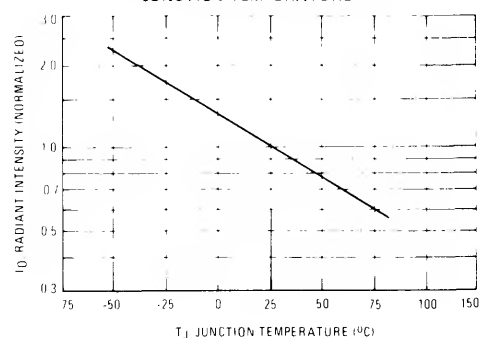
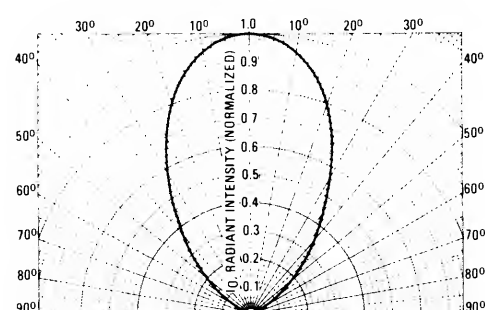


FIGURE 5 – SPATIAL RADIATION PATTERN



Output saturation effects are not evident at currents up to 2 A as shown on Figure 1. However, power output decreases due to heating of the semiconductor as indicated by Figure 3. To estimate output level, average junction temperature may be calculated from:

$$T_J(AV) = T_A + (I_A / V_F) D F_D$$

where D is the duty cycle of the applied current, I_F . Use of the above method should be restricted to drive conditions employing pulses of less than 10 μs duration to avoid errors caused by high peak junction temperatures.



MOTOROLA

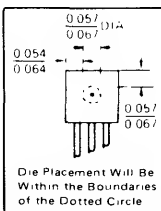
INFRARED-EMITTING DIODE

... designed for industrial processing and control applications such as light modulators, shaft or position encoders, end of tape detectors, and optical coupler applications. Supplied in TO-92 package for ease of mounting and compatibility with existing automatic insertion equipment.

- High Power Output –
 $P_o = 150 \mu\text{W}$ (Typ) @ $I_F = 50 \text{ mA}$
- Infrared Emission – 930 nm (Typ)
- One-Piece, Unibloc Package for High Reliability

MLED92

LOW COST INFRARED-EMITTING DIODE PN GALLIUM ARSENIDE



MAXIMUM RATINGS

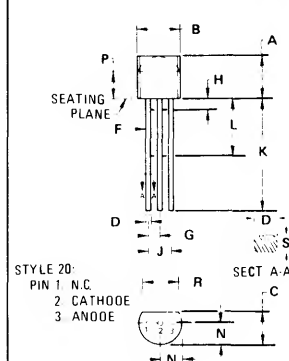
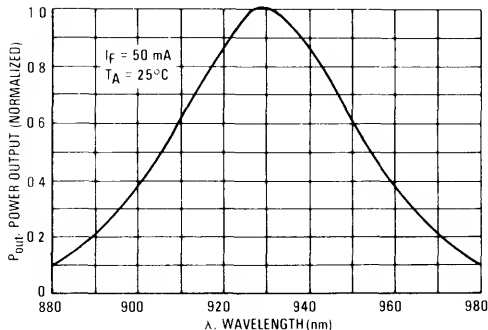
| Rating | Symbol | Value | Unit |
|--|---------------------|-------------|----------------------------|
| Reverse Voltage | V_R | 3.0 | Volts |
| Forward Current-Continuous | I_F | 100 | mA |
| Total Power Dissipation @ $T_A = 25^\circ\text{C}$ | $P_D(1)$ | 215 | mW |
| Derate above 25°C | | 2.86 | $\text{mW}/^\circ\text{C}$ |
| Operating and Storage Junction Temperature Range | $T_{J,T\text{stg}}$ | -65 to +100 | $^\circ\text{C}$ |

THERMAL CHARACTERISTICS

| Characteristic | Symbol | Max | Unit |
|--|--------------------|-----|---------------------------|
| Thermal Resistance Junction to Ambient | $R_{\theta JA}(1)$ | 350 | $^\circ\text{C}/\text{W}$ |

(1) $R_{\theta JA}(1)$ is measured with the device soldered into a typical printed circuit board.

FIGURE 1 – RELATIVE SPECTRAL OUTPUT



NOTES

- 1 CONTOUR OF PACKAGE BEYOND ZONE "P"
- 2 IS UNCONTROLLED
- 3 DIM "F" APPLIES BETWEEN "H" AND "L". DIM "O" & "S" APPLIES BETWEEN "L" & 12.70 mm (0.5") FROM SEATING PLANE. LEAD DIM IS UNCONTROLLED IN "H" & BEYOND 12.70 mm (0.5") FROM SEATING PLANE

| DIM | MILLIMETERS | | INCHES | |
|-----|-------------|------|--------|-------|
| | MIN | MAX | MIN | MAX |
| A | 4.32 | 5.33 | 0.170 | 0.210 |
| B | 4.44 | 5.21 | 0.175 | 0.205 |
| C | 3.18 | 4.19 | 0.125 | 0.165 |
| D | 0.41 | 0.56 | 0.016 | 0.022 |
| F | 0.41 | 0.48 | 0.016 | 0.019 |
| G | 1.14 | 1.40 | 0.045 | 0.055 |
| H | 2.54 | — | 0.100 | — |
| J | 2.41 | 2.67 | 0.095 | 0.105 |
| K | 12.70 | — | 0.500 | — |
| L | 6.35 | — | 0.250 | — |
| N | 2.03 | 2.92 | 0.080 | 0.115 |
| P | 2.92 | — | 0.115 | — |
| R | 3.43 | — | 0.135 | — |
| S | 0.36 | 0.41 | 0.014 | 0.016 |

All JEDEC dimensions and notes apply.
CASE 29-02
TO-92

MLED92

ELECTRICAL CHARACTERISTICS ($T_A = 25^\circ\text{C}$ unless otherwise noted)

| Characteristic | Fig. No | Symbol | Min | Typ | Max | Unit |
|---|---------|------------------|-----|-----|-----|-------|
| Reverse Leakage Current ($V_R = 30\text{ V}$, $R_L = 10\text{ Megohm}$) | - | I_R | - | 50 | - | nA |
| Reverse Breakdown Voltage ($I_R = 100\text{ }\mu\text{A}$) | - | $V(\text{BR})_R$ | 3.0 | - | - | Volts |
| Instantaneous Forward Voltage (Note 3) ($I_F = 50\text{ mA}$) | 2 | V_F | - | 1.2 | 1.5 | Volts |
| Total Capacitance ($V_R = 0\text{ V}$, $f = 1.0\text{ MHz}$) | | C_T | - | 150 | - | pF |

OPTICAL CHARACTERISTICS ($T_A = 25^\circ\text{C}$ unless otherwise noted)

| Characteristic | Fig. No | Symbol | Min | Typ | Max | Unit |
|--|---------|-----------------|-----|------|-----|--------------|
| Total Power Output (Notes 1 and 3) ($I_F = 50\text{ mA}$) | 3-4 | P_O | 50 | 150 | - | µW |
| Radiant Intensity (Note 2) ($I_F = 50\text{ mA}$) | | I_O | -- | 0.66 | - | mW steradian |
| Peak Emission Wavelength | 1 | λ_P | - | 930 | - | nm |
| Spectral Line Half Width | 1 | $\Delta\lambda$ | - | 48 | - | nm |

NOTE

- Power Output, P_O , is the total power radiated by the device into a solid angle of 2π steradians. It is measured by directing all radiation leaving the device within this solid angle onto a calibrated silicon solar cell.
- Irradiance from a Light Emitting Diode (LED) can be calculated by

$$H = \frac{I_O}{d^2}$$
 where H is irradiance in mW/cm^2 , I_O is radiant intensity in mW/steradian ,
 d is distance from LED to the detector in cm.
- Pulse Test. Pulse Width: $300\text{ }\mu\text{s}$. Duty Cycle: 2.0%.

FIGURE 2 - FORWARD CHARACTERISTICS

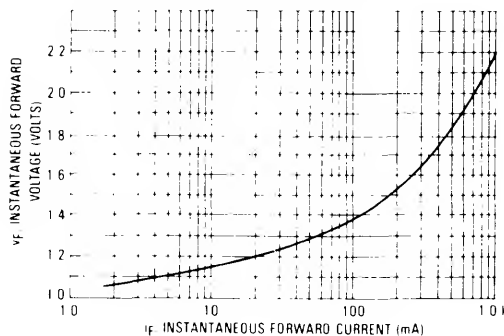


FIGURE 3 - POWER OUTPUT versus JUNCTION TEMPERATURE

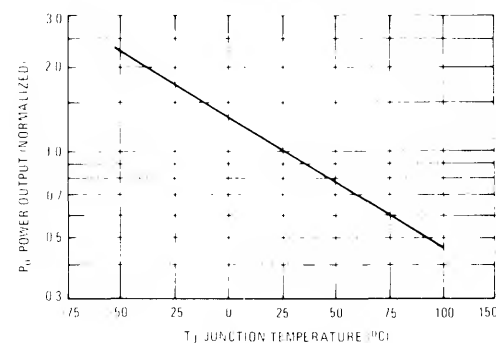


FIGURE 4 - INSTANTANEOUS POWER OUTPUT

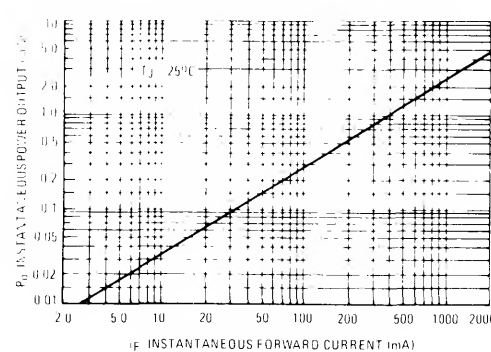
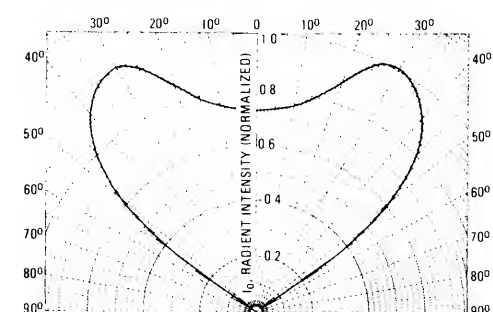


FIGURE 5 - SPATIAL RADIATION PATTERN





MOTOROLA

MLED93 MLED94 MLED95

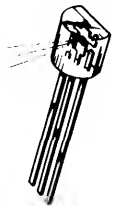
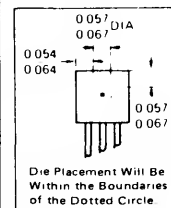
INFRARED-EMITTING DIODE

...designed for industrial processing and control applications such as light modulators, shaft or position encoders, end of tape detectors, and optical coupler applications. Supplied in TO-92 package for ease of mounting and compatibility with existing automatic insertion equipment.

- High Power Output — (Typ)
 - MLED93 — 3.0 mW
 - MLED94 — 5.0 mW
 - MLED95 — 7.0 mW
 - @ $I_F = 100 \text{ mA}$ (duty cycle $\leq 2.0\%$)
- Infrared-Emission — 930 nm (Typ)
- One-Piece, Unibloc Package for High Reliability

LOW COST INFRARED-EMITTING DIODE

PN GALLIUM ARSENIDE



MAXIMUM RATINGS

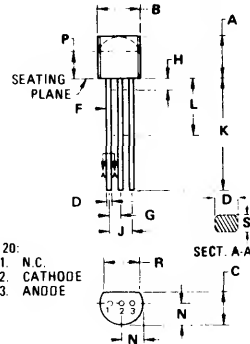
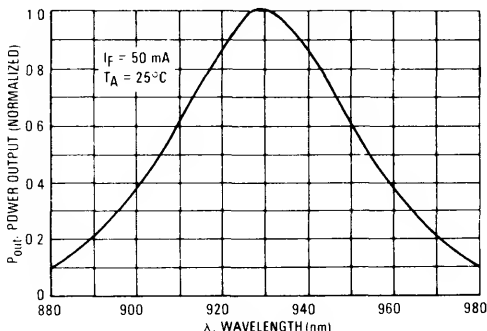
| Rating | Symbol | Value | Unit |
|---|-----------------|-------------|----------------------------|
| Reverse Voltage | V_R | 6.0 | Volts |
| Forward Current-Continuous | I_F | 100 | mA |
| Total Power Dissipation @ $T_A = 25^\circ\text{C}$ Derate above 25°C | $P_D(1)$ | 215 2.86 | mW mW/ $^\circ\text{C}$ |
| Operating and Storage Junction Temperature Range | $T_{J,T_{Stg}}$ | -65 to +100 | $^\circ\text{C}$ |

THERMAL CHARACTERISTICS

| Characteristic | Symbol | Max | Unit |
|--|--------------------|-----|--------------------|
| Thermal Resistance Junction to Ambient | $R_{\theta JA}(1)$ | 350 | $^\circ\text{C/W}$ |

(1) $R_{\theta JA}(1)$ is measured with the device soldered into a typical printed circuit board.

FIGURE 1 — RELATIVE SPECTRAL OUTPUT



NOTES.

- 1 CONTOUR OF PACKAGE BEYOND ZONE "P"
- 2 IS UNCONTROLLED.
- DIM "F" APPLIES BETWEEN "H" AND "L". DIM "O" & "S" APPLIES BETWEEN "L" & 12.70 mm (0.5") FROM SEATING PLANE. LEAD DIM IS UNCONTROLLED IN "H" & BEYOND 12.70 mm (0.5") FROM SEATING PLANE.

| DIM | MILLIMETERS | | INCHES | |
|-----|-------------|------|--------|-------|
| | MIN | MAX | MIN | MAX |
| A | 4.32 | 5.33 | 0.170 | 0.210 |
| B | 4.44 | 5.21 | 0.175 | 0.205 |
| C | 3.18 | 4.19 | 0.125 | 0.165 |
| D | 0.41 | 0.56 | 0.016 | 0.022 |
| F | 0.41 | 0.48 | 0.016 | 0.019 |
| G | 1.14 | 1.40 | 0.045 | 0.055 |
| H | - | 2.54 | - | 0.100 |
| J | 2.41 | 2.67 | 0.095 | 0.105 |
| K | 12.70 | - | 0.500 | - |
| L | 6.35 | - | 0.250 | - |
| N | 2.03 | 2.92 | 0.080 | 0.115 |
| P | 2.92 | - | 0.115 | - |
| R | 3.43 | - | 0.135 | - |
| S | 0.36 | 0.41 | 0.014 | 0.016 |

All JEDEC dimensions and notes apply.

CASE 29-02
TO-92

MLED93, MLED94, MLED95

ELECTRICAL CHARACTERISTICS ($T_A = 25^\circ C$ unless otherwise noted)

| Characteristic | Fig No | Symbol | Min | Typ | Max | Unit |
|--|--------|-------------|-----|-----|-----|-------|
| Reverse Leakage Current ($V_R = 60 V$, $R_L = 1.0 \text{ Megohm}$) | | I_R | | 50 | | nA |
| Reverse Breakdown Voltage ($I_R = 100 \mu A$) | | $V_{(BR)R}$ | 6.0 | | | Volts |
| Instantaneous Forward Voltage ($I_F = 50 \text{ mA}$) | 2 | V_F | | 1.3 | 1.8 | Volts |
| Total Capacitance ($V_R = 0 V$, $f = 10 \text{ MHz}$) | | C_T | | 150 | | pF |

OPTICAL CHARACTERISTICS ($T_A = 25^\circ C$ unless otherwise noted)

| Characteristic | Fig No | Symbol | Min | Typ | Max | Unit |
|--|--------|-----------------|-----|------|-----|--------------|
| Total Power Output (Notes 1 and 3) ($I_F = 100 \text{ mA}$) | 3, 4 | P_O | 2.0 | 3.0 | | mW |
| | MLED93 | | 4.0 | 5.0 | | |
| | MLED94 | | 6.0 | 7.0 | | |
| | MLED95 | | | | | |
| Radiant Intensity (Notes 2 and 3) ($I_F = 100 \text{ mA}$) | MLED93 | I_O | | 13.2 | | mW steradian |
| | MLED94 | | | 22.0 | | |
| | MLED95 | | | 30.8 | | |
| Peak Emission Wavelength | 1 | λ_P | | 930 | | nm |
| Spectral Line Half Width | 1 | $\Delta\lambda$ | | 48 | | nm |

NOTE:

1. Power Output, P_O , is the total power radiated by the device. It is measured by detecting all radiation leaving the device onto a calibrated integrating sphere.
2. Irradiance from a Light Emitting Diode (LED) can be calculated by

$$H = \frac{I_0}{d^2}, \text{ where } H \text{ is irradiance in } \text{mW/cm}^2, I_0 \text{ is radiant intensity in } \text{mW steradian}$$

3. Pulse Test, Pulse Width = 300 μs , Duty Cycle = 2.0

FIGURE 2 – FORWARD CHARACTERISTICS

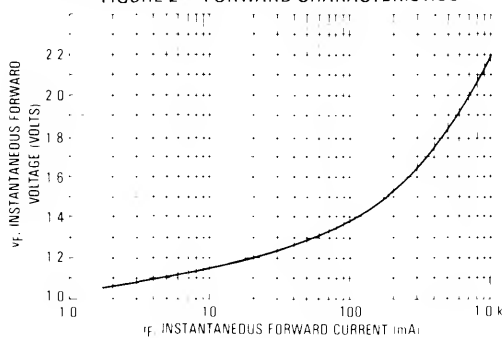


FIGURE 4 – INSTANTANEOUS POWER OUTPUT

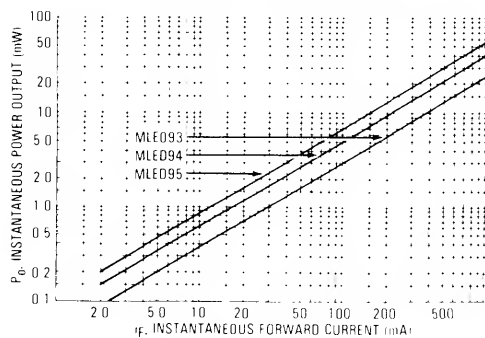


FIGURE 3 – POWER OUTPUT versus JUNCTION TEMPERATURE

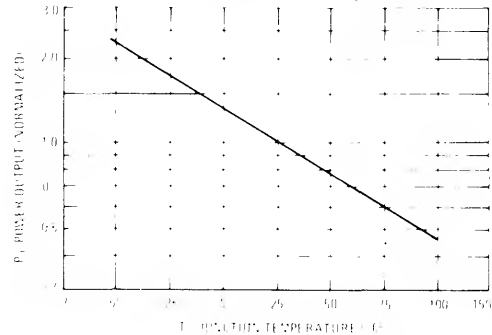
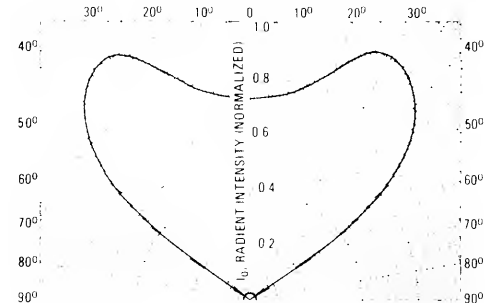


FIGURE 5 – SPATIAL RADIATION PATTERN





MOTOROLA

MLED900

INFRARED-EMITTING DIODE

... designed for applications requiring high power output, low drive power and very fast response time. This device is used in industrial processing and control, light modulators, shaft or position encoders, punched card readers, optical switching, and logic circuits. It is spectrally matched for use with silicon detectors.

- High Power Output – 550 μW (Typ) @ $I_F = 50 \text{ mA}$
- Infrared Emission – 930 nm (Typ)
- Low Drive Current – 10 mA for 120 μW (Typ)
- Unique Molded Lens for Durability and Long Life
- Economical Plastic Package

MAXIMUM RATINGS

| Rating | Symbol | Value | Unit |
|--|-----------------------|-------------|---|
| Reverse Voltage | V_R | 3.0 | Volts |
| Forward Current-Continuous | I_F | 80 | mA |
| Total Device Dissipation @ $T_A = 25^\circ\text{C}$ Derate above 25°C | $P_D(1)$ | 1.20 2.0 | mW $\text{mW}/^\circ\text{C}$ |
| Operating and Storage Junction Temperature Range | $T_{J,T_{stg}}^{(2)}$ | -40 to +85 | $^\circ\text{C}$ |

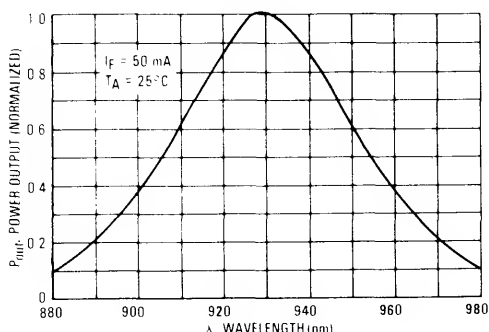
THERMAL CHARACTERISTICS

| Characteristic | Symbol | Max | Unit |
|---|---------------|-----|---------------------------|
| Thermal Resistance, Junction to Ambient | θ_{JA} | 500 | $^\circ\text{C}/\text{W}$ |

(1) Printed Circuit Board Mounting

(2) Heat Sink should be applied to leads during soldering to prevent Case Temperature exceeding 85°C .

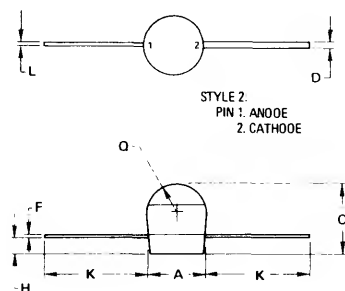
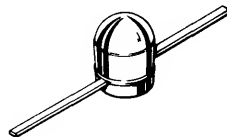
FIGURE 1 – RELATIVE SPECTRAL OUTPUT



INFRARED-EMITTING DIODE
930 nm

PN GALLIUM ARSENIDE

120 MILLIWATTS



NOTE:

1. LEAD IDENTIFICATION SQUARE
BONDING PAO OVER PIN 2.

| DIM | MILLIMETERS | | INCHES | |
|-----|-------------|------|-----------|-------|
| | MIN | MAX | MIN | MAX |
| A | 3.56 | 4.06 | 0.140 | 0.160 |
| C | 4.57 | 5.33 | 0.180 | 0.210 |
| D | 0.46 | 0.61 | 0.018 | 0.024 |
| F | 0.23 | 0.28 | 0.009 | 0.011 |
| H | 1.02 | 1.27 | 0.040 | 0.050 |
| K | 6.35 | — | 0.250 | — |
| L | 0.33 | 0.48 | 0.013 | 0.019 |
| Q | 1.91 NOM | — | 0.075 NOM | — |

CASE 171-02

MLED900

ELECTRICAL CHARACTERISTICS ($T_A = 25^\circ\text{C}$ unless otherwise noted)

| Characteristic | Fig. No. | Symbol | Min | Typ | Max | Unit |
|---|----------|-------------|-----|-----|-----|-------|
| Reverse Leakage Current ($V_R = 3.0 \text{ V}$, $R_L = 1.0 \text{ Megohm}$) | - | I_R | - | 50 | - | nA |
| Reverse Breakdown Voltage ($I_R = 100 \mu\text{A}$) | - | $V_{(BR)R}$ | 3.0 | - | - | Volts |
| Forward Voltage ($I_F = 50 \text{ mA}$) | 2 | V_F | - | 1.2 | 1.5 | Volts |
| Total Capacitance ($V_R = 0 \text{ V}$, $f = 1.0 \text{ MHz}$) | - | C_T | - | 150 | - | pF |

OPTICAL CHARACTERISTICS ($T_A = 25^\circ\text{C}$ unless otherwise noted)

| Characteristics | Fig. No. | Symbol | Min | Typ | Max | Unit |
|--|----------|-----------------|-----|-----|-----|--------------|
| Total Power Output (Note 1) ($I_F = 50 \text{ mA}$) | 3.4 | P_o | 200 | 550 | - | μW |
| Radiant Intensity (Note 2) ($I_o = 10 \text{ mA}$) | | I_o | - | 2.4 | - | mW/steradian |
| Peak Emission Wavelength | 1 | λ_p | - | 930 | - | nm |
| Spectral Line Half Width | 1 | $\Delta\lambda$ | - | 48 | - | nm |

NOTE:

- Power Output, P_o , is the total power radiated by the device into a solid angle of 2π steradians. It is measured by directing all radiation leaving the device, within this solid angle, onto a calibrated silicon solar cell.
- Irradiance from a Light Emitting Diode (LED) can be calculated by:

$$H = \frac{I_o}{d^2} \quad \text{where } H \text{ is irradiance in } \text{mW/cm}^2, I_o \text{ is radiant intensity in } \text{mW/steradian}; \\ d \text{ is distance from LED to the detector in cm.}$$

FIGURE 2 – FORWARD CHARACTERISTICS

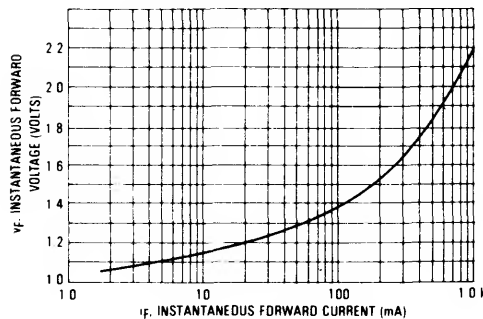


FIGURE 4 – INSTANTANEOUS POWER OUTPUT
versus FORWARD CURRENT

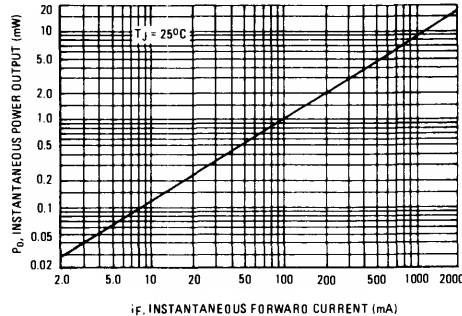


FIGURE 3 – POWER OUTPUT versus JUNCTION TEMPERATURE

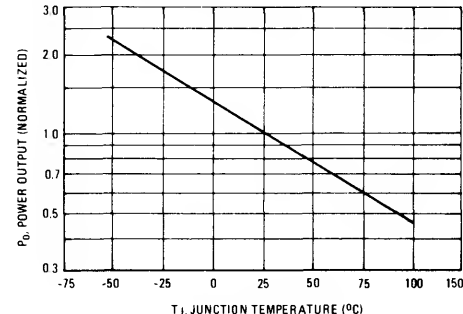
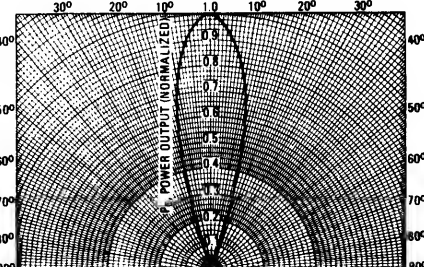


FIGURE 5 – SPATIAL RADIATION PATTERN



Output saturation effects are not evident at currents up to 2 A as shown on Figure 4. However, saturation does occur due to heating of the semiconductor as indicated by Figure 3. To estimate output level, average junction temperature may be calculated from:

$$T_J(AV) = T_A + \theta_{JA} V_F I_F D$$

where D is the duty cycle of the applied current, I_F . Use of the above method should be restricted to drive conditions employing pulses of less than 10 μs duration to avoid errors caused by high peak junction temperatures.



MOTOROLA

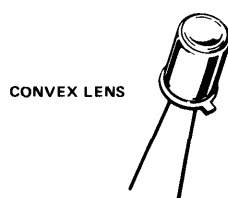
MLED930

INFRARED-EMITTING DIODE

... designed for applications requiring high power output, low drive power and very fast response time. This device is used in industrial processing and control, light modulators, shaft or position encoders, punched card readers, optical switching, and logic circuits. It is spectrally matched for use with silicon detectors.

- High-Power Output – 650, μW (Typ) @ $I_F = 100$ mA
- Infrared-Emission – 900 nm (Typ)
- Low Drive Current – 10 mA for 70 μW (Typ)
- Popular TO-18 Type Package for Easy Handling and Mounting
- Hermetic Metal Package for Stability and Reliability

**INFRARED-EMITTING DIODE
900 nm
PN GALLIUM ARSENIDE
250 MILLIWATTS**



MAXIMUM RATINGS

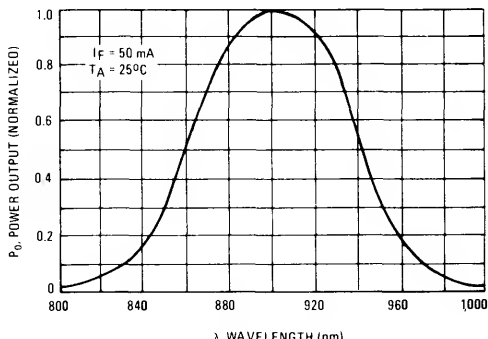
| Rating | Symbol | Value | Unit |
|--|-----------------------|-------------|----------------------------|
| Reverse Voltage | V_R | 3.0 | Volts |
| Forward Current-Continuous | I_F | 150 | mA |
| Total Device Dissipation @ $T_A = 25^\circ\text{C}$ Derate above 25°C | $P_D(1)$ | 250 | mW |
| | | 2.5 | $\text{mW}/^\circ\text{C}$ |
| Operating and Storage Junction Temperature Range | T_J, T_{stg} | -65 to +125 | $^\circ\text{C}$ |

THERMAL CHARACTERISTICS

| Characteristics | Symbol | Max | Unit |
|---|---------------|-----|---------------------------|
| Thermal Resistance, Junction to Ambient | θ_{JA} | 400 | $^\circ\text{C}/\text{W}$ |

(1)Printed Circuit Board Mounting

FIGURE 1 – RELATIVE SPECTRAL OUTPUT



STYLE 1:

PIN 1. ANODE
PIN 2. CATHODE

NOTES:

1. PIN 2 INTERNALLY CONNECTED TO CASE
2. LEADS WITHIN 0.13 mm (0.005)
RADIUS OF TRUE POSITION AT
SEATING PLANE AT MAXIMUM
MATERIAL CONDITION.

| DIM | MILLIMETERS | | INCHES | |
|-----|-------------|------|-----------|-------|
| | MIN | MAX | MIN | MAX |
| A | 5.31 | 5.84 | 0.209 | 0.239 |
| B | 4.52 | 4.95 | 0.178 | 0.195 |
| C | 5.08 | 6.35 | 0.200 | 0.250 |
| D | 0.41 | 0.48 | 0.016 | 0.019 |
| F | 0.51 | 1.02 | 0.020 | 0.040 |
| G | 2.54 BSC | | 0.100 BSC | |
| H | 0.99 | 1.17 | 0.039 | 0.046 |
| J | 0.84 | 1.22 | 0.033 | 0.048 |
| K | 12.70 | — | 0.500 | — |
| L | 3.35 | 4.01 | 0.132 | 0.158 |
| M | 45° BSC | | 45° BSC | |

CASE 209-1

MLED930

ELECTRICAL CHARACTERISTICS ($T_A = 25^\circ\text{C}$ unless otherwise noted)

| Characteristic | Fig. No. | Symbol | Min | Typ | Max | Unit |
|--|----------|-------------|-----|------|-----|-------|
| Reverse Leakage Current ($V_R = 3.0 \text{ V}$) | - | I_R | - | 2.0 | - | nA |
| Reverse Breakdown Voltage ($I_R = 100 \mu\text{A}$) | - | $V_{(BR)R}$ | 3.0 | 8.8 | - | Volts |
| Forward Voltage ($I_F = 50 \text{ mA}$) | 2 | V_F | - | 1.25 | 1.5 | Volts |
| Total Capacitance ($V_R = 0 \text{ V}$, $f = 1.0 \text{ MHz}$) | - | C_T | - | 150 | - | pF |

OPTICAL CHARACTERISTICS ($T_A = 25^\circ\text{C}$ unless otherwise noted)

| Characteristic | Fig. No. | Symbol | Min | Typ | Max | Unit |
|---|----------|-----------------|-----|-----|-----|---------------|
| Total Power Output (Note 1) ($I_F = 100 \text{ mA}$) | 3, 4 | P_O | 200 | 650 | - | μW |
| Radiant Intensity (Note 2) ($I_F = 100 \text{ mA}$) | | I_O | - | 1.5 | - | mW/steradian |
| Peak Emission Wavelength | 1 | λ_P | | 900 | | nm |
| Spectral Line Half Width | 1 | $\Delta\lambda$ | | 40 | | nm |

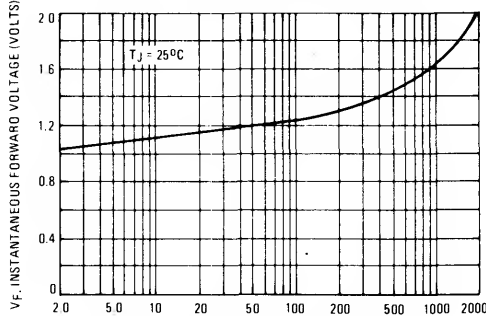
NOTE:

1. Power Output, P_O , is the total power radiated by the device into a solid angle of 2π steradians. It is measured by directing all radiation leaving the device, within this solid angle, onto a calibrated silicon solar cell.

2. Irradiance from a Light Emitting Diode (LED) can be calculated by:

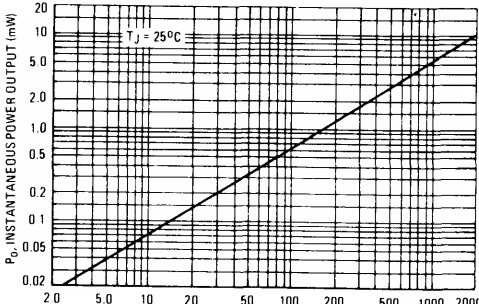
$$H = \frac{I_O}{d^2} \quad \text{where } H \text{ is irradiance in } \text{mW/cm}^2; I_O \text{ is radiant intensity in } \text{mW/steradian}; \\ d \text{ is distance from LED to the detector in cm.}$$

FIGURE 2 – FORWARD CHARACTERISTICS



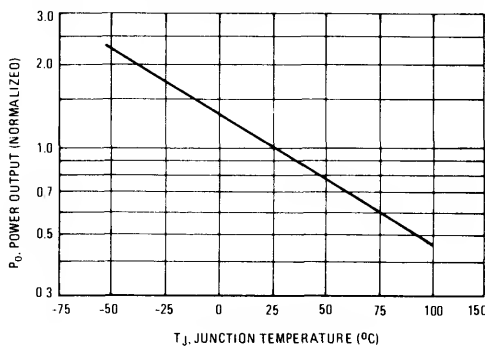
I_F , INSTANTANEOUS FORWARD CURRENT (mA)

FIGURE 4 – INSTANTANEOUS POWER OUTPUT versus FORWARD CURRENT



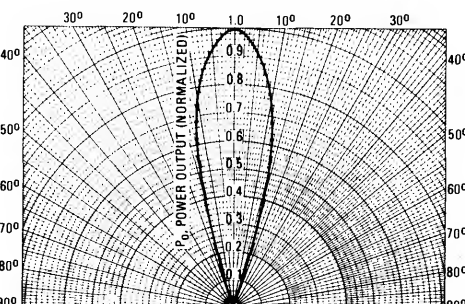
I_F , INSTANTANEOUS FORWARD CURRENT (mA)

FIGURE 3 – POWER OUTPUT versus JUNCTION TEMPERATURE



T_J , JUNCTION TEMPERATURE (°C)

FIGURE 5 – SPATIAL RADIATION PATTERN





MOTOROLA

MOC119

NPN PHOTO DARLINGTON AND PN INFRARED EMITTING DIODE

. . . Gallium Arsenide LED optically coupled to a Silicon Photo Darlington Transistor designed for applications requiring electrical isolation, high-current transfer ratios, small package size and low cost; such as interfacing and coupling systems, phase and feedback controls, solid-state relays and general-purpose switching circuits.

- High Isolation Voltage — $V_{ISO} = 7000$ V (Min)
- Excellent Frequency Response — 30 kHz (Typ)
- High Collector Output Current @ $I_F = 10$ mA — $I_C = 30$ mA (Min)
- Fast Switching Times @ $I_C = 2.5$ mA
 $t_r = 10 \mu s$ (Typ)
 $t_f = 50 \mu s$ (Typ)
- Economical, Compact, Dual-In-Line Package
- Base Not Connected

MAXIMUM RATINGS ($T_A = 25^\circ C$ unless otherwise noted)

| Rating | Symbol | Value | Unit |
|--------|--------|-------|------|
|--------|--------|-------|------|

INFRARED-EMITTING DIODE MAXIMUM RATINGS

| | | | |
|---|-------|-----|---------------|
| Reverse Voltage | V_R | 3.0 | Volts |
| Forward Current — Continuous | I_F | 100 | mA |
| Forward Current — Peak (Pulse Width = 300 μs , 2.0% Duty Cycle) | I_F | 3.0 | Amp |
| Total Power Dissipation @ $T_A = 25^\circ C$ | P_D | 150 | mW |
| Negligible Power in Transistor Derate above $25^\circ C$ | | 2.0 | $mW/^\circ C$ |

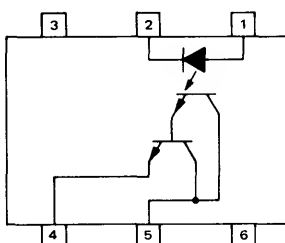
PHOTOTRANSISTOR MAXIMUM RATINGS

| | | | |
|--|-----------|-----|---------------|
| Collector-Emitter Voltage | V_{CEO} | 30 | Volts |
| Emitter-Collector Voltage | V_{ECO} | 7.0 | Volts |
| Collector-Base Voltage | V_{CBO} | 30 | Volts |
| Total Power Dissipation @ $T_A = 25^\circ C$ | P_D | 150 | mW |
| Negligible Power in Diode Derate above $25^\circ C$ | | 2.0 | $mW/^\circ C$ |

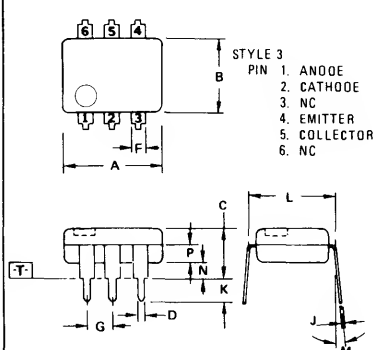
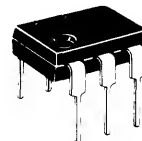
TOTAL DEVICE RATINGS

| | | | |
|---|-----------|-------------|---------------|
| Total Device Dissipation @ $T_A = 25^\circ C$ Equal Power Dissipation in Each Element Derate above $25^\circ C$ | P_D | 250 | mW |
| | | 3.3 | $mW/^\circ C$ |
| Operating Junction Temperature Range | T_J | -55 to +100 | $^\circ C$ |
| Storage Temperature Range | T_{stg} | -55 to +150 | $^\circ C$ |
| Soldering Temperature (10 s) | — | 260 | $^\circ C$ |

FIGURE 1 — DEVICE SCHEMATIC



OPTO COUPLER/ISOLATOR DARLINGTON OUTPUT



NOTES

1. DIMENSIONS A AND B ARE DATUMS.
2. T IS SEATING PLANE.
3. POSITIONAL TOLERANCES FOR LEADS $\phi 0.013 (0.005) M T A M B M$
4. DIMENSION L TO CENTER OF LEADS WHEN FORMED PARALLEL.
5. DIMENSIONING AND TOLERANCING PER ANSI Y14.5, 1973.

| DIM | MILLIMETERS | | INCHES | |
|-----|-------------|------|-----------|-------|
| | MIN | MAX | MIN | MAX |
| A | 8.13 | 8.89 | 0.320 | 0.350 |
| B | 6.10 | 6.60 | 0.240 | 0.260 |
| C | 2.92 | 5.08 | 0.115 | 0.200 |
| D | 0.41 | 0.51 | 0.016 | 0.020 |
| F | 1.02 | 1.78 | 0.040 | 0.070 |
| G | 2.54 BSC | | 0.100 BSC | |
| J | 0.20 | 0.30 | 0.008 | 0.012 |
| K | 2.54 | 3.81 | 0.100 | 0.150 |
| L | 7.62 BSC | | 0.300 BSC | |
| M | 0.0 | 150 | 0.0 | 150 |
| N | 0.38 | 2.54 | 0.015 | 0.100 |
| P | 1.27 | 2.03 | 0.050 | 0.080 |

CASE 730A-01

MOC119

LED CHARACTERISTICS ($T_A = 25^\circ\text{C}$ unless otherwise noted.)

| Characteristic | Symbol | Min | Typ | Max | Unit |
|---|--------|-----|-------|-----|---------------|
| Reverse Leakage Current ($V_R = 3.0 \text{ V}$, $R_L = 1.0 \text{ M ohms}$) | I_R | — | 0.005 | 100 | μA |
| Forward Voltage ($I_F = 10 \text{ mA}$) | V_F | — | 1.2 | 1.5 | Volts |
| Capacitance ($V_R = 0 \text{ V}$, $f = 1.0 \text{ MHz}$) | C | — | 150 | — | pF |

PHOTOTRANSISTOR CHARACTERISTICS ($T_A = 25^\circ\text{C}$ and $I_F = 0$ unless otherwise noted.)

| Characteristic | Symbol | Min | Typ | Max | Unit |
|--|---------------|-----|-----|-----|-------|
| Collector-Emitter Dark Current ($V_{CE} = 10 \text{ V}$, $I_F = 0$) | I_{CEO} | — | 8.0 | 100 | nA |
| Collector-Emitter Breakdown Voltage ($I_C = 100 \mu\text{A}$, $I_B = 0$) | $V_{(BR)CEO}$ | 30 | 60 | — | Volts |
| Emitter-Collector Breakdown Voltage ($I_E = 10 \mu\text{A}$, $I_F = 0$) | $V_{(BR)ECO}$ | 7.0 | 8.0 | — | Volts |

COUPLED CHARACTERISTICS ($T_A = 25^\circ\text{C}$ unless otherwise noted.)

| Characteristic | Symbol | Min | Typ | Max | Unit |
|---|---------------|------|-----------|-----|-------|
| Collector Output Current (1) ($V_{CE} = 2.0 \text{ V}$, $I_F = 10 \text{ mA}$) | I_C | 30 | 70 | — | mA |
| Isolation Surge Voltage (2, 5), 60 Hz ac Peak, 5 Second | V_{ISO} | 7000 | — | — | Volts |
| Isolation Resistance (2) ($V = 500 \text{ V}$) | — | — | 10^{11} | — | Ohms |
| Collector-Emitter Saturation Voltage (1) ($I_C = 10 \text{ mA}$, $I_F = 10 \text{ mA}$) | $V_{CE(sat)}$ | — | 0.8 | 1.0 | Volts |
| Isolation Capacitance (2) ($V = 0$, $f = 1.0 \text{ MHz}$) | — | — | 1.0 | — | pF |

SWITCHING CHARACTERISTICS (Figures 4,5)

| | | | | | |
|--|-------|---|----|---|---------------|
| Rise Time ($V_{CC} = 10 \text{ V}$, $I_C = 2.5 \text{ mA}$, $R_L = 100 \Omega$) | t_r | — | 10 | — | μs |
| Fall Time ($V_{CC} = 10 \text{ V}$, $I_C = 2.5 \text{ mA}$, $R_L = 100 \Omega$) | t_f | — | 50 | — | μs |

(1) Pulse Test: Pulse Width = $300 \mu\text{s}$, Duty Cycle $\leq 2.0\%$.

(2) For this test LED pins 1 and 2 are common and Photo Transistor pins 4 and 5 are common.

(3) I_F adjusted to yield $I_C = 2.0 \text{ mA}$ and $i_c = 2.0 \text{ mA P-P}$ at 10 kHz .

(4) t_d and t_r are inversely proportional to the amplitude of I_F ; t_s and t_f are not significantly affected by I_F .

(5) Isolation Surge Voltage, V_{ISO} , is an internal device dielectric breakdown rating.

MOC119

DC CURRENT TRANSFER CHARACTERISTICS

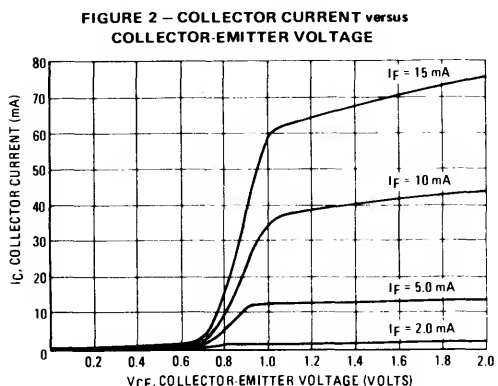
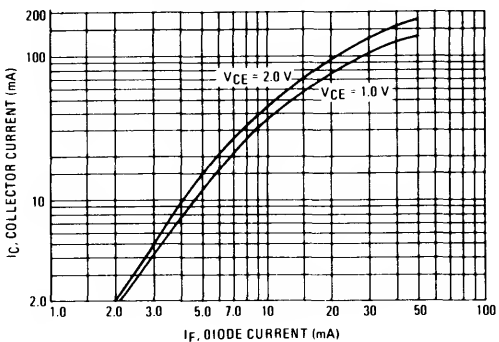


FIGURE 3 – COLLECTOR CURRENT versus DIODE CURRENT



SWITCHING CHARACTERISTICS

FIGURE 4 - SWITCHING TEST CIRCUIT

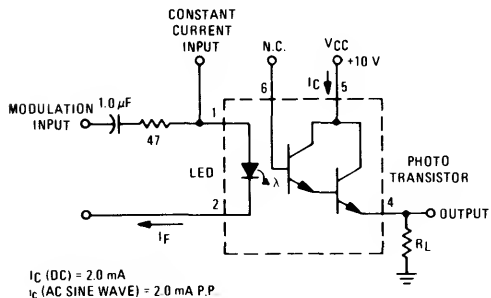


FIGURE 5 – VOLTAGE WAVEFORM

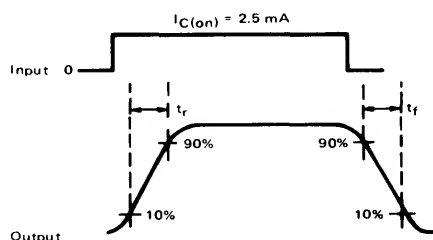
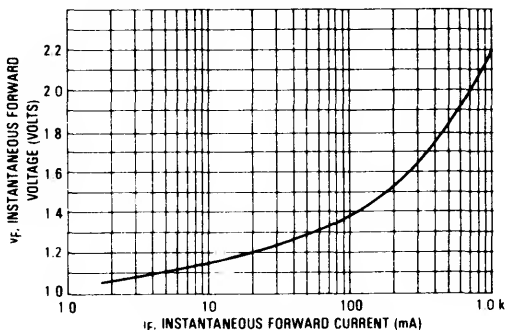
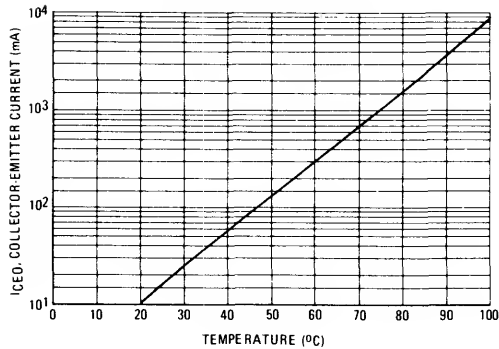
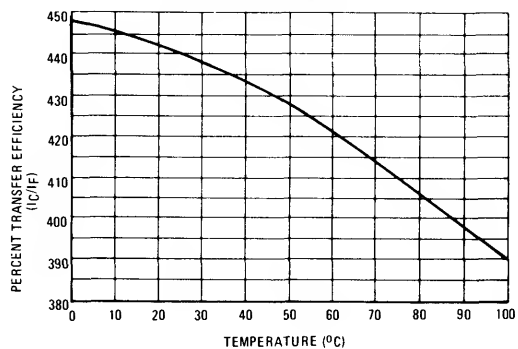


FIGURE 6 – FORWARD CHARACTERISTIC



TEMPERATURE CHARACTERISTICS

**FIGURE 7 – COLLECTOR-EMITTER DARK CURRENT
versus TEMPERATURE****FIGURE 8 – TRANSFER EFFICIENCY
versus TEMPERATURE**



MOTOROLA

**MOC1005
MOC1006**

5000 VOLTS – HIGH ISOLATION COUPLER

. . . Gallium Arsenide LED optically coupled to a Silicon Phototransistor designed for applications requiring high electrical isolation, high transistor breakdown-voltage and low-leakage, small package size and low cost; such as interfacing and coupling systems, logic to power circuit interface, and solid-state relays.

- High Isolation Voltage – $V_{ISO} = 5000$ V (Min)
 - High Collector-Emitter Breakdown Voltage – $V_{(BR)}CEO = 80$ V (Typ) @ $I_C = 1.0$ mA
 - High Collector Output Current @ $I_F = 10$ mA – $I_C = 5.0$ mA (Typ) – MOC1005
= 3.0 mA (Typ) – MOC1006
 - Economical, Compact, Dual-In-Line Plastic Package

MAXIMUM RATINGS ($T_A = 25^\circ\text{C}$ unless otherwise noted).

| Rating | Symbol | Value | Unit |
|--|----------------|-------|-------|
| INFRARED-EMITTING DIODE MAXIMUM RATINGS | | | |
| Reverse Voltage | V _R | 3.0 | Volts |
| Forward Current - Continuous | I _F | 80 | mA |
| Forward Current - Peak Pulse Width = 300 μ s, 2.0% Duty Cycle | I _F | 3.0 | Amp |
| Total Power Dissipation @ T _A = 25°C Negligible Power in Transistor Derate above 25°C | P _D | 150 | mW |
| | | 2.0 | mW/°C |

PHOTOTRANSISTOR MAXIMUM RATINGS

| | | | |
|---|-----------|-----|---------------|
| Collector-Emitter Voltage | V_{CEO} | 30 | Volts |
| Emitter-Collector Voltage | V_{ECO} | 7.0 | Volts |
| Collector-Base Voltage | V_{CBO} | 70 | Volts |
| Total Power Dissipation @ $T_A = 25^\circ C$ Negligible Power in Diode | P_D | 150 | mW |
| Derate above $25^\circ C$ | | 2.0 | $mW/^\circ C$ |

TOTAL DEVICE RATINGS

| | | | |
|--|-----------|-------------|----------------|
| Total Power Dissipation @ $T_A = 25^\circ C$ | P_D | 250 | mW |
| Equal Power Dissipation in Each Element Derate above $25^\circ C$ | | 3.3 | mW/ $^\circ C$ |
| Junction Temperature Range | T_J | -55 to +100 | $^\circ C$ |
| Storage Temperature Range | T_{stg} | -55 to +150 | $^\circ C$ |
| Soldering Temperature (10 s) | | 260 | $^\circ C$ |

FIGURE 1 – MAXIMUM POWER DISSIPATION

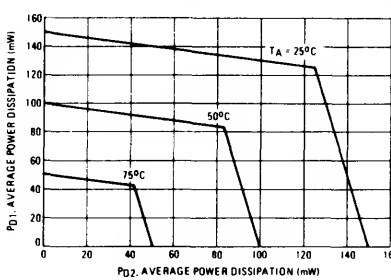


Figure 1 is based upon using limit values in the equation

$$T_{J1} - TA = R_{\theta JA} (P_{D1} + K_{\theta} P_{D2})$$

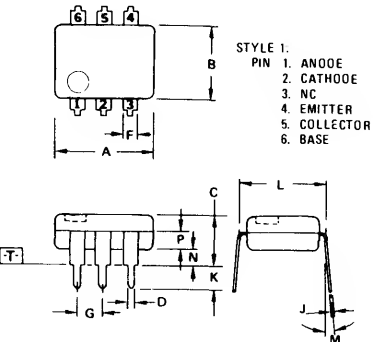
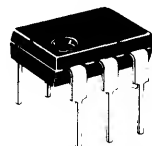
where

- T_{J1} Junction Temperature (100°C)
- T_A Ambient Temperature
- R_{θJA} Junction to Ambient Thermal Resistance (500°C/W)
- P_{D1} Power Dissipation in One Chip
- P_{D2} Power Dissipation in Other Chip
- K_θ Thermal Coupling Coefficient (20%)

Example

With P_{D1} = 90 mW in the LED
 @ T_A = 50°C, the transistor
 P_D (P_{D2}) must be less than 50 mW.

**OPTO
COUPLER/ISOLATOR
TRANSISTOR OUTPUT**



NOTES

- 1 DIMENSIONS A AND B ARE DATUMS.
 - 2 T IS SEATING PLANE.
 - 3 POSITIONAL TOLERANCES FOR LEADS
 0.13 (0.005)  T AND  M
 - 4 DIMENSION L TO CENTER OF LEADS WHEN FORMED PARALLEL.
 - 5 DIMENSIONING AND TOLERANCING PER ANSI Y14.5, 1973.

| | MILLIMETERS | | INCHES | |
|-----|-------------|------|--------|-------|
| DIM | MIN | MAX | MIN | MAX |
| A | 8.13 | 8.89 | 0.320 | 0.350 |
| B | 6.10 | 6.60 | 0.240 | 0.260 |
| C | 2.92 | 5.08 | 0.115 | 0.200 |
| D | 0.41 | 0.51 | 0.016 | 0.020 |
| F | 1.02 | 1.78 | 0.040 | 0.070 |
| G | 2.54 | BSC | 0.100 | BSC |
| J | 0.20 | 0.30 | 0.008 | 0.012 |
| K | 2.54 | 3.81 | 0.100 | 0.150 |
| L | 7.62 | BSC | 0.300 | BSC |
| M | 09 | 150 | 00 | 150 |
| N | 0.38 | 2.54 | 0.015 | 0.100 |
| P | 1.22 | 2.03 | 0.050 | 0.090 |

CASE 730A-01

MOC1005, MOC1006

LED CHARACTERISTICS ($T_A = 25^\circ\text{C}$ unless otherwise noted)

| Characteristic | Symbol | Min | Typ | Max | Unit |
|---|--------|-----|-------|-----|---------------|
| Reverse Leakage Current ($V_R = 3.0 \text{ V}$) | I_R | — | 0.005 | 100 | μA |
| Forward Voltage ($I_F = 10 \text{ mA}$) | V_F | — | 1.2 | 1.5 | Volts |
| Capacitance ($V_R = 0 \text{ V}$, $f = 1.0 \text{ MHz}$) | C | — | 30 | — | pF |

PHOTOTRANSISTOR CHARACTERISTICS ($T_A = 25^\circ\text{C}$ and $I_F = 0$ unless otherwise noted)

| | | | | | |
|--|---------------|----|-----|----|-------|
| Collector-Emitter Dark Current ($V_{CE} = 10 \text{ V}$, Base Open) | I_{CEO} | — | 3.5 | 50 | nA |
| Collector-Base Dark Current ($V_{CB} = 10 \text{ V}$, Emitter Open) | I_{CBO} | — | — | 20 | nA |
| Collector-Base Breakdown Voltage ($I_C = 100 \mu\text{A}$, $I_E = 0$) | $V_{(BR)CBO}$ | 70 | 100 | — | Volts |
| Collector-Emitter Breakdown Voltage ($I_C = 1.0 \text{ mA}$, $I_B = 0$) | $V_{(BR)CEO}$ | 30 | 80 | — | Volts |
| Emitter-Collector Breakdown Voltage ($I_E = 100 \mu\text{A}$, $I_B = 0$) | $V_{(BR)ECO}$ | 70 | — | — | Volts |
| DC Current Gain ($V_{CE} = 5.0 \text{ V}$, $I_C = 500 \mu\text{A}$) | h_{FE} | — | 250 | — | — |

COUPLED CHARACTERISTICS ($T_A = 25^\circ\text{C}$ unless otherwise noted)

| | | | | | | |
|---|--------------------|----------------------|--------------|----------------|-----|-------|
| Collector Output Current (1) ($V_{CE} = 10 \text{ V}$, $I_F = 10 \text{ mA}$, $I_B = 0$) | MOC1005 MOC1006 | I_C | 2.0 1.0 | 5.0 3.0 | — | mA |
| Isolation Surge Voltage, (1) DC (2). AC (3) | | V_{ISO} | 5000 5000 | 10000 10000 | — | Vdc |
| Isolation Resistance (4) ($V = 500 \text{ V}$) | — | — | — | 10^{11} | — | Ohms |
| Collector-Emitter Saturation ($I_C = 2.0 \text{ mA}$, $I_F = 50 \text{ mA}$) | | $V_{CE(\text{sat})}$ | — | 0.2 | 0.5 | Volts |
| Isolation Capacitance (4) ($V = 0$, $f = 1.0 \text{ MHz}$) | — | — | — | 1.3 | — | pF |
| Bandwidth (5) ($I_C = 2.0 \text{ mA}$, $R_L = 100 \text{ Ohms}$, Figure 11) | — | — | — | 300 | — | kHz |

SWITCHING CHARACTERISTICS

| | | | | | | |
|--------------|--------------------|-------|---|--------------|---|---------------|
| Delay Time | MOC1005 MOC1006 | t_d | — | 0.07 0.10 | — | μs |
| Rise Time | MOC1005 MOC1006 | t_r | — | 0.8 2.0 | — | μs |
| Storage Time | MOC1005 MOC1006 | t_s | — | 4.0 2.0 | — | μs |
| Fall Time | MOC1005 MOC1006 | t_f | — | 8.0 8.0 | — | μs |

(1) Pulse Test. Pulse Width = $300 \mu\text{s}$. Duty Cycle $\leq 2.0\%$

(2) Peak DC Voltage — 1.0 Minute

(3) Nonrepetitive Peak AC Voltage — 1 Full Cycle, Sine Wave, 60 Hz

(4) For this test LED pins 1 and 2 are common and Photo Transistor pins 4, 5 and 6 are common

(5) If adjusted to yield $I_C = 2.0 \text{ mA}$ and $I_c = 2.0 \text{ mA}$ p-p at 10 kHz

TYPICAL ELECTRICAL CHARACTERISTICS

FIGURE 2 — MOC1005

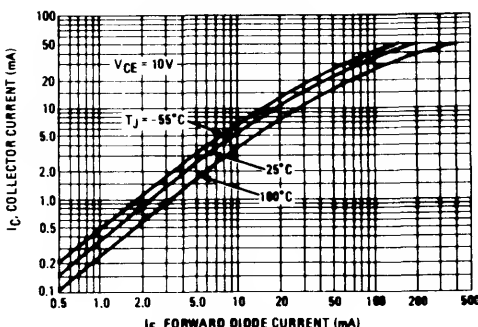
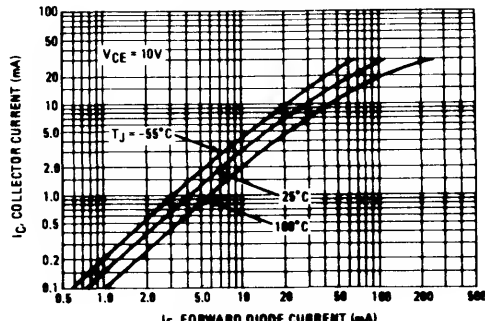


FIGURE 3 — MOC1006



MOC1005, MOC1006

TYPICAL ELECTRICAL CHARACTERISTICS

FIGURE 4 – FORWARD CHARACTERISTICS

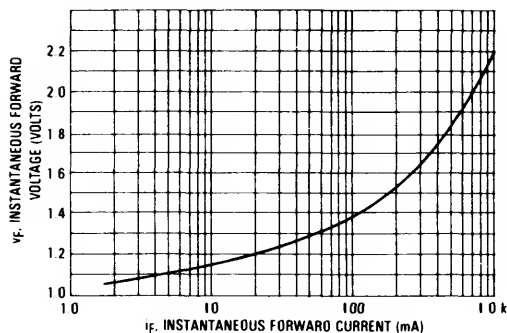


FIGURE 5 – COLLECTOR SATURATION VOLTAGE

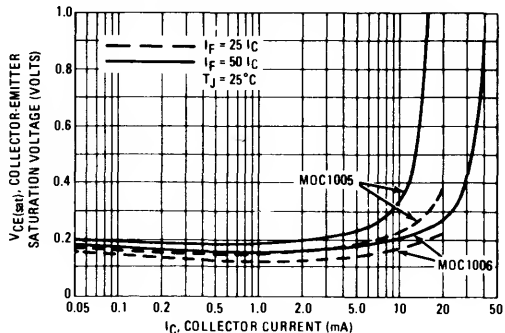


FIGURE 6 – TURN-ON TIME

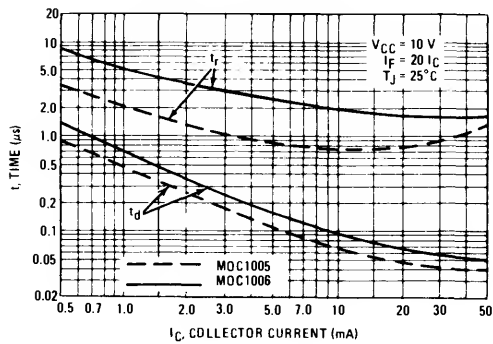


FIGURE 7 – TURN-OFF TIME

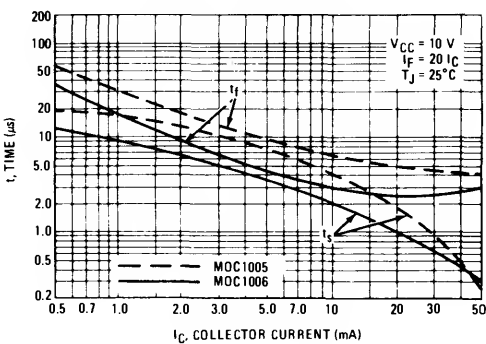


FIGURE 8 – SATURATED SWITCHING TEST CIRCUIT

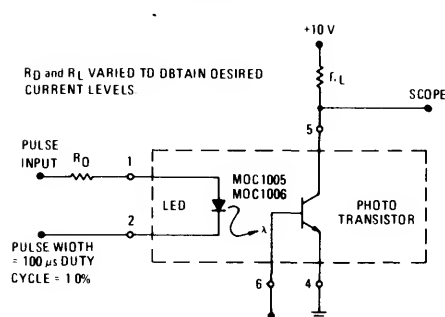
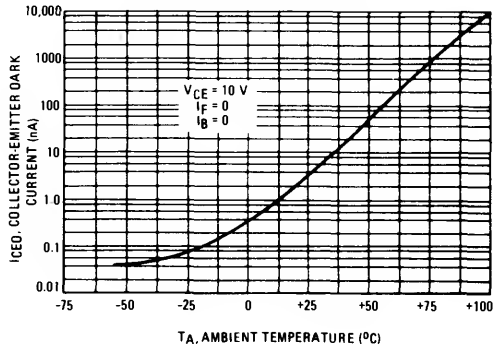


FIGURE 9 – DARK CURRENT versus AMBIENT TEMPERATURE



MOC1005, MOC1006

FIGURE 10 – FREQUENCY RESPONSE

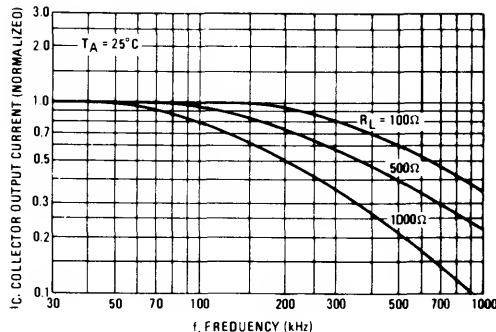


FIGURE 11 – FREQUENCY RESPONSE TEST CIRCUIT

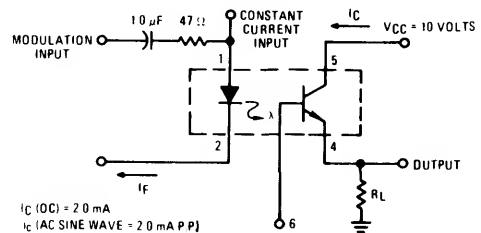


FIGURE 12 – POWER AMPLIFIER

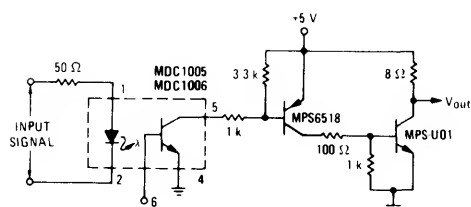


FIGURE 13 – INTERFACE BETWEEN LOGIC AND LOAD

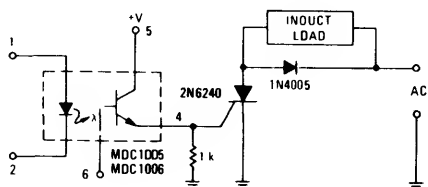


FIGURE 14 – UNIVERSAL CMOS LOGIC TRANSLATOR
(Programmable Constant Current Drive)

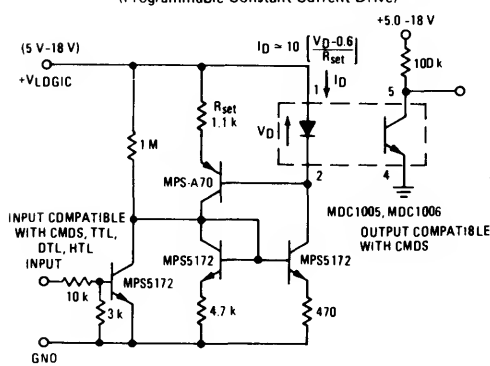
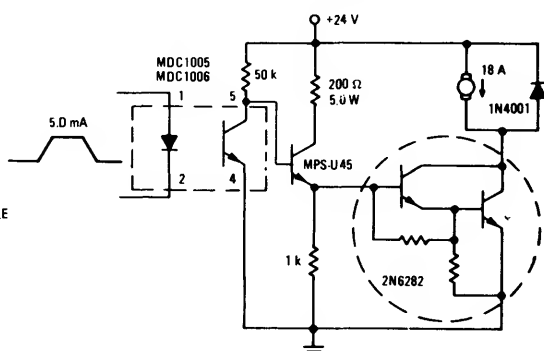


FIGURE 15 – ISOLATED DC MOTOR CONTROLLER





MOTOROLA

**MOC3000
MOC3001
MOC3002
MOC3003**

OPTO SCR COUPLER

These devices consist of a gallium-arsenide infrared emitting diode optically coupled to a photo sensitive silicon controlled rectifier (SCR). They are designed for applications requiring high electrical isolation between low voltage circuitry, like integrated circuits, and the ac line.

- High Blocking Voltage
MOC3000, 3001 — 400 V for 220 Vac Lines
MOC3002, 3003 — 250 V for 1.10 Vac Lines
- Very High Isolation Voltage
 $V_{ISO} = 7500$ V Min
- Standard 6-Pin DIP
- UL Recognized, File Number E54915

MAXIMUM RATINGS ($T_A = 25^\circ\text{C}$ unless otherwise noted)

| Rating | Symbol | Value | Unit |
|--------|--------|-------|------|
|--------|--------|-------|------|

INFRARED EMITTING DIODE MAXIMUM RATINGS

| | | | |
|---|-------|------|----------------------------|
| Reverse Voltage | V_R | 7.0 | Volts |
| Forward Current — Continuous | I_F | 60 | mA |
| Total Power Dissipation @ $T_A = 25^\circ\text{C}$ Negligible Power in Transistor Derate above 25°C | P_D | 100 | mW |
| | | 1.33 | $\text{mW}/^\circ\text{C}$ |

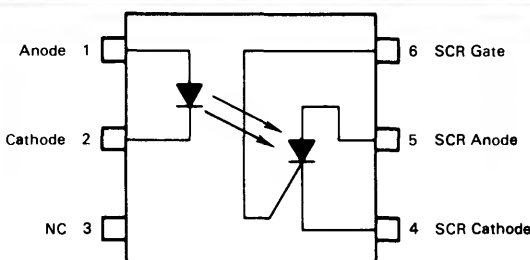
OUTPUT DRIVER MAXIMUM RATINGS

| | | | |
|---|-------------------|-------------|---|
| Peak Forward Voltage MOC3000, 1 MOC3002, 3 | V_{DM} | 400 250 | Volts |
| Forward RMS Current (Full Cycle, 50 to 60 Hz) $T_A = 25^\circ\text{C}$ | $I_T(\text{RMS})$ | 300 | mA |
| Peak Nonrepetitive Surge Current ($P_W = 10$ ms, DC = 10%) | I_{TSM} | 3.0 | A |
| Total Power Dissipation @ $T_A = 25^\circ\text{C}$ Derate above 25°C | P_D | 400 5.33 | mW $\text{mW}/^\circ\text{C}$ |

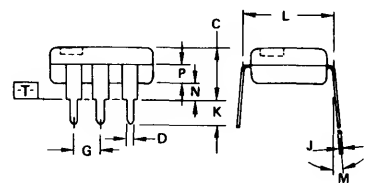
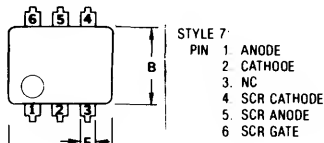
TOTAL DEVICE MAXIMUM RATINGS

| | | | |
|---|-----------|-------------|------------------|
| Isolation Surge Voltage (1) (Peak ac Voltage, 60 Hz, 5 Second Duration) | V_{ISO} | 7500 | Vac |
| Junction Temperature Range | T_J | -40 to +100 | $^\circ\text{C}$ |
| Ambient Operating Temperature Range | T_A | -55 to +100 | $^\circ\text{C}$ |
| Storage Temperature Range | T_{stg} | -55 to +150 | $^\circ\text{C}$ |
| Soldering Temperature (10 s) | — | 260 | $^\circ\text{C}$ |

(1) Isolation surge voltage, V_{ISO} , is an internal device dielectric breakdown rating.



OPTO COUPLER/ISOLATOR with PHOTO SCR OUTPUT 400 and 250 VOLTS



NOTES:

1. DIMENSIONS A AND B ARE DATUMS.
2. T IS SEATING PLANE.
3. POSITIONAL TOLERANCES FOR LEADS:
 ± 0.13 (0.005) T A (0.005)
4. DIMENSION L TD CENTER OF LEADS WHEN FORMED PARALLEL.
5. DIMENSIONING AND TOLERANCING PER ANSI Y14.5, 1973.

| DIM | MILLIMETERS | | INCHES | |
|-----|-------------|------|-----------|-------|
| | MIN | MAX | MIN | MAX |
| A | 8.13 | 8.89 | 0.320 | 0.350 |
| B | 6.10 | 6.60 | 0.240 | 0.260 |
| C | 2.92 | 5.08 | 0.115 | 0.200 |
| D | 0.41 | 0.51 | 0.016 | 0.020 |
| F | 1.02 | 1.78 | 0.040 | 0.070 |
| G | 2.54 BSC | | 0.100 BSC | |
| J | 0.20 | 0.30 | 0.008 | 0.012 |
| K | 2.54 | 3.81 | 0.100 | 0.150 |
| L | 7.62 BSC | | 0.300 BSC | |
| M | 0.0 | 150 | 0.0 | 150 |
| N | 0.38 | 2.54 | 0.015 | 0.100 |
| P | 1.27 | 2.03 | 0.050 | 0.080 |

CASE 730A-01

MOC3000, MOC3001, MOC3002, MOC3003

ELECTRICAL CHARACTERISTICS ($T_A = 25^\circ\text{C}$ unless otherwise noted)

| Characteristic | Symbol | Min | Typ | Max | Unit |
|--|--------|-----|------|-----|---------------|
| LED CHARACTERISTICS | | | | | |
| Reverse Leakage Current ($V_R = 3.0 \text{ V}$) | I_R | — | 0.05 | 10 | μA |
| Forward Voltage ($I_F = 10 \text{ mA}$) | V_F | — | 1.2 | 1.5 | Volts |
| Capacitance ($V = 0, f = 1.0 \text{ MHz}$) | C_J | — | 50 | — | pF |

DETECTOR CHARACTERISTICS

| | | | | | | |
|---|--------------------------------|----------|------------|-----------|-----------|---------------|
| Peak Off-State Voltage ($R_{GK} = 10 \text{ k}\Omega, T_A = 100^\circ\text{C}$) | MOC3000, 3001 MOC3002, 3003 | V_{DM} | 400 250 | — — | — — | Volts |
| Peak Reverse Voltage ($R_{GK} = 10 \text{ k}\Omega, T_A = 100^\circ\text{C}$) | MOC3000, 3001 MOC3002, 3003 | V_{RM} | 400 250 | — — | — — | Volts |
| On-State Voltage ($I_{TM} = 0.3 \text{ A}$) | | V_{TM} | — | 1.1 | 1.3 | Volts |
| Off-State Current ($V_{DM} = 400 \text{ V}, R_{GK} = 10 \text{ k}\Omega, T_A = 100^\circ\text{C}$) ($V_{DM} = 250 \text{ V}, R_{GK} = 10 \text{ k}\Omega, T_A = 100^\circ\text{C}$) | MOC3000, 3001 MOC3002, 3003 | I_{DM} | — — | — — | 150 50 | μA |
| Reverse Current ($V_{RM} = 400 \text{ V}, R_{GK} = 10 \text{ k}\Omega, T_A = 100^\circ\text{C}$) ($V_{RM} = 250 \text{ V}, R_{GK} = 10 \text{ k}\Omega, T_A = 100^\circ\text{C}$) | MOC3000, 3001 MOC3002, 3003 | I_{RM} | — — | — — | 150 50 | μA |
| Capacitance ($V = 0, f = 1.0 \text{ MHz}$) Anode - Gate Gate - Cathode | | C_J | — — | 20 350 | — — | pF |

COUPLED CHARACTERISTICS

| | | | | | | |
|---|--------------------------------|-----------|------------------|------------------------|----------------------|----------------------------|
| LED Current Required to Trigger ($V_{AK} = 50 \text{ V}, R_{GK} = 10 \text{ k}\Omega$) | MOC3001, 3003 MOC3000, 3002 | I_{FT} | — — — — | 10 15 6.0 8.0 | 20 30 11 14 | mA |
| ($V_{AK} = 100 \text{ V}, R_{GK} = 27 \text{ k}\Omega$) | MOC3001, 3003 MOC3000, 3002 | | | | | |
| Isolation Resistance ($V_{IO} = 500 \text{ Vdc}$) | | R_{ISO} | 100 | — | — | $\text{G}\Omega$ |
| Capacitance Input to Output ($V_{IO} = 0, f = 1.0 \text{ MHz}$) | | C_{ISO} | — | — | 2.0 | pF |
| Coupled dv/dt, Input to Output ($R_{GK} = 10 \text{ k}\Omega$) | | dv/dt | — | 500 | — | $\text{Volts}/\mu\text{s}$ |
| Isolation Surge Voltage (Peak ac Voltage, 60 Hz, 5 Second Duration) | | V_{ISO} | 7500 | — | — | Vac |

MOC3000, MOC3001, MOC3002, MOC3003

TYPICAL ELECTRICAL CHARACTERISTICS $T_A = 25^\circ\text{C}$

FIGURE 1 — FORWARD VOLTAGE versus FORWARD CURRENT

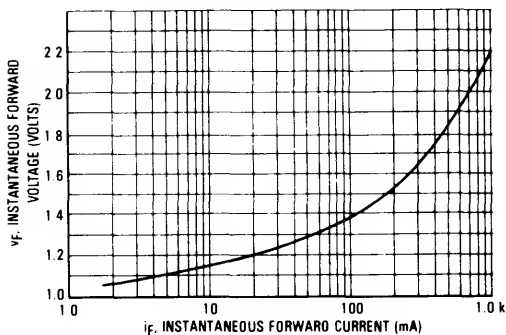


FIGURE 2 — ANODE CURRENT versus ANODE-CATHODE VOLTAGE

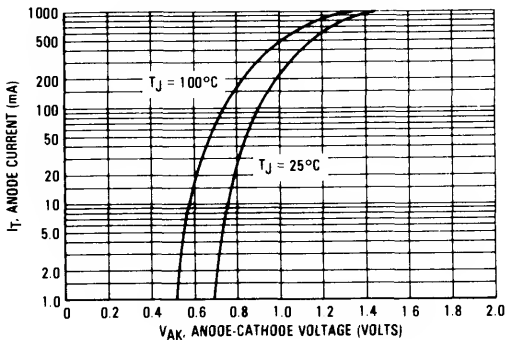


FIGURE 3 — LED TRIGGER CURRENT versus TEMPERATURE

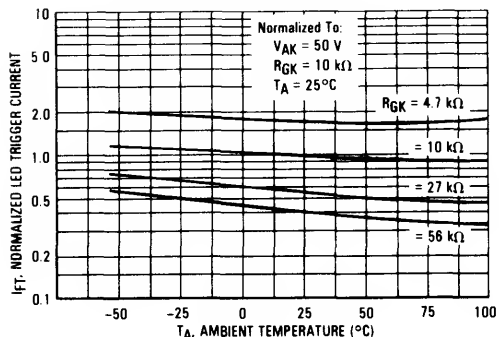
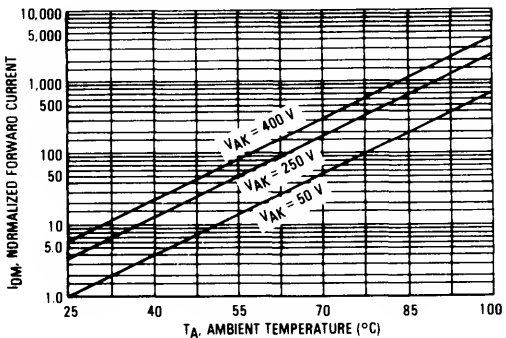


FIGURE 4 — FORWARD LEAKAGE CURRENT versus TEMPERATURE





MOTOROLA

**MOC3009
MOC3010
MOC3011**

OPTICALLY ISOLATED TRIAC DRIVER

These devices consist of a gallium-arsenide infrared emitting diode, optically coupled to a silicon bilateral switch and are designed for applications requiring isolated triac triggering, low-current isolated ac switching, high electrical isolation (to 7500 V peak), high detector standoff voltage, small size, and low cost.

- UL Recognized File Number 54915
- Output Driver Designed for 115 Vac Line
- Standard 6-Pin DIP

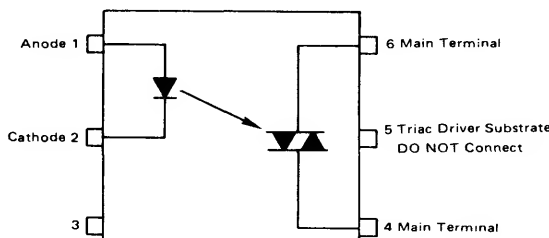
MAXIMUM RATINGS ($T_A = 25^\circ\text{C}$ unless otherwise noted)

| Rating | Symbol | Value | Unit |
|---|-------------------|-------------|----------------------------|
| INFRARED EMITTING DIODE MAXIMUM RATINGS | | | |
| Reverse Voltage | V_R | 3.0 | Volts |
| Forward Current – Continuous | I_F | 50 | mA |
| Total Power Dissipation @ $T_A = 25^\circ\text{C}$ Negligible Power in Transistor Derate above 25°C | P_D | 100 1.33 | mW mW/ $^\circ\text{C}$ |
| OUTPUT DRIVER MAXIMUM RATINGS | | | |
| Off-State Output Terminal Voltage | V_{DRM} | 250 | Volts |
| On-State RMS Current $T_A = 25^\circ\text{C}$ (Full Cycle, 50 to 60 Hz) $T_A = 70^\circ\text{C}$ | $I_T(\text{RMS})$ | 100 50 | mA mA |
| Peak Nonrepetitive Surge Current (PW = 10 ms, DC = 10%) | I_{TSM} | 1.2 | A |
| Total Power Dissipation @ $T_A = 25^\circ\text{C}$ Derate above 25°C | P_D | 300 4.0 | mW mW/ $^\circ\text{C}$ |

TOTAL DEVICE MAXIMUM RATINGS

| | | | |
|---|-----------|-------------|----------------------------|
| Isolation Surge Voltage (1) (Peak ac Voltage, 60 Hz, 5 Second Duration) | V_{ISO} | 7500 | Vac |
| Total Power Dissipation @ $T_A = 25^\circ\text{C}$ Derate above 25°C | P_D | 330 4.4 | mW mW/ $^\circ\text{C}$ |
| Junction Temperature Range | T_J | -40 to +100 | $^\circ\text{C}$ |
| Ambient Operating Temperature Range | T_A | -40 to +70 | $^\circ\text{C}$ |
| Storage Temperature Range | T_{stg} | -40 to +150 | $^\circ\text{C}$ |
| Soldering Temperature (10 s) | — | 260 | $^\circ\text{C}$ |

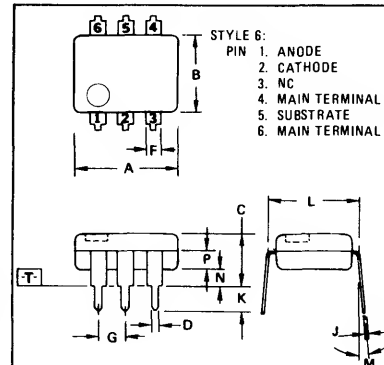
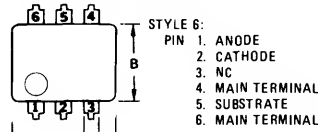
(1) Isolation surge voltage, V_{ISO} , is an internal device dielectric breakdown rating.



OPTO COUPLER/ISOLATOR

PHOTO TRIAC DRIVER OUTPUT

250 VOLTS



NOTES:

1. DIMENSIONS A AND B ARE DATUMS.
2. -T- IS SEATING PLANE.
3. POSITIONAL TOLERANCES FOR LEADS:
 ± 0.13 (0.005) $^{+0.005}_{-0.005}$ T A(M) B(M)
4. DIMENSION L TO CENTER OF LEADS WHEN FORMED PARALLEL.
5. DIMENSIONING AND TOLERANCING PER ANSI Y14.5, 1973.

| DIM | MILLIMETERS | | INCHES | |
|-----|-------------|------|--------|-------|
| | MIN | MAX | MIN | MAX |
| A | 8.13 | 8.89 | 0.320 | 0.350 |
| B | 6.10 | 6.60 | 0.240 | 0.260 |
| C | 2.92 | 5.08 | 0.115 | 0.200 |
| D | 0.41 | 0.51 | 0.016 | 0.020 |
| F | 1.02 | 1.78 | 0.040 | 0.070 |
| G | 2.54 | BSC | 0.100 | 0.150 |
| J | 0.20 | 0.30 | 0.008 | 0.012 |
| K | 2.54 | 3.81 | 0.100 | 0.150 |
| L | 7.62 | BSC | 0.300 | 0.500 |
| M | 0.0 | 150 | 0.0 | 150 |
| N | 0.38 | 2.54 | 0.015 | 0.100 |
| P | 1.27 | 2.03 | 0.050 | 0.080 |

CASE 730A-01

MOC3009 , MOC3010 , MOC3011

ELECTRICAL CHARACTERISTICS ($T_A = 25^\circ\text{C}$ unless otherwise noted)

| Characteristic | Symbol | Min | Typ | Max | Unit |
|--|-------------------------------|----------|------|------------------|------------------------|
| LED CHARACTERISTICS | | | | | |
| Reverse Leakage Current ($V_R = 3.0 \text{ V}$) | I_R | — | 0.05 | 100 | μA |
| Forward Voltage ($I_F = 10 \text{ mA}$) | V_F | — | 1.2 | 1.5 | Volts |
| DETECTOR CHARACTERISTICS ($I_F = 0$ unless otherwise noted) | | | | | |
| Peak Blocking Current, Either Direction (Rated V_{DRM} , Note 1) | I_{DRM} | — | 10 | 100 | nA |
| Peak On-State Voltage, Either Direction ($I_{TM} = 100 \text{ mA}$ Peak) | V_{TM} | — | 2.5 | 3.0 | Volts |
| Critical Rate of Rise of Off-State Voltage, Figure 3 | dv/dt | — | 2.0 | — | $\text{V}/\mu\text{s}$ |
| Critical Rate of Rise of Commutation Voltage, Figure 3 ($I_{load} = 15 \text{ mA}$) | dv/dt | — | 0.15 | — | $\text{V}/\mu\text{s}$ |
| COUPLED CHARACTERISTICS | | | | | |
| LED Trigger Current, Current Required to Latch Output (Main Terminal Voltage = 3.0 V) | MOC3009 MOC3010 MOC3011 | I_{FT} | — | 15 8.0 5.0 | 30 15 10 |
| Holding Current, Either Direction | | I_H | — | 100 | — |
| | | | | | μA |

Note 1. Test voltage must be applied within dv/dt rating.

2. Additional information on the use of the MOC3009/3010/3011 is available in Application Note AN-780.

TYPICAL ELECTRICAL CHARACTERISTICS

$T_A = 25^\circ\text{C}$

FIGURE 1 – ON-STATE CHARACTERISTICS

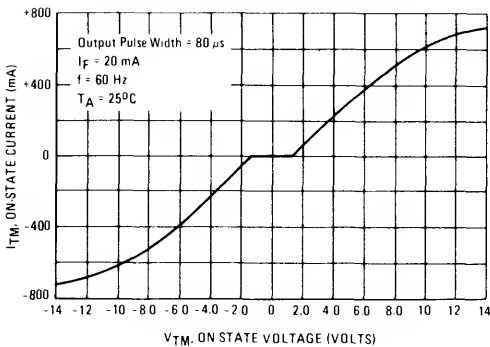
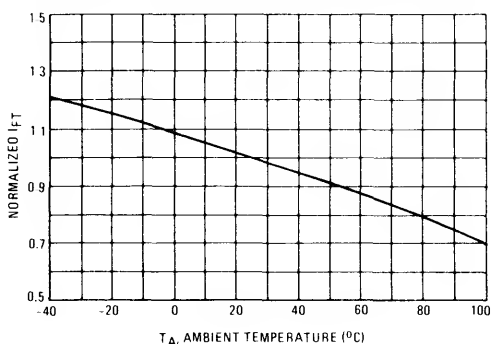


FIGURE 2 – TRIGGER CURRENT versus TEMPERATURE



MOC3009 , MOC3010 , MOC3011

FIGURE 3 – dv/dt TEST CIRCUIT

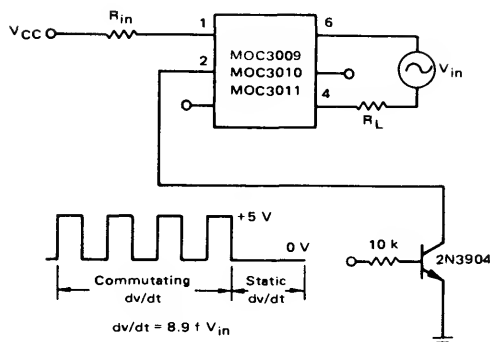


FIGURE 4 – dv/dt versus LOAD RESISTANCE

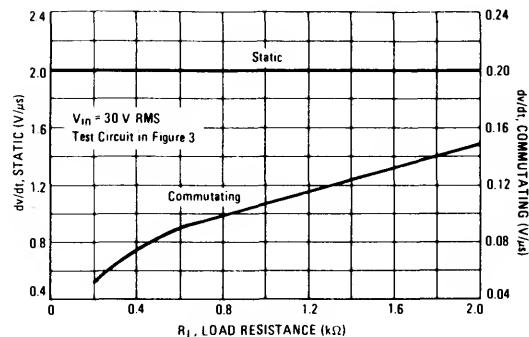


FIGURE 5 – dv/dt versus TEMPERATURE

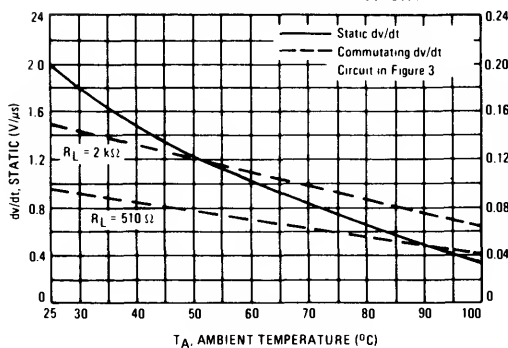


FIGURE 6 – COMMUTATING dv/dt versus FREQUENCY

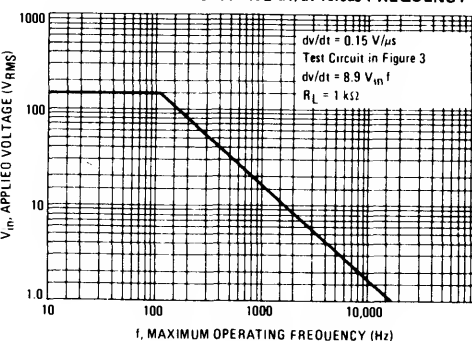
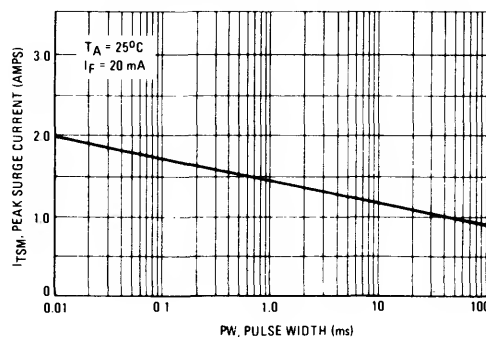


FIGURE 7 – MAXIMUM NONREPETITIVE SURGE CURRENT



MOC3009 , MOC3010 , MOC3011

TYPICAL APPLICATION CIRCUITS

FIGURE 8 – RESISTIVE LOAD

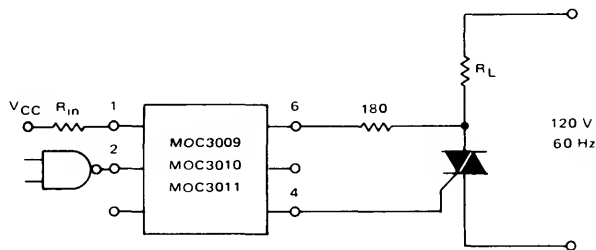


FIGURE 9 – INDUCTIVE LOAD WITH SENSITIVE GATE TRIAC
(I_{GT} ≤ 15 mA)

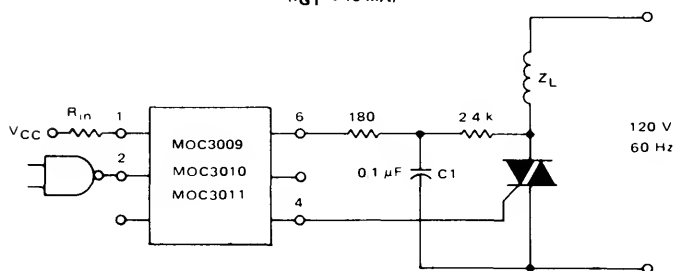
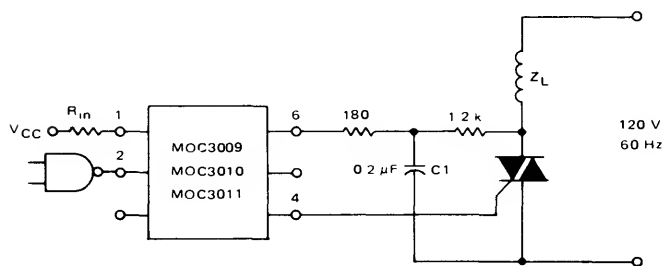


FIGURE 10 – INDUCTIVE LOAD WITH NON-SENSITIVE GATE TRIAC
(15 mA < I_{GT} < 50 mA)





MOTOROLA

**MOC3020
MOC3021**

OPTICALLY ISOLATED TRIAC DRIVER

These devices consist of a gallium-arsenide infrared emitting diode, optically coupled to a silicon bilateral switch. They are designed for applications requiring isolated triac triggering.

- UL Recognized File Number E54915
- Output Driver Designed for 220 Vac Line
- VISO Isolation Voltage of 7500 V Peak
- Standard 6-Pin Plastic DIP

MAXIMUM RATINGS ($T_A = 25^\circ\text{C}$ unless otherwise noted)

| Rating | Symbol | Value | Unit |
|--|--------|-------|------|
| INFRARED EMITTING DIODE MAXIMUM RATINGS | | | |

| | | | |
|---|-------|-------------|----------------------------|
| Reverse Voltage | V_R | 3.0 | Volts |
| Forward Current - Continuous | I_F | 50 | mA |
| Total Power Dissipation @ $T_A = 25^\circ\text{C}$ Negligible Power in Triac Driver Derate above 25°C | P_D | 100 1.33 | mW mW/ $^\circ\text{C}$ |

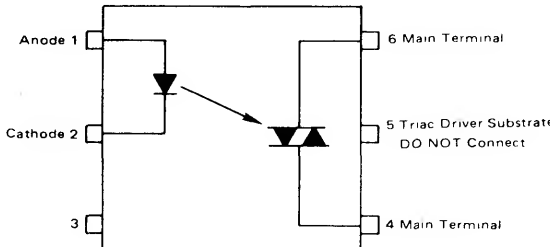
OUTPUT DRIVER MAXIMUM RATINGS

| | | | |
|---|-------------------|------------|----------------------------|
| Off-State Output Terminal Voltage | V_{DRM} | 400 | Volts |
| On-State RMS Current $T_A = 25^\circ\text{C}$ (Full Cycle, 50 to 60 Hz) $T_A = 70^\circ\text{C}$ | $I^T(\text{RMS})$ | 100 50 | mA mA |
| Peak Nonrepetitive Surge Current ($P_W = 10 \text{ ms}, DC = 10\%$) | I^T_{SM} | 1.2 | A |
| Total Power Dissipation @ $T_A = 25^\circ\text{C}$ Derate above 25°C | P_D | 300 4.0 | mW mW/ $^\circ\text{C}$ |

TOTAL DEVICE MAXIMUM RATINGS

| | | | |
|---|-----------|-------------|----------------------------|
| Isolation Surge Voltage (1) (Peak ac Voltage, 60 Hz, 5 Second Duration) | V_{ISO} | 7500 | Vac |
| Total Power Dissipation @ $T_A = 25^\circ\text{C}$ Derate above 25°C | P_D | 330 4.4 | mW mW/ $^\circ\text{C}$ |
| Junction Temperature Range | T_J | -40 to +100 | $^\circ\text{C}$ |
| Ambient Operating Temperature Range | T_A | -40 to +70 | $^\circ\text{C}$ |
| Storage Temperature Range | T_{STG} | -40 to +150 | $^\circ\text{C}$ |
| Soldering Temperature (10 s) | — | 260 | $^\circ\text{C}$ |

(1) Isolation surge voltage, V_{ISO} , is an internal device dielectric breakdown rating.

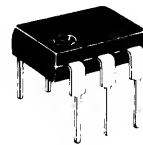


OPTO COUPLER

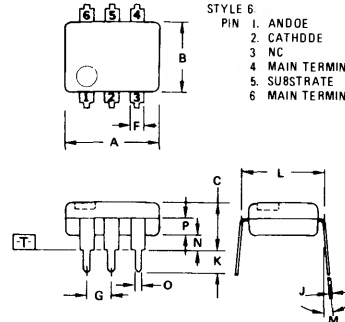
PHOTO TRIAC DRIVER

OUTPUT

400 VOLTS



STYLE 6
PIN
1. ANODE
2. CATHODE
3. NC
4. MAIN TERMINAL
5. SUBSTRATE
6. MAIN TERMINAL



NOTES

1. DIMENSIONS A AND 8 ARE DATUMS
2. T IS SEATING PLANE
3. POSITIONAL TOLERANCES FOR LEADS
 $\phi 0.13 (0.005)$ T A M B Q
4. DIMENSION L TO CENTER OF LEADS WHEN FORMED PARALLEL
5. DIMENSIONING AND TOLERANCING PER ANSI Y14.5, 1973.

| DIM | MILLIMETERS | | INCHES | |
|-----|-------------|------|--------|-------|
| | MIN | MAX | MIN | MAX |
| A | 8.13 | 8.89 | 0.320 | 0.350 |
| B | 6.10 | 6.60 | 0.240 | 0.260 |
| C | 2.92 | 5.08 | 0.115 | 0.200 |
| D | 0.41 | 0.51 | 0.016 | 0.020 |
| F | 1.02 | 1.78 | 0.040 | 0.070 |
| G | 2.54 | 8.5C | 0.100 | 0.85C |
| J | 0.20 | 0.30 | 0.008 | 0.012 |
| K | 2.54 | 3.81 | 0.100 | 0.150 |
| L | 7.62 | 8.5C | 0.300 | 0.85C |
| M | 0.0 | 1.50 | 0.0 | 0.150 |
| N | 0.38 | 2.54 | 0.015 | 0.100 |
| P | 1.27 | 2.05 | 0.050 | 0.080 |

CASE 730A-01

MOC3020, MOC3021

ELECTRICAL CHARACTERISTICS ($T_A = 25^\circ\text{C}$ unless otherwise noted)

| Characteristic | Symbol | Min | Typ | Max | Unit |
|--|-----------|-----|------|------|------------------------|
| LED CHARACTERISTICS | | | | | |
| Reverse Leakage Current ($V_R = 3.0 \text{ V}$) | I_R | | | 0.05 | 100 |
| Forward Voltage ($I_F = 10 \text{ mA}$) | V_F | - | 1.2 | 1.5 | Volts |
| DETECTOR CHARACTERISTICS ($I_F = 0$ unless otherwise noted) | | | | | |
| Peak Blocking Current, Either Direction (Rated V_{DRM} , Note 1) | I_{DRM} | - | 10 | 100 | nA |
| Peak On-State Voltage, Either Direction ($I_{TM} = 100 \text{ mA}$ Peak) | V_{TM} | - | 2.5 | 3.0 | Volts |
| Critical Rate of Rise of Off-State Voltage, $T_A = 85^\circ\text{C}$ | dv/dt | | 10.0 | - | $\text{V}/\mu\text{s}$ |
| <b b="" characteristics<="" coupled=""> | | | | | |
| LED Trigger Current, Current Required to Latch Output (Main Terminal Voltage = 3.0 V, Note 2) | I_{FT} | - | 15 | 30 | mA |
| MOC3020 | | - | 8.0 | 15 | |
| MOC3021 | | - | | | |
| Holding Current, Either Direction | I_H | -- | 100 | - | μA |

Note 1. Test voltage must be applied within dv/dt rating.

2. All devices are guaranteed to trigger at an I_F value less than or equal to max I_{FT} . Therefore, recommended operating I_F lies between max I_{FT} (30 mA for MOC3020, 15 mA for MOC3021) and absolute max I_F (50 mA).

TYPICAL ELECTRICAL CHARACTERISTICS
 $T_A = 25^\circ\text{C}$

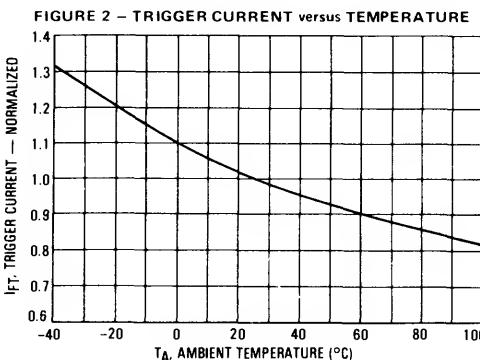
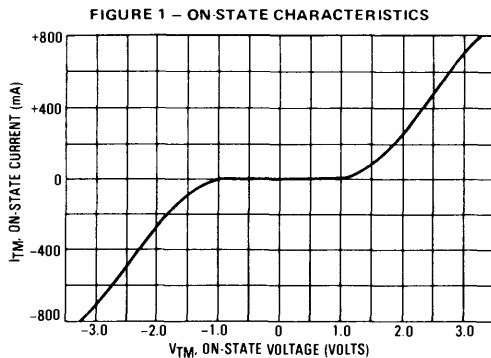
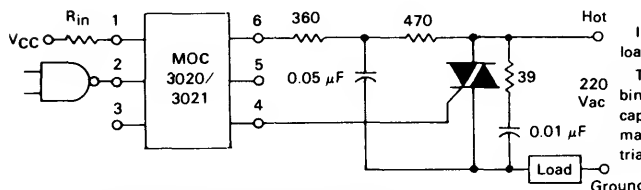


FIGURE 3 – TYPICAL APPLICATION CIRCUIT



In this circuit the "hot" side of the line is switched and the load connected to the cold or ground side.

The 39 ohm resistor and 0.01 μF capacitor are for snubbing of the triac, and the 470 ohm resistor and 0.05 μF capacitor are for snubbing the coupler. These components may or may not be necessary depending upon the particular triac and load used.

Additional information on the use of optically coupled triac drivers is available in Application Note AN-780A.



MOTOROLA

ZERO VOLTAGE CROSSING OPTICALLY ISOLATED TRIAC DRIVER

This device consists of a gallium arsenide infrared emitting diode optically coupled to a monolithic silicon detector performing the function of a Zero Voltage crossing bilateral triac driver.

They are designed for use with a triac in the interface of logic systems to equipment powered from 115 Vac lines, such as teletypewriters, CRTs, printers, motors, solenoids and consumer appliances, etc.

- Simplifies Logic Control of 110 Vac Power
- Zero Voltage Crossing
- High Breakdown Voltage: $V_{DRM} = 250$ V Min
- High Isolation Voltage: $V_{ISO} = 7500$ V Min
- Small, Economical, 6-Pin DIP Package
- Same Pin Configuration as MOC3010/3011
- UL Recognized, File No. E54915
- dv/dt of 100 V/ μ s Typ

MAXIMUM RATINGS ($T_A = 25^\circ\text{C}$ unless otherwise noted)

| Rating | Symbol | Value | Unit |
|--------|--------|-------|------|
|--------|--------|-------|------|

INFRARED EMITTING DIODE MAXIMUM RATINGS

| | | | |
|---|-------|------|----------------------------|
| Reverse Voltage | V_R | 3.0 | Volts |
| Forward Current - Continuous | I_F | 50 | mA |
| Total Power Dissipation @ $T_A = 25^\circ\text{C}$ Negligible Power in Output Driver | P_D | 120 | mW |
| Derate above 25°C | | 1.33 | $\text{mW}/^\circ\text{C}$ |

OUTPUT DRIVER MAXIMUM RATINGS

| | | | |
|---|-------------------|------------|---|
| Off-State Output Terminal Voltage | V_{DRM} | 250 | Volts |
| On-State RMS Current $T_A = 25^\circ\text{C}$ (Full Cycle, 50 to 60 Hz) $T_A = 85^\circ\text{C}$ | $I_T(\text{RMS})$ | 100 50 | mA mA |
| Peak Nonrepetitive Surge Current ($P_W = 10$ ms) | I_{TSM} | 1.2 | A |
| Total Power Dissipation @ $T_A = 25^\circ\text{C}$ Derate above 25°C | P_D | 300 4.0 | mW $\text{mW}/^\circ\text{C}$ |

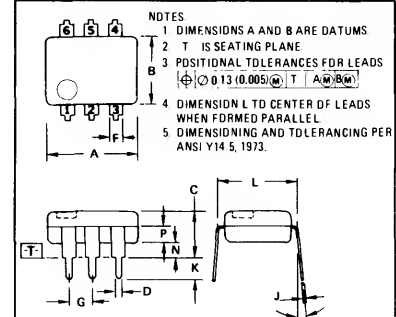
TOTAL DEVICE MAXIMUM RATINGS

| | | | |
|---|-----------|-------------|---|
| Isolation Surge Voltage (1) (Peak ac Voltage, 60 Hz, 5 Second Duration) | V_{ISO} | 7500 | Vac |
| Total Power Dissipation @ $T_A = 25^\circ\text{C}$ Derate above 25°C | P_D | 330 4.4 | mW $\text{mW}/^\circ\text{C}$ |
| Junction Temperature Range | T_J | -40 to +100 | $^\circ\text{C}$ |
| Ambient Operating Temperature Range | T_A | -40 to + 85 | $^\circ\text{C}$ |
| Storage Temperature Range | T_{STG} | -40 to +150 | $^\circ\text{C}$ |
| Soldering Temperature (10 s) | - | 260 | $^\circ\text{C}$ |

(1) Isolation surge voltage, V_{ISO} , is an internal device dielectric breakdown rating.

**MOC3030
MOC3031**

OPTO COUPLER/ISOLATOR ZERO CROSSING TRIAC DRIVER 250 VOLTS

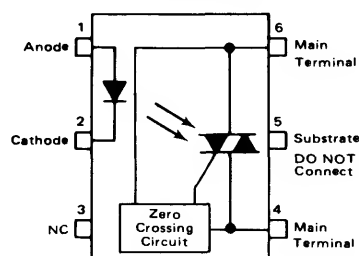


| DIM | MILLIMETERS | | INCHES | |
|-----|-------------|------|-----------|-------|
| | MIN | MAX | MIN | MAX |
| A | 8.13 | 8.89 | 0.320 | 0.350 |
| B | 6.10 | 6.60 | 0.240 | 0.260 |
| C | 2.92 | 5.08 | 0.115 | 0.200 |
| D | 0.41 | 0.51 | 0.016 | 0.020 |
| F | 1.02 | 1.78 | 0.040 | 0.070 |
| G | 2.54 BSC | | 0.100 BSC | |
| J | 0.20 | 0.30 | 0.008 | 0.012 |
| K | 2.54 | 3.81 | 0.100 | 0.150 |
| L | 7.62 BSC | | 0.300 BSC | |
| M | .00 | .150 | .00 | .150 |
| N | .038 | .254 | .015 | .100 |
| P | 1.27 | 2.03 | .050 | .080 |

STYLE 6:
1. ANODE
2. CATHODE
3. NC
4. MAIN TERMINAL
5. SUBSTRATE
6. MAIN TERMINAL

CASE 730A-01

COUPLER SCHEMATIC



MOC3030 , MOC3031

ELECTRICAL CHARACTERISTICS ($T_A = 25^\circ\text{C}$ unless otherwise noted)

| Characteristic | Symbol | Min | Typ | Max | Unit |
|--|-----------|-----|------|-----|------------------------|
| LED CHARACTERISTICS | | | | | |
| Reverse Leakage Current ($V_R = 3.0 \text{ V}$) | I_R | — | 0.05 | 100 | μA |
| Forward Voltage ($I_F = 30 \text{ mA}$) | V_F | — | 1.3 | 1.5 | Volts |
| DETECTOR CHARACTERISTICS ($I_F = 0$ unless otherwise noted) | | | | | |
| Peak Blocking Current, Either Direction (Rated V_{DRM} , Note 1) | I_{DRM} | — | 10 | 100 | nA |
| Peak On-State Voltage, Either Direction ($I_{TM} = 100 \text{ mA}$ Peak) | V_{TM} | — | 1.8 | 3.0 | Volts |
| Critical Rate of Rise of Off-State Voltage | dv/dt | — | 100 | — | $\text{V}/\mu\text{s}$ |

COUPLED CHARACTERISTICS

| | | | | | | |
|--|--------------------|----------|---|-----|----------|---------------|
| LED Trigger Current, Current Required to Latch Output (Main Terminal Voltage = 3.0 V, Note 2) | MOC3030 MOC3031 | I_{FT} | — | — | 30 15 | mA |
| Holding Current, Either Direction | | I_H | — | 100 | — | μA |

ZERO CROSSING CHARACTERISTICS

| | | | | | |
|---|----------|---|-----|-----|---------------|
| Inhibit Voltage ($I_F = \text{Rated } I_{FT}$. MT1-MT2 Voltage above which device will not trigger.) | V_{IH} | — | 15 | 25 | Volts |
| Leakage in Inhibited State ($I_F = \text{Rated } I_{FT}$. Rated V_{DRM} : Off State) | I_R | — | 100 | 200 | μA |

Note 1. Test voltage must be applied within dv/dt rating.

2. All devices are guaranteed to trigger at an I_F value less than or equal to max I_{FT} . Therefore, recommended operating I_F lies between max I_{FT} (30 mA for MOC3030, 15 mA for MOC3031) and absolute max I_F (50 mA).

TYPICAL ELECTRICAL CHARACTERISTICS $T_A = 25^\circ\text{C}$

FIGURE 1 – ON-STATE CHARACTERISTICS

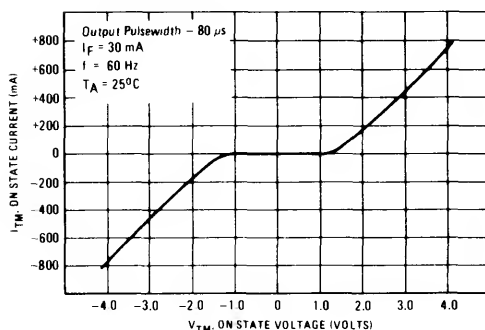
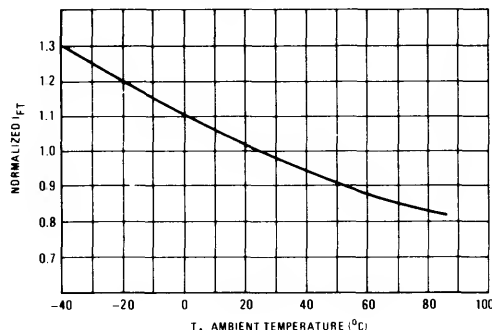
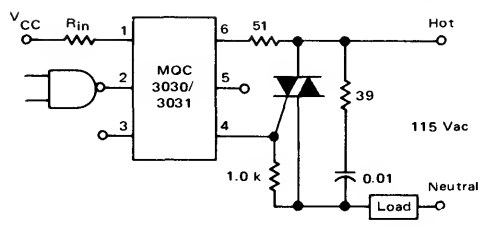


FIGURE 2 – TRIGGER CURRENT versus TEMPERATURE



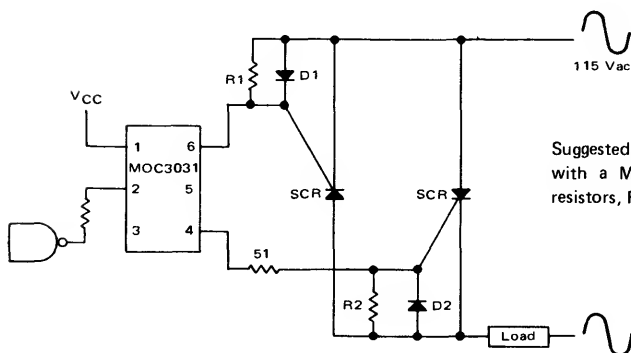
MOC3030 , MOC3031

FIGURE 3 – HOT-LINE SWITCHING APPLICATION CIRCUIT



Typical circuit for use when hot line switching is required. In this circuit the "hot" side of the line is switched and the load connected to the cold or neutral side. The load may be connected to either the neutral or hot line. R_{in} is calculated so that I_F is equal to the rated I_{FT} of the part, 15 mA for the MOC3031 or 30 mA for the MOC3030. The 39 ohm resistor and 0.01 μF capacitor are for snubbing of the triac and may or may not be necessary depending upon the particular triac and load used.

FIGURE 4 – INVERSE-PARALLEL SCR DRIVER CIRCUIT



Suggested method of firing two, back-to-back SCRs, with a Motorola triac driver. Diodes can be 1N4001; resistors, R1 and R2, are optional 1 k ohm.



MOTOROLA

MOC5005 MOC5006

DIGITAL LOGIC COUPLER

... gallium arsenide IRED optically coupled to a high-speed integrated detector. Designed for applications requiring electrical isolation, fast response time, and digital logic compatibility such as interfacing computer terminals to peripheral equipment, digital control of power supplies, motors and other servo machine applications.

Intended for use as a digital inverter, the application of a current to the IRED input results in a LOW voltage; with the IRED off the output voltage is HIGH.

- High Isolation Voltage –
 $V_{ISO} = 7500 \text{ V (Min)}$
- Fast Switching Times @ $I_F = 16 \text{ mA}$, $V_{CC} = 5.0 \text{ V}$
 $t_{on} = 420 \text{ ns (Typ)} - \text{MOC5005}$
 $= 225 \text{ ns (Typ)} - \text{MOC5006}$
 $t_{off} = 320 \text{ ns (Typ)} - \text{MOC5005}$
 $= 270 \text{ ns (Typ)} - \text{MOC5006}$
- Economical, Compact, Dual-In-Line Plastic Package
- Built-In Hysteresis (Figure 2)
- UL Recognized, File No. E54915

MAXIMUM RATINGS ($T_A = 25^\circ\text{C}$ unless otherwise noted)

| Rating | Symbol | Value | Unit |
|--------|--------|-------|------|
|--------|--------|-------|------|

INFRARED-EMITTING DIODE MAXIMUM RATINGS

| | | | |
|---|------------|-------|----------------------------|
| Reverse Voltage | V_R | 3.0 | Volts |
| Forward Current | Continuous | | |
| | Peak | I_F | mA |
| | | 50 | |
| | | 3.0 | Amp |
| Pulse Width = 300 μs , 2.0% Duty Cycle | | | |
| Device Dissipation @ $T_A = 25^\circ\text{C}$ | P_D | 100 | mW |
| Negligible Power in IC | | | |
| Derate above 25 $^\circ\text{C}$ | | 2.0 | $\text{mW}/^\circ\text{C}$ |

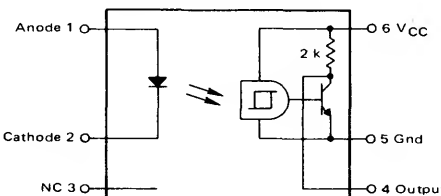
OUTPUT GATE MAXIMUM RATINGS

| | | | |
|---|----------|-----|-------|
| Supply Voltage | V_{CC} | 7.0 | Volts |
| Supply Current @ $V_{CC} = 5.0 \text{ V}$ | I_{CC} | 15 | mA |
| Device Dissipation @ $T_A = 25^\circ\text{C}$ | P_D | 200 | mW |
| Negligible Power in Diode | | | |

TOTAL DEVICE RATINGS

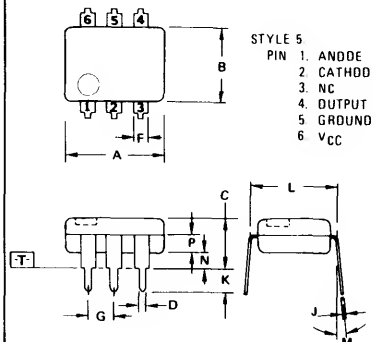
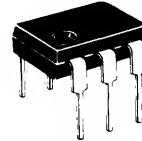
| | | | |
|---|-----------|-------------|------------------|
| Total Device Dissipation @ $T_A = 25^\circ\text{C}$ | P_D | 200 | mW |
| Maximum Operating Temperature | T_A | 85 | $^\circ\text{C}$ |
| Storage Temperature Range | T_{stg} | -55 to +100 | $^\circ\text{C}$ |
| Soldering Temperature (10 s) | | 260 | $^\circ\text{C}$ |

FIGURE 1 – COUPLER SCHEMATIC



OPTO COUPLER/ISOLATOR

HIGH-SPEED DIGITAL OUTPUT



NOTES

1. DIMENSIONS A AND B ARE DATUMS.
2. T IS SEATING PLANE.
3. POSITIONAL TOLERANCES FOR LEADS $(\phi 0.013 \text{ } 0.005)$ T ± 0.005 .
4. DIMENSION L TO CENTER OF LEADS WHEN FORMED PARALLEL.
5. DIMENSIONING AND TOLERANCING PER ANSI Y14.5, 1973.

| DIM | MILLIMETERS | | INCHES | |
|-----|-------------|------|--------|-------|
| | MIN | MAX | MIN | MAX |
| A | 8.13 | 8.89 | 0.320 | 0.350 |
| B | 6.10 | 6.60 | 0.240 | 0.260 |
| C | 2.92 | 5.08 | 0.115 | 0.200 |
| D | 0.41 | 0.51 | 0.016 | 0.020 |
| F | 1.02 | 1.78 | 0.040 | 0.070 |
| G | 2.54 | 8.5C | 0.100 | 0.85C |
| J | 0.20 | 0.30 | 0.008 | 0.012 |
| K | 2.54 | 3.81 | 0.100 | 0.150 |
| L | 7.62 | 8.5C | 0.300 | 0.85C |
| M | .09 | .150 | .00 | .150 |
| N | .38 | 2.54 | 0.015 | 0.100 |
| P | 1.27 | 2.03 | 0.050 | 0.080 |

CASE 730A-01

MOC5005, MOC5006

| Characteristic | Symbol | Min | Typ | Max | Unit |
|----------------|--------|-----|-----|-----|------|
|----------------|--------|-----|-----|-----|------|

IRED CHARACTERISTICS ($T_A = 25^\circ\text{C}$ unless otherwise noted)

| | | | | | |
|---|-------|---|------|-----|---------------|
| Reverse Leakage Current ($V_R = 3.0 \text{ V}$, $R_L = 1.0 \text{ M}\Omega$) | I_R | — | 0.05 | 10 | μA |
| Forward Voltage ($I_F = 10 \text{ mA}$) | V_F | — | 1.2 | 1.5 | Volts |
| Capacitance ($V_R = 0 \text{ V}$, $f = 1.0 \text{ MHz}$) | C | — | 100 | — | pF |

ISOLATION CHARACTERISTICS ($T_A = 25^\circ\text{C}$)

| | | | | | |
|---|-----------|------|-----------|---|-------------|
| Isolation Voltage (1) 60 Hz, AC Peak, 5 s | V_{ISO} | 7500 | — | — | Volts |
| Isolation Resistance ($V = 500 \text{ V}$) (1) | — | — | 10^{11} | — | Ohms |
| Isolation Capacitance ($V = 0 \text{ V}$, $f = 1.0 \text{ MHz}$) (1) | — | — | 1.3 | — | pF |

DEVICE CHARACTERISTICS ($T_A = 25^\circ\text{C}$)

| | | | | | |
|---|----------------------|-----|------|-----|-------------|
| Supply Current ($I_F = 0$, $V_{CC} = 5.0 \text{ V}$) | $I_{CC(\text{off})}$ | 1.5 | 2.5 | 3.5 | mA |
| Supply Current ($I_F = 16 \text{ mA}$, $V_{CC} = 5.0 \text{ V}$) | $I_{CC(\text{on})}$ | 2.5 | 4.0 | 8.0 | mA |
| Output Voltage Low ($I_F = 16 \text{ mA}$, $V_{CC} = 5.0 \text{ V}$, $I_{\text{Sink}} = 10 \text{ mA}$) | V_{OL} | — | 0.35 | 0.6 | Volts |
| Output Voltage High ($I_F = 0 \text{ mA}$, $V_{CC} = 5.0 \text{ V}$, $I_{\text{Source}} = 200 \mu\text{A}$) | V_{OH} | 4.0 | 4.75 | — | Volts |

SWITCHING CHARACTERISTICS

| | | | | | | | |
|---------------|---|---------|-----------|---|-----|-----|----|
| Turn-On Time | (If = 16 mA, $V_{CC} = 5.0 \text{ V}$, Figure 3) | MOC5005 | t_{on} | — | 420 | 700 | ns |
| Fall Time | | MOC5006 | t_f | — | 225 | 350 | ns |
| Turn-Off Time | (If = 16 mA, $V_{CC} = 5.0 \text{ V}$, Figure 3) | MOC5005 | t_{off} | — | 250 | — | ns |
| | | MOC5006 | t_f | — | 200 | — | ns |
| Rise Time | (If = 16 mA, $V_{CC} = 5.0 \text{ V}$, Figure 3) | MOC5005 | t_r | — | 320 | 700 | ns |
| | | MOC5006 | t_r | — | 270 | 350 | ns |

(1) For this test IRED pins 1 and 2 are common and Output Gate pins 4, 5, 6 are common.

FIGURE 2 – TYPICAL OUTPUT VOLTAGE
versus DIODE CURRENT

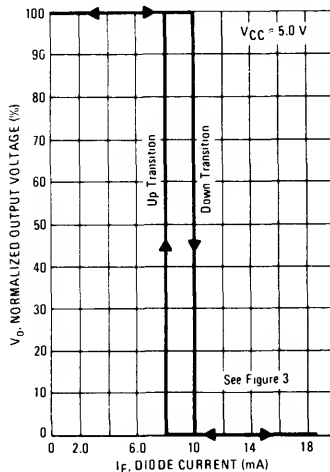
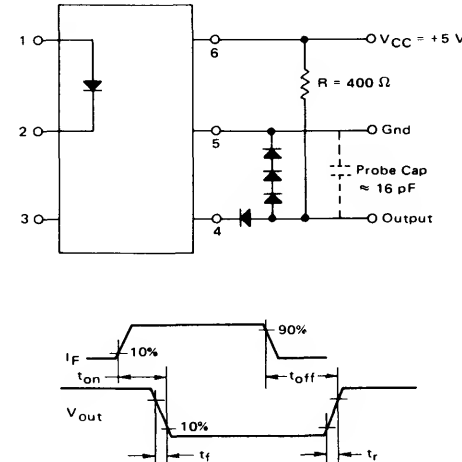


FIGURE 3 – TEST CIRCUIT





MOTOROLA

MOC5010

OPTICALLY ISOLATED AC LINEAR COUPLER

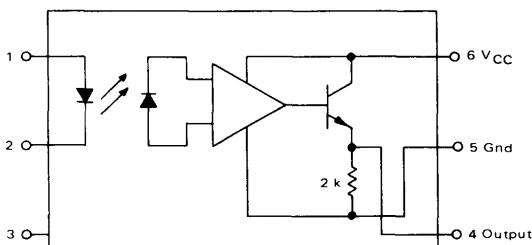
. . . gallium arsenide IRED optically-coupled to a bipolar monolithic amplifier. Converts an input current variation to an output voltage variation while providing a high degree of electrical isolation between input and output. Can be used for line coupling, peripheral equipment isolation, audio, medical, and other applications.

- 250 kHz Bandwidth
- Low Impedance Emitter Follower Output: $Z_O < 200 \Omega$
- High Voltage Isolation: $V_{ISO} = 7500$ V (Min)
- UL Recognized, File Number E54915

MAXIMUM RATINGS ($T_A = 25^\circ\text{C}$ unless otherwise noted)

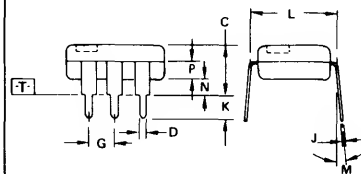
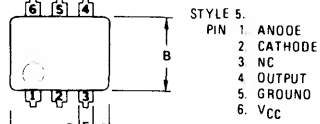
| Rating | Symbol | Value | Unit |
|--|-----------|-------------|----------------------------------|
| INFRARED EMITTING DIODE | | | |
| Reverse Voltage | V_R | 3.0 | Volts |
| Forward Current – Peak Pulse Width = 300 μs , 20% Duty Cycle | I_F | 50 | mA |
| Device Dissipation @ $T_A = 25^\circ\text{C}$ Negligible Power in IC Derate above 25°C | P_D | 100 2.0 | mW $\text{mW}/^\circ\text{C}$ |
| AC AMPLIFIER | | | |
| Supply Voltage | V_{CC} | 15 | Volts |
| Supply Current @ $V_{CC} = 12$ V | I_{CC} | 13 | mA |
| Device Dissipation @ $T_A = 25^\circ\text{C}$ Negligible Power in Diode | P_D | 200 | mW |
| TOTAL DEVICE | | | |
| Device Dissipation @ $T_A = 25^\circ\text{C}$ | P_D | 200 | mW |
| Maximum Operating Temperature | T_A | 85 | $^\circ\text{C}$ |
| Storage Temperature Range | T_{stg} | -55 to +100 | $^\circ\text{C}$ |

FIGURE 1 – COUPLER SCHEMATIC



OPTO COUPLER/ISOLATOR

AC LINEAR AMPLIFIER



NOTES

- 1 DIMENSIONS A AND B ARE DATUMS.
- 2 T IS SEATING PLANE.
- 3 POSITIONAL TOLERANCES FOR LEADS $\Phi 0.13 (0.005)$ T A N B M
- 4 DIMENSION L TO CENTER OF LEADS WHEN FORMED PARALLEL
- 5 DIMENSIONING AND TOLERANCING PER ANSI Y14.5, 1973

| DIM. | MILLIMETERS | | INCHES | |
|------|-------------|------|-----------|-------|
| | MIN | MAX | MIN | MAX |
| A | 8.13 | 8.80 | 0.320 | 0.350 |
| B | 6.10 | 6.60 | 0.240 | 0.260 |
| C | 2.92 | 5.08 | 0.115 | 0.200 |
| D | 0.41 | 0.51 | 0.016 | 0.020 |
| F | 1.02 | 1.78 | 0.040 | 0.070 |
| G | 2.54 BSC | | 0.100 BSC | |
| J | 0.20 | 0.30 | 0.008 | 0.012 |
| K | 2.54 | 3.81 | 0.100 | 0.150 |
| L | 7.62 BSC | | 0.300 BSC | |
| M | 0.0 | 150 | 0.0 | 150 |
| N | 0.38 | 2.54 | 0.015 | 0.100 |
| P | 1.27 | 2.03 | 0.050 | 0.080 |

CASE 730A-01

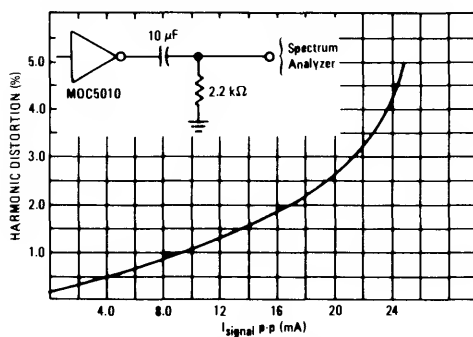
MOC5010

| Characteristic | Symbol | Min | Typ | Max | Unit |
|---|---|--------------|-----------|-----|----------------|
| IRED CHARACTERISTICS ($T_A = 25^\circ\text{C}$ unless otherwise noted) | | | | | |
| Reverse Leakage Current ($V_R = 3.0 \text{ V}$, $R_L = 1.0 \text{ M}\Omega$) | I_R | — | 0.05 | 10 | μA |
| Forward Voltage ($I_F = 10 \text{ mA}$) | V_F | — | 1.2 | 1.5 | Volts |
| Capacitance ($V_R = 0 \text{ V}$, $f = 1.0 \text{ MHz}$) | C | — | 100 | — | pF |
| ISOLATION CHARACTERISTICS ($T_A = 25^\circ\text{C}$) | | | | | |
| Isolation Voltage (1) 60 Hz, AC Peak | V_{ISO} | 7500 | — | — | Volts |
| Isolation Resistance ($V = 500 \text{ V}$) (1) | — | — | 10^{11} | — | Ohms |
| Isolation Capacitance ($V = 0$, $f = 1.0 \text{ MHz}$) (1) | — | — | 1.3 | — | pF |
| DEVICE CHARACTERISTICS ($T_A = 25^\circ\text{C}$) | | | | | |
| Supply Current ($I_F = 0$, $V_{CC} = 12 \text{ V}$) | I_{CC} | 2.0 | 6.0 | 10 | mA |
| Transfer Resistance – Gain $I_{sig} = 1.0 \text{ mA p-p}$, $I_{Bias} = 12 \text{ mA}$ | G_R | — | 100 | — | mV/mA |
| Output Voltage Swing – Single Ended | $(V_{CC} = 6.0 \text{ V})$ $(V_{CC} = 12 \text{ V})$ | V_O | — | 4.0 | Volts |
| Single-Ended Distortion (2) | THD | See Figure 2 | | | |
| Step Response | t | — | 1.4 | — | μs |
| DC Power Consumption | P | — | 30 | — | mW |
| Bandwidth | BW | 100 | 250 | — | kHz |
| DC Output Voltage ($I_{LED} = 0$), $V_{CE} = 12 \text{ V}$ | V_O | 0.2 | 1.0 | 6.0 | Volts |

(1) For this test IRED pins 1 and 2 are common and Output Gate pins 4, 5, 6 are common.

(2) Recommended $I_F = 10$ to 15 mA at $V_{CC} = 12 \text{ V}$.

FIGURE 2 – TYPICAL TOTAL HARMONIC DISTORTION



Typical total harmonic distortion @ 25°C (for units with gain of 200 mV/mA at $I_{bias} = 12 \text{ mA}$, $V_{CC} = 12 \text{ V}$, $f = 50 \text{ kHz}$, Load = [See Insert]).

FIGURE 3 – NORMALIZED FREQUENCY RESPONSE

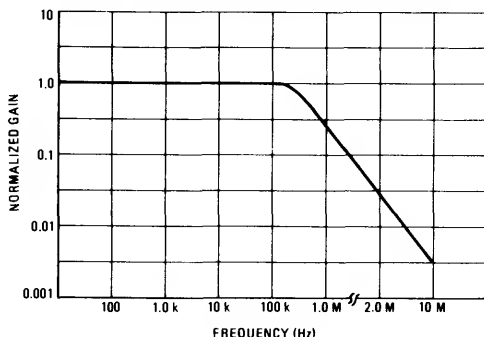
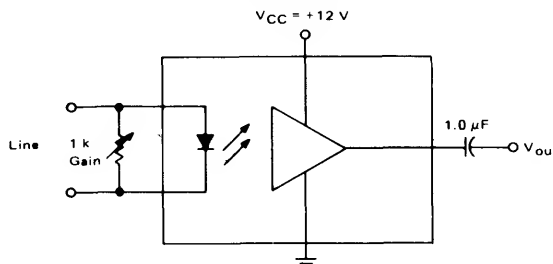


FIGURE 4 – TELEPHONE COUPLER APPLICATION





MOTOROLA

**MOC8020
MOC8021**

HIGH CTR DARLINGTON COUPLER

Gallium Arsenide LED optically coupled to a Silicon Photo Darlington Transistor designed for applications requiring electrical isolation, high breakdown voltage, and high current transfer ratios. Provides excellent performance in interfacing and coupling systems, phase and feedback controls, solid state relays, and general purpose switching circuits.

- High Transfer Ratio
 - 500% — MOC8020
 - 1000% — MOC8021
- High Collector-Emitter Breakdown Voltage —
 $V(BR)CEO = 50$ Vdc (Min)
- High Isolation Voltage —
 $VISO = 7500$ Vac Peak
- UL Recognized, File No. E54915
- Economical Dual-In-Line Package
- Base Not Connected

MAXIMUM RATINGS ($T_A = 25^\circ\text{C}$ unless otherwise noted.)

| Rating | Symbol | Value | Unit |
|--|--------|-------|----------------------------|
| INFRARED-EMITTING DIODE | | | |
| Reverse Voltage | V_R | 3.0 | Volts |
| Forward Current — Continuous | I_F | 50 | mA |
| Forward Current — Peak | I_F | 3.0 | Amp |
| Pulse Width = 300 μs , 2.0% Duty Cycle | | | |
| Total Power Dissipation @ $T_A = 25^\circ\text{C}$ | P_D | 150 | mW |
| Negligible Power in Transistor | | | |
| Derate above 25°C | | 2.0 | $\text{mW}/^\circ\text{C}$ |

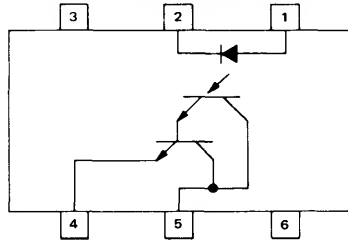
PHOTO DARLINGTON TRANSISTOR

| Collector-Emitter Voltage | V_{CEO} | 50 | Volts |
|--|-----------|-----|----------------------------|
| Emitter-Collector Voltage | V_{ECO} | 5.0 | Volts |
| Collector Current — Continuous | I_C | 150 | mA |
| Total Power Dissipation @ $T_A = 25^\circ\text{C}$ | P_D | 150 | mW |
| Negligible Power in Diode | | 2.0 | $\text{mW}/^\circ\text{C}$ |
| Derate above 25°C | | | |

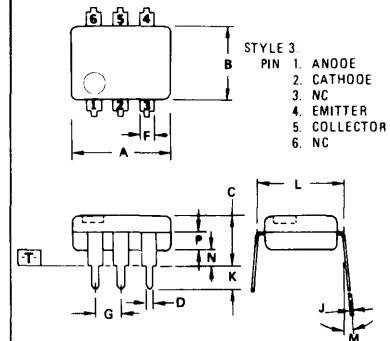
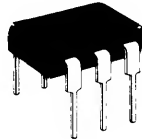
TOTAL DEVICE

| | | | |
|---|-----------|-------------|----------------------------|
| Total Device Dissipation @ $T_A = 25^\circ\text{C}$ | P_D | 250 | mW |
| Equal Power Dissipation in Each Element | | | |
| Derate above 25°C | | 3.3 | $\text{mW}/^\circ\text{C}$ |
| Operating Junction Temperature Range | T_J | -55 to +100 | $^\circ\text{C}$ |
| Storage Temperature Range | T_{stg} | -55 to +150 | $^\circ\text{C}$ |
| Soldering Temperature (10 s) | | 260 | $^\circ\text{C}$ |

FIGURE 1 — DEVICE SCHEMATIC



OPTO COUPLER/ISOLATOR DARLINGTON OUTPUT



NOTES

- 1 DIMENSIONS A AND B ARE DATUMS.
- 2 T IS SEATING PLANE.
- 3 POSITIONAL TOLERANCES FOR LEADS $(\oplus 0.13 / -0.005)$ T A M B Q
- 4 DIMENSION L TO CENTER OF LEADS WHEN FORMED PARALLEL.
- 5 DIMENSIONING AND TOLERANCING PER ANSI Y14.5, 1973.

| | MILLIMETERS | INCHES |
|---|-------------|-----------|
| A | 8.13 | 0.320 |
| B | 6.10 | 0.240 |
| C | 2.92 | 0.115 |
| D | 0.41 | 0.016 |
| F | 1.02 | 0.040 |
| G | 2.54 BSC | 0.100 BSC |
| J | 0.20 | 0.008 |
| K | 2.54 | 0.100 |
| L | 7.62 BSC | 0.300 BSC |
| M | 0.0 | 0.0 |
| N | 0.38 | 0.015 |
| P | 1.27 | 0.050 |

CASE 730A-01

MOC8020, MOC8021

LED CHARACTERISTICS ($T_A = 25^\circ\text{C}$ unless otherwise noted.)

| Characteristic | Symbol | Min | Typ | Max | Unit |
|---|--------|-----|-------|-----|---------------|
| Reverse Leakage Current ($V_R = 3.0 \text{ V}$) | I_R | — | 0.005 | 10 | μA |
| Forward Voltage ($I_F = 10 \text{ mA}$) | V_F | — | 1.2 | 2.0 | Volts |
| Capacitance ($V_R = 0 \text{ V}, f = 1.0 \text{ MHz}$) | C | — | 100 | — | pF |

PHOTO DARLINGTON CHARACTERISTICS ($T_A = 25^\circ\text{C}$ and $I_F = 0$, unless otherwise noted.)

| Characteristic | Symbol | Min | Typ | Max | Unit |
|--|---------------|-----|-----|-----|-------------|
| Collector-Emitter Dark Current ($V_{CE} = 10 \text{ V}$) | I_{CEO} | — | 8.0 | 100 | nA |
| Collector-Emitter Breakdown Voltage ($I_C = 1.0 \text{ mA}$) | $V_{(BR)CEO}$ | 50 | 60 | — | Volts |
| Emitter-Collector Breakdown Voltage ($I_E = 100 \mu\text{A}$) | $V_{(BR)ECO}$ | 5.0 | 8.0 | — | Volts |

COUPLED CHARACTERISTICS ($T_A = 25^\circ\text{C}$ unless otherwise noted.)

| Characteristic | Symbol | Min | Typ | Max | Unit |
|--|-----------|-----------|-----------|-----|-------------|
| Collector Output Current ($V_{CE} = 5.0 \text{ V}, I_F = 10 \text{ mA}$) MOC8020 MOC8021 | I_C | 50 100 | 90 150 | — | mA |
| Isolation Surge Voltage (1, 2), Vac 60 Hz Peak ac, 5 Second | V_{ISO} | 7500 | — | — | Volts |
| Isolation Resistance (1) ($V = 500 \text{ V}$) | — | — | 10^{11} | — | Ohms |
| Isolation Capacitance (1) ($V = 0, f = 1.0 \text{ MHz}$) | — | — | 0.8 | — | pF |

SWITCHING CHARACTERISTICS

| | | | | | |
|--|-----------|---|----|---|---------------|
| Turn-On Time ($I_F = 10 \text{ mA}, V_{CE} = 50 \text{ V}, R_2 = 100 \Omega$) | t_{on} | — | 13 | — | μs |
| Turn-Off Time ($I_F = 10 \text{ mA}, V_{CE} = 50 \text{ V}, R_2 = 100 \Omega$) | t_{off} | — | 60 | — | μs |

(1) For this test LED pins 1 and 2 are common and Photo Transistor pins 4 and 5 are common.

(2) Isolation Surge Voltage, V_{ISO} , is an internal device dielectric breakdown rating.

TYPICAL ELECTRICAL CHARACTERISTICS

FIGURE 2 — FORWARD CHARACTERISTICS

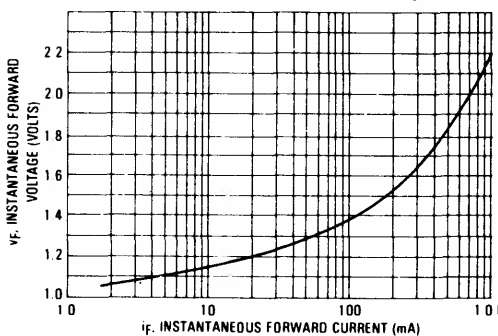
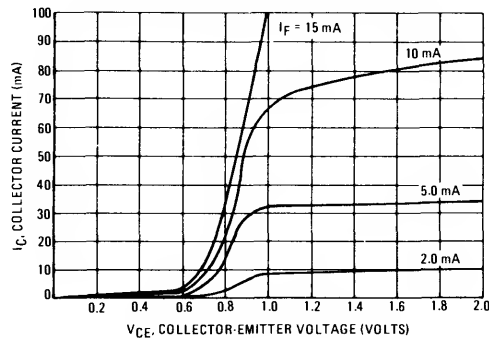


FIGURE 3 — COLLECTOR CURRENT versus COLLECTOR-EMITTER VOLTAGE (MOC8020)





MOTOROLA

**MOC8030
MOC8050**

80-VOLT DARLINGTON COUPLER

Gallium Arsenide LED optically coupled to a Silicon Photo Darlington Transistor designed for applications requiring electrical isolation, high breakdown voltage, and high current transfer ratios. Characterized for use as telephony relay drivers but provides excellent performance in interfacing and coupling systems, phase and feedback controls, solid state relays, and general purpose switching circuits.

- High Transfer Ratio @ Output = 50 mA
 - 300% – MOC8030
 - 500% – MOC8050
- High Collector-Emitter Breakdown Voltage –
 $V(BR)CEO = 80$ Vdc (Min)
- High Isolation Voltage –
 $V_{ISO} = 7500$ Vac Peak
- Excellent Stability Over Temperature
- Economical Dual-In-Line Package
- Base Not Connected

MAXIMUM RATINGS ($T_A = 25^\circ\text{C}$ unless otherwise noted.)

| Rating | Symbol | Value | Unit |
|--------|--------|-------|------|
|--------|--------|-------|------|

INFRARED-EMITTING DIODE

| | | | |
|---|--------|-----|----------------------------|
| Reverse Voltage | V_R | 3.0 | Volts |
| Forward Current – Continuous | I_F | 80 | mA |
| Forward Current – Peak Pulse Width = 300 μs , 2.0% Duty Cycle | I_F' | 3.0 | Amp |
| Total Power Dissipation @ $T_A = 25^\circ\text{C}$ | P_D | 150 | mW |
| Negligible Power in Transistor Derate above 25°C | | 2.0 | $\text{mW}/^\circ\text{C}$ |

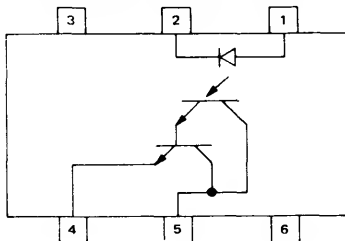
PHOTO DARLINGTON TRANSISTOR

| | | | |
|--|-----------|-----|----------------------------|
| Collector-Emitter Voltage | V_{CEO} | 80 | Volts |
| Emitter-Collector Voltage | V_{ECO} | 5.0 | Volts |
| Collector Current – Continuous | I_C | 150 | mA |
| Total Power Dissipation @ $T_A = 25^\circ\text{C}$ | P_D | 150 | mW |
| Negligible Power in Diode Derate above 25°C | | 2.0 | $\text{mW}/^\circ\text{C}$ |

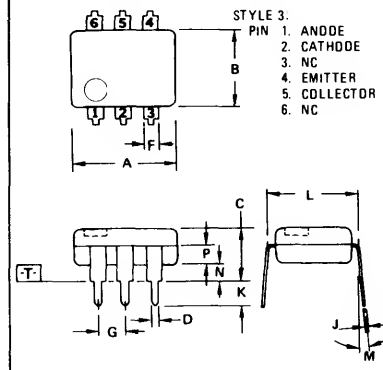
TOTAL DEVICE

| | | | |
|---|-----------|-------------|----------------------------|
| Total Device Dissipation @ $T_A = 25^\circ\text{C}$ Equal Power Dissipation in Each Element Derate above 25°C | P_D | 250 | mW |
| | | 3.3 | $\text{mW}/^\circ\text{C}$ |
| Operating Junction Temperature Range | T_J | -55 to +100 | $^\circ\text{C}$ |
| Storage Temperature Range | T_{stg} | -55 to +150 | $^\circ\text{C}$ |
| Soldering Temperature (10 s) | – | 260 | $^\circ\text{C}$ |

FIGURE 1 – DEVICE SCHEMATIC



OPTO COUPLER/ISOLATOR DARLINGTON OUTPUT



NOTES

1. DIMENSIONS A AND B ARE DATUMS.
2. T IS SEATING PLANE.
3. POSITIONAL TOLERANCES FOR LEADS:
 ± 0.13 (0.005) (M) T A (M) B (M)
4. DIMENSION L TO CENTER OF LEADS WHEN FORMED PARALLEL.
5. DIMENSIONING AND TOLERANCING PER ANSI Y14.5, 1973.

| DIM | MILLIMETERS | | INCHES | |
|-----|-------------|------|--------|-------|
| | MIN | MAX | MIN | MAX |
| A | 8.13 | 8.89 | 0.320 | 0.350 |
| B | 6.10 | 6.60 | 0.240 | 0.260 |
| C | 2.92 | 5.08 | 0.115 | 0.200 |
| D | 0.41 | 0.51 | 0.016 | 0.020 |
| F | 1.02 | 1.78 | 0.040 | 0.070 |
| G | 2.54 | BSC | 0.100 | BSC |
| J | 0.20 | 0.30 | 0.008 | 0.012 |
| K | 2.54 | 3.81 | 0.100 | 0.150 |
| L | 7.62 | BSC | 0.300 | BSC |
| M | 0.0 | 150 | 0.0 | 150 |
| N | 0.38 | 2.54 | 0.015 | 0.100 |
| P | 1.27 | 2.03 | 0.050 | 0.080 |

CASE 730A.01

MOC8030, MOC8050

LED CHARACTERISTICS ($T_A = 25^\circ\text{C}$ unless otherwise noted.)

| Characteristic | Symbol | Min | Typ | Max | Unit |
|--|--------|-----|-------|-----|---------------|
| Reverse Leakage Current ($V_R = 3.0 \text{ V}$) | I_R | — | 0.005 | 10 | μA |
| Forward Voltage ($I_F = 10 \text{ mA}$) | V_F | — | 1.2 | 2.0 | Volts |
| Capacitance ($V_R = 0 \text{ V}$, $f = 1.0 \text{ MHz}$) | C | — | 100 | — | pF |

PHOTO DARLINGTON CHARACTERISTICS ($T_A = 25^\circ\text{C}$ and $I_F = 0$, unless otherwise noted.)

| Characteristic | Symbol | Min | Typ | Max | Unit |
|--|---------------|-----|-----|------|-------------|
| Collector-Emitter Dark Current ($V_{CE} = 60 \text{ V}$) | I_{CEO} | — | 25 | 1000 | nA |
| Collector-Emitter Breakdown Voltage ($I_C = 1.0 \text{ mA}$) | $V_{(BR)CEO}$ | 80 | 95 | — | Volts |
| Emitter-Collector Breakdown Voltage ($I_E = 100 \mu\text{A}$) | $V_{(BR)ECO}$ | 5.0 | 8.0 | — | Volts |

COUPLED CHARACTERISTICS ($T_A = 25^\circ\text{C}$ unless otherwise noted.)

| Characteristic | Symbol | Min | Typ | Max | Unit |
|--|-----------|----------|------------------|-----|-------------|
| Collector Output Current ($V_{CE} = 1.5 \text{ V}$, $I_F = 10 \text{ mA}$) MOC8050 MOC8030 | I_C | 50 30 | 100 50 | — | mA |
| Isolation Surge Voltage (1, 2), Vac 60 Hz Peak ac, 5 Second | V_{ISO} | 7500 | — | — | Volts |
| Isolation Resistance (1) ($V = 500 \text{ V}$) | — | — | 10 ¹¹ | — | Ohms |
| Isolation Capacitance (1) ($V = 0$, $f = 1.0 \text{ MHz}$) | — | — | 0.8 | — | pF |

SWITCHING CHARACTERISTICS

| | | | | | |
|--|-----------|---|----|---|---------------|
| Turn-On Time ($I_F = 10 \text{ mA}$, $V_{CE} = 50 \text{ V}$, $R_2 = 100 \Omega$) | t_{on} | — | 13 | — | μs |
| Turn-Off Time ($I_F = 10 \text{ mA}$, $V_{CE} = 50 \text{ V}$, $R_2 = 100 \Omega$) | t_{off} | — | 60 | — | μs |

(1) For this test LED pins 1 and 2 are common and Photo Transistor pins 4 and 5 are common.

(2) Isolation Surge Voltage, V_{ISO} , is an internal device dielectric breakdown rating.

TYPICAL ELECTRICAL CHARACTERISTICS

FIGURE 2 – FORWARD CHARACTERISTICS

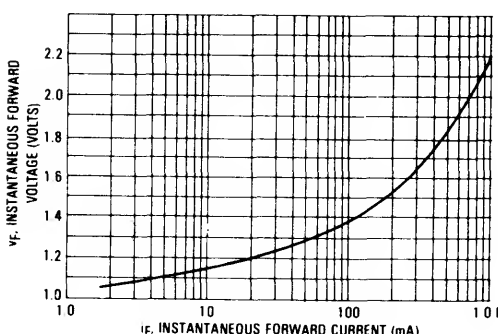
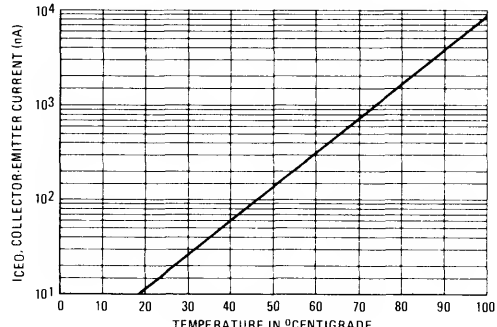


FIGURE 3 – COLLECTOR-EMITTER DARK CURRENT
versus TEMPERATURE



MOC8030, MOC8050

TYPICAL ELECTRICAL CHARACTERISTICS

COLLECTOR CURRENT versus COLLECTOR-EMITTER VOLTAGE

FIGURE 4 – MOC8050

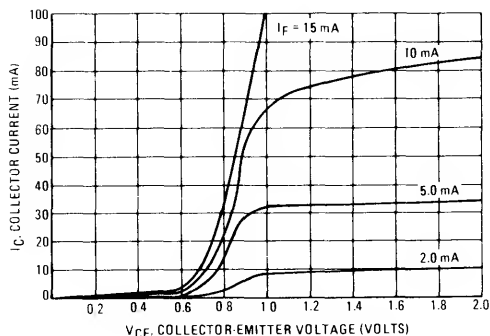
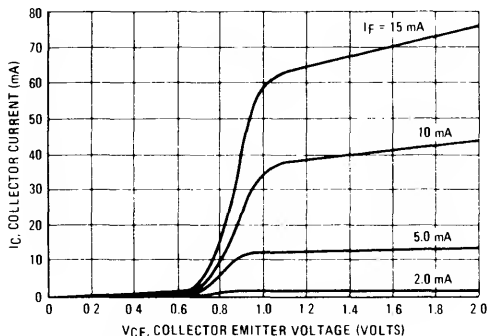


FIGURE 5 – MOC8030



COLLECTOR CURRENT versus COLLECTOR-EMITTER VOLTAGE
(at 25°C and 70°C)

FIGURE 6 – MOC8050

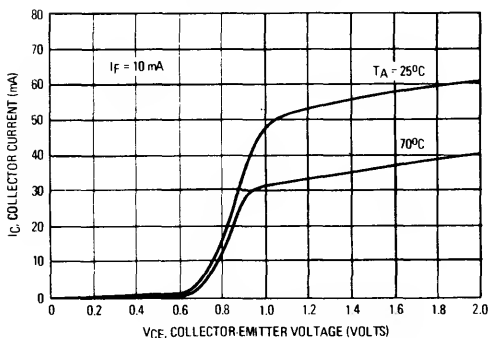
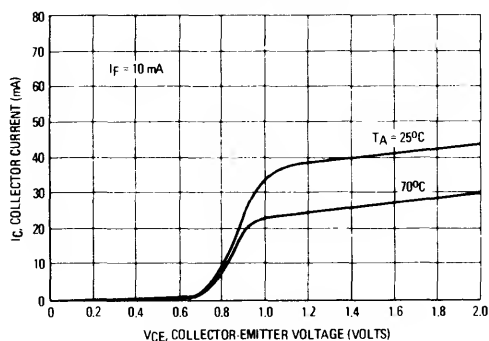


FIGURE 7 – MOC8030



COLLECTOR CURRENT versus DIODE CURRENT

FIGURE 8 – MOC8050

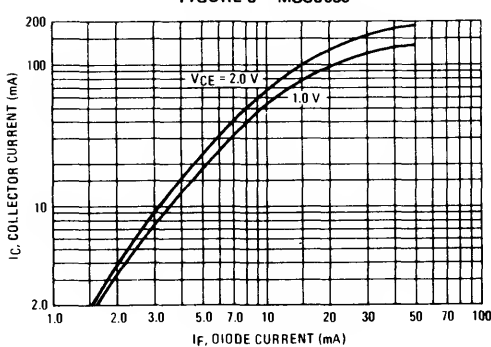
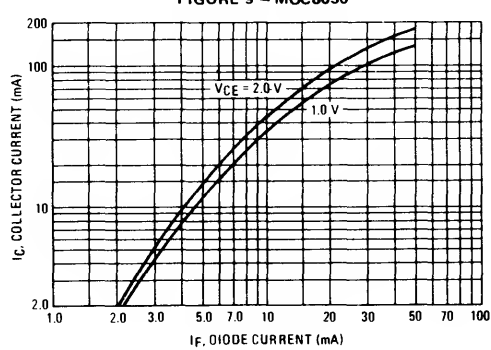


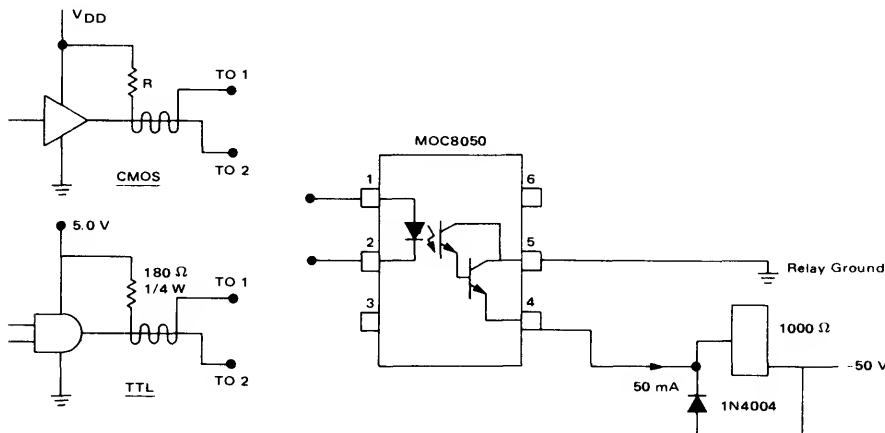
FIGURE 9 – MOC8030



MOC8030, MOC8050

INTERFACING TTL OR CMOS LOGIC TO 50-VOLT, 1000-OHMS RELAY FOR TELEPHONY APPLICATIONS

In order to interface positive logic to negative-powered electromechanical relays, a change in voltage level and polarity plus electrical isolation are required. The MOC8050 can provide this interface and eliminate the external amplifiers and voltage divider networks previously required. The circuit below shows a typical approach for the interface.





MOTOROLA

MRD150

PLASTIC NPN SILICON PHOTO TRANSISTOR

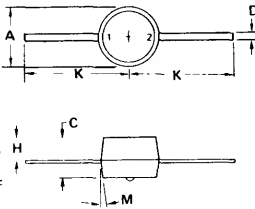
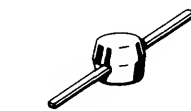
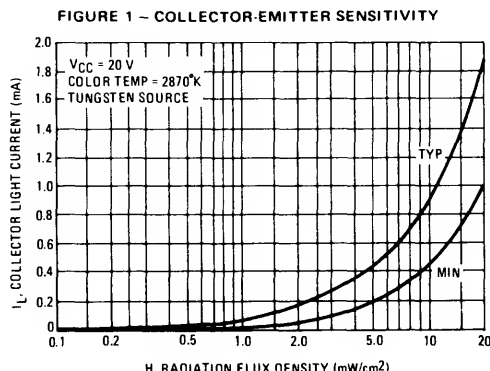
... designed for application in punched card and tape readers, pattern and character recognition equipment, shaft encoders, industrial inspection processing and control, counters, sorters, switching and logic circuits, or any design requiring radiation sensitivity, stable characteristics and high-density mounting.

- Economical Plastic Package
- Sensitive Throughout Visible and Near Infrared Spectral Range for Wide Application
- Small Size for High-Density Mounting
- High Light Current Sensitivity (0.20 mA) for Design Flexibility
- Annular Passivated Structure for Stability and Reliability

MAXIMUM RATINGS

| Rating | Symbol | Value | Unit |
|--|-------------------|-------------|----------------------------|
| Collector-Emitter Voltage | V_{CEO} | 40 | Volts |
| Emitter-Collector Voltage | V_{ECO} | 6.0 | Volts |
| Total Device Dissipation @ $T_A = 25^\circ\text{C}$ Derate above 25°C | P_D | 50 0.67 | mW mW/ $^\circ\text{C}$ |
| Operating and Storage Junction Temperature Range | $T_J(1), T_{stg}$ | -40 to +100 | $^\circ\text{C}$ |

(1) Heat Sink should be applied to leads during soldering to prevent Case Temperature from exceeding 85°C



PIN 1, Emitter
2, Collector

| DIM | MILLIMETERS | | INCHES | |
|-----|-------------|------|--------|-------|
| | MIN | MAX | MIN | MAX |
| A | 1.98 | 2.34 | 0.078 | 0.092 |
| C | 1.22 | 1.47 | 0.048 | 0.058 |
| D | 0.25 | 0.41 | 0.010 | 0.016 |
| F | 0.10 | 0.15 | 0.004 | 0.006 |
| H | 0.51 | 0.76 | 0.020 | 0.030 |
| K | 4.06 | — | 0.160 | — |
| M | 3.0 | 7.0 | 3.0 | 7.0 |

NOTE:

1. INDEX 8 BUTTON ON PACKAGE
BOTTON IS 0.25/0.51 mm (0.010/0.020)
0A & 0.05/0.13 mm (0.002/0.005) OFF SURFACE.

CASE 173-01

MRD150

STATIC ELECTRICAL CHARACTERISTICS ($T_A = 25^\circ\text{C}$ unless noted)

| Characteristic | Fig. No. | Symbol | Min | Typ | Max | Units |
|---|----------|---------------|-----|----------|-----------|---------------|
| Collector Dark Current ($V_{CC} = 20$ V; Base Open) (Note 2) $T_A = 25^\circ\text{C}$ $T_A = 85^\circ\text{C}$ | — | I_{CEO} | — | — 5.0 | 0.10 — | μA |
| Collector-Emitter Breakdown Voltage ($I_C = 100 \mu\text{A}$; Base Open; Note 2) | — | $V_{(BR)CEO}$ | 40 | — | — | Volts |
| Emitter-Collector Breakdown Voltage ($I_E = 100 \mu\text{A}$; Base Open; Note 2) | — | $V_{(BR)ECO}$ | 6.0 | — | — | Volts |

OPTICAL CHARACTERISTICS ($T_A = 25^\circ\text{C}$ unless noted)

| Characteristic | Fig. No. | Symbol | Min | Typ | Max | Units |
|--|----------|-------------------------|------|------|-----|---------------|
| Collector Light Current ($V_{CC} = 20$ V; $R_L = 100$ ohms; Base Open) (Note 1) | 1 | I_L | 0.20 | 0.45 | — | mA |
| Photo Current Rise Time (Note 3) | 2 and 3 | t_r | — | 2.5 | — | μs |
| Photo Current Fall Time (Note 3) | 2 and 3 | t_f | — | 4.0 | — | μs |
| Wavelength of Maximum Sensitivity | 9 | $\lambda_s(\text{typ})$ | — | 0.8 | — | μm |

NOTES:

1. Radiation Flux Density (H) equal to 5.0 mW/cm^2 emitted from a tungsten source at a color temperature of 2870°K .
2. Measured under dark conditions. ($H \approx 0$).
3. For unsaturated response time measurements, radiation is provided by a pulsed GaAs (gallium-arsenide) light-emitting diode ($\lambda = 0.9 \mu\text{m}$) with a pulse width equal to or greater than 10 microseconds (see Figure 2 and Figure 3).

FIGURE 2 – PULSE RESPONSE TEST CIRCUIT

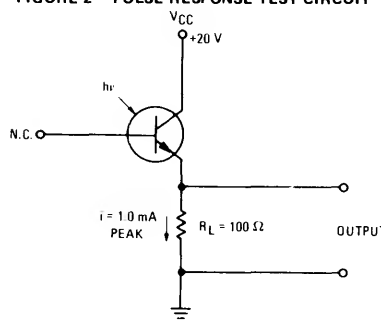
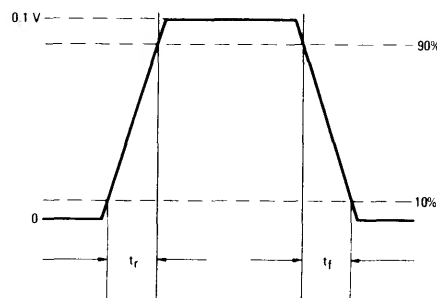


FIGURE 3 – PULSE RESPONSE TEST WAVEFORM



TYPICAL ELECTRICAL CHARACTERISTICS

FIGURE 4 – COLLECTOR-EMITTER CHARACTERISTICS

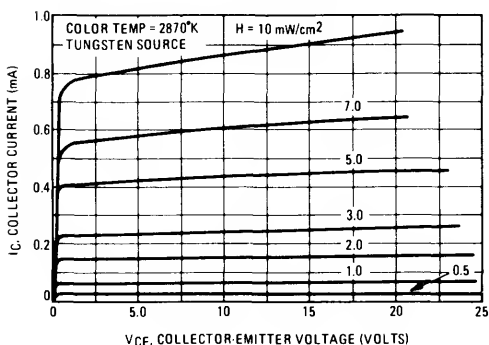


FIGURE 5 – COLLECTOR SATURATION CHARACTERISTICS

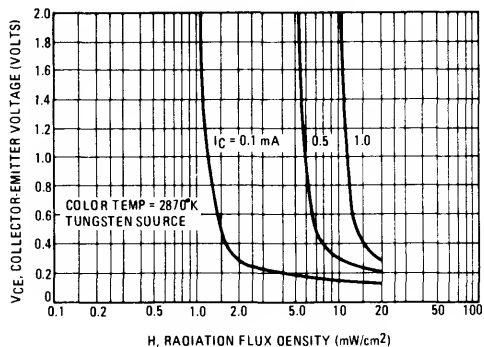


FIGURE 6 – DARK CURRENT versus TEMPERATURE

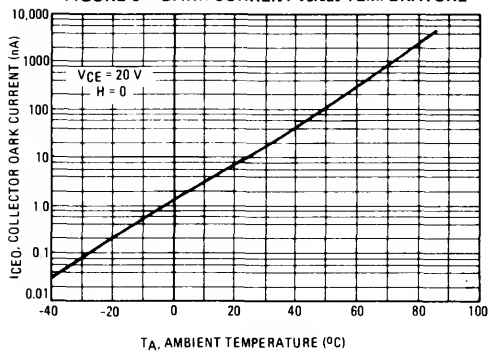


FIGURE 7 – DARK CURRENT versus VOLTAGE

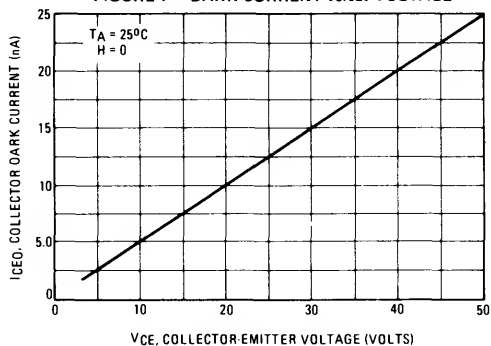


FIGURE 8 – ANGULAR RESPONSE

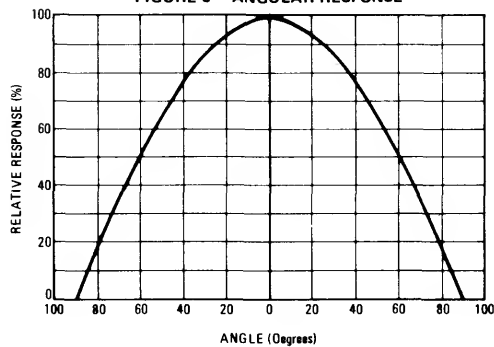
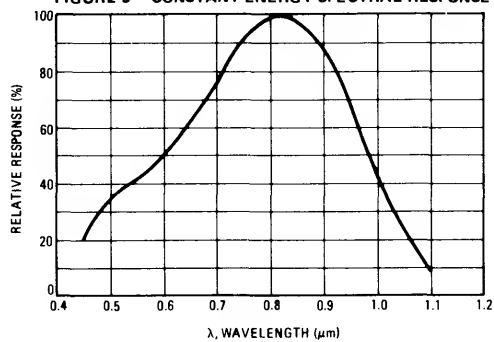


FIGURE 9 – CONSTANT ENERGY SPECTRAL RESPONSE





MOTOROLA

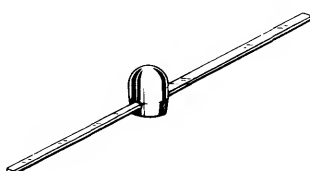
MRD160

PLASTIC NPN SILICON PHOTO TRANSISTOR

. . . designed for application in punched card and tape readers, pattern and character recognition equipment, shaft encoders, industrial inspection processing and control, counters, sorters, switching and logic circuits, or any design requiring radiation sensitivity, stable characteristics and high-density mounting.

- Economical Plastic Package
- Sensitive Throughout Visible and Near Infrared Spectral Range for Wide Application
- Small Size for High-Density Mounting
- High Light Current Sensitivity (0.50 mA) for Design Flexibility
- Annular Passivated Structure for Stability and Reliability
- Complement to MLED60/90 LEDs

40 VOLT PHOTO TRANSISTOR NPN SILICON

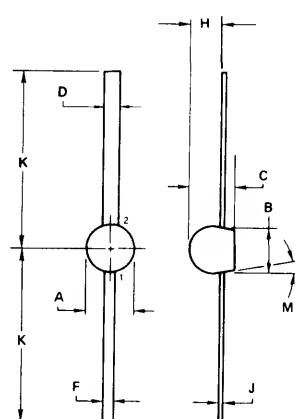
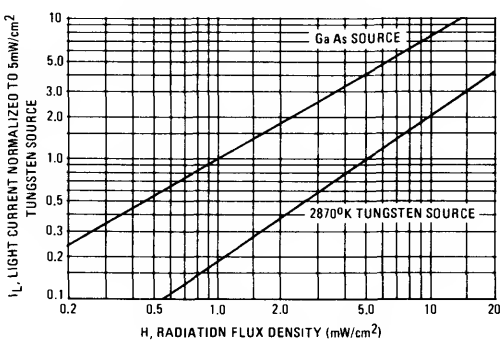


MAXIMUM RATINGS

| Rating | Symbol | Value | Unit |
|---|--------------------------------------|------------|-------------|
| Collector-Emitter Voltage | V _{CEO} | 40 | Volts |
| Emitter-Collector Voltage | V _{ECO} | 6.0 | Volts |
| Total Device Dissipation @ T _A = 25°C Derate above 25°C | P _D | 100 1.3 | mW mW/°C |
| Operating and Storage Junction Temperature Range | T _{J(1)} , T _{stg} | -40 to +85 | °C |

(1) Heat Sink should be applied to leads during soldering to prevent Case Temperature from exceeding 85°C.

**FIGURE 1 – NORMALIZED LIGHT CURRENT versus
RADIATION FLUX DENSITY**



STYLE 2
PIN 1 ANODE
PIN 2 CATHODE

| DIM | MILLIMETERS | | INCHES | |
|-----|-------------|------|--------|-------|
| | MIN | MAX | MIN | MAX |
| A | 2.34 | 2.59 | 0.092 | 0.102 |
| B | 2.11 | 2.36 | 0.083 | 0.093 |
| C | 2.39 | 2.64 | 0.094 | 0.104 |
| D | 0.64 | 0.74 | 0.025 | 0.029 |
| F | 0.46 | 0.56 | 0.018 | 0.022 |
| H | 1.57 | 1.83 | 0.062 | 0.072 |
| J | 0.20 | 0.30 | 0.008 | 0.012 |
| K | 9.65 | — | 0.380 | — |
| M | 90° | 110° | 90° | 110° |

CASE 234-04

MRD160

STATIC ELECTRICAL CHARACTERISTICS ($T_A = 25^\circ\text{C}$ unless noted)

| Characteristic | Fig. No. | Symbol | Min | Typ | Max | Units |
|--|----------|---------------|--------|----------|-----------|---------------|
| Collector Dark Current ($V_{CC} = 20$ V; Note 2) $T_A = 25^\circ\text{C}$ $T_A = 85^\circ\text{C}$ | — | I_{CEO} | — — | — 5.0 | 0.10 — | μA |
| Collector-Emitter Breakdown Voltage ($I_C = 100 \mu\text{A}$; Note 2) | — | $V_{(BR)CEO}$ | 40 | — | — | Volts |
| Emitter-Collector Breakdown Voltage ($I_E = 100 \mu\text{A}$; Note 2) | — | $V_{(BR)ECO}$ | 6.0 | — | — | Volts |

OPTICAL CHARACTERISTICS ($T_A = 25^\circ\text{C}$ unless noted)

| Characteristic | Fig. No. | Symbol | Min | Typ | Max | Units |
|---|----------|--------|------|-----|-----|---------------|
| Collector Light Current ($V_{CC} = 20$ V; $R_L = 100$ ohms; Note 1) | 1 | I_L | 0.50 | 1.5 | — | mA |
| Photo Current Rise Time (Note 3) | 2 and 3 | t_r | — | 2.5 | — | μs |
| Photo Current Fall Time (Note 3) | 2 and 3 | t_f | — | 4.0 | — | μs |

NOTES:

1. Radiation Flux Density (H) equal to 5.0 mW/cm^2 admitted from a tungsten source at a color temperature of 2870°K .
2. Measured under dark conditions. ($H \approx 0$).
3. For unsaturated response time measurements, radiation is provided by a pulsed GaAs (gallium-arsenide) light-emitting diode ($\lambda = 0.9 \mu\text{m}$) with a pulse width equal to or greater than 10 microseconds (see Figure 2 and Figure 3).

FIGURE 2 – PULSE RESPONSE TEST CIRCUIT

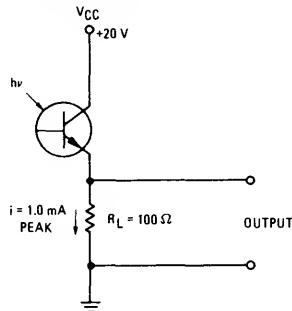
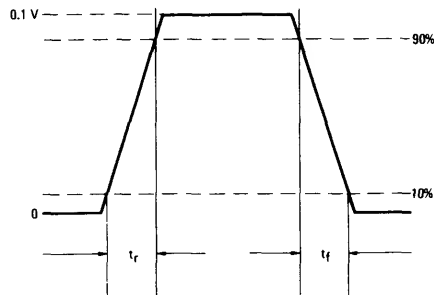


FIGURE 3 – PULSE RESPONSE TEST WAVEFORM



MRD160

TYPICAL ELECTRICAL CHARACTERISTICS

FIGURE 4 – CONTINUOUS LIGHT CURRENT versus DISTANCE

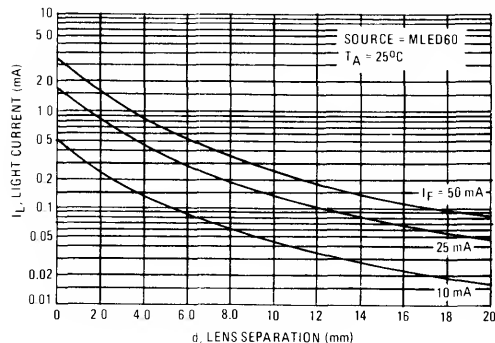


FIGURE 5 – PULSED LIGHT CURRENT versus DISTANCE

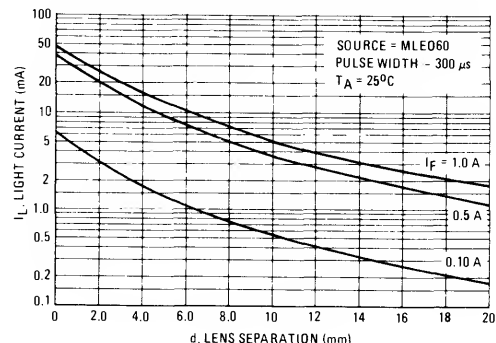


FIGURE 6 – CONSTANT ENERGY SPECTRAL RESPONSE

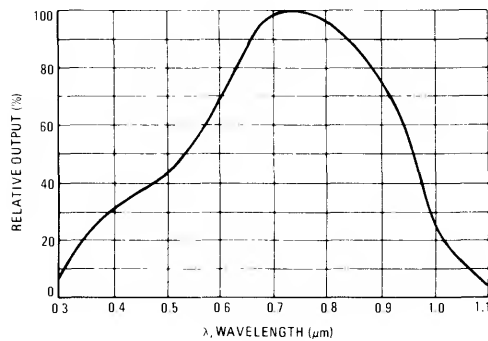


FIGURE 7 – ANGULAR RESPONSE

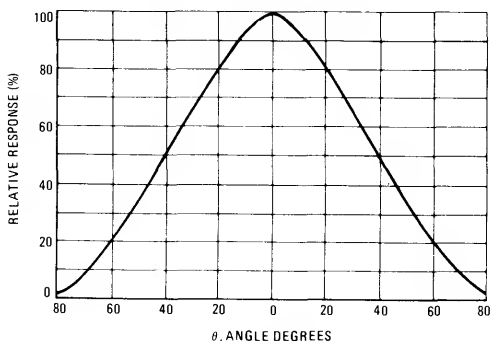
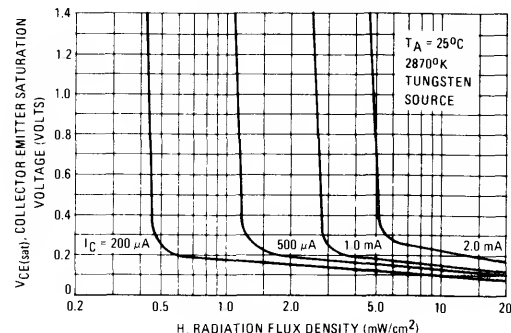


FIGURE 8 – SATURATION CHARACTERISTICS WITH TUNGSTEN SOURCE





MOTOROLA

NPN SILICON HIGH SENSITIVITY PHOTO TRANSISTOR

. . . designed for application in industrial inspection, processing and control, counters, sorters, switching and logic circuits or any design requiring radiation sensitivity, and stable characteristics.

- Popular TO-18 Type Package for Easy Handling and Mounting
- Sensitive Throughout Visible and Near Infrared Spectral Range for Wider Application
- Minimum Light Current 4 mA at $H = 5 \text{ mW/cm}^2$ (MRD300)
- External Base for Added Control
- Annular Passivated Structure for Stability and Reliability

**MRD300
MRD310**

**50 VOLT
PHOTO TRANSISTOR
NPN SILICON**

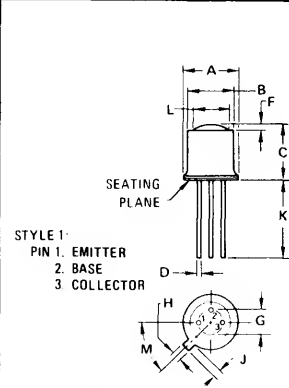
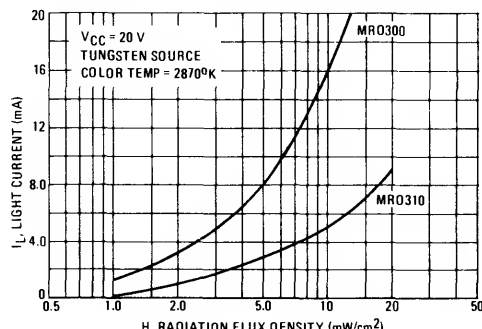
250 MILLIWATTS



MAXIMUM RATINGS ($T_A = 25^\circ\text{C}$ unless otherwise noted)

| Rating (Note 1) | Symbol | Value | Unit |
|--|----------------|-------------|----------------------------|
| Collector-Emitter Voltage | V_{CEO} | 50 | Volts |
| Emitter-Collector Voltage | V_{ECO} | 7.0 | Volts |
| Collector-Base Voltage | V_{CBO} | 80 | Volts |
| Total Device Dissipation @ $T_A = 25^\circ\text{C}$ Derate above 25°C | P_D | 250 1.43 | mW mW/ $^\circ\text{C}$ |
| Operating Junction and Storage Temperature Range | T_J, T_{stg} | -65 to +200 | $^\circ\text{C}$ |

FIGURE 1 – LIGHT CURRENT versus IRRADIANCE



NOTES:

1. LEADS WITHIN .13 mm (.005) RADIUS OF TRUE POSITION AT SEATING PLANE, AT MAXIMUM MATERIAL CONDITION.
2. PIN 3 INTERNALLY CONNECTED TO CASE.

| DIM | MILLIMETERS | | INCHES | |
|-----|-------------|------|--------|-------|
| | MIN | MAX | MIN | MAX |
| A | 5.31 | 5.84 | 0.209 | 0.230 |
| B | 4.52 | 4.95 | 0.178 | 0.195 |
| C | 4.57 | 6.48 | 0.180 | 0.255 |
| D | 0.41 | 0.48 | 0.016 | 0.019 |
| F | — | 1.14 | — | 0.045 |
| G | 2.54 | RSC | 0.100 | RSC |
| H | 0.99 | 1.17 | 0.039 | 0.046 |
| J | 0.84 | 1.22 | 0.033 | 0.048 |
| K | 12.70 | — | 0.500 | — |
| L | 3.35 | 4.01 | 0.132 | 0.158 |
| M | 45° | BSC | 45° | BSC |

CASE 82-05

MRD300, MRD310

STATIC ELECTRICAL CHARACTERISTICS ($T_A = 25^\circ\text{C}$ unless otherwise noted)

| Characteristic | Symbol | Min | Typ | Max | Unit |
|--|---------------|--------|------------|---------|------------------------------|
| Collector Dark Current ($V_{CC} = 20 \text{ V}, H \approx 0$) $T_A = 25^\circ\text{C}$ $T_A = 100^\circ\text{C}$ | I_{CEO} | — — | 5.0 4.0 | 25 — | nA μA |
| Collector-Base Breakdown Voltage ($I_C = 100 \mu\text{A}$) | $V_{(BR)CBO}$ | 80 | 120 | — | Volts |
| Collector-Emitter Breakdown Voltage ($I_C = 100 \mu\text{A}$) | $V_{(BR)CEO}$ | 50 | 85 | — | Volts |
| Emitter-Collector Breakdown Voltage ($I_E = 100 \mu\text{A}$) | $V_{(BR)ECO}$ | 7.0 | 8.5 | — | Volts |

OPTICAL CHARACTERISTICS ($T_A = 25^\circ\text{C}$ unless otherwise noted)

| Characteristic | Device Type | Symbol | Min | Typ | Max | Unit |
|--|------------------|--------|------------|------------|--------|---------------|
| Light Current ($V_{CC} = 20 \text{ V}, R_L = 100 \text{ ohms}$) Note 1 | MRD300 MRD310 | I_L | 4.0 1.0 | 8.0 3.5 | — — | mA |
| Light Current ($V_{CC} = 20 \text{ V}, R_L = 100 \text{ ohms}$) Note 2 | MRD300 MRD310 | I_L | — — | 2.5 0.8 | — — | mA |
| Photo Current Rise Time (Note 3) ($R_L = 100 \text{ ohms}$ $I_L = 1.0 \text{ mA peak}$) | | t_r | — | 2.0 | 2.5 | μs |
| Photo Current Fall Time (Note 3) ($R_L = 100 \text{ ohms}$ $I_L = 1.0 \text{ mA peak}$) | | t_f | — | 2.5 | 4.0 | μs |

NOTES:

1. Radiation flux density (H) equal to 5.0 mW/cm^2 emitted from a tungsten source at a color temperature of 2870°K .
2. Radiation flux density (H) equal to 0.5 mW/cm^2 (pulsed) from a GeAs (gallium-arsenide) source at $\lambda \approx 0.9 \mu\text{m}$.
3. For unsaturated response time measurements, radiation is provided by pulsed GeAs (gallium-arsenide) light-emitting diode ($\lambda \approx 0.9 \mu\text{m}$) with a pulse width equal to or greater than 10 microseconds (see Figure 6) $I_L = 1.0 \text{ mA peak}$.

MRD300, MRD310

TYPICAL ELECTRICAL CHARACTERISTICS

FIGURE 2 – COLLECTOR-EMITTER SATURATION CHARACTERISTIC

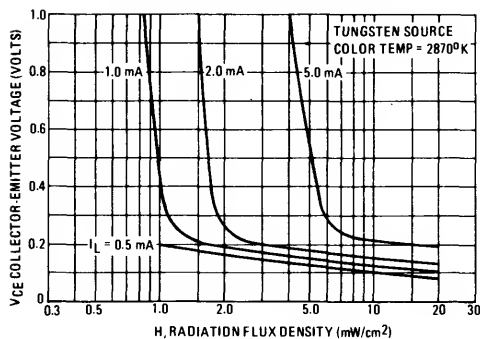


FIGURE 3 – NORMALIZED LIGHT CURRENT versus TEMPERATURE

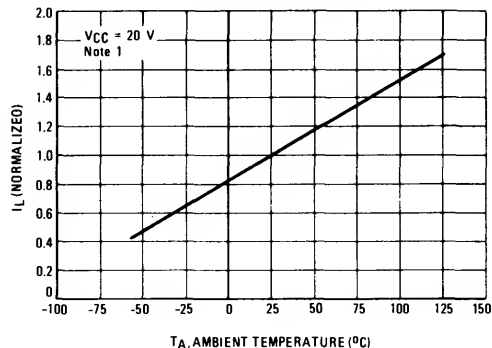


FIGURE 4 – RISE TIME versus LIGHT CURRENT

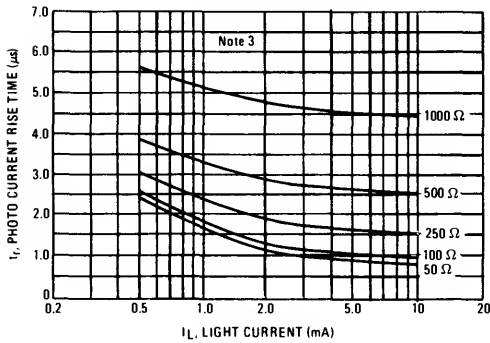


FIGURE 5 – FALL TIME versus LIGHT CURRENT

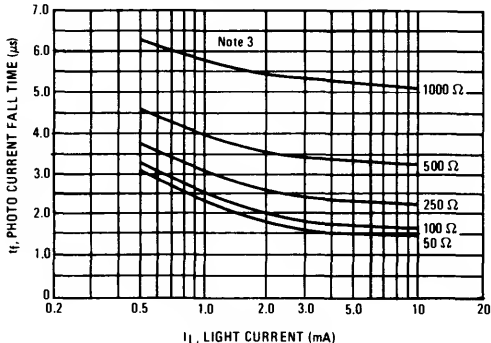
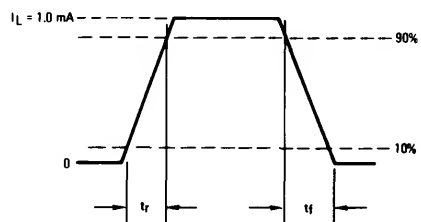
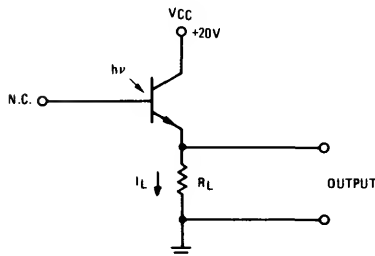


FIGURE 6 – PULSE RESPONSE TEST CIRCUIT AND WAVEFORM



MRD300, MRD310

FIGURE 7 – DARK CURRENT versus TEMPERATURE

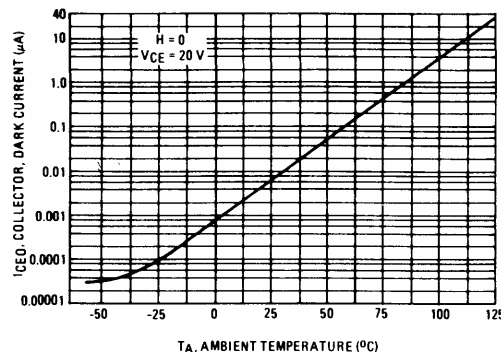


FIGURE 8 – CONSTANT ENERGY SPECTRAL RESPONSE

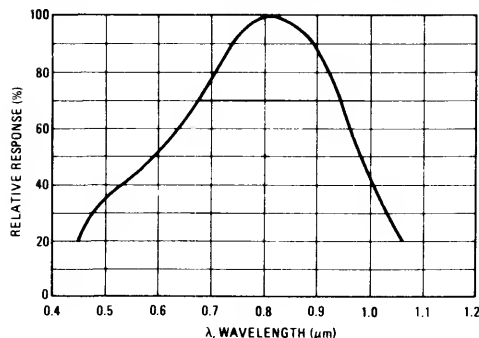
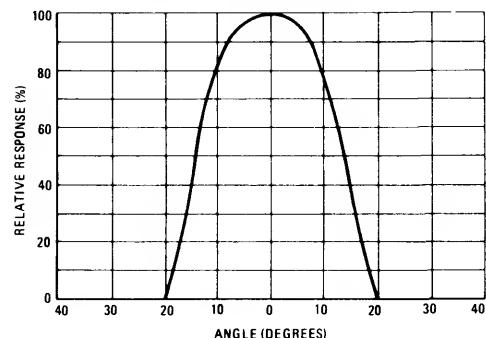


FIGURE 9 – ANGULAR RESPONSE





MOTOROLA

MRD360 MRD370

NPN SILICON HIGH SENSITIVITY PHOTO DARLINGTON TRANSISTORS

. . . designed for application in industrial inspection, processing and control, counters, sorters, switching and logic circuit or any design requiring very high radiation sensitivity at low light levels.

- Popular TO-18 Type Hermetic Package for Easy Handling and Mounting
- Sensitive Throughout Visible and Near Infrared Spectral Range for Wider Application
- Minimum Light Current 12 mA at $H = 0.5 \text{ mW/cm}^2$ (MRD360)
- External Base for Added Control
- Switching Times –
 $t_r @ I_L = 1.0 \text{ mA peak} = 15 \mu\text{s (Typ)} - \text{MRD370}$
 $t_f @ I_L = 1.0 \text{ mA peak} = 25 \mu\text{s (Typ)} - \text{MRD370}$

**PHOTO DARLINGTON
TRANSISTORS
NPN SILICON**

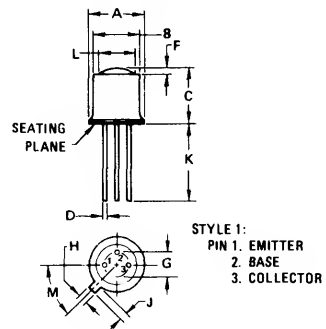
40 VOLTS

250 MILLIWATTS



MAXIMUM RATINGS ($T_A = 25^\circ\text{C}$ unless otherwise noted)

| Rating (Note 1) | Symbol | Value | Unit |
|--|----------------|-------------|----------------------------------|
| Collector-Emitter Voltage | V_{CEO} | 40 | Volts |
| Emitter-Base Voltage | V_{EBO} | 10 | Volts |
| Collector-Base Voltage | V_{CBO} | 50 | Volts |
| Light Current | I_L | 250 | mA |
| Total Device Dissipation @ $T_A = 25^\circ\text{C}$ Derate above 25°C | P_D | 250 1.43 | mW $\text{mW}/^\circ\text{C}$ |
| Operating and Storage Junction Temperature Range | T_J, T_{stg} | -65 to +200 | $^\circ\text{C}$ |

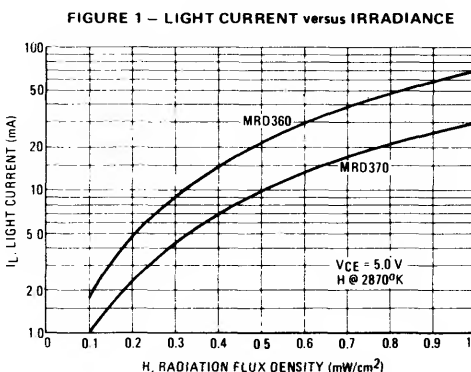


NOTES:

1. LEADS WITHIN .13 mm (.005) RADIUS OF TRUE POSITION AT SEATING PLANE, AT MAXIMUM MATERIAL CONDITION.
2. PIN 3 INTERNALLY CONNECTED TO CASE.

| DIM | MILLIMETERS | | INCHES | |
|-----|-------------|------|-----------|-------|
| | MIN | MAX | MIN | MAX |
| A | 5.31 | 5.84 | 0.209 | 0.230 |
| B | 4.52 | 4.95 | 0.178 | 0.195 |
| C | 4.57 | 6.48 | 0.180 | 0.255 |
| D | 0.41 | 0.48 | 0.016 | 0.019 |
| F | — | 1.14 | — | 0.045 |
| G | 2.54 BSC | — | 0.100 BSC | — |
| H | 0.99 | 1.17 | 0.039 | 0.046 |
| J | 0.84 | 1.22 | 0.033 | 0.048 |
| K | 12.70 | — | 0.500 | — |
| L | 3.35 | 4.01 | 0.132 | 0.158 |
| M | 45° BSC | — | 45° BSC | — |

CASE 82-05
TO-18 Type



MRD360, MRD370

STATIC ELECTRICAL CHARACTERISTICS ($T_A = 25^\circ\text{C}$ unless otherwise noted.)

| Characteristic | Symbol | Min | Typ | Max | Unit |
|---|---------------|-----|------|-----|-------|
| Collector Dark Current ($V_{CE} = 10 \text{ V}, H \approx 0$) $T_A = 25^\circ\text{C}$ | I_{CEO} | — | 10 | 100 | nA |
| Collector-Base Breakdown Voltage ($I_C = 100 \mu\text{A}$) | $V_{(BR)CBO}$ | 50 | 100 | — | Volts |
| Collector-Emitter Breakdown Voltage ($I_C = 100 \mu\text{A}$) | $V_{(BR)CEO}$ | 40 | 80 | — | Volts |
| Emitter-Base Breakdown Voltage ($I_E = 100 \mu\text{A}$) | $V_{(BR)EBO}$ | 10 | 15.5 | — | Volts |

OPTICAL CHARACTERISTICS ($T_A = 25^\circ\text{C}$ unless otherwise noted.)

| Characteristic | Device Type | Symbol | Min | Typ | Max | Unit |
|--|------------------|----------------------|-----------|----------|------------|---------------|
| Light Current $V_{CC} = 5.0 \text{ V}, R_L = 10 \text{ Ohms}$ (Note 1) | MRD360 MRD370 | I_L | 12 3.0 | 20 10 | — — | mA |
| Collector-Emitter Saturation Voltage ($I_L = 10 \text{ mA}, H = 2 \text{ mW/cm}^2$ at 2870°K) | | $V_{CE(\text{sat})}$ | — | 0.6 | 1.0 | Volts |
| Photo Current Rise Time (Note 2) ($R_L = 100 \text{ ohms}$ $I_L = 1.0 \text{ mA peak}$) | MRD360 MRD370 | t_r | — — | 15 15 | 100 100 | μs |
| Photo Current Fall Time (Note 2) ($R_L = 100 \text{ ohms}$ $I_L = 1.0 \text{ mA peak}$) | MRD360 MRD370 | t_f | — — | 65 40 | 150 150 | μs |

NOTES:

1. Radiation flux density (H) equal to 0.5 mW/cm^2 emitted from a tungsten source at a color temperature of 2780°K .
2. For unsaturated response time measurements, radiation is provided by pulsed GaAs (gallium-arsenide) light-emitting diode ($\lambda \approx 0.9 \mu\text{m}$) with a pulse width equal to or greater than 500 microseconds (see Figure 6) $I_L = 1.0 \text{ mA peak}$.

MRD360, MRD370

TYPICAL ELECTRICAL CHARACTERISTICS

FIGURE 2 – COLLECTOR-EMITTER SATURATION CHARACTERISTIC

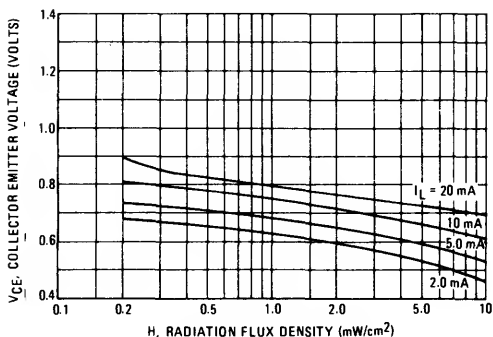


FIGURE 4 – NORMALIZED LIGHT CURRENT versus TEMPERATURE

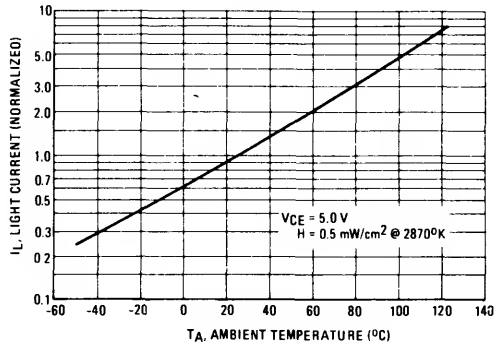


FIGURE 3 – COLLECTOR CHARACTERISTICS

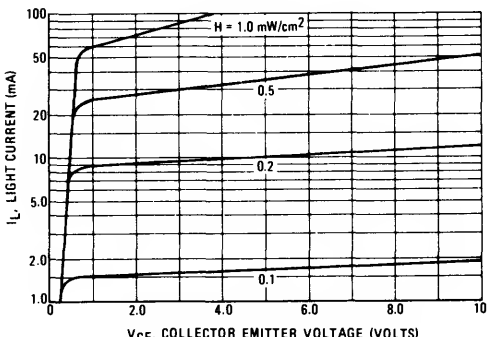


FIGURE 5 – DARK CURRENT versus TEMPERATURE

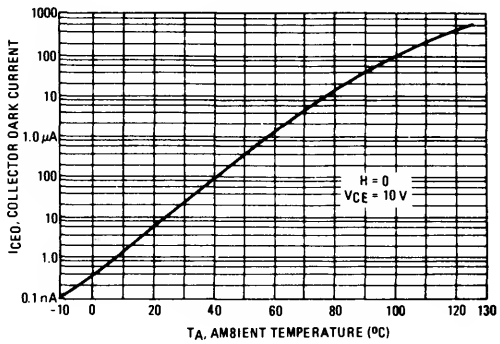
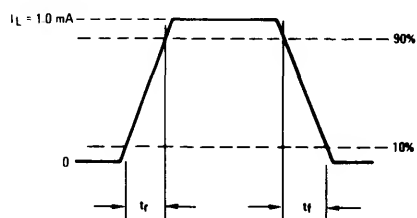
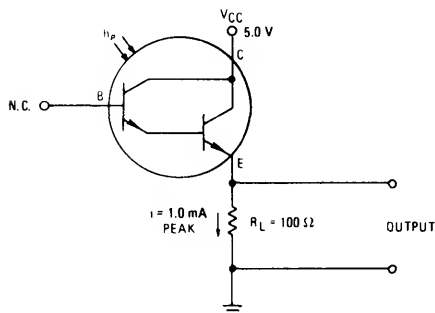


FIGURE 6 – PULSE RESPONSE TEST CIRCUIT AND WAVEFORM



MRD360, MRD370

FIGURE 7 – CONSTANT ENERGY SPECTRAL RESPONSE

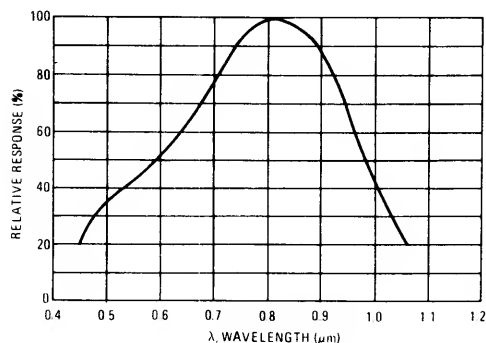
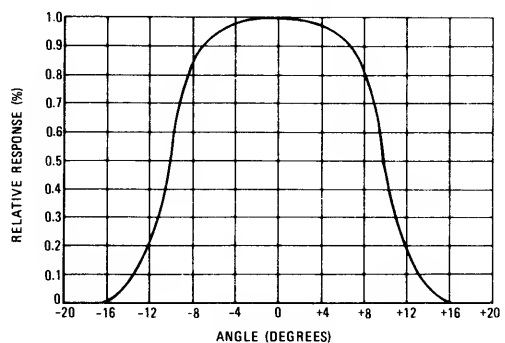


FIGURE 8 – ANGULAR RESPONSE





MOTOROLA

MRD450

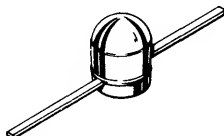
PLASTIC NPN SILICON PHOTO TRANSISTOR

. . . designed for application in industrial inspection, processing and control, counters, sorters, switching and logic circuits or any design requiring radiation sensitivity, and stable characteristics.

- Economical Plastic Package
- Sensitive Throughout Visible and Near Infrared Spectral Range for Wide Application
- Minimum Sensitivity (0.2 mA/mW/cm^2) for Design Flexibility
- Unique Molded Lens for High, Uniform Sensitivity
- Annular Passivated Structure for Stability and Reliability

40 VOLT PHOTO TRANSISTOR NPN SILICON

100 MILLIWATTS

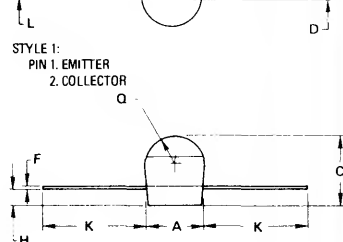
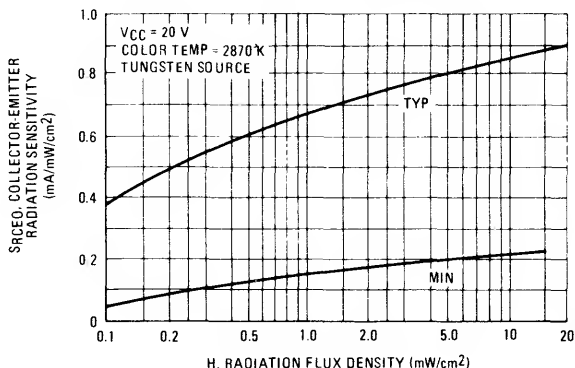


MAXIMUM RATINGS

| Rating (Note 1) | Symbol | Value | Unit |
|---|--------------------|------------|-------------|
| Collector-Emitter Voltage | V _{CEO} | 40 | Volts |
| Emitter-Collector Voltage | V _{ECO} | 6.0 | Volts |
| Total Device Dissipation @ T _A = 25°C Derate above 25°C | P _D | 100 1.3 | mW mW/°C |
| Operating Junction Temperature Range | T _J (1) | -40 to +85 | °C |
| Storage Temperature Range | T _{STG} | -40 to +85 | °C |

(1) Heat Sink should be applied to leads during soldering to prevent Case Temperature from exceeding 85°C

FIGURE 1 – COLLECTOR-EMITTER SENSITIVITY



NOTE
1. LEAD IDENTIFICATION, SQUARE BONDING PAD OVER PIN 2.

| DIM | MILLIMETERS | | INCHES | |
|-----|-------------|------|-----------|-------|
| | MIN | MAX | MIN | MAX |
| A | 3.56 | 4.06 | 0.140 | 0.160 |
| C | 4.57 | 5.33 | 0.180 | 0.210 |
| D | 0.46 | 0.61 | 0.018 | 0.024 |
| F | 0.23 | 0.28 | 0.009 | 0.011 |
| H | 1.02 | 1.27 | 0.040 | 0.050 |
| K | 6.35 | — | 0.250 | — |
| L | 0.33 | 0.48 | 0.013 | 0.019 |
| Q | 1.91 NOM | — | 0.075 NOM | — |

CASE 171-02

MRD450

STATIC ELECTRICAL CHARACTERISTICS ($T_A = 25^\circ\text{C}$ unless otherwise noted)

| Characteristic | Symbol | Min | Typ | Max | Unit |
|---|---------------|-----|----------|-----------|---------------|
| Collector Dark Current ($V_{CC} = 20 \text{ V}$, Note 2) $T_A = 25^\circ\text{C}$ $T_A = 85^\circ\text{C}$ | I_{CEO} | — | — 5.0 | 0.10 — | μA |
| Collector-Emitter Breakdown Voltage ($I_C = 100 \mu\text{A}$; Note 2) | $V_{(BR)CEO}$ | 40 | — | — | Volts |
| Emitter-Collector Breakdown Voltage ($I_E = 100 \mu\text{A}$; Note 2) | $V_{(BR)ECO}$ | 6.0 | — | — | Volts |

OPTICAL CHARACTERISTICS ($T_A = 25^\circ\text{C}$ unless otherwise noted)

| Characteristic | Fig. No. | Symbol | Min | Typ | Max | Unit |
|---|----------|-------------|-----|-----|-----|-----------------------------------|
| Collector-Emitter Radiation Sensitivity ($V_{CC} = 20 \text{ V}$, $R_L = 100 \text{ ohms}$, Note 1) | 1 | S_{RCEO} | 0.2 | 0.8 | — | $\text{mA}/\text{mW}/\text{cm}^2$ |
| Photo Current Rise Time (Note 3) | 2 and 3 | t_r | — | — | 2.5 | μs |
| Photo Current Fall Time (Note 3) | 2 and 3 | t_f | — | — | 4.0 | μs |
| Wavelength of Maximum Sensitivity | 9 | λ_s | — | 0.8 | — | μm |

NOTES:

1. Radiation Flux Density (H) equal to $5.0 \text{ mW}/\text{cm}^2$ emitted from a tungsten source at a color temperature of 2870°K .
2. Measured under dark conditions. ($H \approx 0$).
3. For unsaturated response time measurements, radiation is provided by a pulsed GaAs (gallium-arsenide) light-emitting diode ($\lambda \approx 0.9 \mu\text{m}$) with a pulse width equal to or greater than 10 microseconds (see Figure 2 and Figure 3).

FIGURE 2 – PULSE RESPONSE TEST CIRCUIT

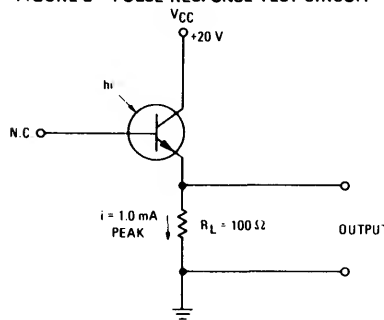
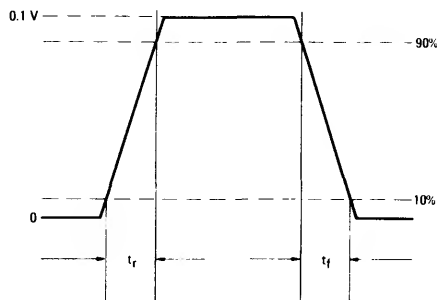


FIGURE 3 – PULSE RESPONSE TEST WAVEFORM



MRD450

TYPICAL ELECTRICAL CHARACTERISTICS

FIGURE 4 – COLLECTOR-EMITTER CHARACTERISTICS

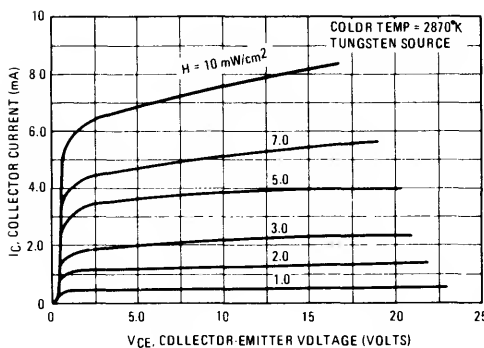


FIGURE 5 – COLLECTOR SATURATION CHARACTERISTICS

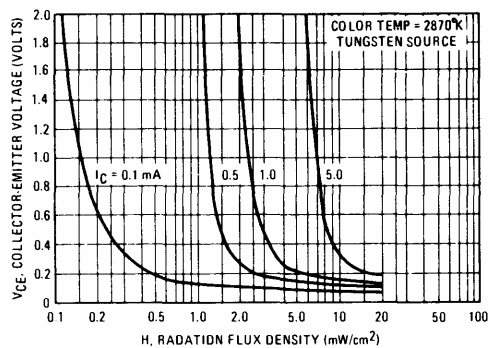


FIGURE 6 – DARK CURRENT versus TEMPERATURE

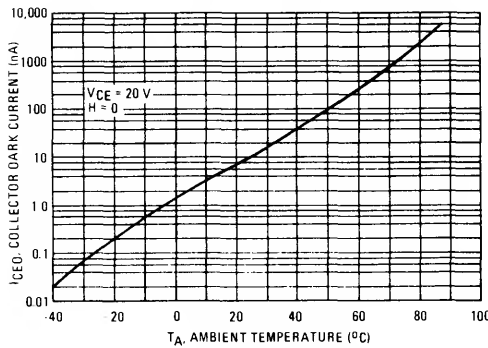


FIGURE 7 – DARK CURRENT versus VOLTAGE

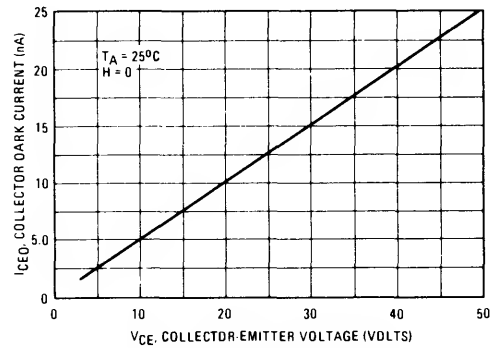


FIGURE 8 – ANGULAR RESPONSE

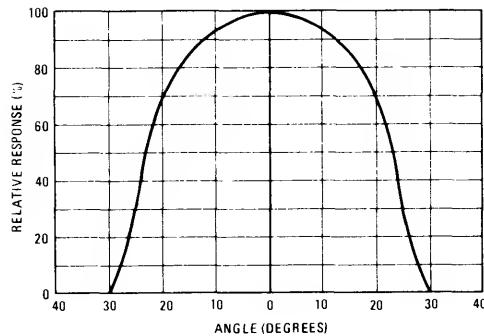
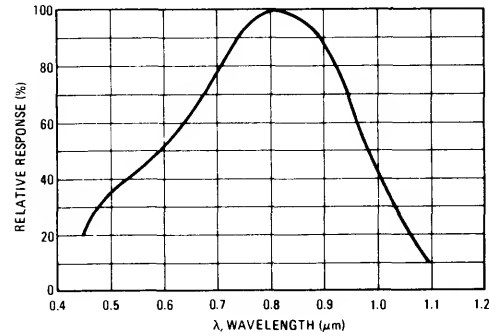


FIGURE 9 – CONSTANT ENERGY SPECTRAL RESPONSE





MOTOROLA

**MRD500
MRD510**

PIN SILICON PHOTO DIODE

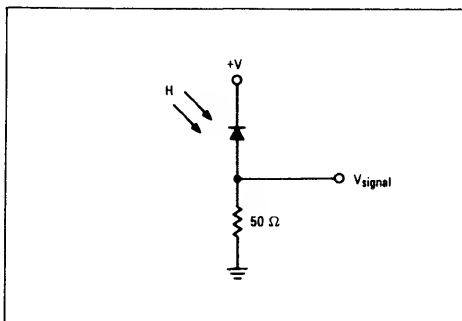
...designed for application in laser detection, light demodulation, detection of visible and near infrared light-emitting diodes, shaft or position encoders, switching and logic circuits, or any design requiring radiation sensitivity, ultra high-speed, and stable characteristics.

- Ultra Fast Response - (<1.0 ns Typ)
- High Sensitivity - MRD500 (1.2 μ A/mW/cm² Min)
MRD510 (0.3 μ A/mW/cm² Min)
- Available With Convex Lens (MRD500) or Flat Glass (MRD510) for Design Flexibility
- Popular TO-18 Type Package for Easy Handling and Mounting
- Sensitive Throughout Visible and Near Infrared Spectral Range for Wide Application
- Annular Passivated Structure for Stability and Reliability

MAXIMUM RATINGS ($T_A = 25^\circ\text{C}$ unless otherwise noted)

| Rating | Symbol | Value | Unit |
|--|----------------|-------------|----------------------------|
| Reverse Voltage | V_R | 100 | Volts |
| Total Device Dissipation @ $T_A = 25^\circ\text{C}$ Derate above 25°C | P_D | 100 0.57 | mW mW/ $^\circ\text{C}$ |
| Operating and Storage Junction Temperature Range | T_J, T_{Stg} | -65 to +200 | $^\circ\text{C}$ |

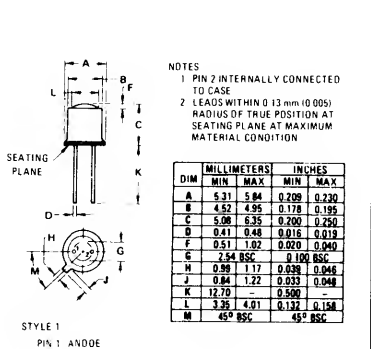
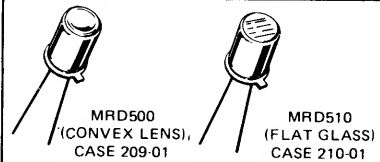
FIGURE 1 – TYPICAL OPERATING CIRCUIT



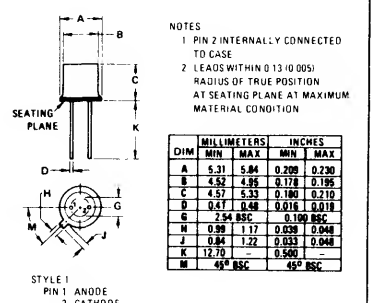
**MRD500
MRD510**

**PHOTO DIODE
PIN SILICON**

**100 VOLTS
100 MILLIWATTS**



CASE 209-01



CASE 210-01

MRD500, MRD510

STATIC ELECTRICAL CHARACTERISTICS ($T_A = 25^\circ\text{C}$ unless otherwise noted)

| Characteristic | Fig. No. | Symbol | Min | Typ | Max | Unit |
|--|----------|-------------|--------|---------|----------|-------|
| Dark Current ($V_R = 20 \text{ V}$, $R_L = 1.0 \text{ megohm}$; Note 2) $T_A = 25^\circ\text{C}$ $T_A = 100^\circ\text{C}$ | 4 and 5 | I_D | — — | — 14 | 2.0 — | nA |
| Reverse Breakdown Voltage ($I_R = 10 \mu\text{A}$) | — | $V_{(BR)R}$ | 100 | 300 | — | Volts |
| Forward Voltage ($I_F = 50 \text{ mA}$) | — | V_F | — | 0.82 | 1.1 | Volts |
| Series Resistance ($I_F = 50 \text{ mA}$) | — | R_s | — | 1.2 | 10 | ohms |
| Total Capacitance ($V_R = 20 \text{ V}$; $f = 1.0 \text{ MHz}$) | 6 | C_T | — | 2.5 | 4 | pF |

OPTICAL CHARACTERISTICS ($T_A = 25^\circ\text{C}$)

| Characteristic | Fig. No. | Symbol | Min | Typ | Max | Unit |
|--|----------|--------------------------------|------------|-------------|--------|-------------------------------------|
| Radiation Sensitivity ($V_R = 20 \text{ V}$, Note 1) MRD500 MRD510 | 2 and 3 | S_R | 1.2 0.3 | 3.0 0.42 | — — | $\mu\text{A}/\text{mW}/\text{cm}^2$ |
| Sensitivity at $0.8 \mu\text{m}$ ($V_R = 20 \text{ V}$, Note 3) MRD500 MRD510 | — — | $S(\lambda = 0.8 \mu\text{m})$ | — | 6.6 1.5 | — — | $\mu\text{A}/\text{mW}/\text{cm}^2$ |
| Response Time ($V_R = 20 \text{ V}$, $R_L = 50 \text{ ohms}$) | — — | $t_{(\text{resp})}$ | | 1.0 | | ns |
| Wavelength of Peak Spectral Response | 7 | λ_s | — | 0.8 | — | μm |

NOTES:

1. Radiation Flux Density (H) equal to 5.0 mW/cm^2 emitted from a tungsten source at a color temperature of 2870°K .
2. Measured under dark conditions. ($H \approx 0$).
3. Radiation Flux Density (H) equal to 0.5 mW/cm^2 at $0.8 \mu\text{m}$.

MRD500, MRD510

TYPICAL ELECTRICAL CHARACTERISTICS

FIGURE 2 – IRRADIATED VOLTAGE – CURRENT CHARACTERISTIC FOR MRD500

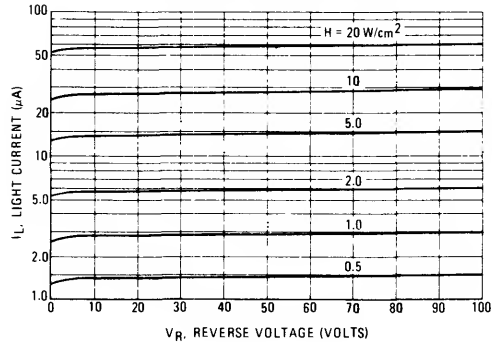


FIGURE 3 – IRRADIATED VOLTAGE – CURRENT CHARACTERISTIC FOR MRD 510

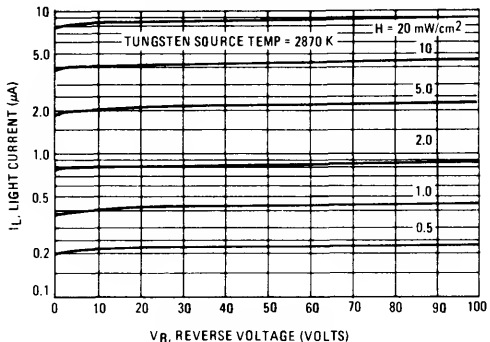


FIGURE 4 – DARK CURRENT versus TEMPERATURE

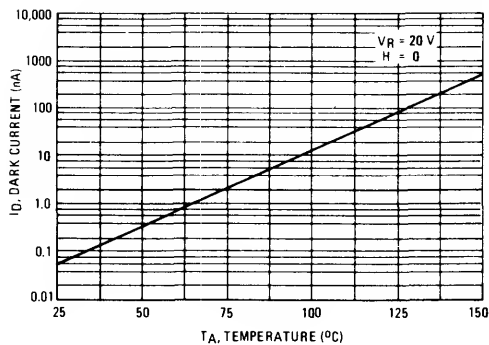


FIGURE 5 – DARK CURRENT versus REVERSE VOLTAGE

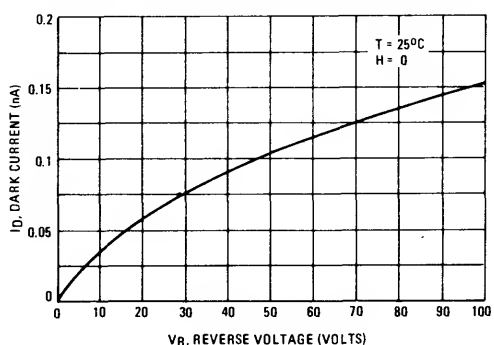


FIGURE 6 – CAPACITANCE versus VOLTAGE

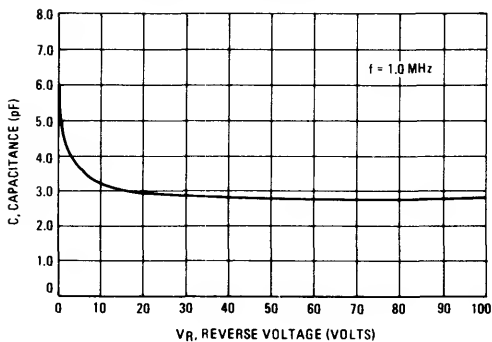
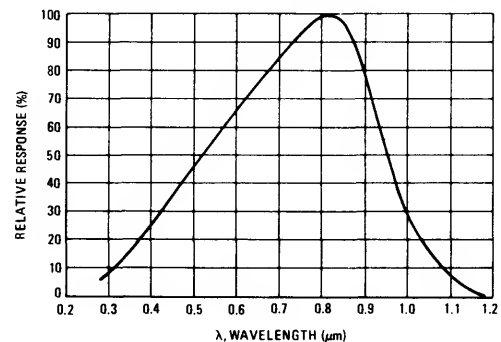


FIGURE 7 – RELATIVE SPECTRAL RESPONSE





MOTOROLA

**MRD3010
MRD3011**

250 V NPN SILICON PHOTO TRIAC DRIVER

...designed for applications requiring light and infrared LED TRIAC triggering, small size, and low cost.

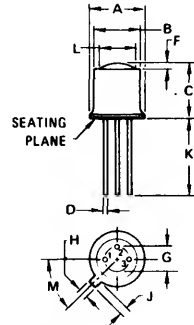
- Hermetic Package at Economy Prices
- Popular TO-18 Type Package for Easy Handling and Mounting
- High Trigger Sensitivity
 $H_{FT} = 0.5 \text{ mW/cm}^2$ (Typ-MRD3011)

OPTICALLY TRIGGERED TRIAC DRIVER



MAXIMUM RATINGS ($T_A = 25^\circ\text{C}$ unless otherwise noted)

| Rating | Symbol | Value | Unit |
|---|---|-------------|----------------------------|
| Off-State Output Terminal Voltage | V_{DRM} | 250 | Volts |
| On-State RMS Current (Full Cycle, 50 to 60 Hz) | $I_T(\text{RMS})$ $T_A = 25^\circ\text{C}$ $T_A = 70^\circ\text{C}$ | 100 50 | mA mA |
| Peak Nonrepetitive Surge Current (PW = 10 ms, DC = 10%) | I_{TSM} | 1.2 | A |
| Total Power Dissipation @ $T_A = 25^\circ\text{C}$ Derate above 25°C | P_D | 400 2.28 | mW mW/ $^\circ\text{C}$ |
| Operating Ambient Temperature Range | T_A | -40 to +70 | $^\circ\text{C}$ |
| Junction Temperature Range | T_J | -40 to +100 | $^\circ\text{C}$ |
| Storage Temperature Range | T_{stg} | -40 to +150 | $^\circ\text{C}$ |
| Soldering Temperature (10 s) | - | 260 | $^\circ\text{C}$ |



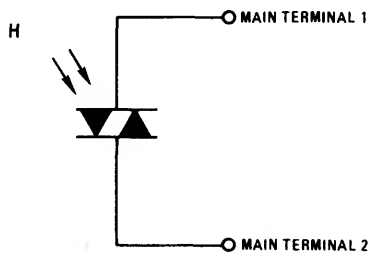
STYLE 3:
 1. MAIN TERMINAL
 2. MAIN TERMINAL
 3. SUBSTRATE
 (do not connect)

NOTES:

1. LEADS WITHIN .13 mm (.005) RADIUS OF TRUE POSITION AT SEATING PLANE, AT MAXIMUM MATERIAL CONDITION.
2. PIN 3 INTERNALLY CONNECTED TO CASE.

| DIM | MILLIMETERS | | INCHES | |
|-----|-------------|------|-----------|-------|
| | MIN | MAX | MIN | MAX |
| A | 5.31 | 5.84 | 0.209 | 0.230 |
| B | 4.52 | 4.95 | 0.178 | 0.195 |
| C | 4.57 | 6.48 | 0.180 | 0.255 |
| D | 0.41 | 0.48 | 0.016 | 0.019 |
| F | — | 1.14 | — | 0.045 |
| G | 2.54 BSC | — | 0.100 BSC | — |
| H | 0.99 | 1.17 | 0.039 | 0.046 |
| J | 0.84 | 1.22 | 0.033 | 0.048 |
| K | 12.70 | — | 0.500 | — |
| L | 3.35 | 4.01 | 0.132 | 0.158 |
| M | 45° BSC | — | 45° BSC | — |

CASE 82-05



MRD3010, MRD3011

ELECTRICAL CHARACTERISTICS ($T_A = 25^\circ\text{C}$ unless otherwise noted)

| Characteristic | Symbol | Min | Typ | Max | Unit |
|---|-----------|-----|------------|------------|-------------------------|
| DETECTOR CHARACTERISTICS ($I_F = 0$ unless otherwise noted) | | | | | |
| Peak Blocking Current, Either Direction (Rated V_{DRM} , Note 1) | I_{DRM} | — | 10 | 100 | nA |
| Peak On-State Voltage, Either Direction ($ I_{TM} = 100 \text{ mA Peak}$) | V_{TM} | — | 2.5 | 3.0 | Volts |
| Critical Rate of Rise of Off-State Voltage, Figure 3 | dv/dt | — | 2.0 | — | $\text{V}/\mu\text{s}$ |
| Critical Rate of Rise of Commutation Voltage, Figure 3 ($I_{load} = 15 \text{ mA}$) | dv/dt | — | 0.15 | — | $\text{V}/\mu\text{s}$ |
| OPTICAL CHARACTERISTICS | | | | | |
| Maximum Irradiance Level Required to Latch Output (Main Terminal Voltage 3.0 V, $R_L = 150 \Omega$) MRD3010 Color Temperature = 2870°K MRD3011 | HFT | — | 1.0 0.5 | 5.0 2.0 | mW/cm^2 |
| Holding Current, Either Direction Initiating Flux Density = $5.0 \text{ mW}/\text{cm}^2$ | I_H | — | 100 | — | μA |

NOTE 1. Test voltage must be applied within dv/dt rating.

FIGURE 1 – ON STATE CHARACTERISTICS

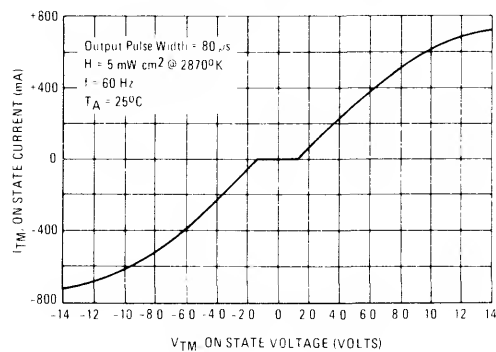


FIGURE 2 – dv/dt TEST CIRCUIT

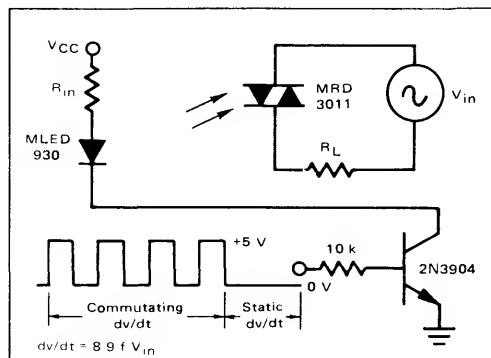


FIGURE 3 – dv/dt versus LOAD RESISTANCE

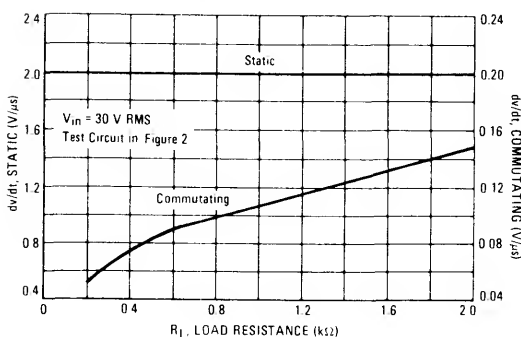
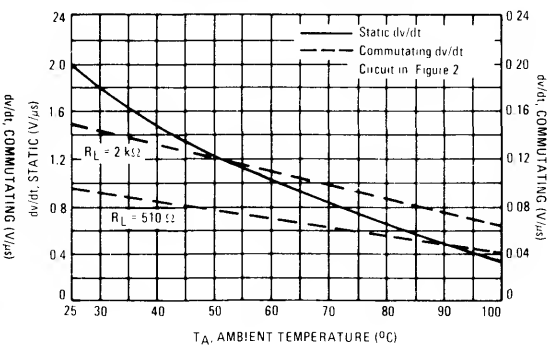


FIGURE 4 – dv/dt versus TEMPERATURE



MRD3010, MRD3011

FIGURE 5 – COMMUTATING dv/dt versus FREQUENCY

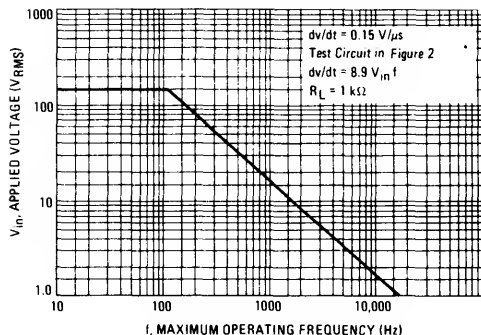
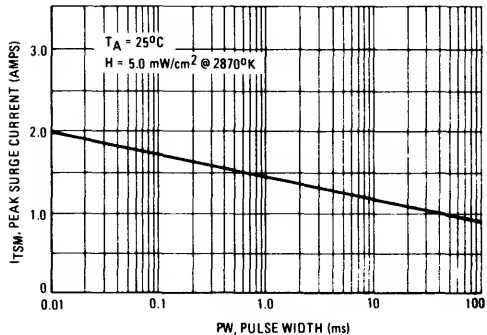
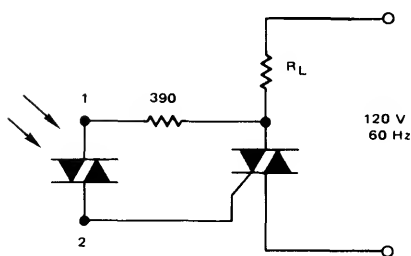


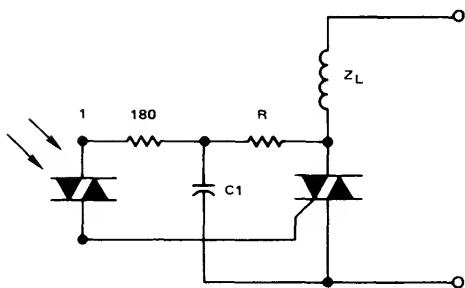
FIGURE 6 – MAXIMUM NONREPETITIVE SURGE CURRENT



RESISTIVE LOAD



INDUCTIVE LOAD



TRIAC $I_{GT} < 15 \text{ mA}$

$R = 2.4 \text{ k}\Omega$

$C1 = 0.1 \mu\text{F}$

TRIAC $I_{GT} > 15 \text{ mA}$

$R = 1.2 \text{ k}\Omega$

$C1 = 0.2 \mu\text{F}$



MOTOROLA

**MRD3050, MRD3051,
MRD3054,
MRD3055, MRD3056**

NPN SILICON PHOTO TRANSISTORS

. . . designed for application in industrial inspection, processing and control, counters, sorters, switching and logic circuits or any design requiring radiation sensitivity, and stable characteristics.

- Hermetic Package at Economy Prices
- Popular TO-18 Type Package for Easy Handling and Mounting
- Sensitive Throughout Visible and Near Infrared Spectral Range for Wider Application
- Range of Radiation Sensitivities for Design Flexibility
- External Base for Added Control
- Annular Passivated Structure for Stability and Reliability

**30 VOLT
PHOTO TRANSISTORS
NPN SILICON**

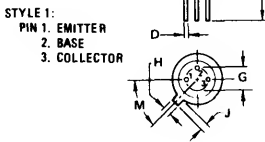
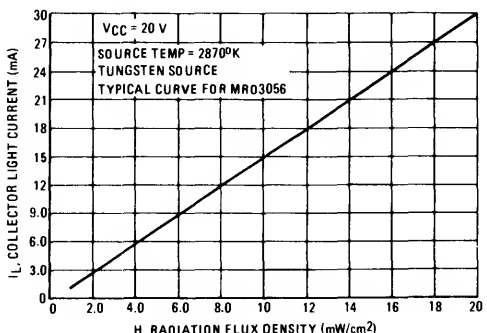


MAXIMUM RATINGS ($T_A = 25^\circ\text{C}$ unless otherwise noted)

| Rating | Symbol | Value | Unit |
|---|-----------------|-------------|----------------------------|
| Collector-Emitter Voltage | V_{CEO} | 30 | Volts |
| Emitter-Collector Voltage | V_{ECO} | 5.0 | Volts |
| Collector-Base Voltage | V_{CBO} | 40 | Volts |
| Total Power Dissipation @ $T_A = 25^\circ\text{C}$ Derate above 25°C | P_D | 400 2.28 | mW mW/ $^\circ\text{C}$ |
| Operating and Storage Junction Temperature Range | $T_{J,T_{stg}}$ | -65 to +200 | $^\circ\text{C}$ |

THERMAL CHARACTERISTICS

| Characteristic | Symbol | Max | Unit |
|---|-----------------|-----|---------------------------|
| Thermal Resistance, Junction to Ambient | $R_{\theta JA}$ | 438 | $^\circ\text{C}/\text{W}$ |



- NOTES:**
1. LEADS WITHIN .13 mm (.005) RADIUS OF TRUE POSITION AT SEATING PLANE, AT MAXIMUM MATERIAL CONDITION.
 2. PIN 3 INTERNALLY CONNECTED TO CASE.

| DIM | MILLIMETERS | | INCHES | |
|-----|-------------|------|-----------|-------|
| | MIN | MAX | MIN | MAX |
| A | 5.31 | 5.84 | 0.209 | 0.230 |
| B | 4.52 | 4.95 | 0.178 | 0.195 |
| C | 4.57 | 6.48 | 0.180 | 0.255 |
| D | 0.41 | 0.48 | 0.016 | 0.018 |
| F | — | 1.14 | — | 0.045 |
| G | 2.54 BSC | | 0.100 BSC | |
| H | 0.98 | 1.17 | 0.039 | 0.046 |
| J | 0.84 | 1.22 | 0.033 | 0.048 |
| K | 12.70 | — | 0.500 | — |
| L | 3.35 | 4.01 | 0.132 | 0.158 |
| M | 45° BSC | | 45° BSC | |

CASE 82-05

MRD3050, MRD3051, MRD3054, MRD3055, MRD3056

STATIC ELECTRICAL CHARACTERISTICS ($T_A = 25^\circ\text{C}$ unless otherwise noted)

| Characteristic | Symbol | Min | Typ | Max | Unit |
|--|---------------|--------|-------------|----------|---------------|
| Collector Dark Current ($V_{CC} = 20\text{ V}$, $R_L = 1.0$ Megohm, Note 2) $T_A = 25^\circ\text{C}$ $T_A = 85^\circ\text{C}$ | I_{CEO} | — — | 0.02 5.0 | 0.1 — | μA |
| Collector-Base Breakdown Voltage ($I_C = 100\ \mu\text{A}$) | $V_{(BR)CBO}$ | 40 | 100 | — | Volts |
| Collector-Emitter Breakdown Voltage ($I_C = 100\ \mu\text{A}$) | $V_{(BR)CEO}$ | 30 | 75 | — | Volts |
| Emitter-Collector Breakdown Voltage ($I_E = 100\ \mu\text{A}$) | $V_{(BR)ECO}$ | 5.0 | 8.0 | — | Volts |

OPTICAL CHARACTERISTICS ($T_A = 25^\circ\text{C}$ unless otherwise noted)

| Characteristic | Fig. No. | Symbol | Min | Typ | Max | Unit |
|--|----------|-------------------|---------------------------------|-------------------------|-----------------------|---------------|
| Collector-Light Current ($V_{CC} = 20\text{ V}$, $R_L = 100$ ohms, Note 1) MRD3050 MRD3051 MRD3054 MRD3055 MRD3056 | 1 | I_L | 0.1 0.2 0.5 1.5 2.0 | — — — — 8.0 | — — — — — | mA |
| Photo Current Saturated Rise Time (Note 3) | 4 | $t_r(\text{sat})$ | — | 1.0 | — | μs |
| Photo Current Saturated Fall Time (Note 3) | 4 | $t_f(\text{sat})$ | — | 1.0 | — | μs |
| Photo Current Rise Time (Note 4) | 4 | t_r | — | 2.0 | — | μs |
| Photo Current Fall Time (Note 4) | 4 | t_f | — | 2.5 | — | μs |
| Wavelength of Maximum Sensitivity | — | λ_s | — | 0.8 | — | μm |

NOTES:

1. Radiation flux density (H) equal to $5.0\ \text{mW/cm}^2$ emitted from a tungsten source at a color temperature of 2870°K .
2. Measured under dark conditions. ($H \approx 0$).
3. For saturated switching time measurements, radiation is provided by a pulsed xenon arc lamp with a pulse width of

approximately 1.0 microsecond (see Figure 4).

4. For unsaturated switching time measurements, radiation is provided by a pulsed GaAs (gallium-arsenide) light-emitting diode ($\lambda \approx 0.9\ \mu\text{m}$) with a pulse width equal to or greater than 10 microseconds (see Figure 4).

MRD3050, MRD3051, MRD3054, MRD3055, MRD3056

TYPICAL ELECTRICAL CHARACTERISTICS

**FIGURE 2 – COLLECTOR Emitter
CHARACTERISTICS – MRD3056**

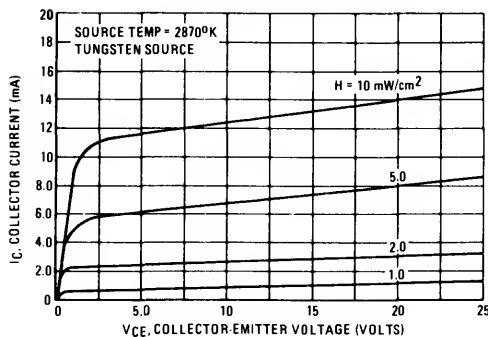


FIGURE 3 – PHOTO CURRENT versus TEMPERATURE

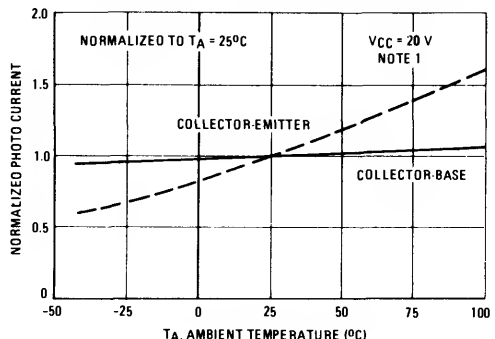


FIGURE 4 – PULSE RESPONSE TEST CIRCUIT AND WAVEFORM

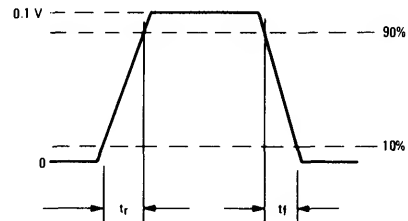
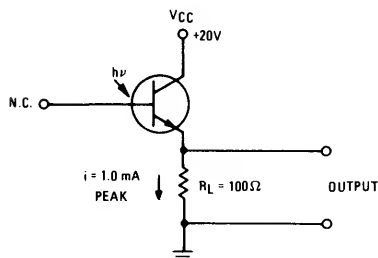
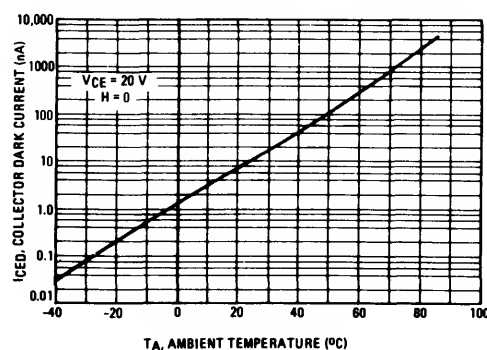


FIGURE 5 – DARK CURRENT versus TEMPERATURE



MRD3050, MRD3051, MRD3054, MRD3055, MRD3056

TYPICAL CIRCUIT APPLICATIONS

(Extracted from Motorola Application Note AN-508, "Applications of Phototransistors in Electro-Optic Systems")

FIGURE 6 – STROBEFLASH SLAVE ADAPTER

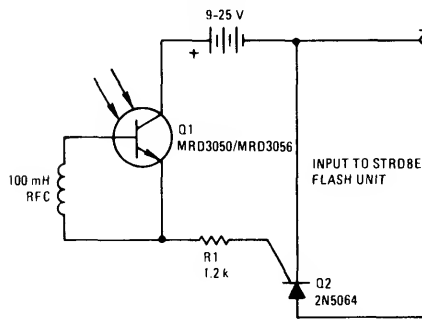


FIGURE 7 – LIGHT OPERATED SCR ALARM USING
SENSITIVE-GATE SCR

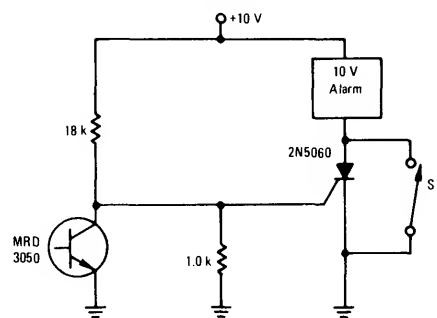
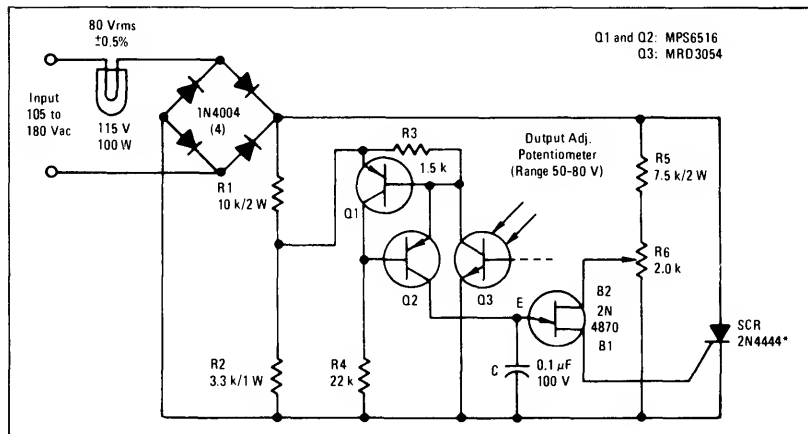


FIGURE 8 – CIRCUIT DIAGRAM OF VOLTAGE REGULATOR FOR PROJECTION LAMP.



*2N4444 to be used with a heat sink.



MOTOROLA

OPTO COUPLERS/ISOLATORS

PHOTOTRANSISTOR AND PHOTODARLINGTON OPTO COUPLERS

Extensive series of popular industry couplers in the standard dual-in-line plastic package.

- **High Isolation Voltage — 7500 V**

All Motorola couplers are specified at 7500 V ac peak (5 seconds). This usually exceeds the originator's specification.

- **Specifications Correspond to Originator's Specifications**

All parameters other than isolation voltages are tested to the originator's specifications (both condition and limits), including parameters which may not be shown on this data sheet.

- **UL Recognition, File No. E54915**

All Motorola devices shown here are UL Recognized.

Transistor Couplers

H11A1, 2, 3, 4, 5

H11A520, 550, 5100

IL1, 12, 15, 74

MCT2, 2E, 26

MCT271, 272, 273

MCT274, 275, 277

TIL111, 112, 114, 115

TIL116, 117

TIL124, 125, 126

TIL153, 154, 155

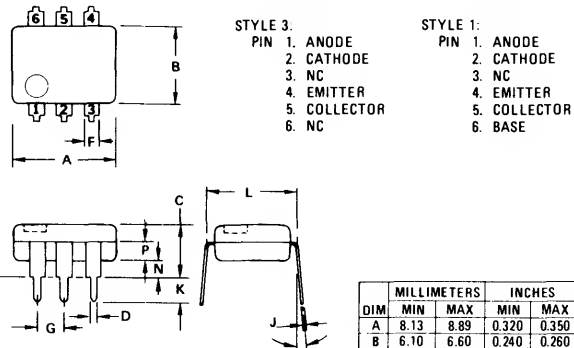
Darlington Couplers

H11B1, 2, 3, 255

MCA230, 231, 255

TIL113, 119, 127, 128

TIL156, 157



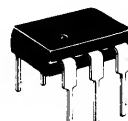
NOTES

1. DIMENSIONS A AND 8 ARE DATUMS
2. T IS SEATING PLANE.
3. POSITIONAL TOLERANCES FOR LEADS: $\phi \text{ } 0.13 (0.005)$ T A(M)B(M)
4. DIMENSION L TO CENTER OF LEADS WHEN FORMED PARALLEL.
5. DIMENSIONING AND TOLERANCING PER ANSI Y14.5, 1973.

| DIM | MILLIMETERS | | INCHES | |
|-----|-------------|------|--------|-------|
| | MIN | MAX | MIN | MAX |
| A | 8.13 | 8.89 | 0.320 | 0.350 |
| B | 6.10 | 6.60 | 0.240 | 0.260 |
| C | 2.92 | 5.08 | 0.115 | 0.200 |
| D | 0.41 | 0.51 | 0.016 | 0.020 |
| F | 1.02 | 1.78 | 0.040 | 0.070 |
| G | 2.54 | 8SC | 0.100 | 8SC |
| J | 0.20 | 0.30 | 0.008 | 0.012 |
| K | 2.54 | 3.81 | 0.100 | 0.150 |
| L | 7.62 | 8SC | 0.300 | 8SC |
| M | 0.0 | 150 | 0.0 | 150 |
| N | 0.38 | 2.54 | 0.015 | 0.100 |
| P | 1.27 | 2.03 | 0.050 | 0.080 |

CASE 730A-01

PLASTIC PACKAGE



CASE 730A-01

OPTO COUPLERS ISOLATORS

ELECTRICAL CHARACTERISTICS ($T_A = 25^\circ C$ unless otherwise noted)

| PARAMETER | Current Transfer Ratio | | | Isolation Voltage (1) | Saturation Voltage | | | Collector Dark Current | Collector-Emitter Breakdown Voltage | | LED Forward Voltage | | |
|----------------|-----------------------------|----------|----------------|-----------------------|--------------------------|----------|----------|------------------------|-------------------------------------|-------------|---------------------|----------------|----------|
| TEST CONDITION | I_F and V_{CE} as shown | | | Input to Output | I_F and I_C as shown | | | V_{CE} as shown | $I_F = 0$ | $I_F = 0$ | I_C as shown | I_F as shown | |
| SYMBOL | CTR % | | | V_{ISO} Volts Peak | $V_{CE(SAT)}$ Volts | | | I_{CEO} nA | $V_{(BR)CEO}$ Volts | V_F Volts | | | |
| Device Type | Min | I_F mA | V_{CE} Volts | Min | Max | I_F mA | I_C mA | Max | V_{CE} Volts | Min | I_C | Max | I_F mA |
| H11A1 | 50 | 10 | 10 | 7500 | 0.4 | 10 | 0.5 | 50 | 10 | 30 | 10 | 1.5 | 10 |
| H11A2 | 20 | 10 | 10 | 7500 | 0.4 | 10 | 0.5 | 50 | 10 | 30 | 10 | 1.5 | 10 |
| H11A3 | 20 | 10 | 10 | 7500 | 0.4 | 10 | 0.5 | 50 | 10 | 30 | 10 | 1.5 | 10 |
| H11A4 | 10 | 10 | 10 | 7500 | 0.4 | 10 | 0.5 | 50 | 10 | 30 | 10 | 1.5 | 10 |
| H11A5 | 30 | 10 | 10 | 7500 | 0.4 | 10 | 0.5 | 100 | 10 | 30 | 10 | 1.7 | 10 |
| H11A520 | 20 | 10 | 10 | 7500 | 0.4 | 20 | 2.0 | 50 | 10 | 30 | 10 | 1.5 | 10 |
| H11A550 | 50 | 10 | 10 | 7500 | 0.4 | 20 | 2.0 | 50 | 10 | 30 | 10 | 1.5 | 10 |
| H11A5100 | 100 | 10 | 10 | 7500 | 0.4 | 20 | 2.0 | 50 | 10 | 30 | 10 | 1.5 | 10 |
| H11B1* | 500 | 1.0 | 5.0 | 7500 | 1.0 | 1.0 | 1.0 | 100 | 10 | 25 | 10 | 1.5 | 10 |
| H11B2* | 200 | 1.0 | 5.0 | 7500 | 1.0 | 1.0 | 1.0 | 100 | 10 | 25 | 10 | 1.5 | 10 |
| H11B3* | 100 | 1.0 | 5.0 | 7500 | 1.0 | 1.0 | 1.0 | 100 | 10 | 25 | 10 | 1.5 | 50 |
| H11B255* | 100 | 10 | 5.0 | 7500 | — | — | — | 100 | 10 | 55 | 0.1 | 1.5 | 20 |
| IL1 | 20 | 10 | 10 | 7500 | 0.5 | 16 | 1.6 | 50 | 10 | 30 | 1.0 | 1.5 | 60 |
| IL12 | 10 | 10 | 5.0 | 7500 | — | — | — | 250 | 5.0 | 20 | 1.0 | 1.5 | 10 |
| IL15 | 6.0 | 10 | 10 | 7500 | 0.5 | 50 | 2.0 | 100 | 5.0 | 30 | 1.0 | 1.5 | 60 |
| IL74 | 12.5 | 16 | 5.0 | 7500 | 0.5 | 16 | 2.0 | 500 | 5.0 | 20 | 1.0 | 1.75 | 10 |
| MCA230* | 100 | 10 | 5.0 | 7500 | 1.0 | 50 | 50 | 100 | 10 | 30 | 0.1 | 1.5 | 20 |
| MCA231* | 200 | 1.0 | 1.0 | 7500 | 1.2 | 10 | 50 | 100 | 10 | 30 | 1.0 | 1.5 | 20 |
| MCA255* | 100 | 10 | 5.0 | 7500 | 1.0 | 50 | 50 | 100 | 10 | 55 | 0.1 | 1.5 | 20 |
| MCT2 | 20 | 10 | 10 | 7500 | 0.4 | 16 | 2.0 | 50 | 10 | 30 | 1.0 | 1.5 | 20 |
| MCT2E | 20 | 10 | 10 | 7500 | 0.4 | 16 | 2.0 | 50 | 10 | 30 | 1.0 | 1.5 | 20 |
| MCT26 | 6.0 | 10 | 10 | 7500 | 0.5 | 60 | 16 | 100 | 5.0 | 30 | 1.0 | 1.5 | 20 |
| MCT271 | 45 | 10 | 10 | 7500 | 0.4 | 16 | 2.0 | 50 | 10 | 30 | 1.0 | 1.5 | 20 |
| MCT272 | 75 | 10 | 10 | 7500 | 0.4 | 16 | 2.0 | 50 | 10 | 30 | 1.0 | 1.5 | 20 |
| MCT273 | 125 | 10 | 10 | 7500 | 0.4 | 16 | 2.0 | 50 | 10 | 30 | 1.0 | 1.5 | 20 |
| MCT274 | 225 | 10 | 10 | 7500 | 0.4 | 16 | 2.0 | 50 | 10 | 30 | 1.0 | 1.5 | 20 |
| MCT275 | 70 | 10 | 10 | 7500 | 0.4 | 16 | 2.0 | 50 | 10 | 80 | 1.0 | 1.5 | 20 |
| MCT277 | 100 | 10 | 10 | 7500 | — | — | — | 50 | 10 | 30 | 1.0 | 1.5 | 20 |
| TIL111 | 8.0 | 16 | 0.4 | 7500 | 0.4 | 16 | 2.0 | 50 | 10 | 30 | 1.0 | 1.4 | 16 |
| TIL112 | 2.0 | 10 | 5.0 | 7500 | 0.5 | 50 | 2.0 | 100 | 5.0 | 20 | 1.0 | 1.5 | 10 |
| TIL113* | 300 | 10 | 1.0 | 7500 | 1.0 | 125 | 50 | 100 | 10 | 30 | 1.0 | 1.5 | 10 |
| TIL114 | 8.0 | 16 | 0.4 | 7500 | 0.4 | 16 | 2.0 | 50 | 10 | 30 | 1.0 | 1.4 | 16 |
| TIL115 | 2.0 | 10 | 5.0 | 7500 | 0.5 | 50 | 2.0 | 100 | 5.0 | 20 | 1.0 | 1.5 | 10 |
| TIL116 | 20 | 10 | 10 | 7500 | 0.4 | 15 | 2.2 | 50 | 10 | 30 | 1.0 | 1.5 | 60 |
| TIL117 | 50 | 10 | 10 | 7500 | 0.4 | 10 | 0.5 | 50 | 10 | 30 | 1.0 | 1.4 | 16 |
| TIL119* | 300 | 10 | 2.0 | 7500 | 1.0 | 10 | 1.0 | 100 | 10 | 30 | 1.0 | 1.5 | 10 |
| TIL124 | 10 | 10 | 10 | 7500 | 0.4 | 10 | 1.0 | 50 | 10 | 30 | 1.0 | 1.4 | 10 |
| TIL125 | 20 | 10 | 10 | 7500 | 0.4 | 10 | 1.0 | 50 | 10 | 30 | 1.0 | 1.4 | 10 |
| TIL126 | 50 | 10 | 10 | 7500 | 0.4 | 10 | 1.0 | 50 | 10 | 30 | 1.0 | 1.4 | 10 |
| TIL127* | 300 | 10 | 1.0 | 7500 | 1.0 | 50 | 125 | 100 | 10 | 30 | 1.0 | 1.5 | 10 |
| TIL128* | 300 | 10 | 2.0 | 7500 | 1.0 | 10 | 1.0 | 100 | 10 | 30 | 1.0 | 1.5 | 10 |
| TIL153 | 10 | 10 | 10 | 7500 | 0.4 | 10 | 1.0 | 50 | 10 | 30 | 1.0 | 1.4 | 10 |
| TIL154 | 20 | 10 | 10 | 7500 | 0.4 | 10 | 1.0 | 50 | 10 | 30 | 1.0 | 1.4 | 10 |
| TIL155 | 50 | 10 | 10 | 7500 | 0.4 | 10 | 1.0 | 50 | 10 | 30 | 1.0 | 1.4 | 10 |
| TIL156* | 300 | 10 | 1.0 | 7500 | 1.0 | 50 | 125 | 100 | 10 | 30 | 1.0 | 1.5 | 10 |
| TIL157* | 300 | 10 | 2.0 | 7500 | 1.0 | 10 | 1.0 | 100 | 10 | 30 | 1.0 | 1.5 | 10 |

*Darlington

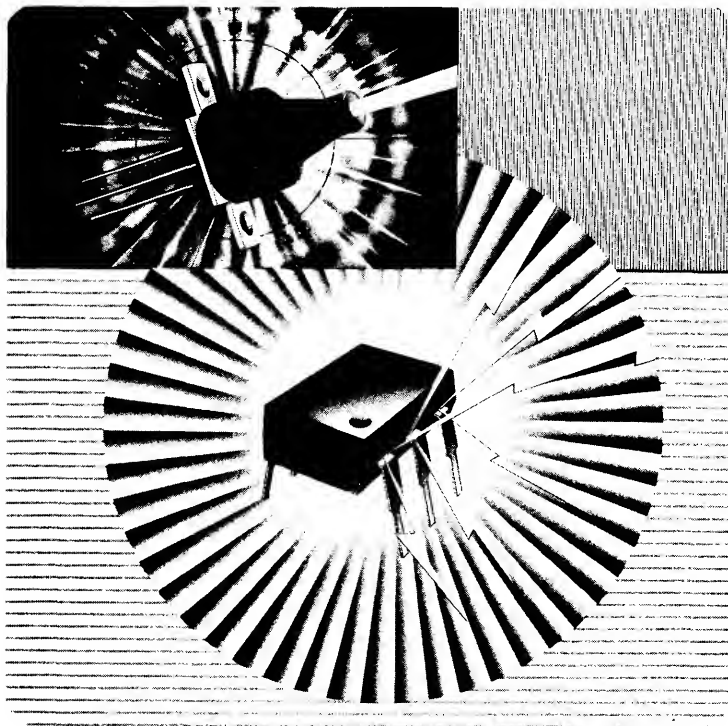
(1) Isolation Surge Voltage V_{ISO} is an internal device dielectric breakdown rating.

For this test LED pins 1 and 2 are common and phototransistor pins 4, 5, and 6 are common.

(2) See Case 730A-01, Style 3.

OPTOELECTRONICS

Applications Information



THEORY AND CHARACTERISTICS OF PHOTOTRANSISTORS

Prepared By:
John Bliss

INTRODUCTION

Phototransistor operation is based on the sensitivity of a pn junction to radiant energy. If radiant energy of proper wave-length is made to impinge on a junction, the current through that junction will increase. This optoelectronic phenomenon has provided the circuit designer with a device for use in a wide variety of applications. However, to make optimum use of the phototransistor, the designer should have a sound grasp of its operating principles and characteristics.

HISTORY

The first significant relationships between radiation and electricity were noted by Gustav Hertz in 1887. Hertz observed that under the influence of light, certain surfaces were found to liberate electrons.

In 1900, Max Planck proposed that light contained energy in discrete bundles or packets which he called photons. Einstein formulated this theory in 1905, showing that the energy content of each photon was directly proportional to the light frequency:

$$E = hf, \quad (1)$$

where E is the photon energy,
h is Planck's constant, and
f is the light frequency.

Planck theorized that a metal had associated with it a work function, or binding energy for free electrons. If a photon could transfer its energy to a free electron, and that energy exceeded the work function, the electron could be liberated from the surface. The presence of an electric field could enhance this by effectively reducing the work function. Einstein extended Planck's findings by showing that the velocity, and hence the momentum of an emitted electron, depended on the work function and the light frequency.

PHOTO EFFECT IN SEMICONDUCTORS

Bulk Crystal

If light of proper wavelength impinges on a semiconductor crystal, the concentration of charge carriers is found to increase. Thus, the crystal conductivity will increase:

$$\sigma = q (\mu_e n + \mu_h p), \quad (2)$$

where σ is the conductivity,

q is the electron charge,

μ_e is the electron mobility,

μ_h is the hole mobility,

n is the electron concentration, and

p is the hole concentration.

The process by which charge-carrier concentration is increased is shown in Figure 1. The band structure of the semiconductor is shown, with an energy gap, or forbidden region, of E_g electron volts. Radiation from two light sources is shown striking the crystal. Light frequency f_1 is sufficiently high that its photon energy, hf_1 , is slightly greater than the energy gap. This energy is transferred to a bound electron at site one in the valence band, and the electron is excited to a higher energy level, site one in the conduction band, where it is free to serve as a current carrier. The hole left behind at site one in the valence band is also free to serve as a current carrier.

The photon energy of the lower-frequency light, hf_2 , is less than the band gap, and an electron freed from site two in the valence band will rise to a level in the forbidden region, only to release this energy and fall back into the valence band and recombine with a hole at site three.

The above discussion implies that the energy gap, E_g , represents a threshold of response to light. This is true, however, it is not an abrupt threshold. Throughout the photo-excitation process, the law of conservation of mo-

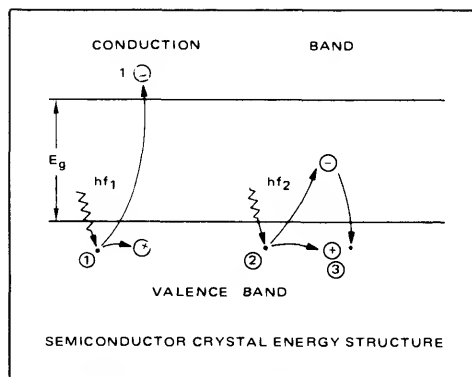


FIGURE 1 – Photoeffect in a Semiconductor

mentum applies. The momentum and density of hole-electron sites are highest at the center of both the valence and conduction bands, and fall to zero at the upper and lower ends of the bands. Therefore, the probability of an excited valence-band electron finding a site of like momentum in the conduction band is greatest at the center of the bands and lowest at the ends of the bands. Consequently, the response of the crystal to the impinging light is found to rise from zero at a photon energy of E_g electron volts, to a peak at some greater energy level, and then to fall to zero again at an energy corresponding to the difference between the bottom of the valence band and the top of the conduction band.

The response is a function of energy, and therefore of frequency, and is often given as a function of reciprocal frequency, or, more precisely, of wave length. An example is shown in Figure 2 for a crystal of cadmium-selenide. On the basis of the information given so far, it would seem reasonable to expect symmetry in such a curve; however, trapping centers and other absorption phenomena affect the shape of the curve¹.

The optical response of a bulk semiconductor can be modified by the addition of impurities. Addition of an acceptor impurity, which will cause the bulk material to become p-type in nature, results in impurity levels which lie somewhat above the top of the valence band. Photo-excitation can occur from these impurity levels to the conduction band, generally resulting in a shifting and reshaping of the spectral response curve. A similar modification of response can be attributed to the donor impurity levels in n-type material.

PN Junctions

If a pn junction is exposed to light of proper frequency, the current flow across the junction will tend to increase. If the junction is forward-biased, the net increase will be relatively insignificant. However, if the junction is reverse-biased, the change will be quite appreciable. Figure 3 shows the photo effect in the junction for a frequency well within the response curve for the device.

1. See references for a detailed discussion of these.

Photons create hole-electron pairs in the crystal on both sides of the junction. The transferred energy promotes the electrons into the conduction band, leaving the holes in the valence band. The applied external bias provides an electric field, \mathcal{E} , as shown in the figure. Thus the photo-induced electrons in the p-side conduction band will flow down the potential hill at the junction into the n-side and from there to the external circuit. Likewise, holes in the valence band of the n-side will flow across the junction into the p-side where they will add to the external current.

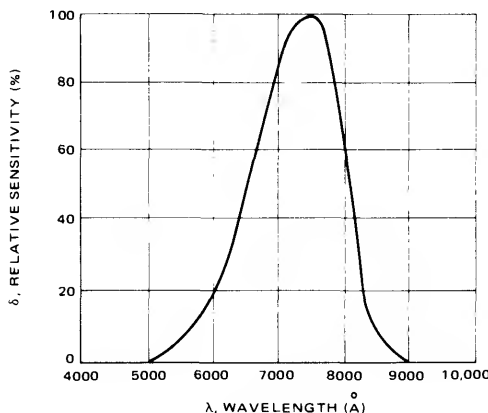


FIGURE 2 – Spectral Response of Cadmium Selenide

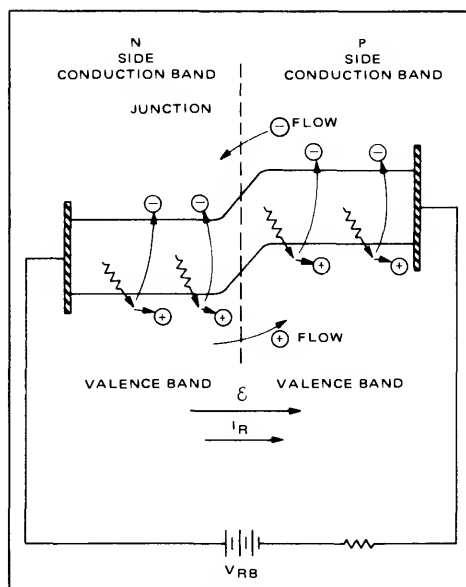


FIGURE 3 – Photo Effect in a Reverse-Biased PN Junction

Under dark conditions, the current flow through the reverse-biased diode is the reverse saturation current, I_o . This current is relatively independent of the applied voltage (below breakdown) and is basically a result of the thermal generation of hole-electron pairs.

When the junction is illuminated, the energy transferred from photons creates additional hole-electron pairs. The number of hole-electron pairs created is a function of the light intensity.

For example, incident monochromatic radiation of H (watts/cm²) will provide P photons to the diode:

$$P = \frac{\lambda H}{hc}, \quad (3)$$

where λ is the wavelength of incident light,

h is Planck's constant, and

c is the velocity of light.

The increase in minority carrier density in the diode will depend on P , the conservation of momentum restriction, and the reflectance and transmittance properties of the crystal. Therefore, the photo current, I_λ , is given by

$$I_\lambda = \eta F q A, \quad (4)$$

where η is the quantum efficiency or ratio of current carriers to incident photons,

F is the fraction of incident photons transmitted by the crystal,

q is the charge of an electron, and

A is the diode active area.

Thus, under illuminated conditions, the total current flow is

$$I = I_o + I_\lambda. \quad (5)$$

If I_λ is sufficiently large, I_o can be neglected, and by using the spectral response characteristics and peak spectral sensitivity of the diode, the total current is given approximately by

$$I \approx \delta S R H, \quad (6)$$

where δ is the relative response and a function of radiant wavelength,

S_R is the peak spectral sensitivity, and

H is the incident radiation.

The spectral response for a silicon photo-diode is given in Figure 4.

Using the above relations, an approximate model of the diode is given in Figure 5. Here, the photo and thermally generated currents are shown as parallel current sources. C represents the capacitance of the reverse-biased junction while G represents the equivalent shunt conductance of the diode and is generally quite small. This model applies only for reverse bias, which, as mentioned above, is the normal mode of operation.

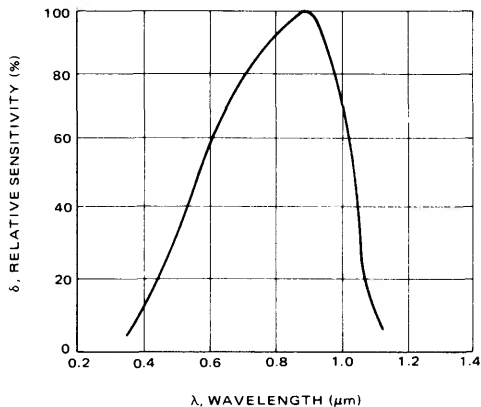


FIGURE 4 – Spectral Response of Silicon Photodiode

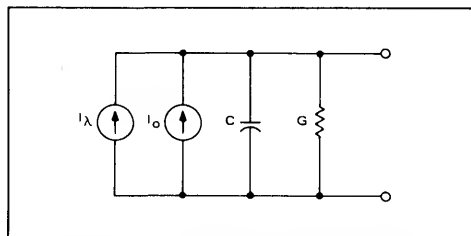


FIGURE 5 – Approximate Model of Photodiode

Photo Transistor

If the pn junction discussed above is made the collector-base diode of a bipolar transistor, the photo-induced current is the transistor base current. The current gain of the transistor will thus result in a collector-emitter current of

$$I_C = (h_{fe} + 1) I_\lambda, \quad (7)$$

where I_C is the collector current,

h_{fe} is the forward current gain, and

I_λ is the photo induced base current.

The base terminal can be left floating, or can be biased up to a desired quiescent level. In either case, the collector-base junction is reverse biased and the diode current is the reverse leakage current. Thus, photo-stimulation will result in a significant increase in diode, or base current, and with current gain will result in a significant increase in collector current.

The energy-band diagram for the photo transistor is shown in Figure 6. The photo-induced base current is returned to the collector through the emitter and the external circuitry. In so doing, electrons are supplied to the base region by the emitter where they are pulled into the collector by the electric field E .

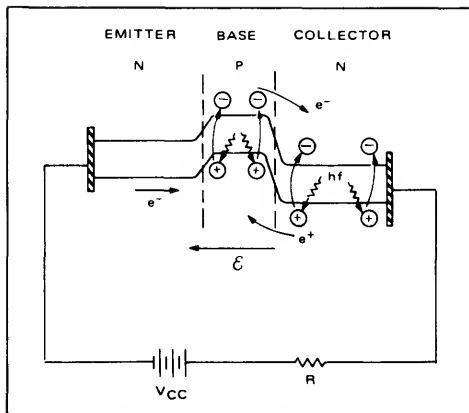


FIGURE 6 – Photoeffect in a Transistor

The model of the photo diode in Figure 5 might also be applied to the phototransistor, however, this would be severely limited in conveying the true characteristics of the transistor. A more useful and accurate model can be obtained by using the hybrid-pi model of the transistor and adding the photo-current generator between collector and base. This model appears in Figure 7.

Assuming a temperature of 25°C, and a radiation source at the wave length of peak response (i.e., $\delta = 1$), the following relations apply:

$$I_\lambda \approx SRCBO \cdot H, \quad (8a)$$

$$gm = 40 i_c, \text{ and} \quad (8b)$$

$$r_{be} = h_{fe}/gm, \quad (8c)$$

where SRCBO is the collector-base diode radiation sensitivity with open emitter,

gm is the forward transconductance,

i_c is the collector current, and

r_{be} is the effective base-emitter resistance.

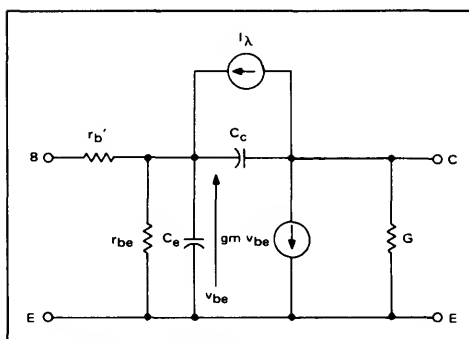


FIGURE 7 – Hybrid-pi Model of Phototransistor

In most cases $r'_b \ll r_{be}$, and can be neglected. The open-base operation is represented in Figure 8. Using this model, a feel for the high-frequency response of the device may be obtained by using the relationship

$$f_t \approx \frac{gm}{2\pi C_e}, \quad (9)$$

where f_t is the device current-gain-bandwidth product.

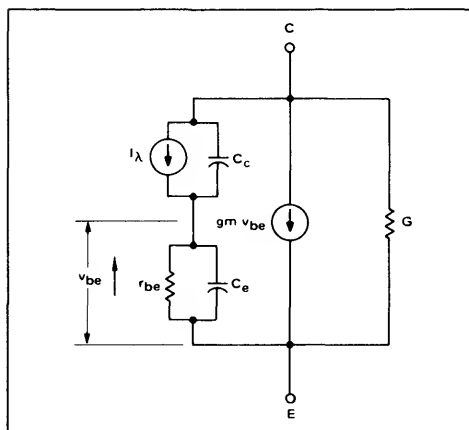


FIGURE 8 – Floating Base Approximate Model of Phototransistor

STATIC ELECTRICAL CHARACTERISTICS OF PHOTOTRANSISTORS

Spectral Response

As mentioned previously, the spectral response curve provides an indication of a device's ability to respond to radiation of different wave lengths. Figure 9 shows the spectral response for constant energy radiation for the Motorola MRD300 phototransistor series. As the figure indicates, peak response is obtained at about 8000 Å (Angstroms), or 0.8 μm.

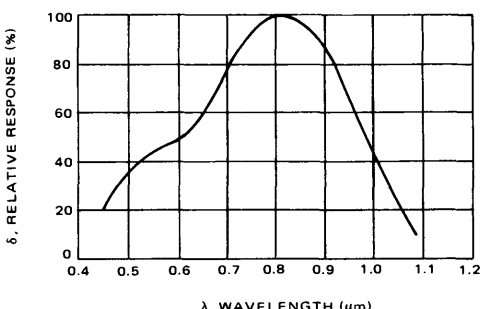


FIGURE 9 – Constant Energy Spectral Response for MRD300

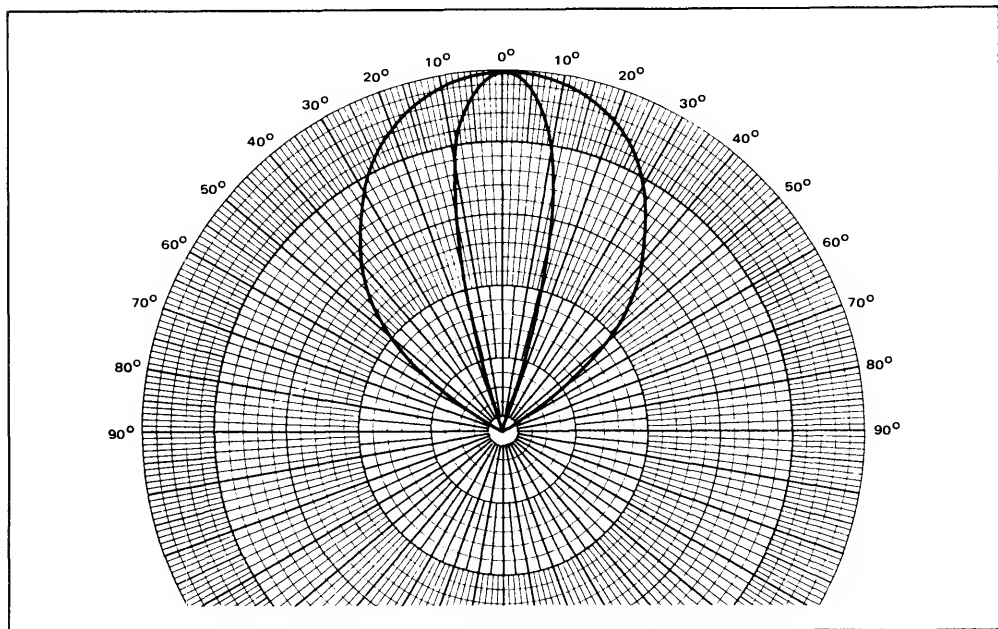


FIGURE 10 – Polar Response of MRD300. Inner Curve with Lens, Outer Curve with Flat Glass.

Angular Alignment

Lambert's law of illumination states that the illumination of a surface is proportional to the cosine of the angle between the normal to the surface and the direction of the radiation. Thus, the angular alignment of a phototransistor and radiation source is quite significant. The cosine proportionality represents an ideal angular response. The presence of an optical lens and the limit of window size further affect the response. This information is best conveyed by a polar plot of the device response. Such a plot in Figure 10 gives the polar response for the MRD300 series.

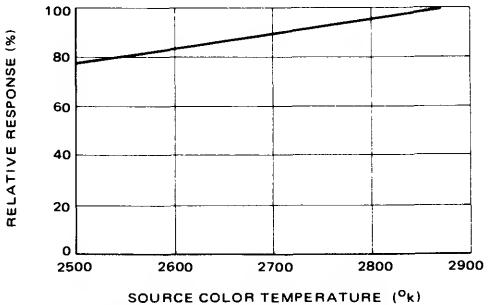


FIGURE 12 – Relative Response of MRD300 versus Color Temperature

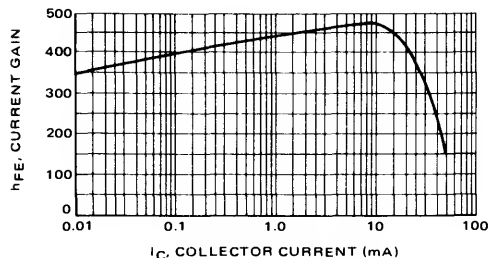


FIGURE 11 – DC Current Gain versus Collector Current

DC Current Gain

The sensitivity of a photo transistor is a function of the collector-base diode quantum efficiency and also of the dc current gain of the transistor. Therefore, the overall sensitivity is a function of collector current. Figure 11 shows the collector current dependence of dc current gain.

Color Temperature Response

In many instances, a photo transistor is used with a broad band source of radiation, such as an incandescent lamp. The response of the photo transistor is therefore dependent on the source color temperature. Incandescent

sources are normally operated at a color temperature of 2870°K, but, lower-color-temperature operation is not uncommon. It therefore becomes desirable to know the result of a color temperature difference on the photo sensitivity. Figure 12 shows the relative response of the MRD300 series as a function of color temperature.

Temperature Coefficient of I_p

A number of applications call for the use of phototransistors in temperature environments other than normal room temperature. The variation in photo current with temperature changes is approximately linear with a positive slope of about 0.667%/°C.

The magnitude of this temperature coefficient is primarily a result of the increase in h_{FE} versus temperature, since the collector-base photo current temperature coefficient is only about 0.1%/°C.

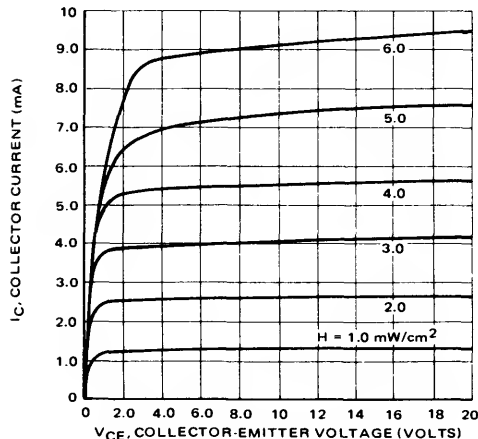


FIGURE 13 – Collector Characteristics for MRD300

Collector Characteristics

Since the collector current is primarily a function of impinging radiation, the effect of collector-emitter voltage, below breakdown, is small. Therefore, a plot of the I_C – V_{CE} characteristics with impinging radiation as a parameter, are very similar to the same characteristics with I_B as a parameter. The collector family for the MRD300 series appears in Figure 13.

Radiation Sensitivity

The capability of a given phototransistor to serve in a given application is quite often dependent on the radiation sensitivity of the device. The open-base radiation sensitivity for the MRD300 series is given in Figure 14. This indicates that the sensitivity is approximately linear with respect to impinging radiation. The additional capability of the MRD300 to be pre-biased gives rise to interest in the sensitivity as a function of equivalent base resistance. Figure 15 gives this relationship.

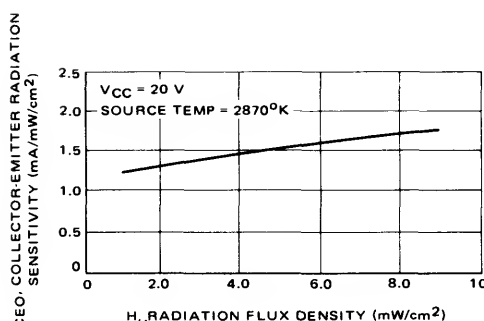


FIGURE 14 – Open Base Sensitivity versus Radiation for MRD300

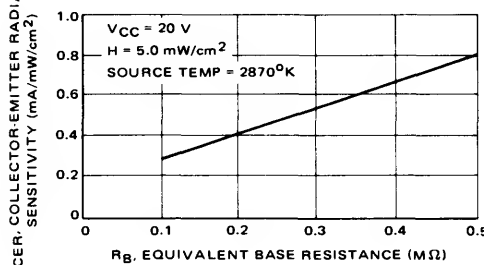


FIGURE 15 – Effect of Base Resistance on Sensitivity of MRD300

Capacitance

Junction capacitance is the significant parameter in determining the high frequency capability and switching speed of a transistor. The junction capacitances of the MRD300 as a function of junction voltages are given in Figure 16.

DYNAMIC CHARACTERISTICS OF PHOTOTRANSISTORS

Linearity

The variation of h_{FE} with respect to collector current results in a non-linear response of the photo transistor over

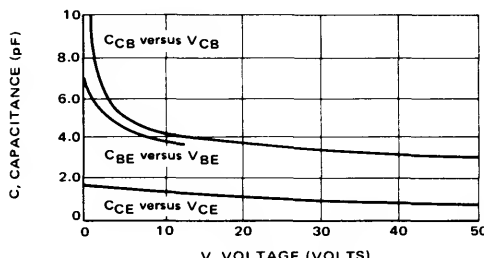


FIGURE 16 – Junction Capacitances versus Voltage for MRD300

large signal swings. However, the small-signal response is approximately linear. The use of a load line on the collector characteristic of Figure 13 will indicate the degree of linearity to be expected for a specific range of optical drive.

Frequency Response

The phototransistor frequency response, as referred to in the discussion of Figures 7 and 8, is presented in Figure 17. The device response is flat down to dc with the rolloff frequency dependent on the load impedance as well as on the device. The response is given in Figure 17 as the 3-dB frequency as a function of load impedance for two values of collector current.

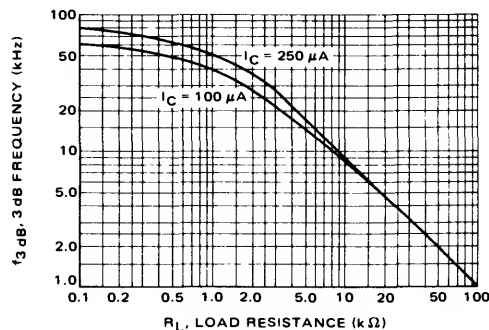


FIGURE 17 – 3 dB Frequency versus Load Resistance for MRD300

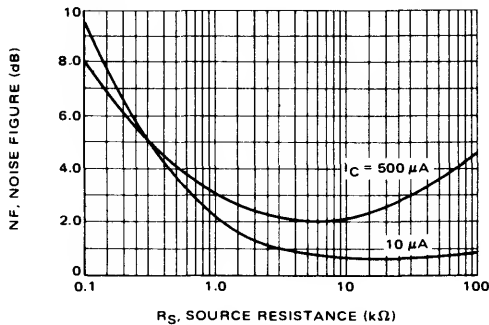


FIGURE 18 – MRD300 Noise Figure versus Source Resistance

Noise Figure

Although the usual operation of the phototransistor is in the floating base mode, a good qualitative feel for the device's noise characteristic can be obtained by measuring noise figure under standard conditions. The 1 kHz noise figure for the MRD300 is shown in Figure 18.

Small Signal h Parameters

As with noise figure, the small-signal h-parameters, measured under standard conditions, give a qualitative feel for

the device behavior. These are given as functions of collector current in Figure 19. With this information, the device can be analyzed in the standard hybrid model of Figure 20(a); by use of the conversions of Table I, the equivalent r-parameter model of Figure 20(b) can be used.

TABLE I – Parameter Conversions

$$h_{fb} = \frac{h_{fe}}{1 + h_{fe}}$$

$$r_c = \frac{h_{fe} + 1}{h_{oe}}$$

$$r_e = \frac{h_{re}}{h_{oe}}$$

$$r_b = h_{ie} - \frac{h_{re}(1 + h_{fe})}{h_{oe}}$$

SWITCHING CHARACTERISTICS OF PHOTOTRANSISTORS

In switching applications, two important requirements of a transistor are:

- (1) speed
- (2) ON voltage

Since some optical drives for phototransistors can provide fast light pulses, the same two considerations apply.

Switching Speed

If reference is made to the model of Figure 8, it can be seen that a fast rise in the current I_λ will not result in an equivalent instantaneous increase in collector-emitter current. The initial flow of I_λ must supply charging current to C_{CB} and C_{BE} . Once these capacitances have been charged, I_λ will flow through r_{be} . Then the current generator, $g_m \cdot V_{be}$, will begin to supply current. During turn-off, a similar situation occurs. Although I_λ may instantaneously drop to zero, the discharge of C_{CB} and C_{BE} through r_{be} will maintain a current flow through the collector. When the capacitances have been discharged, V_{be} will fall to zero and the current, $g_m \cdot V_{be}$, will likewise drop to zero. (This discussion assumes negligible leakage currents). These capacitances therefore result in turn-on and turn-off delays, and in rise and fall times for switching applications just as found in conventional bipolar switching transistors. And, just as with conventional switching, the times are a function of drive. Figure 21 shows the collector current (or drive) dependence of the turn-on delay and rise times. As indicated the delay time is dependent on the device only; whereas the rise-time is dependent on both the device and the load.

If a high-intensity source, such as a xenon flash lamp, is used for the optical drive, the device becomes optically saturated unless large optical attenuation is placed between source and detector. This can result in a significant storage time during the turn off, especially in the floating-base mode since stored charge has no direct path out of the

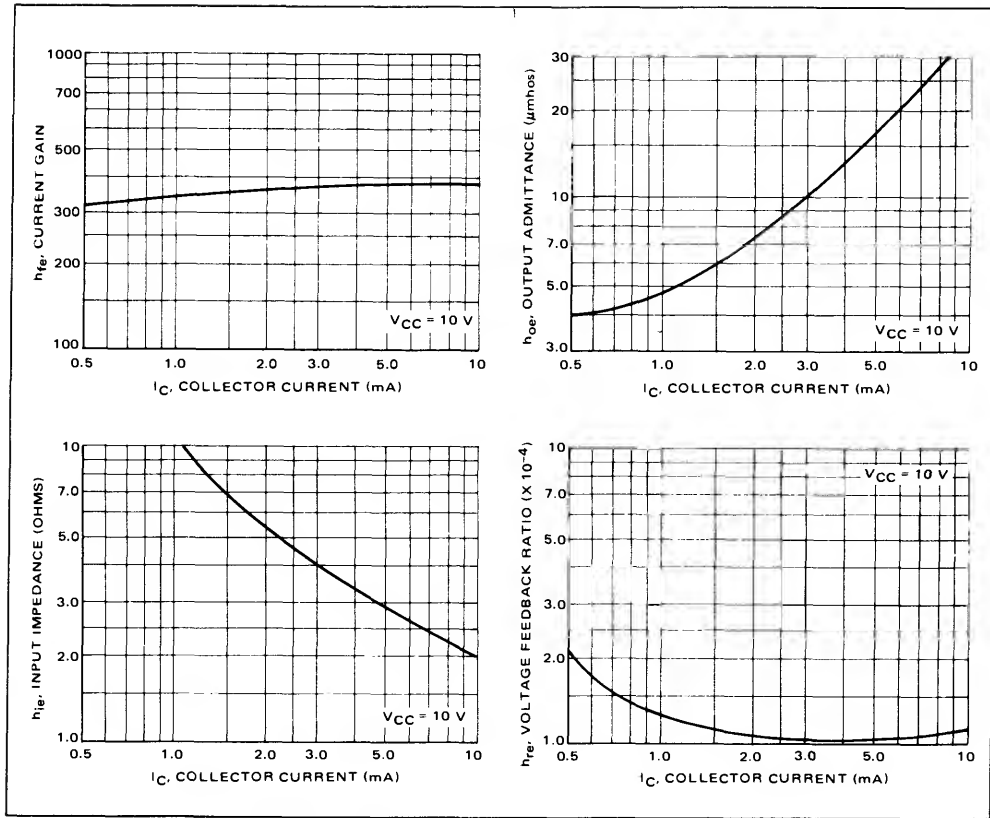


FIGURE 19 – 1 kHz h-Parameters versus Collector Current for MRD300

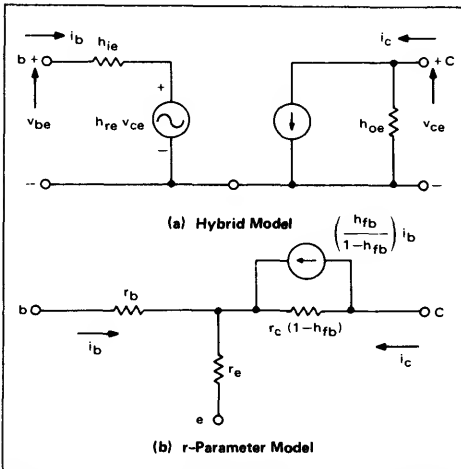


FIGURE 20 – Low Frequency Analytical Models of Phototransistor Without Photo Current Generator

base region. However, if a non-saturating source, such as a GaAs diode, is used for switching drive, the storage, or turn-off delay time is quite low as shown in Figure 22.

Saturation Voltage

An ideal switch has zero ON impedance, or an ON voltage drop of zero. The ON saturation voltage of the MRD300 is relatively low, approximately 0.2 volts. For a given collector current, the ON voltage is a function of drive, and is shown in Figure 23.

APPLICATIONS OF PHOTOTRANSISTORS

As mentioned previously, the phototransistor can be used in a wide variety of applications. Figure 24 shows two phototransistors in a series-shunt chopper circuit. As Q₁ is switched ON, Q₂ is OFF, and when Q₁ is switched OFF, Q₂ is driven ON.

Logic circuitry featuring the high input/output electrical isolation of photo transistors is shown in Figure 25.

Figure 26 shows a linear application of the phototransistor. As mentioned previously, the linearity is obtained for small-signal swings.

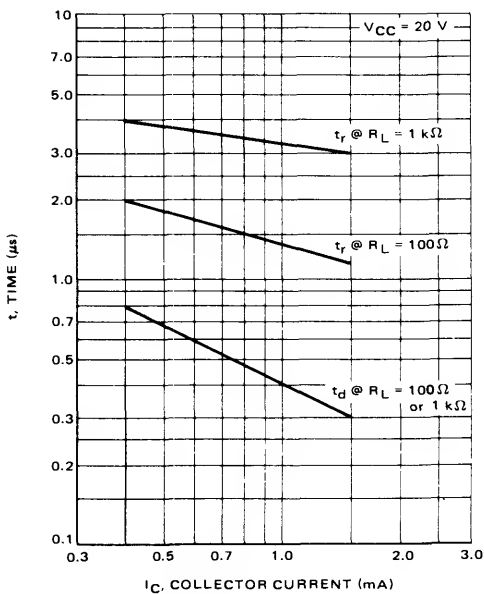


FIGURE 21 – Switching Delay and Rise Times for MRD300

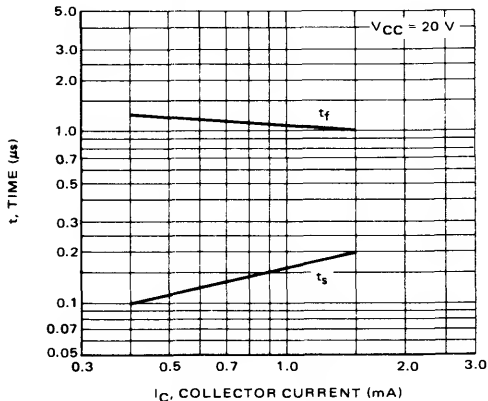


FIGURE 22 – Switching Storage and Fall Times for MRD300

A double-pole, single-throw relay is shown in Figure 27. In general, the phototransistor can be used in counting circuitry, level indications, alarm circuits, tachometers, and various process controls.

Conclusion

The phototransistor is a light-sensitive active device of moderately high sensitivity and relatively high speed. Its response is both a function of light intensity and wavelength, and behaves basically like a standard bipolar transistor with an externally controlled collector-base leakage current.

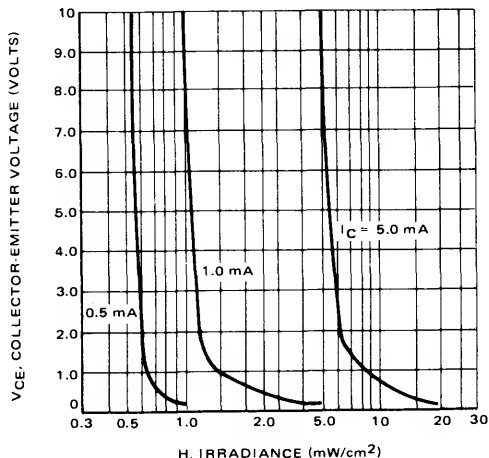


FIGURE 23 – Collector Emitter Saturation Voltage as a Function of Irradiance for MRD300

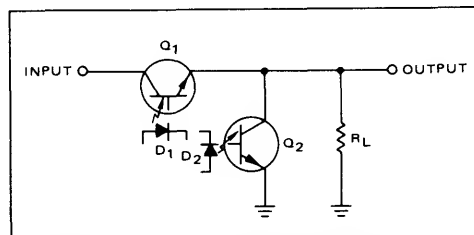


FIGURE 24 – Series-Shunt Chopper Circuit Using MRD300 Phototransistors and GaAs Light Emitting Diodes (LEDs)

APPENDIX I

Radiant energy covers a broad band of the electromagnetic spectrum. A relatively small segment of the band is the spectrum of visible light. A portion of the electromagnetic spectrum including the range of visible light is shown in Figure I-1.

The portion of radiant flux, or radiant energy emitted per unit time, which is visible is referred to as luminous flux. This distinction is due to the inability of the eye to respond equally to like power levels of different visible wavelengths. For example, if two light sources, one green and one blue are both emitting like wattage, the eye will perceive the green light as being much brighter than the blue. Consequently, when speaking of visible light of varying color, the watt becomes a poor measure of brightness. A more meaningful unit is the lumen. In order to obtain a clear understanding of the lumen, two other definitions are required.

The first of these is the standard source (Fig. I-2). The standard source, adopted by international agreement, con-

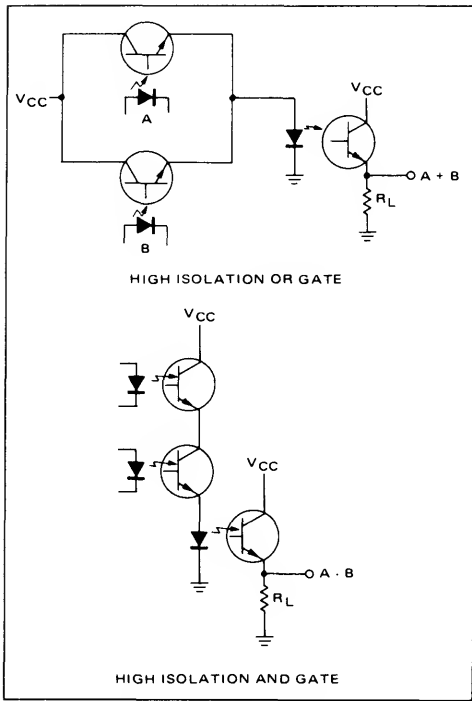


FIGURE 25 – Logic Circuits Using the MRD300 and LEDs

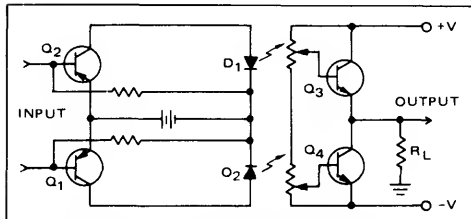


FIGURE 26 – Small Signal Linear Amplifier Using MRD300 and LEDs

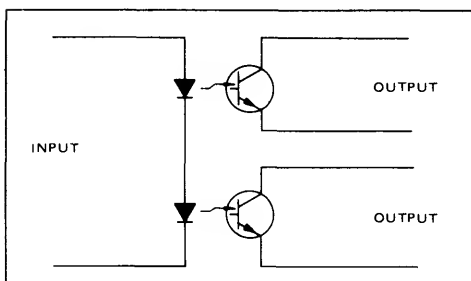


FIGURE 27 – DPST Relay Using MRD300s and LEDs

sists of a segment of fused thorium immersed in a chamber of platinum. When the platinum is at its melting point, the light emitted from the chamber approximates the radiation of a black body. The luminous flux emitted by the source is dependent on the aperture and cone of radiation. The cone of radiation is measured in terms of the solid angle.

The concept of a solid angle comes from spherical geometry. If a point is enclosed by a spherical surface and a set of radial lines define an area on the surface, the radial lines also subtend a solid angle. This angle, ω , is shown in Figure I-3, and is defined as

$$\omega = \frac{A}{r^2}, \quad (I-1)$$

where A is the described area and r is the spherical radius.

If the area A is equal to r^2 , then the solid angle subtended is one unit solid angle or one steradian, which is nothing more than the three-dimensional equivalent of a radian.

With the standard source and unit solid angle established, the lumen can be defined.

A lumen is the luminous flux emitted from a standard source and included within one steradian.

Using the concept of the lumen, it is now possible to define other terms of illumination.

Illuminance

If a differential amount of luminous flux, dF , is impinging on a differential area, dA , the illuminance, E , is given by

$$E = \frac{dF}{dA} \quad (I-2)$$

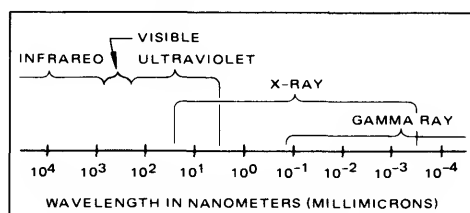


FIGURE I-1 – Portion of Electromagnetic Spectrum

Illuminance is most often expressed in lumens per square foot, or foot-candles. If the illuminance is constant over the area, (I-2) becomes

$$E = F/A. \quad (I-3)$$

Luminous Intensity

When the differential flux, dF , is emitted through a differential solid angle, $d\omega$, the luminous intensity, I , is given by

$$I = \frac{dF}{d\omega} \quad (I-4)$$

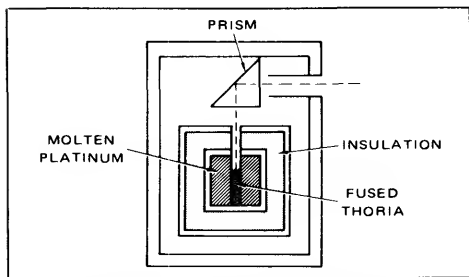


FIGURE I-2 – International Standard Source

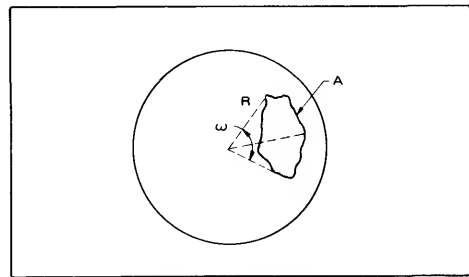


FIGURE I-3 – Solid Angle, ω

Luminous intensity is most often expressed in lumens per steradian or candela. If the luminous intensity is constant with respect to the angle of emission, (I-4) becomes:

$$I = \frac{F}{\omega} \quad (I-5)$$

If the wavelength of visible radiation is varied, but the illumination is held constant, the radiative power in watts will be found to vary. This again illustrates the poor quality of the watt as a measure of illumination. A relation between illumination and radiative power must then be specified at a particular frequency. The point of specification has been taken to be at a wavelength of $0.555 \mu\text{m}$, which is the peak of spectral response of the human eye. At this wavelength, 1 watt of radiative power is equivalent to 680 lumens.

APPENDIX II OPTOELECTRONIC DEFINITIONS

- F. Luminous Flux: Radiant flux of wavelength within the band of visible light.
- Lumen: The luminous flux emitted from a standard source and included within one steradian (solid angle equivalent of a radian).
- H. Radiation Flux Density (Irradiance): The total incident radiation energy measured in power per unit area (e.g., mW/cm^2).
- E. Luminous Flux Density (Illuminance): Radiation flux density of wavelength within the band of visible light. Measured in lumens/ ft^2 or foot candles. At the wavelength of peak response of the human eye, $0.555 \mu\text{m}$ ($0.555 \times 10^{-6} \text{m}$), 1 watt of radiative power is equivalent to 680 lumens.
- S_R. Radiation Sensitivity: The ratio of photo-induced current to incident radiant energy, the latter measured at the plane of the lens of the photo device.
- S_I. Illumination Sensitivity: The ratio of photo-induced current to incident luminous energy, the latter measured at the plane of the lens of the photo device.

Spectral Response: Sensitivity as a function of wavelength of incident energy. Usually normalized to peak sensitivity.

Constants

Planck's constant: $h = 4.13 \times 10^{-15} \text{ eV}\cdot\text{s}$.

electron charge: $q = 1.60 \times 10^{-19} \text{ coulomb}$.

velocity of light: $c = 3 \times 10^8 \text{ m/s}$.

Illumination Conversion Factors

| Multiply | By | To Obtain |
|-------------------------|-----------------------|------------------|
| lumens/ ft^2 | 1 | ft. candles |
| lumens/ ft^2 * | 1.58×10^{-3} | mW/cm^2 |
| candlepower | 4π | lumens |

*At $0.555 \mu\text{m}$.

BIBLIOGRAPHY AND REFERENCES

1. Fitchen, Franklin C., *Transistor Circuit Analysis and Design*, D. Van Nostrand Company, Inc., Princeton 1962.
2. Hunter, Lloyd P., ed., *Handbook of Semiconductor Electronics*, Sect 5., McGraw-Hill Book Co., Inc., New York 1962.
3. Jordan, A.G. and A.G. Milnes, "Photoeffect on Diffused PN Junctions with Integral Field Gradients", *IRE Transactions on Electron Devices*, October 1960.
4. Millman, Jacob, *Vacuum-tube and Semiconductor Electronics*, McGraw-Hill Book Co., Inc., New York 1958.
5. Sah, C.T., "Effect of Surface Recombination and Channel on PN Junction and Transistor Characteristics", *IRE Transactions on Electron Devices*, January 1962.
6. Sears, F.W. and M.W. Zemansky, *University Physics*, Addison-Wesley Publishing Co., Inc., Reading, Massachusetts 1962.
7. Shockley, William, *Electrons and Holes in Semiconductors*, D. Van Nostrand Company, Inc., Princeton 1955.

APPLICATIONS OF PHOTOTRANSISTORS IN ELECTRO-OPTIC SYSTEMS

INTRODUCTION

A phototransistor is a device for controlling current flow with light. Basically, any transistor will function as a phototransistor if the chip is exposed to light, however, certain design techniques are used to optimize the effect in a phototransistor.

Just as phototransistors call for special design techniques, so do the circuits that use them. The circuit designer must supplement his conventional circuit knowledge with the terminology and relationships of optics and radiant energy. This note presents the information necessary to supplement that knowledge. It contains a short review of phototransistor theory and characteristics, followed by a detailed discussion of the subjects of irradiance, illuminance, and optics and their significance to phototransistors. A distinction is made between low-frequency/steady-state design and high-frequency design. The use of the design information is then demonstrated with a series of typical electro-optic systems.

PHOTOTRANSISTOR THEORY¹

Phototransistor operation is a result of the photo-effect in solids, or more specifically, in semiconductors. Light of a proper wavelength will generate hole-electron pairs within the transistor, and an applied voltage will cause these carriers to move, thus causing a current to flow. The intensity of the applied light will determine the number of carrier pairs generated, and thus the magnitude of the resultant current flow.

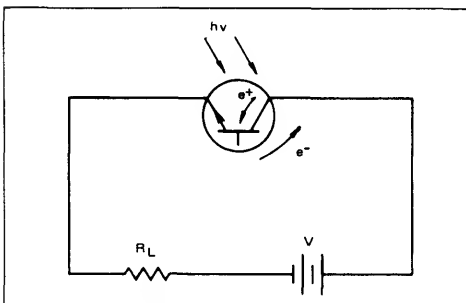


FIGURE 1 – Photo-Generated Carrier Movement
in a Phototransistor

In a phototransistor the actual carrier generation takes place in the vicinity of the collector-base junction. As shown in Figure 1 for an NPN device, the photo-generated holes will gather in the base. In particular, a hole generated in the base will remain there, while a hole generated in the collector will be drawn into the base by the strong field at the junction. The same process will result in electrons tending to accumulate in the collector. Charge will not really accumulate however, and will try to evenly distribute throughout the bulk regions. Consequently, holes will diffuse across the base region in the direction of the emitter junction. When they reach the junction they will be injected into the emitter. This in turn will cause the emitter to inject electrons into the base. Since the emitter injection efficiency is much larger than the base injection efficiency, each injected hole will result in many injected electrons.

It is at this point that normal transistor action will occur. The emitter injected electrons will travel across the base and be drawn into the collector. There, they will combine with the photo-induced electrons in the collector to appear as the terminal collector current.

Since the actual photogeneration of carriers occurs in the collector base region, the larger the area of this region, the more carriers are generated, thus, as Figure 2 shows, the transistor is so designed to offer a large area to impinging light.

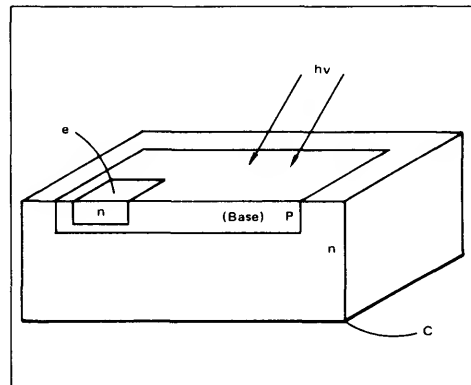


FIGURE 2 – Typical Double-Diffused Phototransistor Structure

¹ For a detailed discussion see Motorola Application Note AN-440, "Theory and Characteristics of Phototransistors."

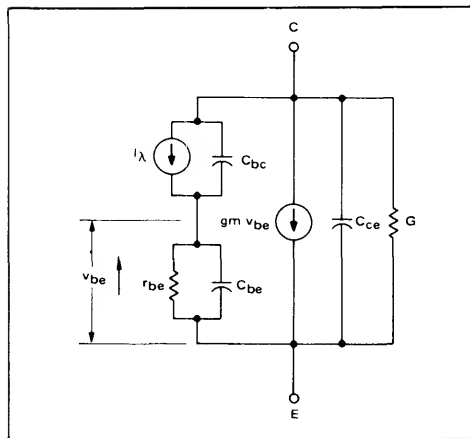


FIGURE 3 – Floating Base Approximate Model of Phototransistor

PHOTOTRANSISTOR STATIC CHARACTERISTICS

A phototransistor can be either a two-lead or a three-lead device. In the three-lead form, the base is made electrically available, and the device may be used as a standard bipolar transistor with or without the additional capability of sensitivity to light. In the two-lead form the base is not electrically available, and the transistor can only be used with light as an input. In most applications, the only drive to the transistor is light, and so the two-lead version is the most prominent.

As a two-lead device, the phototransistor can be modeled as shown in Figure 3. In this circuit, current generator I_λ represents the photo generated current and is approximately given by

$$I_\lambda = \eta F q A \quad (1)$$

where

η is the quantum efficiency or ratio of current carriers to incident photons,

F is the fraction of incident photons transmitted by the crystal,

q is the electronic charge, and

A is the active area.

The remaining elements should be recognized as the component distribution in the hybrid-pi transistor model. Note that the model of Figure 3 indicates that under dark conditions, I_λ is zero and so v_{be} is zero. This means that the terminal current $I \approx gm v_{be}$ is also zero.

In reality there is a thermally generated leakage current, I_0 , which shunts I_λ . Therefore, the terminal current will be non-zero. This current, I_{CEO} , is typically on the order of 10 nA at room temperature and may in most cases be neglected.

As a three lead device, the model of Figure 3 need only have a resistance, r_b' , connected to the junction of C_{bc} and C_{be} . The other end of this resistance is the base terminal. As mentioned earlier, the three lead phototransistor is less common than the two lead version. The only advantages of having the base lead available are to stabilize the device operation for significant temperature excursions, or to use the base for unique circuit purposes.

Mention is often made of the ability to optimize a phototransistor's sensitivity by using the base. The idea is that the device can be electrically biased to a collector current at which hFE is maximum. However, the introduction of any impedance into the base results in a net decrease in photo sensitivity. This is similar to the effect noticed when I_{CEO} is measured for a transistor and found to be greater than I_{CER} . The base-emitter resistor shunts some current around the base-emitter junction, and the shunted current is never multiplied by hFE .

Now when the phototransistor is biased to peak hFE , the magnitude of base impedance is low enough to shunt an appreciable amount of photo current around the base-emitter. The result is actually a lower device sensitivity than found in the open base mode.

Spectral Response – As mentioned previously, a transistor is sensitive to light of a proper wavelength. Actually, response is found for a range of wavelengths. Figure 4 shows the normalized response for a typical phototransistor series (Motorola MRD devices) and indicates that peak response occurs at a wavelength of 0.8 μm . The warping in the response curve in the vicinity of 0.6 μm results from adjoining bands of constructive and destructive interference in the SiO_2 layer covering the transistor surface.

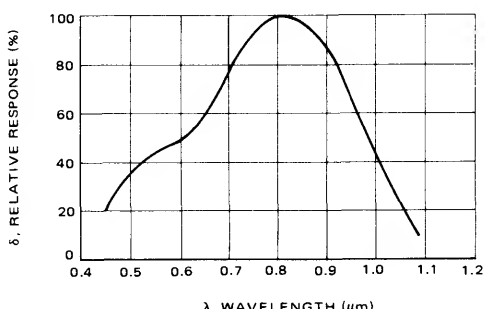


FIGURE 4 – Constant Energy Spectral Response for MRD Phototransistor Series

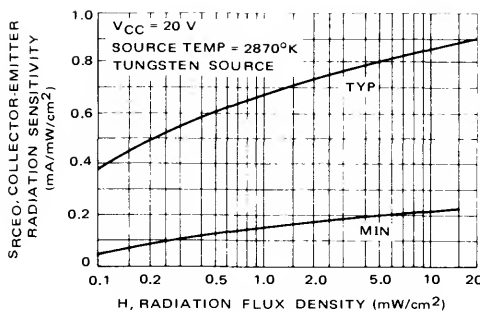


FIGURE 5 – Radiation Sensitivity for MRD450

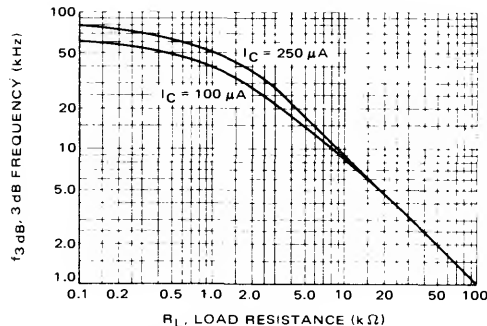


FIGURE 7 – 3 dB Frequency versus Load Resistance for MRD Phototransistor Series

Radiation Sensitivity – The absolute response of the MRD450 phototransistor to impinging radiation is shown in Figure 5. This response is standardized to a tungsten source operating at a color temperature of 2870°K. As subsequent discussion will show, the transistor sensitivity is quite dependent on the source color temperature.

Additional static characteristics are discussed in detail in AN-440, and will not be repeated here.

LOW-FREQUENCY AND STEADY-STATE DESIGN APPROACHES

For relatively simple circuit designs, the model of Figure 3 can be replaced with that of Figure 6. The justification for eliminating consideration of device capacitance is based on restricting the phototransistor's use to d.c. or low frequency applications. The actual frequency range of validity is also a function of load resistance. For example, Figure 7 shows a plot of the 3 dB response frequency as a function of load resistance.

Assume a modulated light source is to drive the phototransistor at a maximum frequency of 10 kHz. If the resultant photo current is 100 μA, Figure 7 shows a 3-dB frequency of 10 kHz at a load resistance of 8 kilohms. Therefore, in this case, the model of Figure 6 can be used with acceptable results for a load less than 8

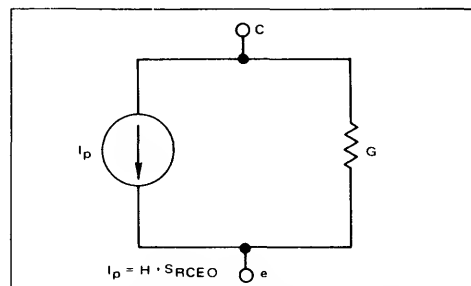


FIGURE 6 – Low-Frequency and Steady-State Model for Floating-Base Phototransistor

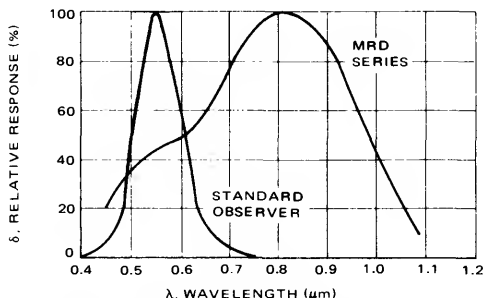


FIGURE 8 – Spectral Response for Standard Observer and MRD Series

kilohms. For larger loads, the hybrid-pi model must be used.

For the remainder of the discussion of low frequency and steady state design, it is assumed that the simplified model of Figure 6 is valid.

RADIATION AND ILLUMINATION SOURCES

The effect of a radiation source on a photo-transistor is dependent on the transistor spectral response and the spectral distribution of energy from the source. When discussing such energy, two related sets of terminology are available. The first is radiometric which is a physical system; the second is photometric which is a physiological system.

The photometric system defines energy relative to its visual effect. As an example, light from a standard 60 watt-bulb is certainly visible, and as such, has finite photometric quantity, whereas radiant energy from a 60-watt resistor is not visible and has zero photometric quantity. Both items have finite radiometric quantity.

The defining factor for the photometric system is the spectral response curve of a standard observer. This is shown in Figure 8 and is compared with the spectral response of the MRD series. The defining spectral response of the radiometric system can be imagined as unit response for all wavelengths.

A comparison of the terminology for the two systems is given in Table I.

There exists a relationship between the radiometric and photometric quantities such that at a wavelength of 0.55 μm , the wavelength of peak response for a standard observer, one watt of radiant flux is equal to 680 lumens of luminous flux. For a broadband of radiant flux, the visually effective, or photometric flux is given by:

$$F = K \int P(\lambda) \delta(\lambda) d\lambda \quad (2a)$$

where

K is the proportionality constant (of 680 lumens/watt),

$P(\lambda)$ is the absolute spectral distribution of radiant flux,

$\delta(\lambda)$ is the relative response of the standard observer,

and

$d\lambda$ is the differential wavelength,

A similar integral can be used to convert incident radiant flux density, or irradiance, to illuminance:

$$E = K \int H(\lambda) \delta(\lambda) d\lambda \quad (2b)$$

In Equation(2b) if $H(\lambda)$ is given in watts/ cm^2 , E will be in lumens/ cm^2 . To obtain E in footcandles (lumens/ ft^2), the proportionality constant becomes

$$K = 6.3 \times 10^5 \text{ footcandles/mW/cm}^2$$

Fortunately, it is usually not necessary to perform the above integrations. The photometric effect of a radiant source can often be measured directly with a photometer.

Unfortunately, most phototransistors are specified for use with the radiometric system. Therefore, it is often necessary to convert photometric source data, such as the candle power rating of an incandescent lamp to radiometric data. This will be discussed shortly.

GEOMETRIC CONSIDERATIONS

In the design of electro-optic systems, the geometrical relationships are of prime concern. A source will effectively appear as either a point source, or an area source, depending upon the relationship between the size of the source and the distance between the source and the detector.

Point Sources — A point source is defined as one for which the source diameter is less than ten percent of the distance between the source and the detector, or,

$$\alpha < 0.1r, \quad (3)$$

where

α is the diameter of the source, and

r is the distance between the source and the detector.

Figure 9 depicts a point source radiating uniformly in every direction. If equation (3) is satisfied, the detector area, AD , can be approximated as a section of the area of a sphere of radius r whose center is the point source.

The solid angle, ω , in steradians² subtended by the detector area is

$$\omega = \frac{AD}{r^2} \quad (4)$$

Since a sphere has a surface area of $4\pi r^2$, the total solid angle of a sphere is

$$\omega_S = \frac{4\pi r^2}{r^2} = 4\pi \text{ steradians.}$$

Table II lists the design relationships for a point source in terms of both radiometric and photometric quantities.

The above discussion assumes that the photodetector is aligned such that its surface area is tangent to the sphere with the point source at its center. It is entirely possible that the plane of the detector can be inclined from the

TABLE I — Radiometric and Photometric Terminology

| Description | Radiometric | Photometric |
|---|--|---|
| Total Flux | Radiant Flux, P , in Watts | Luminous Flux, F , in Lumens |
| Emitted Flux Density at a Source Surface | Radiant Emissance, W , in Watts/cm ² | Luminous Emissance, L , in Lumens/ft ² (foot lamberts), or lumens/cm ² (Lamberts) |
| Source Intensity (Point Source) | Radiant Intensity, I_r , in Watts/Steradian | Luminous Intensity, I_L , in Lumens/Steradian (Candela) |
| Source Intensity (Area Source) | Radiance, B_r , in (Watts/Steradian)/cm ² | Luminance, B_L , in (Lumens/Steradian)/ft ² (footlambert) |
| Flux Density Incident on a Receiver Surface | Irradiance, H , in Watts/cm ² | Illuminance, E , in Lumens/ft ² (footcandle) |

TABLE II — Point Source Relationships

| Description | Radiometric | Photometric |
|-----------------------------------|--|--|
| Point Source Intensity | I_r , Watts/Steradian | I_L , Lumens/Steradian |
| Incident Flux Density | H (Irradiance) = $\frac{I_r}{r^2}$, watts/distance ² | E (Illuminance) = $\frac{I_L}{r^2}$, lumens/distance ² |
| Total Flux Output of Point Source | $P = 4\pi I_r$, Watts | $F = 4\pi I_L$, Lumens |

TABLE III — Design Relationships for an Area Source

| Description | Radiometric | Photometric |
|-----------------------|---|--|
| Source Intensity | B_r , Watts/cm ² /steradian | B_L , Lumens/cm ² /steradian |
| Emitted Flux Density | $W = \pi B_r$, Watts/cm ² | $L = \pi B_L$, Lumens/cm ² |
| Incident Flux Density | $H = \frac{B_r A_s}{r^2 + (\frac{D}{2})^2}$, Watts/cm ² | $E = \frac{B_L A_s}{r^2 + (\frac{D}{2})^2}$, Lumens/cm ² |

²Steradian: The solid equivalent of a radian.

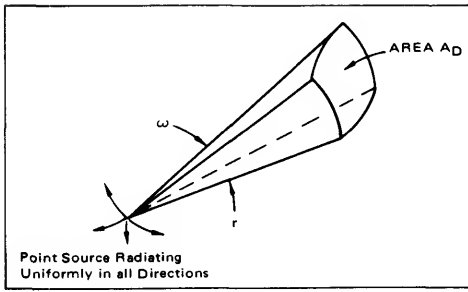


FIGURE 9 – Point Source Geometry

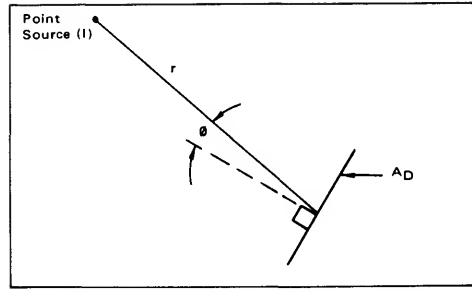


FIGURE 10 – Detector Not Normal to Source Direction

tangent plane. Under this condition, as depicted in Figure 10, the incident flux density is proportional to the cosine of the inclination angle, ϕ . Therefore,

$$H = \frac{I_r}{r^2} \cos \phi, \text{ and} \quad (5a)$$

$$E = \frac{I_L}{r^2} \cos \phi. \quad (5b)$$

AREA SOURCES

When the source has a diameter greater than 10 percent of the separation distance,

$$\alpha \gg 1/r, \quad (6)$$

it is considered to be an area source. This situation is shown in Figure 11. Table III lists the design relationships for an area source.

A special case that deserves some consideration occurs when

$$\frac{\alpha}{2} \gg r, \quad (7)$$

that is, when the detector is quite close to the source. Under this condition,

$$H = \frac{B_r A_s}{r^2 + \left(\frac{\alpha}{2}\right)^2} \approx \frac{B_r A_s}{\left(\frac{\alpha}{2}\right)^2}, \quad (8)$$

but, the area of the source,

$$A_s = \pi \left(\frac{\alpha}{2}\right)^2, \quad (9)$$

Therefore,

$$H \approx B_r \pi = W, \quad (10)$$

That is, the emitted and incident flux densities are equal. Now, if the area of the detector is the same as the area of the source, and equation (7) is satisfied, the total incident energy is approximately the same as the total

radiated energy, that is, unity coupling exists between source and detector.

LENS SYSTEMS

A lens can be used with a photodetector to effectively increase the irradiance on the detector. As shown in Figure 12a, the irradiance on a target surface for a point source of intensity, I , is

$$H = I/d^2, \quad (11)$$

where d is the separation distance.

In Figure 12b a lens has been placed between the source and the detector. It is assumed that the distance d' from the source to the lens is approximately equal to d :

$$d' \approx d, \quad (12)$$

and the solid angle subtended at the source is sufficiently small to consider the rays striking the lens to be parallel.

If the photodetector is circular in area, and the distance from the lens to the detector is such that the image of the source exactly fills the detector surface area, the radiant flux on the detector (assuming no lens loss) is

$$P_D = P_L = H' \pi r_L^2, \quad (13)$$

where

P_D is the radiant flux incident on the detector,

P_L is the radiant flux incident on the lens,

H' is the flux density on the lens, and

r_L is the lens radius.

Using equation (12),

$$H' = I/d^2 = H. \quad (14)$$

The flux density on the detector is

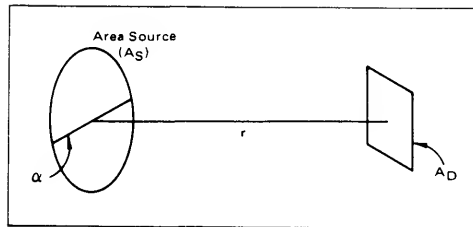


FIGURE 11 – Area Source Geometry

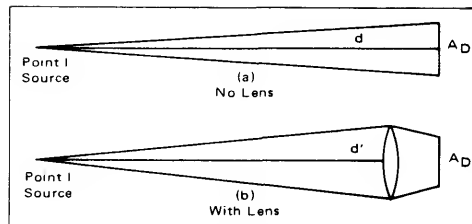


Figure 12 – Use of a Lens to Increase Irradiance on a Detector

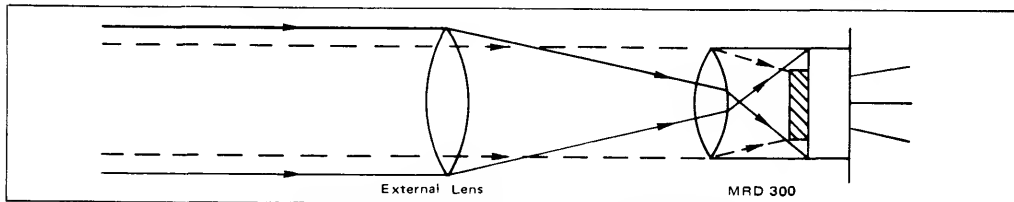


FIGURE 13 – Possible Misalignment Due to Arbitrary Use of External Lens Dotted Rays Indicate Performance Without External Lens

$$H_D = P_D / A_D, \quad (15)$$

where A_D is the detector area, given by

$$A_D = \pi r_d^2. \quad (16)$$

Using (13), (14), and (16) in (15) gives

$$H_D = \frac{1}{d^2} \left(\frac{r_L}{r_d} \right)^2 \quad (17)$$

Now dividing (17) by (11) gives the ratio of irradiance on the detector with a lens to the irradiance without a lens.

$$\frac{H_D}{H} = \frac{\frac{1}{d^2} \left(\frac{r_L}{r_d} \right)^2}{\frac{I}{d^2}} = \left(\frac{r_L}{r_d} \right)^2. \quad (18)$$

As (18) shows, if the lens radius is greater than the detector radius, the lens provides an increase in incident irradiance on the detector. To account for losses in the lens, the ratio is reduced by about ten percent.

$$R = 0.9 \left(\frac{r_L}{r_d} \right)^2 \quad (19)$$

where R is the gain of the lens system.

It should be pointed out that arbitrary placement of a lens may be more harmful than helpful. That is, a lens system must be carefully planned to be effective.

For example, the MRD300 phototransistor contains a lens which is effective when the input is in the form of parallel rays (as approximated by a uniformly radiating point source). Now, if a lens is introduced in front of the MRD300 as shown in Figure 13, it will provide a non-

parallel ray input to the transistor lens. Thus the net optical circuit will be misaligned. The net irradiance on the phototransistor chip may in fact be less than without the external lens. The circuit of Figure 14 does show an effective system. Lens 1 converges the energy incident on its surface to lens 2 which reconverts this energy into parallel rays. The energy entering the phototransistor lens as parallel rays is the same (neglecting losses) as that entering lens 1. Another way of looking at this is to imagine that the phototransistor surface has been increased to a value equal to the surface area of lens 1.

FIBER OPTICS

Another technique for maximizing the coupling between source and detector is to use a fiber bundle to link the phototransistor to the light source. The operation of fiber optics is based on the principle of total internal reflection.

Figure 15 shows an interface between two materials of different indices of refraction. Assume that the index of refraction, n , of the lower material is greater than that, n' , of the upper material. Point P represents a point source of light radiating uniformly in all directions. Some rays from P will be directed at the material interface.

At the interface, Snell's law requires:

$$n \sin \theta = n' \sin \theta', \quad (20)$$

where

θ is the angle between a ray in the lower material and the normal to the interface,

and

θ' is the angle between a refracted ray and the normal.

Rearranging (20),

$$\sin \theta' = \frac{n}{n'} \sin \theta. \quad (21)$$

By assumption, n/n' is greater than one, so that

$$\sin \theta' > \sin \theta. \quad (22)$$

However, since the maximum value of $\sin \theta'$ is one and occurs when θ' is 90° , θ' will reach 90° before θ does. That is, for some value of θ , defined as the critical angle, θ_C , rays from P do not cross the interface. When $\theta > \theta_C$, the rays are reflected entirely back into the lower material, or total internal reflection occurs.

Figure 16 shows the application of this principle to fiber optics. A glass fiber of refractive index n is clad with a layer of glass of lower refractive index, n' . A ray of light entering the end of the cable will be refracted as shown. If, after refraction, it approaches the glass interface at an angle greater than θ_C , it will be reflected within the fiber. Since the angle of reflection must equal the angle of incidence, the ray will bounce down the fiber and emerge, refracted, at the exit end.

The numerical aperture, NA, of a fiber is defined as the sin of the half angle of acceptance. Application of Snell's law at the interface for θ_C , and again at the fiber end will give

$$NA \equiv \sin \phi = \sqrt{n^2 - n'^2}. \quad (23)$$

For total internal reflection to occur, a light ray must enter the fiber within the half angle ϕ .

Once a light ray is within the fiber, it will suffer some attenuation. For glass fibers, an absorption rate of from five to ten per cent per foot is typical. There is also an entrance and exit loss at the ends of the fiber which typically result in about a thirty per cent loss.

As an example, an illuminance E at the source end of a three-foot fiber bundle would appear at the detector as

$$E_D = 0.7 E e^{-aL} = 0.7 E e^{-(0.1)(3)} = 0.51 E, \quad (24)$$

where E is the illuminance at the source end,

E_D is the illuminance at the detector end,

a is the absorption rate, and

L is the length.

This assumes an absorption loss of ten percent per foot.

TUNGSTEN LAMPS

Tungsten lamps are often used as radiation sources for photodetectors. The radiant energy of these lamps is distributed over a broad band of wavelengths. Since the eye and the phototransistor exhibit different wavelength-dependent response characteristics, the effect of a tungsten lamp will be different for both. The spectral output of a tungsten lamp is very much a function of color temperature.

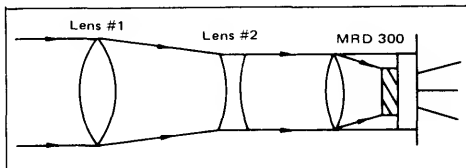


FIGURE 14 – Effective Use of External Optics with the MRD 300

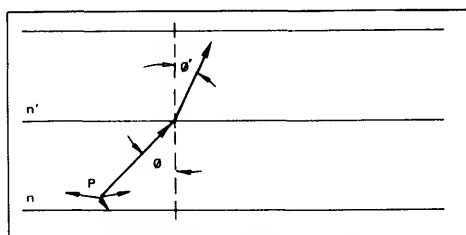


FIGURE 15 – Ray Refraction at an Interface

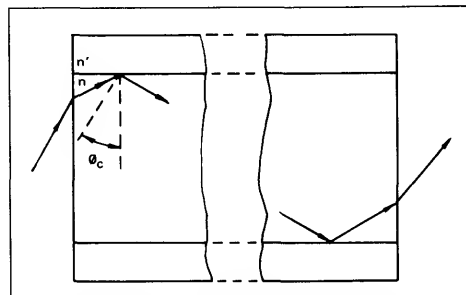


FIGURE 16 – Refraction in an Optical Fiber

Color temperature of a lamp is the temperature required by an ideal blackbody radiator to produce the same visual effect as the lamp. At low color temperatures, a tungsten lamp emits very little visible radiation. However, as color temperature is increased, the response shifts toward the visible spectrum. Figure 17 shows the spectral distribution of tungsten lamps as a function of color temperature. The lamps are operated at constant wattage and the response is normalized to the response at 2800°K . For comparison, the spectral response for both the standard observer and the MRD phototransistor series are also plotted. Graphical integration of the product of the standard observer response and the pertinent source distribution from Figure 17 will provide a solution to equations (2a) and (2b).

Effective Irradiance – Although the sensitivity of a photodetector to an illuminant source is frequently provided, the sensitivity to an irradiant source is more common. Thus, it is advisable to carry out design work in

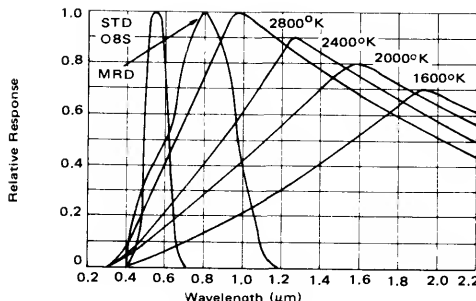


FIGURE 17 – Radiant Spectral Distribution of Tungsten Lamp

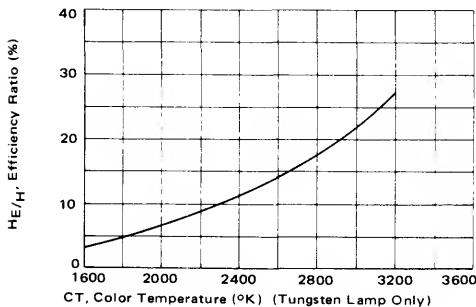


FIGURE 18 – MRD Irradiance Ratio versus Color Temperature

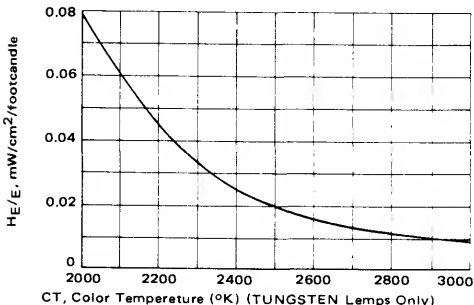


FIGURE 19 – MRD Irradiance/Illuminance Ratio versus Color Temperature

terms of irradiance. However, since the spectral response of a source and a detector are, in general, not the same, a response integration must still be performed. The integral is similar to that for photometric evaluation.

$$PE = \int P(\lambda) Y(\lambda) d\lambda \quad (25)$$

where

PE is the effective radiant flux on the detector, $P(\lambda)$ is the spectral distribution of source flux

and

$Y(\lambda)$ is the spectral response of the detector.

Again, such an integration is best evaluated graphically. In terms of flux density, the integral is

$$HE = \int H(\lambda) Y(\lambda) d\lambda \quad (26)$$

where HE is the effective flux density (irradiance) on the detector
and $H(\lambda)$ is the absolute flux density distribution of the source on the detector.

Graphical integration of equations (2b) and (26) has been performed for the MRD series of phototransistors for several values of lamp color temperature. The results are given in Figures 18 and 19 in terms of ratios. Figure 18 provides the irradiance ratio, HE/H versus color temperature. As the curve shows, a tungsten lamp operating at 2600°K is about 14% effective on the MRD series devices. That is, if the broadband irradiance of such a lamp is measured at the detector and found to be 20 mW/cm^2 , the transistor will effectively see

$$HE = 0.14 (20) = 2.8 \text{ mW/cm}^2 \quad (27)$$

The specifications for the MRD phototransistor series include the correction for effective irradiance. For example, the MRD450 is rated for a typical sensitivity of 0.8 mA/mW/cm^2 . This specification is made with a tungsten source operating at 2870°K and providing an irradiance at the transistor of 5.0 mW/cm^2 . Note that this will result in a current flow of 4.0 mA.

However, from Figure 18, the effective irradiance is

$$HE = (5.0)(.185) = 0.925 \text{ mW/cm}^2 \quad (28)$$

By using this value of HE and the typical sensitivity rating it can be shown that the device sensitivity to a monochromatic irradiance at the MRD450 peak response of $0.8 \mu\text{m}$ is

$$S = \frac{IC}{HE} = \frac{4.0 \text{ mA}}{0.925 \text{ mW/cm}^2} = 4.33 \text{ mA/mW/cm}^2 \quad (29)$$

Now, as shown previously, an irradiance of 20 mW/cm^2 at a color temperature of 2600°K looks like monochromatic irradiance at $0.8 \mu\text{m}$ of 2.8 mW/cm^2 (Equation 27). Therefore, the resultant current flow is

$$I = S HE (4.33)(2.8) = 12.2 \text{ mA} \quad (30)$$

An alternate approach is provided by Figure 20. In this figure, the relative response as a function of color temperature has been plotted. As the curve shows, the response is down to 83% at a color temperature of 2600°K. The specified typical response for the MRD450 at 20 mW/cm^2 for a 2870°K tungsten source is 0.9 mA/mW/cm^2 . The current flow at 2600°K and 20 mW/cm^2 is therefore

$$I = (0.83)(0.9)(20) = 14.9 \text{ mA} \quad (31)$$

This value agrees reasonably well with the result obtained in Equation 30. Similarly, Figure 19 will show that a current flow of 6.67 mA will result from an illuminance of 125 foot candles at a color temperature of 2600°K.

Determination of Color Temperature – It is very likely that a circuit designer will not have the capability to measure color temperature. However, with a voltage measuring capability, a reasonable approximation of color temperature may be obtained. Figure 21 shows the classical variation of lamp current, candlepower and lifetime for a tungsten lamp as a function of applied voltage. Figure 22 shows the variation of color temperature as a function of the ratio

$$\rho = \frac{\text{MSCP}}{\text{WATT}} \quad (32)$$

where

MSCP is the mean spherical candlepower at the lamp operating point and WATT is the lamp IV product at the operating point.

As an example, suppose a type 47 indicator lamp is used as a source for a phototransistor. To extend the lifetime, the lamp is operated at 80% of rated voltage.

| Lamp | Rated Volts | Rated Current | MSCP |
|------|-------------|---------------|-------------|
| 47 | 6.3V | 150 mA | 0.52 approx |

Geometric Considerations – The candlepower ratings on most lamps are obtained from measuring the total lamp output in an integrating sphere and dividing by the unit solid angle. Thus the rating is an average, or mean-spherical-candlepower. However, a tungsten lamp cannot radiate uniformly in all directions, therefore, the candlepower varies with the lamp orientation. Figure 23 shows the radiation pattern for a typical frosted tungsten lamp. As shown, the maximum radiation occurs in the horizontal direction for a base-down or base-up lamp. The circular curve simulates the output of a uniform radiator, and contains the same area as the lamp polar plot. It indicates that the lamp horizontal output is about 1.33

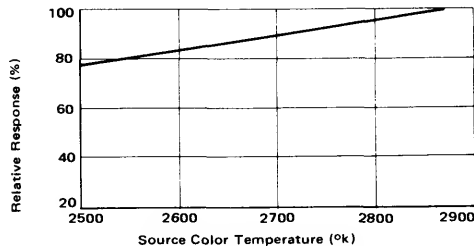


FIGURE 20 – Relative Response of MRD Series versus Color Temperature

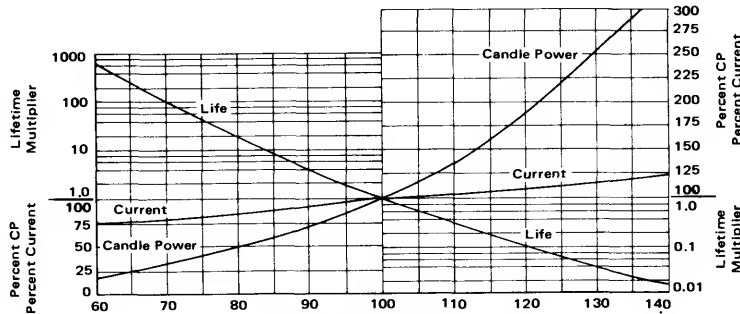


FIGURE 21 – Tungsten Lamp Parameter Variations versus Variations about Rated Voltage

From Figure 21 for 80% rated voltage,
 (Rated Current) (Percent current) = (.15)(0.86) = 0.129 ampere
 (Rated CP) (Percent CP) = (0.5)(0.52) = 0.26 CP
 (Rated Voltage) (Percent Voltage) = (6.3)(0.8) = 5.05 V

$$\text{WATTS} = (5.05)(0.129) = 0.65$$

$$\rho = \frac{0.26}{0.65} = 0.4,$$

From Figure 22, for $\rho = 0.4$,

$$CT = 2300^{\circ}\text{K},$$

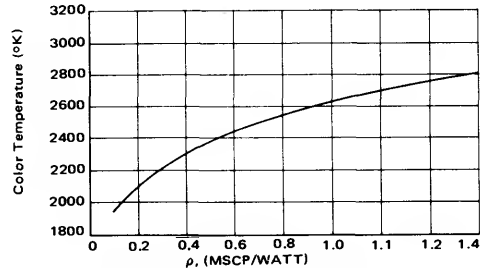


FIGURE 22 – Color Temperature versus Candle Power/Power Ratio

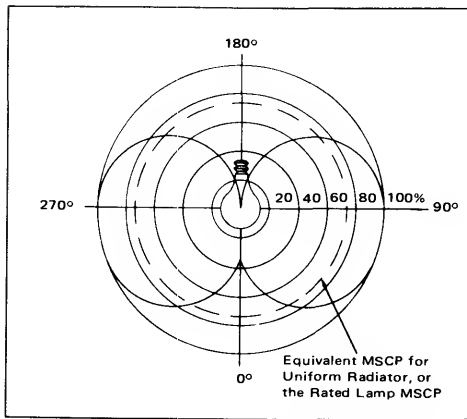


FIGURE 23 – Typical Radiation Pattern for a Frosted Incandescent Lamp

times the rated MSCP, while the vertical output, opposite the base, is 0.48 times the rated MSCP.

The actual polar variation for a lamp will depend on a variety of physical features such as filament shape, size and orientation and the solid angle intercepted by the base with respect to the center of the filament.

If the lamp output is given in horizontal candlepower (HCP), a fairly accurate calculation can be made with regard to illuminance on a receiver.

A third-form of rating is beam candlepower, which is provided for lamps with reflectors.

In all three cases the rating is given in lumens/steradian or candlepower.

SOLID STATE SOURCES

In contrast with the broadband source of radiation of the tungsten lamp, solid state sources provide relatively narrow band energy. The gallium arsenide (GaAs) light-emitting-diode (LED) has spectral characteristics which make it a favorable mate for use with silicon photodetectors. LED's are available for several wavelengths, as

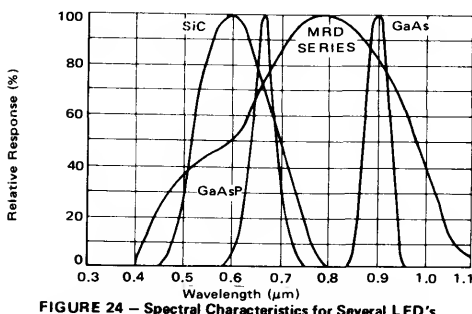


FIGURE 24 – Spectral Characteristics for Several LED's Compared with MRD Series

shown in Figure 24, but as the figure shows, the GaAs diode and the MRD phototransistor series are particularly compatible. Application of Equation (26) to the GaAs response and the MRD series response indicates that the efficiency ratio, H_E/H , is approximately 0.9 or 90%. That is, an irradiance of 4.0 mW/cm^2 from an LED will appear to the phototransistor as 3.6 mW/cm^2 . This means that a typical GaAs LED is about 3.5 times as effective as a tungsten lamp at 2870°K . Therefore, the typical sensitivity for the MRD450 when used with a GaAs LED is approximately

$$S = (0.8)(3.5) = 2.8 \text{ mA/mW/cm}^2. \quad (33)$$

An additional factor to be considered in using LED's is the polar response. The presence of a lens in the diode package will confine the solid angle of radiation. If the solid angle is θ , the resultant irradiance on a target located at a distance d is

$$H = \frac{4P}{\pi\theta^2 d^2} \text{ watts/cm}^2, \quad (34)$$

where

P is the total output power of the LED in watts

θ is the beam angle

d is the distance between the LED and the detector in cm.

LOW FREQUENCY AND STEADY STATE APPLICATIONS

Light Operated Relay – Figure 25 shows a circuit in which presence of light causes a relay to operate. The relay used in this circuit draws about 5 mA when Q2 is in saturation. Since h_{FE} (min) for the MPS3394 is 55 at a collector current of 2mA, a base current of 0.5 mA is sufficient to ensure saturation. Phototransistor Q1 provides the necessary base drive. If the MRD300 is used, the minimum illumination sensitivity is 4 $\mu\text{A}/\text{footcandle}$, therefore,

$$E = \frac{I_C}{S_{ICEO}} = \frac{0.5 \text{ mA}}{4 \times 10^{-3} \text{ mA/footcandle}} \quad (35)$$

$E = 125 \text{ footcandles}$

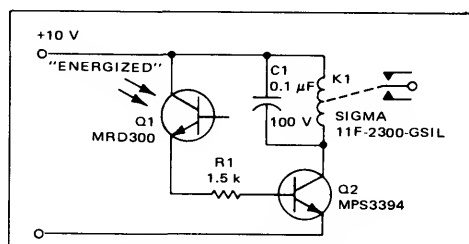


FIGURE 25 – Light-Operated Relay

This light level can be supplied by a flashlight or other equivalent light source.

The equivalent irradiance is obviously that value of irradiance which will cause the same current flow. Assume the light source is a flashlight using a PR2 lamp. The ratings for this lamp are

| Lamp | Rated Volts | Rated Current | MSCP |
|------|-------------|---------------|------|
| PR2 | 2.38 | 0.50 A | 0.80 |

If the flashlight has new batteries the lamp voltage is

$$V_L = 2(1.55) = 3.1 \text{ volts} \quad (36)$$

This means that the lamp is operated at 130 per cent of rated voltage. From Figure 21 for 130% rated voltage, (Rated Current) (Percent Current) = (0.5)(1.15) = 0.575 ampere

$$(\text{Rated CP}) (\text{Percent CP}) = (0.80)(2.5) = 2 \text{ CP}$$

$$(\text{Rated Voltage}) (\text{Percent Voltage}) = (2.38)(1.3) = 3.1 \text{ volts.}$$

Therefore, the MSCP/watt rating is 1.12. From Figure 22, the color temperature is 2720°K.

Now, from Figure 20, the response at a color temperature of 2720°K is down to 90% of its reference value. At the reference temperature, the minimum SRCEO for the MRD300 is 0.8 mA/mW/cm², so at 2720°K it is

$$\text{SRCEO (MIN)} = (0.9)(0.8) = 0.72 \text{ mA/mW/cm}^2 \quad (37)$$

and

$$I_C = \frac{0.5}{\text{SRCEO}} = \frac{0.5}{0.72} = 0.65 \text{ mW/cm}^2 \quad (38)$$

However, sensitivity is a function of irradiance, and at 0.695 mW/cm² it has a minimum value (at 2720°K) of about 0.45 mA/mW/cm², therefore

$$H_E = \frac{0.5}{0.45} = 1.11 \text{ mW/cm}^2 \quad (39)$$

Again, we note that at an irradiance of 1.11 mW/cm², the minimum SRCEO is about 0.54 mA/mW/cm². Several applications of the above process eventually result in a convergent answer of

$$H_E \approx 1.0 \text{ mW/cm}^2 \quad (40)$$

Now, from the MRD450 data sheet, SRCEO (min) at an irradiance of 1.0 mW/cm² and color temperature of 2720°K is

$$\text{SRCEO} = (0.15)(0.9) = 0.135 \text{ mA/mW/cm}^2 \quad (41)$$

At 1.0 mW/cm², we can expect a minimum IC of 0.135 mA. This is below the design requirement of 0.5 mA. By looking at the product of SRCEO (min) and H on the data sheet curve, the minimum H for 0.5 mA for using the MRD450 can now be calculated.

$$\frac{H}{H_E} = \frac{3.0}{1.0} = \frac{I(\text{MRD450})}{I(\text{MRD300})} = \frac{I(\text{MRD450})}{125} \quad (42)$$

or

$$I(\text{MRD450}) = 375 \text{ footcandles} \quad (43)$$

This value is pretty high for a two D-cell flashlight, but the circuit should perform properly since about 200 footcandles can be expected from a flashlight, giving a resultant current flow of approximately

$$I = \frac{220}{275} (0.5 \text{ mA}) = 0.293 \text{ mA} \quad (44)$$

This will be the base current of Q2, and since the relay requires 5 mA, the minimum hFE required for Q2 is

$$hFE(Q2) = \frac{5}{0.293} = 17. \quad (45)$$

This is well below the hFE (min) specification for the MPS3394 (55) so proper circuit performance can be expected.

A variation of the above circuit is shown in Figure 26. In this circuit, the presence of light deenergizes the relay. The same light levels are applicable. The two relay circuits can be used for a variety of applications such as automatic door activators, object or process counters, and intrusion alarms. Figure 27, for example, shows the circuit of Figure 26 used to activate an SCR in an alarm system. The presence of light keeps the relay deenergized, thus denying trigger current to the SCR gate. When the light is interrupted, the relay energizes, providing the SCR with trigger current. The SCR latches ON, so only a momentary interruption of light is sufficient to cause the alarm to ring continuously. S1 is a momentary contact switch for resetting the system.

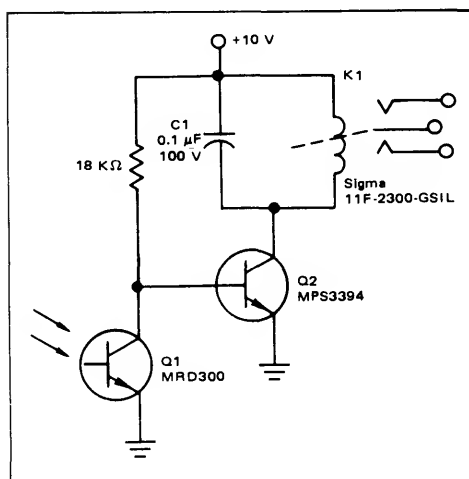


FIGURE 26 – Light De-energized Relay

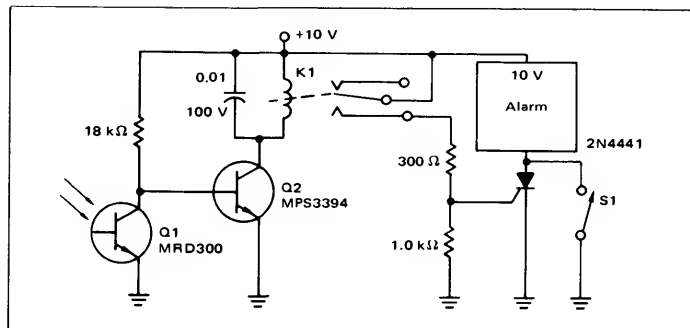


FIGURE 27 – Light-Relay
Operated SCR Alarm Circuit

If the SCR has a sensitive gate, the relay can be eliminated as shown in Figure 28. The phototransistor holds the gate low as long as light is present, but pulls the gate up to triggering level when the light is interrupted. Again, a reset switch appears across the SCR.

Voltage Regulator – The light output of an incandescent lamp is very dependent on the RMS voltage applied to it. Since the phototransistor is sensitive to light changes, it can be used to monitor the light output of a lamp, and in a closed-loop system to control the lamp voltage. Such a regulator is particularly useful in a projection system where it is desired to maintain a constant brightness level despite line voltage variations.

Figure 29 shows a voltage regulator for a projection lamp. The RMS voltage on the lamp is set by the firing angle of the SCR. This firing angle in turn is set by the unijunction timing circuit. Transistors Q1 and Q2 form a constant-current source for charging timing capacitor C.

The magnitude of the charging current, the capacitance, C, and the position of R6 set the firing time of the UJT oscillator which in turn sets the firing angle of the SCR. Regulation is accomplished by phototransistor Q3. The brightness of the lamp sets the current level in Q3, which diverts current from the timing capacitor. Potentiometer R6 is set for the desired brightness level.

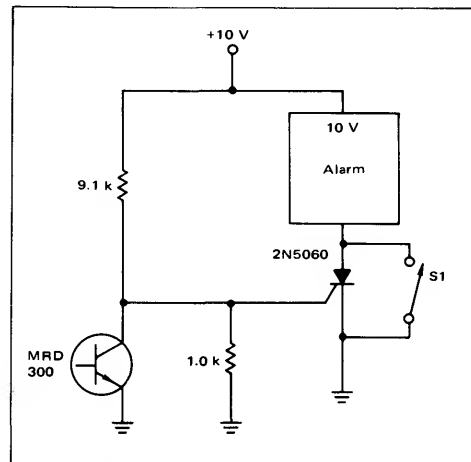


FIGURE 28 – Light Operated SCR Alarm
Using Sensitive-Gate SCR

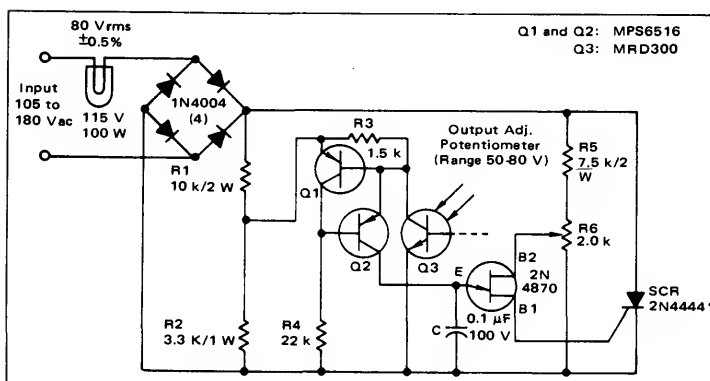


FIGURE 29 – Circuit Diagram of
Voltage Regulator for
Projection Lamp.

*2N4444 to be used with a heat sink.

If the line voltage rises, the lamp tends to become brighter, causing an increase in the current of Q3. This causes the unijunction to fire later in the cycle, thus reducing the conduction time of the SCR. Since the lamp RMS voltage depends on the conduction angle of the SCR, the increase in line voltage is compensated for by a decrease in conduction angle, maintaining a constant lamp voltage.

Because the projection lamp is so bright, it will saturate the phototransistor if it is directly coupled to it. Either of two coupling techniques are satisfactory. The first is to attenuate the light to the phototransistor with a translucent material with a small iris. The degree of attenuation or translucency must be experimentally determined for the particular projection lamp used.

The second coupling technique is to couple the lamp and phototransistor by a reflected path. The type of reflective surface and path length will again depend on the particular lamp being used.

Switching Characteristics — When the phototransistor changes state from OFF to ON, a significant time delay is associated with the $r_{be} C_{be}$ time constant. As shown in Figure 30, the capacitance of the emitter-base junction is appreciable. Since the device photocurrent is $gm V_{be}$ (from Figure 3), the load current can change state only as fast as V_{be} can change. Also, V_{be} can change only as fast as C_{be} can charge and discharge through the load resistance. Figure 31 shows the variations in rise and fall time with load resistance. This measurement was made using a GaAs light emitting diode for the light source. The LED output power and the separation distance between the LED and the phototransistor were adjusted for an ON phototransistor current of 1.5 mA. The rise time was also measured for a short-circuited load and found to be about 700 ns.

The major difficulty encountered in high-frequency applications is the load-dependent frequency response. Since the phototransistor is a current source, it is desirable to use a large load resistance to develop maximum output voltage. However, large load resistances limit the useful frequency range. This seems to present the designer with a tradeoff between voltage and speed. However, there is a technique available to eliminate the need for such a tradeoff.

Figure 32 shows a circuit designed to optimize both speed and output voltage. The common-base stage Q2 offers a low-impedance load to the phototransistor, thus maximizing response speed. Since Q2 has near-unity current gain, the load current in R_L is approximately equal to the phototransistor current. Thus the impedance transformation provided by Q2 results in a relatively load-independent frequency response.

The effect of Q2 is shown in Figures 33 and 34. In Figure 33, the 3-dB frequency response as a function of load is shown. Comparing this with Figure 7, the effect of Q2 is quite evident. Comparison of Figures 31 and 34 also demonstrates the effect of Q2.

Remote Strobeflash Slave Adapter — At times when using an electronic strobe flash, it is desirable to use a remote, or "slave" flash synchronized with the master. The circuit in Figure 35 provides the drive needed to trigger a slave unit, and eliminates the necessity for

synchronizing wires between the two flash units.

The MRD300 phototransistor used in this circuit is cut off in a VCER mode due to the relatively low dc resistance of rf choke L1 even under high ambient light conditions. When a fast-rising pulse of light strikes the base region of this device, however, L1 acts as a very high impedance to the ramp and the transistor is biased into conduction by the incoming pulse of light.

When the MRD300 conducts, a signal is applied to the gate of SCR Q2. This triggers Q2, which acts as a solid-state relay and turns on the attached strobeflash unit.

In tests this unit was unaffected by ambient light conditions. It fired up to approximately 20 feet from strobe-light flashes using only the lens of the MRD300 for light pickup.

CONCLUSION

The phototransistor provides the circuit or system designer with a unique component for use in dc and linear or digital-time-varying applications. Use of a phototransistor yields extremely high electrical and mechanical isolation. The proper design of an electro-optical system requires a knowledge of both the radiation source characteristics and the phototransistor characteristics. This knowledge, coupled with an adequately defined distance and geometric relationship, enables the designer to properly predict the performance of his designs.

REFERENCES

1. Motorola Application Note AN-440, *Theory and Characteristics of Phototransistors*.
2. Francis W. Sears, *Optics*, Addison-Wesley Publishing Company, Inc., 1948.
3. IES Lighting Handbook, 3rd Edition, Illuminating Engineering Society, 1959.

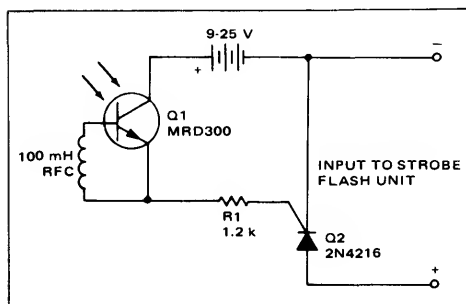


FIGURE 35 – Strobeflash Slave Adapter

ISOLATION TECHNIQUES USING OPTICAL COUPERS

Prepared by
Francis Christian

INTRODUCTION

The optical coupler is a new device that offers the design engineer new freedoms in designing circuits and systems. Problems such as ground loop isolation, common mode noise rejection, power supply transformations, and many more problems can be solved or simplified with the use of an optical coupler.

Operation is based on the principle of detecting emitted light. The input to the coupler is connected to a light emitter and the output is a photodetector, the two elements being separated by a transparent insulator and housed in a light-excluding package. There are many types of optical couplers; for example, the light source could be an incandescent lamp or a light emitting diode (LED). Also, the detector could be photovoltaic cell, photoconductive cell, photodiode, phototransistor, or a light-sensitive SCR. By various combinations of emitters and detectors, a number of different types of optical couplers could be assembled.

Once an emitter and detector have been assembled as a coupler, the optical portion is permanently established so that device use is only electronic in nature. This eliminates the need for the circuit designer to have knowledge of optics. However, for effective application, he must know something of the electrical characteristics, capabilities, and limitations, of the emitter and detector.

COUPLER CHARACTERISTICS

The 4N25 is an optical coupler consisting of a gallium arsenide (GaAs) LED and a silicon phototransistor. (For more information on LEDs and phototransistors, see References 1 and 2).

The coupler's characteristics are given in the following sequence: LED characteristics, phototransistor characteristics, coupled characteristics, and switching characteristics. Table I shows all four for the 4N25 series.

INPUT

For most applications the basic LED parameters I_F and V_F are all that are needed to define the input. Figure 1 shows these forward characteristics, providing the necessary information to design the LED drive circuit. Most circuit applications will require a current limiting resistor in series with the LED input. The circuit in Figure 2 is a typical drive circuit.

The current limiting resistor can be calculated from the following equation:

$$R = \frac{V_{IN} - V_F}{I_F},$$

where

V_F = diode forward voltage
 I_F = diode forward current

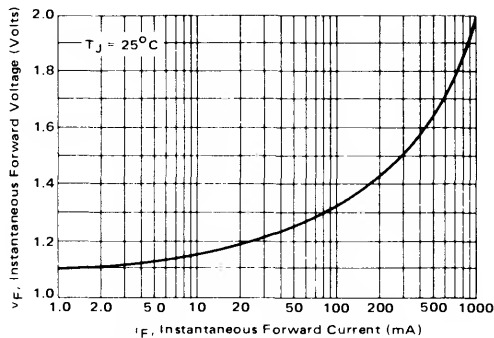


FIGURE 1 – Input Diode Forward Characteristic

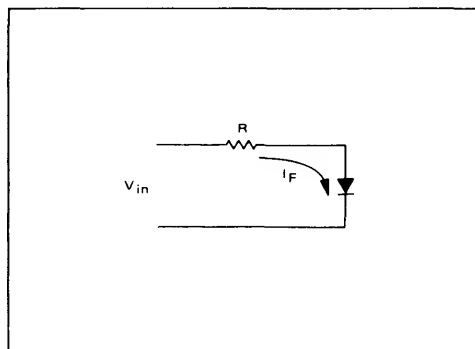


FIGURE 2 – Simple Drive Circuit For An LED

TABLE I

LED CHARACTERISTICS ($T_A = 25^\circ C$ unless otherwise noted)

| Characteristic | Symbol | Min | Typ | Max | Unit |
|--|--------|-----|------|-----|---------|
| *Reverse Leakage Current ($V_B = 30 V$, $R_L = 1.0 M\Omega$) | I_R | — | 0.05 | 100 | μA |
| *Forward Voltage ($I_F = 50 mA$) | V_F | — | 1.2 | 1.5 | Volts |
| Capacitance ($V_B = 0 V$, $f = 1.0 MHz$) | C | — | 150 | — | pF |

PHOTOTRANSISTOR CHARACTERISTICS ($T_A = 25^\circ C$ and $I_F = 0$ unless otherwise noted)

| Characteristic | Symbol | Min | Typ | Max | Unit |
|---|---------------|-----|-----|-----|-------|
| *Collector Emitter Dark Current ($V_{CE} = 10 V$, Base Open) 4N25, 4N26, 4N27 4N28 | I_{CEO} | — | 3.5 | 50 | nA |
| *Collector Base Dark Current ($V_{CB} = 10 V$, Emitter Open) | I_{CBO} | — | — | 100 | nA |
| *Collector Base Breakdown Voltage ($I_C = 100 \mu A$, $I_E = 0$) | $V_{(BR)CBO}$ | 70 | — | — | Volts |
| *Collector Emitter Breakdown Voltage ($I_C = 1.0 mA$, $I_E = 0$) | $V_{(BR)CEO}$ | 30 | — | — | Volts |
| *Emitter Collector Breakdown Voltage ($I_E = 100 \mu A$, $I_B = 0$) | $V_{(BR)ECO}$ | 7.0 | — | — | Volts |
| OC Current Gain ($V_{CE} = 5.0 V$, $I_C = 500 \mu A$) | β_{FE} | — | 250 | — | — |

COUPLED CHARACTERISTICS ($T_A = 25^\circ C$ unless otherwise noted)

| Characteristic | Symbol | Min | Typ | Max | Unit |
|--|---------------|---------------------|-------------|-----|-------|
| *Collector Output Current (1) ($V_{CE} = 10 V$, $I_F = 10 mA$, $I_B = 0$) 4N25, 4N26 4N27, 4N28 | I_C | 2.0 1.0 | 5.0 3.0 | — | mA |
| *Isolation Voltage (2) 4N25 4N26, 4N27 4N28 | V_{ISO} | 2500 1500 500 | — — — | — | Volts |
| Isolation Resistance (2) ($V = 500 V$) | — | — | 10^{11} | — | Ohms |
| *Collector Emitter Saturation ($I_C = 2.0 mA$, $I_F = 50 mA$) | $V_{CE(sat)}$ | — | 0.2 | 0.5 | Volts |
| Isolation Capacitance (2) ($V = 0$, $f = 1.0 MHz$) | — | — | 1.3 | — | pF |
| Bandwidth (3) ($I_C = 2.0 mA$, $R_L = 100 \Omega$, Figure 11) | — | — | 300 | — | kHz |

SWITCHING CHARACTERISTICS

| | | | | | | | |
|--------------|--|--------------------------|-------|---|--------------|---|---------|
| Delay Time | $I_C = 10 mA$, $V_{CC} = 10 V$ Figures 6 and 8 | 4N25, 4N26 4N27, 4N28 | t_d | — | 0.07 0.10 | — | μs |
| Rise Time | — | — | t_r | — | 0.8 2.0 | — | μs |
| Storage Time | $I_C = 10 mA$, $V_{CC} = 10 V$ Figures 7 and 8 | 4N25, 4N26 4N27, 4N28 | t_s | — | 4.0 2.0 | — | μs |
| Fall Time | — | — | t_f | — | 7.0 3.0 | — | μs |

*Indicates JEDEC Registered Data. (1) Pulse Test. Pulse Width = 300 μs . Duty Cycle = 20%.
 (2) For this test LED pins 1 and 2 are common and Photo Transistor pins 4, 5 and 6 are common.
 (3) If adjusted to yield $I_C = 2.0 mA$ and $I_C = 2.0 mA$ p.p. at 10 kHz.

OUTPUT

The output of the coupler is the phototransistor. The basic parameters of interest are the collector current I_C and collector emitter voltage, V_{CE} . Figure 3 is a curve of $V_{CE(sat)}$ versus I_C for two different drive levels.

COUPLING

To fully characterize the coupler, a new parameter, the dc current transfer ratio or coupling efficiency (η) must be defined. This is the ratio of the transistor collector current to diode current I_C/I_F . Figures 4A and 4B show the typical dc current transfer functions for the couplers at $V_{CE} = 10$ volts. Note that η varies with I_F and V_{CE} .

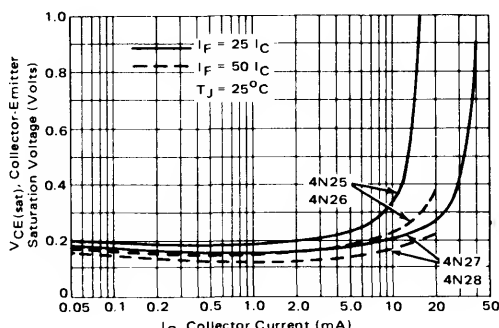


FIGURE 3 – COLLECTOR SATURATION VOLTAGE

Once the required output collector current I_C is known, the input diode current can be calculated by

$$I_F = I_C/\eta,$$

where I_F is the forward diode current
 I_C is the collector current
 η is the coupling efficiency or transfer ratio.

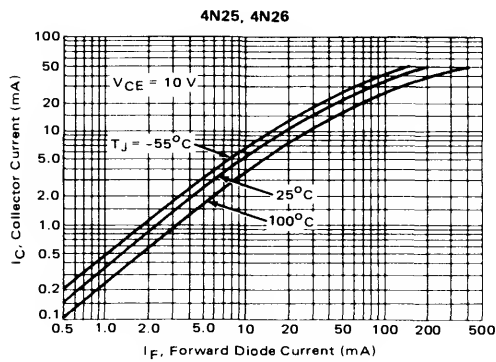


FIGURE 4A – DC Current Transfer Ratio

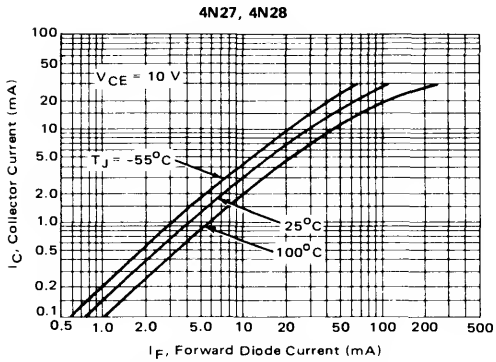


FIGURE 4B – DC Current Transfer Ratio

RESPONSE TIME

The switching times for the couplers are shown in Figures 5A and 5B. The speed is fairly slow compared to switching transistors, but is typical of phototransistors because of the large base-collector area. The switching time or bandwidth of the coupler is a function of the load resistor R_L because of the $R_L C_O$ time constant where C_O is the parallel combination of the device and load capacitances. Figure 6 is a curve of frequency response versus R_L .

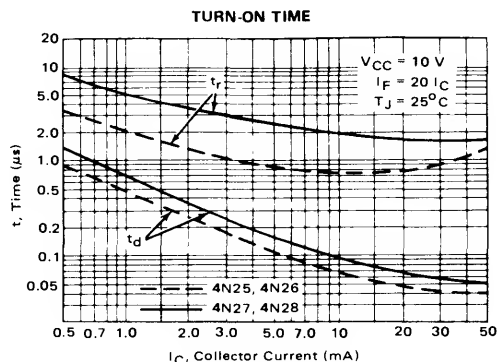


FIGURE 5A – Switching Times

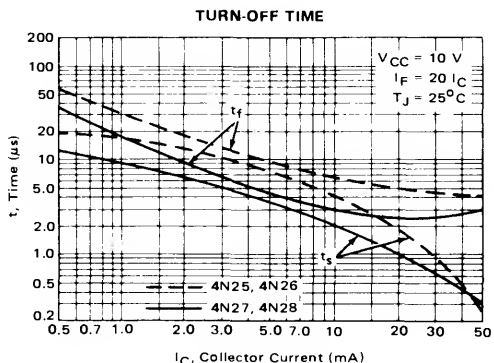


FIGURE 5B – Switching Times

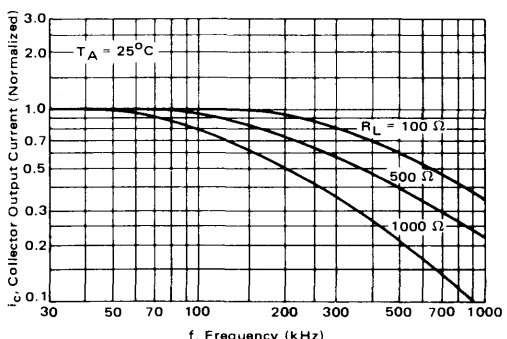


FIGURE 6 – Frequency Response

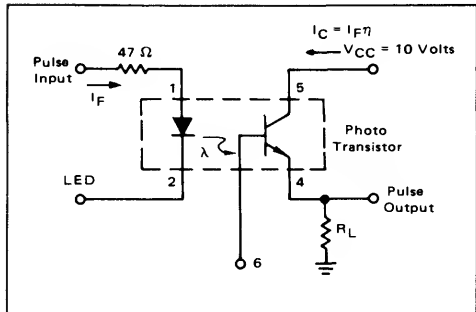


FIGURE 7 – Pulse Mode Circuit

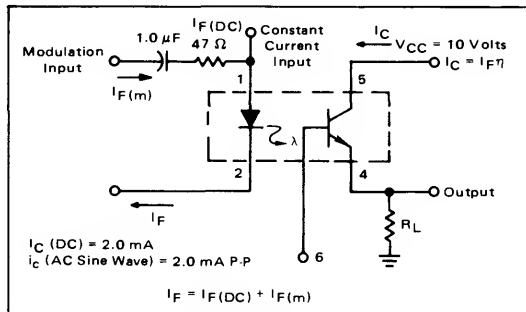


FIGURE 8 – Linear Mode Circuit

OPERATING MODE

The two basic modes of operation are pulsed and linear. In the pulsed mode of operation, the LED will be switched on or off. The output will also be pulses either in phase or 180° out of phase with the input depending on where the output is taken. The output will be 180° out of phase if the collector is used and in phase if the emitter is used for the output.

time for a diode-transistor coupler is in the order of 2 to 5 μ s, where the diode-diode coupler is 50 to 100 ns. The one disadvantage with the diode-diode coupler is that the output current is much lower than the diode-transistor coupler. This is because the base current is being used as signal current and the β multiplication of the transistor is omitted. Figure 10 is a graph of I_B versus I_F using the coupler in the diode-diode mode.

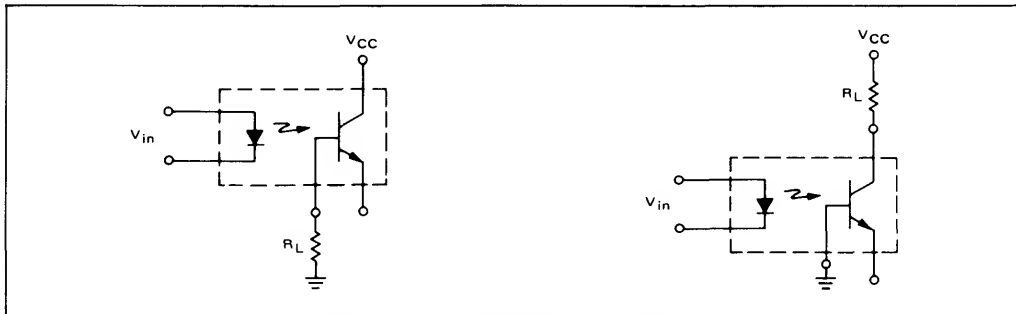


FIGURE 9 – Circuit Connections for Using the 4N26 As a Diode-Diode Coupler

In the linear mode of operation, the input is biased at a dc operating point and then the input is changed about this dc point. The output signal will have an ac and dc component in the signal.

Figures 7 and 8 show typical circuits for the two modes of operation.

THE 4N26 AS A DIODE-DIODE COUPLER

The 4N26 which is a diode-transistor coupler, can be used as a diode-diode coupler. To do this the output is taken between the collector and base instead of the collector and emitter. The circuits in Figure 9 show the connections to use the coupler in the diode-diode mode.

The advantage of using the 4N26 as a diode-diode coupler is increased speed. For example, the pulse rise

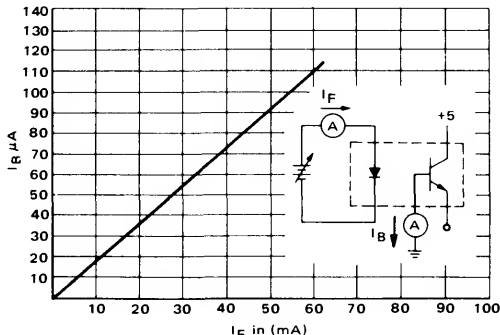


FIGURE 10 – I_B versus I_F Curve for Using the 4N26 As a Diode-Diode Coupler

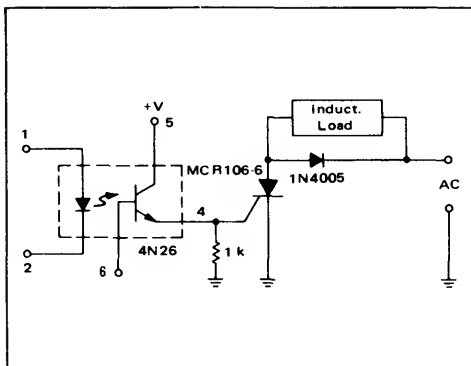


FIGURE 11 – Coupler-Driven SCR

APPLICATIONS

The following circuits are presented to give the designer ideas of how the 4N26 can be used. The circuits have been bread-boarded and tested, but the values of the circuit components have not been selected for optimum performance over all temperatures.

Figure 11 shows a coupler driving a silicon controlled rectifier (SCR). The SCR is used to control an inductive load, and the SCR is driven by a coupler. The SCR used is a sensitive gate device that requires only 1 mA of gate current and the coupler has a minimum current transfer ratio of 0.2 so the input current to the coupler, I_F , need only be 5 mA. The 1 k resistor connected to the gate of the SCR is used to hold off the SCR. The 1N4005 diode is used to suppress the self-induced voltage when the SCR turns off.

Figure 12 is a circuit that couples a high voltage load to a low voltage logic circuit. To insure that the voltage to the MTTL flip-flop exceeds the logic-one level, the coupler

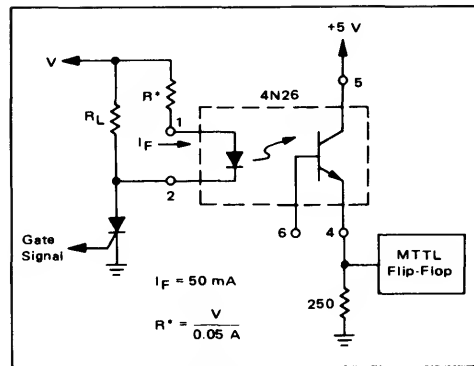


FIGURE 12 – Opto Coupler In A Load To Logic Translation

output current must be at least 10 mA. To guarantee 10 mA of output current, the input current to the LED must be 50 mA. The current limiting resistor R can be calculated from the equation $R = \frac{V - VF}{0.05}$. If the power supply voltage, V , is much greater than VF , the equation for R reduces to $R = \frac{V}{0.05}$.

The circuit of Figure 13 shows a coupler driving an operational amplifier. In this application an ac signal is passed through the coupler and then amplified by the op amp. To pass an ac signal through the coupler with minimum distortion, it is necessary to bias the LED with a dc current. The ac signal is summed with the dc current so the output voltage of the coupler will have an ac and a dc component. Since the op amp is capacitively coupled to the coupler, only the ac signal will appear at the output.

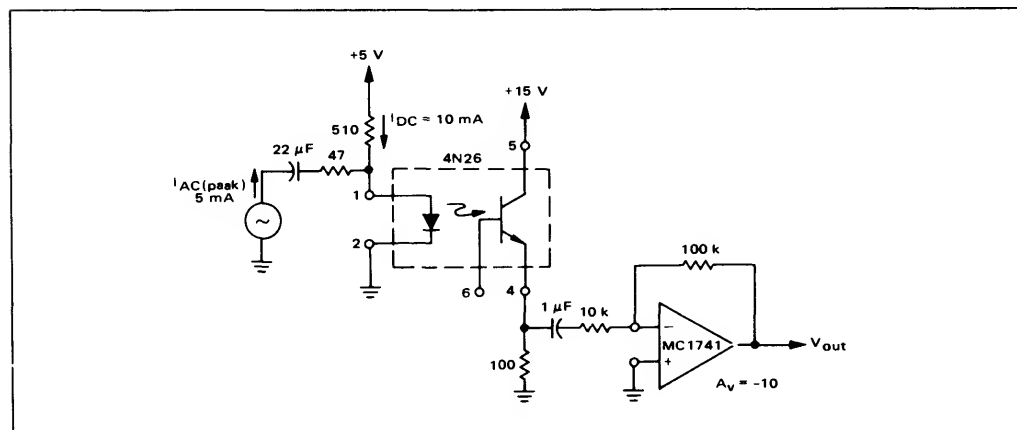


FIGURE 13 – Coupling An AC Signal to an Operational Amplifier

The circuit of Figure 14 shows the 4N26 being used as a diode-diode coupler, the output being taken from the collector-base diode. In this mode of operation, the emitter is left open, the load resistor is connected between the base and ground, and the collector is tied to the positive voltage supply. Using the coupler in this way reduces the switching time from 2 to 3 μ s to 100 ns.

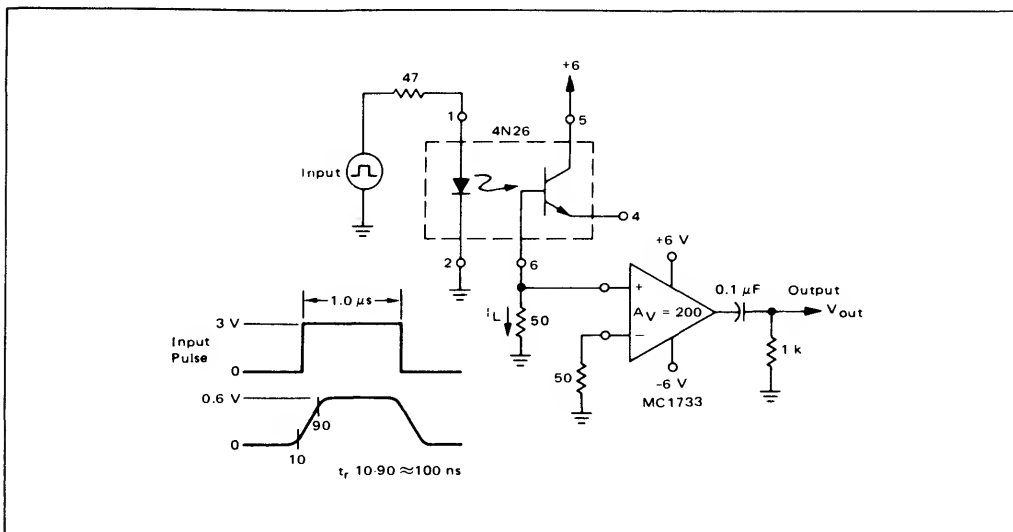


FIGURE 14 – Using the 4N26 as a Diode-Diode Coupler

The circuit of Figure 15 is a standard two-transistor one-shot, with one transistor being the output transistor of the coupler. The trigger to the one-shot is the LED input to the coupler. A pulse of 3 μ s in duration and 15 mA will trigger the circuit. The output pulse width (PW_O) is equal to $0.7 RC + PW_1 + 6 \mu s$ where PW_1 is the input pulse width and 6 μ s is the turn-off delay of the coupler. The amplitude of the output pulse is a function of the power supply voltage of the output side and independent of the input.

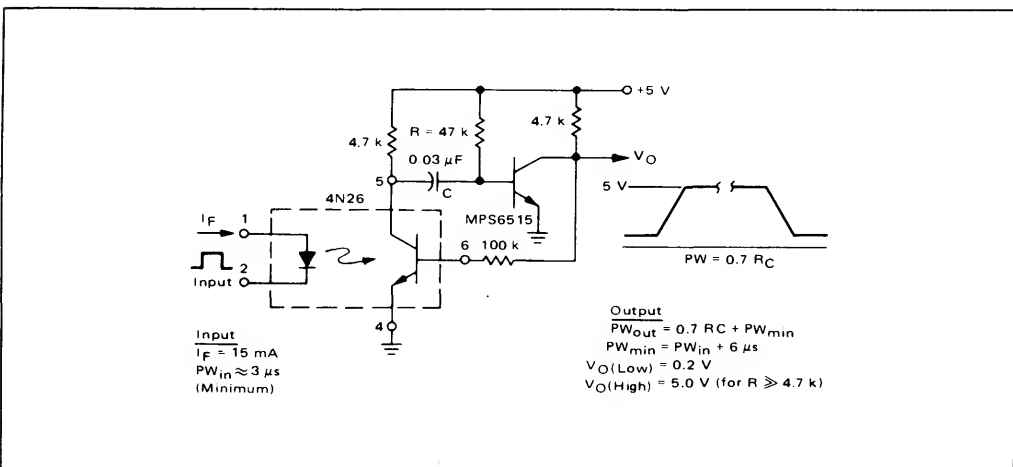


FIGURE 15 – Pulse Stretcher

The circuit of Figure 16 is basically a Schmitt trigger. One of the Schmitt trigger transistors is the output transistor of a coupler. The input to the Schmitt trigger is the LED of the coupler. When the base voltage of the coupler's transistor exceeds $V_{t1} + V_{be}$ the output transistor of

the coupler will switch on. This will cause Q2 to conduct and the output will be in a high state. When the input to the LED is removed, the coupler's output transistor will shut off and the output voltage will be in a low state. Because of the high impedance in the base of the coupler

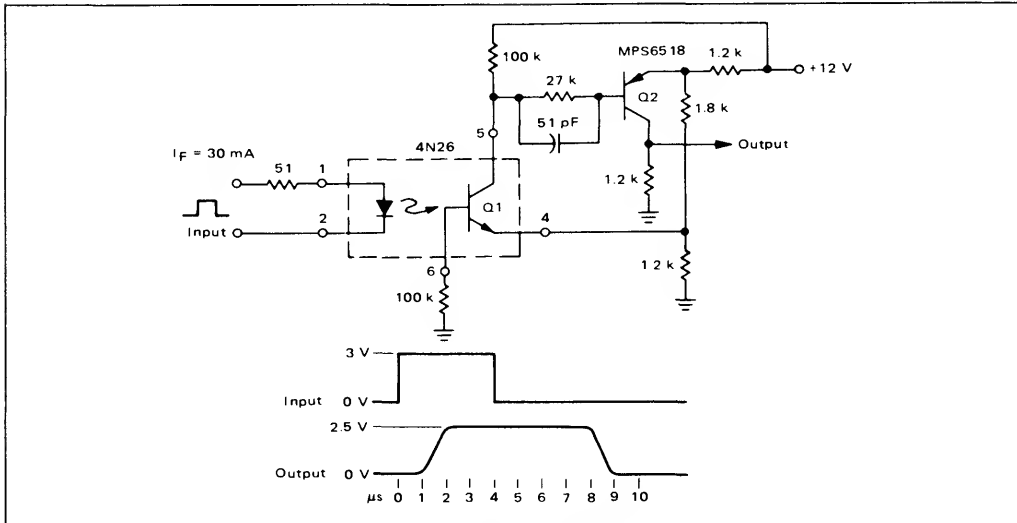


FIGURE 16 – Optically Coupled Schmitt Trigger

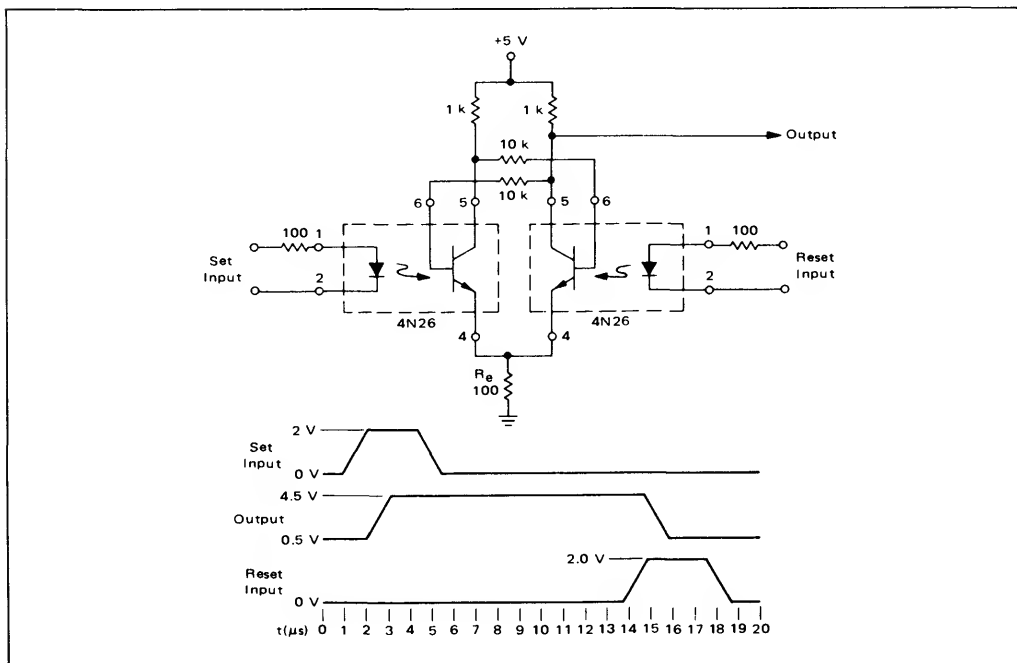


FIGURE 17 – Optically Coupled R-S Flip-Flop

transistor, the turn-off delay is about 6 μ s. The high base impedance (100 k ohms) represents a compromise between sensitivity (input drive required) and frequency response. A low value base resistor would improve speed but would also increase the drive requirements.

The circuit in Figure 17 can be used as an optically coupled R-S flip-flop. The circuit uses two 4N26 couplers cross coupled to produce two stable states. To change the output from a low state to a high state requires a positive 2 V pulse at the set input. The minimum width of the set pulse is 3 μ s. To switch the output back to the low state needs only a pulse on the reset input. The reset-operation is similar to the set operation.

Motorola integrated voltage regulators provide an input

for the express purpose of shutting the regulator off. For large systems, various subsystems may be placed in a standby mode to conserve power until actually needed. Or the power may be turned OFF in response to occurrences such as overheating, over-voltage, shorted output, etc.

With the use of the 4N26 optically coupler, the regulator can be shut down while the controlling signal is isolated from the regulator. The circuit of Figure 18 shows a positive regulator connected to an optical coupler.

To insure that the drive to the regulator shut down control is 1 mA, (the required current), it is necessary to drive the LED in the coupler with 5 mA of current, an adequate level for logic circuits.

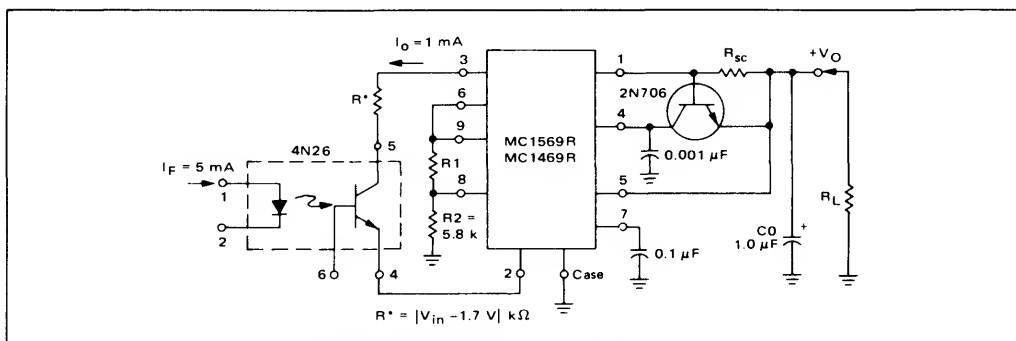


FIGURE 18 – Optical Coupler Controlling the Shut Down of MC1569 Voltage Regulator

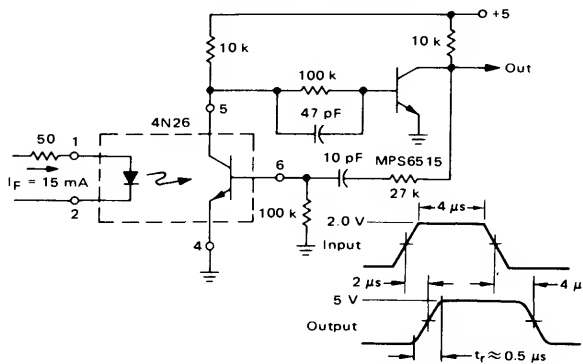


FIGURE 19 – Simple Pulse Amplifier

The circuit in Figure 19 is a simple pulse amplifier using positive, ac feedback into the base of the 4N26. The advantage of the feedback is in faster switching time. Without the feedback, the pulse rise time is about 2.0 μ s, but with the positive feedback, the pulse rise time is about 0.5 μ s. Figure 17A shows the input and output waveforms of the pulse amplifier.

REFERENCES

1. "Theory and Characteristics of Phototransistors," Motorola Application Note AN-440.
2. "Motorola Switching Transistor Handbook."
3. Deboo, G.J. and C.N. Burrous, Integrated Circuits and Semiconductor Devices Theory and Application, McGraw-Hill, 1971.

APPLICATIONS OF THE MOC3011 TRIAC DRIVER

Prepared by:
Pat O'Neill

DESCRIPTIONS OF THE MOC3011

Construction

The MOC3011 consists of a gallium arsenide infrared LED optically exciting a silicon detector chip, which is especially designed to drive triacs controlling loads on the 115 Vac power line. The detector chip is a complex device which functions in much the same manner as a small triac, generating the signals necessary to drive the gate of a larger triac. The MOC3011 allows a low power exciting signal to drive a high power load with a very small number of components, and at the same time provides practically complete isolation of the driving circuitry from the power line.

The construction of the MOC3011 follows the same highly successful coupler technology used in Motorola's broad line of plastic couplers (Figure 1). The dual lead

frame with an epoxy undermold provides a stable dielectric capable of sustaining 7.5 kV between the input and output sides of the device. The detector chip is passivated with silicon nitride and uses Motorola's annular ring to maintain stable breakdown parameters.

Basic Electrical Description

The GaAs LED has nominal 1.3 V forward drop at 10 mA and a reverse breakdown voltage greater than 3 V. The maximum current to be passed through the LED is 50 mA.

The detector has a minimum blocking voltage of 250 Vdc in either direction in the off state. In the on state, the detector will pass 100 mA in either direction with less than 3 V drop across the device. Once triggered into the on (conducting) state, the detector will remain there until the current drops below the holding current (typically 100 μ A) at which time the detector reverts to the off (non-conducting) state. The detector may be triggered into the on state by exceeding the forward blocking voltage, by voltage ramps across the detector at rates exceeding the static dv/dt rating, or by photons from the LED. The LED is guaranteed by the specifications to trigger the detector into the on state when 10 mA or more is passed through the LED. A similar device, the MOC3010, has exactly the same characteristics except it requires 15 mA to trigger.

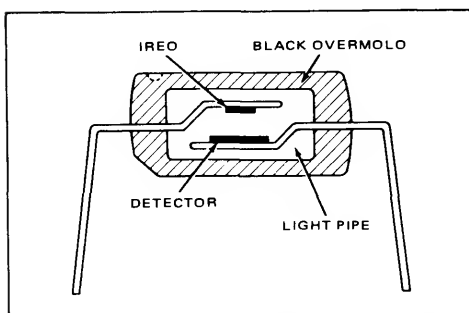


FIGURE 1 – Motorola Double-Molded Coupler Package

Since the MOC3011 looks essentially like a small optically triggered triac, we have chosen to represent it as shown on Figure 2.

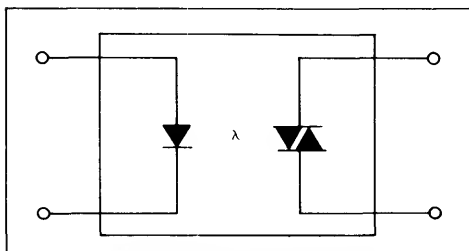


FIGURE 2 – Schematic Representation of MOC3011 and MOC3010

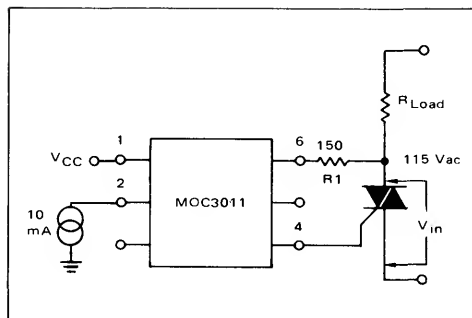


FIGURE 3 – Simple Triac Gating Circuit

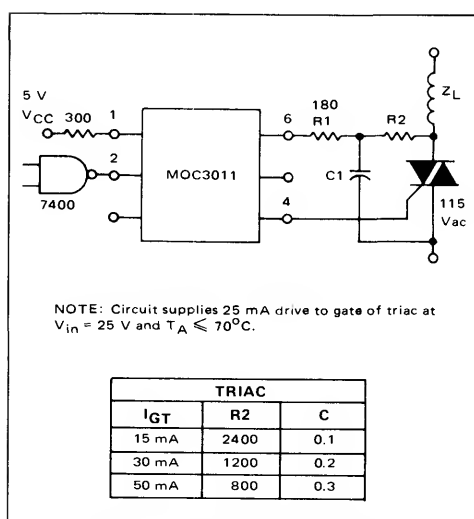


FIGURE 4 – Logic to Inductive Load Interface

USING THE MOC3011 AS A TRIAC DRIVER

Triac Driving Requirements

Figure 3 shows a simple triac driving circuit using the MOC3011. The maximum surge current rating of the MOC3011 sets the minimum value of R1 through the equation:

$$R1(\min) = V_{in}(pk)/1.2 \text{ A}$$

If we are operating on the 115 Vac nominal line voltage, $V_{in}(pk) = 180 \text{ V}$, then

$$R1(\min) = V_{in}(pk)/1.2 \text{ A} = 150 \text{ ohms.}$$

In practice, this would be a 150 or 180 ohm resistor. If the triac has $I_{GT} = 100 \text{ mA}$ and $V_{GT} = 2 \text{ V}$, then the voltage V_{in} necessary to trigger the triac will be given by $V_{inT} = R1 \cdot I_{GT} + V_{GT} + V_{TM} = 20 \text{ V}$.

Resistive Loads

When driving resistive loads, the circuit of Figure 3 may be used. Incandescent lamps and resistive heating elements are the two main classes of resistive loads for which 115 Vac is utilized. The main restriction is that the triac must be properly chosen to sustain the proper inrush loads. Incandescent lamps can sometimes draw a peak current known as "flashover" which can be extremely high, and the triac should be protected by a fuse or rated high enough to sustain this current.

Line Transients—Static dv/dt

Occasionally transient voltage disturbance on the ac line will exceed the static dv/dt rating of the MOC3011. In this case, it is possible that the MOC3011 and the associated triac will be triggered on. This is usually not a problem, except in unusually noisy environments, because the MOC3011 and its triac will commute off at the next zero crossing of the line voltage, and most loads are not noticeably affected by an occasional single half-cycle of applied power. See Figure 5 for typical dv/dt versus temperature curves.

Inductive Loads—Commutating dv/dt

Inductive loads (motors, solenoids, magnets, etc.) present a problem both for triacs and for the MOC3011 because the voltage and current are not in phase with each other. Since the triac turns off at zero current, it may be trying to turn off when the applied current is zero but the applied voltage is high. This appears to the triac like a sudden rise in applied voltage, which turns on the triac if the rate of rise exceeds the commutating dv/dt of the triac or the static dv/dt of the MOC3011.

Snubber Networks

The solution to this problem is provided by the use of "snubber" networks to reduce the rate of voltage rise seen by the device. In some cases, this may require two snubbers—one for the triac and one for the MOC3011. The triac snubber is dependent upon the triac and load used and will not be discussed here. In many applications

the snubber used for the MOC3011 will also adequately protect the triac.

In order to design a snubber properly, one should really know the power factor of the reactive load, which is defined as the cosine of the phase shift caused by the load. Unfortunately, this is not always known, and this makes snubbing network design somewhat empirical. However a method of designing a snubber network may be defined, based upon a typical power factor. This can be used as a "first cut" and later modified based upon experiment.

Assuming an inductive load with a power factor of PF = 0.1 is to be driven. The triac might be trying to turn off when the applied voltage is given by

$$V_{to} = V_{pk} \sin \phi \approx V_{pk} \approx 180 \text{ V}$$

First, one must choose R1 (Figure 4) to limit the peak capacitor discharge current through the MOC3011. This resistor is given by

$$R1 = V_{pk}/I_{max} = 180/1.2 \text{ A} = 150 \Omega$$

A standard value, 180 ohm resistor can be used in practice for R1.

It is necessary to set the time constant for $\tau = R_2 C$. Assuming that the triac turns off very quickly, we have a peak rate of rise at the MOC3011 given by

$$dv/dt = V_{to}/\tau = V_{to}/R_2 C$$

Setting this equal to the worst case dv/dt (static) for the MOC3011 which we can obtain from Figure 5 and solving for R2C:

$$dv/dt(T_j = 70^\circ\text{C}) = 0.8 \text{ V}/\mu\text{s} = 8 \times 10^5 \text{ V/s}$$

$$R_2 C = V_{to}/(dv/dt) = 180/(8 \times 10^5) \approx 230 \times 10^{-6}$$

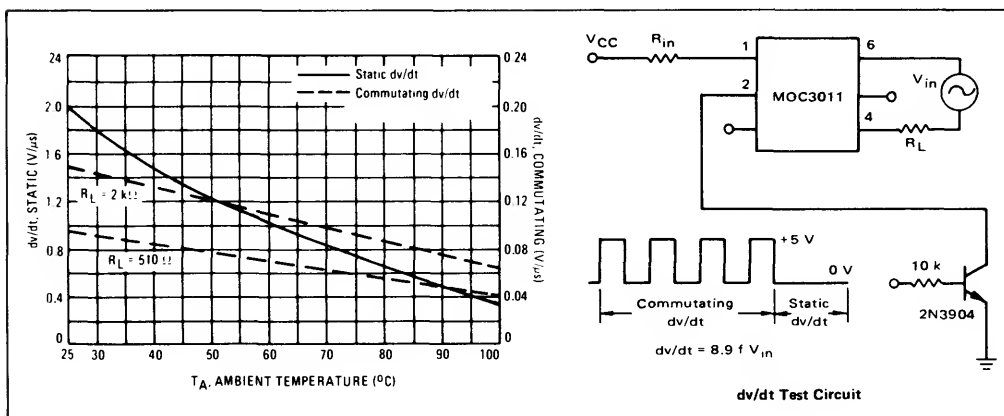


FIGURE 5 – dv/dt versus Temperature

The largest value of R₂ available is found, taking into consideration the triac gate requirements. If a sensitive gate triac is used, such as a 2N6071B, I_{GT} = 15 mA @ -40°C. If the triac is to be triggered when V_{in} ≤ 40 V

$$(R_1 + R_2) \approx V_{in}/I_{GT} \approx 40/0.015 \approx 2.3 \text{ k}$$

If we let R₂ = 2400 ohms and C = 0.1 μF, the snubbing requirements are met. Triacs having less sensitive gates will require that R₂ be lower and C be correspondingly higher as shown in Figure 4.

INPUT CIRCUITRY

Resistor Input

When the input conditions are well controlled, as for example when driving the MOC3011 from a TTL, DTL, or HTL gate, only a single resistor is necessary to interface the gate to the input LED of the MOC3011. This resistor should be chosen to set the current into the LED to be a minimum of 10 mA but no more than 50 mA. 15 mA is a suitable value, which allows for considerable degradation of the LED over time, and assures a long operating life for the coupler. Currents higher than 15 mA do not improve performance and may hasten the aging process inherent in LED's. Assuming the forward drop to be 1.5 V at

15 mA allows a simple formula to calculate the input resistor.

$$R_i = (V_{CC} - 1.5)/0.015$$

Examples of resistive input circuits are seen in Figures 2 and 6.

Increasing Input Sensitivity

In some cases, the logic gate may not be able to source or sink 15 mA directly. CMOS, for example, is specified to have only 0.5 mA output, which must then be increased to drive the MOC3011. There are numerous ways to increase this current to a level compatible with the MOC3011 input requirements; an efficient way is to use the MC14049B shown in Figure 6. Since there are six such buffers in a single package, the user can have a small package count when using several MOC3011's in one system.

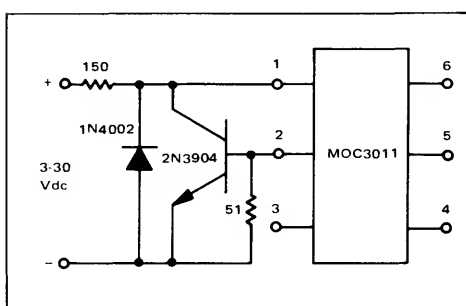


FIGURE 7 – MOC3011 Input Protection Circuit

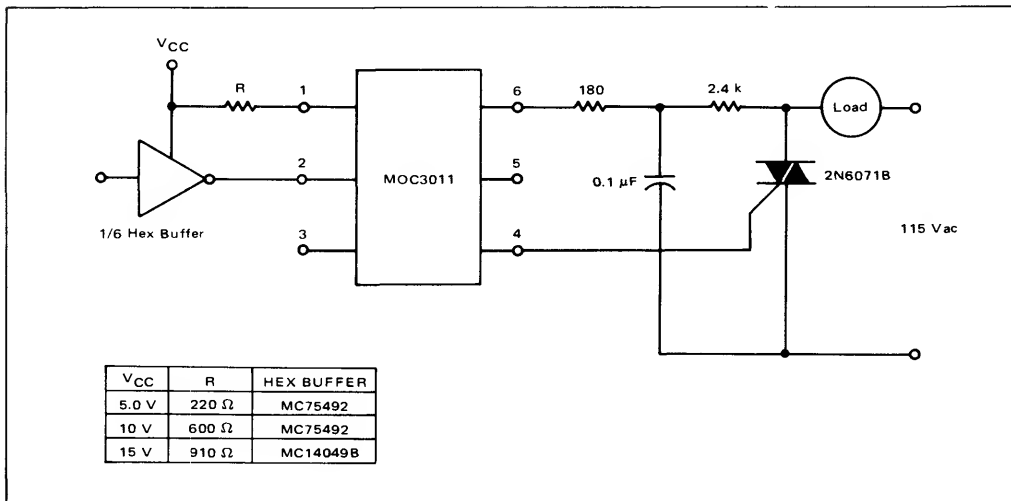


FIGURE 6 – MOS to ac Load Interface

Input Protection Circuits

In some applications, such as solid state relays, in which the input voltage varies widely the designer may want to limit the current applied to the LED of the MOC3011. The circuit shown in Figure 7 allows a non-critical range of input voltages to properly drive the MOC3011 and at the same time protects the input LED from inadvertent application of reverse polarity.

LED Lifetime

All light emitting diodes slowly decrease in brightness during their useful life, an effect accelerated by high temperatures and high LED currents. To allow a safety margin and insure long service life, the MOC3011 is actually tested to trigger at a value lower than the specified 10 mA input threshold current. The designer can therefore design the input circuitry to supply 10 mA to the LED and still be sure of satisfactory operation over

a long operating lifetime. On the other hand, care should be taken to insure that the maximum LED input current (50 mA) is not exceeded or the lifetime of the MOC3011 may be shortened.

APPLICATIONS EXAMPLES

Using the MOC3011 on 240 Vac Lines

The rated voltage of a MOC3011 is not sufficiently high for it to be used directly on 240 Vac line; however, the designer may stack two of them in series. When used this way, two resistors are required to equalize the voltage dropped across them as shown in Figure 8.

Remote Control of ac Voltage

Local building codes frequently require all 115 Vac light switch wiring to be enclosed in conduit. By using a MOC3011, a triac, and a low voltage source, it is

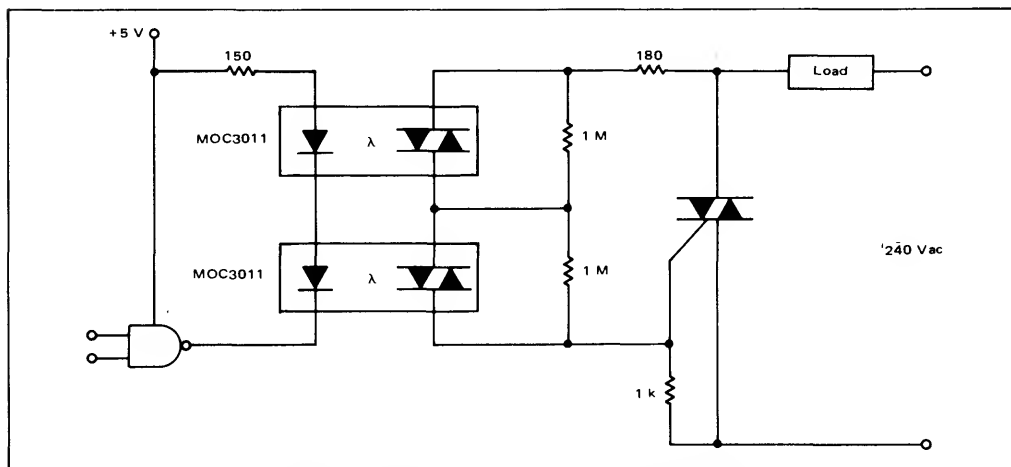


FIGURE 8 – 2 MOC3011 Triac Drivers in Series to Drive 240 V Triac

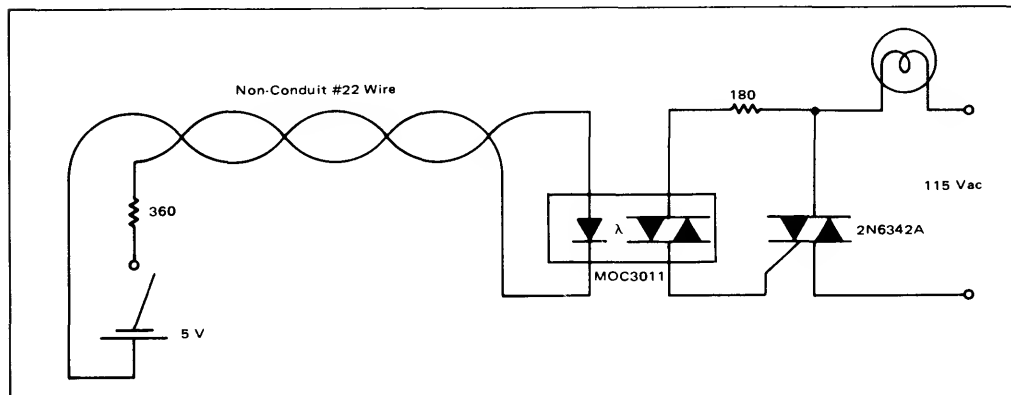


FIGURE 9 – Remote Control of ac Loads Through Low Voltage Non-Conduit Cable

possible to control a large lighting load from a long distance through low voltage signal wiring which is completely isolated from the ac line. Such wiring usually is not required to be put in conduit, so the cost savings in installing a lighting system in commercial or residential buildings can be considerable. An example is shown in Figure 9. Naturally, the load could also be a motor, fan, pool pump, etc.

Solid State Relay

Figure 10 shows a complete general purpose, solid state relay snubbed for inductive loads with input protection. When the designer has more control of the input and output conditions, he can eliminate those components which are not needed for his particular application to make the circuit more cost effective.

Interfacing Microprocessors to 115 Vac Peripherals

The output of a typical microcomputer input-output

(I/O) port is a TTL-compatible terminal capable of driving one or two TTL loads. This is not quite enough to drive the MOC3011, nor can it be connected directly to an SCR or triac, because computer common is not normally referenced to one side of the ac supply. Standard 7400 series gates can provide an input compatible with the output of an MC6820, MC6821, MC6846 or similar peripheral interface adaptor and can directly drive the MOC3011. If the second input of a 2 input gate is tied to a simple timing circuit, it will also provide energization of the triac only at the zero crossing of the ac line voltage as shown in Figure 11. This technique extends the life of incandescent lamps, reduces the surge current strains on the triac, and reduces EMI generated by load switching. Of course, zero crossing can be generated within the microcomputer itself, but this requires considerable software overhead and usually just as much hardware to generate the zero-crossing timing signals.

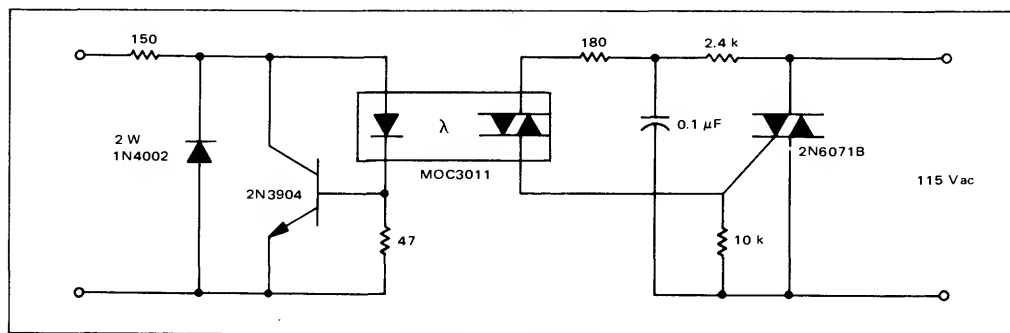
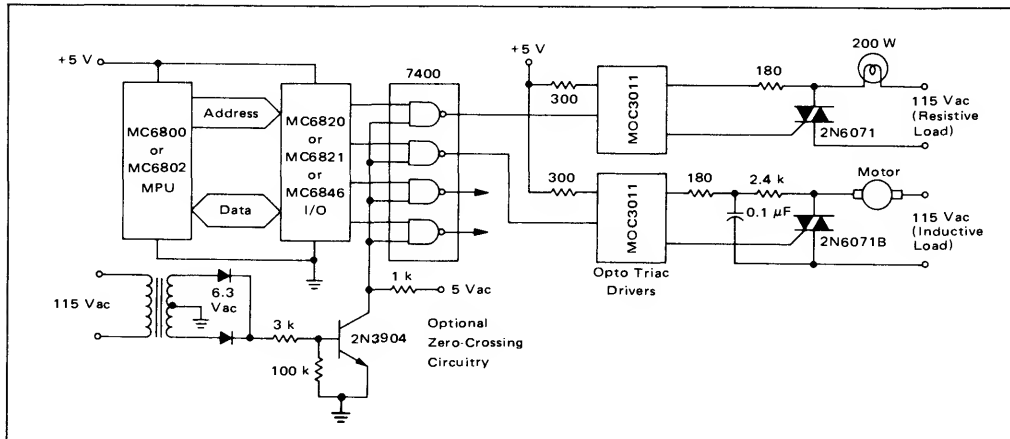
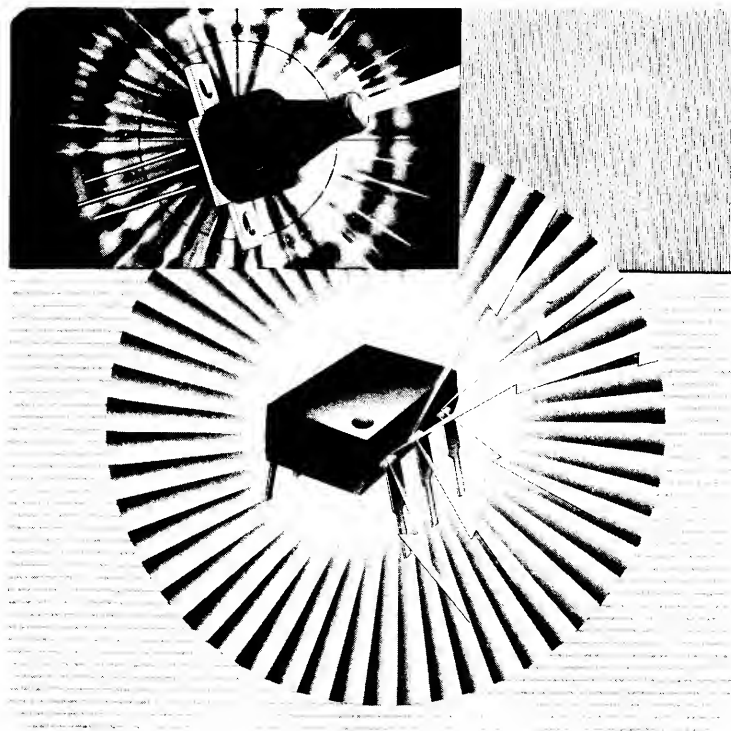


FIGURE 10 – Solid-State Relay



FIBER OPTICS



General Information

The Motorola Fiber Optic product portfolio is intended principally to address fiber optic communications systems in the computer, industrial controls, medical electronics, consumer and automotive applications.

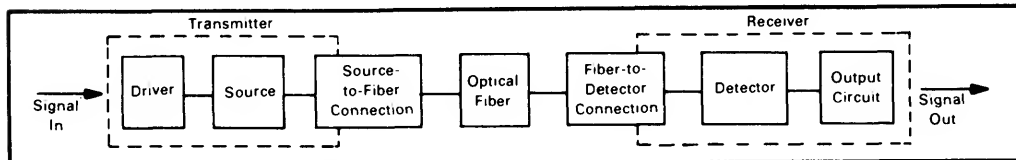
Analog and digital modulation schemes at bandwidths through 50 MHz and system lengths through several kilometers may be achieved using Motorola fiber optic semiconductor devices.

The semiconductors are housed in packages suitable for high-volume production and low cost. Most important, however, the packages are standardized, permitting interchangeability, speedy field maintenance, and easy assembly into systems.

FIBER OPTICS . . .

a new method of cabled communication and data transmission using modulated light through an optical cable.

Basic Fiber-Optic Link

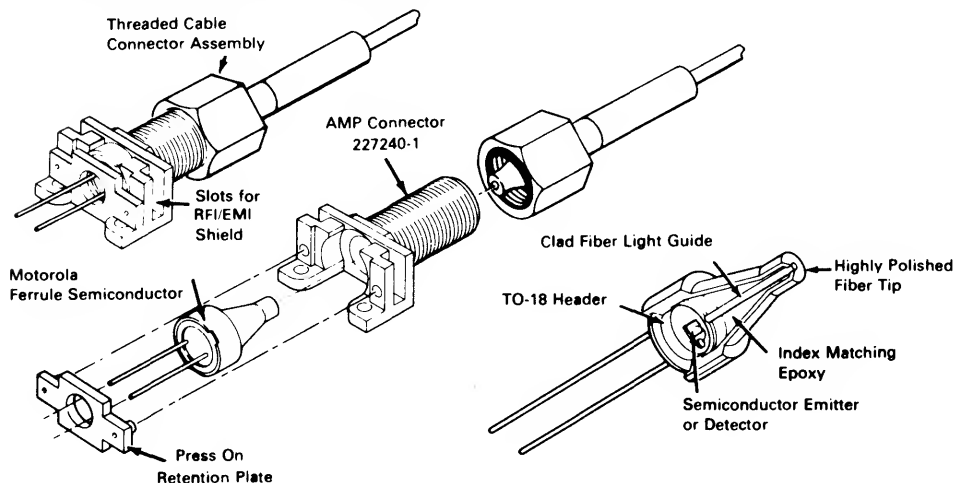


Fiber optics systems offer many advantages in terms of performance and cost over traditional electrical, coaxial or hard-wired transmission systems.

Fiber optic systems inherently provide:

- Ability to transmit a great deal of data on a single fiber
- Electrical isolation
- EMI/RFI noise immunity, no electromagnetic coupling
- No signal radiation or noise emission
- No spark or fire hazard
- Short circuit protection, no current flow
- Transmission security
- Lightweight, small diameter cable
- Lightning surge current and transient immunity
- Cost effectiveness

The fiber optic emitters and detectors are in the new and unique ferrule package and in the standard lensed TO-18 type package. This ferrule package was developed to provide maximum coupling of light between the die and the fiber. The package is small, rugged and producable in volume. The ferrule mates with the AMP ferrule connector #227240-1 for easy assembly into systems and precise fiber-to-fiber alignment. This assembly permits the efficient coupling of semiconductor-to-fiber cable and allows the use of any fiber type or diameter.



BASIC CONCEPTS OF FIBER OPTICS AND FIBER OPTIC COMMUNICATIONS

Prepared By:
John Bliss

Introduction

This note presents an introduction to the main principles of fiber optics. Its purpose is to review some basic concepts from physics that relate to fiber optics and the application of semiconductor devices to the generation and detection of light transmitted by optical fibers. The discussion begins with a description of a fiber optic link and the inherent advantages of fiber optics over wire.

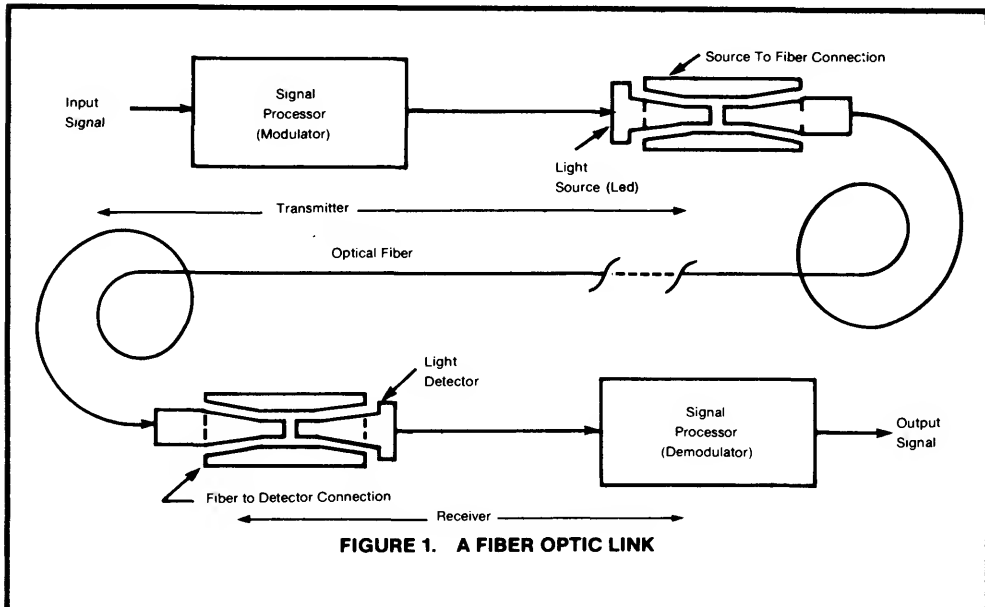
A fiber optic link .

Webster gives as one definition of a link "something which binds together or connects." In fiber optics, a link is the assembly of hardware which connects a source of a signal with

its ultimate destination. The items which comprise the assembly are shown in Figure 1. As the figure indicates, an input signal, for example, a serial digital bit stream, is used to modulate a light source, typically an LED (light emitting diode). A variety of modulation schemes can be used. These will be discussed later. Although input signal is assumed to be a digital bit stream, it could just as well be an analog signal, perhaps video.

The modulated light must then be coupled into the optical fiber. This is a critical element of the system. Based on the coupling scheme used, the light coupled into the fiber could be two orders of magnitude down from the total power of source.

Once the light has been coupled into the fiber, it is attenuated as it travels along the fiber. It is also subject to distortion. The degree of distortion limits the maximum data rate that can be transmitted.



At the receive end of the fiber, the light must now be coupled into a detector element (like a photo diode). The coupling problem at this stage, although still of concern, is considerably less severe than at the source end. The detector signal is then reprocessed or decoded to reconstruct the original input signal.

A link like that described in Figure 1 could be fully transparent to the user. That is, everything from the input signal connector to the output signal connector could be prepackaged. Thus, the user need only be concerned with supplying a signal of some standard format (like T1-L) and extracting a similar signal. Such a T1-in/T1-out system obviates the need for a designer to understand fiber optics. However, by analyzing the problems and concepts internal to the link, the user is better prepared to apply fiber optics technology to his system.

Advantages of Fiber Optics

There are both performance and cost advantages to be realized by using fiber optics over wire.

Greater Bandwidth. The higher the carrier frequency in a communications system, the greater its potential signal bandwidth. Since fiber optics work with carrier frequencies on the order of 10^9 - 10^{14} Hz as compared to radio frequencies of 10^6 - 10^8 Hz, signal bandwidths are potentially 10⁶ times greater.

Smaller size and weight. A single fiber is capable of replacing a very large bundle of individual copper wires. For example, a typical telephone cable may contain close to 1,000 pairs of copper wire and have a cross-sectional diameter of seven to ten centimeters. A single glass fiber cable capable of handling the same amount of signal might be only one-half centimeter in diameter. The actual fiber may be as small as 50 μ -meters. The additional size would be the jacket and strength elements. The weight reduction in this example should be obvious.

Lower attenuation. Length for length, optical fiber exhibits

less attenuation than does twisted wire or coaxial cable. Also, the attenuation of optical fibers, unlike that of wire, is not frequency dependent.

Freedom from EMI. Unlike wire, glass does not pick up nor generate electro-magnetic interference (EMI). Optical fibers do not require expensive shielding techniques to desensitize them to stray fields.

Ruggedness. Since glass is relatively inert in the kind of environments normally seen by wired systems, the corrosive nature of such environments is of less concern.

Safety. In many wired systems, the potential hazard of short circuits between wires or from wires to ground, requires special precautionary designs. The dielectric nature of optic fibers eliminates this requirement and the concern for hazardous sparks occurring during interconnects.

Lower Cost. Optical fiber costs are continuing to decline while the cost of wire is increasing. In many applications today, the total system cost for a fiber optic design is lower than for a comparable wired design. As time passes, more and more systems will be decidedly less expensive with optical fibers.

Physics of light

The performance of optical fibers can be fully analyzed by application of Maxwell's Equation for electromagnetic field theory. However, these are necessarily complex and, fortunately, can be bypassed for most users by the application of ray tracing and analysis. When considering LED's and photo detectors, the particle theory of light is used. The change from ray to particle theory is fortunately a simple step.

Over the years, it has been demonstrated that light (in fact, all electromagnetic energy) travels at approximately 300,000 Km/second in free space. It has also been demonstrated that in materials denser than free space, the speed of light is reduced. This reduction in the speed of light as it passes from free space

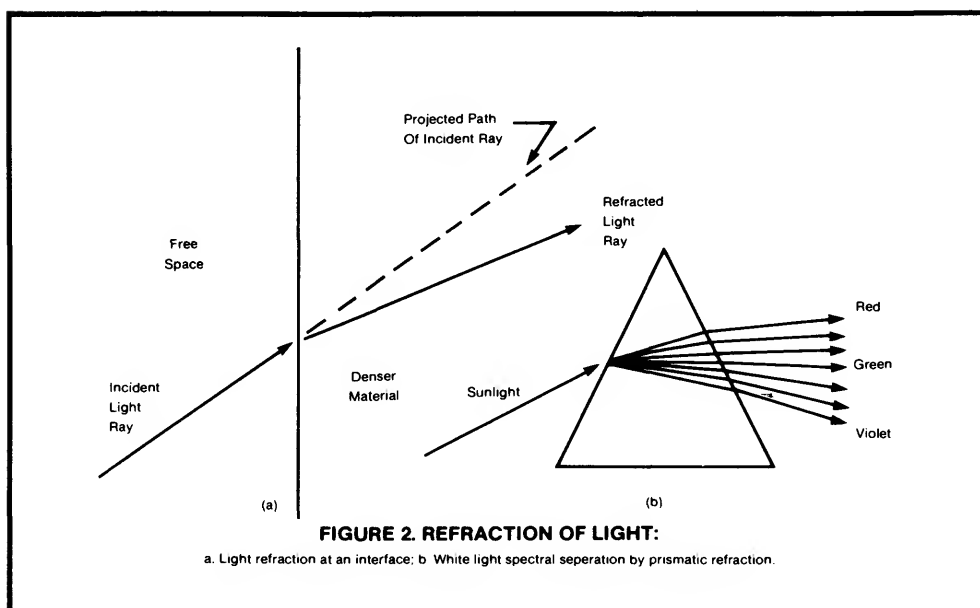


FIGURE 2. REFRACTION OF LIGHT:

a. Light refraction at an interface; b. White light spectral separation by prismatic refraction.

into a denser material results in refraction of the light. Simply stated, the light ray is bent at the interface. This is shown in Figure 2a. In fact, the reduction of the speed of light is different for different wavelengths; and, therefore, the degree of bending is different for each wavelength. It is this variation in effect for different wavelengths that results in rainbows. Water droplets in the air act like small prisms (Figure 2b) to split white sunlight into the visible spectrum of colors.

The actual bend angle at an interface is predictable and depends on the **refractive index** of the dense material. The **refractive index**, usually given the symbol n , is the ratio of the speed of light in free space to its speed in the denser material:

$$n = \frac{\text{speed of light in free space}}{\text{speed of light in given material}} \quad (1)$$

Although n is also a function of wavelength, the variation in many applications is small enough to be ignored and a single value is given. Some typical values of n are given in Table 1:

Table 1
Representative Indices of Refraction

| | |
|------------------------|--------------|
| Vacuum | 1.0 |
| Air | 1.0003 (1.0) |
| Water | 1.33 |
| Fused Quartz | 1.46 |
| Glass | 1.5 |
| Diamond | 2.0 |
| Silicon | 3.4 |
| Gallium-Arsenide | 3.6 |

It is interesting to consider what happens to a light ray as it meets the interface between two transmissive materials. Figure 3 shows two such materials of refractive indices n_1 and n_2 . A light ray is shown in material 1 and incident on the interface at point P. Snell's law states that:

$$n_1 \sin\theta_1 = n_2 \sin\theta_2 \quad (2)$$

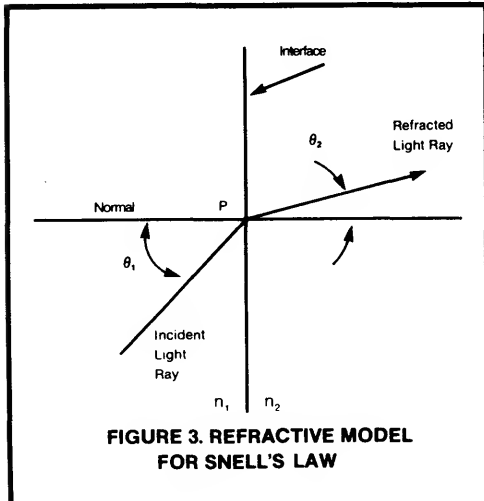


FIGURE 3. REFRACTIVE MODEL FOR SNELL'S LAW

The angle of refraction, θ_2 , can be determined:

$$\sin\theta_2 = \frac{n_1}{n_2} \sin\theta_1 \quad (3)$$

If material 1 is air, n_1 has the value of 1; and since n_2 is greater than 1, θ_2 is seen to be less than θ_1 ; that is, in passing through the interface, the light ray is refracted (bent) toward the normal.

If material 1 is not air but still an index of refraction less than material 2, the ray will still be bent toward the normal. Note that if n_2 is less than n_1 , θ_2 is greater than θ_1 , or the ray is refracted away from the normal.

Consider Figure 4 in which an incident ray is shown at an angle such that the refracted ray is along the interface, or the angle of refraction is 90°. Note that $n_1 > n_2$. Using Snell's law:

$$\sin\theta_2 = \frac{n_1}{n_2} \sin\theta_1 \quad (4)$$

or, with θ_2 equal to 90°:

$$\sin\theta_1 = \frac{n_2}{n_1} \sin\theta_2 \quad (5)$$

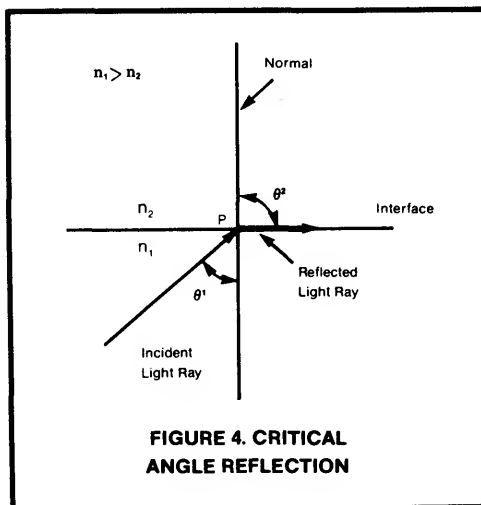


FIGURE 4. CRITICAL ANGLE REFLECTION

The angle, θ_c , is known as the critical angle and defines the angle at which incident rays will not pass through the interface. For angles greater than θ_c , 100 percent of the light rays are reflected (as shown in Figure 5), and the angle of incidence equals the angle of reflection.

This characteristic of reflection for light incident at greater than the critical angle is a fundamental concept in fiber optics.

Optical Fibers

Figure 6 shows the typical construction of an optical fiber. The central portion, or core, is the actual propagating path for light. Although the core is occasionally constructed of plastic, it is more typically made of glass. The choice of material will be discussed later. Bonded to the core is a cladding layer -- again, usually glass, although plastic cladding of glass core is not uncommon. The composition of glass can be tailored during

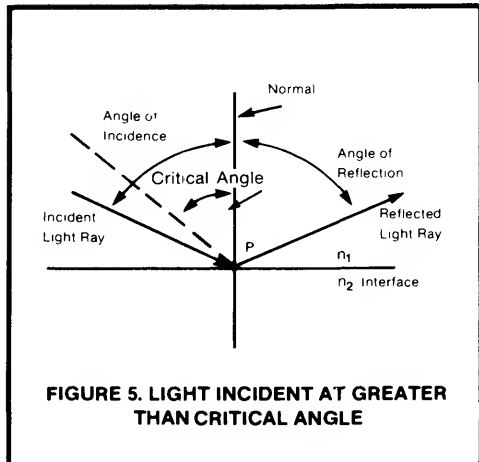


FIGURE 5. LIGHT INCIDENT AT GREATER THAN CRITICAL ANGLE

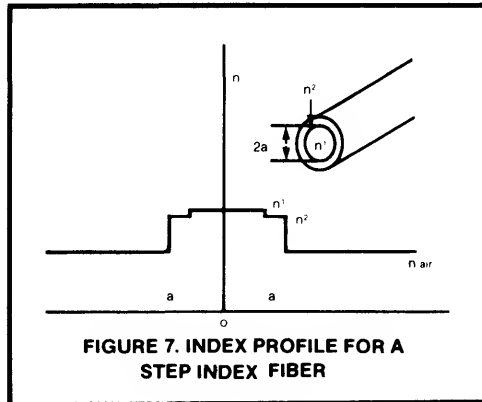


FIGURE 7. INDEX PROFILE FOR A STEP INDEX FIBER

processing to vary the index of refraction. For example, an all-glass, or silica-clad fiber, may have the compositions set so that the core material has an index of refraction of 1.5; and the clad has an index of refraction of 1.485. To protect the clad fiber, it is typically enclosed in some form of protective rubber or plastic jacket. This type of optical fiber is called a "step index multimode" fiber. Step index refers to the profile of the index of refraction across the fiber (as shown in Figure 7). The core has an essentially constant index n_1 . The classification "multimode" should be evident shortly.

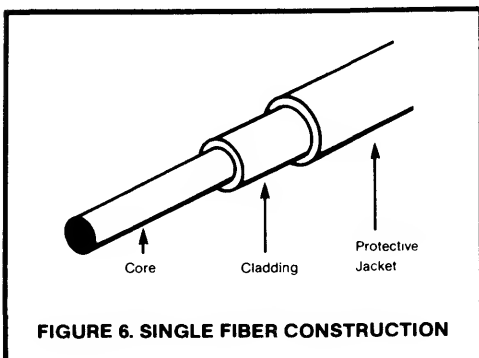


FIGURE 6. SINGLE FIBER CONSTRUCTION

Numerical Aperture

Applying the concept of total internal reflection at the n_1, n_2 interface, we can now demonstrate the propagation of light along the fiber core and the constraint on light incident on the fiber end to ensure propagation. Figure 8 illustrates the analysis. As the figure shows, ray propagation results from the continuous reflection at the core/clad interface such that the ray bounces down the fiber length and ultimately exits at the far end. If the principle of total internal reflection is applied at

point P, the critical angle value for θ_3 is found by Snell's law:

$$\theta_c = \theta_3 (\min) = \sin^{-1} \frac{n_2}{n_1} \quad (6)$$

Now, since θ_3 is a complementary angle to θ_2 ,

$$\theta_2 (\max) = \sin^{-1} \frac{(n_1^2 - n_2^2)^{1/2}}{n_1} \quad (7)$$

Again applying Snell's law at the entrance surface (recall $n_{\text{air}} = 1$).

$$\sin \theta_{\text{in}} (\max) = n_1 \sin \theta_2 (\max) \quad (8)$$

Combining (7) and (8),

$$\sin \theta_{\text{in}} (\max) = (n_1^2 - n_2^2)^{1/2} \quad (9)$$

$\theta_{\text{in}} (\max)$ represents the largest angle with the normal to the fiber end for which total internal reflection will occur at the core-clad interface. Light rays entering the fiber end at angles greater than $\theta_{\text{in}} (\max)$ will pass through the interface at P and be lost. The value $\sin \theta_{\text{in}} (\max)$ is one of the fundamental parameters for an optical fiber. It defines the half-angle of the cone of acceptance for light to be propagated along the fiber and is called the "numerical aperture," usually abbreviated N.A.

$$\text{N.A.} = \sin \theta_{\text{in}} (\max) = (n_1^2 - n_2^2)^{1/2} \quad (10)$$

There are several points to consider about N.A. and equation (10). Recall that in writing (8), we assumed that the material at the end of the fiber was air with an index of 1. If it were some other material, (8) would be written (with n_3 representing the material):

$$n_3 \sin \theta_{\text{in}} (\max) = n_1 \sin \theta_2 (\max) \quad (11)$$

and combining (7) and (11)

$$\sin_{\text{in}} (\max) = \frac{(n_1^2 - n_2^2)^{1/2}}{n_3} = \text{N.A.} \quad (12)$$

That is, the N.A. would be reduced by the index of refraction of the end material. When fiber manufacturers specify N.A., it is usually given for an air interface unless otherwise stated.

The second point concerns the absoluteness of N.A. The analysis assumed that the light rays entered the fiber, and in propagating along it, they continually passed through the central axis of the fiber. Such rays are called "meridional" rays. It is

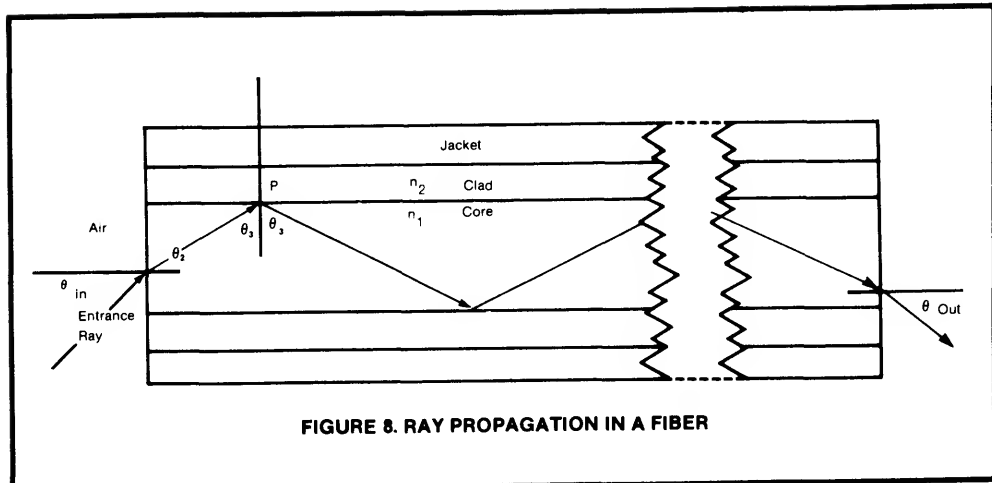


FIGURE 8. RAY PROPAGATION IN A FIBER

entirely possible that some rays may enter the fiber at such an angle that in passing down the fiber, they never intercept the axis. Such rays are called "skew" rays. An example is shown in both side and end views in Figure 9.

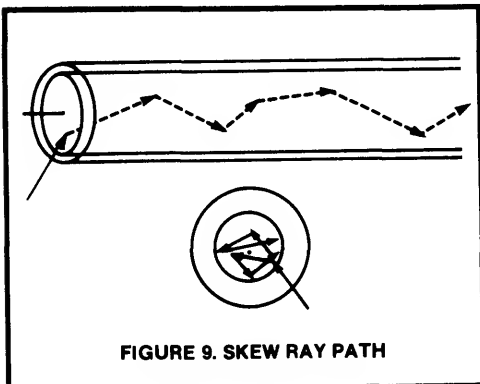


FIGURE 9. SKEW RAY PATH

1 meter to allow the attenuation of elad and high order modes¹) is connected to a high N.A. radiometric sensor, such as a large-area photodiode. The power detected by the sensor is read on a radiometer power meter. The other end of the fiber is mounted on

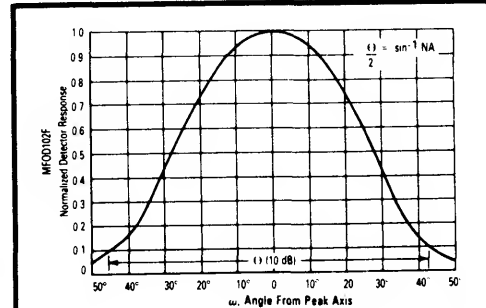


FIGURE 10. GRAPHICAL DEFINITION OF NUMERICAL APERTURE.

Also, some rays may enter at angles very close to the critical angle. In bouncing along the fiber, their path length may be considerably longer than rays at shallower angles. Consequently, they are subject to a larger probability of absorption and may, therefore, never be recovered at the output end. However, for very short lengths of fiber, they may not be lost. These two effects, plus the presence of light in the cladding for short lengths, results in the N.A. not cutting off sharply according to equations (10) and (12) and of appearing larger for short lengths. It is advisable to define some criteria for specifying N.A. At Motorola, N.A. is taken as the acceptance angle for which the response is no greater than 10dB down from the peak value. This is shown in Figure 10. Figure 11 shows a typical method of measuring a fiber's N.A. In the measurement, a sample to be measured (at least

a rotatable fixture such that the axis of rotation is the end of the fiber. A collimated light source is directed at the end of the fiber. This can be a laser or other source, such as an LED, at a sufficient distance to allow the rays entering the fiber to be paraxial. The fiber end is adjusted to find the peak response position. Ideally, this will be at zero degrees; but manufacturing variations could result in a peak slightly offset from zero. The received power level is noted at the peak. The fiber end is then rotated until the two points are found at which the received power is one-tenth the peak value. The sin of half the angle between these two points is the N.A.

The apparent N.A. of a fiber is a function of the N.A. of the

¹High order modes refers to steep angle rays.

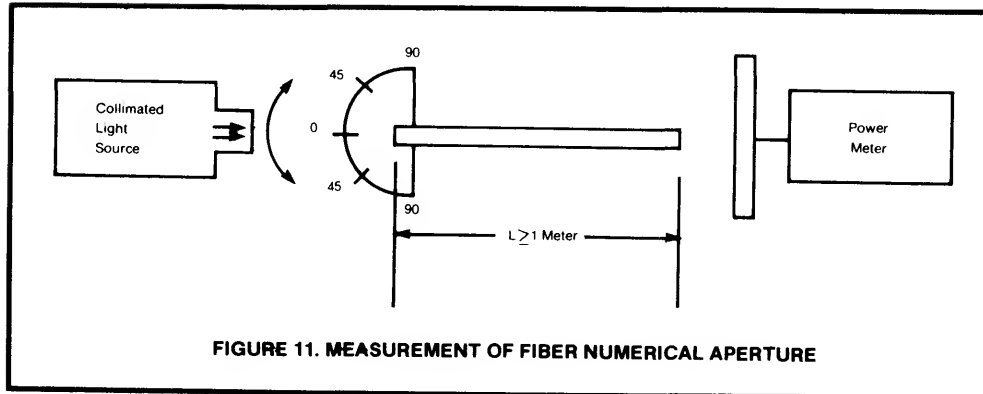


FIGURE 11. MEASUREMENT OF FIBER NUMERICAL APERTURE

source that is driving it. For example, Figures 12a and 12b are plots of N.A. versus length for the same fiber. In (12a) the source has a broad N.A. (0.7), while in (12b) the source N.A. is 0.32. Note that in both cases, the N.A. at 100m is about 0.31; but at 1 meter, the apparent N.A. is 0.42 in (12a) but 0.315 in (12b). The high order modes entering the fiber from the 0.7 N.A. source take nearly the full 100 meters to be stripped out by attenuation. Thus, a valid measurement of a fiber's true N.A. requires a collimated, or very low, N.A. source or a very long-length sample.

Fiber Attenuation

Mention was made above of the "stripping" or attenuation of high order modes due to their longer path length. This suggests that the attenuation of power in a fiber is a function of length. This is indeed the case. A number of factors contribute to the attenuation: imperfections at the core-clad interface; flaws in the consistency of the core material; impurities in the composition. The surface imperfections and material flaws tend to affect all wavelengths. The impurities tend to be selective in the

wavelength they affect. For example, hydroxyl molecules (OH^-) are strong absorbers of light at 900nm. Therefore, if a fiber manufacturer wants to minimize losses at 900nm, he will have to take exceptional care in his process to eliminate moisture (the source of OH^-). Other impurities are also present in any manufacturing process. The degree to which they are controlled will determine the attenuation characteristic of a fiber. The cumulative effect of the various impurities results in plots of attenuation versus wavelength exhibiting peaks and valleys. Four examples of attenuation (given in dB/Km) are shown in Figure 13.

Fiber Types

It was stated at the beginning of this section that fibers can be made of glass or plastic. There are three varieties available today:

1. Plastic core and cladding;
2. Glass core with plastic cladding -- often called 'PCS' (plastic-clad silica);
3. Glass core and cladding -- silica-clad silica.

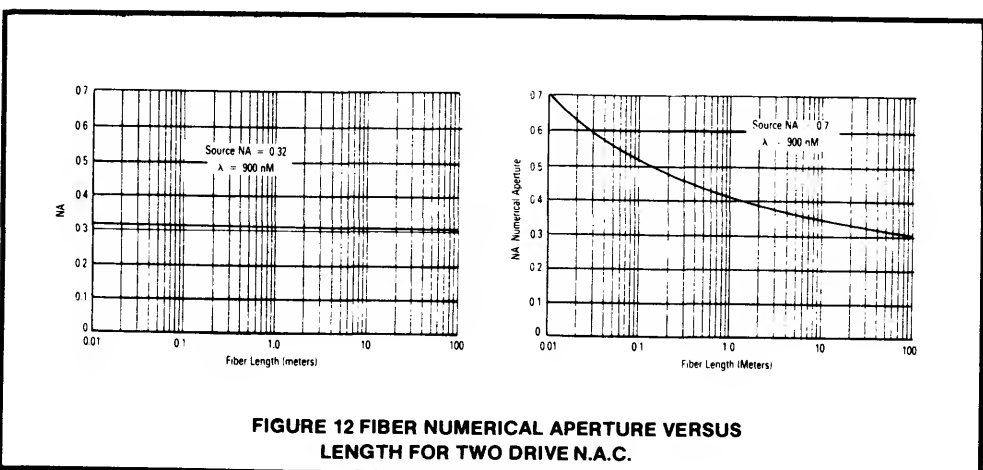


FIGURE 12 FIBER NUMERICAL APERTURE VERSUS LENGTH FOR TWO DRIVE N.A.C.

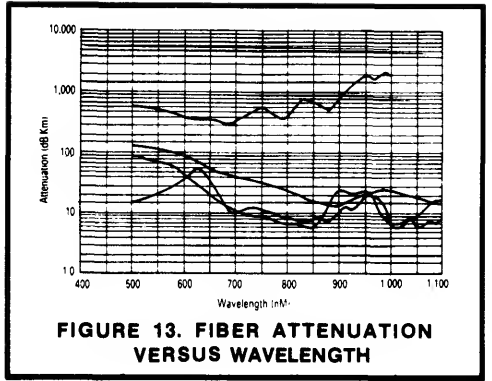


FIGURE 13. FIBER ATTENUATION VERSUS WAVELENGTH

All plastic fibers are extremely rugged and useful for systems where the cable may be subject to rough day-after-day treatment. They are particularly attractive for benchtop interconnects. The disadvantage is their high attenuation characteristic.

PCS cables offer the better attenuation characteristics of glass and are less affected by radiation than all-glass fibers.² They see considerable use in military-grade applications.

All glass fibers offer low attenuation performance and good concentricity, even for small-diameter cores. They are generally easy to terminate, relative to PCS. On the down side, they are usually the least rugged, mechanically, and more susceptible to increases in attenuation when exposed to radiation.

The choice of fiber for any given application will be a function of the specific system's requirements and trade-off options.

So far, the discussion has addressed single fibers. Fibers, particularly all-plastic, are frequently grouped in bundles. This is usually restricted to very low-frequency, short-distance applications. The entire bundle would interconnect a single light source and sensor or could be used in a fan-out at either end. Bundles are also available for interconnecting an array of sources with a matched

²It should be noted that the soft clad material should be removed and replaced by a hard clad material for best fiber core-to-connector termination.

array of detectors. This enables the interconnection of multiple discrete signal channels without the use of multiplex techniques. In this type of cable, the individual fibers are usually separated in individual jackets and, perhaps, each embedded in clusters of strength elements, like Kevlar. In one special case bundle, the fibers are arrayed in a ribbon configuration. This type cable is frequently seen in telephone systems using fiber optics.

In Figure 7, the refractive index profile was shown as constant over the core cross-section with a step reduction at the core-clad interface. The core diameter was also large enough that many modes (low and high order) are propagated along its path. In Figure 14, a section of this fiber is shown with three discrete modes shown propagating down the fiber. The lowest order mode is seen traveling along the axis of the fiber (or at least parallel to it). The middle order mode is seen to bounce several times at the interface. The total path length of this mode is certainly greater than that of the mode along the axis. The high order mode is seen to make many trips across the fiber, resulting in an extremely long path length.

The signal input to this fiber is seen as a step pulse of light. However, since all the light that enters the fiber at a fixed time does not arrive at the end at one time (the higher modes take longer to traverse their longer path), the net effect is to stretch or distort the pulse. This is characteristic of a multimode, step-index fiber and tends to limit the range of frequency for the data being propagated.

Figure 15 shows what this pulse stretching can do. An input pulse train is seen in (15a). At some distance (say 100 meters), the pulses (due to dispersion) are getting close to running together but are still distinguishable and recoverable. However, at some greater distance (say 200 meters), the dispersion has resulted in the pulses running together to the degree that they are indistinguishable. Obviously, this fiber would be unusable at 200 meters for this data rate. Consequently, fiber specifications usually give bandwidth in units of MHz-Km – that is, a 200 MHz-Km cable can send 200-MHz data up to 1 Km or 100-MHz data up to 2 Km etc.

To overcome the distortion due to path length differences, fiber manufacturers have developed graded index fiber. An example of multimode, graded-index fiber is shown in Figure 16.

In the fiber growth process, the profile of the index of refraction is tailored to follow the parabolic profile shown in the figure. This results in low order modes traveling through a constant density material. High order modes see lower density

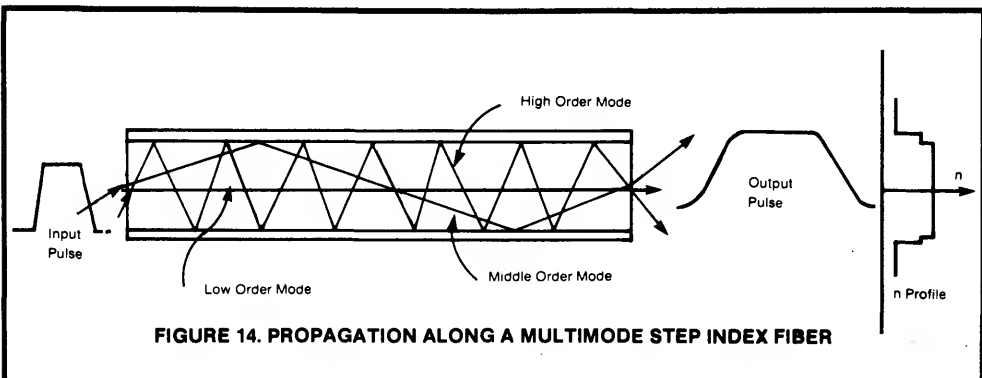
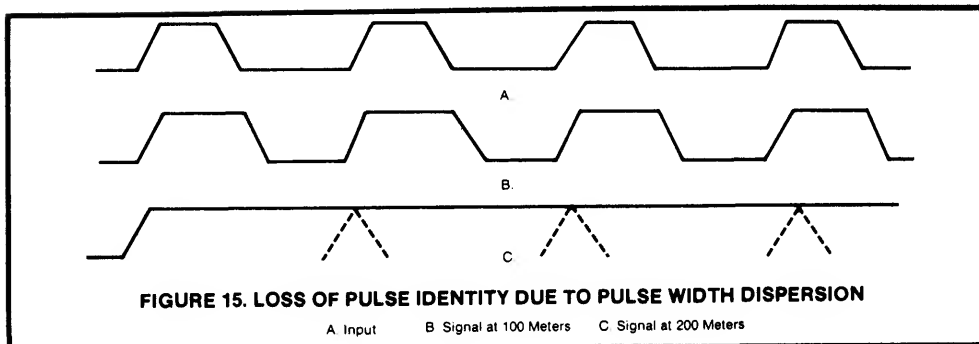


FIGURE 14. PROPAGATION ALONG A MULTIMODE STEP INDEX FIBER



material as they get further away from the axis of the core. Thus, the velocity of propagation increases away from the center. The result is that all modes, although they may travel different distances, tend to cover the length of the fiber in the same amount of time. This yields a fiber with higher bandwidth capability than multimode stepped index.

One more fiber type is also available. This is the single mode, step-index fiber shown in Figure 17. In this fiber, the core is extremely small (on the order of just a few micrometers). This type accepts only the lowest order mode and suffers no modal dispersion. It is an expensive fiber and requires a very high-power, highly-directional source like a laser diode. Consequently, applications for this type of fiber are the very high data rate, long-distance systems.

As a final statement on fiber properties, it is interesting to compare optical fiber with coax cable. Figure 18 show the loss versus frequency characteristics for a low-loss fiber compared with the characteristics of several common coax cables. Note that the attenuation of optical fiber is independent of frequency (up to the point where modal dispersion comes into play).

Active Components For Fiber Optics

Propagation through fiber optics is in the form of light or, more specifically, electromagnetic radiation in the spectral range of near-infrared or visible light. Since the signal levels to

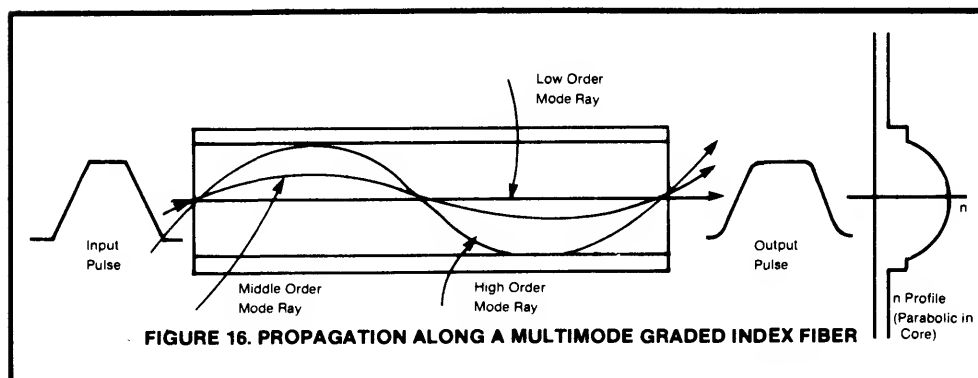
be dealt with are generally electrical in nature (like serial digital logic at standard T²L levels), it is necessary to convert the source signal into light at the transmitter end and from light back to T²L at the receive end. There are several components which can accomplish these conversions. This discussion will concentrate on light emitting diodes (LED's) as sources of PIN photodiodes and Integrated Detector Preampifiers (IDP's) as sensors.

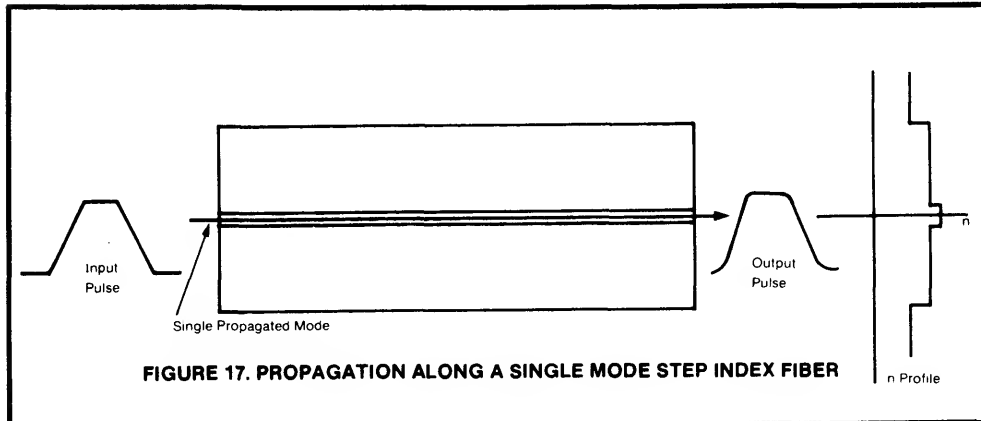
Light Emitting Diodes

Most people are familiar with LED's in calculator displays. Just as they are optimized geometrically and visually for the function of displaying characters, some LED's are specifically designed and processed to satisfy the requirements of generating light, or near-light (that is, infrared), for coupling into fibers. There are several criteria of importance for LED's used with fibers:

1. Output power;
2. Wavelength;
3. Speed;
4. Emission pattern.

Output power. Manufacturers are continually striving to increase the output power or efficiency of LED's. The more efficient an LED, the lower its drive requirements, or the greater the losses that can be accommodated elsewhere in the system.





However, total power emitted by an LED is not the whole picture (see **Emission Pattern**)

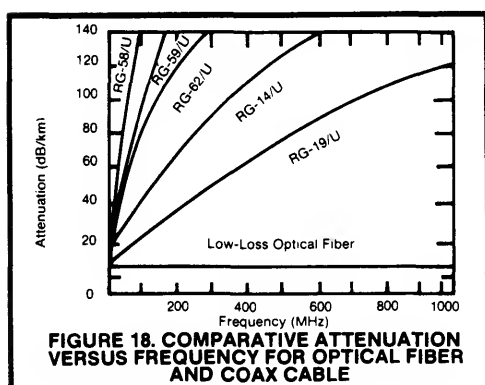
Wavelength. As shown earlier, optical fibers exhibit an attenuation characteristic that varies with wavelength. Figure 19 is a repeat of one of the sample curves from Figure 13. If this fiber were to be used in a system, the desired wavelength of operation would be about 875nm where the attenuation is down to about 7dB Km. The most undesirable wavelength for use in this fiber's range is 630nm where the loss is about 600dB Km. Therefore, all other considerations being satisfied, an LED with a characteristic emission wavelength of 875nm would be used.

to select the fastest diode available but rather the fastest required to do the job, with some margin designed in.

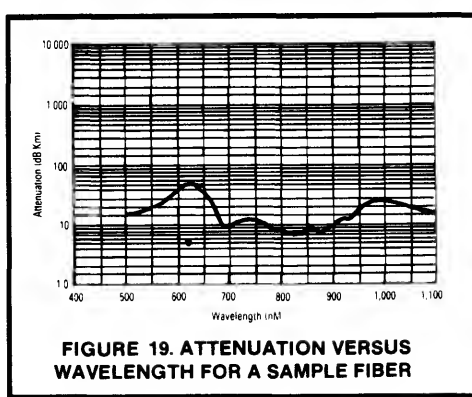
Emission Pattern. In typical data communications systems the light from the LED is coupled into a fiber with a core diameter of 100 to 200um. If the emission pattern of a particular LED is a collimated beam of 100um or less diameter, it might be possible to couple nearly all the power into the fiber. Thus, a 100uW LED with such an emission pattern might be a better choice than a 5mW LED with a lambertian³ pattern.

Light Generation

Light is emitted from an LED as a result of the recombining of electrons and holes. Electrically, an LED is just a P-N junction. Under forward bias, minority carriers are injected across the junction. Once across, they recombine with majority carriers and give up their energy in the process. The energy given up is approximately equal to the energy gap for the material. The same injection/recombination process occurs in any P-N junction; but in certain materials, the nature of the process is typically radiative -- that is, a light photon is produced. In other materials (silicon and germanium, for



Speed. LED's exhibit finite turn-on and turn-off times. A device with a response of 100nsec would never work in a 20-MHz system. (In general, the 3dB bandwidth is equal to 0.35 divided by the risetime.) In a symmetrical RTZ system (see data encoding later in this paper), the pulse width for a single bit would be 25nsec. A 100nsec LED would hardly have begun to turn on when it would be required to turn off. There is often a trade-off between speed and power, so it would not be advisable



example), the process is primarily non-radiative and no photons are generated.

Light emitting materials do have a distribution of non-radiative sites -- usually crystal lattice defects, impurities, etc. Minimizing these is the challenge to the manufacturer in his attempt to produce more efficient devices. It is also possible for non-radiative sites to develop over time and, thus, reduce efficiency. This is what gives LED's finite lifetimes, although 10^5 to 10^6 -hour lifetimes are essentially infinite compared with some other components of many systems.

The simplest LED structures are homojunction, epitaxially-grown devices and single-diffused devices. These structures are shown in Figure 20.

The epitaxially-grown LED is generally constructed of silicon-doped gallium-arsenide. A melt of elemental gallium containing arsenic and silicon dopant is brought in contact at high temperature with the surface of an n-type gallium-arsenide wafer. At the initial growth temperature, the silicon atoms in the dopant replace some of the gallium atoms in the crystal lattice. In so doing, they contribute an excess electron to the bond. This results in the grown layer being n-type. During the growth, the temperature is systematically reduced. At a certain critical temperature, the silicon atoms begin to replace some of the arsenic atoms in the crystal. This removes an electron from the bond, resulting in the formation of a p-type layer. As a finished diode, the entire surface, as well as the four sides, radiate light. The characteristic wavelength of this type of device is 940nm, and it typically radiates a total power of 3mW at 100mA forward current. It is relatively slow with turn-on and turn-off times on the order of 150nsec. The non-directionality of its emission makes it a poor choice as a light source for use with optical fibers.

The planar diffused LED is formed by controlled diffusion of zinc into a tellurium-doped n-gallium-arsenide wafer. A finished diode has a typical power output of 500uW at a wavelength of 900nm. Turn-on and turn-off times are usually around 15-20nsec. The emission pattern is lambertian, similar to the grown

¹Lambertian: The spatial pattern of reflected light from a sheet of paper, e.g. The intensity of light in any direction from a plane lambertian surface is equal to the intensity in the direction of the normal to the surface times the cos of the angle between the direction and the normal.

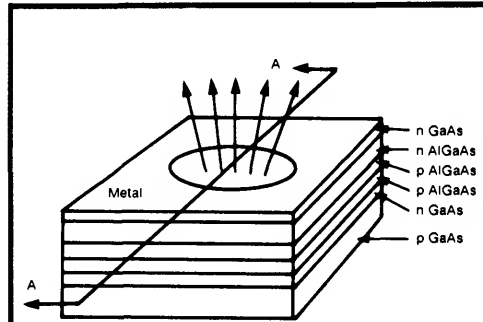


FIGURE 21. PLANAR HETEROJUNCTION LED

junction LED above.

Both of the above structures, although they can be used in fiber optics, are not optimized for the purpose of coupling into small fibers. Several variations of LED structures are currently used to improve the efficiency of light coupling into fibers. The two basic structures for fiber optic LED's are surface emitting and edge emitting. Surface-emitting devices are further broken down to planar and etched-well devices. The material used for these devices could be gallium-arsenide or any material which exhibits efficient photon-generating ability. The most common material in use today is the ternary crystal aluminum-gallium-arsenide. It is used extensively because it results in very efficient devices and has a characteristic wavelength around 820nm⁴ at which many fibers give lowest attenuation. (Many fibers are even better around 1300nm, but the materials technology for LED's at this wavelength -- InGaAsP -- is still on the front end of the learning curve; and devices are very expensive.)

Planar Fiber Optic LED

The planar heterojunction LED is somewhat similar to the grown junction LED of Figure 20a. Both utilize the liquid-phase epitaxial process to fabricate the device. The LED shown in Figure 21 is a heterojunction aluminum-gallium-arsenide

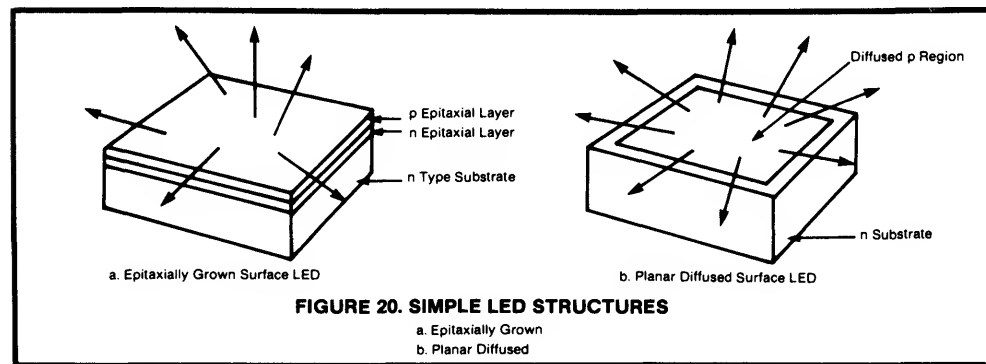


FIGURE 20. SIMPLE LED STRUCTURES

- a. Epitaxially Grown
- b. Planar Diffused

structure. The geometry is designed so that the device current is concentrated in a very small area of the active layer. This accomplishes several things: (1) the increase in current density makes for a brilliant light spot; (2) the small emitting area is well suited to coupling into small core fibers; and (3) the small effective area has a low capacitance and, thus, higher speed.

In Figure 21, the device appears to be nothing more than a multilayer version of the device in Figure 20a with a top metal layer containing a small opening. However, as the section view of AA shows in Figure 22, the internal construction provides some interesting features. To achieve concentration of the light emission in a small area, a method must be incorporated to confine the current to the desired area. Since the individual layers are grown across the entire surface of the wafer, a separate process must be used to confine the current. First an n-type tellurium-doped layer is grown on a zinc-doped p-type substrate. Before any additional layers are grown, a hole is etched through the n-layer and just into the substrate. The diameter of the hole defines the ultimate light-emitting area. Next, a p-type layer of Al_xGa_{1-x}As is grown. This layer is doped such that its resistivity is quite high; this impedes carrier flow in a horizontal direction, but vertical flow is not impeded since the layer is so thin. This ensures that current flow from the substrate will be confined to the area of the etched hole. The next layer to be grown is the p-type active layer. The aluminum-gallium mix of this layer gives it an energy gap corresponding to 820nm wavelength photons. The actual P-N junction is then formed by growth of an n-type tellurium-doped aluminum-gallium-arsenide. The doping and aluminum-gallium mix of this layer is set to give it a larger energy gap than the p-layer just below it. This makes it essentially transparent to the 820nm photons generated below. A final cap layer of gallium-arsenide is grown to enable ohmic contact by the top metal. The end result is an 820nm planar LED of small emission area. The radiation pattern is still lambertian, however.

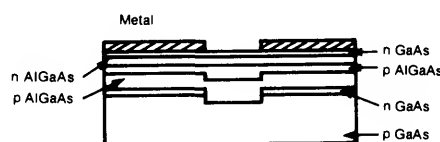


FIGURE 22. SECTION AA OF PLANAR HETEROJUNCTION LED

If a fiber with a core equal in area to the emission area is placed right down on the surface, it might seem that all the emitted light would be collected by the fiber; but since the emission pattern is lambertian, high order mode rays will not be launched into the fiber.

There is a way to increase the amount of light coupled. If a spherical lens is placed over the emitting area, the collimating

effect will convert high order modes to low order modes (see Figure 23).

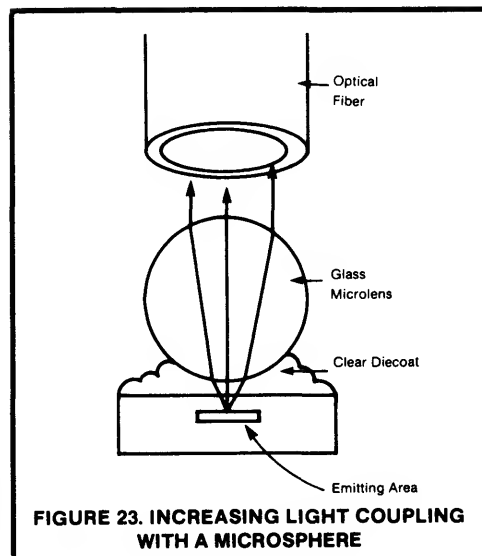


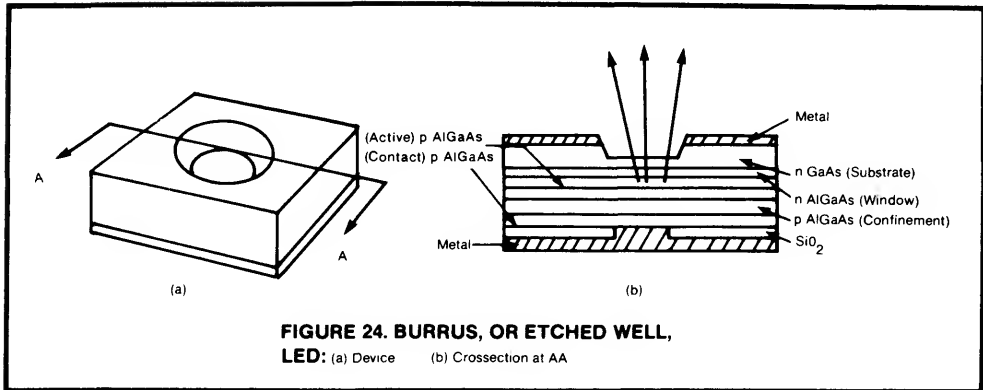
FIGURE 23. INCREASING LIGHT COUPLING WITH A MICROSPHERE

Etched-Well Surface LED

For data rates used in telecommunications (100 MHz), the planar LED becomes impractical. These higher data rates usually call for fibers with cores on the order of 50-62um. If a planar LED is used, the broad emission pattern of several hundred micro-meters will only allow a few percent of the power to be launched into the small fiber. Of course, the emission area of the planar device could be reduced; but this can lead to reliability problems. The increase in current density will cause a large temperature rise in the vicinity of the junction, and the thermal path from the junction to the die-attach header (through the confining layer and substrate) is not good enough to help draw the heat away from the junction. Continuous operation at higher temperature would soon increase the non-radiative sites in the LED and the efficiency would drop rapidly. If the chip is mounted upside down, the hot spot would be closer to the die-attach surface; but the light would have to pass through the thick substrate. The photon absorption in the substrate would reduce the output power significantly. The solution to this problem was developed by Burris and Dawson, of Bell Labs. The etched-well, or "Burris" diode, is shown in Figure 24.

The thick n-type substrate is the starting wafer. Successive layers of aluminum-gallium-arsenide are grown epitaxially on the substrate. The layer functions (confinement, active, window) are essentially the same as in the planar structure. After the final p-type layer (contact) is grown, it is covered with a layer of SiO₂. Small openings are then cut in the SiO₂ to define the active emitting area. Metal is then evaporated over the wafer and contacts the p-layer through the small openings. The final

*This is adjustable by varying the mix of aluminum in the aluminum-gallium-arsenide crystal.



processing consists of etching through the substrate. The etched wells are aligned over the active areas defined by the SiO_2 openings on the underside of the wafer and remove the heavily-photon-absorptive substrate down to the window layer. As an indication of the delicacy of this operation, it requires double-sided alignment on a wafer about 0.1m thick with a final thickness in the opening of about 0.025mm.

The radiation pattern from the Burrus diode is still lambertian. However, it is a remarkably-small emitting area and enables coupling into very small fibers (down to 50 μm). The close proximity of the hot spot (0.025mm) to the heat sink at the die attach makes it a reliable structure.

Several methods can be used for launching the emitted power into a fiber. These are shown in Figure 25.

The Burrus structure is superior to the planar for coupling to small fibers (<100 μm) but considerably more expensive due to its delicate structure.

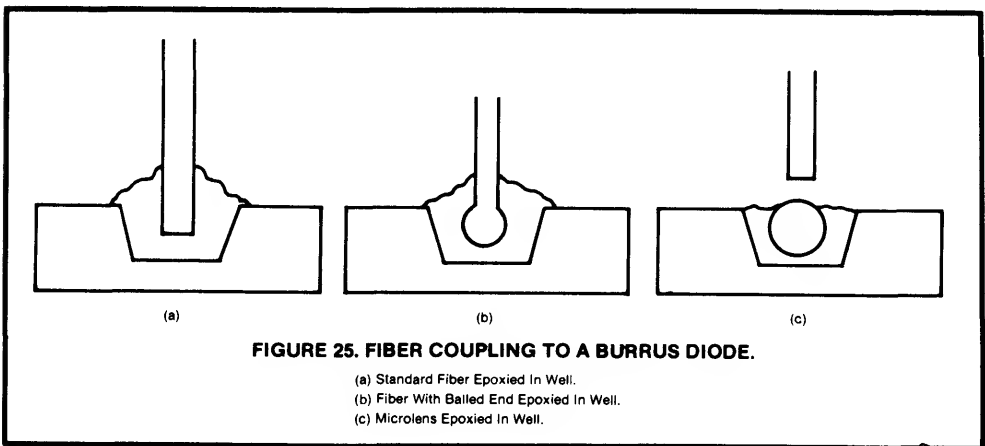
Edge-Emitting LED

The surface structures discussed above are lambertian

sources. A variation of the heterojunction family that emits a highly-directional pattern is the edge-emitting diode. This is shown in Figure 26. The layer structure is similar to the planar and Burrus diodes, but the emitting area is a stripe rather than a confined circular area. The emitted light is taken from the edge of the active stripe and forms an elliptical beam. The edge-emitting diode is quite similar to the diode lasers used for fiber optics. Although the edge emitter provides a very efficient source for coupling into small fibers, its structure calls for significant differences in packaging from the planar or Burrus.

Photo Detectors

PIN Photodiodes. Just as a P-N junction can be used to generate light, it can also be used to detect light. If a P-N junction is reverse-biased and under dark conditions, very little current flows through it. However, when a light shines on the device, photon energy is absorbed and hole-electron pairs are created. If the carriers are created in or near the depletion region at the junction, they are swept across the junction by the electric field. This movement of charge carriers across the junction



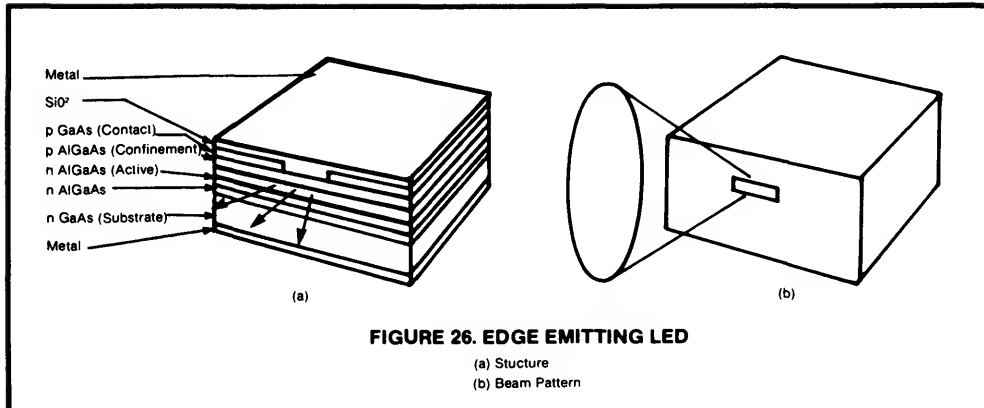


FIGURE 26. EDGE EMITTING LED

(a) Structure
(b) Beam Pattern

causes a current flow in the circuitry external to the diode. The magnitude of this current is proportional to the light power absorbed by the diode and the wavelength. A typical photodiode structure is shown in Figure 27, and the IV characteristic and spectral sensitivity are given in Figure 28.

In Figure 28a, it is seen that under reverse-bias conditions, the current flow is noticeable a function of light power density on the device. Note that in the forward-bias mode, the device eventually acts like an ordinary forward-biased diode with an exponential IV characteristic.

Although this type of P-N photodiode could be used as a fiber optic detector, it exhibits three undesirable features. The noise performance is generally not good enough to allow its use in sensitive systems; it is usually not fast enough for high-speed data applications; and due to the depletion width, it is not sensitive enough. For example, consider Figure 29. The depletion is indicated by the plot of electric field. In a typical device, the p-anode is very heavily doped; and the bulk of the depletion region is on the n-cathode side of the junction. As light shines on the device, it will penetrate through the p-region

toward the junction. If all the photon absorption takes place in the depletion region, the generated holes and electrons will be accelerated by the field and will be quickly converted to circuit current. However, hole-electron pair generation occurs from the surface to the back side of the device. Although most of it occurs within the depletion region, enough does occur outside this region to cause a problem in high-speed applications. This problem is illustrated in Figure 30. A step pulse of light is applied to a photodiode. Because of distributed capacitance and bulk resistance, and exponential response by the diode is expected. The photocurrent wave form show this as a ramp at turn-on. However, there is a distinct tail that occurs starting at point "a." The initial ramp up to "a" is essentially the response within the depletion region. Carriers that are generated outside the depletion region are not subject to acceleration by the high electric field. They tend to move through the bulk by the process of diffusion, a much slower travel. Eventually, these carriers reach the depletion region and are sped up. The effect can be eliminated, or at least substantially reduced by using a PIN structure. This is shown in Figure 31, and the electric field

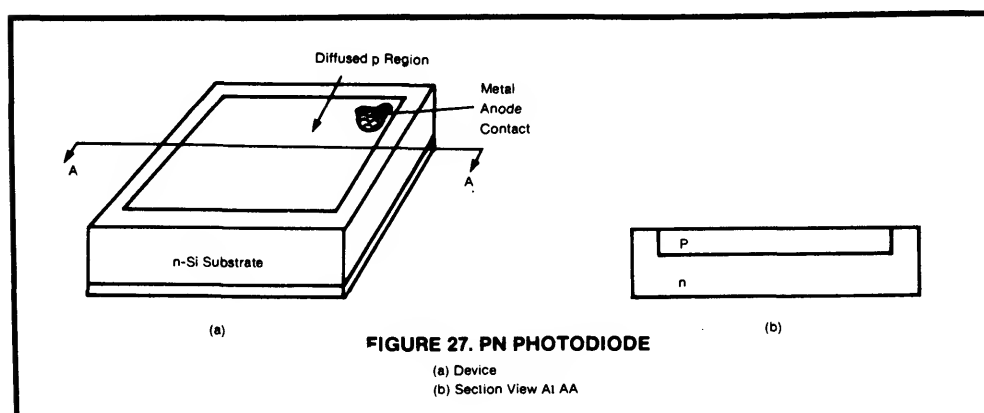


FIGURE 27. PN PHOTODIODE

(a) Device
(b) Section View At AA

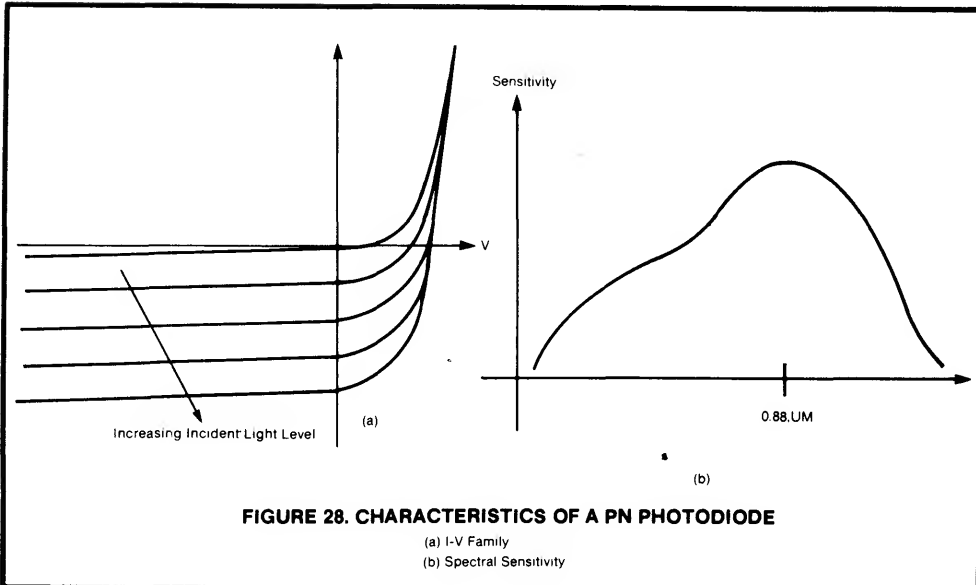


FIGURE 28. CHARACTERISTICS OF A PN PHOTODIODE

(a) I-V Family
 (b) Spectral Sensitivity

distribution is shown in Figure 32. Almost the entire electric field is across the intrinsic (I) region so that very few photons are absorbed in the p- and n- region. The photocurrent response in such a structure is essentially free of the tailing effect seen in Figure 30.

In addition to the response time improvements, the high resistivity I-region gives the PIN diode lower noise performance.

The critical parameters for a PIN diode in a fiber optic application are:

1. Responsivity;
2. Dark current;
3. Response speed;
4. Spectral response.

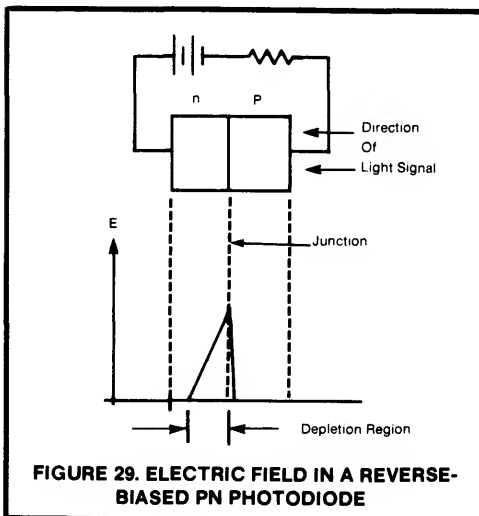


FIGURE 29. ELECTRIC FIELD IN A REVERSE-BIASED PN PHOTODIODE

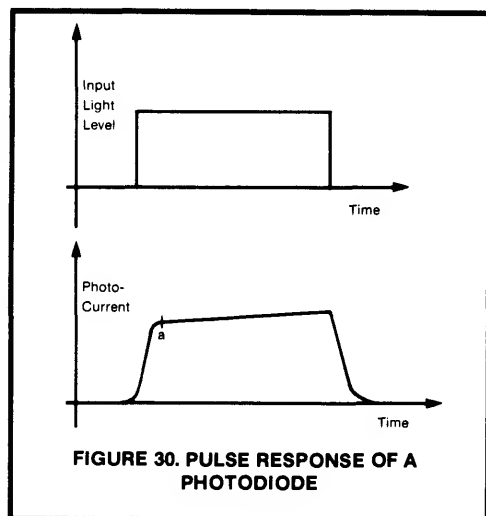


FIGURE 30. PULSE RESPONSE OF A PHOTODIODE

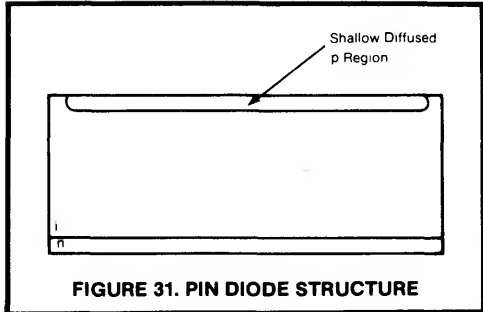


FIGURE 31. PIN DIODE STRUCTURE

Responsivity is usually given in amps/watt at a particular wavelength. It is a measure of the diode output current for a given power launched into the diode. In a system, the designer must then be able to calculate the power level coupled from the system to the diode (see AN-804, listed in Bibliography).

Dark current is the thermally-generated reverse leakage current in the diode. In conjunction with the signal current calculated from the responsivity and incident power, it gives the designer the on-off ratio to be expected in a system.

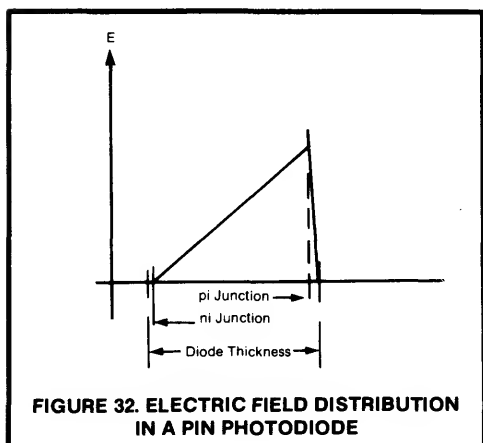


FIGURE 32. ELECTRIC FIELD DISTRIBUTION IN A PIN PHOTODIODE

Response Speed determines the maximum data rate capability of the diode; and in conjunction with the response of other elements of the system, it sets the maximum system data rate.⁵

Spectral Response determines the range, or system length, that can be achieved relative to the wavelength at which responsivity is characterized. For example, consider Figure 33. The responsivity of the MFOD102F is given as 0.15A/W at 900nm. As the curve indicates, the response at 900nm is 78 percent of the peak response. If the diode is to be used in a

system with an LED operating at 820nm, the response (or system length) would be:

$$R(820) = \frac{.98}{.78} R(900) = 1.26 R(900) \quad (13)$$

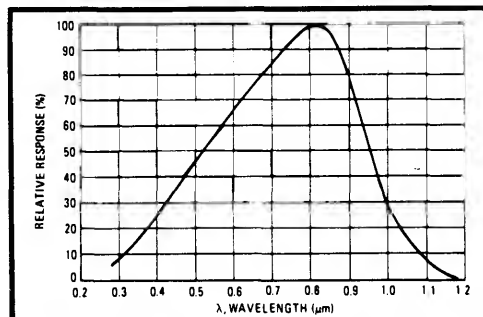


FIGURE 33. RELATIVE SPECTRAL RESPONSE MFOD 102F PIN PHOTODIODE

Integrated Detector Preamplifiers. The PIN photodiode mentioned above is a high output impedance current source. The signal levels are usually on the order of tens of nanoamps to tens of microamps. The signal requires amplification to provide data at a usable level like T²L. In noisy environments, the noise-insensitive benefits of fiber optics can all be lost at the receiver connection between diode and amplifier. Proper shielding can prevent this. An alternative solution is to integrate the follow-up amplifier into the same package as the photo diode. This device is called an integrated detector preamplifier (IDP). An example of this is given in Figure 34.

Incorporating an intrinsic layer into the monolithic structure is not practical with present technology, so a P-N junction photodiode is used. The first two transistors form a transimpedance amplifier. A third stage emitter follower is used to provide resistive negative feedback. The amplifier gives a low impedance voltage output which is then fed to a phase splitter. The two outputs are coupled through emitter followers.

The MFOD404F IDP has a responsivity greater than 20mV/uW at 900nm. The response rise and fall times are 50nS maximum, and the input light power can go as high as 30uW before noticeable pulse distortion occurs. Both outputs offer a typical impedance of 200Ω.

The IDP can be used directly with a voltage comparator or, for more sophisticated systems, could be used to drive any normal voltage amplifier. Direct drive of a comparator is shown in Figure 35.

A Fiber Optics Communications System

Now that the basic concepts and advantages of fiber optics and the active components used with them have been discussed, it is of interest to go through the design of a system. The system will be a simple point-to-point application operating in the simplex⁶ mode. The system will be analyzed for three aspects:

⁵Device capacitance also impacts this. See "Designer's Guide to Fiber-Optic Data Links" listed in Bibliography.

⁶In a simplex system, a single transmitter is connected to a single receiver by a single fiber. In a half duplex system, a single

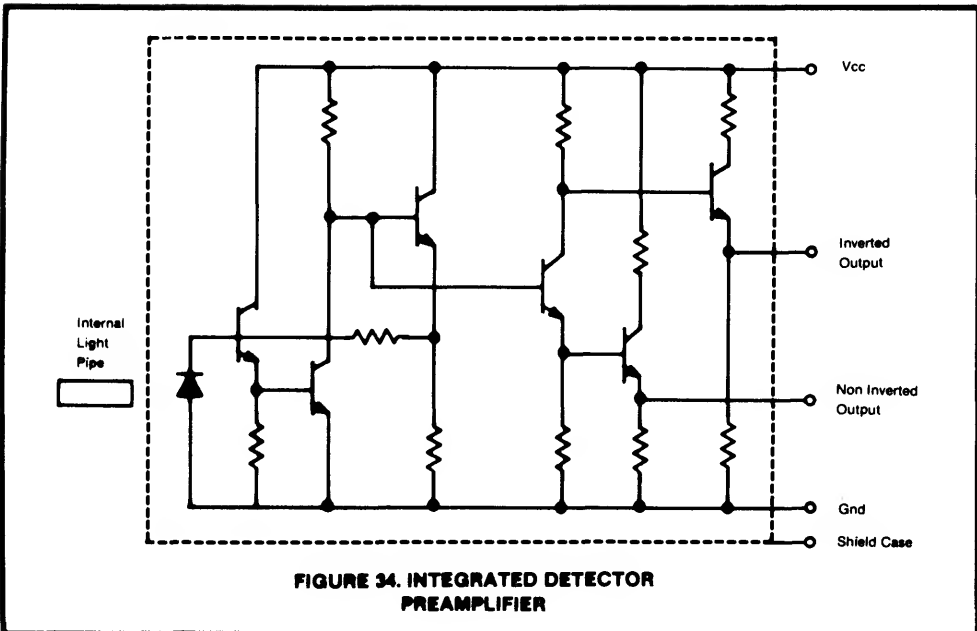


FIGURE 34. INTEGRATED DETECTOR PREAMPLIFIER

1. Loss budget:
2. Rise time budget:
3. Data encoding format.

Loss Budget. If no in-line repeaters are used, every element of the system between the LED and the detector introduces some loss into the system. By identifying and quantifying each loss, the designer can calculate the required transmitter power to ensure a given signal power at the receiver, or conversely, what signal power will be received for a given transmitter power. The process is referred to as calculating the system loss budget.

This sample system will be based on the following individual characteristics:

Transmitter: MFOE102F, characteristics in data sheet.

Fiber: Silica-clad silica fiber with a core diameter of 200 μm ; step index multimode; 20dB / Km attenuation at 900 nm; N.A. of 0.35; and a 3dB bandwidth of 5MHz-Km.

Receiver: MFOD404F, characteristics in data sheet.

The system will link a transmitter and receiver over a distance of 250 meters and will use a single section of fiber (no splices).

*cont. from pg. 5-17

fiber provides a bidirectional alternate signal flow between a transmitter/receiver pair at each end. A full duplex system would consist of a transmitter and receiver at each end and a pair of fibers connecting them.

Some additional interconnect loss information is required.⁷

1. Whenever a signal is passed from an element with an N.A. greater than the N.A. of the receiving element, the loss incurred is given by:

$$\text{N.A. Loss} = 20 \log (\text{NA}_1 / \text{NA}_2) \quad (14)$$

where: NA₁ is the exit numerical aperture of the signal source;
 where: NA₂ is the acceptance N.A. of the element|receiving the signal.
2. Whenever a signal is passed from an element with a cross-sectional area greater than the area of the receiving element, the loss incurred is given by:

$$\text{Area Loss} = 20 \log (\text{Diameter}_1 / \text{Diameter}_2) \quad (15)$$

where: Diameter₁ is the diameter of the signal source (assumes a circular fiber port);
 where: Diameter₂ is the diameter of the element receiving the signal.
3. If there is any space between the sending and receiving elements, a loss is incurred. For example: an LED with an exit N.A. of 0.7 will result in a gap loss of 2dB if it couples into a fiber over a gap of 0.15mm.
4. If the source and receiving elements have their axes offset, there is an additional loss. This loss is also dependent on the separation gap. For an LED with an exit N.A. of 0.7 and a gap with its receiving fiber of 0.15mm, there will be a loss of 2.5dB for an axial misalignment of 0.035mm.

⁷For a detailed discussion of all these loss mechanisms, see AN-804.

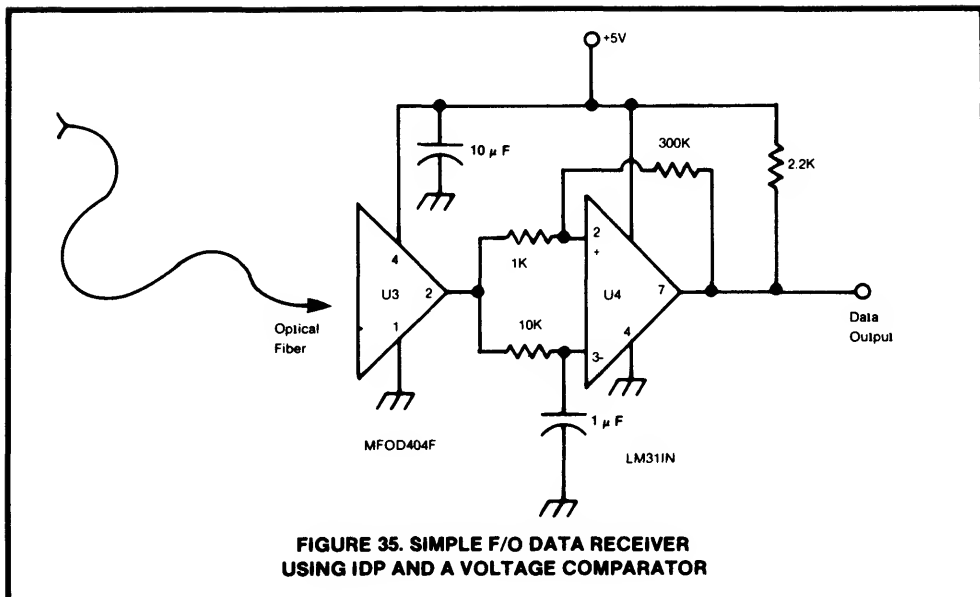


**FIGURE 35. SIMPLE F/O DATA RECEIVER
USING IDP AND A VOLTAGE COMPARATOR**

5. If the end surfaces of the two elements are not parallel, an additional loss can be incurred. If the non-parallelity is held below 2-3 degrees, this loss is minimal and can generally be ignored.
6. As light passes through any interface, some of it is reflected. This loss, called Fresnel loss, is a function of the indices of refraction of the materials involved. For the devices in this example, this loss is typically 0.2dB/interface.

The system loss budget is now ready to be calculated. Figure 38 shows the system configuration. Table II presents the individual loss contribution of each element in the link.

TABLE II
Fiber Optic Link Loss Budget

| | Loss Contribution |
|--|-------------------|
| MFOE102F to Fiber N.A. Loss | 6.02dB |
| MFOE102F to Fiber Area Loss | 0 |
| Transmitter Gap Loss (see text) | 2.00dB |
| Transmitter Misalignment Loss (see text) | 2.50dB |
| Fiber Entry Fresnel Loss | 0.20dB |
| Fiber Attenuation (250 meters) | 5.00dB |
| Fiber Exit Fresnel Loss | 0.20dB |
| Receiver Gap Loss | 2.00dB |
| Receiver Misalignment Loss | 2.50dB |
| Detector Fresnel Loss | 0.20dB |
| Fiber to Detector N.A. Loss | 0 |
| Fiber to Detector Area Loss | 0 |
| Total Path Loss | 20.62dB |

Note that in Table II no Fresnel loss was considered for the LED. This loss, although present, is included in specifying the

output power in the data sheet.

In this system, the LED is operated at 100 mA. MFOE102F shows that at this current the instantaneous output power is typically 130uW. This assumes that the junction temperature is maintained at 25°C. The output power from the LED is then converted to a reference level relative to 1mW:

$$P_o = 10 \log \frac{0.13mW}{1.0mW} \quad (16)$$

$$P_o = -8.86dBm \quad (17)$$

The power received by the MFOD404F is then calculated:

$$P_R = P_o - \text{loss} \quad (18)$$

$$P_R = 10(-2.948)mW = 0.001mW \quad (19)$$

This reference level is now converted back to absolute power:

$$P_R = 10(-2.948)mW = 0.001mW \quad (20)$$

Based on the typical responsivity of the MFOD404F, the expected output signal will be:

$$V_o = (30mV/uW)(1uW) = 30mV \quad (21)$$

As shown in MFOD404F, the output signal will be typically seventy-five times above the noise level.

In many cases, a typical calculation is insufficient. To perform a worst-case analysis, assume that the signal-to-noise ratio at the MFOD404F output must be 20dB. The maximum noise output voltage is 1.0mV. Therefore, the output signal must be 10mV. With a worst-case responsivity of 20mV/uW, the received power must be:

$$P_R = \frac{V_o}{R} = \frac{10mV}{20mV/uW} = 0.5uW \quad (22)$$

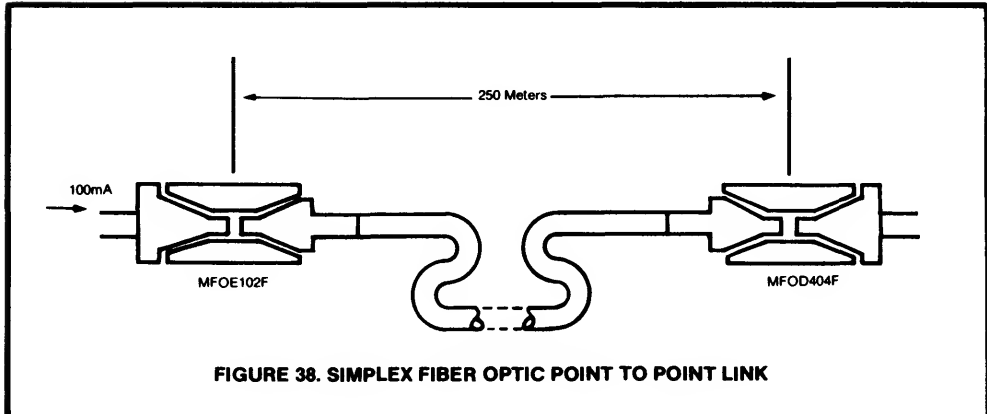


FIGURE 38. SIMPLEX FIBER OPTIC POINT TO POINT LINK

$$P_R = 10 \log \frac{0.0005 \text{mW}}{1 \text{mW}} = -33 \text{dBm} \quad (23)$$

The link loss was already performed as worst case, so:

$$P_o(\text{LED}) = -33 \text{dBm} + 20.62 \text{dB} = -12.39 \text{dBm} \quad (24)$$

$$P_o = 10(-1.23) \text{mW} = 0.0577 \text{mW} = 57.7 \mu\text{W} \quad (25)$$

MFOE102F includes a derating curve for LED output versus junction temperature. At 100mA drive, the forward voltage will be greater than 1.5V worst case. Although it will probably be less than 2.0V, using 2.0V will give a conservative analysis:

$$P_{DSS} = (0.1A)(2V) = 200 \text{mW} \quad (26)$$

This is within the maximum rating for operation at 25°C ambient. If we assume the ambient will be 25°C or less, the junction temperature can be conservatively calculated:

$$\Delta T_j = (400 \text{C/W})(0.2 \text{W}) = 80^\circ\text{C} \quad (27)$$

If we are transmitting digital data, we can assume an average duty cycle of 50 percent so that the ΔT_j will likely be 40°C. This gives:

$$T_j = T_A + \Delta T_j = 65^\circ\text{C} \quad (28)$$

The power output derating curve shows a value of 0.65 at 65°C. Thus, the DC power level will be:

$$P_o(\text{DC}) = \frac{57.7 \mu\text{W}}{0.65} = 88.77 \mu\text{W} \quad (29)$$

As MFOE102F indicates, at 50mA DC the minimum power is 40μW. Doubling the current should approximately double the output power, giving 80μW.

Since the required DC equivalent power is 87.77μW, the link may be marginal under worst case conditions. The designer may be required to compromise somewhat on S/N ratio for the output signal or set higher minimum output power* or responsivity specifications on the LED and detector devices. Use of a lower attenuation cable, or higher N/A cable, would also help by reducing the length loss or N/A loss at the

transmitter end.

Rise Time Budget. The cable for this system was specified to have a bandwidth of 5 MHz-Km. Since the length of the system is 250 meters, the system bandwidth, if limited by the cable, is 20 MHz. Data links are usually rated in terms of a rise time budget. The system rise time is found by taking the square root of the sum of the squares of the individual elements. In this system the only two elements to consider are the LED and the detector. Thus:

$$t_{Rise} = \sqrt{(t_{Rise, \text{LED}})^2 + (t_{Rise, \text{detector}})^2} \quad (30)$$

Using the typical values of MFOD404F and MFOE102F:

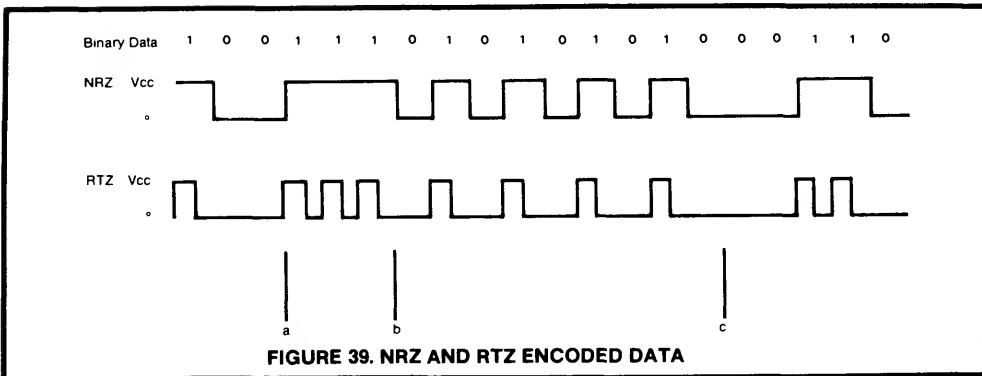
$$t_{Rise} = \sqrt{(25)^2 + (50)^2} = 60 \text{nS} \quad (31)$$

Total system performance may be impacted by including the rise time of additional circuit elements. Additional considerations are covered in detail in AN-794 and the Designer's Guide mentioned earlier (see Bibliography).

Data Encoding Format. In a typical digital system, the coding format is usually NRZ, or non-return to zero. In this format, a string of ones would be encoded as a continuous high level. Only when there is a change of state to a "0" would the signal level drop to zero. In RTZ (return to zero) encoding, the first half of a clock cycle would be high for a "1" and low for a "0." The second half would be low in either case. Figure 39 shows an NRZ and RTZ waveform for a binary data stream. Note between a-b the RTZ pulse rate repetition rate is at its highest. The highest bit rate requirement for an RTZ system is a string of "1's". The highest bit rate for an NRZ system is for alternating "1's" and "0's," as shown from b-c. Note that the highest NRZ bit rate is half the highest RTZ bit rate, or an RTZ system would require twice the bandwidth of an NRZ system for the same data rate.

However, to minimize drift in a receiver, it will probably be AC coupled; but if NRZ encoding is used and a long string of "1's" is transmitted, the AC coupling will result in lost data in the receiver. With RTZ data, data is not lost with AC coupling since only a string of "0's" results in a constant signal level; but that level is itself zero. However, in the case of both NRZ and RTZ, for any continuous string of either "1's" or "0's" for NRZ or "0's" RTZ will prevent the receiver from recovering any

*It might also be advisable to allow for LED degradation over time. A good design may include 3.0dB in the loss budget for long-term degradation.

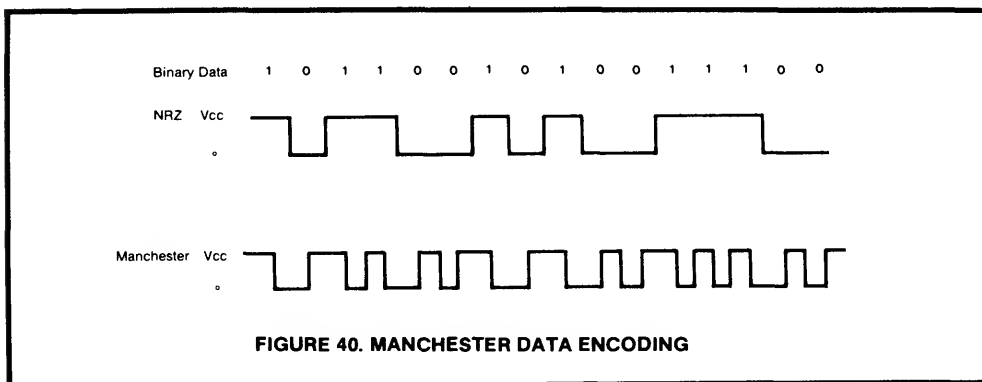


clock signal.

Another format, called Manchester encoding, solves this problem, by definition, in Manchester, the polarity reverses once each bit period regardless of the data. This is shown in Figure 40. The large number of level transitions enables the receiver to derive a clock signal even if all "1's" or all "0's" are being received.

the receiver may saturate. A good encoding scheme for these applications is pulse bipolar encoding. This is shown in Figure 41. The transmitter runs at a quiescent level and is turned on harder for a short duration during a data "0" and is turned off for a short duration during a data "1".

Additional details on encoding schemes can be obtained from recent texts on data communications or pulse code modulation.



In many cases, clock recovery is not required. It might appear that RTZ would be a good encoding scheme for these applications. However, many receivers include automatic gain control (AGC). During a long stream of "0's," the AGC could crank the receiver gain up; and when "1's" data begin to appear,

Summary

This note has presented the basic principles that govern the coupling and transmission of light over optical fibers and the design considerations and advantages of using optical fibers for communication information in the form of modulated light.

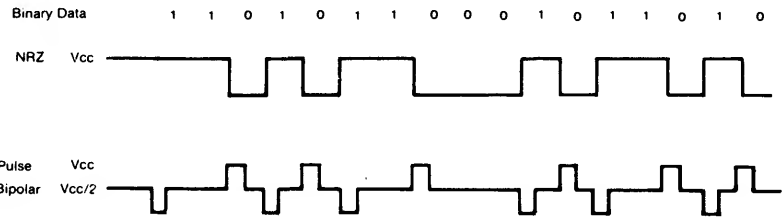


FIGURE 41. PULSE BIPOLAR ENCODING

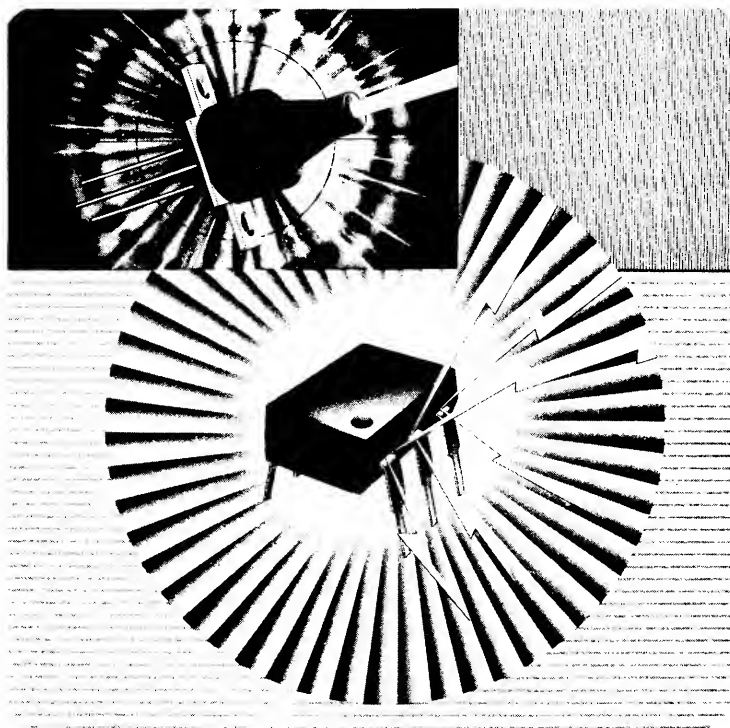
Bibliography

1. Gempe, Horst: "Applications of Ferruled Components to Fiber Optic Systems." Motorola Application Note AN-804; Phoenix, Arizona; 1980.
2. Mirtich, Vincent L.: "A 20-MBaud Full Duplex Fiber Optic Data Link Using Fiber Optic Active Components." Motorola Application Note AN-794; Phoenix, Arizona, 1980.
3. Mirtich, Vincent L.: "Designer's Guide to: Fiber-Optic Data Links," Parts 1, 2, & 3; EDN June 20, 1980; August 5, 1980; and August 20, 1980.

BASIC FIBER OPTIC TERMINOLOGY

| | |
|---------------------------------|---|
| FIBER: | The glass, plastic-clad silica or plastic medium by which light is conducted or transmitted. Can be multi-mode (capable of propagating more than one mode of a given wavelength) or single-mode (one that supports propagation of only one mode of a given wavelength). |
| CABLE: | The jacketed combination of fiber or fiber bundles with cladding and strength reinforcing components. |
| CLADDING: | A covering for the core of an optical fiber that provides optical insulation and protection. Generally fused to the fiber, it has a low index of refraction. |
| CORE: | The light transmitting portion of the fiber optic cable. It has a higher index of refraction than the cladding. |
| ACCEPTANCE ANGLE: | A measure of the maximum angle within which light may be coupled from a source or emitter. It is measured relative to the fiber's axis. |
| NUMERICAL APERTURE (NA): | A number that indicates a fiber's ability to accept light and shows how much light can be off-axis and still be accepted by the fiber. |
| FRESNEL LOSS: | Reflection losses which occur at the input and output interfaces of an optical fiber and are caused by differences in the index of refraction between the core material and immersion media. |
| INDEX OF REFRACTION: | Compares the velocity of light in a vacuum to its velocity in a material. The index or ratio varies with wavelength. |
| EMITTER: | Converts the electrical signal into an optical signal. Lasers or LED's are commonly used. |
| DETECTOR: | Converts light signals from optical fibers to electrical signals that can be further amplified to allow reproduction of the original signal. |

FIBER OPTICS



Selector Guide

INFRARED EMITTERS

Designed as infrared sources for fiber optic communication systems. These devices are designed to conveniently fit within compatible AMP connectors. (TO-18 type packages fit AMP connector 227015; ferruled semiconductors fit AMP connector 227240-1.)

Both 820 nm and 900 nm wavelengths are available. Unless otherwise noted, the optical port of the ferruled devices is 200 μm fiber optic core diameter.

| Package | | Device Type | Total Power Output | | λ nm | Fiber Core Diameter | NA | Response Time t_r/t_f Typ ns |
|----------|---------|-------------|--------------------|--------------|-----------------|---------------------|------|--------------------------------------|
| | | | Typ | @ I_F (mA) | | | | |
| TO-18 | 209-02 | MFOE100 | 550 μW | 50 | 900 | — | — | 50 |
| | | MFOE200 | 1.6 mW | 50 | 940 | — | — | 250 |
| FERRULED | 338-02 | MFOE102F | 140 μW | 100 | 900 | 200 | 0.7 | 25 |
| | | MFOE103F | 140 μW | 100 | 900 | 200 | 0.7 | 15 |
| | 338D-01 | MFOE106F | 700 μW | 100 | 820 | 200 | 0.58 | 12 |

PHOTO DETECTORS

Designed for the detection of infrared radiation in fiber optic communication systems. A family of detectors including PIN diodes, photo transistors (XSTR), photo Darlintons (DARL), and monolithic Integrated Detector Preamplifiers (IDP) are provided. The Integrated Detector Preamplifiers contain light detectors, transimpedance preamplifiers, and quasi-complementary outputs. These devices are designed to conveniently fit within compatible AMP connectors. (TO-18 type packages fit AMP connector 227015; ferruled semiconductors fit AMP connector 227240-1.)

The optical port of the ferruled devices is 200 μm fiber optic core diameter.

| Package | | Device | | Responsivity Typ | | Operating Voltage Volts | Response Time Typ t_r/t_f |
|----------|---------|--------|----------|--|--|----------------------------|-----------------------------------|
| | | Type | Number | 820 nm | 900 nm | | |
| TO-18 | 209-02 | PIN | MFOD100 | 20 $\mu\text{A}/\text{mW}/\text{cm}^2$ | 18 $\mu\text{A}/\text{mW}/\text{cm}^2$ | 20 | 10 ns/10 ns |
| | | XSTR | MFOD200 | 8.4 mA/mW/cm ² | 5.6 mA/mW/cm ² | 20 | 2.5 $\mu\text{s}/4.0 \mu\text{s}$ |
| FERRULED | 82-04 | DARL | MFOD300 | 85 mA/mW/cm ² | 75 mA/mW/cm ² | 5.0 | 40 $\mu\text{s}/60 \mu\text{s}$ |
| | | PIN | MFOD102F | 0.5 $\mu\text{A}/\mu\text{W}$ | 0.4 $\mu\text{A}/\mu\text{W}$ | 20 | 25 ns/25 ns |
| | 338-02 | PIN | MFOD104F | 0.5 $\mu\text{A}/\mu\text{W}$ | 0.4 $\mu\text{A}/\mu\text{W}$ | 5.0 | 6.0 ns/6.0 ns |
| | | XSTR | MFOD202F | 115 $\mu\text{A}/\mu\text{W}$ | 100 $\mu\text{A}/\mu\text{W}$ | 20 | 2.5 $\mu\text{s}/4.0 \mu\text{s}$ |
| | 338A-02 | DARL | MFOD302F | 6800 $\mu\text{A}/\mu\text{W}$ | 6000 $\mu\text{A}/\mu\text{W}$ | 5.0 | 40 $\mu\text{s}/60 \mu\text{s}$ |
| | | IDP | MFOD402F | 1.7 mV/ μW | 1.5 mV/ μW | 15 | 20 ns/20 ns |
| | 338B-01 | IDP | MFOD404F | 34 mV/ μW | 30 mV/ μW | 5.0 | 40 ns/40 ns |
| | | IDP | MFOD405F | 5.0 mV/ μW | 4.0 mV/ μW | 5.0 | 10 ns/10 ns |

TRANSMITTERS

Complete signal processing circuitry is used to translate electrical energy to optical energy for fiber optic systems. This family includes monolithic integrated circuit drivers and complete fiber optic modules with infrared source.

| Package | Device Type | Bandwidth | Operating Voltage Volts | Drive Current | P_o | λ nm | Optical Port |
|---|-------------|----------------------------|-------------------------|----------------|-------------|--------------|--------------|
|  620-06 | MFOC700* | 10 Mbit TTL 20 Mbit ECL | +5.0 | Thru 100 mA | — | — | — |
|  343-01 | MFOLO2T | 200 kbit TTL | +5.0 | 100 mA | 140 μ W | 900 | 200 μ m |

*To be introduced.

RECEIVERS

Devices used to convert optical energy to conditioned electrical impulses in fiber optic systems. This family includes monolithic integrated circuit signal processing circuits with AGC and complete modules with TTL and ECL outputs.

| Package | Device Type | Bandwidth | Operating Voltage Volts | AGC | Dynamic Range | Detector | Min Input for 10 ⁻⁹ BER |
|---|-------------|----------------------------|-------------------------|-----|---------------|------------|------------------------------------|
|  620-06 | MFOC600* | 10 Mbit TTL 20 Mbit ECL | +5.0 | yes | >20 dB | IDP or PIN | — |
|  343-01 | MFOLO2R | 200 kbit TTL | +5.0 | no | >20 dB | PIN | 10 nW -50 dBm |

*To be introduced.



LINKS

Fiber optic Links are designed as educational tools but are usable in real system applications. Tutorial in nature, they include the necessary parts to construct fiber optic communication links. They include preterminated fiber optic cable, connectors, source, and detector. In the MFOL02 are complete TTL transmitter and receiver modules.

| Device Type | Transmitter | Receiver | Cable | Data Rate |
|-------------|-------------|----------|-----------|----------------|
| MFOL01 | MFOE103F | MFOD402F | 1 meter | 20 megabit NRZ |
| MFOL02 | MFOL02T | MFOL02R | 10 meters | 200 kbit NRZ |

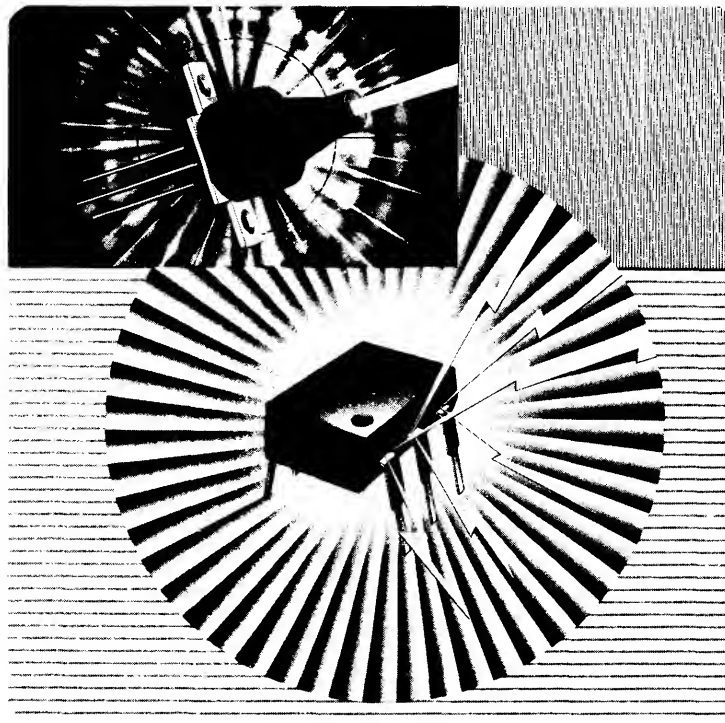


ACCESSORIES

A complement of parts are made available to ease the design of fiber optic systems using the Motorola ferruled semiconductor components, and are convenient items to the customer's purchasing cycle.

| Device Type | Description |
|-------------|---|
| MFOA02 | Connector, AMP 227240-1 |
| MFOA03 | Cable, 1 meter DuPont S120, Terminated |
| MFOA10 | Cable, 10 meters DuPont RFAQ PIR140, Terminated |

FIBER OPTICS



Data Sheets

FIBER OPTIC DATA SHEETS

| | Page | |
|----------|--|------|
| MFOD100 | PIN Photo Diode for Fiber Optic Systems | 7-3 |
| MFOD102F | PIN Photo Diode for Fiber Optic Systems | 7-5 |
| MFOD104F | PIN Photo Diode for Fiber Optic Systems | 7-7 |
| MFOD200 | Phototransistor for Fiber Optic Systems | 7-9 |
| MFOD202F | Phototransistor for Fiber Optic Systems | 7-11 |
| MFOD300 | Photodarlington Transistor for Fiber Optic Systems | 7-13 |
| MFOD302F | Photodarlington Transistor for Fiber Optic Systems | 7-15 |
| MFOD402F | Integrated Detector/Preamplifier for Fiber Optic Systems | 7-17 |
| MFOD404F | Integrated Detector/Preamplifier for Fiber Optic Systems | 7-21 |
| MFOD405F | Integrated Detector/Preamplifier for Fiber Optic Systems | 7-25 |
| MFOE100 | Infrared-Emitting Diode for Fiber Optic Systems | 7-29 |
| MFOE102F | Infrared-Emitting Diode for Fiber Optic Systems | 7-31 |
| MFOE103F | Infrared-Emitting Diode for Fiber Optic Systems | 7-33 |
| MFOE106F | New Generation AlGaAs LED | 7-35 |
| MFOE200 | Infrared-Emitting Diode for Fiber Optic Systems | 7-37 |
| MFOL01 | The Link | 7-39 |
| MFOL02 | Link II | 7-41 |



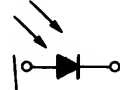
MOTOROLA

MFOD100

PIN PHOTO DIODE FOR FIBER OPTICS SYSTEMS

...designed for infrared radiation detection in short length, high frequency Fiber Optics Systems. Typical applications include: medical electronics, industrial controls, M6800 Microprocessor systems, security systems, etc.

- Spectral Response Matched to MFOE100, 200
- Hermetic Metal Package for Stability and Reliability
- Ultra Fast Response – 1.5 ns typ
- Very Low Leakage
 $I_D = 2.0 \text{ nA (max)} @ V_R = 20 \text{ Volts}$
- Compatible with AMP Mounting Bushing #227015

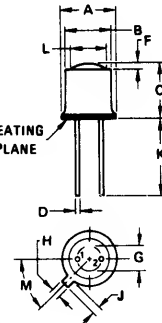


**FIBER OPTICS
PIN PHOTO DIODE**



MAXIMUM RATINGS ($T_A = 25^\circ\text{C}$ unless otherwise noted)

| Rating | Symbol | Value | Unit |
|--|-----------------|-------------|----------------------------|
| Reverse Voltage | V_R | 150 | Volts |
| Total Device Dissipation @ $T_A = 25^\circ\text{C}$ Derate above 25°C | P_D | 100 0.57 | mW mW/ $^\circ\text{C}$ |
| Operating and Storage Junction Temperature Range | $T_{J,T_{stg}}$ | -55 to +175 | $^\circ\text{C}$ |



STYLE I:

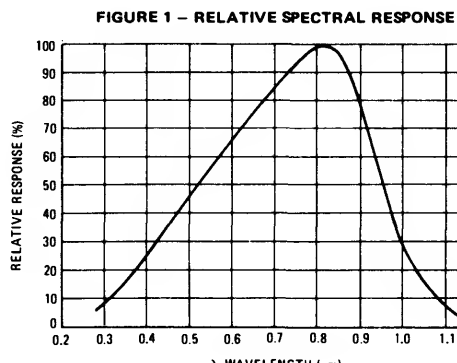
PIN 1. ANODE
PIN 2. CATHODE

NOTES:

1. PIN 2 INTERNALLY CONNECTED TO CASE
2. LEADS WITHIN 0.13 mm (0.005) RADIUS OF TRUE POSITION AT SEATING PLANE AT MAXIMUM MATERIAL CONDITION.

| DIM | MILLIMETERS | | INCHES | |
|-----|-------------|------|-----------|-------|
| | MIN | MAX | MIN | MAX |
| A | 5.31 | 5.84 | 0.209 | 0.230 |
| B | 4.52 | 4.95 | 0.178 | 0.195 |
| C | 6.22 | 6.98 | 0.245 | 0.275 |
| D | 0.41 | 0.48 | 0.016 | 0.019 |
| F | 1.19 | 1.60 | 0.047 | 0.063 |
| G | 2.54 BSC | | 0.100 BSC | |
| H | 0.99 | 1.17 | 0.039 | 0.046 |
| J | 0.84 | 1.22 | 0.033 | 0.048 |
| K | 12.70 | — | 0.500 | — |
| L | 3.35 | 4.01 | 0.132 | 0.158 |
| M | 45° BSC | | 45° BSC | |

CASE 209-02



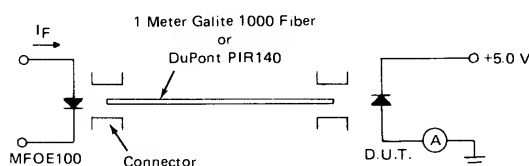
MFOD100

ELECTRICAL CHARACTERISTICS

| Characteristic | Symbol | Min | Typ | Max | Unit |
|---|-----------------------|--------|------------|---------|---------------|
| Dark Current ($V_R = 20$ V, $R_L = 1.0$ M, Note 1) $T_A = 25^\circ C$ $T_A = 100^\circ C$ | I_D | — — | 1.0 14 | 10 — | nA |
| Reverse Breakdown Voltage ($I_R = 10 \mu A$) | $V_{(BR)R}$ | 100 | 200 | — | Volts |
| Forward Voltage ($I_F = 50$ mA) | V_F | — | — | 1.1 | Volts |
| Series Resistance ($I_F = 50$ mA) | R_s | — | — | 10 | ohms |
| Total Capacitance ($V_R = 20$ V, $f = 1.0$ MHz) | C_T | — | — | 4.0 | pF |
| Responsivity (Figure 2) | R | 0.4 | 0.5 | — | $\mu A/\mu W$ |
| Response Time ($V_R = 20$ V, $R_L = 50$ ohms) | t_{on} t_{off} | — — | 1.0 1.0 | — — | ns ns |

1. Measured under dark conditions. $H = 0$

FIGURE 2 – RESPONSIVITY TEST CONFIGURATION



TYPICAL CHARACTERISTICS

COUPLED SYSTEM PERFORMANCE versus FIBER LENGTH*

FIGURE 3 – MFOE100 SOURCE

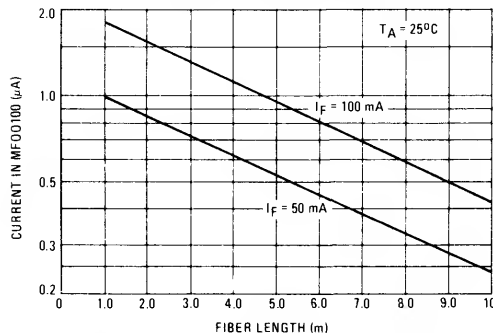
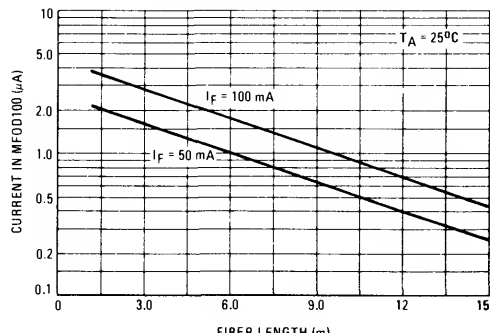


FIGURE 4 – MFOE200 SOURCE



* 0.045" Dia. Fiber Bundle, N.A. ≈ 0.67 , Attenuation at 900 nm ≈ 0.6 dB/m



MOTOROLA

MFOD102F

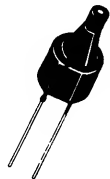
Advance Information

PIN PHOTO DIODE FOR FIBER OPTIC SYSTEMS

. . . designed for infrared radiation detection in high frequency Fiber Optic Systems. It is packaged in Motorola's Fiber Optic Active Component (FOAC) case, and fits directly into AMP Incorporated fiber optic connectors. These metal connectors provide excellent RFI immunity. Typical applications include medical electronics, industrial controls, M6800 microprocessor systems, security systems, computer and peripheral equipment, etc.

- Fast Response – 25 ns Typ
- May Be Used with MFOExxx Emitters
- FOAC Package – Small and Rugged
- Fiber Input Port Greatly Enhances Coupling Efficiency
- Prepolished Optical Port
- Compatible with AMP Connector #227240-1
- 200 μm (8 mil) Diameter Optical Port

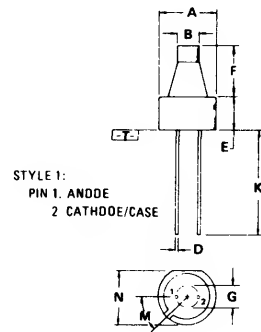
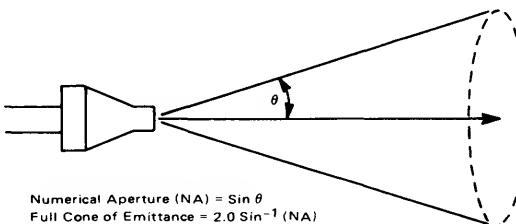
FIBER OPTICS PIN PHOTO DIODE



MAXIMUM RATINGS ($T_A = 25^\circ\text{C}$ Unless otherwise noted)

| Rating | Symbol | Value | Unit |
|--|-----------|-------------|----------------------------|
| Reverse Voltage | V_R | 100 | Volts |
| Total Device Dissipation @ $T_A = 25^\circ\text{C}$ Derate above 25°C | P_D | 100 0.57 | mW mW/ $^\circ\text{C}$ |
| Operating Temperature Range | T_A | -30 to +85 | $^\circ\text{C}$ |
| Storage Temperature Range | T_{stg} | -30 to +100 | $^\circ\text{C}$ |

FIGURE 1 – CONE OF ACCEPTANCE



NOTES:

1. \boxed{T} IS SEATING PLANE.
2. POSITIONAL TOLERANCE FOR LEADS:
 $\boxed{\Delta} \pm .36(0.014) \odot T$
3. DIMENSIONING AND TOLERANCING PER Y14.5, 1973.

| DIM | MILLIMETERS | | INCHES | |
|-----|-------------|------|-----------|-------|
| | MIN | MAX | MIN | MAX |
| A | 6.86 | 7.11 | 0.270 | 0.280 |
| B | 2.54 | 2.64 | 0.100 | 0.104 |
| D | 0.40 | 0.48 | 0.016 | 0.019 |
| E | 3.94 | 4.44 | 0.155 | 0.175 |
| F | 6.17 | 6.38 | 0.243 | 0.251 |
| G | 2.54 BSC | | 0.100 BSC | |
| K | 12.70 | — | 0.500 | — |
| M | 45° | NOM | 45° | NOM |
| N | 6.22 | 6.73 | 0.245 | 0.265 |

CASE 338-02

MFOD102F

ELECTRICAL CHARACTERISTICS ($T_A = 25^\circ\text{C}$)

| Characteristic | Symbol | Min | Typ | Max | Unit |
|--|-------------|-----|-----|-----|------------------------|
| Dark Current ($V_R = 20 \text{ V}$, $R_L = 1.0 \text{ M}$, $H \approx 0$) | I_D | — | — | 2.0 | nA |
| Reverse Breakdown Voltage ($I_R = 10 \mu\text{A}$) | $V_{(BR)R}$ | 100 | 200 | — | Volts |
| Forward Voltage ($I_F = 50 \text{ mA}$) | V_F | — | — | 1.1 | Volts |
| Series Resistance ($I_F = 50 \text{ mA}$) | R_s | — | — | 10 | ohms |
| Total Capacitance ($V_R = 20 \text{ V}$, $f = 1.0 \text{ MHz}$) | C_T | — | — | 4.0 | pF |
| Noise Equivalent Power | NEP | — | 50 | — | fW/ $\sqrt{\text{Hz}}$ |

OPTICAL CHARACTERISTICS ($T_A = 25^\circ\text{C}$)

| | | | | | |
|--|-----------------------|--------|----------|--------|---------------------------|
| Responsivity @ 900 nm ($V_R = 20 \text{ V}$, $R_L = 10 \Omega$, $P = 10 \mu\text{W}^*$) | R | 0.15 | 0.40 | — | $\mu\text{A}/\mu\text{W}$ |
| Response Time @ 900 nm ($V_R = 20 \text{ V}$, $R_L = 50 \Omega$) | t_{on} t_{off} | — — | 25 25 | — — | ns ns |
| Numerical Aperture of Input Port (200 μm [8 mil] diameter core) | NA | — | 0.48 | — | — |

*Power launched into Optical Input Port. The designer must account for interface coupling losses.

TYPICAL CHARACTERISTICS

FIGURE 2 – RELATIVE SPECTRAL RESPONSE

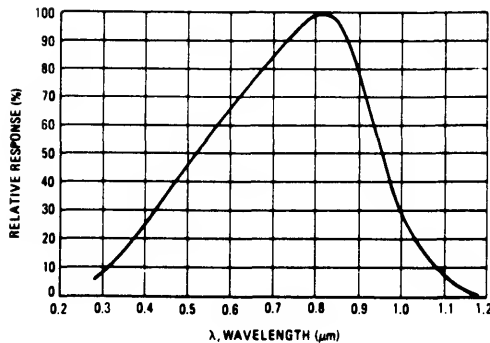
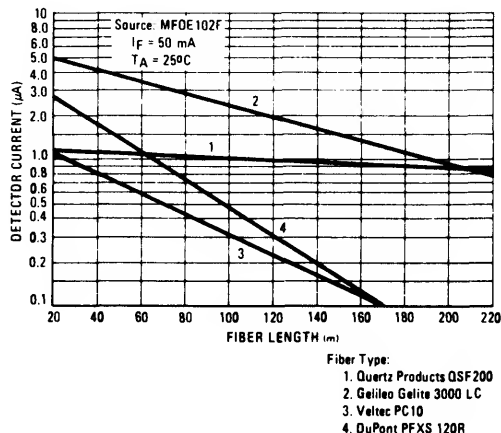


FIGURE 3 – DETECTOR CURRENT versus FIBER* LENGTH





MOTOROLA

MFOD104F

Advance Information

PIN PHOTO DIODE FOR FIBER OPTIC SYSTEMS

... designed for infrared radiation detection in high frequency Fiber Optic Systems. It is packaged in Motorola's Fiber Optic Active Component (FOAC) case, and fits directly into AMP Incorporated fiber optic connectors. These metal connectors provide excellent RFI immunity. Typical applications include medical electronics, industrial controls, M6800 microprocessor systems, security systems, computer and peripheral equipment, etc.

- Fast Response - 6.0 ns Typ @ 5.0 V
- May Be Used with MFOExxx Emitters
- FOAC Package - Small and Rugged
- Fiber Input Port Greatly Enhances Coupling Efficiency
- Prepolished Optical Port
- Compatible with AMP Connector #227240-1
- 200 μm (8 mil) Diameter Optical Port

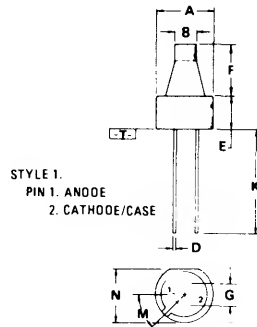
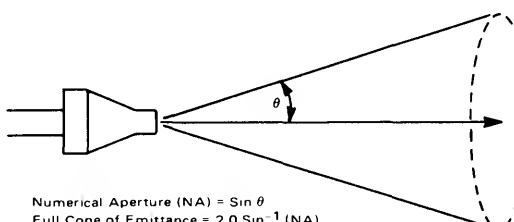
FIBER OPTICS PIN PHOTO DIODE



MAXIMUM RATINGS ($T_A = 25^\circ\text{C}$ Unless otherwise noted)

| Rating | Symbol | Value | Unit |
|--|-----------|-------------|----------------------------|
| Reverse Voltage | V_R | 100 | Volts |
| Total Device Dissipation @ $T_A = 25^\circ\text{C}$ Derate above 25°C | P_D | 100 0.57 | mW mW/ $^\circ\text{C}$ |
| Operating Temperature Range | T_A | -30 to +85 | $^\circ\text{C}$ |
| Storage Temperature Range | T_{stg} | -30 to +100 | $^\circ\text{C}$ |

FIGURE 1 – CONE OF ACCEPTANCE



NOTES:

1. T IS SEATING PLANE.
 2. POSITIONAL TOLERANCE FOR LEADS:
-
3. DIMENSIONING AND TOLERANCING PER Y14.5, 1973

| DIM | MILLIMETERS | | INCHES | |
|-----|-------------|------|-----------|-------|
| | MIN | MAX | MIN | MAX |
| A | 6.86 | 7.11 | 0.270 | 0.280 |
| B | 2.54 | 2.64 | 0.100 | 0.104 |
| D | 0.40 | 0.48 | 0.016 | 0.019 |
| E | 3.94 | 4.44 | 0.155 | 0.175 |
| F | 6.17 | 6.38 | 0.243 | 0.251 |
| G | 2.54 BSC | | 0.100 BSC | |
| K | 12.70 | — | 0.500 | — |
| M | 45° | NOM | 45° | NOM |
| N | 6.22 | 6.73 | 0.245 | 0.265 |

CASE 338-02

This is advance information and specifications are subject to change without notice.

MFOD104F

ELECTRICAL CHARACTERISTICS ($T_A = 25^\circ\text{C}$)

| Characteristic | Symbol | Min | Typ | Max | Unit |
|--|-------------|-----|------|-----|------------------------|
| Dark Current ($V_R = 20 \text{ V}$, $R_L = 1.0 \text{ M}$, $H \approx 0$) | I_D | — | — | 2.0 | nA |
| Reverse Breakdown Voltage ($I_R = 10 \mu\text{A}$) | $V_{(BR)R}$ | 100 | 200 | — | Volts |
| Forward Voltage ($I_F = 50 \text{ mA}$) | V_F | — | 0.82 | 1.2 | Volts |
| Total Capacitance ($V_R = 5.0 \text{ V}$, $f = 1.0 \text{ MHz}$) | C_T | — | — | 4.0 | pF |
| Noise Equivalent Power | NEP | — | 50 | — | fW/ $\sqrt{\text{Hz}}$ |

OPTICAL CHARACTERISTICS ($T_A = 25^\circ\text{C}$)

| | | | | | |
|--|-------------------|------|------|---|---------------------------|
| Responsivity @ 900 nm ($V_R = 5.0 \text{ V}$, $P = 10 \mu\text{W}^*$) | R | 0.15 | 0.40 | — | $\mu\text{A}/\mu\text{W}$ |
| Response Time @ 900 nm $V_R = 5.0 \text{ V}$ 12 V 20 V | t_{on}, t_{off} | — | 6.0 | — | ns |
| Numerical Aperture of Input Port, 3.0 dB ($200 \mu\text{m}$ [8 mil] diameter core) | NA | — | 0.48 | — | — |

*Power launched into Optical Input Port. The designer must account for interface coupling losses.

TYPICAL CHARACTERISTICS

FIGURE 2 – RELATIVE SPECTRAL RESPONSE

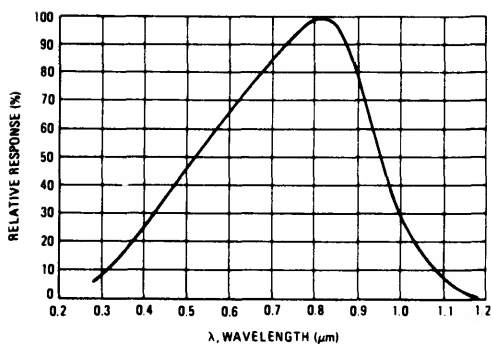
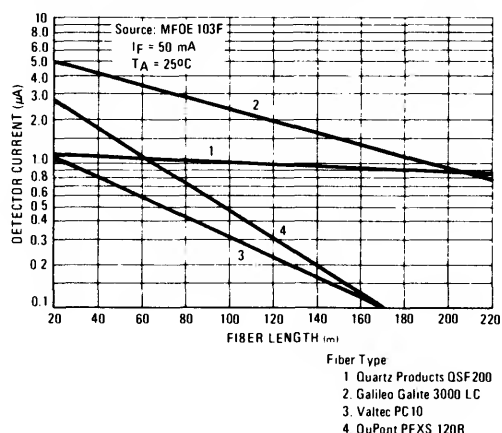


FIGURE 3 – DETECTOR CURRENT versus FIBER* LENGTH





MOTOROLA

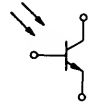
MFOD200

PHOTOTRANSISTOR FOR FIBER OPTICS SYSTEMS

... designed for infrared radiation detection in medium length, medium frequency Fiber Optic Systems. Typical applications include: medical electronics, industrial controls, security systems, M6800 Microprocessor systems, etc.

- Spectral Response Matched to MFOE100, 200
- Hermetic Metal Package for Stability and Reliability
- High Sensitivity for Medium Length Fiber Optic Control Systems
- Compatible with AMP Mounting Bushing #227015

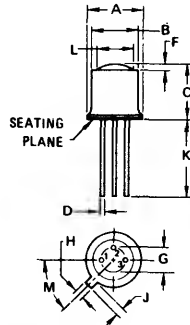
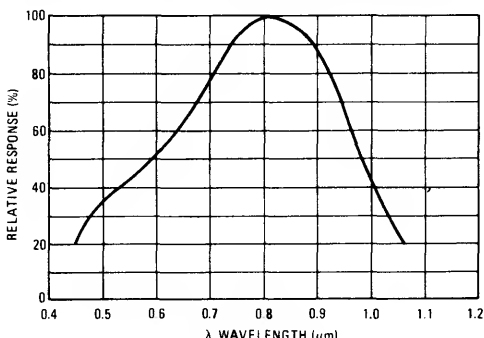
FIBER OPTICS NPN SILICON PHOTOTRANSISTOR



MAXIMUM RATINGS ($T_A = 25^\circ\text{C}$ unless otherwise noted).

| Rating (Note 1) | Symbol | Value | Unit |
|--|----------------|-------------|----------------------------|
| Collector-Emitter Voltage | V_{CEQ} | 40 | Volts |
| Emitter-Base Voltage | V_{EBO} | 10 | Volts |
| Collector-Base Voltage | V_{CBO} | 70 | Volts |
| Light Current | I_L | 250 | mA |
| Total Device Dissipation @ $T_A = 25^\circ\text{C}$ Derate above 25°C | P_D | 250 1.43 | mW mW/ $^\circ\text{C}$ |
| Operating and Storage Junction Temperature Range | T_J, T_{stg} | -55 to +175 | $^\circ\text{C}$ |

FIGURE 1 – CONSTANT ENERGY SPECTRAL RESPONSE



- STYLE 1:
 1. Emitter
 2. Base
 3. Collector

NOTES:

1. LEADS WITHIN .13 mm (.005) RADIUS OF TRUE POSITION AT SEATING PLANE, AT MAXIMUM MATERIAL CONDITION.
2. PIN 3 INTERNALLY CONNECTED TO CASE.

| | MILLIMETERS | | INCHES | |
|------|-------------|------|-----------|-------|
| DIM. | MIN. | MAX. | MIN. | MAX. |
| A | 5.31 | 5.84 | 0.209 | 0.230 |
| B | 4.52 | 4.95 | 0.176 | 0.195 |
| C | 6.22 | 6.98 | 0.245 | 0.275 |
| D | 0.41 | 0.48 | 0.016 | 0.019 |
| F | 1.19 | 1.60 | 0.047 | 0.063 |
| G | 2.54 BSC | | 0.100 BSC | |
| H | 0.99 | 1.17 | 0.039 | 0.046 |
| J | 0.84 | 1.22 | 0.033 | 0.048 |
| K | 12.70 | | 0.500 | — |
| L | 3.35 | 4.01 | 0.132 | 0.158 |
| M | 45° BSC | | 45° BSC | |

CASE 82-04

MFOD200

STATIC ELECTRICAL CHARACTERISTICS ($T_A = 25^\circ\text{C}$ unless otherwise noted)

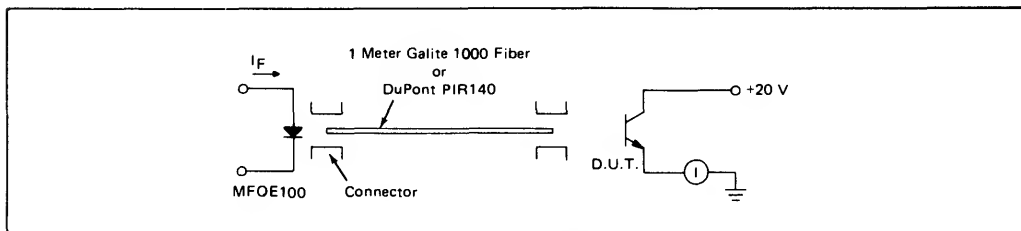
| Characteristic | Symbol | Min | Typ | Max | Unit |
|--|---------------|-----|-----|-----|------------------------------|
| Collector Dark Current ($V_{CC} = 20 \text{ V}$, $H \approx 0$) $T_A = 25^\circ\text{C}$ $T_A = 100^\circ\text{C}$ | I_{CEO} | — | — | 25 | nA μA |
| Collector-Base Breakdown Voltage ($I_C = 100 \mu\text{A}$) | $V_{(BR)CBO}$ | 50 | — | — | Volts |
| Collector-Emitter Breakdown Voltage ($I_C = 100 \mu\text{A}$) | $V_{(BR)CEO}$ | 30 | — | — | Volts |
| Emitter-Collector Breakdown Voltage ($I_E = 100 \mu\text{A}$) | $V_{(BR)ECO}$ | 7.0 | — | — | Volts |

OPTICAL CHARACTERISTICS ($T_A = 25^\circ\text{C}$)

| Characteristic | Symbol | Min | Typ | Max | Unit |
|--|--------|------|-----|-----|---------------------------|
| Responsivity (Figure 2) | R | 14.5 | 18 | — | $\mu\text{A}/\mu\text{W}$ |
| Photo Current Rise Time (Note 1) ($R_L = 100 \text{ ohms}$) | t_r | — | 2.5 | — | μs |
| Photo Current Fall Time (Note 1) ($R_L = 100 \text{ ohms}$) | t_f | — | 4.0 | — | μs |

Note 1. For unsaturated response time measurements, radiation is provided by pulsed GaAs (gallium-arsenide) light-emitting diode ($\lambda \approx 900 \text{ nm}$) with a pulse width equal to or greater than 10 microseconds, $I_C = 1.0 \text{ mA}$ peak.

FIGURE 2 – RESPONSIVITY TEST CONFIGURATION



TYPICAL CHARACTERISTICS

COUPLED SYSTEM PERFORMANCE versus FIBER LENGTH*

FIGURE 3 – MFOE100 SOURCE

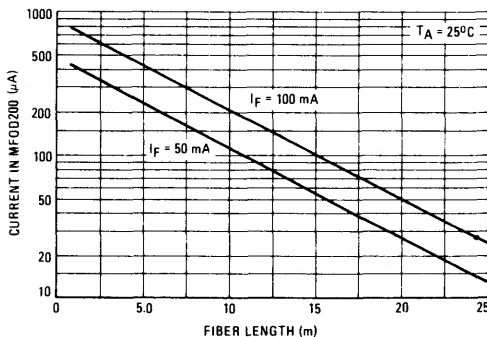
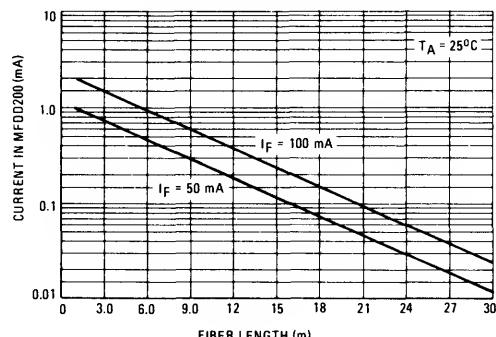


FIGURE 4 – MFOE200 SOURCE



*0.045" Dia. Fiber Bundle, N.A. ≈ 0.67 , Attenuation at 900 nm $\approx 0.6 \text{ dB/m}$



MOTOROLA

MFOD202F

Advance Information

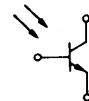
PHOTOTRANSISTOR FOR FIBER OPTIC SYSTEMS

... designed for infrared radiation detection in medium frequency Fiber Optic Systems. It is packaged in Motorola's Fiber Optic Active Component (FOAC) case, and fits directly into AMP Incorporated fiber optic connectors. These metal connector's provide excellent RFI immunity. Typical applications include medical electronics, industrial controls, security systems, computer and peripheral equipment, etc.

- High Sensitivity for Medium Frequency Fiber Optic Systems
- May Be Used with MFOExxx Emitters
- FOAC Package - Small and Rugged
- Fiber Input Port Greatly Enhances Coupling Efficiency
- Prepolished Optical Port
- Compatible with AMP Connector #227240-1
- 200 μm [8 mil] Diameter Core Optical Port

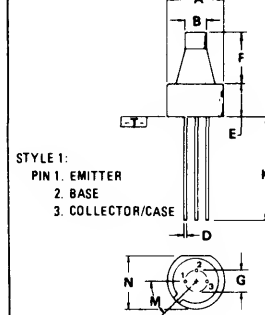
FIBER OPTICS

NPN SILICON
PHOTOTRANZISTOR



MAXIMUM RATINGS ($T_A = 25^\circ\text{C}$ unless otherwise noted).

| Rating | Symbol | Value | Unit |
|--|-----------|-------------|----------------------|
| Collector-Emitter Voltage | V_{CEO} | 50 | Volts |
| Emitter-Base Voltage | V_{EBO} | 10 | Volts |
| Collector-Base Voltage | V_{CBO} | 50 | Volts |
| Light Current | I_L | 250 | mA |
| Total Device Dissipation @ $T_A = 25^\circ\text{C}$ Derate above 25°C | P_D | 250 | mW |
| | | 1.43 | mW/ $^\circ\text{C}$ |
| Operating Temperature Range | T_A | -30 to +85 | $^\circ\text{C}$ |
| Storage Temperature Range | T_{stg} | -30 to +100 | $^\circ\text{C}$ |

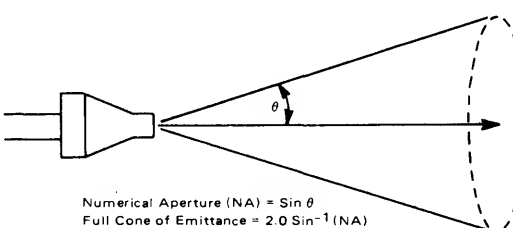


- NOTES:
1. IS SEATING PLANE.
 2. POSITIONAL TOLERANCE FOR LEADS:
 $\pm .36(0.014)$
 3. DIMENSIONING AND TOLERANCING PER Y14.5, 1973.

| DIM | MILLIMETERS | | INCHES | |
|-----|-------------|------|--------|-------|
| | MIN | MAX | MIN | MAX |
| A | 6.86 | 7.11 | 0.270 | 0.280 |
| B | 2.54 | 2.64 | 0.100 | 0.104 |
| D | 0.40 | 0.48 | 0.016 | 0.019 |
| E | 3.94 | 4.44 | 0.155 | 0.175 |
| F | 6.17 | 6.38 | 0.243 | 0.251 |
| G | 2.54 | 2.62 | 0.100 | 0.102 |
| K | 12.70 | — | 0.500 | — |
| M | 45° | NOM | 45° | NOM |
| N | 6.22 | 6.73 | 0.245 | 0.265 |

CASE 338A-02

FIGURE 1 – CONE OF ACCEPTANCE



STATIC ELECTRICAL CHARACTERISTICS ($T_A = 25^\circ\text{C}$ unless otherwise noted)

| Characteristic | Symbol | Min | Typ | Max | Unit |
|--|---------------|-----|-----|-----|-------|
| Collector Dark Current ($V_{CC} = 20 \text{ V}, V_H \approx 0$) | I_{CEO} | — | 5.0 | 50 | nA |
| Collector-Base Breakdown Voltage ($I_C = 100 \mu\text{A}$) | $V_{(BR)CBO}$ | 50 | — | — | Volts |
| Collector-Emitter Breakdown Voltage ($I_C = 100 \mu\text{A}$) | $V_{(BR)CEO}$ | 50 | — | — | Volts |

OPTICAL CHARACTERISTICS ($T_A = 25^\circ\text{C}$)

| Characteristic | Symbol | Min | Typ | Max | Unit |
|---|--------|-----|------|-----|---------------------------|
| Responsivity ($V_{CC} = 20 \text{ V}, R_L = 10 \Omega, \lambda \approx 900 \text{ nm}, P = 1.0 \mu\text{W}^*$) | R | 70 | 100 | — | $\mu\text{A}/\mu\text{W}$ |
| Photo Current Rise Time ($R_L = 100 \Omega$) | t_r | — | 2.5 | — | μs |
| Photo Current Fall Time ($R_L = 100 \Omega$) | t_f | — | 4.0 | — | μs |
| Numerical Aperture of Input Port -- Figure 1 (200 μm [B mil] diameter core) | NA | — | 0.48 | — | — |

*Power Launched into Optical Input Port. The designer must account for interface coupling losses.

TYPICAL CHARACTERISTICS

FIGURE 2 – CONSTANT ENERGY SPECTRAL RESPONSE

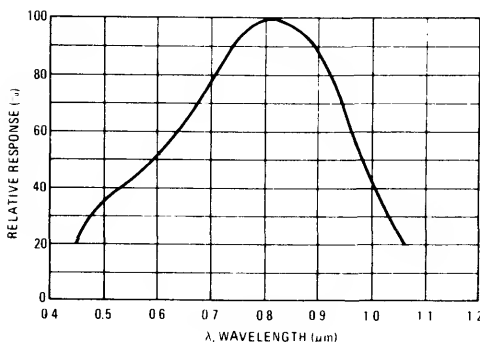
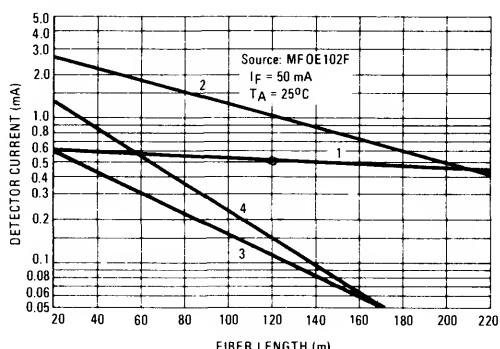


FIGURE 3 – DETECTOR CURRENT versus FIBER* LENGTH



- *Fiber Type
- 1. Quartz Products QS200
- 2. Galileo Galilei 3000 LC
- 3. Valtec PC10
- 4. DuPont PFXS 120R



MOTOROLA

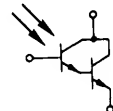
MFOD300

**PHOTODARLINGTON TRANSISTOR
FOR FIBER OPTICS SYSTEMS**

... designed for infrared radiation detection in long length, low frequency Fiber Optics Systems. Typical applications include: industrial controls, security systems, medical electronics, M6800 Microprocessor Systems, etc.

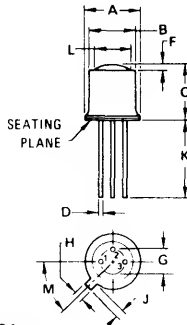
- Spectral Response Matched to MFOE100, 200
- Hermetic Metal Package for Stability and Reliability
- Very High Sensitivity for Long Length Fiber Optics Control Systems
- Compatible With AMP Mounting Bushing #227015

**FIBER OPTICS
NPN SILICON
PHOTODARLINGTON
TRANSISTOR**



MAXIMUM RATINGS ($T_A = 25^\circ\text{C}$ unless otherwise noted)

| Rating | Symbol | Value | Unit |
|--|----------------|-------------|----------------------------------|
| Collector-Emitter Voltage | V_{CEO} | 40 | Volts |
| Emitter-Base Voltage | V_{EBO} | 10 | Volts |
| Collector-Base Voltage | V_{CBO} | 70 | Volts |
| Light Current | I_L | 250 | mA |
| Total Device Dissipation @ $T_A = 25^\circ\text{C}$ Derate above 25°C | P_D | 250 1.43 | mW $\text{mW}/^\circ\text{C}$ |
| Operating and Storage Junction Temperature Range | T_J, T_{stg} | -55 to +175 | °C |



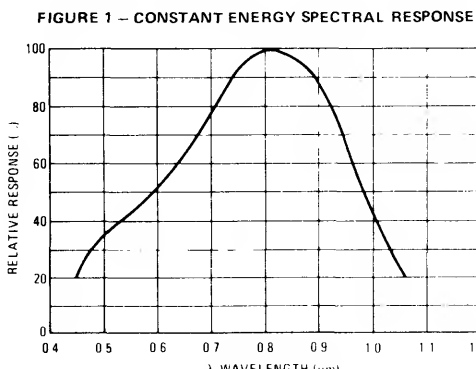
STYLE 1:
PIN 1 Emitter
2 Base
3 Collector

NOTES

- 1 LEADS WITHIN .13 mm (.005) RADIUS OF TRUE POSITION AT SEATING PLANE, AT MAXIMUM MATERIAL CONDITION.
- 2 PIN 3 INTERNALLY CONNECTED TO CASE

| | MILLIMETERS | | INCHES | |
|-----|-------------|------|--------|-------|
| DIM | MIN | MAX | MIN | MAX |
| A | 5.31 | 5.84 | 0.209 | 0.230 |
| B | 4.52 | 4.95 | 0.178 | 0.195 |
| C | 6.22 | 6.98 | 0.245 | 0.275 |
| D | 0.41 | 0.48 | 0.016 | 0.019 |
| F | 1.19 | 1.60 | 0.047 | 0.063 |
| G | 2.54 | 2.85 | 0.100 | 0.112 |
| H | 0.99 | 1.17 | 0.039 | 0.046 |
| J | 0.84 | 1.22 | 0.033 | 0.048 |
| K | 12.70 | - | 0.500 | - |
| L | 3.35 | 4.01 | 0.132 | 0.158 |
| M | 45° | 85C | 45° | 85C |

CASE 82-04



MFOD300

STATIC ELECTRICAL CHARACTERISTICS ($T_A = 25^\circ\text{C}$)

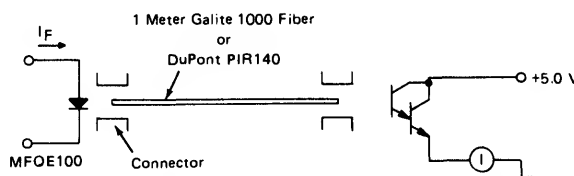
| Characteristic | Symbol | Min | Typ | Max | Unit |
|--|---------------|-----|-----|-----|-------|
| Collector Dark Current ($V_{CE} = 10 \text{ V}, H \approx 0$) | I_{CEO} | — | 10 | 100 | nA |
| Collector-Base Breakdown Voltage ($I_C = 100 \mu\text{A}$) | $V_{(BR)CBO}$ | 50 | — | — | Volts |
| Collector-Emitter Breakdown Voltage ($I_C = 100 \mu\text{A}$) | $V_{(BR)CEO}$ | 30 | — | — | Volts |
| Emitter-Base Breakdown Voltage ($I_E = 100 \mu\text{A}$) | $V_{(BR)EBO}$ | 10 | — | — | Volts |

OPTICAL CHARACTERISTICS ($T_A = 25^\circ\text{C}$)

| Characteristic | Symbol | Min | Typ | Max | Unit |
|--|--------|-----|-----|-----|---------------------------|
| Responsivity (Figure 2) | R | 400 | 500 | — | $\mu\text{A}/\mu\text{W}$ |
| Photo Current Rise Time (Note 1) ($R_L = 100 \text{ ohms}$) | t_r | — | 40 | — | μs |
| Photo Current Fall Time (Note 1) ($R_L = 100 \text{ ohms}$) | t_f | — | 60 | — | μs |

Note 1. For unsaturated response time measurements, radiation is provided by pulsed GaAs (gallium-arsenide) light-emitting diode ($\lambda \approx 900 \text{ nm}$) with a pulse width equal to or greater than 500 microseconds, $I_C = 1.0 \text{ mA peak}$.

FIGURE 2 – RESPONSIVITY TEST CONFIGURATION



TYPICAL CHARACTERISTICS

COUPLED SYSTEM PERFORMANCE versus FIBER LENGTH*

FIGURE 3 – MFOE100 SOURCE

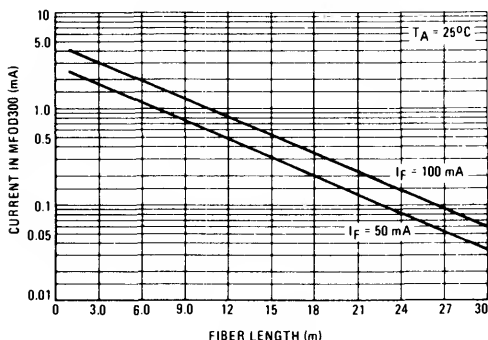
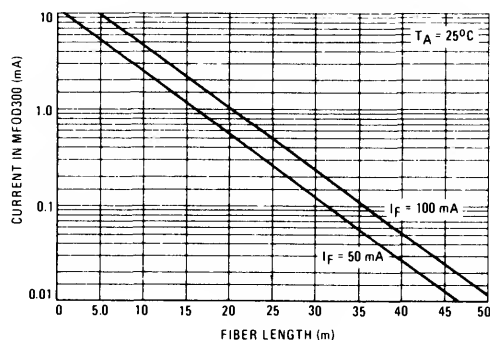


FIGURE 4 – MFOE200 SOURCE



*0.045" Dia. Fiber Bundle, N.A. ≈ 0.67 , Attenuation at 900 nm $\approx 0.6 \text{ dB/m}$



MOTOROLA

MF0D302F

Advance Information

PHOTODARLINGTON TRANSISTOR FOR FIBER OPTIC SYSTEMS

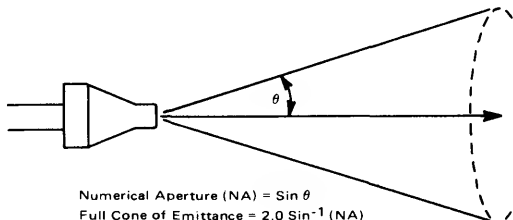
. . . designed for infrared radiation detection in low frequency Fiber Optic Systems. It is packaged in Motorola's Fiber Optic Active Component (FOAC) case, and fits directly into AMP Incorporated fiber optic connectors. These metal connectors provide excellent RFI immunity. Typical applications include medical electronics, industrial controls, security systems, computer and peripheral equipment, etc.

- High Sensitivity for Low Frequency Long Length Fiber Optic Control Systems
- May Be Used with MFOExxx Emitters
- FOAC Package — Small and Rugged
- Fiber Input Port Greatly Enhances Coupling Efficiency
- Prepolished Optical Port
- Compatible with AMP Connector #227240-1
- 200 μm (8 mil) Diameter Core Optical Port

MAXIMUM RATINGS ($T_A = 25^\circ\text{C}$ unless otherwise noted).

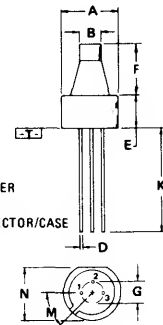
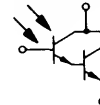
| Rating | Symbol | Value | Unit |
|--|-----------|-------------|----------------------|
| Collector-Emitter Voltage | V_{CEO} | 40 | Volts |
| Emitter-Base Voltage | V_{EBO} | 10 | Volts |
| Collector-Base Voltage | V_{CBO} | 50 | Volts |
| Light Current | I_L | 250 | mA |
| Total Device Dissipation @ $T_A = 25^\circ\text{C}$ Derate above 25°C | P_D | 250 | mW |
| | | 1.43 | mW/ $^\circ\text{C}$ |
| Operating Temperature Range | T_A | -30 to +85 | $^\circ\text{C}$ |
| Storage Temperature Range | T_{stg} | -30 to +100 | $^\circ\text{C}$ |

FIGURE 1 – CONE OF ACCEPTANCE



FIBER OPTICS

NPN SILICON
PHOTODARLINGTON
TRANSISTOR



NOTES:

1. \boxed{T} IS SEATING PLANE.
2. POSITIONAL TOLERANCE FOR LEADS:
 ± 0.36 (0.014) \boxed{T}
3. DIMENSIONING AND TOLERANCING PER Y14.5, 1973.

| DIM | MILLIMETERS | | INCHES | |
|-----|-------------|------|-----------|-------|
| | MIN | MAX | MIN | MAX |
| A | 6.86 | 7.11 | 0.270 | 0.280 |
| B | 2.54 | 2.64 | 0.100 | 0.104 |
| D | 0.40 | 0.48 | 0.016 | 0.019 |
| E | 3.94 | 4.44 | 0.155 | 0.175 |
| F | 6.17 | 6.38 | 0.243 | 0.251 |
| G | 2.54 BSC | | 0.100 BSC | |
| K | 12.70 | — | 0.500 | — |
| M | 45° | NOM | 45° | NOM |
| N | 6.22 | 6.73 | 0.245 | 0.265 |

CASE 338A-02

MFOD302F

STATIC ELECTRICAL CHARACTERISTICS ($T_A = 25^\circ\text{C}$)

| Characteristic | Symbol | Min | Typ | Max | Unit |
|--|---------------|-----|-----|-----|-------|
| Collector Dark Current ($V_{CC} = 12 \text{ V}$, $H \approx 0$, $T_A = 25^\circ\text{C}$) | I_{CEO} | — | 10 | 100 | nA |
| Collector-Base Breakdown Voltage ($I_C = 100 \mu\text{A}$) | $V_{(BR)CBO}$ | 50 | — | — | Volts |
| Collector-Emitter Breakdown Voltage ($I_C = 100 \mu\text{A}$) | $V_{(BR)CEO}$ | 40 | — | — | Volts |
| Emitter-Base Breakdown Voltage ($I_E = 100 \mu\text{A}$) | $V_{(BR)EBO}$ | 10 | — | — | Volts |

OPTICAL CHARACTERISTICS ($T_A = 25^\circ\text{C}$)

| Characteristic | Symbol | Min | Typ | Max | Unit |
|---|--------|------|------|-----|---------------------------|
| Responsivity ($V_{CC} = 5.0 \text{ V}$, $R_L = 10 \Omega$, $\lambda \approx 900 \text{ nm}$, $P = 1.0 \mu\text{W}^*$) | R | 2000 | 6000 | — | $\mu\text{A}/\mu\text{W}$ |
| Photo Current Rise Time ($R_L = 100 \text{ ohms}$) | t_r | — | 40 | — | μs |
| Photo Current Fall Time ($R_L = 100 \text{ ohms}$) | t_f | — | 60 | — | μs |
| Numerical Aperture of Input Port — Figure 1 (200 μm [8 mil] diameter core) | NA | — | 0.48 | — | — |

*Power launched into Optical Input Port. The designer must account for interface coupling losses.

TYPICAL CHARACTERISTICS

FIGURE 2 – CONSTANT ENERGY SPECTRAL RESPONSE

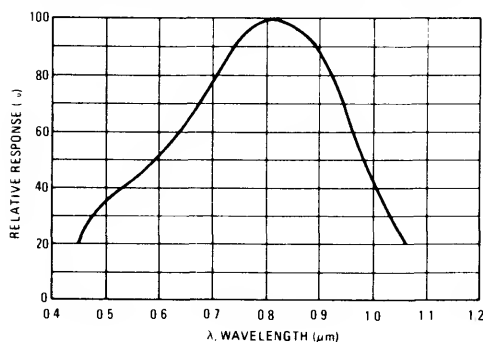
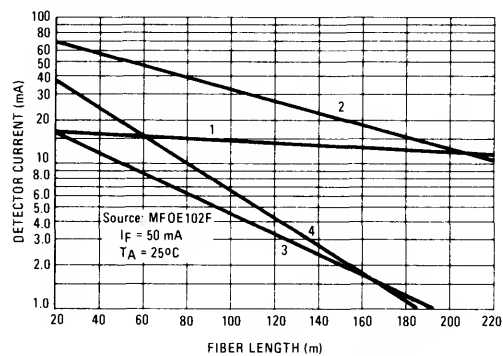


FIGURE 3 – DETECTOR CURRENT versus FIBER* LENGTH



**MOTOROLA****MFOD402F****INTEGRATED DETECTOR/PREAMPLIFIER
FOR FIBER OPTIC SYSTEMS**

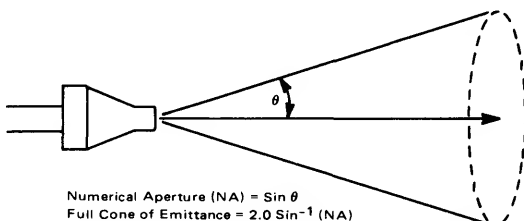
. . . designed as a monolithic integrated circuit containing both detector and preamplifier for use in medium bandwidth, medium distance systems. Packaged in Motorola's Fiber Optic Active Component (FOAC) case, the device fits directly into AMP Incorporated fiber optic connectors which also provide excellent RFI immunity. The output of the device is low impedance to provide even less sensitivity to stray interference. The MFOD402F has a 200 μm [8 mil] fiber input with a high numerical aperture.

- Usable for Data Systems Up to 30 Megabaud
- Dynamic Range Greater Than 100:1
- RFI Shielded in AMP Connector #227240-1
- May Be Used with MFOExxx Emitters
- FOAC Package – Small and Rugged
- Fiber Input Port Greatly Enhances Coupling Efficiency
- Prepolished Optical Port

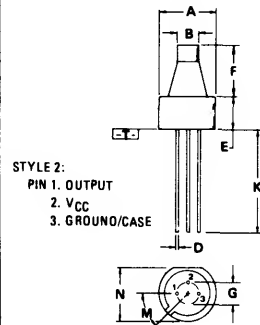
FIBER OPTICS**INTEGRATED DETECTOR
PREAMPLIFIER****MAXIMUM RATINGS** ($T_A = 25^\circ\text{C}$ unless otherwise noted).

| Rating | Symbol | Value | Unit |
|---|------------------|-------------|----------------------------|
| Operating Voltage | V _{CC} | 20 | Volts |
| *Total Device Dissipation @ $T_A = 25^\circ\text{C}$ Derate above 25°C | P _D | 250 1.43 | mW mW/ $^\circ\text{C}$ |
| Operating Temperature Range | T _A | -30 to +85 | $^\circ\text{C}$ |
| Storage Temperature Range | T _{stg} | -30 to +100 | $^\circ\text{C}$ |

*Package Limitations.

FIGURE 1 – CONE OF ACCEPTANCE

Patent applied for.

**NOTES:**

1. \square IS SEATING PLANE.
2. POSITIONAL TOLERANCE FOR LEADS:
 $\pm .36 (0.014)$ \odot \square T
3. DIMENSIONING AND TOLERANCING PER Y14.5, 1973.

| DIM | MILLIMETERS | | INCHES | |
|-----|-------------|------|-----------|-------|
| | MIN | MAX | MIN | MAX |
| A | 6.86 | 7.11 | 0.270 | 0.280 |
| B | 2.54 | 2.64 | 0.100 | 0.104 |
| D | 0.40 | 0.48 | 0.016 | 0.019 |
| E | 3.94 | 4.44 | 0.155 | 0.175 |
| F | 6.17 | 6.38 | 0.243 | 0.251 |
| G | 2.54 BSC | | 0.100 BSC | |
| K | 12.70 | — | 0.500 | — |
| M | 45° | NOM | 45° | NOM |
| N | 6.22 | 6.73 | 0.245 | 0.265 |

CASE 338A-02

MFOD402F

ELECTRICAL CHARACTERISTICS ($V_{CC} = 15 \text{ V}$, $T_A = 25^\circ\text{C}$)

| Characteristics | Symbol | Conditions | Value | | | Units |
|-----------------------------|-----------------|------------|-------|------|-----|------------------------|
| | | | Min | Typ | Max | |
| Power Supply Current | I_{CC} | Circuit A | 1.4 | 1.7 | 2.0 | mA |
| Quiescent dc Output Voltage | V_q | Circuit A | 0.6 | 0.7 | 0.9 | Volts |
| Resistive Load | $R_O\text{Max}$ | | 300 | — | — | Ohms |
| Capacitive Load | $C_O\text{Max}$ | | — | — | 20 | pF |
| Output Impedance | z_O | | — | 200 | — | Ohms |
| RMS Noise Output | V_{NO} | Circuit A | — | 0.3 | — | mV |
| Noise Equivalent Power | NEP | | — | 57 | — | pW/ $\sqrt{\text{Hz}}$ |
| Operating Voltage Range | V_{CC} | | 5.0 | — | 15 | Volts |
| Bandwidth * (3.0 dB) | BW | | — | 17.5 | — | MHz |

OPTICAL CHARACTERISTICS ($T_A = 25^\circ\text{C}$)

| | | | | | | |
|---|------------|-----------|-----|------|---|-------------------------|
| Responsivity ($V_{CC} = 15 \text{ V}$, $\lambda = 900 \text{ nm}$, $P = 10 \mu\text{W}^{**}$) | R | Circuit B | 0.6 | 1.5 | — | $\text{mV}/\mu\text{W}$ |
| Pulse Response | t_r, t_f | Circuit B | — | 20 | — | ns |
| Numerical Aperture of Input Core (200 μm [8 mil] diameter core) | NA | | — | 0.70 | — | — |

*Calculated from Step Response.

**Power launched into Optical Input Port. The designer must account for interface coupling losses.
See Application Note AN-804.

FIGURE 2 – EQUIVALENT SCHEMATIC

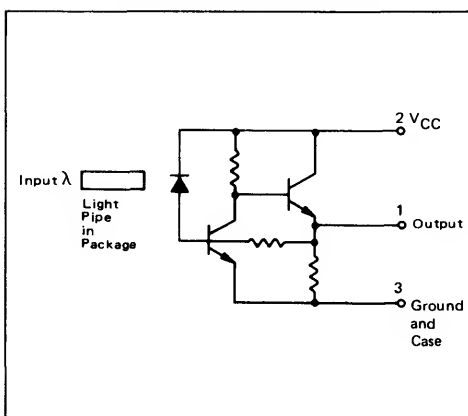
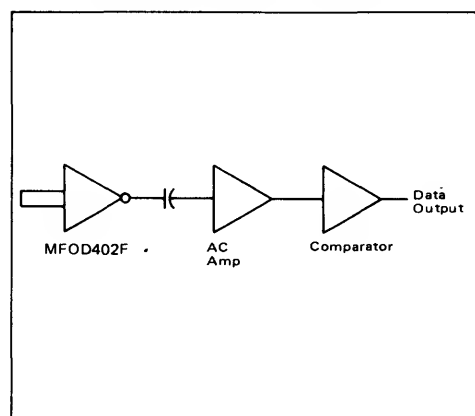
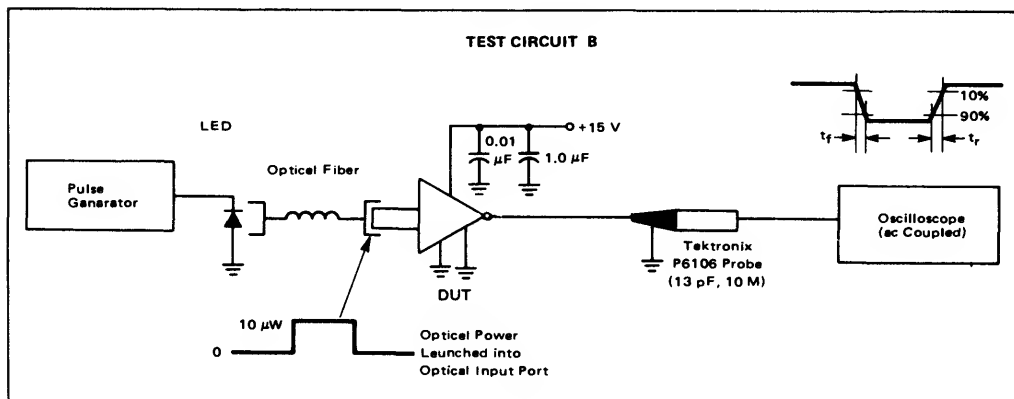
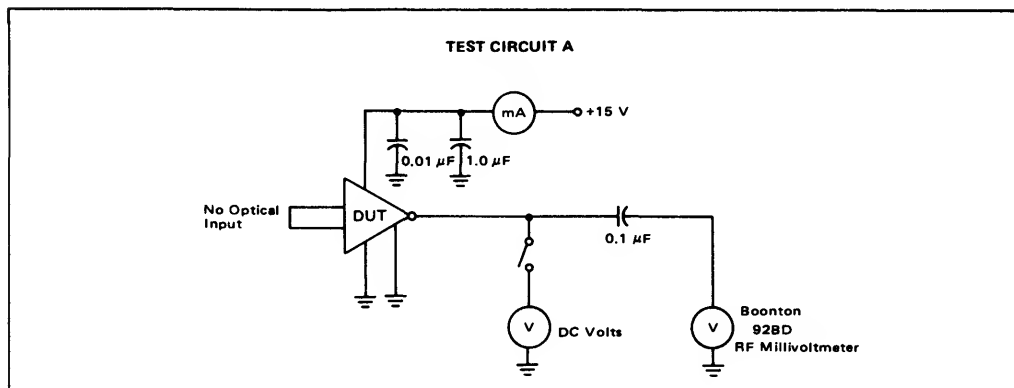


FIGURE 3 – TYPICAL APPLICATIONS



MFOD402F



APPLICATIONS INFORMATION

The MFOD402F is designed primarily for use in ac coupled fiber optic receivers as shown in Figure 3. Best performance is to be obtained with receivers in approximately the 10 MHz (20 Mbs) range. The output is an ac voltage in the range of 1-100 mV riding on a 700 mV quiescent dc level. The ac signal should be amplified by a high-gain amplifier such as an MC1733 or MC1590 and applied to suitable comparators to transform it into the desired logic form.

The device is designed for use with 8 mil (200 μ m) fiber optic cables. This size is becoming standard in computer use and is well designed for the frequency range common in this equipment.

A typical operating system should be designed to deliver a suitable amount of power to provide at least a 10 dB signal to noise ratio. If the system is operated at maximum

bandwidth, approximately 3 μ W of power from an 8 mil fiber will typically provide this ratio.

The performance of the device is affected by the capacitance seen at the output port to ground. This should be held below 20 pF to provide lowest noise operation. Values above about 50 pF may cause it to oscillate. Lower capacitance values will cause less overshoot in the transient response. The transient response is also affected by the operating voltage. The recommended operating voltage is 15 V, although the device can be operated at 5 V if the overshoot is tolerable in the particular system. (Figures 4 and 5.) See Application Note AN-794.

For best results, the MFOD402F should be inserted into an AMP metal fiber optics connector with the case, circuit ground, and metal connector all grounded. This will minimize RFI and lower the error rate observed in the system.

MFOD402F

FIGURE 4 – OUTPUT WAVEFORM WITH $V_{CC} = 15$ V

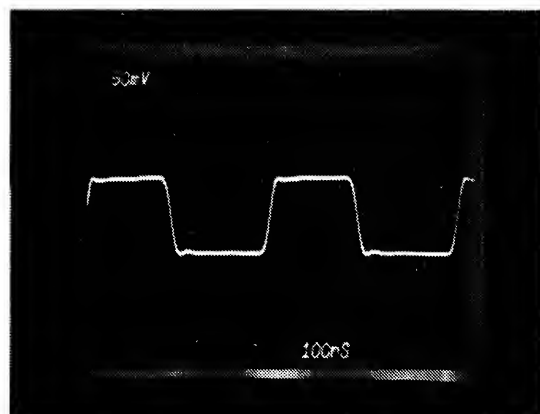
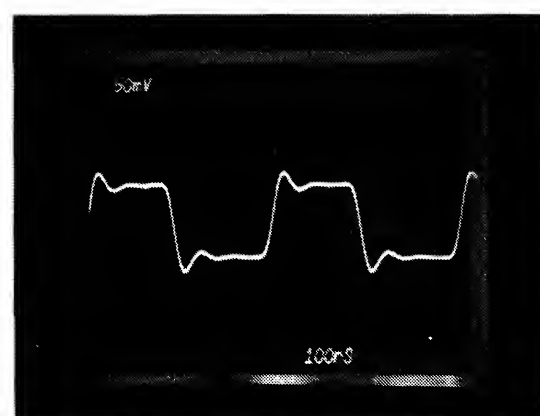


FIGURE 5 – OUTPUT WAVEFORM WITH $V_{CC} = 5.0$ V





MOTOROLA

MFOD404F

INTEGRATED DETECTOR/PREAMPLIFIER FOR FIBER OPTIC SYSTEMS

... designed as a monolithic integrated circuit containing both detector and preamplifier for use in medium bandwidth, medium distance systems. It joins Motorola family of Straight Shooter devices packaged in the Fiber Optic Ferrule case. The device fits directly into AMP Incorporated fiber optic connectors which also provide excellent RFI immunity. The output of the device is low impedance to provide even less sensitivity to stray interference. The MFOD404F has a 200 μ m (8 mil) fiber input with a high numerical aperture.

- Usable for Data Systems up to 10 Megabaud
 - Dynamic Range Greater than 100:1
 - RFI Shielded in AMP Connector #227240-1
 - May be Used with MFOExxx Emitters
 - Ferrule Package — Small and Rugged
 - Fiber Input Port Greatly Enhances Coupling Efficiency
 - Prepolished Optical Port

FIBER OPTICS

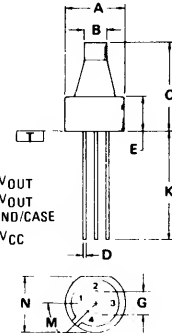
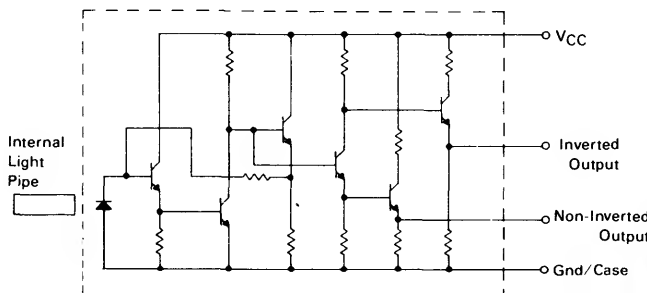
INTEGRATED DETECTOR PREAMPLIFIER



MAXIMUM RATINGS ($T_A = 25^\circ\text{C}$ unless otherwise noted)

| Rating | Symbol | Value | Unit |
|-----------------------------|------------------|-------------|-------|
| Supply Voltage | V _{CC} | 7.5 | Volts |
| Operating Temperature Range | T _A | -30 to +85 | °C |
| Storage Temperature Range | T _{sta} | -30 to +100 | °C |

FIGURE 1 – EQUIVALENT SCHEMATIC



NOTES

1. **T** IS SEATING PLANE.
 2. POSITIONAL TOLERANCE FOR LEADS:

| | | | | |
|--|--|--------------|-----|---|
| | | 0.36 (0.014) | (M) | T |
|--|--|--------------|-----|---|
 3. DIMENSIONING AND TOLERANCING
PER Y14.5, 1973

| DIM | MILLIMETERS | | INCHES | |
|-----|-------------|---------|--------|---------|
| | MIN | MAX | MIN | MAX |
| A | 6.86 | 7.11 | 0.270 | 0.280 |
| B | 2.54 | 2.64 | 0.100 | 0.104 |
| C | 10.16 | 10.80 | 0.400 | 0.425 |
| D | 0.40 | 0.48 | 0.016 | 0.019 |
| E | 3.94 | 4.44 | 0.155 | 0.175 |
| G | 2.54 | 2.88 | 0.100 | 0.112 |
| K | 12.70 | — | 0.500 | — |
| M | 450 | 450 BSC | 450 | 450 BSC |
| N | 6.22 | 6.73 | 0.245 | 0.265 |

CASE 338B-01

MFOD404F

ELECTRICAL CHARACTERISTICS ($V_{CC} = 5.0$ V, $T_A = 25^\circ\text{C}$)

| Characteristics | Symbol | Conditions | ' Min | Typ | Max | Units |
|--|----------|------------|-------|-----|-----|-------|
| Power Supply Current | I_{CC} | Circuit A | 3.0 | 3.5 | 5.0 | mA |
| Ouiescent dc Output Voltage (Non-Inverting Output) | V_q^- | Circuit A | 0.5 | 0.6 | 0.7 | Volts |
| Ouiescent dc Output Voltage (Inverting Output) | V_q^+ | Circuit A | 2.7 | 3.0 | 3.3 | Volts |
| Output Impedance | z_o | | — | 200 | — | Ohms |
| RMS Noise Output | V_{NO} | Circuit A | — | 0.4 | 1.0 | mV |

OPTICAL CHARACTERISTICS ($T_A = 25^\circ\text{C}$)

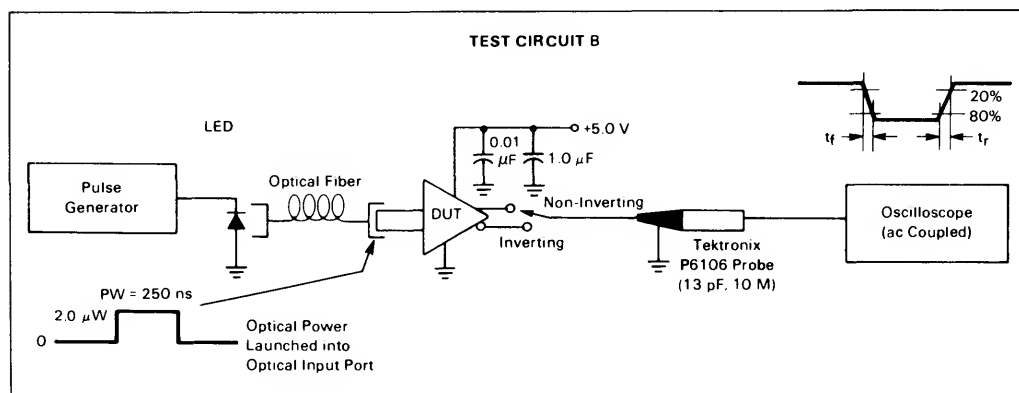
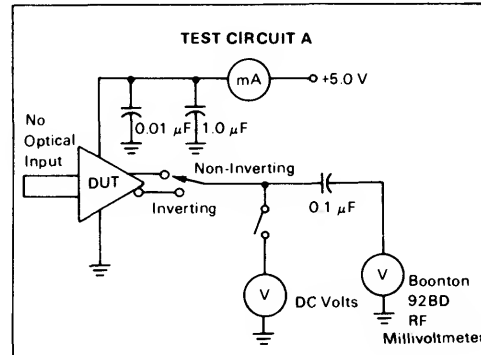
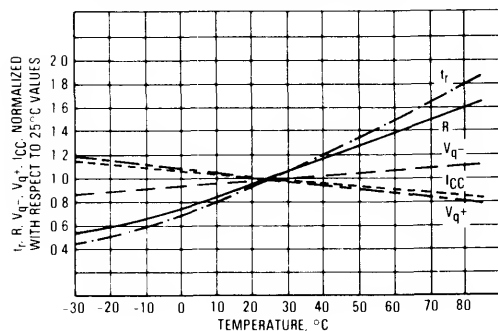
| | | | | | | |
|--|------------|-----------|---------|----------|---------|-------------------------|
| Responsivity ($V_{CC} = 5.0$ V, $P = 2.0 \mu\text{W}^*$) $\lambda = 900$ nm $\lambda = 820$ nm | R | Circuit B | 20 — | 30 35 | 50 — | $\text{mV}/\mu\text{W}$ |
| Pulse Response | t_f, t_r | Circuit B | — | 35 | 50 | ns |
| Numerical Aperture of Input Core (200 μm [8 mil] diameter core) | NA | | — | 0.70 | — | — |
| Signal-to-Noise Ratio @ $P_{in} = 1.0 \mu\text{W}$ peak* | S/N | | — | 35 | — | dB |
| Maximum Input Power for Negligible Distortion in Output Pulse* | | | — | — | 30 | μW |

RECOMMENDED OPERATING CONDITIONS

| | | | | | |
|------------------|-----------|-----|-----|-----|-------|
| Supply Voltage | V_{CC} | 4.0 | 5.0 | 6.0 | Volts |
| Capacitive Load | C_L | — | — | 100 | pF |
| Input Wavelength | λ | — | 900 | — | nm |

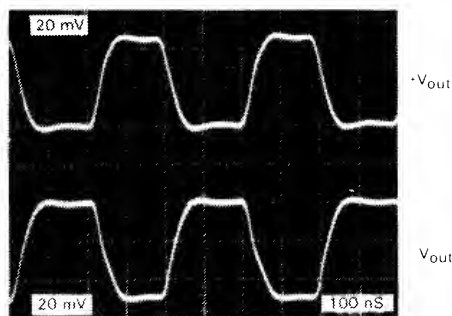
*Power launched into Optical Input Port. The designer must account for interface coupling losses.

FIGURE 2 — TYPICAL PERFORMANCE OVER
OPERATING TEMPERATURE RANGE



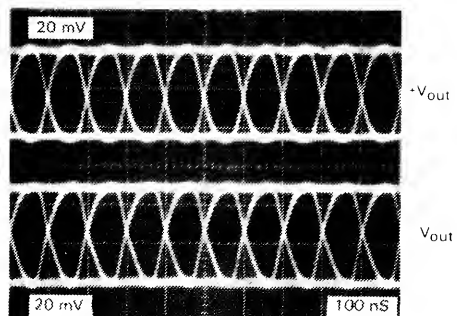
MFOD404F

FIGURE 3



Pulse response of MFOD404F to square wave input with peak optical input power of 2.0 microwatts at $V_{CC} = 5.0$ V

FIGURE 4



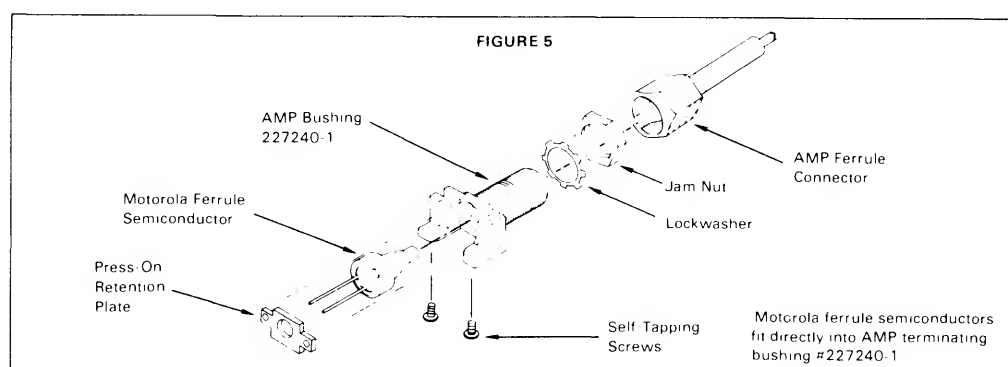
MFOD404F response to pseudo random bit stream input with average optical input power of 1.0 microwatt. Note the good quality eye pattern at 10 Mbits per second. $V_{CC} = 5.0$ V

APPLICATIONS INFORMATION

The basic function of the MFOD404F integrated detector preamplifier is to convert an optical input into a voltage level proportional to the received optical power. Within the package is a monolithic chip having the detector diode and a transimpedance amplifier with emitter follower isolation amplifiers on both the inverted and non-inverted outputs. A high level of RFI EMI immunity is provided by this detector circuit.

The MFOD404F is in the Motorola ferrule fiber optic semiconductor package with a 200 μ m fiber core input. With the AMP connector, #227240-1, these ferrule devices are easily and precisely assembled into systems, can be connected to plastic or glass cable of almost any diameter and are easily interchanged for system modification or upgrade. Mechanics of the use of the ferrule devices and basic optic system losses are presented in the Motorola Application Note AN-804.

FIGURE 5



MFOD404F

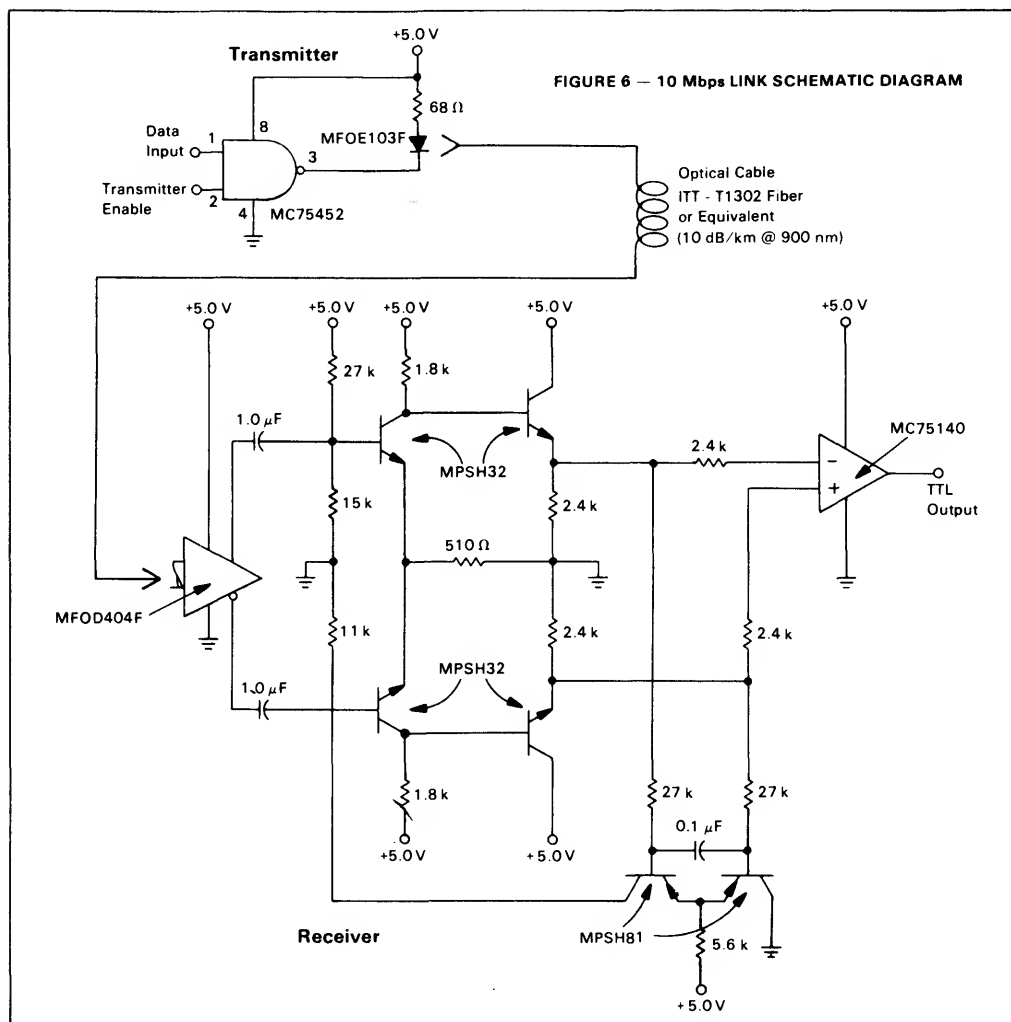
APPLICATIONS INFORMATION (continued)

A Simple, 10 Mbps Fiber Optic Link

The schematic diagram in Figure 6 illustrates how easily a high performance fiber optic link can be constructed with low-cost commercially available components when based on the MFOD404F integrated detector/preamplifier.

When used with the fiber indicated in Figure 6, the MFOE103F conservatively launches a peak power of 5.0 microwatts when driven with a peak current of only 50

milliamperes. Since the receiver's sensitivity is 0.1 micro-watts average power for 10^{-9} BER (Bit Error Rate) at data rates up to 10 Mbps NRZ, reliable communications links can be constructed up to 500 meters in length while providing both a 6.0 dB power margin for LED time and temperature degradation and 3.0 dB for connector loss at the receiver (worst case design). In addition, since the receiver dynamic range exceeds 20 dB, there is no danger of overloading the receiver in short link length applications.





MOTOROLA

INTEGRATED DETECTOR/PREAMPLIFIER FOR FIBER OPTIC SYSTEMS

designed as a monolithic integrated circuit containing both detector and preamplifier for use in computer, industrial control, and other communications systems.

Packaged in Motorola's Ferrule case, the device fits directly into AMP Incorporated fiber optic connectors which also provide excellent RFI immunity. The output of the device is low impedance to provide even less sensitivity to stray interference. The MFOD405F has a 200 μm (8 mil) fiber input with a high numerical aperture.

- Usable for Data Systems Through 40 Megabaud
- Dynamic Range Greater than 100:1
- RFI Shielded in AMP Connector #227240-1
- May be Used with MFOExxx Emitters
- Ferrule Package — Small and Rugged
- Fiber Input Port Greatly Enhances Coupling Efficiency
- Prepolished Optical Port

MFOD405F

FIBER OPTICS

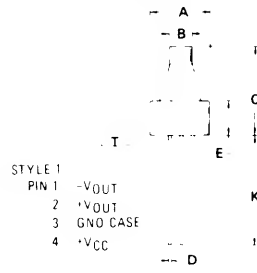
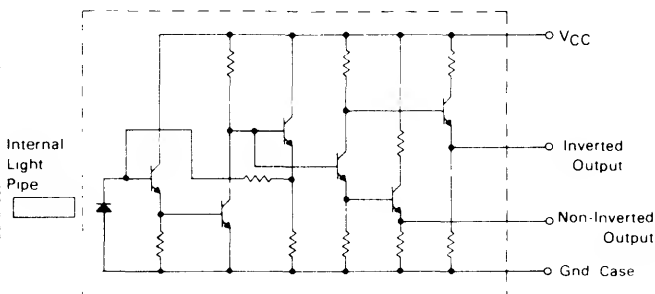
INTEGRATED DETECTOR PREAMPLIFIER



MAXIMUM RATINGS ($T_A = 25^\circ\text{C}$ unless otherwise noted)

| Rating | Symbol | Value | Unit |
|-----------------------------|------------------|-------------|-------|
| Supply Voltage | V _{CC} | 7.5 | Volts |
| Operating Temperature Range | T _A | -30 to +85 | °C |
| Storage Temperature Range | T _{Stg} | -30 to +100 | °C |

FIGURE 1 — EQUIVALENT SCHEMATIC



NOTES

- 1 T IS SEATING PLANE
- 2 POSITIONAL TOLERANCE FOR LEADS ± 0.36 (0.014) ± 0.175 T
- 3 DIMENSIONING AND TOLERANCING PER Y14.5-1973

| DIM | MILLIMETERS | | INCHES | |
|-----|-------------|-------|-----------|-------|
| | MIN | MAX | MIN | MAX |
| A | 6.86 | 7.11 | 0.270 | 0.280 |
| B | 2.54 | 2.64 | 0.100 | 0.104 |
| C | 10.16 | 10.80 | 0.400 | 0.425 |
| D | 0.40 | 0.48 | 0.016 | 0.019 |
| E | 3.94 | 4.44 | 0.155 | 0.175 |
| G | 2.54 BSC | | 0.100 BSC | |
| K | 12.70 | | 0.500 | |
| M | 450 BSC | | 450 BSC | |
| N | 6.22 | 6.73 | 0.245 | 0.265 |

CASE 338B-01

MFOD405F

ELECTRICAL CHARACTERISTICS ($V_{CC} = 5.0$ V, $T_A = 25^\circ\text{C}$)

| Characteristics | Symbol | Conditions | Min | Typ | Max | Units |
|--|----------|------------|-----|-----|-----|-------|
| Power Supply Current | I_{CC} | Circuit A | 3.0 | 4.5 | 6.0 | mA |
| Quiescent dc Output Voltage (Non-Inverting Output) | V_Q^- | Circuit A | 0.6 | 0.7 | 0.8 | Volts |
| Quiescent dc Output Voltage (Inverting Output) | V_Q^+ | Circuit A | 2.7 | 3.0 | 3.3 | Volts |
| Output Impedance | z_o | | — | 200 | — | Ohms |
| RMS Noise Output | V_{NO} | Circuit A | — | 0.5 | 1.0 | mV |

OPTICAL CHARACTERISTICS ($T_A = 25^\circ\text{C}$)

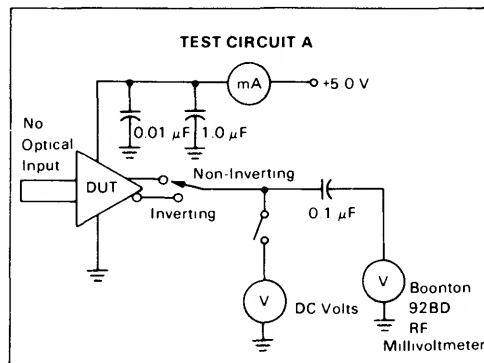
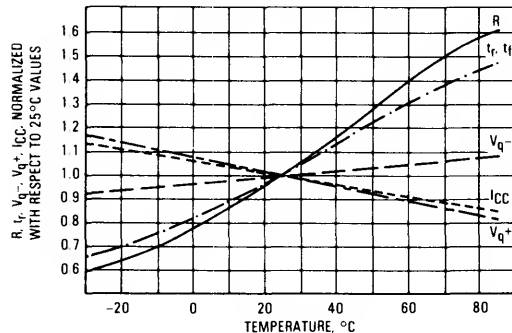
| | | | | | | |
|---|------------|-----------|-----|------|-----|-------------------------|
| Responsivity ($V_{CC} = 5.0$ V, $\lambda = 820$ nm, $P = 10 \mu\text{W}^*$) | R | Circuit B | 3.0 | 4.5 | 7.0 | $\text{mV}/\mu\text{W}$ |
| Pulse Response | t_r, t_f | Circuit B | — | 10 | 15 | ns |
| Numerical Aperture of Input Core (200 μm [8 mil] diameter core) | NA | | — | 0.70 | — | — |
| Signal-to-Noise Ratio @ $P_{in} = 2.0 \mu\text{W}$ peak* | S/N | | — | 24 | — | dB |
| Maximum Input Power for Negligible Distortion in Output Pulse* | | Circuit B | — | — | 120 | μW |

RECOMMENDED OPERATING CONDITIONS

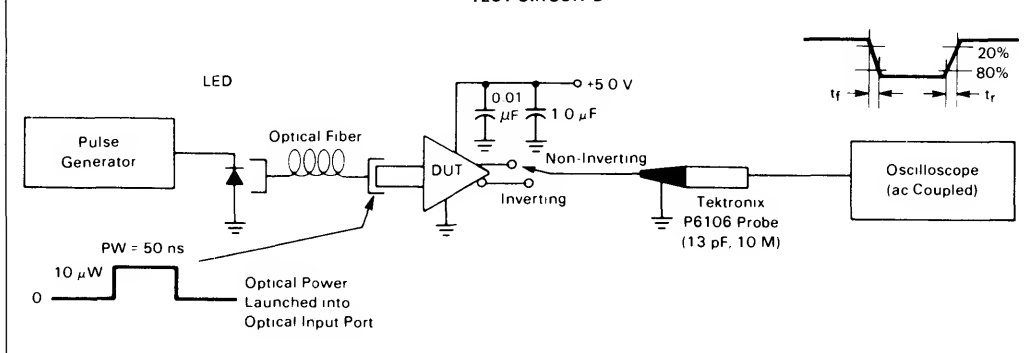
| | | | | | |
|---------------------------------|-----------|-----|-----|-----|---------------|
| Supply Voltage | V_{CC} | 4.0 | 5.0 | 6.0 | Volts |
| Capacitive Load (Either Output) | C_L | — | — | 100 | μF |
| Input Wavelength | λ | — | 820 | — | nm |

*Power launched into Optical Input Port. The designer must account for interface coupling losses as discussed in AN-804

FIGURE 2 — TYPICAL PERFORMANCE OVER
OPERATING TEMPERATURE RANGE

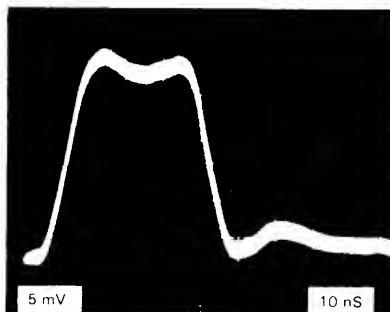


TEST CIRCUIT B



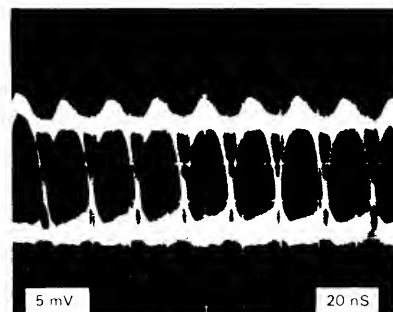
MFOD405F

FIGURE 3



Output waveform in response to a 50 nanosecond, 6.0 microwatt optical input pulse

FIGURE 4



Eye pattern generated by pseudo-random bit stream at 40 Mb/s

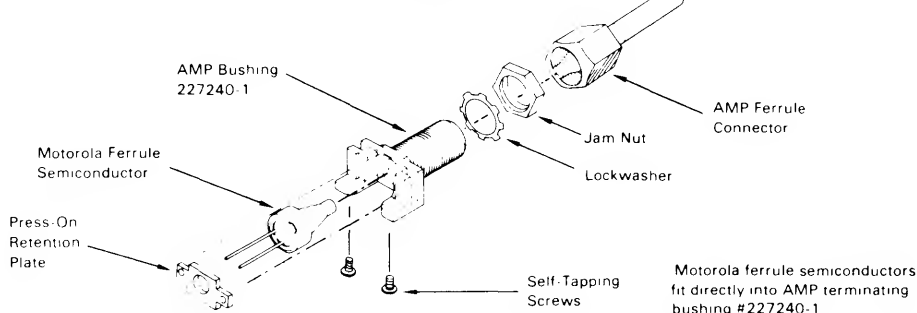
APPLICATIONS INFORMATION

The basic function of the MFOD405F integrated detector/preamplifier is to convert an optical input into a voltage level proportional to the received optical power. Within the package is a monolithic chip having the detector diode and a transimpedance amplifier with emitter follower isolation amplifiers on both the inverted and non-inverted outputs. The device in the connector assembly is virtually immune to RFI/EMI. The IDP circuit itself provides a high level of RFI/EMI immunity. EMI pickup at the input of a fiber optic receiver can be a potential problem, but as the MFOD405F is a single monolithic chip this function between the optical port and the receiver

is quite small and essentially eliminates this source of EMI. Finally, the whole device is mounted inside the AMP metal connector with a special RFI/EMI shielding option.

The MFOD405F is in the Motorola ferrule fiber optic semiconductor package with a 200 μm fiber core input. With the AMP connector, #227240-1, these ferrule devices are easily and precisely assembled into systems, can be connected to plastic or glass cable of almost any diameter and are easily interchanged for system modification or upgrade. Mechanics of the use of the ferrule devices and basic fiber optic system losses are presented in the Motorola Application Note AN-804.

FIGURE 5



MFOD405F

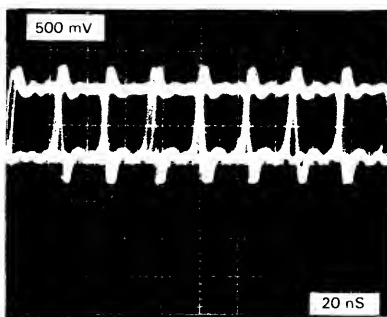
APPLICATIONS INFORMATION (continued)

40 Mb/s FIBER OPTIC LINK USING MFOD405F DETECTOR

The attached figure shows a receiver capable of operation at data rates in excess of 40 Mbps when driven by a suitably fast LED. The quasi-differential output of the MFOD405F is amplified by a two-stage differential amplifier consisting of two stages of an MC10116 MECL line receiver. It is important to utilize MECL layout practices in this receiver because of the very high data rates of which it is capable. The receiver requires about 5.0 microwatts of optical input power to drive the output to full MECL logic levels. The attached photograph of the eye-pattern at 40 Mb/s shows the capability of very clean data transmission at this speed. The transmitter shown can drive fast LED's to suitable speeds for use with this receiver.

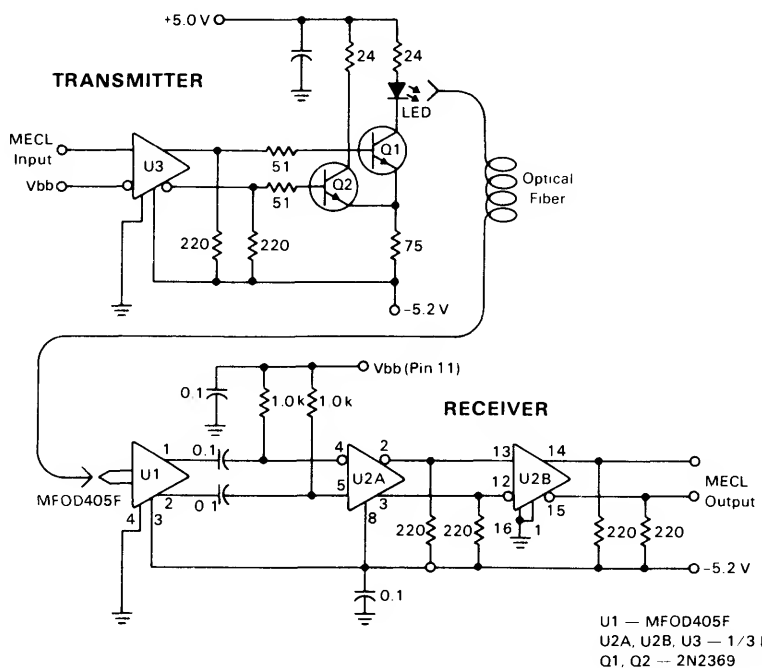
Further suggestions for circuits using the MFOD405F can be found in an article by R. Kirk Moulton in *Electronic Design* of March 1, 1980.

FIGURE 6



Eye-pattern output of receiver operating at 40 Mb/s

FIGURE 7





MOTOROLA

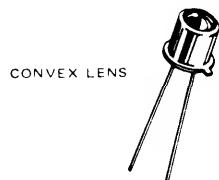
MF0E100

INFRARED EMITTING DIODE FOR FIBER OPTICS SYSTEMS

...designed as an infrared source in medium frequency, short length Fiber Optics Systems. Typical applications include: medical electronics, industrial controls, M6800 Microprocessor systems, security systems, etc.

- Spectral Response Matched to MFOD100, 200, 300
- Hermetic Metal Package for Stability and Reliability
- Fast Response - 50 ns typ
- Compatible With AMP Mounting Bushing =227015

IR-EMITTING DIODE FOR FIBER OPTICS SYSTEMS



MAXIMUM RATINGS

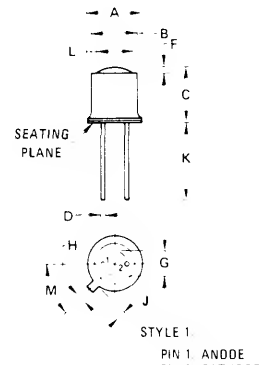
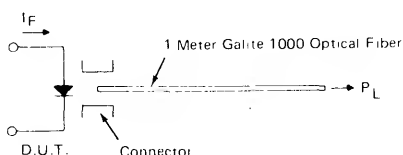
| Rating | Symbol | Value | Unit |
|--|----------------|-------------|----------------------------|
| Reverse Voltage | V_R | 3.0 | Volts |
| Forward Current - Continuous | I_F | 100 | mA |
| Total Device Dissipation @ $T_A = 25^\circ\text{C}$ Derate above 25°C | $P_D(1)$ | 250 2.5 | mW mW/ $^\circ\text{C}$ |
| Operating and Storage Junction Temperature Range | T_J, T_{stg} | -55 to +125 | $^\circ\text{C}$ |

THERMAL CHARACTERISTICS

| Characteristics | Symbol | Max | Unit |
|---|---------------|-----|--------------------|
| Thermal Resistance, Junction to Ambient | θ_{JA} | 400 | $^\circ\text{C/W}$ |

(1) Printed Circuit Board Mounting

FIGURE 1 – LAUNCHED POWER TEST CONFIGURATION



NOTES

- 1 PIN 2 INTERNALLY CONNECTED TO CASE
- 2 LEADS WITHIN 0.13 mm (0.005)
RADIUS OF TRUE POSITION AT SEATING PLANE AT MAXIMUM MATERIAL CONDITION

| DIM | MILLIMETERS | | INCHES | |
|-----|-------------|------|-----------|-------|
| | MIN | MAX | MIN | MAX |
| A | 5.31 | 5.84 | 0.209 | 0.230 |
| B | 4.52 | 4.95 | 0.178 | 0.195 |
| C | 6.22 | 6.98 | 0.245 | 0.275 |
| D | 0.41 | 0.48 | 0.016 | 0.019 |
| F | 1.19 | 1.60 | 0.047 | 0.063 |
| G | 2.54 BSC | | 0.100 BSC | |
| H | 0.99 | 1.17 | 0.039 | 0.046 |
| J | 0.84 | 1.22 | 0.033 | 0.048 |
| K | 12.70 | - | 0.500 | - |
| L | 3.35 | 4.01 | 0.132 | 0.158 |
| M | 4.59 BSC | | 0.180 BSC | |

CASE 209-02

MFOE100

ELECTRICAL CHARACTERISTICS ($T_A = 25^\circ\text{C}$)

| Characteristic | Fig. No. | Symbol | Min | Typ | Max | Unit |
|---|----------|-------------|-----|-----|-----|-------|
| Reverse Leakage Current ($V_R = 3.0 \text{ V}$, $R_L = 1.0 \text{ Megohm}$) | — | I_R | — | 50 | — | nA |
| Reverse Breakdown Voltage ($I_R = 100 \mu\text{A}$) | — | $V_{(BR)R}$ | 3.0 | — | — | Volts |
| Forward Voltage ($I_F = 100 \text{ mA}$) | — | V_F | — | 1.5 | 1.7 | Volts |
| Total Capacitance ($V_R = 0 \text{ V}$, $f = 1.0 \text{ MHz}$) | — | C_T | — | 100 | — | pF |

OPTICAL CHARACTERISTICS ($T_A = 25^\circ\text{C}$)

| | | | | | | |
|--|------|---------------|-----|------|---|---------------|
| Total Power Output (Note 1) ($I_F = 100 \text{ mA}$, $\lambda \approx 900 \text{ nm}$) | 1, 2 | P_o | 700 | 1000 | — | μW |
| Power Launched (Note 2) ($I_F = 100 \text{ mA}$) | 3 | P_L | 14 | 20 | — | μW |
| Optical Turn-On and Turn-Off Time | — | $t_{on, off}$ | — | 50 | — | ns |

1. Total Power Output, P_o , is defined as the total power radiated by the device into a solid angle of 2π steradians.
2. Power Launched, P_L , is the optical power exiting one meter of 0.045" diameter optical fiber bundle having NA = 0.67, Attenuation = 0.6 dB/m @ 900 nm, terminated with AMP connectors. (See Figure 1.)

TYPICAL CHARACTERISTICS

FIGURE 2 – INSTANTANEOUS POWER OUTPUT versus FORWARD CURRENT

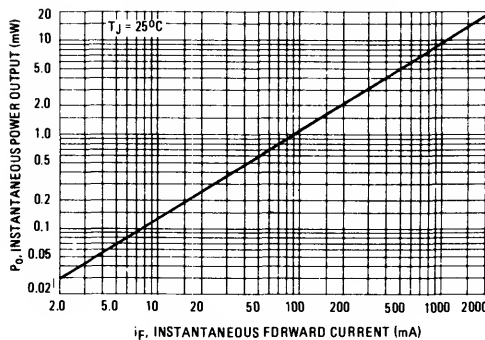
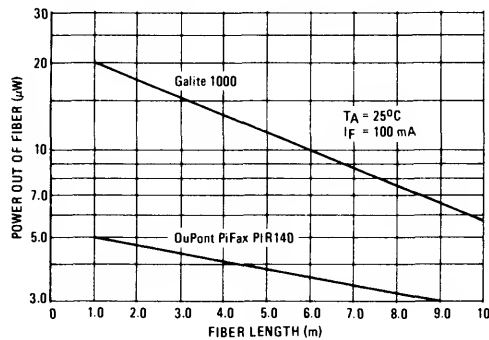


FIGURE 3 – POWER OUT OF FIBER versus FIBER LENGTH





MOTOROLA

MF0E102F

Advance Information

INFRARED EMITTING DIODE FOR FIBER OPTIC SYSTEMS

... designed as an infrared source for Fiber Optic Systems. It is packaged in Motorola's Fiber Optic Active Component (FOAC) case, and fits directly into AMP Incorporated fiber optics connectors for easy interconnect and use. Typical applications include medical electronics, industrial controls, M6800 microprocessor systems, security systems, computer and peripheral equipment, etc.

- Fast Response -- 25 ns typ
- May Be Used with MFODxxx Detectors
- FOAC Package -- Small and Rugged
- Fiber Output Port Greatly Enhances Coupling Efficiency
- Optical Port is Prepolished
- Compatible with AMP Connector #227240-1
- 200 μm [8 mil] Diameter Core Optical Port

FIBER OPTICS IR-EMITTING DIODE

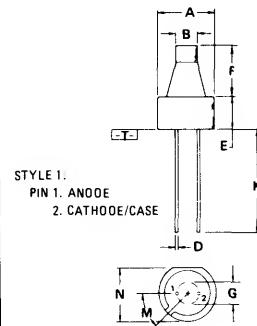


MAXIMUM RATINGS

| Rating | Symbol | Value | Unit |
|--|-----------|-------------|----------------------|
| Reverse Voltage | V_R | 3.0 | Volts |
| Forward Current—Continuous | I_F | 100 | mA |
| Total Device Dissipation @ $T_A = 25^\circ\text{C}$ Derate above 25°C | P_D | 250 | mW |
| | | 2.5 | mW/ $^\circ\text{C}$ |
| Operating Temperature Range | T_A | -30 to +85 | $^\circ\text{C}$ |
| Storage Temperature Range | T_{stg} | -30 to +100 | $^\circ\text{C}$ |

THERMAL CHARACTERISTICS

| Characteristics | Symbol | Max | Unit |
|---|---------------|-----|--------------------|
| Thermal Resistance, Junction to Ambient | θ_{JA} | 400 | $^\circ\text{C/W}$ |



NOTES

1. --- IS SEATING PLANE.
2. POSITIONAL TOLERANCE FOR LEADS:

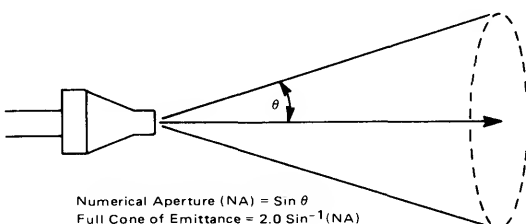
$\pm 0.36(0.014)$ \ominus T

3. DIMENSIONING AND TOLERANCING PER Y14.5, 1973.

| DIM | MILLIMETERS | | INCHES | |
|-----|-------------|------|-----------|-------|
| | MIN | MAX | MIN | MAX |
| A | 6.86 | 7.11 | 0.270 | 0.280 |
| B | 2.54 | 2.64 | 0.100 | 0.104 |
| D | 0.40 | 0.48 | 0.016 | 0.019 |
| E | 3.94 | 4.44 | 0.155 | 0.175 |
| F | 6.17 | 6.38 | 0.243 | 0.251 |
| G | 2.54 BSC | | 0.100 BSC | |
| K | 12.70 | — | 0.500 | — |
| M | 45° | NOM | 45° | NOM |
| N | 6.22 | 6.73 | 0.245 | 0.265 |

CASE 338-02

FIGURE 1 – CONE OF RADIATION



MFOE102F

ELECTRICAL CHARACTERISTICS ($T_A = 25^\circ\text{C}$)

| Characteristic | Symbol | Min | Typ | Max | Unit |
|---|-------------|-----|-----|-----|-------|
| Reverse Leakage Current ($V_R = 3.0 \text{ V}$, $R_L = 1.0 \text{ Megohm}$) | I_R | — | 50 | — | nA |
| Reverse Breakdown Voltage ($I_R = 100 \mu\text{A}$) | $V_{(BR)R}$ | 3.0 | — | — | Volts |
| Forward Voltage ($I_F = 50 \text{ mA}$) | V_F | — | 1.2 | 1.5 | Volts |
| Total Capacitance ($V_R = 0 \text{ V}$, $f = 1.0 \text{ MHz}$) | C_T | — | 45 | — | pF |

OPTICAL CHARACTERISTICS ($T_A = 25^\circ\text{C}$)

| | | | | | |
|--|-------------------|----|------|---|---------------|
| Total Power Output From Optical Port ($I_F = 50 \text{ mA}$, $\lambda \approx 900 \text{ nm}$) | P_o | 40 | 70 | — | μW |
| Numerical Aperture of Output Port (Figure 1) (200 μm [8 mil] diameter core) | NA | — | 0.48 | — | — |
| Wavelength of Peak Emission | — | — | 900 | — | nm |
| Spectral Line Half Width | — | — | 50 | — | nm |
| Optical Turn-On or Turn-Off Time | t_{on}, t_{off} | — | 25 | — | ns |

TYPICAL CHARACTERISTICS

FIGURE 2 – INSTANTANEOUS POWER OUTPUT
versus FORWARD CURRENT

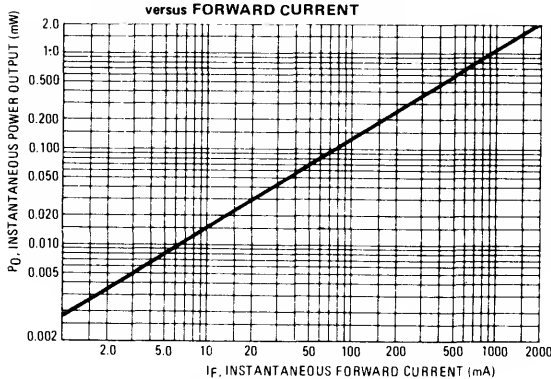


FIGURE 3 – POWER OUT OF FIBER* versus FIBER LENGTH

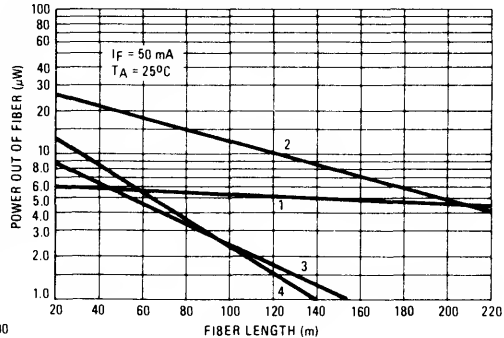
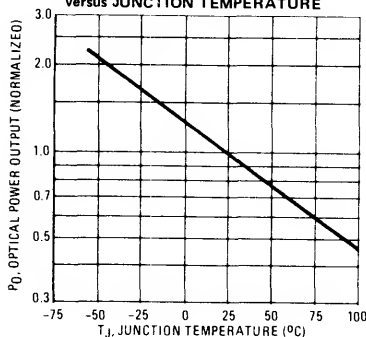


FIGURE 4 – OPTICAL POWER OUTPUT
versus JUNCTION TEMPERATURE



*Fiber Type
 1. Quartz Products OSF200
 2. Galileo Galilei 3000 LC
 3. Valtec PC10
 4. DuPont PF XS 120R



MOTOROLA

MF0E103F

Advance Information

INFRARED EMITTING DIODE FOR FIBER OPTIC SYSTEMS

... designed as an infrared source for Fiber Optic Systems. It is packaged in Motorola's Fiber Optic Active Component (FOAC) case, and fits directly into AMP Incorporated fiber optics connectors for easy interconnect and use. Typical applications include medical electronics, industrial controls, M6800 microprocessor systems, security systems, computer and peripheral equipment, etc.

- Fast Response - 15 ns typ
- May Be Used with MFODxxx Detectors
- FOAC Package - Small and Rugged
- Fiber Output Port Greatly Enhances Coupling Efficiency
- Optical Port is Prepolished
- Compatible with AMP Connector #227240-1
- 200 μm [8 mil] Diameter Core Optical Port

FIBER OPTICS IR-EMITTING DIODE



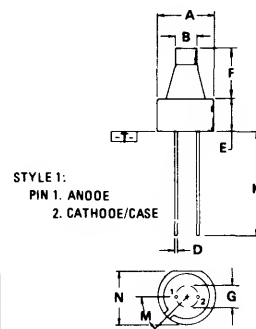
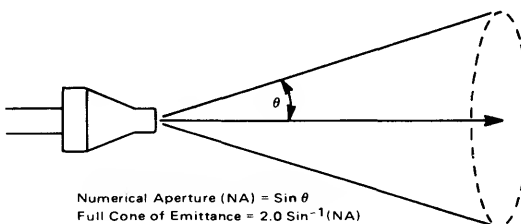
MAXIMUM RATINGS

| Rating | Symbol | Value | Unit |
|--|-----------|-------------|------------------|
| Reverse Voltage | V_R | 3.0 | Volts |
| Forward Current - Continuous | I_F | 100 | mA |
| Total Device Dissipation @ $T_A = 25^\circ\text{C}$ Derate above 25°C | P_D | 250 2.5 | mW mW/W |
| Operating Temperature Range | T_A | -30 to +85 | $^\circ\text{C}$ |
| Storage Temperature Range | T_{stg} | -30 to +100 | $^\circ\text{C}$ |

THERMAL CHARACTERISTICS

| Characteristics | Symbol | Max | Unit |
|---|---------------|-----|---------------------------|
| Thermal Resistance, Junction to Ambient | θ_{JA} | 400 | $^\circ\text{C}/\text{W}$ |

FIGURE 1 - CONE OF RADIATION



NOTES:

1. \square IS SEATING PLANE.
2. POSITIONAL TOLERANCE FOR LEADS:
 $\downarrow \pm .36(0.014) \square T$
3. DIMENSIONING AND TOLERANCING PER Y14.5, 1973.

| DIM | MILLIMETERS | | INCHES | |
|-----|-------------|------|-----------|-------|
| | MIN | MAX | MIN | MAX |
| A | 6.86 | 7.11 | 0.270 | 0.280 |
| B | 2.54 | 2.64 | 0.100 | 0.104 |
| D | 0.40 | 0.48 | 0.016 | 0.019 |
| E | 3.94 | 4.44 | 0.155 | 0.175 |
| F | 6.17 | 6.38 | 0.243 | 0.251 |
| G | 2.54 BSC | | 0.100 BSC | |
| K | 12.70 | - | 0.500 | - |
| M | 45° NOM | | 45° NOM | |
| N | 6.22 | 6.73 | 0.245 | 0.265 |

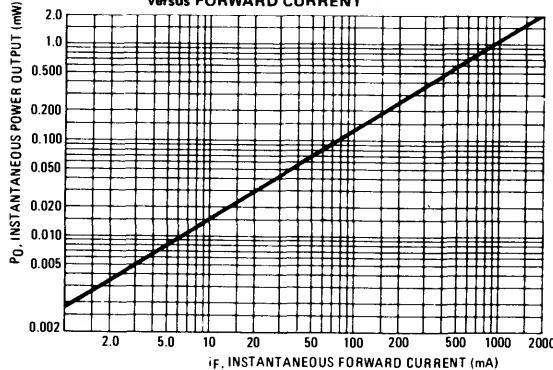
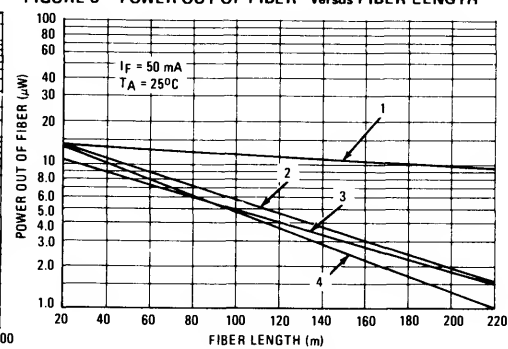
CASE 338-02

ELECTRICAL CHARACTERISTICS ($T_A = 25^\circ\text{C}$)

| Characteristic | Symbol | Min | Typ | Max | Unit |
|---|-------------|-----|-----|-----|-------|
| Reverse Leakage Current ($V_R = 3.0 \text{ V}$, $R_L = 1.0 \text{ Megohm}$) | I_R | — | 50 | — | nA |
| Reverse Breakdown Voltage ($I_R = 100 \mu\text{A}$) | $V_{(BR)R}$ | 3.0 | — | — | Volts |
| Forward Voltage ($I_F = 50 \text{ mA}$) | V_F | — | 1.2 | 1.5 | Volts |
| Total Capacitance ($V_R = 0 \text{ V}$, $f = 1.0 \text{ MHz}$) | C_T | — | 45 | — | pF |

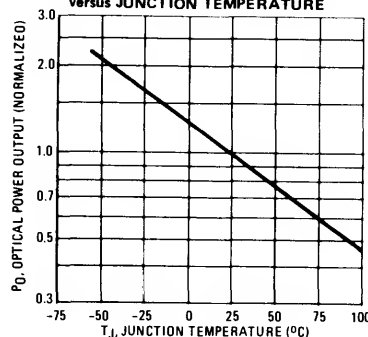
OPTICAL CHARACTERISTICS ($T_A = 25^\circ\text{C}$)

| | | | | | |
|--|---------------------------------|----|------|----|---------------|
| Total Power Output From Optical Port ($I_F = 50 \text{ mA}$, $\lambda \approx 900 \text{ nm}$) | P_O | 40 | 70 | — | μW |
| Numerical Aperture of Output Port (Figure 1) 10.0 dB (200 μm [8 mil] diameter core) | NA | — | 0.70 | — | — |
| Wavelength of Peak Emission | — | — | 900 | — | nm |
| Spectral Line Half Width | — | — | 50 | — | nm |
| Optical Turn-On or Turn-Off Time ($I_F = 100 \text{ mA}$) | $t_{\text{on}}, t_{\text{off}}$ | — | 15 | 22 | ns |

TYPICAL CHARACTERISTICS
FIGURE 2 – INSTANTANEOUS POWER OUTPUT versus FORWARD CURRENT

FIGURE 3 – POWER OUT OF FIBER* versus FIBER LENGTH


*Fiber Type

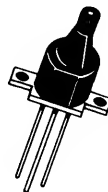
1. Maxlight KSC200B
2. Galite 3000 LC
3. Siecor 155
4. DuPont PFXS 120R

FIGURE 4 – OPTICAL POWER OUTPUT versus JUNCTION TEMPERATURE


**MOTOROLA****MF0E106F****Advance Information****NEW GENERATION AlGaAs LED**

Specifically designed for Fiber Optics. This high-power, 820 nm LED is packaged in Motorola's Fiber Optic Ferrule case, and fits directly into AMP, Incorporated fiber optics connector #227240-1 for easy interconnect use. Typical applications include medical electronics, industrial controls, M6800 microprocessor systems, security systems, computer and peripheral systems, etc.

- Fast Response - 12 ns typ
- May Be Used with MFODxxx Detectors
- Ferrule Package - Small and Rugged
- Fiber Output Port Greatly Enhances Coupling Efficiency
- Optical Port is Prepolished
- Compatible with AMP Connector #227240-1
- 200 μ m [8 mil] Diameter Core Optical Port

**FIBER OPTICS
IR-EMITTING DIODE**

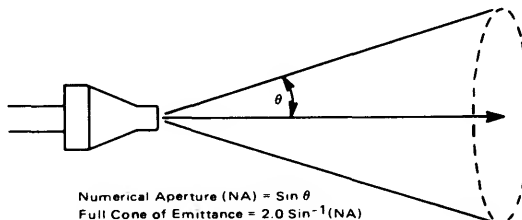
CASE 338D-01

MAXIMUM RATINGS

| Rating | Symbol | Value | Unit |
|--|-----------|-------------|----------------------|
| Reverse Voltage | V_R | 3.0 | Volts |
| Forward Current—Continuous | I_F | 150 | mA |
| Total Device Dissipation @ $T_A = 25^\circ\text{C}$ Derate above 25°C | P_D | 250 | mW |
| | | 2.5 | mW/ $^\circ\text{C}$ |
| Operating Temperature Range | T_A | -30 to +85 | $^\circ\text{C}$ |
| Storage Temperature Range | T_{stg} | -30 to +100 | $^\circ\text{C}$ |

THERMAL CHARACTERISTICS

| Characteristics | Symbol | Max | Unit |
|---|---------------|-----|--------------------|
| Thermal Resistance, Junction to Ambient | θ_{JA} | 175 | $^\circ\text{C/W}$ |

FIGURE 1 – CONE OF RADIATION

Numerical Aperture (NA) = $\sin \theta$
Full Cone of Emittance = $2.0 \sin^{-1}(NA)$

This is advance information and specifications are subject to change without notice.
Patent applied for.

MFOE106F

ELECTRICAL CHARACTERISTICS ($T_A = 25^\circ\text{C}$)

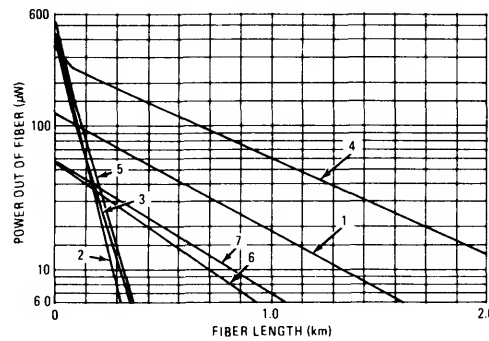
| Characteristic | Symbol | Min | Typ | Max | Unit |
|---|-------------|-----|-----|-----|-------|
| Reverse Leakage Current ($V_R = 3.0 \text{ V}$, $R_L = 1.0 \text{ Megohm}$) | I_R | — | 50 | — | nA |
| Reverse Breakdown Voltage ($I_R = 100 \mu\text{A}$) | $V_{(BR)R}$ | 3.0 | — | — | Volts |
| Forward Voltage ($I_F = 50 \text{ mA}$) | V_F | — | 1.2 | 1.5 | Volts |
| Total Capacitance ($V_R = 0 \text{ V}$, $f = 1.0 \text{ MHz}$) | C_T | — | 450 | — | pF |

OPTICAL CHARACTERISTICS ($T_A = 25^\circ\text{C}$)

| | | | | | |
|---|---------------------------------|---|------|----|---------------|
| Total Power Output From Optical Port ($I_F = 100 \text{ mA}$, $\lambda \approx 820 \text{ nm}$) | P_o | — | 700 | — | μW |
| Numerical Aperture of Output Port (Figure 1) 10.0 dB (200 μm [8 mil] diameter core) | NA | — | 0.50 | — | — |
| Wavelength of Peak Emission | — | — | 820 | — | nm |
| Spectral Line Half Width | — | — | 35 | — | nm |
| Optical Turn-On or Turn-Off Time | $t_{\text{on}}, t_{\text{off}}$ | — | 12 | 20 | ns |

TYPICAL CHARACTERISTICS

FIGURE 2 – POWER OUT OF FIBER* versus FIBER LENGTH



- * Fiber Type
 - 1. Belden 220001
 - 2. DuPont S120
 - 3. Siecor 155B
 - 4. Maxlight KSC200B
 - 5. Galite 3000LC
 - 6. Siecor 142
 - 7. I.T.T. T1302
 - 7. Galite 5020



MOTOROLA

MF0E200

INFRARED EMITTING DIODE FOR FIBER OPTICS SYSTEMS

...designed as an infrared source in low frequency, short length Fiber Optics Systems. Typical applications include: medical electronics, industrial controls, M6800 Microprocessor systems, security systems, etc.

- High Power Output Liquid Phase Epitaxial Structure
- Spectral Response Matched to MFOD100, 200, 300
- Hermetic Metal Package for Stability and Reliability
- Compatible With AMP Mounting Bushing #227015

HIGH-POWER IR-EMITTING DIODE FOR FIBER OPTICS SYSTEMS



MAXIMUM RATINGS

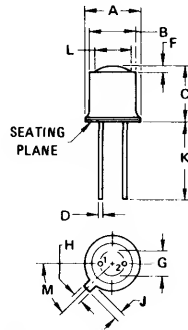
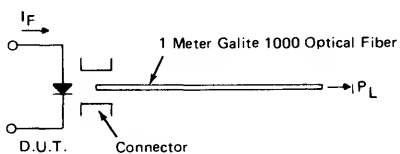
| Rating | Symbol | Value | Unit |
|--|-----------------------|-------------|----------------------------|
| Reverse Voltage | V_R | 3.0 | Volts |
| Forward Current—Continuous | I_F | 100 | mA |
| Total Device Dissipation @ $T_A = 25^\circ\text{C}$ Derate above 25°C | $P_D(1)$ | 250 2.5 | mW mW/ $^\circ\text{C}$ |
| Operating and Storage Junction Temperature Range | T_J, T_{stg} | -55 to +125 | $^\circ\text{C}$ |

THERMAL CHARACTERISTICS

| Characteristics | Symbol | Max | Unit |
|---|---------------|-----|---------------------------|
| Thermal Resistance, Junction to Ambient | θ_{JA} | 400 | $^\circ\text{C}/\text{W}$ |

(1) Printed Circuit Board Mounting

FIGURE 1 – LAUNCHED POWER TEST CONFIGURATION



**STYLE 1:
PIN 1. ANODE
2. CATHODE**

NOTES:

1. PIN 2 INTERNALLY CONNECTED TO CASE.
2. LEADS WITHIN 0.13 mm (0.005) RADIUS OF TRUE POSITION AT SEATING PLANE AT MAXIMUM MATERIAL CONDITION.

| DIM | MILLIMETERS | | INCHES | |
|-----|-------------|------|---------|-------|
| | MIN | MAX | MIN | MAX |
| A | 5.31 | 5.84 | 0.209 | 0.230 |
| B | 4.52 | 4.95 | 0.178 | 0.195 |
| C | 6.22 | 6.98 | 0.245 | 0.275 |
| D | 0.41 | 0.48 | 0.016 | 0.019 |
| F | 1.19 | 1.60 | 0.047 | 0.063 |
| G | 2.54 | BSC | 0.100 | BSC |
| H | 0.99 | 1.17 | 0.039 | 0.046 |
| J | 0.84 | 1.22 | 0.033 | 0.048 |
| K | 12.70 | — | 0.500 | — |
| L | 3.35 | 4.01 | 0.132 | 0.158 |
| M | 45° BSC | — | 45° BSC | — |

CASE 209-02

ELECTRICAL CHARACTERISTICS ($T_A = 25^\circ\text{C}$)

| Characteristic | Fig. No. | Symbol | Min | Typ | Max | Unit |
|---|----------|-------------|-----|-----|-----|-------|
| Reverse Leakage Current ($V_R = 3.0 \text{ V}$, $R_L = 1.0 \text{ Megohm}$) | — | I_R | — | 50 | — | nA |
| Reverse Breakdown Voltage ($I_R = 100 \mu\text{A}$) | — | $V_{(BR)R}$ | 3.0 | — | — | Volts |
| Forward Voltage ($I_F = 100 \text{ mA}$) | — | V_F | — | 1.5 | 1.7 | Volts |
| Total Capacitance ($V_R = 0 \text{ V}$, $f = 1.0 \text{ MHz}$) | — | C_T | — | 150 | — | pF |

OPTICAL CHARACTERISTICS ($T_A = 25^\circ\text{C}$)

| | | | | | | |
|--|------|-------------------|-----|-----|---|---------------|
| Total Power Output (Note 1) ($I_F = 100 \text{ mA}$, $\lambda \approx 940 \text{ nm}$) | 1, 2 | P_o | 2.0 | 3.0 | — | mW |
| Power Launched (Note 2) ($I_F = 100 \text{ mA}$) | 3 | P_L | 35 | 45 | — | μW |
| Optical Turn-On and Turn-Off Time | — | t_{on}, t_{off} | — | 250 | — | ns |

1. Total Power Output, P_o , is defined as the total power radiated by the device into a solid angle of 2π steradians.
2. Power Launched, P_L , is the optical power exiting one meter of 0.045" diameter optical fiber bundle having NA = 0.67, Attenuation = 0.6 dB/m @ 940 nm, terminated with AMP connectors. (See Figure 1.)

TYPICAL CHARACTERISTICS

FIGURE 2 – INSTANTANEOUS POWER OUTPUT
versus FORWARD CURRENT

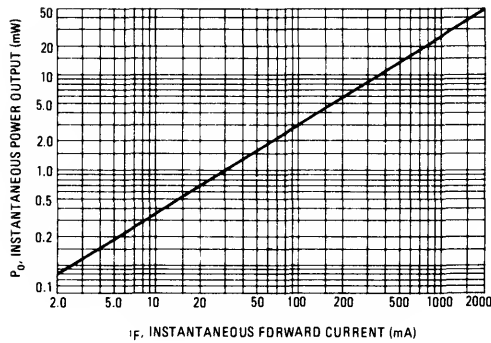
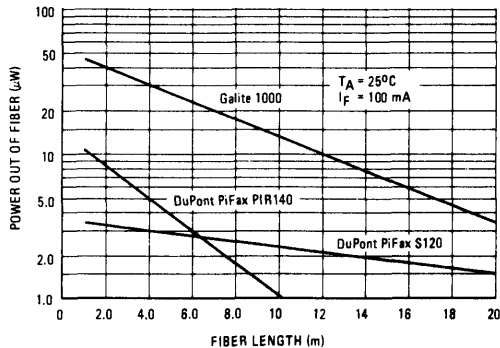


FIGURE 3 – POWER OUT OF FIBER
versus FIBER LENGTH





MOTOROLA

MFOL01

THE LINK

A complete Fiber Optic one way transmission path component assembly.

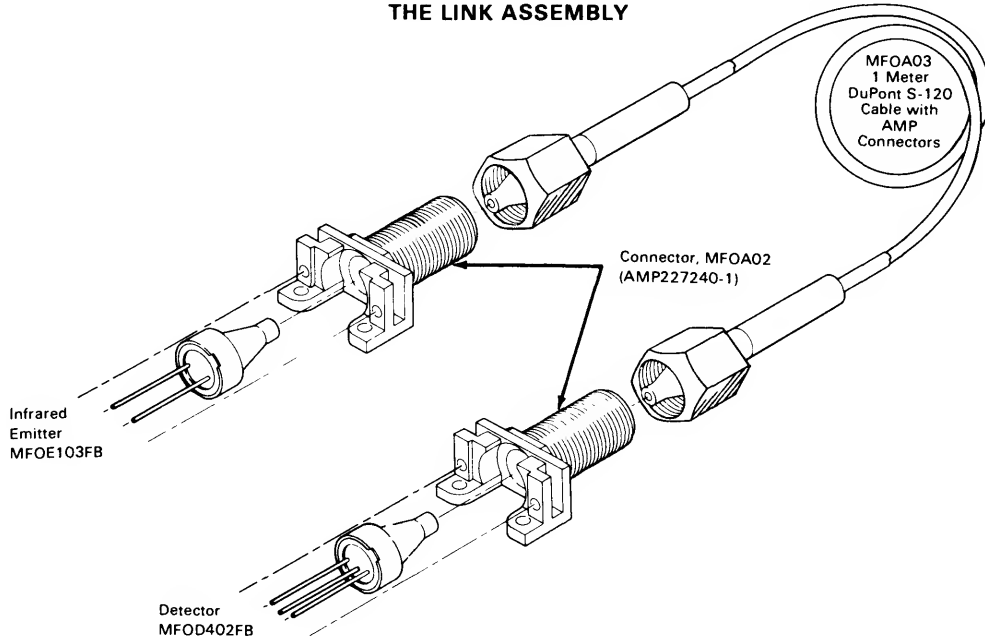
The Link includes an infrared emitter, one meter of cable with connectors, an integrated detector preamplifier and the compatible ferrule semiconductor connectors.

Also included are basic design formulas, system design examples, descriptive material on fiber optics, circuit ideas, several application suggestions, and device data sheets.

- 17 MHz Linear Capability
- NRZ Data to 20 Mb/s
- Expandable System Lengths (cable loss dependant)
- Rugged, Prepolished, Ferrule Semiconductors
- No Optical Expertise Needed
- RFI Shielded Detector

FIBER OPTICS KIT

THE LINK ASSEMBLY



MFOL01

MFOE103FB IR Emitter

MAXIMUM RATINGS

| Rating | Symbol | Value | Unit |
|-----------------------------|----------------|------------|-------|
| Reverse Voltage | V _R | 30 | Volts |
| Forward Current—Continuous | I _F | 100 | mA |
| Operating Temperature Range | T _A | -30 to +85 | °C |

ELECTRICAL CHARACTERISTICS (T_A = 25°C)

| Characteristic | Symbol | Min | Typ | Max | Unit |
|---|--------------------|-----|-----|-----|-------|
| Reverse Leakage Current (V _R = 30 V, R _L = 1.0 Megohm) | I _R | — | 50 | — | nA |
| Reverse Breakdown Voltage (I _R = 100 μA) | V _{(BR)R} | 30 | — | — | Volts |
| Forward Voltage (I _F = 50 mA) | V _F | — | 1.2 | 1.5 | Volts |
| Total Capacitance (V _R = 0 V, f = 1.0 MHz) | C _T | — | 45 | — | pF |

OPTICAL CHARACTERISTICS (T_A = 25°C)

| | | | | | |
|---|------------------------------------|----|-----------|----|----|
| Total Power Output From Optical Port I _P = 50 mA (λ ≈ 900 nm) | P _O | 40 | 70 140 | — | μW |
| Numerical Aperture of Output Port 3.0 dB (200 μm [8 mil] diameter core) | NA | — | 0.48 | — | — |
| Optical Turn-On or Turn-Off Time | t _{on} , t _{off} | — | 15 | 22 | ns |

MFDOD402FB INTEGRATED DETECTOR PREAMPLIFIER

MAXIMUM RATINGS (T_A = 25°C unless otherwise noted)

| Rating | Symbol | Value | Unit |
|-----------------------------|-----------------|------------|-------|
| Operating Voltage | V _{CC} | 20 | Volts |
| Operating Temperature Range | T _A | -30 to +85 | °C |

ELECTRICAL CHARACTERISTICS (V_{CC} = 15 V, T_A = 25°C)

| Characteristic | Symbol | Min | Value Typ | Max | Unit |
|-----------------------------|--------------------|-----|--------------|-----|--------|
| Power Supply Current | I _{CC} | 1.4 | 1.7 | 2.0 | mA |
| Quiescent dc Output Voltage | V _Q | 0.6 | 0.7 | 0.9 | Volts |
| Resistive Load | R _O Max | 300 | — | — | Ohms |
| Capacitive Load | C _O Max | — | — | 20 | pF |
| Output Impedance | Z _O | — | 200 | — | Ohms |
| RMS Noise Output | V _{NO} | — | 0.3 | — | mV |
| Noise Equivalent Power | NEP | — | 57 | — | pW/√Hz |
| Operating Voltage Range | V _{CC} | 5.0 | — | 15 | Volts |
| Bandwidth (3.0 dB) | BW | — | 17.5 | — | MHz |

OPTICAL CHARACTERISTICS (T_A = 25°C)

| | | | | | |
|--|---------------------------------|-----|------|---|-------|
| Responsivity (V _{CC} = 15 V, λ = 900 nm, P = 10 λW*) | R | 0.6 | 1.5 | — | mV/μW |
| Pulse Response | t _r , t _f | — | 20 | — | ns |
| Numerical Aperture of Input Core (200 μm [8 mil] diameter core) | NA | — | 0.48 | — | — |

*Power launched into Optical Input Port. The designer must account for interface coupling losses.

MFOA03 FIBER OPTIC CABLE ASSEMBLY

| |
|---|
| Type: DuPont S-120 |
| Number of Fibers: 1 |
| Fiber Core Diameter, nominal: 200 μm (8 mil) |
| Numerical Aperture, nominal: 0.4 |
| Attenuation: 100 dB/Km @ 900 nm |
| Cable Connectors: AMP Optimate metal connectors compatible with AMP 227240-1 Connectors |



MOTOROLA

MFOL02

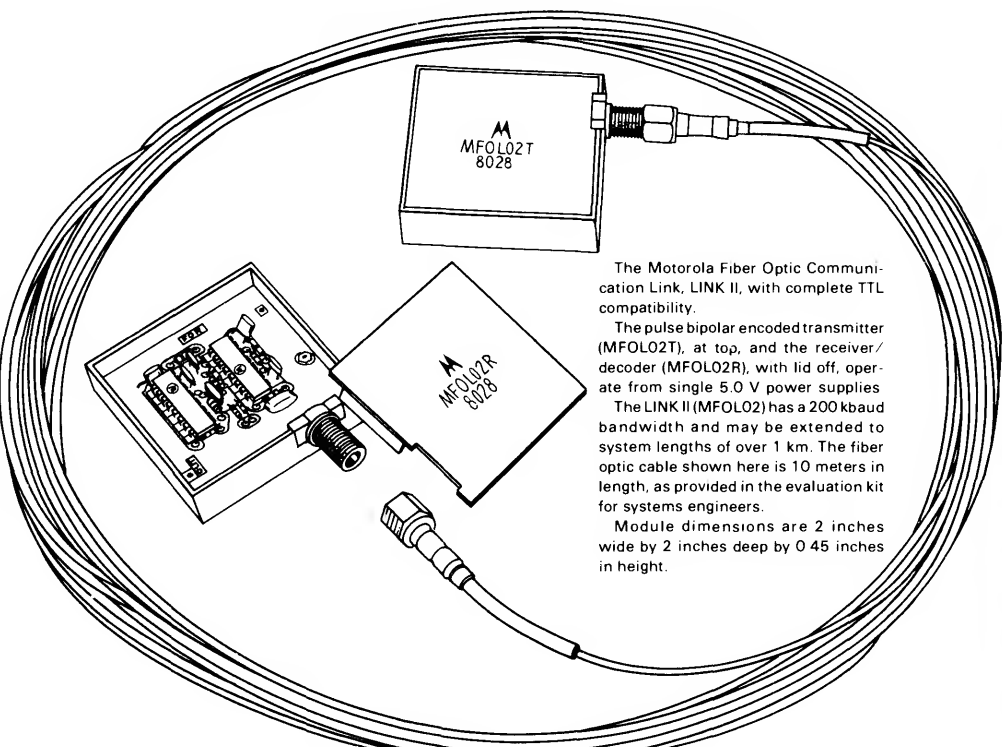
LINK II

A Complete Fiber Optic Simplex TTL communication data link. Link II features a transmitter and receiver module, 10 meters of fiber cable, preterminated with appropriate matching AMP connectors.

Link II includes complete component specifications, extensive application literature discussing The Theory of Operation of LINK II, and the "basic concepts" of fiber optics and fiber optic communications.

- Simplex TTL 200 kHz BW Data Link
- TTL Transmitter and Receiver Modules
- Preterminated 10 meters of Fiber Optic Cable (Expandable to 2 km)
- Link II Theory of Operation
- System Design Considerations, Data Sheets, Application Notes

**TTL
FIBER OPTIC
DATA
LINK**



The Motorola Fiber Optic Communication Link, LINK II, with complete TTL compatibility.

The pulse bipolar encoded transmitter (MFOL02T), at top, and the receiver/decoder (MFOL02R), with lid off, operate from single 5.0 V power supplies.

The LINK II (MFOL02) has a 200 kbaud bandwidth and may be extended to system lengths of over 1 km. The fiber optic cable shown here is 10 meters in length, as provided in the evaluation kit for systems engineers.

Module dimensions are 2 inches wide by 2 inches deep by 0.45 inches in height.

MFOLO2

MFOLO2T TRANSMITTER

ELECTRICAL CHARACTERISTICS ($T_A = 25^\circ C$)

| Characteristic | Symbol | Min | Typ | Max | Unit |
|---|----------|------|------|-----|---------------|
| Power Supply Voltage | V_{CC} | — | 5.0 | — | Volts |
| Power Supply Current (Idle Mode) | I_{CC} | — | 80 | — | mA |
| Total Power Output From Output Port * ($\lambda = 900 \text{ nm}$, Idle Mode $I_F = 50 \text{ mA}$) | P_o | 40 | 70 | — | μW |
| Numerical Aperture of Output Port | NA | — | 0.70 | — | — |
| Bandwidth | BW | D.C. | — | 200 | Kbit |

*Transmitter features MFOE102F

MFOLO2R RECEIVER

ELECTRICAL CHARACTERISTICS ($T_A = 25^\circ C$)

| Characteristic | Symbol | Min | Typ | Max | Unit |
|----------------------------------|----------|------|------|-----|---------------|
| Power Supply Voltage | V_{CC} | — | 5.0 | — | Volts |
| Power Supply Current (Idle Mode) | I_{CC} | — | 8.0 | — | mA |
| Receiver Sensitivity* | S | — | 0.01 | — | μW |
| Numerical Aperture of Input Port | NA | — | 0.70 | — | — |
| Bandwidth | BW | D.C. | — | 200 | Kbit |
| Dynamic Range (NRZ) | — | — | 25 | — | dB |

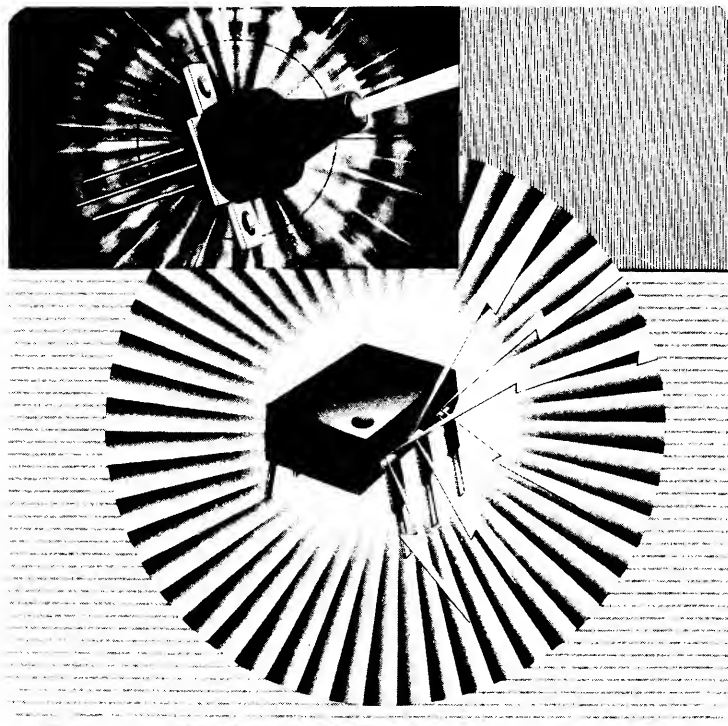
*Receiver features MFOD102F

MFOA10 CABLE ASSEMBLY

10 meters of single fiber core preterminated cable.

LINK II can be expanded to several km by
utilization of other Motorola FOAC Devices
ie: MFOE106F/MFOD405F (820/nm system)

FIBER OPTICS



Applications Information

A 20-MBAUD FULL DUPLEX FIBER OPTIC DATA LINK USING FIBER OPTIC ACTIVE COMPONENTS

Prepared By:
Vincent L. Mirtich

INTRODUCTION

This application note describes an optical transceiver which is designed to be used in a full duplex data communications link. Its electrical interface with the outside world is TTL. The optical interface between modules consists of separate transmit and receive ports, which use the Motorola Fiber Optic Active Component (FOAC) for the optical to electrical transducers. Two modules can optically communicate via either two separate fibers or via an optical duplexer such as a three-port directional coupler and a single fiber. The data rate can be anything from 20 Mbaud on down as long as the transmitter input rise times are compatible with TTL specifications. For NRZ data where one baud per bit is required, data can be transferred at rates up to 20 Mbits. For RZ data where 2 bauds per bit are required, data can be transferred at rates up to 10 Mbits. The small-signal 3.0 dB bandwidth of the system is 10 MHz minimum. The unit can also be configured as an optical repeater by connecting the receiver electrical output to the transmitter electrical input.

The receiver is edge coupled and therefore places no constraints on data format. Since the edge coupling removes the data base line variation, there is no baseline tracking required. Consequently, there is no limit on the length of a string of ones or zeroes. The receiver latches and remembers the polarity of the last received data edge. The use of the Motorola FOAC for the transmitter and receiver transducers greatly simplifies the optical interface. It eliminates

the handling of delicate fiber pigtails, the need for terminating and polishing such pigtails, and is compatible with the AMP connector system.

This application note will follow the following format:

- I. Transmitter Description
 - A. Block diagram and functional description
 - B. Schematic diagram and design considerations
 - C. Transmitter performance
- II. Receiver Description
 - A. Functional block diagram and design considerations
 - B. Amplitude detector coupling and required S/N
 - C. Schematic diagram and circuit implementation
 - D. Receiver performance
- III. Building the Boards
 - A. Parts list and unique parts
 - B. Working with FOACs and AMP connectors
 - C. Shielding requirements
- IV. Testing the Boards
 - A. Test equipment required
 - B. Looping transmitter to receiver. Caution with LED
 - C. Waveform analysis
 - D. Setting hysteresis
- V. System Performance
 - A. Interpreting fiber, emitter, and detector specifications
 - B. Calculating system performance. Loss budget, dispersion limit.

TRANSMITTER DESCRIPTION

Transmitter Block Diagram and Functional Description

Figure 1 shows the functional block diagram of the optical transmitter. The first block is the logic interface. Since the transmitter is intended for use in data communications applications, it has to interface a common logic family and provide some standard load and input signal requirements. Also, since it is intended for use at data rates of up to 20 Mbaud, TTL is a good choice for the logic family. The logic interface function then could be implemented by one of the standard TTL gates, inverters, etc., to provide an electrical port which can be driven from any TTL output.

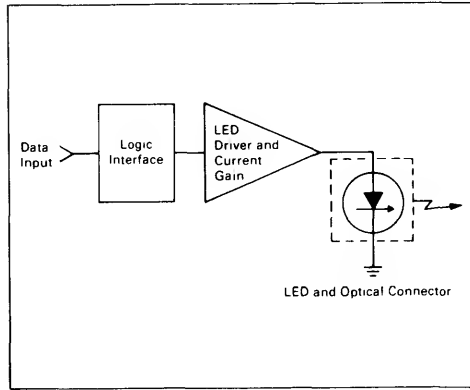


FIGURE 1 — Optical Transmitter Functional Block Diagram

The second block in Figure 1, the **LED Driver and Current Gain**, has several functions. First, it must provide the forward current required by the LED for the particular optical output power desired. Secondly, it must switch that current on and off in response to the input data with rise and fall times consistent with the maximum baud rate expected. Third, it must provide enough current gain to amplify the limited source and sink current of the logic interface block up to the needed LED current.

The third block, the **LED and Optical Connector** could be broken into two separate functions, as is usually the case. However, through the use of a well thought out and economically advantageous approach to the electrical to optical fiber translation, the electrical to optical transducer and the fiber coupling functions have been addressed in concert. The electro/optical transducer is an LED which emits pulses of optical energy in response to the data input. In this case, the optical energy is near infrared which is invisible to the unaided eye. The LED package, a FOAC, efficiently couples as much emitted energy as possible into a short internal pre-polished pigtail fiber. The coupler or connector then mounts the FOAC so that its optical port is aligned with the core of the system fiber. In this way, the percentage of emitted optical power that is launched into the system fiber is maximized without any special preparation of the transducer by the user. Refer to Figure 2.

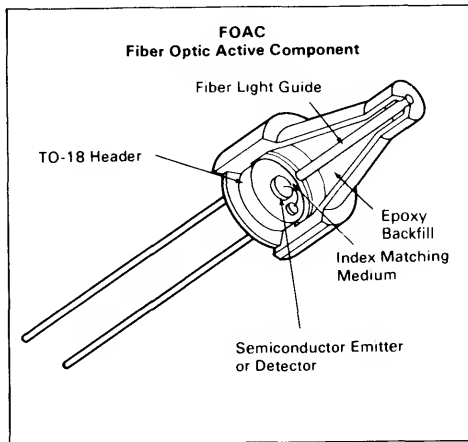


FIGURE 2 — FOAC Construction

In addition to these functions, it would be nice if the transmitter had the following features. It would be convenient if the LED current were easily set to whatever value was desired. It would be desirable if the LED current were not influenced greatly by power supply fluctuations or temperature variations. Since this transmitter is to be operating beside a receiver operating on the same power supply, it would greatly simplify transmitter/receiver isolation if the transmitter didn't cause large supply current variations which modulated the power supply lines. Finally, it would be useful if the transmitter could easily be gated off by another logic signal so that the LED did not respond to the data input.

Transmitter Schematic and Design Considerations

Figure 3 shows the transmitter circuit schematic and indicates which portion of the circuit performs each of the previously mentioned functions.

The **logic interface** has been implemented using the two sections of the SN74LS40 dual four input NAND gate in cascade. The LS40 was chosen as the particular part because of its buffered output. Since it can sink 24 mA instead of the normal 8.0 mA (typical LS output) and still provide 0.5 V for a low output, it puts less of a current gain requirement on the following circuitry. The reason two sections were used in cascade rather than one is that every TTL gate introduces some differential prop delay. This is a difference in propagation times through the gate for positive and negative transitions. It is primarily a function of the gates' output transistor configuration and how hard they are driven by internal circuitry. In some instances, it can be very near zero, and in other parts it can be as high as 10 ns. However, on a particular chip, all sections will tend to have differential prop delays of the same polarity and very nearly equal. If two inverting functions on the same chip are then cascaded, the differential prop delay through the pair will tend to null to zero since both polarities of incoming data edges are processed as positive transitions by one gate and as negative transitions by the other gate.

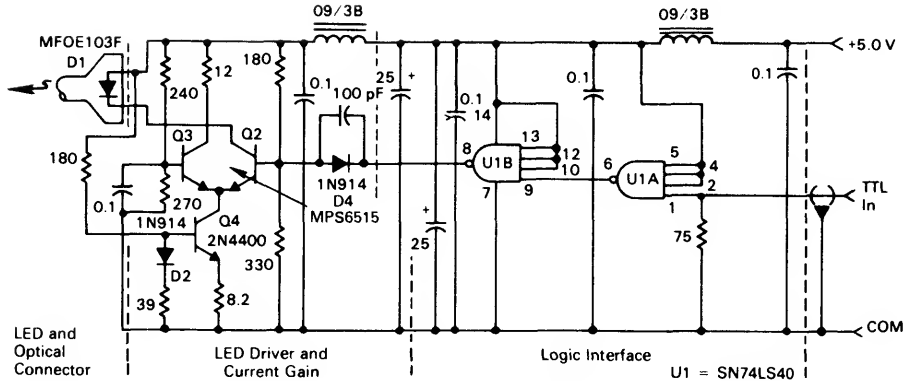


FIGURE 3 — Transmitter Schematic

The effect of a 10 ns longer propagation delay for high to low transitions on a 20 Mbaud squarewave is shown in Figure 4. It will be noted that processing the distorted signal through a second gate having prop delays equal to those of the first gate corrects the duty cycle distortion at the expense of a little higher absolute prop delay. The distorted waveform is delayed by t_{PHL} only whereas the undistorted waveform is delayed by $t_{PHL} + t_{PLH}$. This slight increase in absolute prop delay is usually insignificant compared to the absolute prop delay through the transmission medium. It will also be noted that if the distortion is not corrected, then the waveform applied to the LED driver is of a higher baud rate, thus requiring wider system bandwidth.

The cascading of two identical inverting gates also provides a way of balancing their power supply currents and avoids putting transients on the +5.0 V power line. The schematic shows different loads on

the two NAND gate sections so that the currents are not equal for the two logic input levels. However, if additional power supply decoupling were needed to further reduce transmitter and receiver crosstalk, putting a $430\ \Omega$ pull-up resistor from Pin 6 of U1A to +5.0 V would improve the balance of transmitter power supply current between the two logic states at the expense of another 10 mA or so in transmitter current drain.

The gating function mentioned earlier is also not shown in the schematic but can be easily implemented by tying one of Pins 2, 4, or 5 of U1A to +5.0 V through a suitable pull-up resistor and then providing this pin to the outside world for a logic low to gate off the data. This data off condition would also produce an LED off condition.

The 75Ω termination across the data input is to terminate an expected 75Ω coaxial cable. If data rates significantly lower than 20 Mbaud are transmitted

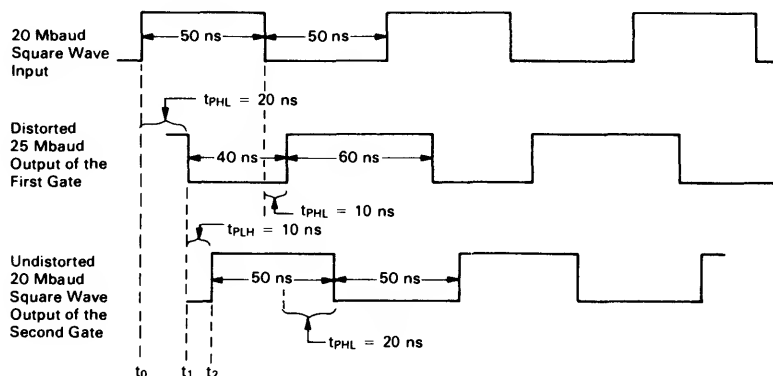


FIGURE 4 — Correction of Duty Cycle Distortion Caused by Gate Differential Prop Delay

then a coaxial cable may not be necessary and a different termination can be used. The reader is cautioned, however, that an unshielded data line into the transmitter could cause crosstalk to the receiver and thereby destroy the system error rate performance. Therefore, if an unshielded lead-in is desired, it should be implemented while monitoring hit errors in the receive channel.

The **LED driver** and **current gain** function is implemented with a discrete current limited differential amplifier with the LED as one of the collector loads. The amplifier's emitter coupled configuration is well known for providing fast switching speeds. Its non-saturating characteristic prevents any stored charge accumulation in the transistor base region and the corresponding degradation in turn off time. Therefore, rise and fall times of this driver are fast and very nearly the same. Since these driver transistors don't saturate, they also preserve their high small-signal current gain and consequently minimize base drive requirements.

The current source, Q4, is biased so that its collector current is equal to the peak LED current desired. The emitter resistor of Q4 sets the current and the component values shown in Figure 3 bias Q4 at 100 mA. Diode D2 matches the thermal drift in the emitter voltage of Q4 which holds its collector current constant over temperature.

Once this current is fixed, the logic state at Pin 8 of UIB determines if it flows through Q2 and the LED or through Q3 and the $12\ \Omega$ resistor. A logic high at Pin 8 reverse biases D4 and allows the Q2 base current to be supplied by the resistor divider network and consequently turns on the LED. A logic low at Pin 8 biases Q2 and the LED off.

The required logic condition at the TTL input to turn on the LED can easily be switched 180° by driving the LED with the opposite side of the differential amplifier. It should be pointed out that this is the preferred way of switching the transmitter phase rather than adding another stage of logic inversion which would introduce differential prop delay and hence duty cycle distortion.

The use of a differential driver does cause the transmitter current drain to be relatively constant even when the LED is off. However, the disadvantage of higher standby drain is far outweighed by the reduction in power line transients on the +5.0 V line due to no significant power supply current switching. This greatly enhances the isolation between the transmitter and receiver.

The **LED and connector** used is the MFOE103F in the ferruled package and the AMP 227240-1 connector. This LED has a maximum rise time of 22 ns and a typical power out of $70\ \mu\text{W}$ at 50 mA drive current.

Transmitter Performance

Figure 5 shows the calculated exit power expected for six different fibers when driven from the transmitter. This chart can be used to determine which fiber delivers the most exit power for a given path length.

Figure 6 shows the variation in LED current and transmitter output power over temperature. This was measured at the end of a 20 foot length of the Seicor cable, with the LED biased for continuous operation.

Figure 7 displays the duty cycle distortion introduced by the transmitter logic interface and LED driver. Figure 7(a) shows a 50% duty cycle square-wave at the transmitter TTL input and Figure 7(b)

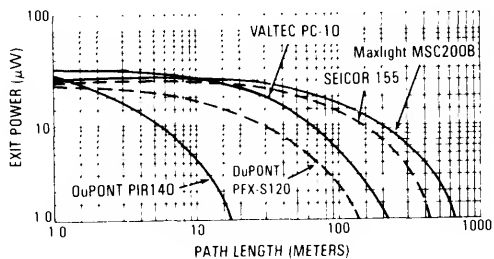


FIGURE 5 — Calculated Peak Exit Power versus Fiber Path

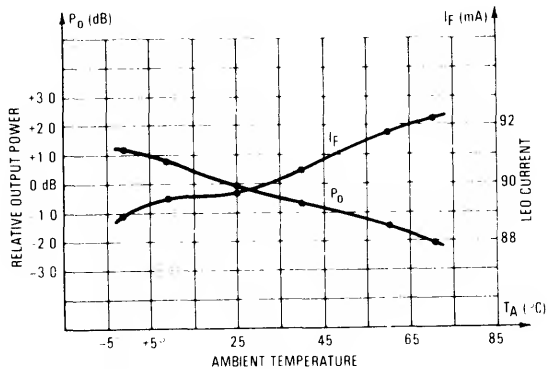


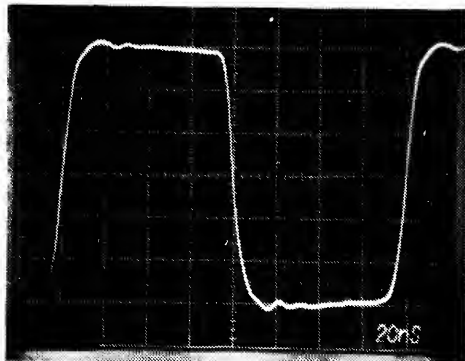
FIGURE 6 — Optical Output Power and LED Current versus Temperature

shows the corresponding LED current waveform measured with a high frequency current probe. It will be noted that the current waveform exhibits an indiscernible amount of duty cycle distortion.

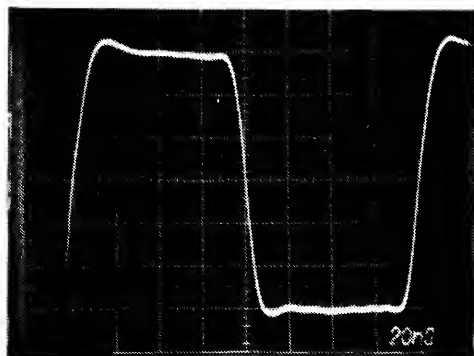
The biasing of the base of Q2 in both logic states relative to the bias at the base of Q1 can be another source of duty cycle distortion. If this is critical to the application and must be held to less than a couple of nanoseconds, these resistors may be selected to tighter tolerances. Also, replacing the LS40 NAND gate with an S40 (standard, Schottky) NAND gate will reduce distortion contributed by that source.

Figure 8 shows the absolute prop delay through the transmitter. It will be noted that both positive and negative transitions are delayed about 43 ns.

Figure 9 shows the 10%-90% rise and fall times of the LED current waveform to be about 17 ns and 13 ns respectively.



(a) Transmitter TTL Input



(b) LED Current

FIGURE 7 — Transmitter Duty Cycle Distortion

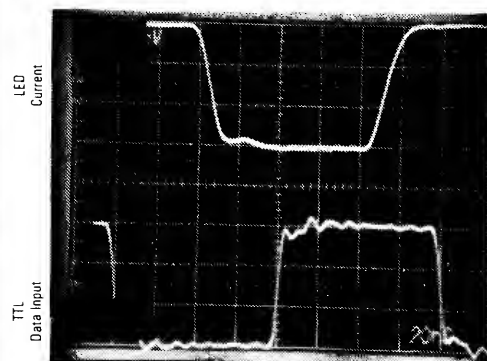


FIGURE 8 — Transmitter Absolute Prop Delay

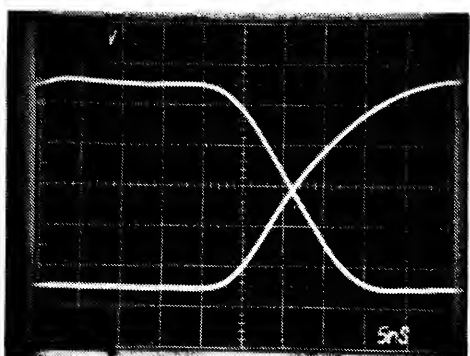


FIGURE 9 — LED Current Rise and Fall Time

RECEIVER DESCRIPTION

Functional Block Diagram and Design Considerations

Figure 10 shows the receiver functional block diagram.

The first element is the **optical detector** which receives pulses of optical energy emanating from the end of a fiber. It typically looks like a current source (see Figure 11) whose magnitude is dependent on the incident optical energy and a parallel capacitor whose value is dependent on device design

and the magnitude of reverse bias across it. This capacity adds in parallel with any external load capacity to form a net load capacity which must be charged and discharged by the minute photo current from the detector. Because this detector output is a high impedance source and its signal is very small, it is a difficult point to interface without introducing noise, RFI, and reactive loads which degrade the signal quality.

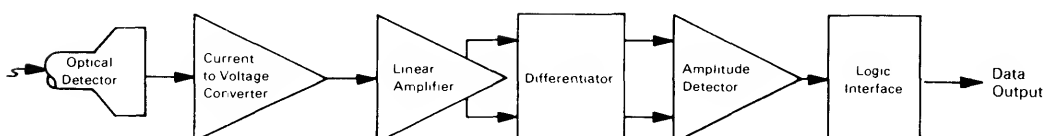


FIGURE 10 -- Optical Receiver Functional Block Diagram

For this reason, the second element shown in the block diagram, the **current to voltage converter**, is usually coupled as closely as possible to the optical detector and very often this interface is then shielded from outside interference. This converter is typically a transimpedance amplifier circuit built from an op amp or other high gain amplifier with negative current feedback. This circuit does three things. First, it provides signal gain by producing an output voltage proportional to the input current. Second, by virtue of its high open loop gain and negative feedback, it provides a low output impedance. Third, it provides a virtual ground at its signal input. That is to say, it has a very low input impedance. Because of this, there is little or no voltage swing at its input. Since the capacitive load on the optical detector has to be charged by the photo current, the relationship of

$$I \sim C \frac{\Delta V}{\Delta t} \quad (1)$$

$$\Delta t = C \frac{\Delta V}{I} \quad (2)$$

holds true. This says that for a capacitor C , being charged by a constant current I , the change in voltage across it, ΔV , will occur in time interval Δt . Thus, for the model in Figure 11,

$$\begin{aligned} \text{if } I &= 50 \text{ nA} \\ C &= 10 \text{ pF} \\ \Delta V &= 1.0 \text{ mV} \\ \text{then } \Delta t &= 200 \text{ ns} \end{aligned}$$

Naturally, if the virtual ground input of the current to voltage converter reduces ΔV to very nearly zero, the transition time, Δt , also approaches zero and much faster rise times can be recovered. Also, by reducing the capacitance, C , one can improve the rise time.

This capacitance is the parallel equivalent of the optical detector capacitance, the amplifier input capacitance, and parasitic capacitance of the printed circuit board. An integrated detector/preamp (IDP) reduces the component capacitances to a minimum and completely eliminates the PCB capacitance, thereby minimizing rise time and providing a low impedance voltage source to which interfacing is easily accomplished.

Now that the optical signal has been converted into a voltage pulse coming from a low source impedance and having fast rising and falling edges, it can be processed by more conventional means. For this

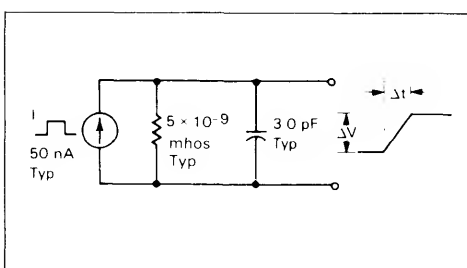


FIGURE 11 — Practical Photo Detector Model

reason, the third element in the block diagram is a linear **voltage amplifier**. This amplifier should have sufficient gain to amplify the expected noise from the current to voltage converter up to the minimum level detectable by the amplitude detector. The reason for this will be seen later.

With this consideration in mind, the minimum gain of the voltage amplifier can then be defined as

$$A_{v_{min}} = \frac{\text{Amplitude Detector Threshold (V}_pp)}{\text{I to V Converter Noise Output (V}_pp)} \quad (3)$$

Having more gain than this merely amplifies signal and noise together beyond the minimum amplitude detector threshold and accomplishes nothing but a higher required detector threshold. Thus, it would be better for the designer to have a voltage gain block whose gain tracked detector threshold from unit to unit or else a voltage gain and detector threshold which did not vary significantly from unit to unit. The latter is much easier to accomplish.

The next characteristic of the linear amplifier that must be considered is its bandwidth or rise time. Rise time will be considered here because data links are usually characterized by a rise time budget rather than a bandwidth budget. The system rise time is defined as the rise time of the signal appearing at the amplitude detector input which in this case is the voltage amplifier's output. For reasons explained later, a well designed system has its bandwidth determined in the optical detector and preamp so the voltage gain block's rise time should not degrade system rise time by more than 10%. Rise time contributions through the system add as the square root of the sum of the squares. System rise time is exhibited by the output waveform of the voltage amplifier. It is usually determined by contributions from the current to voltage converter and the voltage amplifier such that:

$$t_{R_{SYS}} = \sqrt{(t_{R_{IDP}})^2 + (t_{R_{AV}})^2} \quad (4)$$

where $t_{R_{SYS}}$ is the system rise time desired at the voltage amplifier's output

$t_{R_{IDP}}$ is the rise time of the integrated detector preamp

$t_{R_{AV}}$ is the required rise time of the voltage amplifier

This is only true if all other rise times in the system, such as the LED driver, the LED, and the fiber dispersion, are fast enough so as not to contribute significantly to the system rise time.

Now, if the voltage amplifier rise time should not degrade the well designed system by more than 10%, then using equation (4)

$$t_{R_{SYS}} \leq (1.1) t_{R_{IDP}}$$

$$\sqrt{(t_{R_{IDP}})^2 + (t_{R_{AV}})^2} \leq 1.1 t_{R_{IDP}}$$

$$\text{and } t_{R_{AV}} \leq (0.458) t_{R_{IDP}} \quad (5)$$

There is also a lower limit on this voltage amplifier's rise time which precludes it from having as fast a rise time as is available. That is, as the noise from each noise source in the receiver is added, its relative contribution is a function of its bandwidth. For example, if the IDP is characterized as having a noise bandwidth B_1 , an input noise of $e_{n1} \text{ V}/\sqrt{\text{Hz}}$, and a gain of A_{v1} and if the voltage amplifier similarly has equivalent parameters of B_2 , e_{n2} , and A_{v2} , then the noise presented to the amplitude detector in volts is

$$e_{n\text{DET}} = [e_{n1} \sqrt{B_1} A_{v1} + e_{n2} \sqrt{B_2}] A_{v2} \quad (6)$$

From equation (6) it can be seen that if the voltage amplifier's noise bandwidth, B_2 , is too large in relation to the IDP's bandwidth, B_1 , its noise contribution can be significant or even dominant in which case a much wider noise spectrum and higher noise levels are available at the amplitude detector to degrade S/N. The upper limit on the voltage amplifier's bandwidth then is the point at which the noise contribution of the voltage amplifier is about 50% of the IDP noise. This will enable the IDP noise to still determine amplitude detector threshold.

$$\begin{aligned} e_{n1} \sqrt{B_1} A_{v1} A_{v2} &= 2e_{n2} \sqrt{B_2} A_{v2} \\ B_2 &= B_1 \left[\frac{(A_{v1})(e_{n1})}{2e_{n2}} \right]^2 \end{aligned}$$

To sum up the characteristics of the voltage gain block, it should have sufficient gain to amplify the IDP noise up to minimum amplitude detector

threshold as well as gain which doesn't vary more than amplitude detector threshold from unit to unit. It should have a rise time fast enough so as not to degrade system rise time by more than 10% but not so fast a rise time that its noise bandwidth contributes significantly to system noise.

The next component in the block diagram of Figure 10 is the **differentiator**. As was mentioned in the Introduction, this edge coupled receiver strips off the base line variations with duty cycle from the data stream. This is the function of the differentiator and there are a few considerations to be made in picking the values of R and C. Figure 12 compares the waveforms through an ac coupling network with those through a differentiator. Figures 12(a) and 12(b) each show a 20% duty cycle pulse train and an 80% duty cycle pulse train as two possible extremes in data format for a particular system. When passed through the ac coupling network shown in Figure 12(c), the resulting waveforms will have the levels shown in 12(e). Note the 3.0 V variation in "logic 1" levels and the same variation in "logic 0" levels as the duty cycle varies from 20% to 80%. In practice, an even wider range in duty cycle is often encountered, thereby making the lowest "logic 1" and the highest "logic 0" even less distinguishable from one another. As a result, if a level detector such as a comparator is used to decide whether a "logic 1" or a "0" is present, it must compare the data stream to a floating reference which tracks the reference level of the data stream so that it is always centered between the peaks. For best noise immunity, this reference would have to be at the midpoint of the peak to peak amplitude of the data. Under this condition, the noise immunity would be equal to the amplitude of the data pulses. If the data should lapse for a period of time,

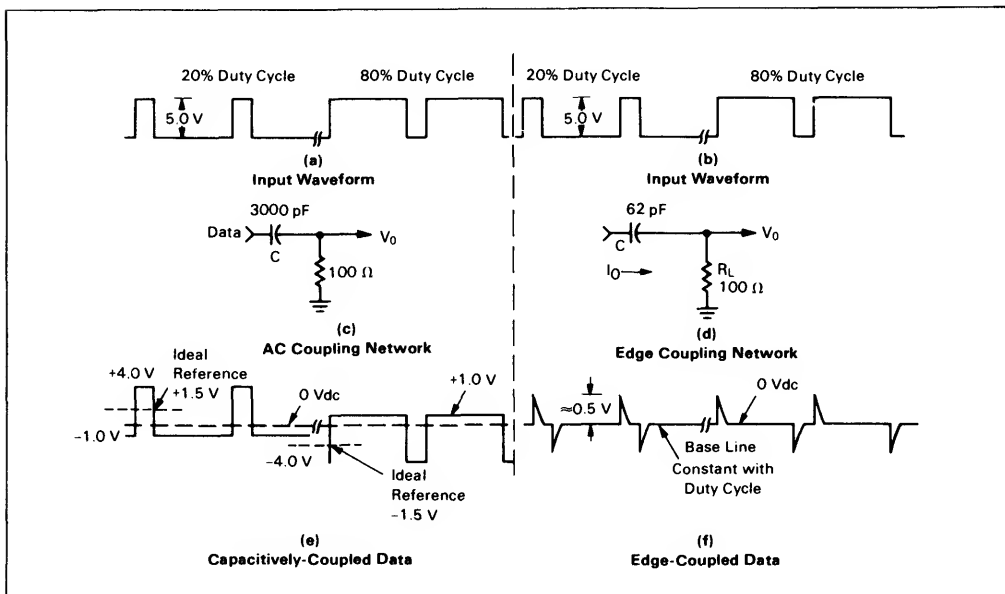


FIGURE 12 — Comparison of Data Stream Waveforms Through AC-Coupled and Edge-Coupled Systems

this floating reference would decay to its appropriate limit for minimum or maximum duty cycle. Once transmission resumed, depending on the initial duty cycle, the first few bits of data could be missed until the reference returned to its proper level.

A much more versatile system which is tolerant of any duty cycle from continuous "logic 1's" to continuous "logic 0's" is the edge coupled system. As can be seen from Figures 12(b), (d), and (f), only the edges of the data pulses are passed by the coupling network. These pass at reduced amplitude and then the recovery or discharge of the network occurs before the next data edge comes along. Since the V_0 out of the network in Figure 12(d) is the drive signal for the amplitude detector, it should be maximized. Since V_0 is the product of the load resistor and the capacitor current, I_0 should be maximized. Therefore,

$$\text{since } V_0 = R_L I_0 \\ \text{and } I_0 = C \frac{dV_C}{dt}, \quad (7)$$

$$V_0 = R_L \cdot C \cdot \frac{dV_C}{dt}$$

where V_C is the voltage across the differentiator capacitors. Hence, the $R_L C$ time constant should be maximized to provide maximum amplitude detector drive. If the input waveform to the edge coupling network appears as Figure 13(a), V_0 will appear as that shown in 13(b).

However, in maximizing the $R_L C$ time constant, it cannot be increased without limit. As can be seen from Figure 13(b), within the minimum bit time, the differentiator must be allowed to recover fully. Allowing 4 time constants ($4 R_L C$) after the system rise time t_{RSYS} has occurred will permit sufficient recovery. Hence the minimum bit time, T , is given by

$$T = t_{RSYS} + 4 R_L C \max$$

$$\text{and } R_L C \max = \frac{T - t_{RSYS}}{4} \quad (8)$$

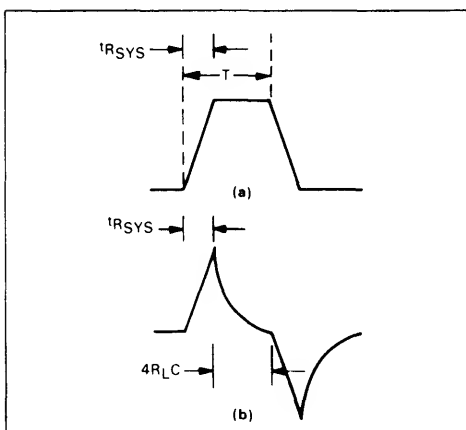


FIGURE 13 — Differentiator Waveforms

There is an implication here that may not be obvious. That is, to provide the required input to the amplitude detector, two requirements must be satisfied. The differentiator input signal must have adequate amplitude and it must have an adequately fast rise time. Looking back at equation 7, it will be noted that it is $\frac{dV_C}{dt}$ which determines V_0 and

therefore there is a myriad of combinations of amplitude and rise time which will provide adequate results. However, if the transition height of the input waveform is so small that its peak value is below detector threshold, or if the rise time is so slow that the $R_L C$ time constant decays significantly before the transition is complete, then the pulse will go undetected. An example of this occurs if the fiber link is disrupted during the transmission of an LED "ON" condition ("logic 1"). That disruption generates so slow a transition that it will not couple through the differentiator and the receiver will indicate that the LED is still on until the link is restored and a fast LED "OFF" transition is received.

There is another subtlety implied here and that is that all coupling capacitor time constants ahead of the differentiator must be long enough so as not to decay, during a long string of ones or zeroes, so fast as to generate an edge that is differentiable. A coupling time constant of one or two orders of magnitude longer than the differentiator time constant is suitable.

From a practical point of view the output impedance level of the differentiator should be kept low so that measurements with scope probes can be made without destroying the waveshape of the differentiator output signal. It was found that an R value of 500Ω or less was needed to keep a conventional $10X$, 7.0 pF probe from severely loading differentiators having time constants in the 5 to 20 ns range.

With the data stream now differentiated, the next block in Figure 10, the **amplitude detector** can be considered. Refer to Figure 14. Since each differentiated edge returns to the reference voltage level from

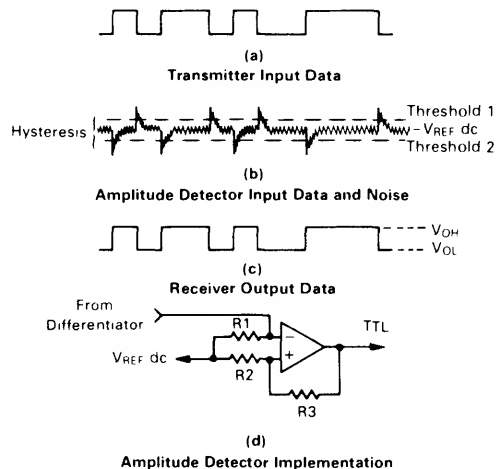


FIGURE 14 — Edge Detector Operation

either polarity of pulse, what is required is an amplitude detector with two thresholds, one above the reference voltage and one below; in essence a Schmitt Trigger function which has hysteresis and whose threshold is dependent on the output state. Looking at the next block of Figure 10 and noting that it must generate a logic interface, in this case a TTL interface, it can be seen that both blocks can be accomplished by using a comparator or line receiver with positive feedback as the amplitude detector. Figure 14 describes the operation and implementation of this amplitude detector with hysteresis. As can be seen, when a positive edge crosses threshold 1, the output switches low and the feedback to the non-inverting input causes threshold 2 to now apply. Since the positive edge decays back to V_{REF}, threshold 2 is not crossed and the output is latched low. The next edge to come along must be negative and when it occurs it crosses threshold 2 causing the output to switch high. Similarly, it latches in this state and reinstates threshold 1.

In order for the hysteresis to be symmetrical about V_{REF}, it must be centered between the limits of the TTL output swing. That is,

$$V_{\text{REF}} = \frac{V_{\text{OH}} + V_{\text{OL}}}{2} \quad (9)$$

Referring to Figure 14(d), the hysteresis is determined by:

$$H = (V_{\text{OH}} - V_{\text{OL}}) \left(\frac{R_2}{R_2 + R_3} \right) \quad (10)$$

R₁ is made equal to R₂ so as not to introduce voltage offsets due to the input current of the amplitude detector. In practice, R₁ and R₂ should be made fairly low values so that the actual input voltages do not have a step between the two states due to the voltage drop of these resistors and the amplitude detector input current. Because they are low values, 100–500 Ω is typical, R₁ also becomes the load of the differentiator.

As can be seen from Figure 14(b), the hysteresis must be made greater than the peak-to-peak noise riding on the data stream. The amplitude detector used in this 20-Mbaud system is similar to this but is driven differentially. To afford a better understanding of why this type of amplitude detector was chosen, a discussion of different amplitude detector implementations and their relative merits follow.

Amplitude Detector Coupling and Required S/N

Just how much larger than the noise the hysteresis must be depends on the probability of error one is willing to accept. That probability, or Bit Error Rate performance, directly relates to the required signal-to-noise ratio. These two parameters of BER and S/N have been related by Curve A shown in Figure 15. This curve is derived by evaluating the error function for a normal distribution which defines the probability of a noise pulse being some factor, N, times the rms noise level for various values of N. However, this curve is only applicable to amplitude detector performance if certain assumptions are made. The first is that the amplitude detector threshold or decision level is always midway between the two extremes of the data stream level. The second

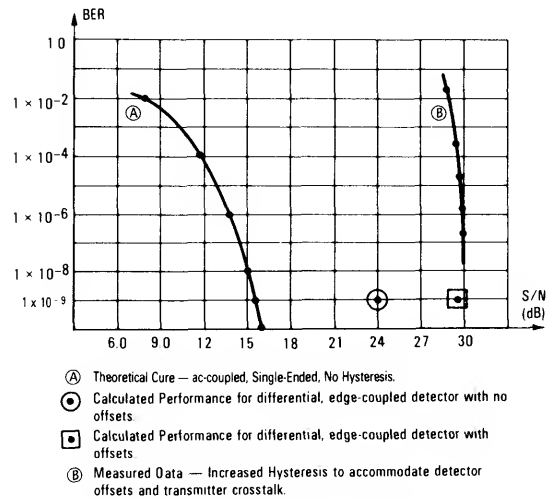


FIGURE 15 — BER versus S/N Performance

assumption is either that during the absence of data it is acceptable for noise crossing threshold to cause output transitions or else that data is never absent. The third is that there is no hysteresis around the threshold. The expected waveforms are shown in Figure 16(a).

This S/N versus BER curve and the waveforms of Figure 16(a) apply to both ac-coupled as well as dc-coupled systems as long as the above assumptions prevail. However, because of the difficulty of controlling the amplified thermal drifts in a dc-coupled system, ac coupling is usually used in an optical data transmission system. Therefore dc-coupled systems will not be considered here.

Referring to Figure 16(a), as long as the waveform is above threshold the data bit is labeled a "logic 1" and if the waveform is below threshold, the data bit is labeled a "logic 0." As long as data is always present, that is idle channel condition is marked with a flag, a squarewave or some other recognizable pattern, the only time an error will occur is when a noise pulse is large enough to reach threshold. Looking at Figure 16(a) it can be seen that when the noise peak equals or exceeds the threshold voltage, a bit error is made. The amplitude to which noise peaks will rise only once in 1×10^{-9} attempts is 6.15 times the rms noise amplitude. Therefore, the required peak signal amplitude for a 1×10^{-9} BER is 6.15 times the rms noise. If the signal is any smaller than that, a noise pulse riding on the data which is large enough to cross threshold and cause a bit error will occur more often and the BER will be less than 1×10^{-9} . Expressing this in more conventional terms then, the required S/N ratio for a 1×10^{-9} BER is:

$$\text{S/N} = 20 \log \left(\frac{e_{\text{peak}}}{e_{\text{nrms}}} \right) = 20 \log \left(\frac{6.15 e_{\text{nrms}}}{e_{\text{nrms}}} \right)$$

$$\text{S/N} = 15.8 \text{ dB}$$

This can be seen to lie on Curve A in Figure 15. This S/N is not a true power ratio but merely 20 times the log of a ratio of a peak voltage to an rms voltage.

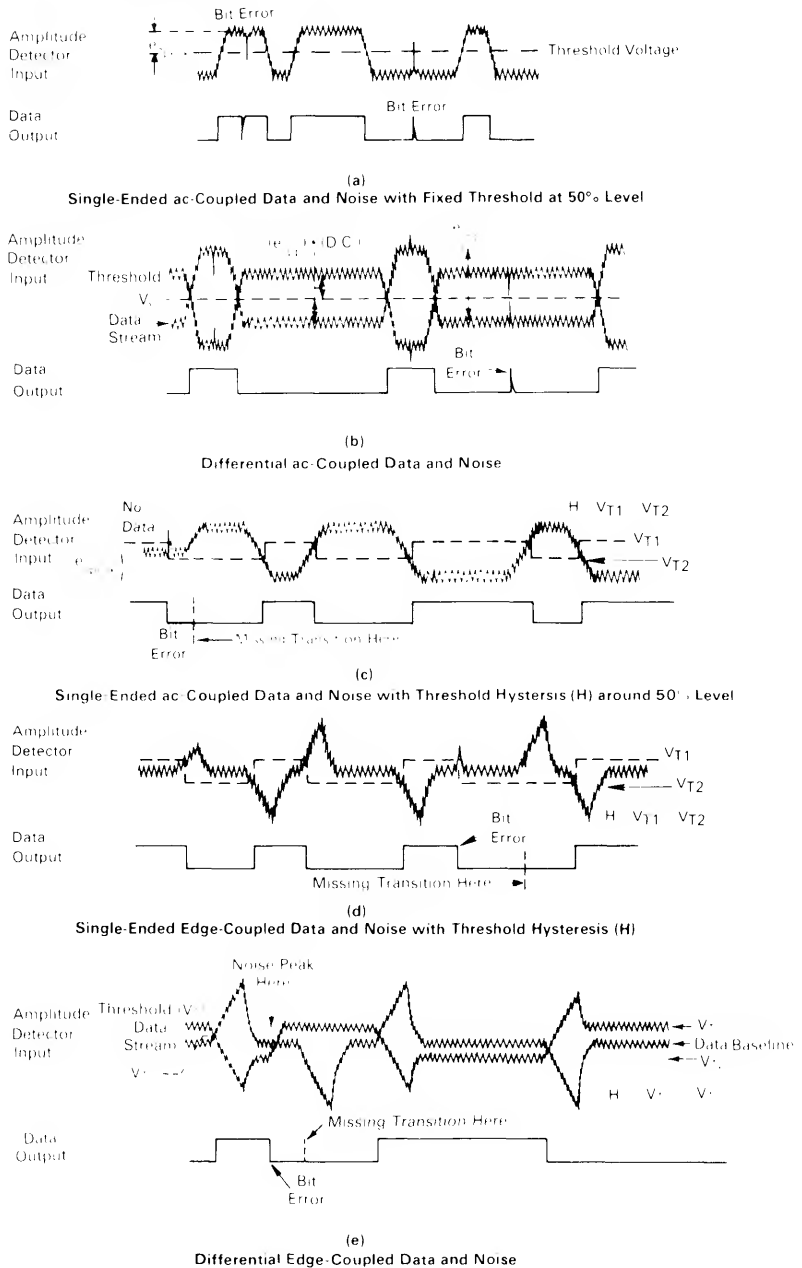


FIGURE 16

However, by convention these units are called dBs of signal-to-noise.

If the data in Figure 16(a) drives the detector differentially, then the waveforms of Figure 16(b) apply. Here, rather than comparing data to a fixed noise free threshold centered between the voltage extremes of the data stream, the data is compared to a threshold voltage which is different for a logic one bit than it is for a logic zero bit. This threshold is the data stream inverted. That is, it is data plus noise which is equal in amplitude to the data stream data plus noise, but opposite in phase. Since both the data stream and the threshold are capacitively coupled, their base lines float to maintain an average value of zero. Thus, referring to Figure 16(b), the data stream and threshold levels are separated from each other by a voltage difference which is a function of the incoming duty cycle (D.C.). The amplitude of noise this system can tolerate without making bit errors is, therefore, a function of duty cycle. This means the peak signal to rms noise required by this system to insure a 1×10^{-9} BER is also a function of duty cycle.

Looking at Figure 16(b) it can be seen that the data stream is in a logic one state for a small percentage of the time and in a logic zero state the rest of the time. This represents a low duty cycle pulse train. As the duty cycle is increased so that the data stream remains in a logic one state for a longer percentage of the time, the entire data stream waveform will float downward, so that the logic zero voltage level will move farther from and the logic one voltage level will move closer to the quiescent bias level V_Q . As this happens the threshold waveform on the other hand will remain in the logic zero state for the same increased percentage of time and the waveform will move upward a corresponding amount. Thus, the two waveforms will be close to one another and noise immunity will be relatively low for large duty cycles as well as for low duty cycles and their separation from each other and the noise immunity will be maximized when the duty cycle is 50%.

Thus, the proximity of the threshold and data stream waveforms depends on the limit of incoming duty cycle furthest from 50%. If this limit is less than 50%, the value of D.C. to be used in equation (11) is equal to the decimal equivalent of the duty cycle itself. If the limit of duty cycle is greater than 50%, then the value of D.C. is the decimal equivalent of 100% minus the duty cycle.

That is

$$(e_{s_{pp}}) \cdot (D.C.) = 6.15(e_{n_{rms}})$$

$$2(e_{s_{peak}}) = \frac{6.15(e_{n_{rms}})}{D.C.} \quad (11)$$

$$(e_{s_{peak}}) = \frac{6.15(e_{n_{rms}})}{2(D.C.)}$$

for a square wave or 50% duty cycle,

$$e_{s_{peak}} = 6.15(e_{n_{rms}})$$

$$\text{or } S/N = 15.8 \text{ dB}$$

For a 20% to 70% variation in duty cycle, the limit is 20% and the value of D.C. is 0.2.

$$e_{s_{peak}} = \frac{6.15(e_{n_{rms}})}{2(2)}$$

$$\text{or } S/N = 20 \log \left[\frac{e_{s_{peak}}}{e_{n_{rms}}} \right]$$

$$S/N = 23.7 \text{ dB}$$

For a 30% to 80% variation in duty cycle, the limit is 80% and the value of D.C. is 1.00 - 0.8 = 0.2. Hence,

$$e_{s_{peak}} = \frac{6.15(e_{n_{rms}})}{2(2)}$$

$$\text{and } S/N = 20 \log \left[\frac{e_{s_{peak}}}{e_{n_{rms}}} \right]$$

$$S/N = 23.7 \text{ dB}$$

for the general case and a 1×10^{-9} BER requirement,

$$S/N = 20 \log \left[\frac{6.15}{2(D.C.)} \right] = 20 \log \left[\frac{(6.15)(.5)}{(D.C.)} \right]$$

$$S/N = 15.8 \text{ dB} + 20 \log \left(\frac{.5}{D.C.} \right) \quad (12)$$

where D.C. is always ≤ 0.5 .

The added benefit of differential drive is the common mode rejection of extraneous signals being radiated or conducted into the amplitude detector inputs.

The idle channel pattern is not always a continuation of constant amplitude transitions. In some cases it is a continuous logic state and in such cases idle channel noise can be rejected by hysteresis in the amplitude detector. Such is the case in Figure 16(c). In this case the data stream is compared to a threshold which is different for a logic one output than it is for a logic zero output. This threshold is not generated by inverting the data stream. It is generated by feeding back a portion of the output data signal to the non-inverting input of the amplitude detector. Since the threshold is not a linear function of the input data stream, there is no noise riding on it. The difference in threshold voltage for the two states is called the hysteresis. The hysteresis must be wide enough to reject all noise spikes of amplitudes which occur more often than once in 10^9 when no data is present. That is to maintain a BER of 1×10^{-9} ,

$$H \geq 2 e_{s_{peak}} \text{ or } 2 (6.15 e_{n_{rms}})$$

Once this condition is satisfied a detection will occur every time the peak signal plus noise exceeds one-half the hysteresis. However, if this is all that is required, there will be much greater edge ambiguity or jitter in this system than in the previous ones because of the increased proximity between the noise and the amplitude detector threshold. Therefore, in order for this edge jitter to be no worse than before, the peak signal must exceed the threshold by the same amount as it did before or,

$$\begin{aligned} e_{speak} &= \frac{1}{2} H + e_{npeak} \\ e_{speak} &= 6.15e_{nrms} + 6.15e_{nrms} \\ e_{speak} &= 12.3e_{nrms} \end{aligned}$$

In other words, imposing the condition of idle channel noise rejection has caused a degradation in system sensitivity for the same BER performance. The signal-to-noise ratio required for this idle channel noise rejection is,

$$S/N = 20 \log \left(\frac{e_{speak}}{e_{nrms}} \right) = 20 \log \left(\frac{12.3 e_{nrms}}{e_{nrms}} \right)$$

$$S/N = 21.8 \text{ dB}$$

This system is 6.0 dB less sensitive than those previously discussed. Its benefit is freedom from data format constraints such as the maximum length of a string of ones or zeroes or having to present an appropriate idle channel pattern for noise rejection.

The effect of edge coupling or differentiation rather than ac coupling can be examined by referring to Figure 16(d). The first thing to be noticed is that the data is compared to the same type of threshold as in the previous case; that is a two state threshold generated by feedback from the amplitude detector output to non-inverting input. The difference between these two thresholds is the hysteresis H . Referring to Figure 16(d), it will be noticed that after the edge or transition is coupled through to the detector, the differentiation network immediately begins to discharge according to its time constant. This forces the amplitude detector input to return to its base line level midway between the two threshold levels during every bit cell. Because of this, the hysteresis H must once again be greater than the peak to peak noise level for the required probability of error regardless of the idle channel condition. Otherwise noise would toggle the detector during almost every bit interval after the network discharge was complete. Since this system should have no more jitter than the others, the signal should exceed threshold by the same amount as before or e_{npeak} . Thus the required signal level at the amplitude detector input is

$$\begin{aligned} e_{speak} &= \frac{H}{2} + e_{npeak} = 6.15e_{nrms} + 6.15e_{nrms} \\ e_{speak} &= 12.3e_{nrms} \end{aligned}$$

Since this is after the differentiation, the effect of the differentiator on the signal to noise ratio must be taken into account in order to compare sensitivities at the same point in the circuit. It has been experimentally determined that the loss of the differentiator is 8.2 dB for the rms noise. When measuring the differentiator's loss to the signal, it must be remembered that the differentiator's peak output transition is the response to the peak to peak input transition. The amplitudes of those two transitions have been compared and it has been determined that the input was 10.4 dB larger than the output. Therefore, the S/N has been degraded by 10.4 dB less 8.2 dB or 2.2 dB. Therefore, the required S/N ratio into the differentiator for a BER of 1×10^{-9} is

$$S/N = 2.2 \text{ dB} + 20 \log \left(\frac{e_{speak}}{e_{nrms}} \right) = 2.2 \text{ dB} + 20 \log (12.3)$$

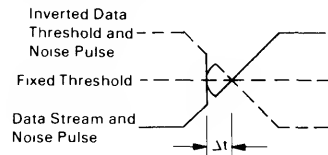
$$S/N = 24.0 \text{ dB}$$

This relatively high signal to noise requirement is 8.2 dB higher than the originally proposed approach of Figure 16(a) but this loss of sensitivity buys the freedom from idle channel noise and simplicity of no base line variation with duty cycle.

Finally, the edge coupled system differentially driven will be examined. Refer to Figure 16(e). Once again as in the case described in Figure 16(b), the threshold for this differentially driven edge coupled case is generated by inverting the incoming data stream plus noise. However, unique to this case, is the fact that there is hysteresis in the threshold as well. This hysteresis limits the levels to which the threshold can decay after the inverted data edges couple through the differentiator network. This hysteresis, H , is the difference between the two threshold levels, VT_1 and VT_2 . These levels can be seen clearly in Figure 16(e) only if the data edges are separated in time long enough to allow the RC differentiators to discharge completely. The noise on these threshold levels can also be noticed. Assuming the data base line is centered between VT_1 and VT_2 , the hysteresis must be

$$H = 2(e_{npeak} + e_{npeak}) = 4e_{npeak}$$

to insure that noise doesn't toggle the output. As can be seen from the inset below, a noise pulse riding on the data stream will cause the same ambiguity in zero crossing (i.e. Δt) whether the threshold is fixed or is inverted data plus noise.



In order to keep edge jitter the same in this system as it was in previous systems then, the peak signal must exceed threshold by the same amount or e_{npeak} . Therefore referring to Figure 16(e) the peak signal required is

$$e_{speak} = V_{TS} + e_{npeak}$$

where V_{TS} is the threshold at the time of switching.

However, the threshold doesn't remain at VT_1 but starts moving in opposite phase with the data edge with the same rise time as the data edge. Because of this, the data edge and threshold edge will cross each other and thereby cause an output transition when they have traversed equal voltage increments. Since the data stream baseline is assumed to be centered between VT_1 and VT_2 , this crossover will occur halfway between VT_1 and the baseline and so the actual threshold voltage level will be VT_1 or $1/2 H$ less $1/4 H$ (H). That is

$$\begin{aligned}
 V_{TS} &= (\frac{1}{2}H - \frac{1}{4}H) = \frac{1}{4}H \\
 \text{therefore } e_{speak} &= \frac{1}{4}H + e_{npeak} \\
 e_{speak} &= e_{npeak} + e_{npeak} \\
 e_{speak} &= 2e_{npeak}
 \end{aligned}$$

and for a BER = 1×10^{-9}

$$S/N = 20 \log \left(\frac{e_{speak}}{e_{nrm}} \right) = 20 \log \left(\frac{6.15 e_{nrm}}{e_{nrm}} \right)$$

$$S/N = 21.8 \text{ dB}$$

Once again this is out of the differentiator and to translate it to the differentiator input an additional degradation in S/N of 2.2 dB must be taken into account. Therefore for the differentially driven edge coupled detector the S/N ratio required for a 1×10^{-9} BER is

$$S/N = 21.8 \text{ dB} + 2.2 \text{ dB}$$

$$S/N = 24.0 \text{ dB}$$

Table I below summarizes the pros and cons of these amplitude detector approaches.

It can be seen looking at Table I that the differentially driven edge coupled detector accommodates the most variation in data format and idle channel signalling. In addition it provides common mode rejection of extraneous signals thereby providing better performance under full duplex conditions. For these reasons it was chosen as the detector for this receiver which needed such flexibility. The price for this versatility is about 8.2 dB in S/N sensitivity. Certainly this is not insignificant and if the data format and idle channel signalling in a particular application permitted, the system designer would do well to consider the ac coupled approaches.

One practical factor not considered here is that the amplitude detector device itself will have input offset

specifications which vary from unit to unit. This means that in all of the amplitude detectors described, a certain amount of additional signal will be required to insure that threshold is always crossed regardless of the offset for a particular unit. For the device used here, the MC75107, a potential difference of 25 mV or greater between inputs must exist to guarantee states. This directly affects the required hysteresis. The two amplitude detector inputs which are separated by H/2 volts must now be separated by $2e_{npeak} + 25 \text{ mV}$ rather than by $2e_{npeak}$ in the previous comparison. Similarly, the peak signal must now exceed the reference level, V_T , by $2e_{npeak} + 25 \text{ mV}$.

That is: $e_{speak} = V_T + (2e_{npeak} + 25 \text{ mV})$

and $V_T = \frac{1}{2}H - e_{speak}$

Therefore $e_{speak} = 2e_{npeak} + 25 \text{ mV}$

for a BER of 1×10^{-9}

$$e_{speak} = 12.3e_{nrm} + 25 \text{ mV}$$

The value of e_{nrm} was experimentally determined to be 2.4 mV rms. Since 25 mV is 10.4 times the 2.4 mV rms measured at the detector input,

$$e_{speak} = 12.3e_{nrm} + 10.4e_{nrm}$$

$$e_{speak} = 22.7e_{nrm}$$

$$20 \log \left(\frac{e_{speak}}{e_{nrm}} \right) = 27.1 \text{ dB}$$

Taking into account the 2.2 dB degradation in S/N due to the differentiator, the required S/N is

$$S/N = 27.1 \text{ dB} + 2.2 \text{ dB}$$

$$S/N = 29.3 \text{ dB}$$

to accommodate all MC75107 detector chips. This point is also plotted on Figure 15.

The remaining function in the block diagram of

TABLE I

| DETECTOR APPROACH | S/N SENSITIVITY FOR 1×10^{-9} BER | ADVANTAGES | DISADVANTAGES |
|---|--|--|---|
| Single Ended ac Coupled. No hysteresis | 15.8 dB | Maximum sensitivity. | Requires continuous idle channel pattern and duty cycle limits to reject noise as well as a reference voltage that tracks data base line. No common mode rejection. |
| Differential ac Coupled | * 15.8 dB + $20 \log \left(\frac{0.5}{D.C.} \right)$ | No base line tracking required. Common mode rejection. | Requires continuous idle channel pattern and duty cycle limits to reject noise. Sacrifice in sensitivity dependent on duty cycle limits. |
| Single Ended ac Coupled with hysteresis | 21.8 dB | Doesn't require continuous idle pattern and duty cycle limits for noise rejection. | Sacrifices 6 dB in sensitivity. Requires threshold which tracks data stream base line. No common mode rejection. |
| Single Ended Edge Coupled with hysteresis | 24.0 dB | Doesn't require idle channel pattern or duty cycle limits to reject noise. Doesn't require tracking reference voltage. | Sacrifices 8.2 dB in sensitivity. No common mode rejection. |
| Differential Edge Coupled with hysteresis | 24.0 dB | Doesn't require idle channel pattern or duty cycle limits. Doesn't require tracking reference voltage. Offers common mode rejection. | Sacrifices 8.2 dB in sensitivity. |

*See text for definition of D.C.

Figure 10 is the **logic interface**. Its purpose is to generate a standard logic level and provide sufficient drive capability for simple interfacing. The TTL logic level in this receiver is actually generated by the amplitude detector. However, in order to buffer the amplitude detector's output, another line receiver section is used for isolation and the interface to the TTL world. In addition, an emitter follower provides the needed drive for a $75\ \Omega$ coaxial line to the external test equipment.

Receiver Schematic Diagram and Circuit Implementation

Figure 17 shows the receiver schematic and indicates which portions perform each of the functions outlined in the functional block diagram description.

The first active component in the receiver schematic is the MFOD402F integrated detector preamp (IDP). It performs both the **optical detector** and **current to voltage converter** functions described earlier. It also affords all the isolation advantages of the integrated structure that were outlined in a previous section. Its transfer function is typically 1.0 mV of output amplitude per μW of optical input power. Output impedance is specified as $200\ \Omega$ typical and although its maximum real and reactive loads are also specified, it was found that these loads caused excessive ringing of the IDP output. There-

fore, in this circuit, the real load was kept above $500\ \Omega$ and the capacitive load was minimized by careful printed circuit layout. The output rise time of the MFOD402F is specified as typically 20 ns and that is about what appears at the output of the linear amplifier where the signal is sufficiently large in amplitude to measure. The supply voltage of $+15\text{ V}$ was chosen so that operation on the flat portion of the IDP's ΔR curve was guaranteed. Below 10 V , ΔV_{CC}

the IDP's rise time begins to degrade rapidly.

The shield over the optical connector and IDP is required for isolation from the receiver's own TTL output and the crosstalk of the transmitter. Its contribution to performance may only be measurable in terms of improved bit error rate.

The noise out of the IDP is specified as $300\ \mu\text{V}$ rms typical, and is a good number to use in calculating the amplitude detector hysteresis required.

Linear Amplifier

The MC1733 was chosen as the linear amplifier primarily because of its wide gain bandwidth and its reasonably low noise. It was used at a gain of 100 because that provides sufficient gain to amplify the IDP noise up to minimum amplitude detector threshold, as will be seen later, and it also allows the simple strapping of Pins 3 and 12 together using a

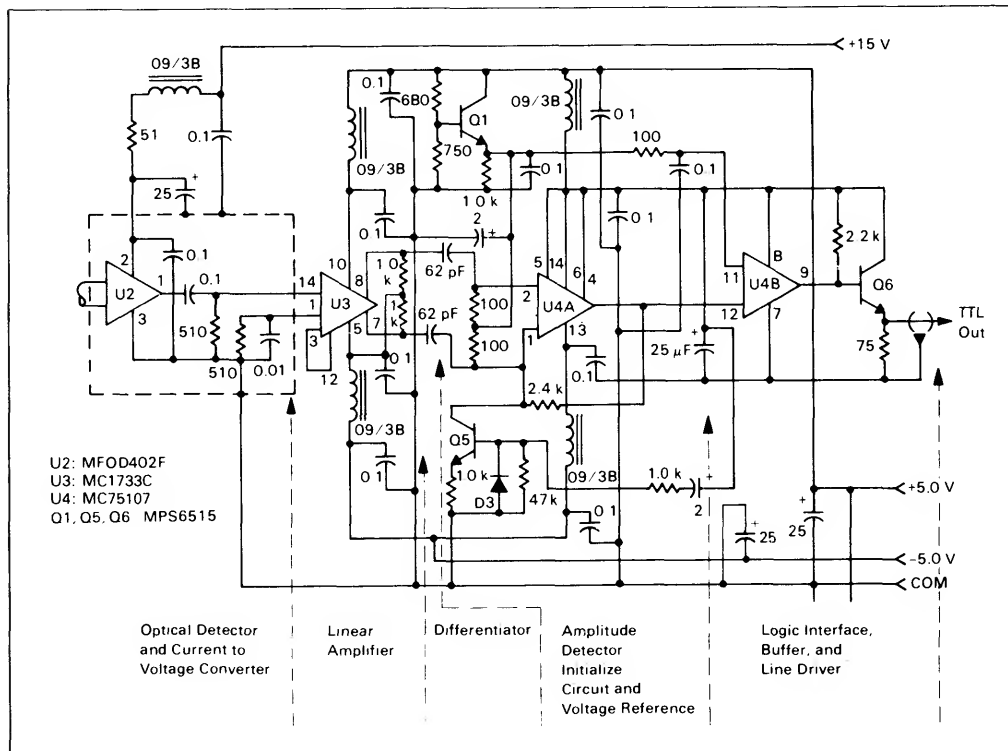


FIGURE 17 — Receiver Schematic

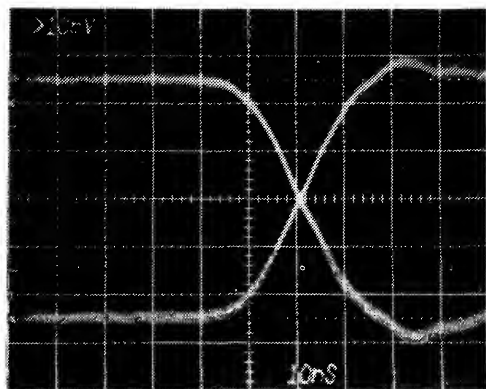
foil runner beneath the chip itself. This proved simpler than bringing Pins 4 and 11 out around the chip and tying them together with an external gain setting resistor. Pins 4 and 11 are the emitters of the input differential amplifier and proved very susceptible to the injection of noise and positive feedback from the TTL output.

Output Pins 7 and 8 provide the data stream waveforms which are the vital signs of the system. They provide information about the system signal to noise ratio, the system rise and fall time, and an indication of received signal level. See Figure 18. With the MC1733 strapped for a differential gain of 100, each output will deliver a single ended signal 50 times larger than the IDP output.

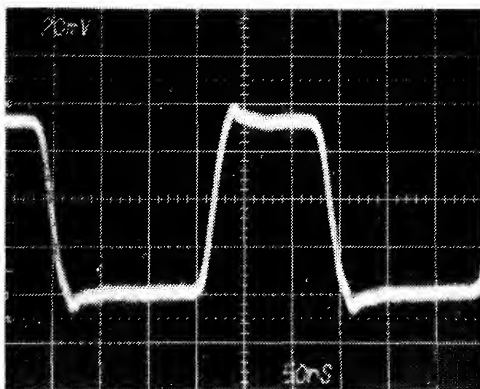
With this gain strapping on the MC1733, the rise time out of this amplifier is typically 10 ns when driven from a fast pulse generator. The input bias resistors were chosen to be as low as the IDP could drive so as to enhance gain stability of the MC1733.

The differentiators consist of the 62 pF capacitors and the 100 Ω resistors for the amplitude detector's input bias. Since the output of the MC1733 is taken differentially, there are two such networks required. The impedance of these networks was made low so as to minimize the voltage step at the detector input pins caused by the drop across the 100 Ω resistors. This step results from the change in base current of the amplitude detector between the ON and OFF states. Specified as a total worst case base current change of 80 μ A, the 100 Ω differentiator will cause an 8.0 mV step at Pin 2 of the amplitude detector and a subtracting of 8.0 mV from the hysteresis at Pin 1 of the amplitude detector. Another reason to keep the differentiator impedance low is to prevent instrument loading. A 10X scope probe, for example, will load a 1000 Ω differentiator enough so as to make time constant measurements meaningless and waveform analysis unreliable.

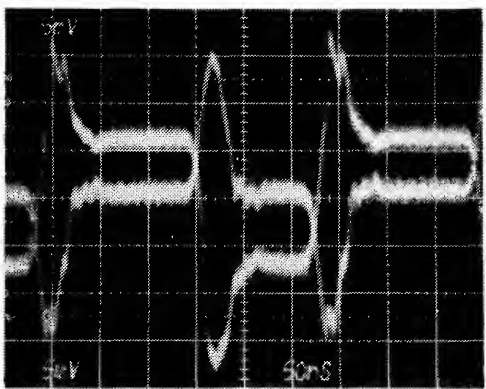
As mentioned earlier, in equation (8), the differenti-



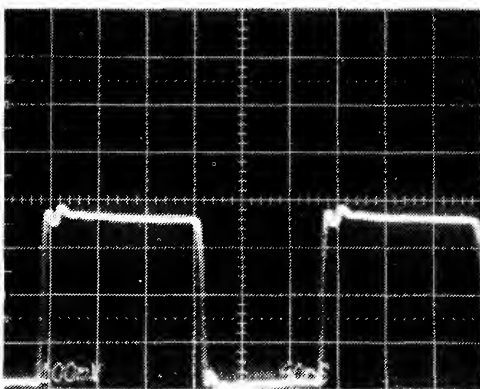
(a)
System Rise and Fall Time at Pin 8 of MC1733



(b)
System S/N at Pin 8 of MC1733 for a BER of $<1 \times 10^{-9}$



(c)
Typical Waveforms at Amplitude Detector Inputs
Pins 1 and 2 of MC75107



(d)
Amplitude Detector Output

FIGURE 18 — Receiver Waveforms

ator time constant is controlled by the minimum bit time and the system rise time. From equation (8)

$$4R_L C_{\max} = T - t_{R_{SYS}}$$

where T is the minimum bit time and $t_{R_{SYS}}$ is the system rise time. Assuming for now that the system rise time, which is measured at the MC1733 output is 30 ns worst case, the maximum RC time constant consistent with a 20 Mbaud bit cell is

$$R_L C_{\max} = \frac{T - t_{R_{SYS}}}{4} = \frac{50 \text{ ns} - 30 \text{ ns}}{4}$$

$$R_L C_{\max} = 5.0 \text{ ns}$$

The values used are 62 pF and 100 Ω giving a time constant of 6.2 ns. This hedging by 1.2 ns means that the required transition height from the MC1733 will have to be slightly higher to be detected for transitions spaced 50 ns apart than they will be if spaced by 55 ns or greater.

The MC75107 line receiver is the **amplitude detector** and Q1 and Q5 perform the voltage reference and initialize functions, respectively. The amplitude detector is basically a high speed comparator with positive feedback to perform a Schmitt Trigger function. Its output swing is 0.1 to 3.6 Vdc, limited by the active pullup. With that output swing the hysteresis is 130 mV. With this output swing, the optimum reference voltage is using equation (9)

$$V_{REF} = \frac{V_{OH} + V_{OL}}{2} = \frac{3.6 \text{ V} + 0.1 \text{ V}}{2}$$

$$V_{REF} = +1.85 \text{ V}$$

As was mentioned previously, the 100 Ω input bias resistors were that low to minimize the voltage step at the amplitude detector inputs when the output changed state. Similarly, to reduce the step in reference voltage when the output switches, the current in the reference transistor, Q1, has been set to 4.0 mA and its base to ground impedance (r_b) has been lowered to about 360 Ω . This makes the voltage reference output impedance approximately

$$R_O = r_e + \frac{r_b}{H_{FE}} \quad \text{or} \quad \frac{26 \Omega \cdot \text{mA}}{4.0 \text{ mA}} + \frac{360 \Omega}{150}$$

$$R_O = 8.9 \Omega$$

To evaluate the step change in reference voltage when the data output changes states, the amount of current that the voltage reference, Q1, must source and sink must first be found.

$$I_{SOURCE} = \frac{V_{REF} - V_{OL}}{R_H} = \frac{1.85 - 0.1}{2.5 \text{ k}} = 0.7 \text{ mA}$$

where R_H is the sum of the feedback resistor and bias resistor for the amplitude detector. From Figure 21, $R_H = R_{11} + R_{10} = 2.4 \text{ k} + 100 \Omega = 2.5 \text{ k}$. Similiarly,

$$I_{SINK} = \frac{V_{OH} - V_{REF}}{R_H} = \frac{3.6 - 1.85}{2.5 \text{ k}} = 0.7 \text{ mA}$$

Thus, the total change in reference current between logic states is 1.4 mA. With $R_0 = 8.9 \Omega$, the step in V_{REF} = 12.5 mV. This step is almost completely a common mode signal which is about 0.6% of V_{REF} and thus insignificant. The voltage divider formed by the 2.4 k hysteresis resistor and the 100 Ω bias resistor does introduce a differential signal of 1/25 of this step in reference voltage. Therefore, the differential signal at the amplitude detector input resulting from this 12.5 mV step in V_{REF} is only 0.5 mV. Refer to Figure 18 for typical waveforms at the amplitude detector input and output.

The sensitivity specification on the MC75107 is $\pm 25 \text{ mV}$ over temperature and unit to unit variations. It will be noted from Figure 18(c) that the hysteresis must be large enough so as to keep the voltage difference between the data base line and the threshold always greater than 25 mV, including the noise peaks, except during transitions. When the absolute difference between these two inputs to the MC75107 falls below 25 mV, the output state is not defined and thus errors can be made. Consequently, the hysteresis was empirically set to 130 mV to insure this 25 mV separation between inputs at all points on the waveform. Only when this is accomplished does the BER approach 1×10^{-9} or less as was discussed in the section on amplitude detectors.

The **initializing circuit**, Q5, which does not appear on the simplified block diagram of Figure 10, merely injects a pulse of approximately 250 μs in duration into the amplitude detector during power up to insure that the output always turns on to the low state in the absense of optical transitions. By pulling down on the positive input of the amplitude detector a logic high at Pin 4 of the MC75107 is inhibited. After the discharge of C16, the leakage current and depletion capacity of the Q5 collector base junction are inconsequential to the performance of the circuit.

The **logic interface, buffer, and line driver** have been implemented using the other section of the MC75107 and Q6. The MC75107 section regenerates the TTL level already at Pin 4 but isolates the positive feedback from the external loading conditions. Q6 provides the additional drive required to the 75 Ω cable used in the test set up. At 20 Mbaud, the shielding of this lead is essential. Since the error detector used provided a 75 Ω coaxial interface, RG-59 cable was selected.

Receiver Performance

Figure 18, once again, shows the typical waveforms one should expect at key points in the receiver, as well as system rise time and the S/N ratio required for good BER performance.

Figure 15, Curve B, shows the typical BER versus S/N at the differentiator input. Curve B represents performance that can be expected when amplitude detector input offsets and transmitter crosstalk are accounted for. Figure 19 relates S/N to optical input power for this 20 Mbaud receiver. This curve was generated by measuring S/N and then calculating backwards from the measured signal level out of the MC1733 amplifier through the receiver gain of 50 mV/ μW .

The dynamic range of the receiver is precisely defined as the ratio of the amplitude of the maximum usable signal detected to the amplitude of the

minimum usable signal detected. There the precision ends, however, because what is usable in one application is not in another. The minimum usable signal can be picked off of the curve in Figure 19 for whatever S/N is required to achieve the desired BER. The maximum usable signal is where distortion gets to be prohibitive. Duty cycle distortion versus output level of the MC1733 is plotted in Figure 20.

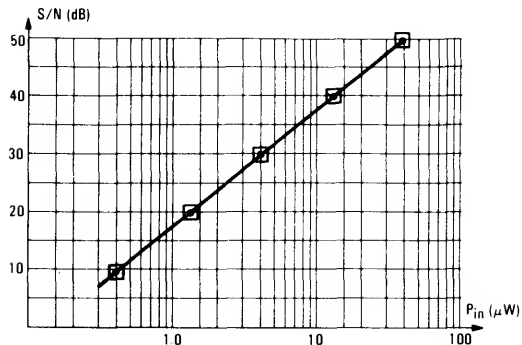


FIGURE 19 — Signal-to-Noise versus Optical Input Power

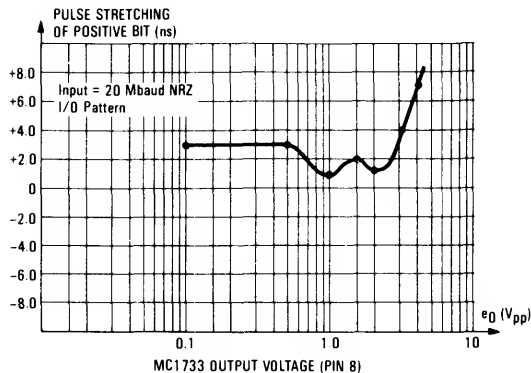


FIGURE 20 — Receiver Overload Characteristic

This curve was measured by simulating high level optical inputs with a pulse generator in place of the IDP and having equivalent output impedance and transition times. The distortion occurs in the MC1733 output before the IDP overloads and thus this is a valid test. The dynamic range can be deduced then by dividing the optical input power needed to cause the intolerable level of distortion, say 5.0 ns, by the optical input power needed to provide the required BER, say 1×10^{-9} , and taking 10 log of the ratio. To find the optical input power that causes overload, refer to Figure 20 and divide the output voltage in mV by 50 mV/μW. To find the optical input power required for a 1×10^{-9} BER, refer to Figure 15, Curve B, and then use that S/N ratio to find optical power required from Figure 19. For this example then, the dynamic range would be

$$\text{Dynamic Range} = 10 \log \left(\frac{70 \mu\text{W}}{4.0 \mu\text{W}} \right)$$

$$\text{Dynamic Range} = 12.4 \text{ dB}$$

Temperature testing indicated that over the 0°C to 70°C temperature range, no significant degradations in performance occurred. Nominal drifts in detector offsets did not cause any significant changes in sensitivity.

BUILDING THE BOARDS

In building the boards, the last components to be inserted should be the optical transducers and mounting bushings. This will reduce their handling and thus the probability of scratching or contaminating the optical ports with particles commonly found in a work bench environment.

To begin building the boards, refer to the parts list and complete schematic (Figure 21), the component overlay (Figure 22) and the photograph of the completed board (Figure 27). It is recommended that the IC sockets mentioned in the part list be used at least on the first pair of boards to allow looking at system performance versus tolerances in device parameters and to allow for the misfortune of damaging an IC during construction. The decoupling chokes should be available from Ferroxcube. When installing them, care should be taken so as to position them so that the turns protruding from the ends of the ferrite are not shorted together. When ordering electrolytic capacitors to fit the board layout, the approximate dimensions on the parts list should be used as a guide. Where there is ground foil on the component side of the board, care must be used when inserting all components so that no leads are shorted to ground.

It will be noted in the schematic of Figure 21 and in the parts list, that a shield can be specified for shielding the receiver optical transducer. This is to prevent the sensitive receiver input from picking up energy radiating from the receivers TTL output as well as from the transmitter circuitry. The can part number listed must be notched out to fit over the AMP mounting bushing and then sweat soldered down to the ground foil pattern on the component side of the board. Refer to Figure 24 for details of shield preparation. Without the shield, there will probably be more ringing in the waveform at the detector input and the bit error rate will be significantly degraded. To accommodate this shield, capacitor C4 may have to be installed on the solder side of the board depending on the vintage of the actual board used. Before any components are installed, it is recommended that the holes for the BNC connectors first be enlarged to a 0.375 inch diameter and the holes for the +5.0 V, -5.0 V, and ground wires be enlarged to about a 0.070 inch diameter in order to accommodate #18 AWG stranded wire.

After all other components are mounted to the PCB, and before the receiver shield is put on, the FOAC's and their bushings must be assembled.

It will be noted that the FOAC, shown in Figure 23(a), has a flat spot on the circumference of the ferrule and this flat spot affords it a stable position on the PC board. Therefore, when assembling the FOAC and bushing, refer to Figure 23(b), the FOAC is first inserted into the connector so that the flat spot is facing down toward the PC board. Large coupling losses will be encountered if the FOAC is

not seated properly in the bushing. To eliminate the uncertainty of whether or not these parts are seated properly, the distance between the back of the FOAC and plane "A" of the bushing, shown in Figure 23(b), can be measured. It should be no greater than 0.130

inches. The plastic retention plate puts sufficient tension on the FOAC's so as to maintain proper seating.

Once the FOAC is properly seated, its leads can be formed to fit the foot print on the PC board. The

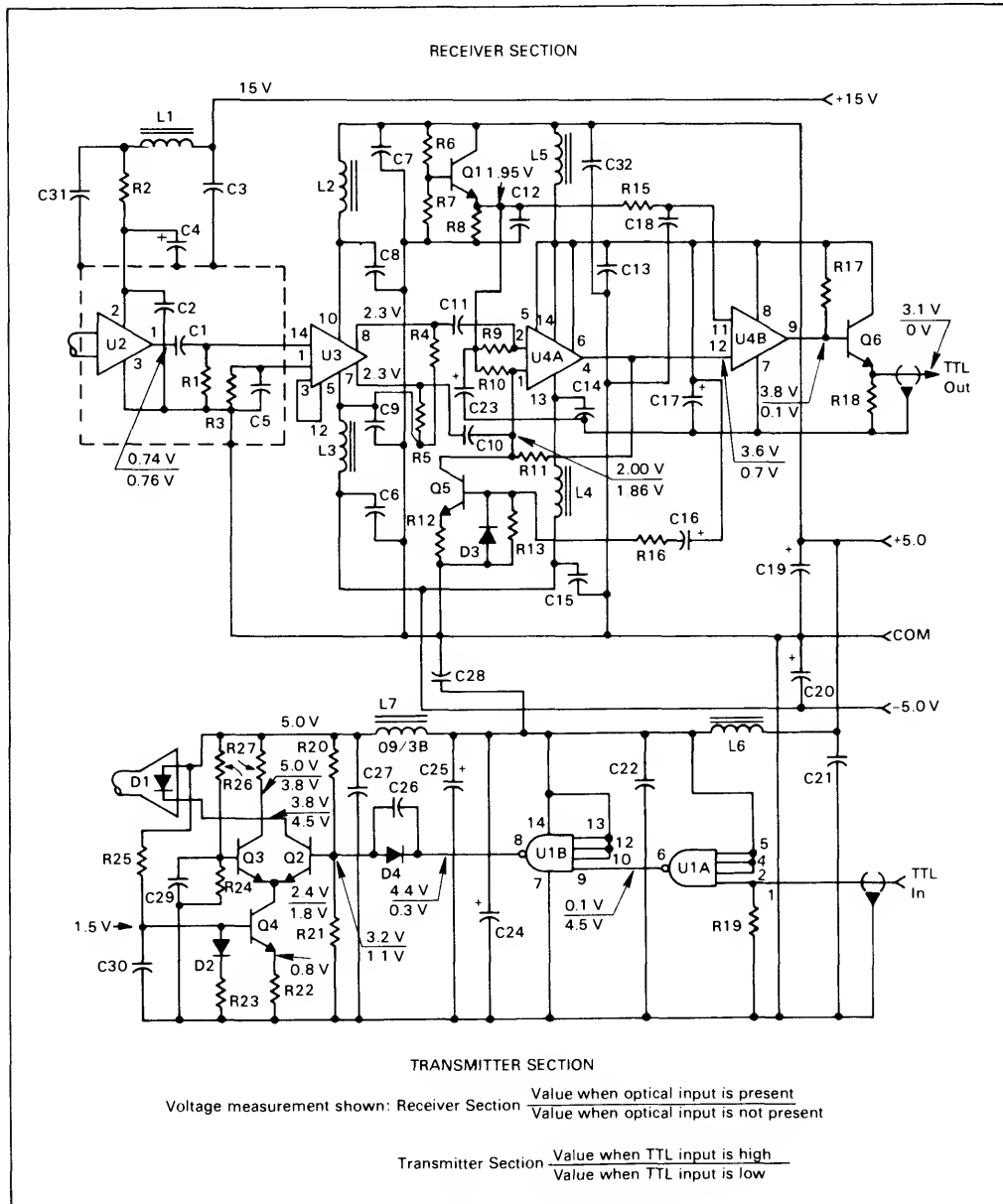


FIGURE 21 — Complete Transceiver Schematic

PARTS LIST

| Reference Symbol | Description |
|--|---|
| Capacitors | |
| C1, C2, C3, C6, C7, C8, C9, C12, C13, C14, C15, C18, C21, C22, C27, C28, C29, C30, C31, C32 | 0.1 μ F — ≥ 50 V Ceramic Capacitors, 0.250" lead spacing, Mallory C25C104M101CA |
| C5 | 0.01 μ F — 50 V Disk Ceramic Capacitors, 0.250" lead spacing, 290" OD, Sprague UK50-103 |
| C10, C11 | 62 pF 5% Dipped Mica Capacitor |
| C16, C23 | 2.0 μ F, 25 W Vdc — 0.250" OD \times 9/16" long, Sprague TE-1201 |
| C4, C17, C19, C20, C24, C25 | 25 μ F, 25 W Vdc, 0.25" OD \times 0.625", Mallory TT25X25B |
| C26 | 100 pF 5% Dipped Mica Capacitor |
| Diodes | |
| D1 | MFOE103F, Infrared LED |
| D2, D3, D4 | 1N914, High-Speed Switching Diode |
| Chokes | |
| L1, L2, L3, L4, L5, L6, L7 | Ferroxcube VK200-09/3B |
| Transistors | |
| Q1, Q2, Q3, Q5, Q6 Q4 | MPS6515 General-Purpose High-Gain NPN Transistor 2N4400, Low V_{CE} (sat) Switching Transistor |
| Resistors (1/4 W, 5%, Carbon composition) | |
| R1, R3 | 510 Ω |
| R2 | 51 Ω |
| R4, R5, R8, R12, R16 | 1 k Ω |
| R6 | 680 Ω |
| R7 | 750 Ω |
| R9, R10 | 100 Ω |
| R11 | 2.4 k Ω |
| R13 | 47 k Ω |
| R17 | 2.2 k Ω |
| R15 | 100 Ω |
| R18, R19 | 75 Ω |
| R20, R25 | 180 Ω |
| R21 | 330 Ω |
| R22 | 8.2 Ω |
| R23 | 39 Ω |
| R24 | 270 Ω |
| R26 | 240 Ω |
| R27 | 12 Ω |
| Integrated Circuits | |
| U1 | SN74LS40B, Dual 4-Input Buffered NAND Gate |
| U2 | MFOD402F, Integrated Photodetector Preamp |
| U3 | MC1733, Wide Band Linear Video Amp |
| U4 | MC75107, Dual TTL Line Receiver |
| Non-Referenced Items | |
| 3 | Low Profile IC Sockets, AMP #530177-1 |
| 1 | Shield Can, Hudson Tool & Die Co., #HU5655, 0.734" long, steel |
| 2 | BNC Bulkhead Connectors, UG1094/U Female |
| 2 | Active Device Mounting Kits, AMP Part #227240-1 |

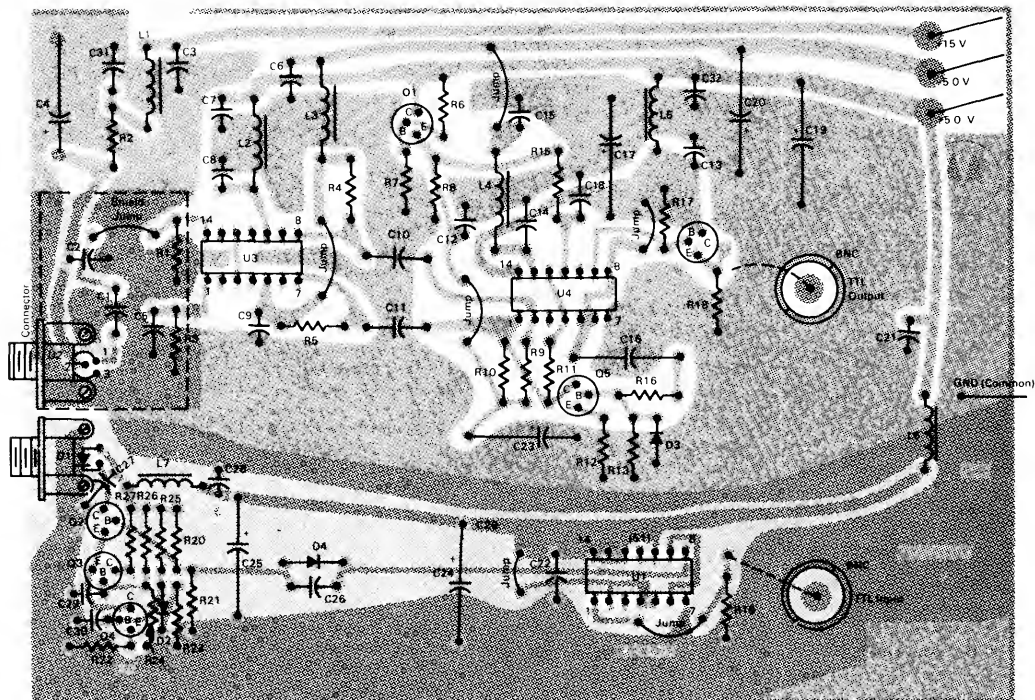


FIGURE 22 — PCB Component Overlay

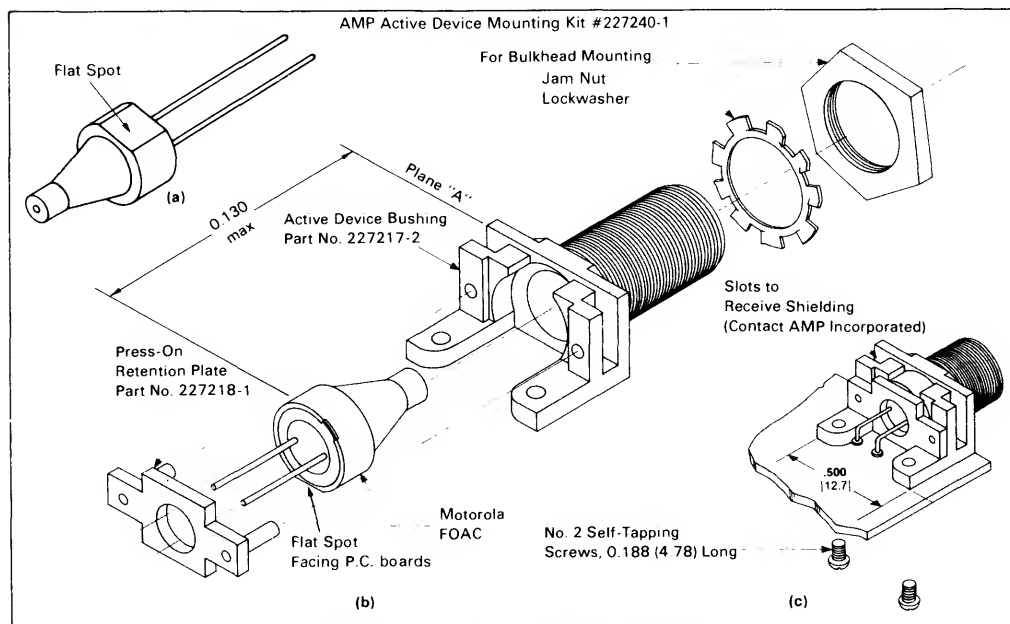


FIGURE 23 — Assembly of the FOAC and Connector

bushing is then fastened down to the PC board using the two self-tapping screws included with it, and the leads appropriately soldered. See Figure 23(c).

The bushing, retention plate, self-tapping screws, lockwasher, and jam nut are available as kit #227240-1 from AMP, Inc. Additional FOAC's i.e., the MFOE103F and MFOD402F, are available through Motorola distributors.

Once the MFOD402F is mounted in its bushing and the assembly is mounted on the PC board, the shield can be mounted over the receiver front end. The cover specified in the parts list must be notched as shown in Figure 24 in order to fit over the AMP bushing. Once it is notched it can be sweat soldered at the corners to the component side ground foil provided for this purpose.

If more printed circuit boards are required, it should be kept in mind that the PC layout with its bus ground structure and component side shielding is an integral part of the circuit. Any deviation from this layout can be expected to cause changes in isolation between the receiver TTL output and the receiver input as well as between the transmitter and receiver. Figure 30 shows the full size artwork which can be used to make a photomaster in order to duplicate the boards.

The artwork shown is positive with the emulsion side down so that a photo negative of this should provide the proper photomaster. Alignment of the two photomasters can be achieved by drilling through the photomasters and the board at the hole locations for the optical connector mounting screws and the +5.0 V and the -5.0 V power connection pads.

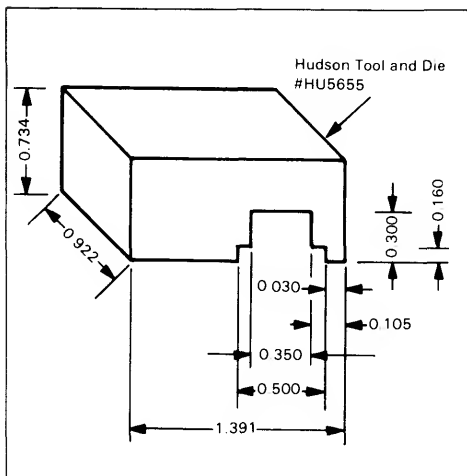


FIGURE 24 — Shield Preparation

TESTING THE BOARDS

To test the completed boards to their full capability, the following equipment is required:

1. One known-good 1 meter fiber of $200 \mu\text{m}$ core (See Figure 28 for suggested types).
2. Tektronix 475 oscilloscope or equivalent with two 10X, 7.0 pF probes.

3. Two compliments of power supplies each consisting of:

- 1-HP 6205 dual power supply, or equivalent, for ± 5.0 V
- 1-HP 6218A power supply, or equivalent, for $+15$ V
4. One Tektronix 6042 DC to 50 MHz current probe, or equivalent
5. One HP 3780A Pattern Generator/Error Detector, or equivalent
6. One E.H. Research Labs Model 139 Pulse Generator, or equivalent
7. One Wavetek Model 142 Function Generator, or equivalent
8. Assorted RG-59 coaxial cables, 1-4 ft. long, and two 75Ω BNC terminations
9. DC Multimeter General Purpose type $100 \text{k}\Omega/\text{volt}$ or greater

10. Two system fibers (see section on System Performance)

11. One Photodyne Model 22 XL Optical Power meter, or equivalent

If the two boards in the kit are built correctly, and connected as shown in Figure 25, with appropriate lengths of the system fiber chosen, then a 1×10^{-9} BER or better should be measurable in both directions.

It must be kept in mind that this receiver is sensitive to electrical signal variations at the interface to the electro-optic transducer, regardless of their source. Because of this, the unshielded receiver is sensitive to EMI.

Before any attempt at measuring system performance is made, each module should be given a cursory check by comparing dc voltage levels to those typical dc voltages shown on the schematic in Figure 21.

CAUTION

An inadvertent short from the LED cathode or Q2 collector to ground will place a momentary 5.0 V of forward bias across the LED and DESTROY IT. Care should be taken in probing this portion of the circuit. Probing the collector of Q3 rather than Q2 will provide an indication of proper switching without the danger of shorting the LED.

If meaningful BER measurements are to be made, either a shielded enclosure for the receiver or a shielded environment such as a screen room will be required. The latter enables lower bit error rates to be measured because it allows the pattern generator/error detector which is also sensitive to EMI and line transients to be shielded as well.

If the above BER performance is not achieved, then some troubleshooting must be done. Each module should be first checked out individually by looping a transmitter back to its own receiver with the known-good 1 meter fiber. The testing sequence listed below can be used.

TROUBLE SHOOTING TEST SEQUENCE

1. Test Module A in loop mode with 1 meter fiber. If data output is good proceed to Step 2. If bad, follow module troubleshooting tree to locate problem and retest.
2. Test Module B in loop mode with 1 meter fiber. If data output is good, proceed to Step 3. If bad, follow module troubleshooting tree to locate problem and then retest.

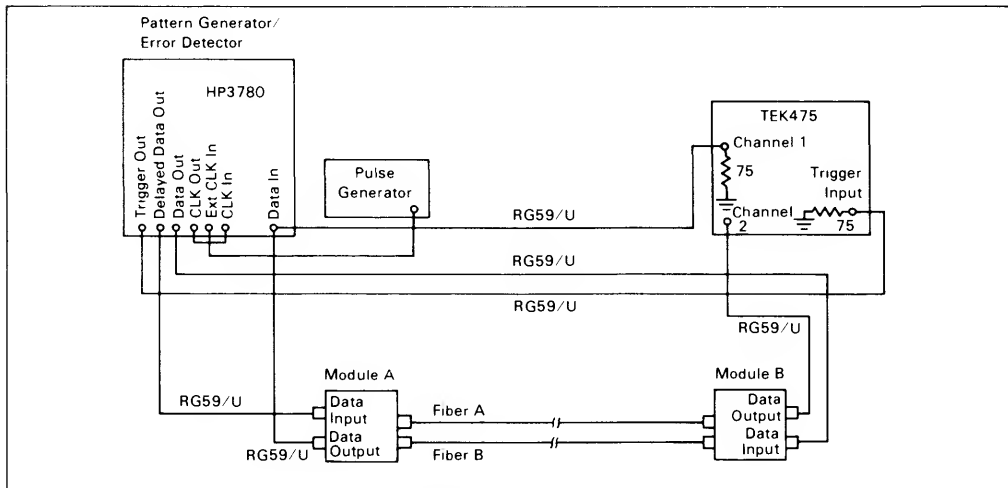


FIGURE 25 — BER Test Setup

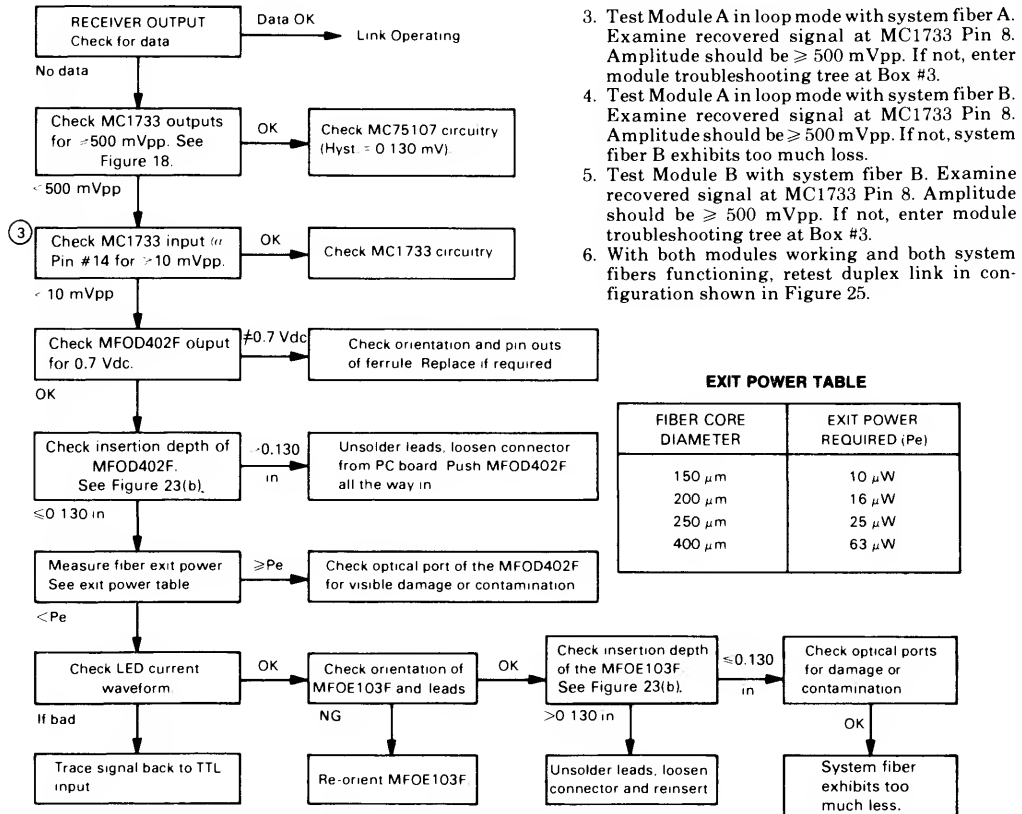


FIGURE 26 — Module Troubleshooting Tree

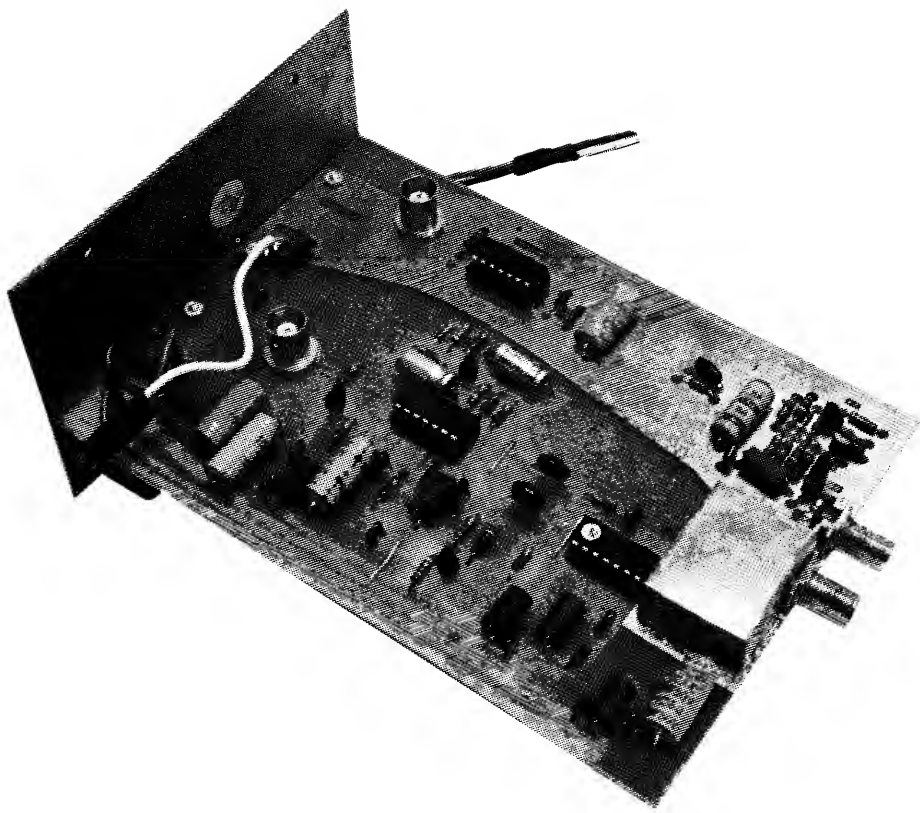


FIGURE 27 — The Completed Transceiver

SYSTEM PERFORMANCE

Before system performance is calculated, the elements of system loss will be reviewed. (Refer to Figure 28.)

L_{CM} is clad mode loss which reflects the portion of the LED's measured output that exits from the clad of the FOAC and is essentially unusable.

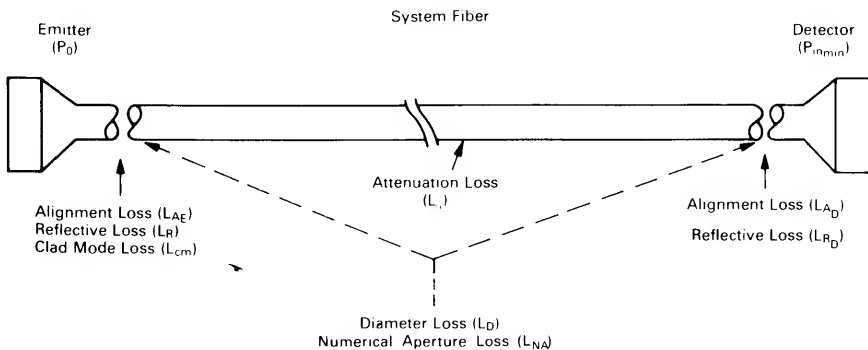


FIGURE 28 — Components of Loss Budget

L_D is the diameter loss which is the portion of light lost when the system fiber has a different core diameter than the $200 \mu\text{m}$ core of the FOAC.

L_{AE} and L_{AD} are the alignment losses at the emitter and detector respectively due to mechanical tolerances of the connector and ferrule.

L_R is the reflective loss at the interface between two fiber ends.

L_{NA} is the NA loss incurred when the system fiber NA, which is a function of fiber length, is different from the NA of the FOAC.

L_a is the signal attenuation loss due to the attenuation of the fiber per unit length.

These loss components will be evaluated in a sample calculation using MaxLight MSC200B fiber.

First, the clad mode loss has been measured experimentally. For very short systems using $200 \mu\text{m}$ core fibers or systems having fiber core diameters of $250 \mu\text{m}$ or more, the clad mode loss would be ignored since light exiting the clad of the FOAC would be usable. In most systems, however, this is not the case. Therefore, the power out of the LED must be reduced by 5% which is the amount of the FOAC output that exits from the clad. Therefore, the clad mode loss is given by:

$$L_{CM} = 10 \log \left(\frac{P_{core}}{P_{total}} \right) = 10 \log \left(\frac{(0.95 P_{total})}{P_{total}} \right)$$

$$L_{CM} = 0.2 \text{ dB}$$

L_D , or diameter loss, is proportional to the relative cross sectional areas of the system fiber core and the FOAC core. If the system fiber is of a smaller core diameter than the FOAC, the diameter loss will be incurred at the emitter/fiber interface. If the system fiber is of a larger core diameter than the FOAC, the diameter loss will be incurred at the fiber/detector interface. The loss across this type of diameter step is given by:

$$L_D = 10 \log \left(\frac{\text{larger diameter}}{\text{smaller diameter}} \right)^2$$

for MSC200B fiber,

$$L_D = 10 \log \left(\frac{200 \mu\text{m}}{200 \mu\text{m}} \right)^2$$

$$L_D = 0.0 \text{ dB}$$

L_A , or alignment loss, is incurred at each interconnect whether that is between two fibers, a fiber and a FOAC, or two FOAC's. It is due to finite tolerances in the mechanical dimensions of the mounting bushing, the ferrule, and the FOAC. These tolerances allow some axial and angular misalignment as well as some longitudinal tip to tip separation between the fiber and the FOAC. Measurements indicate that this loss component is typically 2 dB at the emitter/fiber interface and 1 dB at the detector/fiber interface. The reason it is less at the receive end is that the cone of light exiting the fiber subtends a smaller solid angle than the cone of light exiting the LED FOAC. Therefore, the fiber/detector interface is more tolerant of longitudinal tip to tip separation. Thus, the values of alignment loss are:

$$L_{AE} = 2 \text{ dB}$$

$$L_{AD} = 1 \text{ dB}$$

L_R , the reflective loss, is due to the loss of light incurred by the reflection off of the surface of the fiber core at both the emitter and detector interfaces. These losses amount to about 0.5 dB for each interface. However, where the IDP is used as the photo detector component, its transfer function in mV per μW already includes the reflective loss at its optical port, so that a receiver sensitivity calculation includes this loss. Therefore, with that type of detector the reflective loss need only be accounted for at the emitter interface. With other detectors, namely the PIN photodiode, photo transistor, or photo darlington, reflective loss has to be accounted for at both ends of the system. For this system using the IDP then,

$$L_R = 0.5 \text{ dB}$$

L_{NA} is the loss incurred when light emitted from an LED or fiber subtends a larger solid angle than the acceptance cone of the mating fiber or detector. If the LED source has a numerical aperture (NA) larger than the NA of the system fiber, then the loss will occur at the LED end of the system. If on the other hand the system fiber has an NA larger than the LED and photo detector, then all of the light emitted by the LED will be accepted by the system fiber but the NA loss will occur at the fiber/detector interface.

A complicating facet of NA loss is that fiber NA decreases as fiber length increases and each fiber has a different characteristic. Some fiber manufacturers plot it as a function of length and others specify it only at a kilometer. Some fibers have a slow variation of NA over path length and others apparently vary exponentially. The path length must be known so that the fiber NA can be defined by the fiber manufacturer. Once the NA is defined, the NA loss can be calculated from:

$$L_{NA} = 10 \log \left(\frac{\text{larger NA}}{\text{smaller NA}} \right)^2$$

The NA's used here are the 10% intensity NA's for the FOAC and fiber. The 10% NA's provide much closer correlation to measured results than do the 50% NA's. This formula is based on certain assumptions and provides a good first order approximation to the actual NA loss. In this example, the component of NA loss will be left undefined until later.

Next, L_a , the signal attenuation loss, is merely the product of the cable attenuation factor in dB per unit length and the path length needed. It is expressed by:

$$L_a = (\alpha \text{ in } \frac{\text{dB}}{\text{m}}) \cdot (l \text{ in meters})$$

For MSC200B fiber, the attenuation factor is typically 18 dB/KM.

Finally, the last component of the loss budget is the system gain margin. This is the amount of excess signal desired at the receiver input. Some amount of signal above sensitivity level should be supplied to the receiver to insure that the system still performs well through out the LED aging and expected variations in ambient conditions. For this example a gain margin of 3 dB will be assumed. That is:

$$GM = 3 \text{ dB}$$

The sum of all of these loss components is the system loss budget. That is:

$$\text{Loss Budget} = L_B = L_{CM} + L_D + L_{AE} + L_{AD} + L_{RE} + L_{RD} + L_{NA} + L_\alpha + GM$$

For MSC200B fiber then:

$$L_B = 0.2 \text{ dB} + 0 \text{ dB} + 2 \text{ dB} + 1 \text{ dB} + 0.5 \text{ dB} + 0 \text{ dB} + L_{NA} + L_\alpha + 3 \text{ dB}$$

$$L_B = 6.7 \text{ dB} + L_{NA} + L_\alpha$$

This loss budget must now be compared to the difference in power levels between the transmitter output power and the receiver minimum input power. This difference in power levels is called system gain. If the loss budget exceeds this system gain then there is no excess system gain and the desired performance cannot be obtained. Either a shorter path length must be used or less Gain Margin must be specified or the transmitter output power or receiver input sensitivity must be increased. If, on the other hand, the loss budget doesn't exceed the system gain, then there will be excess system gain and the desired performance will be obtained.

The output power of the transmitter described here can be taken from the MFOE103F data sheet. At 100 mA, the typical output power is 125 μW . Referenced to 1 mW, this is -9.0 dBm. The receiver input sensitivity is defined by the measure of BER performance required. From Figure 15, curve B, a S/N ratio of about 30 dB is required for a BER of 1×10^{-9} . From Figure 19, a S/N ratio of 30 dB requires an optical input power of 4 μW . Referenced to 1 mW, this is -24.0 dBm. Therefore, the system gain is:

$$G_{sys} = P_o - P_{in,min} = 9 \text{ dBm} - (-24 \text{ dBm})$$

$$G_{sys} = 15 \text{ dB}$$

If a specific path length is known, the NA loss and signal attenuation loss can be evaluated. For example, assume 100 feet or 31 meters is the desired path length. From the Maxlight MSC200B data sheet,

at 31 meters, the NA ≈ 0.40 .

$$\text{therefore, from eq. (13)} \quad L_{NA} = 10 \log \left(\frac{0.63}{0.40} \right)^2$$

$$L_{NA} = 3.9 \text{ dB}$$

It will be noted that 0.63 was used for the NA of the FOAC. This is the 10% NA which, as explained earlier, must be used in this formula. What appears on the present MFOE103F data sheet is the 50% NA of 0.48. Use of this 50% NA will give erroneous results for the NA loss. Now that L_{NA} has been evaluated, L_α can be determined.

$$L_\alpha = (18 \text{ dB/kM}) \cdot (0.031 \text{ kM})$$

$$L_\alpha = 0.6 \text{ dB}$$

Now the loss budget for this fiber is found using equation (14).

$$L_B = 6.7 \text{ dB} + 3.9 \text{ dB} + 0.6 \text{ dB}$$

$$L_B = 11.2 \text{ dB}$$

Now the excess system gain can be found. It is given by:

$$\Delta G_{sys} = G_{sys} - L_B.$$

For this 31 meter system,

$$\Delta G_{sys} = 15 \text{ dB} - 11.2 \text{ dB}$$

$$\Delta G_{sys} = 3.8 \text{ dB}$$

Since ΔG_{sys} is a positive number, the system will perform better than expected. If ΔG_{sys} were zero, the system would perform as expected with typical connectors and components. If ΔG_{sys} were negative, the system would not have performed as expected or may not have performed at all if ΔG_{sys} were a large negative number.

Since a ΔG_{sys} was positive, that 3.8 dB of excess system gain can be spent in a variety of ways. One way is that the fiber path length can be increased by an amount which will cause L_{NA} plus L_α to increase the loss budget by 3.8 dB. Another way is that a splice can be inserted in the system fiber path which will use up about 2.5 dB of the 3.8 dB. A third way of spending the 3.8 dB of excess system gain is to reduce LED current until the P_o drops 3.8 dB and thereby increase LED reliability. Or the 3.8 dB can be left unspent and allowed to provide extra gain margin for less susceptibility to disruption of communications.

In this example the path length was known and the loss budget was easily calculated in order to determine excess system gain. Very often the path length is the unknown and the maximum path length is what needs to be determined. In this case a re-iterative calculation is necessary. This is done by assuming a path length such as the length that has been calculated already and then calculating the ΔG_{sys} . If ΔG_{sys} turns out to be positive, as in this example, the fiber length can be increased until the L_{NA} and L_α increase by an amount equal to ΔG_{sys} according to the fiber manufacturers plots of NA and L_α vs. length. If on the other hand this guess at path length yields a negative ΔG_{sys} , then the length should be reduced until the sum of L_{NA} and L_α is reduced by an amount equal to ΔG_{sys} . Once this second guess at fiber length has been made, a recalculation of ΔG_{sys} is made and should be much closer to zero. When ΔG_{sys} is essentially zero, then that path length is L_{MAX} .

For example, since a 31m length of MSC200B fiber yielded a ΔG_{sys} of 3.8 dB, a second guess of path length of 200 m will be made in order to find L_{MAX} . When the length is increased from 33 m to 200 m, the NA drops from 0.40 to 0.36 according to the fiber data sheets. That means the new value of L_{NA} is:

$$L_{NA} = 10 \log \left(\frac{0.63}{0.36} \right)^2 = 4.9 \text{ dB}$$

The signal attenuation loss is also increased to:

$$L_\alpha = (18 \text{ dB/kM}) \cdot (0.2 \text{ kM}) = 3.6 \text{ dB}$$

Therefore, the new loss budget using equation 14 is:

$$L_B = 6.7 \text{ dB} + 4.9 \text{ dB} + 3.6 \text{ dB} = 15.2 \text{ dB}$$

Using equation 15, the excess system gain for 200 meters is:

$$\Delta G_{sys} = 15 \text{ dB} - 15.2 \text{ dB}$$

$$\Delta G_{sys} = -0.2 \text{ dB}$$

That is 200 meters is slightly longer than the maximum path length that will provide the desired performance. Reducing this new path length sufficiently to reduce the loss budget by 0.2 dB will cause an insignificant decrease in L_{NA} . Therefore, this 0.2 dB can be spent by shortening the system by approximately:

$$\Delta \ell = \frac{0.2 \text{ dB}}{18 \text{ dB/km}} = 11 \text{ m}$$

In other words, with Maxlight MSC200B fiber and typical characteristics for connectors, transmitter and receiver, the maximum path length that will allow 1×10^{-9} BER performance with a 3 dB gain margin is:

$$L_{MAX} = 189 \text{ meters}$$

Figure 29 summarizes similar calculations for a variety of other fibers.

All of these calculations assume that the system under consideration is attenuation limited. But there is another limitation relating to the maximum data rate that can be transmitted over a given distance. The source of this limitation is a transit time phenomenon of fiber propagation called modal dispersion.

Because of the relatively short system path lengths summarized in Figure 28, modal dispersion is not a factor in these systems. At what path length modal dispersion in a particular fiber begins to degrade system rise time can be calculated if the pulse spreading specification or dispersion for the fiber is known. For example, Valtec PC-10 has a pulse broadening specification of 40 ns/km. This represents the pulse width at the 50% points of a pulse exiting the

fiber in response to a sub-nanosecond wide pulse being launched into the fiber. Since the pulse exiting the fiber is Gaussian in shape, the 10%-90% rise time is about 72% of this 50% pulse width. Therefore, if the short system rise time of this 20-Mbaud system is 30 ns, the rise time of the fiber for less than 10% degradation due to modal dispersion is:

$$t_{R_{SYS}(long)} \leq 1.1 t_{R_{SYS}(short)}$$

$$\sqrt{(30 \text{ ns})^2 + (t_{R_fiber})^2} \leq 1.1 (30 \text{ ns})$$

$$900 \text{ ns}^2 + (t_{R_fiber})^2 \leq 1089 \text{ ns}^2$$

$$(t_{R_fiber})^2 \leq 189 \text{ ns}^2$$

$$t_{R_fiber} \leq 13.7 \text{ ns}$$

The length of PC-10 which will cause this much degradation is given by:

$$t_{R_fiber}(\text{ns}) = (0.72) (\text{Dispersion} \frac{\text{ns}}{\text{km}}) \times (\text{length})$$

$$\text{length} = \frac{t_{R_fiber}}{0.72(\text{Disp})} \text{ km} = \frac{13.7 \text{ ns}}{0.72 (40 \text{ ns/km})}$$

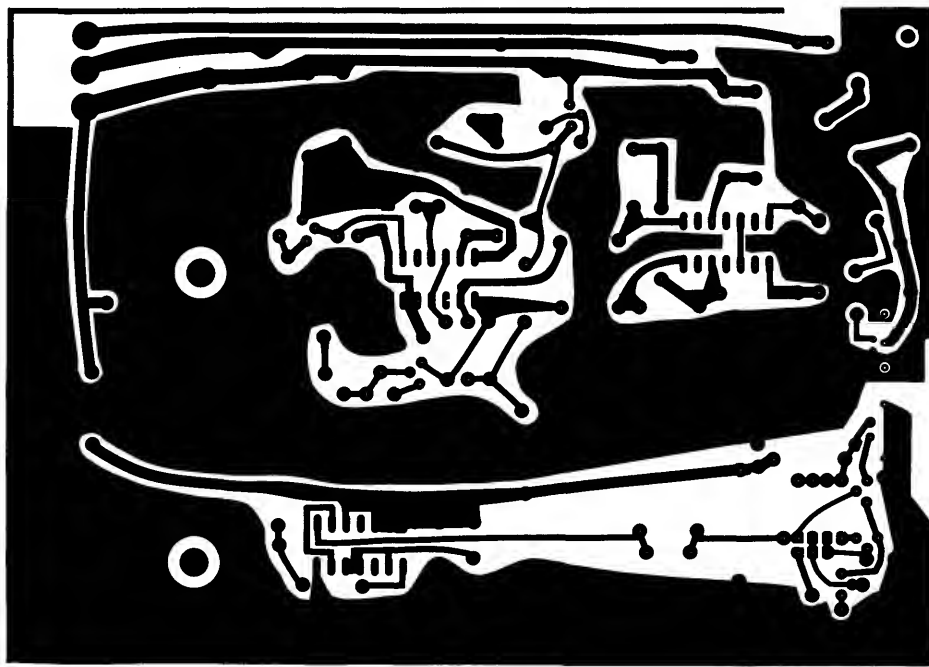
$$\text{length} = 476 \text{ meters}$$

In other words, if a 10% degradation in system performance is all that is tolerable and improvements in this 20-Mbaud system extend the use of PC-10 to beyond 476 meters, then 476 meters will remain as the maximum allowable path length. The system will no longer be attenuation limited but will now be dispersion limited.

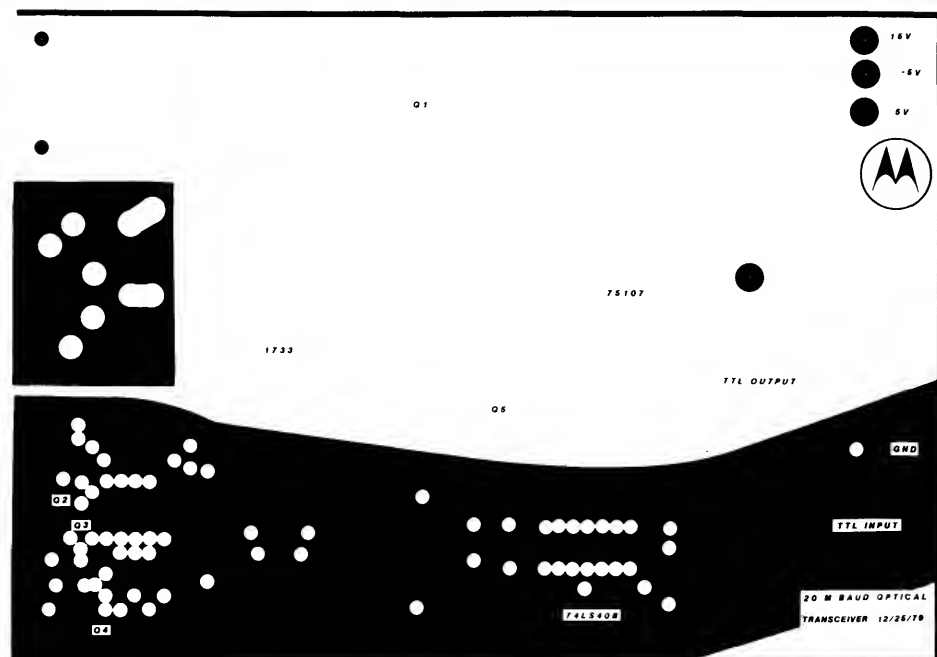
| Fiber/System Parameters | Maxlight MSC200B | Seicor 155 | Valtec ¹ PC-08 | Valtec ¹ PC-10 | DuPont ¹ PIR 140 | DuPont ¹ S-120 Type 30 |
|---|---------------------|-------------------|------------------------------|------------------------------|--------------------------------|--------------------------------------|
| Fiber Core Diameter | 200 μm | 200 μm | 200 μm | 250 μm | 368 μm | 200 μm |
| Clad Mode Loss (L_{CM}) | 0.2 dB | 0.2 dB | 0.2 dB | 0.0 dB | 0.0 dB | 0.2 dB |
| Diameter Loss (L_D) | 0.0 dB | 0.0 dB | 0.0 dB | 1.9 dB | 5.3 dB | 0.0 dB |
| Alignment Loss ($L_{AE} + L_{AD}$) | 3.0 dB | 3.0 dB | 3.0 dB | 0.5 dB | 0.5 dB | 3.0 dB |
| Reflective Loss (L_R) (Using IDP) | 0.5 dB | 0.5 dB | 0.5 dB | 0.5 dB | 0.5 dB | 0.5 dB |
| Loss Budget (L.B.) without L_{NA} or L_n , including 3 dB G.M. | 6.7 dB | 6.7 dB | 6.7 dB | 5.9 dB | 9.3 dB | 6.7 dB |
| Fiber NA $\approx \ell_{max}$ | 0.36 | 0.40 | 0.38 | 0.38 | 0.44 | 0.38 |
| NA Loss (L_{NA}) | 4.9 dB | 3.9 dB | 4.4 dB | 4.4 dB | 3.1 dB | 4.4 dB |
| Allowable Attenuation Loss (L_n) (15 dB - L.B. - L_{NA}) | 3.4 dB | 4.4 dB | 3.9 dB | 4.7 dB | 2.6 dB | 3.9 dB |
| Fiber Attenuation Factor (α) | 18 dB/km | 35 dB/km | 70 dB/km | 70 dB/km | 950 dB/km | 95 dB/km |
| Maximum Path Length (ℓ_{max}) | 189 m | 126 m | 55 m | 67 m | 2.7 m | 41 m |

¹ Calculations for this fiber are based on measured NA versus length data which is available from the fiber manufacturer but is as yet unpublished.

FIGURE 29 — Maximum Path Length Calculations with 15 dB of System Gain



(a) Solder Side



(b) Component Side

FIGURE 30 — Printed Circuit Artwork

SUMMARY

The fiber optic data link described herein is quite versatile. With a TTL interface, no data format constraints, 0-20 Mbaud capability, and full duplex operation, it can be inserted into almost any system as a transparent link for the purpose of evaluating the contribution of fiber optics to improved system performance. In addition, it can be configured as a simplex optical repeater by strapping the receiver data output to the transmitter data input.

This application note has also introduced the reader to the Motorola Fiber Optic Active Component, or FOAC, and some of the mechanical and optical considerations involved in its proper use. The necessary functional blocks as well as some of the desirable characteristics of an optical data transmitter

and receiver have also been discussed. The text and waveform diagrams dealing with signal detection schemes should offer insight into whether or not edge coupling is appropriate for a particular application.

The data shown here on transmitter, receiver, and system performance was generated from measurements on two units in a system. It should be considered typical performance and normal variations around these values should be expected.

ACKNOWLEDGEMENTS

The author would like to acknowledge the laboratory assistance of John Toney in gathering data and generating several iterations of printed circuit board design.

APPLICATIONS OF FERRULED COMPONENTS TO FIBER OPTIC SYSTEM

Prepared By:
Horst Gempe

THE MOTOROLA FERRULED LED Construction and Optical Characteristics

This device is constructed by assembling an infrared light emitting diode (LED) in a package suitably configured to mate with and become an integral part of a fiber

optic connector. This active connector concept is illustrated in Figure 1(a). The ferruled semiconductor and its exploded view are illustrated in Figures 1(b) and 1(c).

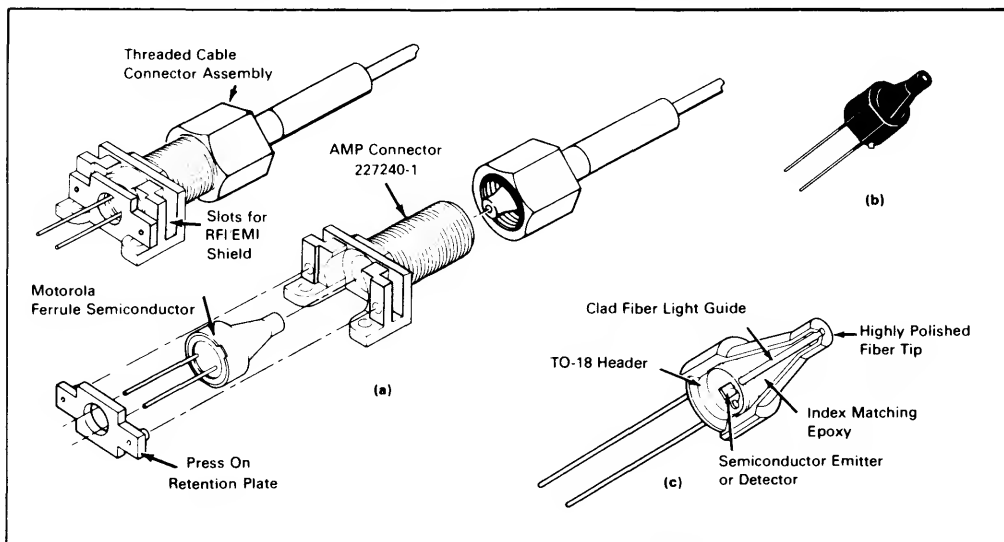


FIGURE 1 — Motorola Fiber Optic Active Component (FOAC)

- (a) Package/Connector Concept
- (b) External View of FOAC
- (c) Exploded View of FOAC

A depiction of the light emission pattern of the LED is shown in Figure 2. The fiber cladding carries less than five percent of the total output power since most clad modes are absorbed by the high index of refraction epoxy.

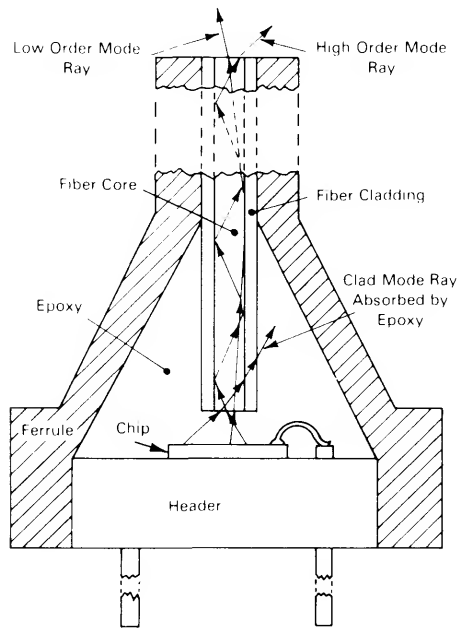


FIGURE 2 — Light Ray Patterns in FOAC LED

The core carries high- and low-order modes with the distribution of total energy as shown in Figure 3. The presence of high-order modes makes the effective numerical aperture (NA) greater than would be found for a fiber length longer than about one meter.

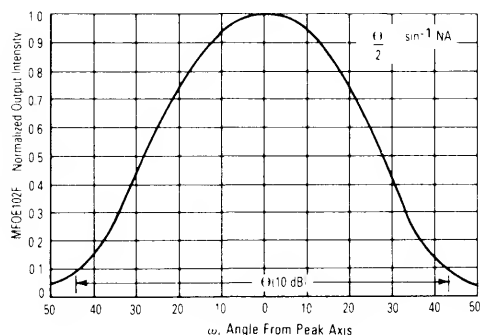


FIGURE 3 — Light Emission Pattern for FOAC LED

Measurement of Output Power

There are several methods currently in use for measuring the output of FO sources.

The integrating sphere method shown in Figure 4 collects the power radiated from the source in all directions and directs it to the silicon detector cell of a radiometer. It is the most repeatable technique of measurement since it is effectively independent of geometry. However, since it is not sensitive to the NA of the source, it does not enable the user to predict the amount of the measured power that can be coupled from the source into a fiber.

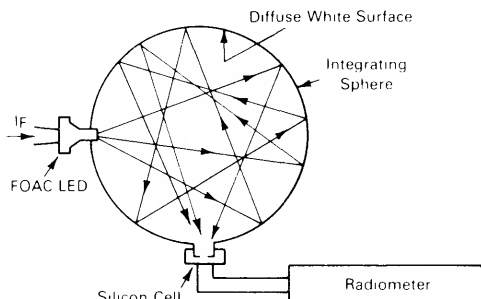


FIGURE 4 — Integrating Sphere/Radiometer Measurement Method

The barrel method, Figure 5, simulates the condition of coupling into a fiber. Only the power that passes through the aperture is measured. Repeatability requires exact duplication of the aperture size, the distance between the source and the silicon cell, and the accurate positioning of the source orthogonal to the direction between source and cell.

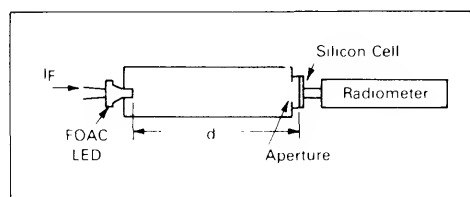


FIGURE 5 — Barrel/Radiometer Measurement System

As an example of measurement difference between the integrating sphere and barrel methods, a device was measured under like-drive conditions in the integrating sphere of a PhotoResearch PR 1000 Radiometer and a barrel type Photodyne Radiometer. The results are given in Table I.

| Measurement Method | MFOE102F Measured Power |
|------------------------------|-------------------------|
| Integrating Sphere (PR 1000) | 73 microwatts |
| Barrel (Photodyne) | 67 microwatts |

For the MFOE102F ($NA = 0.7$) the correction factor between the barrel and the integrating sphere is 0.91. Devices with smaller NAs will have a correction factor approaching 1.0.

THE MOTOROLA FERRULED DETECTOR

Construction and Optical Characteristics

The detector members of the FOAC family utilize the same construction as the LED. Again, because of the short length of the fiber in the ferrule, the effective NA is larger than found for longer sections of the same type of fiber. The angular response for the detector is similar to the emission pattern for the LED, Figure 6.

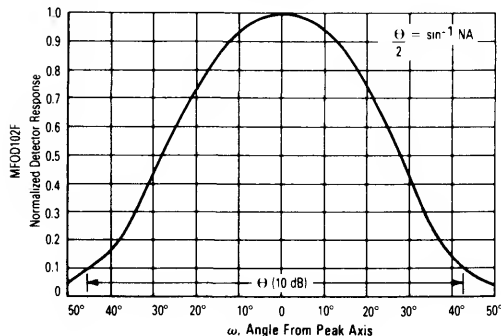


FIGURE 6 — Light Response Pattern for FOAC Detector

Measurement of Responsivity

The response of the detectors is given in output voltage or current per unit of optical power coupled into the detector's input port. It does not include losses (see Fresnel and connector losses later in this bulletin) between the power source and the input port since these are a function of each individual system's variables.

The FOAC detector responsivity is measured by connecting a FOAC LED to a one meter length of fiber that is connected to a simulated detector ferrule, see Figure 7. The power launched from the simulated ferrule is measured in an integrating sphere, and is a true measure of the actual power coupled into a ferrule detector. The power measured by the sphere/radiometer is recorded.

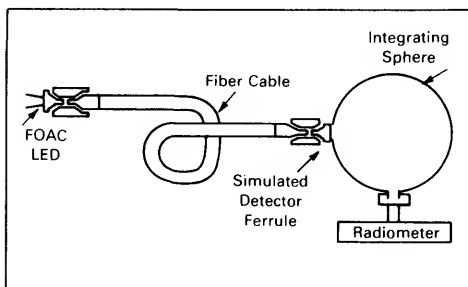


FIGURE 7 — Calibration of Light Source for Detector Responsivity Measurement

The detector to be measured is then connected to the fiber in place of the simulated ferrule, Figure 8, and the output voltage or current is noted. The responsivity for the detector is taken as the ratio of the output voltage or current to the power as measured by the integrating sphere.

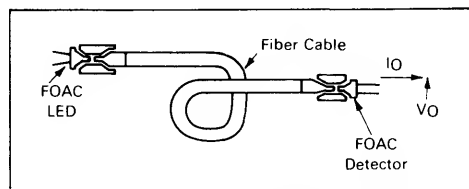


FIGURE 8 — Detector Responsivity Measurement

OPTICAL FIBERS

To calculate the total losses for a system, it is important to know and understand the parameters of the system fiber. The two most critical parameters are:

1. Output NA of the fiber
2. Fiber attenuation

Output NA of a Fiber

The output NA of a fiber is a function of its length, as shown in Figure 9. Most fiber manufacturers specify NA. If it is not available for a particular fiber, it can be measured as shown later in this bulletin.

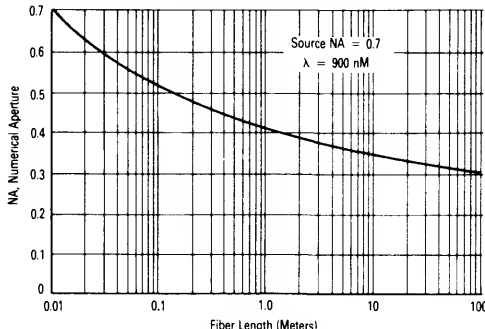


FIGURE 9 — NA versus Length for a Sample Fiber

Fiber Attenuation

The attenuation characteristic of a fiber is usually specified in dB per meter or dB per kilometer. If it is given as a single value, the manufacturer will specify the wavelength of measurement. Usually the attenuation is given graphically as a function of wavelength. Figure 10 shows several examples. The specified attenuation does not contain losses due to NA changes, since

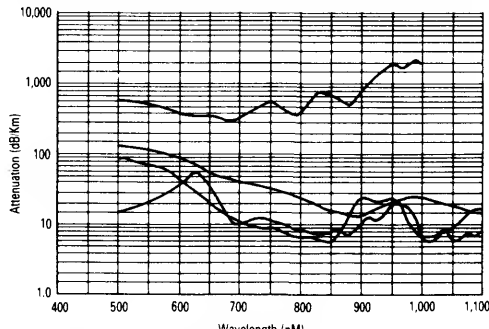


FIGURE 10 — Attenuation versus Wavelength for Several Fibers

it is usually measured with a very narrow angle (small NA) source. In many applications, the NA of the system source is greater than the NA of the system fiber. This means additional loss is incurred which will have to be added to the total attenuation loss when calculating a system flux budget.

THE MEASUREMENT OF NA

Source NA

The measurement of NA for an LED source can be made as shown in Figure 11(a). The power from the source is measured by a silicon cell radiometer through a very small aperture. The peak power level is measured and recorded. The source is rotated and the angle between the two points at which the power level drops to one tenth the peak power level (-10 dB) is noted. Signifying this angle as Θ , the source NA is calculated:

$$NA(\text{source}) = \sin(\Theta/2) \quad (1)$$

Detector NA

The NA for a detector is measured in a similar arrangement, see Figure 11(b). The silicon cell radiometer is replaced by a stable light source. The peak detector response is measured and recorded, and the angle between the two points at which the response is one tenth the peak (-10 dB) is noted. Again signifying this angle as Θ :

$$NA(\text{detector}) = \sin(\Theta/2) \quad (2)$$

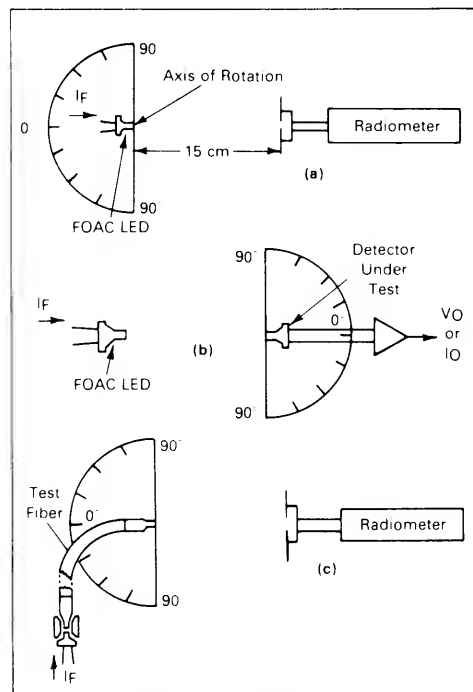


FIGURE 11 — NA Measurement

- (a) For FOAC LED
- (b) For FOAC Detector
- (c) For Fiber

Fiber NA

If the NA of a fiber is not known, it can be measured. The fiber to be tested is terminated in standard cable connectors (AMP Part #530954). One end of the fiber to be measured is connected to a FOAC LED. The other end of the fiber is directed at a silicon cell/radiometer, Figure 11(c). The peak power level from the fiber is recorded. The end of the fiber is then rotated and the angle between the points at which the power level is one tenth the peak (-10 dB) is noted. Again, using this angle, Θ :

$$NA(\text{fiber}) = \sin(\Theta/2) \quad (3)$$

CONNECTOR LOSSES

There are a variety of losses that can occur in the interconnections in a system. These are:

- NA loss
- Diameter loss
- Gap loss
- Axial misalignment loss
- Fresnel loss
- Angular loss

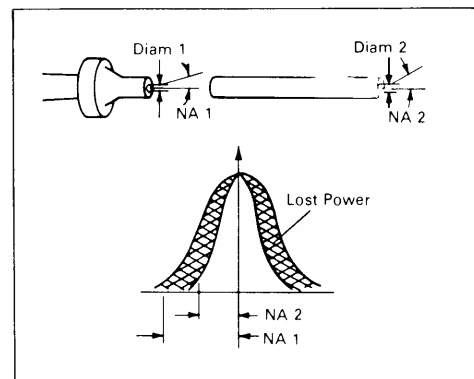


FIGURE 12 — NA Loss

NA Loss

It was shown earlier that presence of high order modes in the FOAC LED give it an effective NA higher than a long length of the same type of fiber, Figure 9. As shown in Figure 12, the difference in the two areas of the spatial patterns represents lost power due to different NAs. The magnitude of this loss is given by:

$$NA\text{ Loss} = 20 \log(NA_1 NA_2) \quad (4)$$

Note that in the case of coupling from a small NA fiber to a larger NA fiber, no energy is lost due to NA difference so that the loss in equation 4 becomes zero. (Example: coupling from a system fiber into a FOAC detector!)

Diameter Loss

If two fibers of different diameters are coupled, an additional loss may be incurred. It is given by:

$$\text{Diameter Loss} = 20 \log(Dia_1 Dia_2) \quad (5)$$

Again, if the receiving fiber has a diameter greater than the source fiber, Figure 12, the diameter loss reduces to zero.

Gap Loss

Ideally, two fibers would be joined such that no gap exists between them. In practice a small gap is intentionally introduced to prevent mechanical damage to the fiber surfaces. The Motorola FOAC devices and AMP connector bushings are designed to hold this gap to about 0.1 mm. The result of variations in the gap for several sample NAs is given in Figure 13.

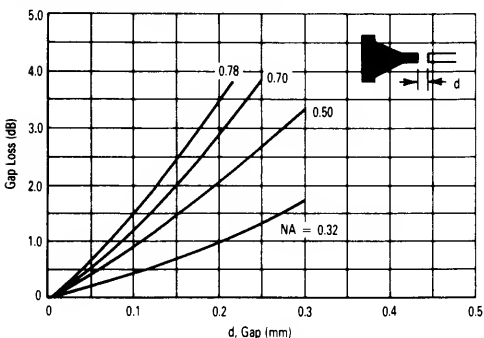


FIGURE 13 — Gap Loss

Axial Misalignment Loss

If two connected fibers are not concentric there will be an obvious loss of power. The effect of this misalignment for several NAs is shown in Figures 14(a), 14(b), and 14(c). The effect of gap separation is also included in these graphs.

FIGURE 14(a)

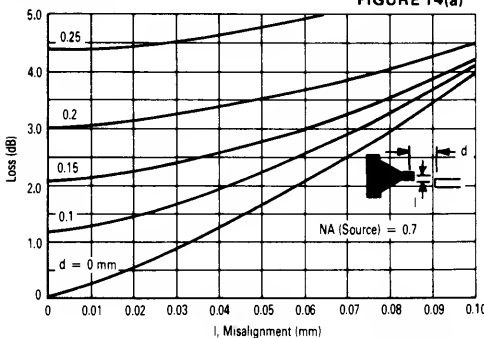


FIGURE 14(b)

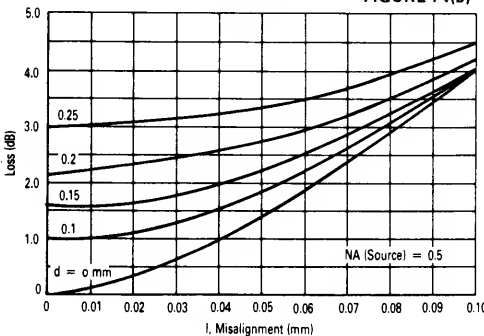


FIGURE 14(c)

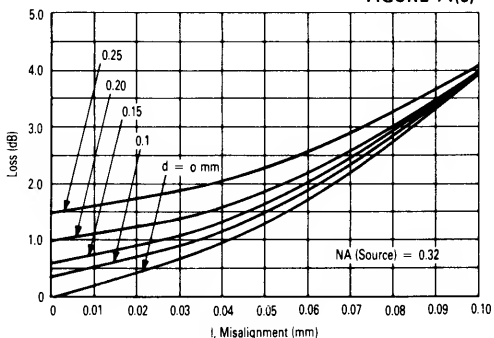


FIGURE 14 — Misalignment Loss

Fresnel Loss

As light passes through any interface, some energy is transmitted and some reflected. The amount of energy lost is a function of the indices of refraction of the materials forming the interface. For the FOAC family of devices and glass core fibers this loss is a fairly consistent 0.2 dB per interface.

Angular Loss

If the surfaces of the two connected fiber ends are not parallel, an additional loss is incurred. The magnitude of this is shown in Figure 15.

FLUX BUDGET

Once the various losses in a system have been identified and quantified, it is a relatively simple exercise to calculate the total system loss and thus predict system performance. To illustrate this, and to highlight a major loss element in systems, two examples will be considered. In each case an MFOE102F LED is used for the source and an MFOD102F PIN diode as the detector. System A uses a 50 meter length of cable, while system B uses two 50 meter lengths joined by a fiber/fiber splice.

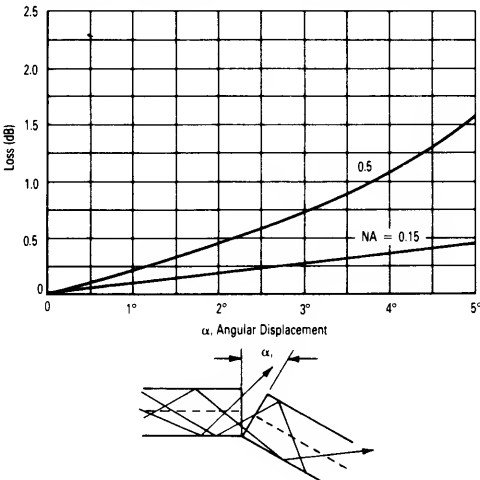


FIGURE 15 — Angular Loss

System A Flux Budget

System A is shown in Figure 16. A proper flux budget should consider all significant losses. These include:

1. Connector losses: gap, misalignment and Fresnel (angular losses are usually quite small so the very low loss that results will be ignored).
2. Numerical aperture loss
3. Fiber attenuation
4. Diameter loss — the two systems being analyzed will use the same diameter fiber throughout so that diameter loss can be considered to be zero

The following specifications apply:

MFOE102F: $P_o = 125 \mu\text{W}$ @ 100 mA
 NA (10 dB effective) = 0.7
 Core diameter = 200 μm
 Wavelength = 900 nm

MFOD102F: $R = 0.4 \mu\text{A}/\mu\text{W}$ @ 900 nm
 NA (10 dB effective) = 0.7
 Core diameter = 200 μm
 $I_{dark} = 2.0 \text{nA}$ @ 25°C

Fiber: Length = 50 M
 Attenuation = 25 dB Km @ 900 nm.

Figure 10
 NA @ 50 M = 0.32
 Core diameter = 200 μm

Connectors: Gap = 0.15 mm typical
 Misalignment = 0.05 mm typical

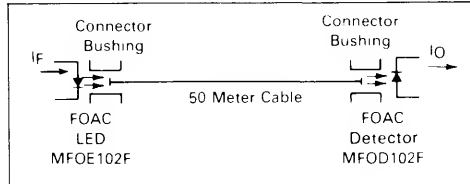


FIGURE 16 — 50 Meter F/O System

The total system loss can now be calculated.

| | |
|--|----------|
| LED to Fiber Connector Loss, Figure 14(a) | 2.7 dB |
| LED to Fiber Fresnel Loss | 0.2 dB |
| LED to Fiber NA Loss | |
| $[20 \log NA /LED] \cdot NA(FIBER) $ | 6.79 dB |
| Fiber Attenuation (50 Meters) | 1.25 dB |
| Fiber to Detector Connector Loss, Figure 14(c) | 1.5 dB |
| Fiber Exit Fresnel Loss | 0.2 dB |
| Detector Entry Fresnel Loss | 0.2 dB |
| Total System A Loss | 12.84 dB |

(Note that no NA loss was included at the detector end since the detector NA is greater than the fiber NA. Also, no LED exit Fresnel loss was considered since it is already accounted for in the P_o specification for the LED).

To determine total system performance we can construct a table. For this analysis we will use power units in dBm similar to the volume units (vW) used in audio work. We will define a power unit of zero dBm for an optical power of one milliwatt. For any power level we then have:

$$\text{dBm} = 10 \log (P_1 \text{ mW}) \quad (6)$$

$$\text{dBM} = 10 \log P(\text{mW}) \quad (7)$$

The table for system analysis now becomes:

TABLE II

| Point in the System | Power Units (dBm) | P (μW) |
|---|-------------------|---------------------|
| P1 LED @ 100 mA | 9.03 | 125 |
| P2 Power in Fiber | 11.93 | |
| (P1 — Connector loss — Fresnel loss) | | |
| P3 Power from Fiber | -20.17 | |
| (P2 — NA loss — Attenuation — exit Fresnel) | | |
| P4 Power into Detector | -21.87 | 6.5 |
| (P3 — Connector loss — entry Fresnel) | | |

Of course, this could have just as easily been calculated from the total system loss of 12.6 dB:

$$\text{System Loss} = 10 \log |P(\text{in})/P(\text{out})| \quad (8)$$

$$12.84 = 10 \log [125 \mu\text{W}/P(\text{out})] \quad (9)$$

$$P(\text{out}) = 6.50 \mu\text{W} \quad (10)$$

However, partitioning the power level at any point in the system, as in Table II, enables us to plot the power level over the system as shown in Figure 17.

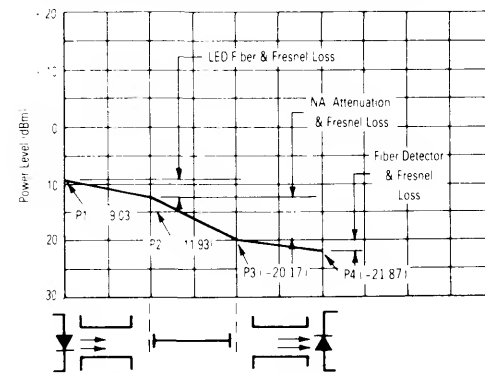


FIGURE 17 — Power Level Along System A

Using the detector responsivity, the output signal current can now be determined:

$$I_o = P(\text{in}/\text{detector}) \times R \quad (11)$$

$$I_o = 6.5 \mu\text{W} \times 0.4 \mu\text{A}/\mu\text{W} \quad (12)$$

$$I_o = 2.60 \mu\text{A} \quad (13)$$

Since the detector dark current, I_d , of the MFOD102F is 2.0 nA at 25°C, the signal-to-noise ratio is:

$$\text{SNR} = 10 \log (2.60/0.002) \quad (14)$$

$$\text{SNR} = 31.1 \text{ dB} \quad (15)$$

System B Flux Budget

System B is shown in Figure 18. It is identical to System A except for the addition of a second 50 meter length of fiber and a fiber fiber splice.

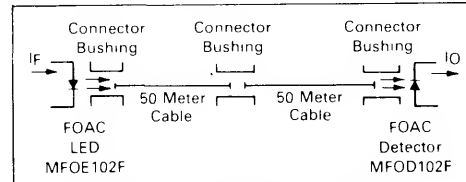


FIGURE 18 — 100 Meter, 2 Cable System

In calculating system losses it is important to note that the NA of 100 meters of fiber is 0.31, per Figure 9. It is independent of the presence of the splice at the midpoint, since the second 50 meters continues to strip high order modes. Another way of looking at it is to consider a replot of Figure 9. This is shown in Figure 19. The difference is that the NA at zero is the NA of the source, in this case the 0.32 exit NA of the first 50 meter length. At long distances the cable will still approach the same asymptotic value as in Figure 9. In Figure 19 it can be seen that the curve passes through 0.31 at 50 meters. So a 50 meter cable starting with an NA of 0.32, and a 100 meter cable starting with an NA of 0.7 will both have an exit NA of 0.31. (This is true of course only for this particular cable)

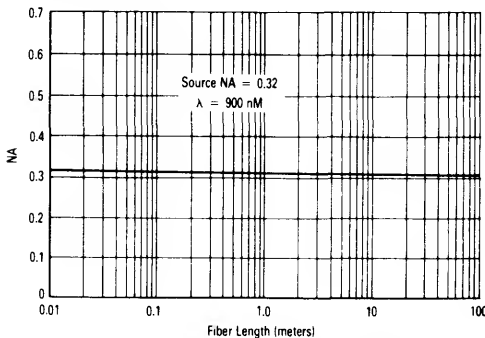


FIGURE 19 — NA versus Length for a Sample Fiber

Calculating system loss:

| | |
|---|----------|
| LED to Fiber Connector Loss, Figure 14(a) | 2.7 dB |
| Fiber 1 Entry Fresnel Loss | 0.2 dB |
| LED to Fiber 1 NA Loss | 6.79 dB |
| Fiber 1 Attenuation | 1.25 dB |
| Fiber 1 Exit Fresnel Loss | 0.2 dB |
| Fiber/Fiber Connector Loss | 1.50 dB |
| Fiber 2 Entry Fresnel Loss | 0.2 dB |
| Fiber 1/Fiber 2 NA Loss | 0.28 dB |
| Fiber 2 Attenuation | 1.25 dB |
| Fiber 2 Exit Fresnel Loss | 0.2 dB |
| Fiber to Detector Connector Loss | 1.5 dB |
| Detector Entry Fresnel Loss | 0.2 dB |
| Total System B Loss | 16.27 dB |

The power level system analysis is:

TABLE III

| Point in the System | Power Units (dBm) | P (μ W) |
|---|-------------------|--------------|
| P1: LED (\sim 100 mA) | -9.03 | 125 |
| P2: Power in Fiber 1 (P1 — Connector Loss — Fresnel Loss) | -11.93 | |
| P3: Power from Fiber 1 (P2 — NA loss — Attenuation — Fresnel Loss) | -20.17 | |
| P4: Power in Fiber 2 (P3 — Connector Loss — Fresnel Loss) | -21.87 | |
| P5: Power from Fiber 2 (P4 — NA Loss — Attenuation — Fresnel Loss) | -23.6 | |
| P6: Power into Detector (P5 — Connector Loss — Fresnel Loss) | -25.30 | 2.95 |

The power level along System B is plotted in Figure 20.

The output signal is now calculated:

$$I_0 = 2.95 \mu\text{W} \times 0.4 \frac{\mu\text{A}}{\mu\text{W}} \quad (16)$$

$$I_0 = 1.18 \mu\text{A} \quad (17)$$

The SNR for System B is:

$$\text{SNR} = 10 \log (1.18/0.002) \quad (18)$$

$$\text{SNR} = 28 \text{ dB} \quad (19)$$

It is now of interest to compare the losses in System A with those in System B. At first thought, it might seem that doubling the system length should approximately double the system loss. If the dominant loss mechanism were fiber attenuation, this might be true.

However, as Figures 17 and 20 show, the greatest loss occurs in the first 50 meters of fiber. Since the fiber attenuation and Fresnel loss for any 50 meter length of this cable is essentially constant at fixed wavelength, the major loss has to be a result of the NA loss from the FOAC LED to the fiber. As shown in the analysis of the two systems this loss is 6.79 dB. As a percentage of the total loss in the two systems, it represents 53% in System A and 42% in System B.

Therefore, in designing a system, the greatest loss will usually be incurred at the front end of the system where the LED couples to the system fiber. One way to combat this is to select fibers with large NAs. However, this will reduce the high frequency capability of the system by increasing pulse dispersion distortion, so the designer is faced with making a tradeoff between system length, or SNR and high-frequency performance.

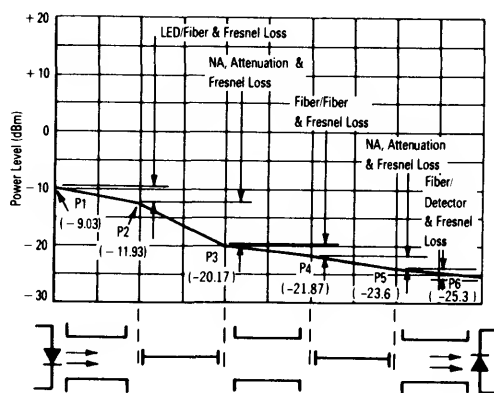


FIGURE 20 — Power Level Along System B

SUMMARY

The packaging concept used in the Motorola FOAC line of products enables the user to quickly design and assemble an F/O system. A full understanding of the device characteristics and the characteristics of cables and connectors used with FOACs, gives the designer the capability to perform a flux budget analysis of his system and thus predict performance.

Specific conclusions drawn from this study are:

- | | |
|------------|--|
| LED | — in most cases not all power as specified on typical data sheets is usable due to NA differences. |
| Fiber | — NA is not constant in short lengths of fiber when used with high NA sources. |
| Connectors | — Connector losses are dependent upon the NA conditions combined with the mechanical tolerances. |
| Detector | — Detector responsivity is specified as a function of the actual power launched into the optical input port. |

BIBLIOGRAPHY

1. Barnoski, Michael K., ed., *Fundamentals of Optical Fiber Communications*, Academic Press, Inc., New York, 1976.
2. "Introduction to Fiber Optics and AMP Fiber-Optic Products," HB5444, AMP, Inc., Harrisburg, PA, 1979.
3. Mirtich, Vince, "A 20-MBaud Full Duplex Fiber Optic Data Link Using Fiber Optic Active Components," Motorola Application Note AN-794, Phoenix, AZ, 1980.

MFOL02 THEORY OF OPERATION

Prepared By:
David Stevenson

The design of Link II™ is such that it appears transparent to the user. In other words, the designer that wishes to take advantage of some of the benefits of fiber optics digital data transmission need not know any more about these modules other than they take TTL in and give TTL out. This means that Motorola's Link II™ modules are suited for immediate applications requiring bandwidths from D.C. to 200k bits and point-to-point system lengths of up to 1000 meters.

For the more curious user, or those who wish to use the modules as an educational tool to learn more about fiber optics circuit design, the modules have been designed to allow easy access to the circuit boards within.

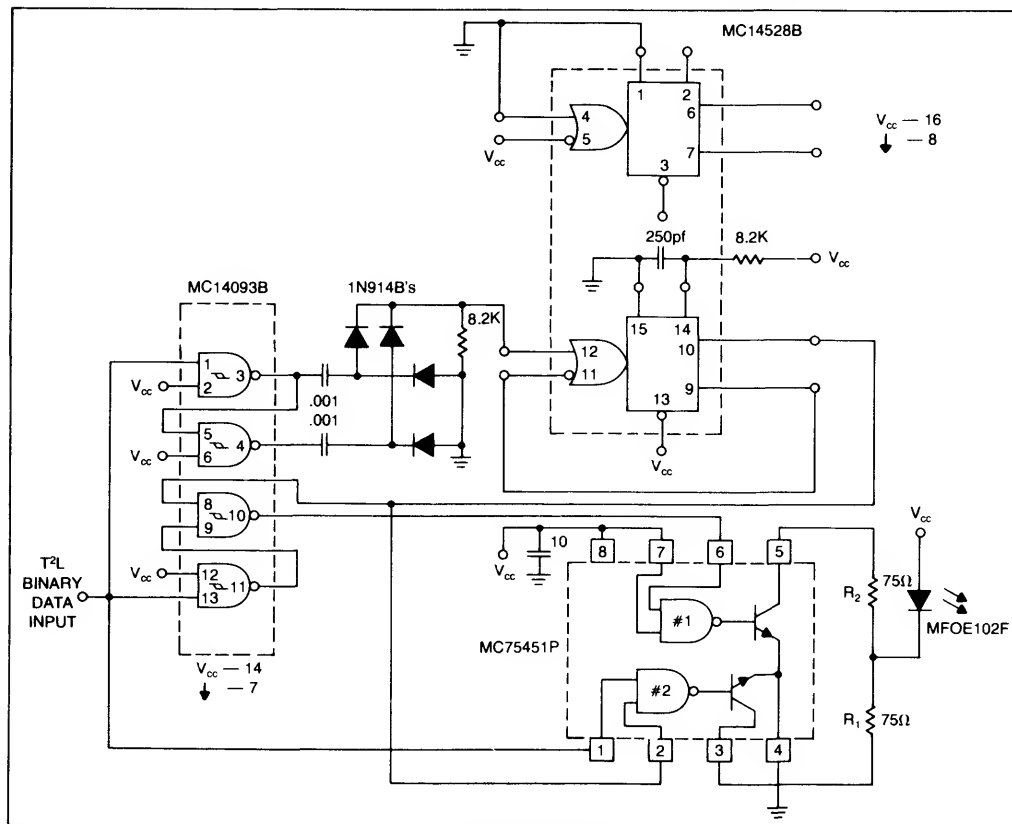
Before beginning with the circuit analysis, the general specifications of the modules should be highlighted. First of all, both the transmitter and the receiver circuits are designed for single 5 volt power supply operation. As previously stated, the bandwidth capability is D.C. to

200k bits and depending on the particular optical fiber that is used, the transmission path can be extended up to 1000 meters.

Physically, both module housings are identical, being approximately 2 inches by 2 inches by .45 inches. The module base is configured similar to a large dual inline package having 8 pins fixed in two rows of 4 each. Spacing between the pins is .400 inches and spacing between the two rows is 1.670 inches. Optical input and output ports are provided using AMP Optimate fiber connectors. The modules are designed with removable covers so that the printed circuit boards and associated components can be accessed even when the circuits are in operation.

TRANSMITTER

Circuit analysis will begin with the transmitter. The basic requirement of this circuit is to convert TTL voltage levels to corresponding current pulses through the light



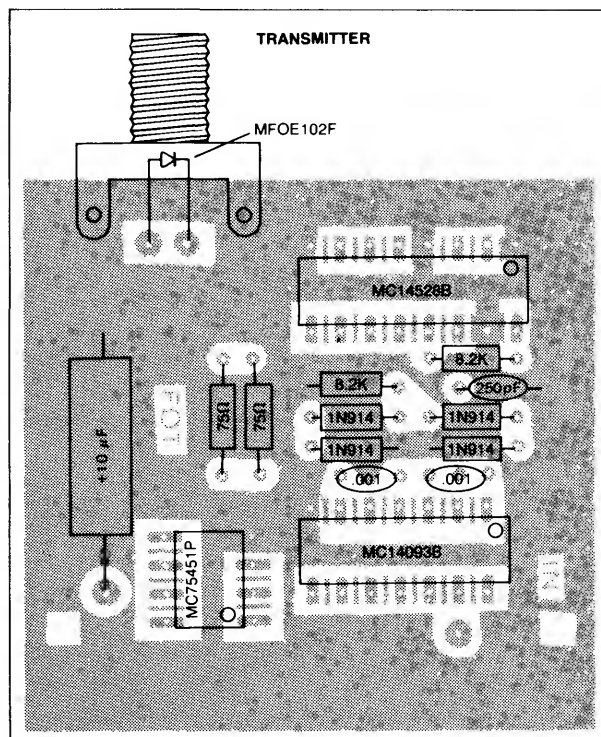
TRANSMITTER CIRCUIT
FIGURE 1.

emitting diode MFOE102F. Furthermore, the transmitter provides for ternary or pulse bipolar encoding format. Basically, with the pulse bipolar encoding format, the LED operates in three distinct states. During idle modes in data transmission the LED drive assumes a median level which is midway between logic 1 and logic 0. During positive going transitions on the input (logic 0 to logic 1) the LED is momentarily turned off. During negative going transitions (logic 1 to logic 0) the LED is momentarily driven at approximately twice the median or quiescent level. The advantage of the pulse bipolar format over the standard binary return to zero format is that the transmitter always transmits data at a fixed pulse width so it places no restrictions on the input signal other than maximum frequency. Another advantage of this type of transmission is that during idle modes of data transmission the light source is not turned off so if the receiver incorporates automatic gain control it always maintains a reference level.

Beginning at the transmitter input (Figure 1), the binary TTL signal drives the input of a two input NAND Schmitt trigger (1/4 MC14093). This gate forms an inverter by virtue of its second input being tied to V_{cc} . This inverted signal is then split and part of it is inputted to

pin 5 of the second NAND Schmitt trigger. The result is that the signal at pin 4 is essentially the input waveform and the signal at pin 3 is its complement. These two complementary signals are differentiated by $.001\mu F$ capacitors and rectified by a full wave bridge formed by the four 1N914B diodes. The result is that for every transition of the input, either 0 to 1 or 1 to 0, a positive pulse is applied to the 'set' input of the MC14528B monostable multivibrator. The MC14528B multivibrator is programmable so that the output pulse width can be determined by an external R-C time constant at pin 14. The values chosen give a pulse width of approximately $2\mu Sec$ which is adequate for 200k-bit transmission. This then, will be the pulse width of the current pulses applied to the LED to represent logic 0 and logic 1 transmission. Notice that the MC14528B is actually a dual monostable, only one half of which is used.

The remaining two Nand Schmitt triggers are used to gate the proper timing pulses to the MC75451P dual NAND input peripheral driver. The operation of this device is such that when the transmitter is in its idle mode, that is, the current through the LED is at the median level, the current path in this state is shown in Figure 3.



COMPONENT LAYOUT
FIGURE 2.

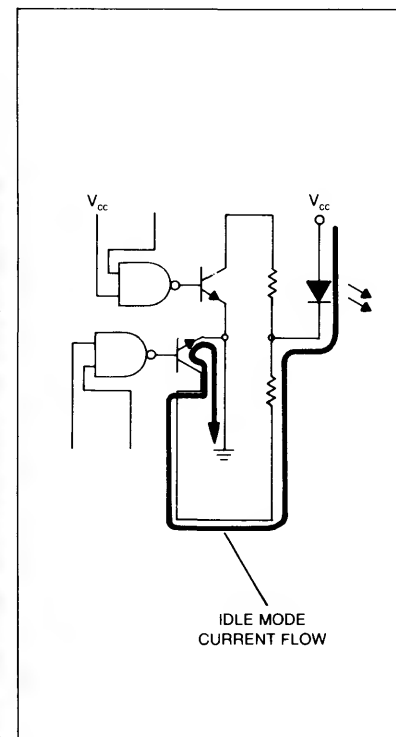
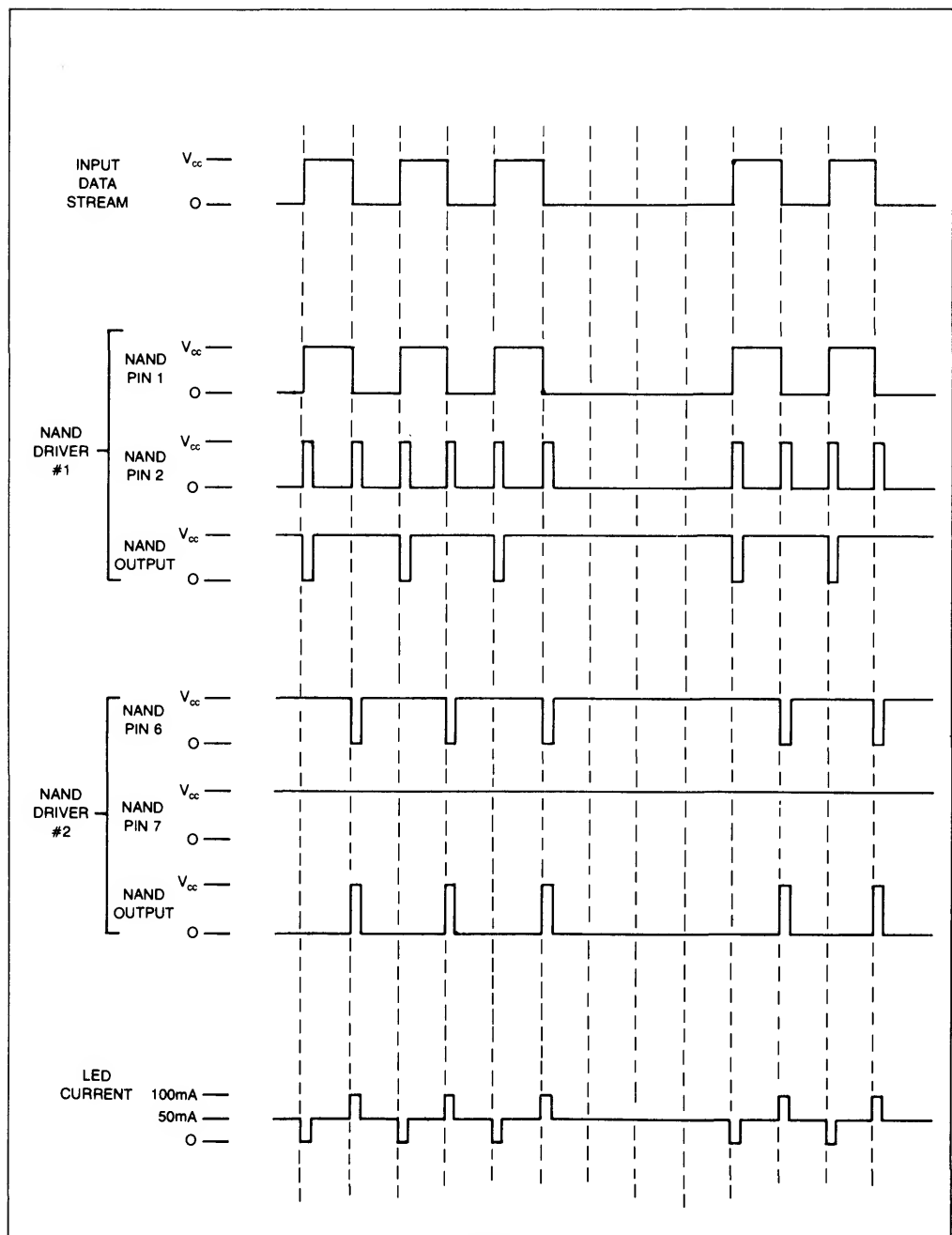


FIGURE 3.



CIRCUIT WAVEFORMS
FIGURE 4.

The value of idle current flowing through the LED is a function of Vcc and R1 and can be calculated by:

$$I_{idle} = \frac{V_{cc} - V_f - V_{sat}}{R_1}$$

where: V_f is the forward voltage drop of the LED
 V_{sat} is the 'on' state voltage of the MC75451
 $V_{cc} = 5$ volts, $R1 = 75$ and $V_f = 1.2$ volts yield an idle current of approximately 50mA.

In order to understand the other two states of the pulse bipolar transmitter it is necessary to evaluate the signals present at the inputs to both NAND drivers at each transition point of the input data stream. The waveform at pin 1 of NAND driver #1 is that of the input data. The waveform at pin 2 is the $2\mu\text{Sec}$ pulse produced by the monostable multivibrator. Before the waveform at pin 6 can be derived it is necessary to evaluate the action of the other two Nand Schmitt trigger gates. The input waveform is buffered and inverted by NAND #4 (input pin 13 output pin 11). This inverted waveform is NAND'ed with the $2\mu\text{Sec}$ pulse output of the monostable and the result is a $2\mu\text{Sec}$ negative pulse at each negative transition of the input (1 to 0). This signal at NAND #3 pin 10 is connected to pin 6 of NAND driver #2. Since pin 7 is held at Vcc this results in the output of the NAND gate going high (logic 1) for $2\mu\text{Sec}$ at every negative transition of the input waveform. The resulting outputs of both NAND drivers are shown with respect to the input waveform in Figure 4. It can be seen that for every positive transition of the input both NAND gate outputs are low, meaning the LED is turned off for a period of $2\mu\text{Sec}$. For each negative transition of the input both NAND outputs are high and since R2 is equal to R1, the LED is driven at twice the median current level for $2\mu\text{Sec}$. At all other times the LED is driven at the median level.

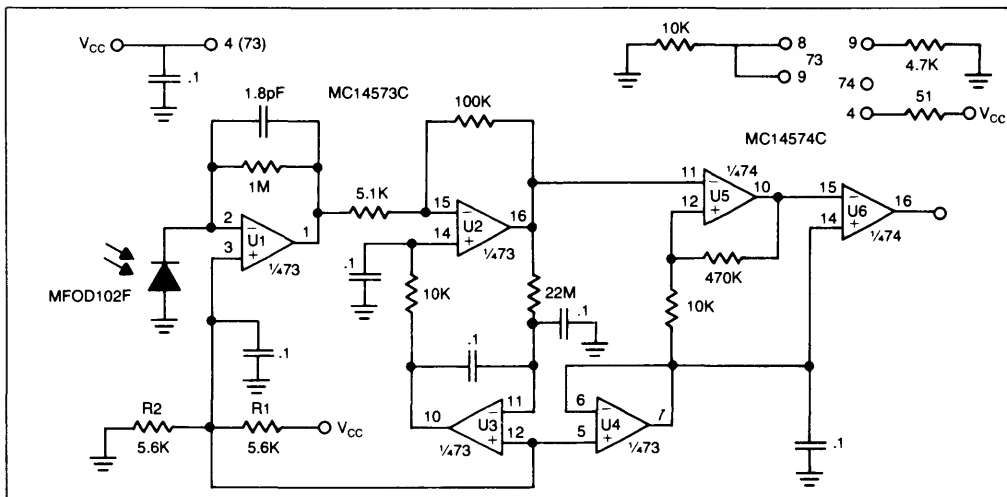
RECEIVER

The entire receiver is constructed using two CMOS integrated circuits. The MC14573C is a quad operational amplifier and the MC14574C is a quad comparator.

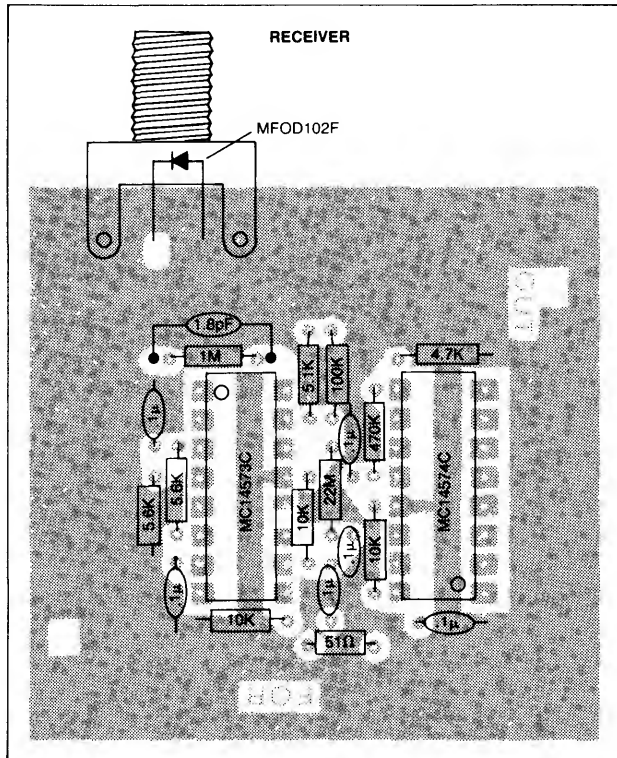
The detector used for this receiver is the MFOD102F PIN photodiode. This detector can be thought of as a current source whose output current is proportional to the input optical flux or light level. The receiver output device is a voltage comparator so between the two some kind of current to voltage conversion and amplification must take place. The current to voltage conversion takes place at U1. (Figure 5.) The theoretical gain of this amplifier which is fixed by the 1 Meg Ω feedback resistor, is 1 volt/ μ Amp. This in turn is followed by amplifier U2 whose gain is fixed at 20 by the 5.1k Ω input resistor and the 100k Ω feedback resistor. The integrating amplifier formed by U3 clamps the output reference level of U2 to a voltage fixed by the values of R1 and R2. In this case these are both 5.1k Ω so the reference voltage is one half of Vcc or 2.5v. U3 also tends to cancel voltage offsets produced by U2 by feeding this back to U2's input. This allows the receiver to be D.C. coupled which reduces component count and cost.

The output of U2 is then fed to comparator U5 which provides additional amplification and boosts the signal to TTL levels. Comparator U6 is used to improve hysteresis and invert the signal so that the output waveform is in phase with the original data stream applied to the transmitter. Finally, the 2.5 volt reference voltage is buffered by U4 to prevent transients produced by the comparators from interfering with the front end amplifiers and reducing the need for additional filtering.

MFOL02 was designed as a 1kM Link. Motorola's MFOE106F will greatly improve the performance capabilities of the MFOL02 Link. Use of this high power AlGaAs 820nm source extends the system length capability to several kilometers with no loss of bandwidth.



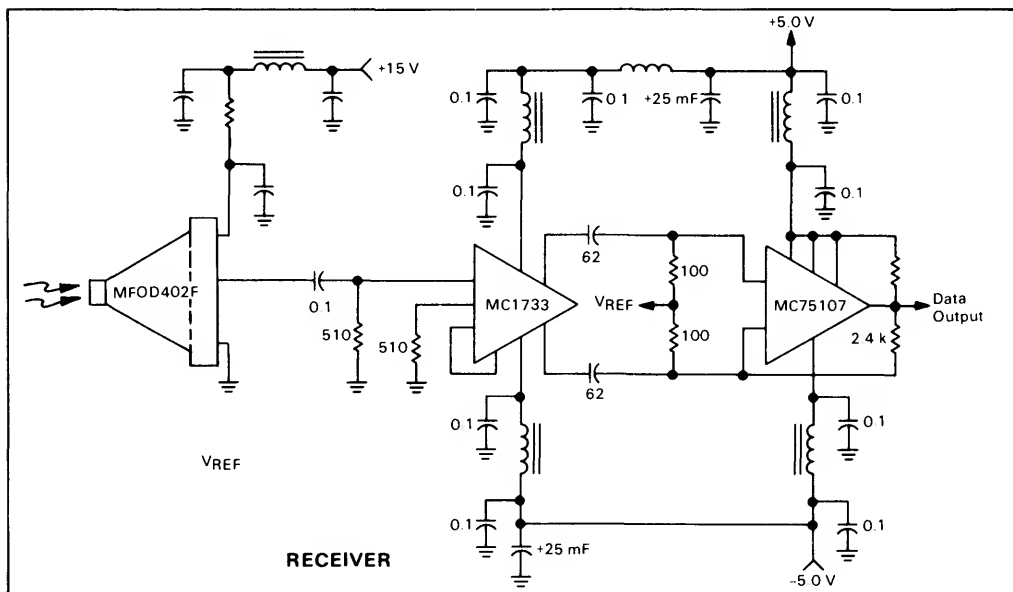
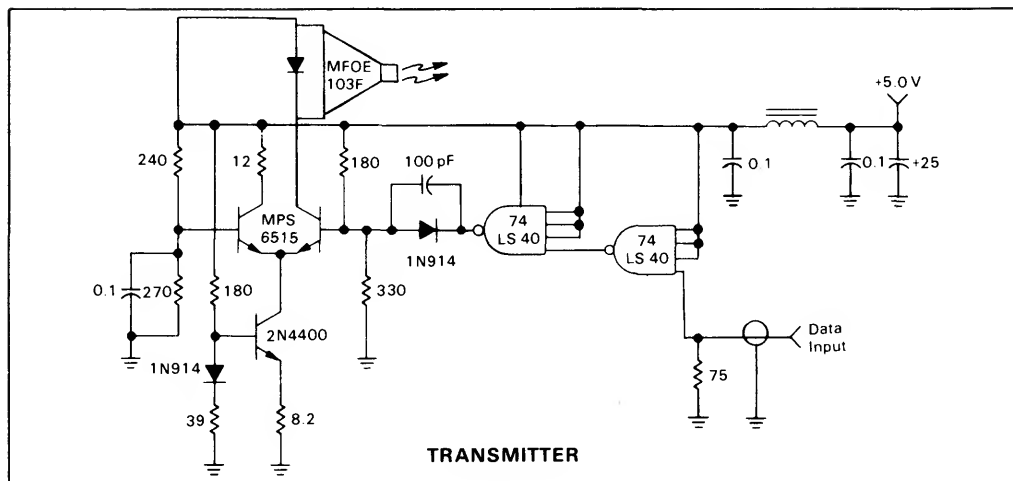
**RECEIVER CIRCUIT
FIGURE 5.**



COMPONENT LAYOUT
FIGURE 6.

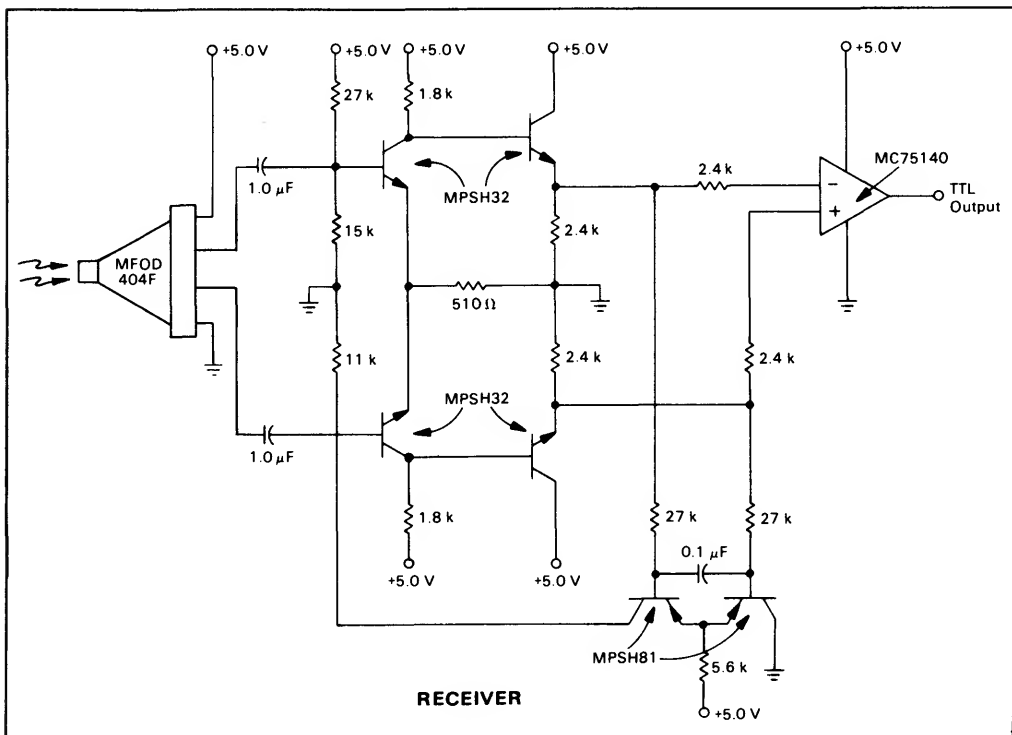
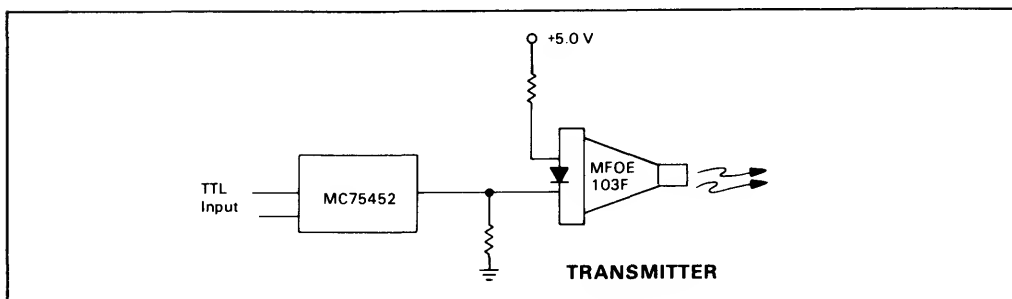
FIBER OPTIC CIRCUIT IDEAS

20 MBaud Data Link
Emitter — MFOE103F
Detector — MFOE402F



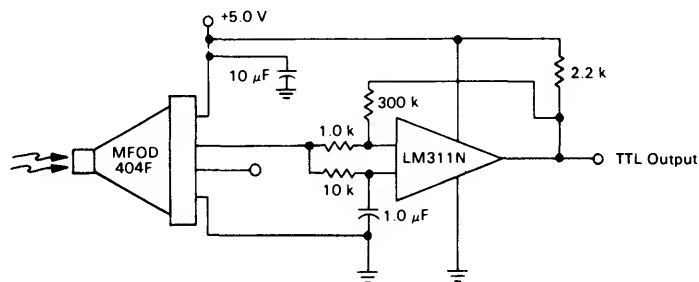
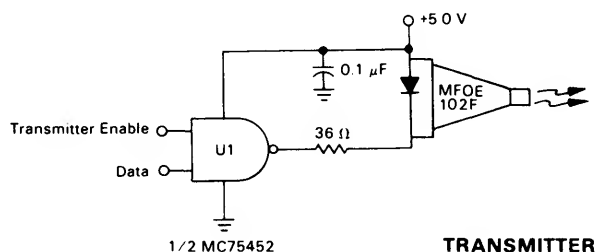
FIBER OPTIC CIRCUIT IDEAS

**10 MBaud Data Link
Emitter — MFOE103F
Detector — MFOD404F**



FIBER OPTIC CIRCUIT IDEAS

2.0 MBaud Data Link
Emitter — MFOE102F
Detector — MFOD404F



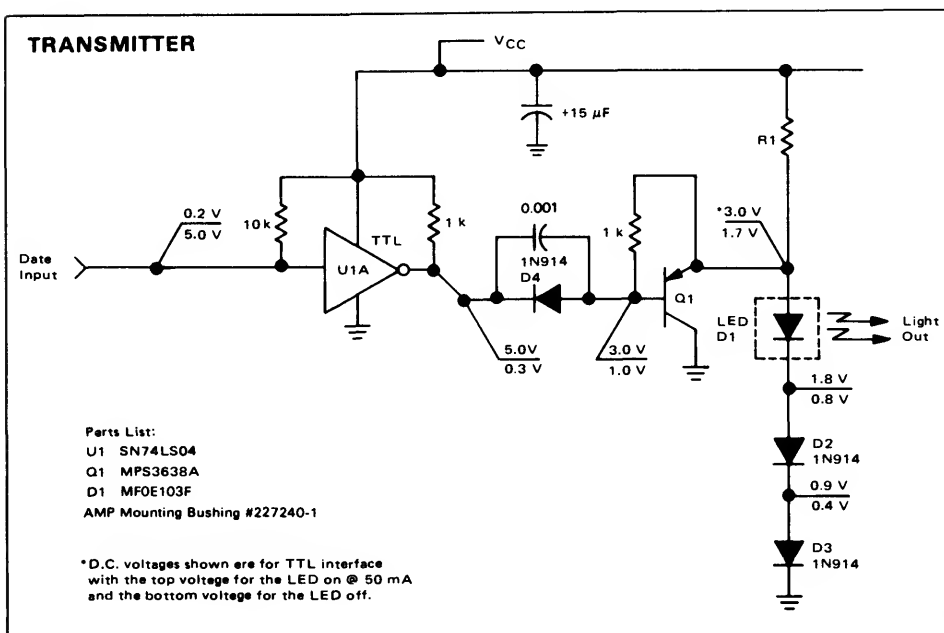
RECEIVER

FIBER OPTIC CIRCUIT IDEAS

1.0 MEGABIT SYSTEM

Microcomputer and microprocessor data links may be constructed using fiber optics. These data links offer all the advantages of fiber optics (transient/surge current immunity, high voltage isolation, no ground loops, RFI/EMI isolation, etc.) The links have been demonstrated in point of sale terminals, microprocessor controlled industrial controls, petro chemical applications, RS232 and many other areas. Full duplex links with system lengths greater than 1 Km have been constructed.

The transmitter and receiver circuits are depicted below with recommended parts list:



TRANSMITTER:

This fiber optic transmitter handles NRZ data rates to 10 Mbits or square wave frequencies to 5 MHz, and is TTL compatible.

Powered from +5V supply for TTL operation, the transmitter requires only 150 mA total current.

The LED drive current may be adjusted by resistor R1, and should be set for the proper LED power output level needed for system operation. (see LED data sheets.)

Resistor (R1) value may be calculated as follows:

$$\frac{R1 + V_{CC} - 3.0\text{ V}}{I_F} \text{ ohms}$$

Where: V_{CC} = Power Supply Voltage
 I_F = Desired LED forward current

FIBER OPTIC CIRCUIT IDEAS

1.0 MEGABIT SYSTEM — Cont.

The LED is turned off when transistor Q1 is driven on. Diodes D2 and D3 are used to assure the turn-off.

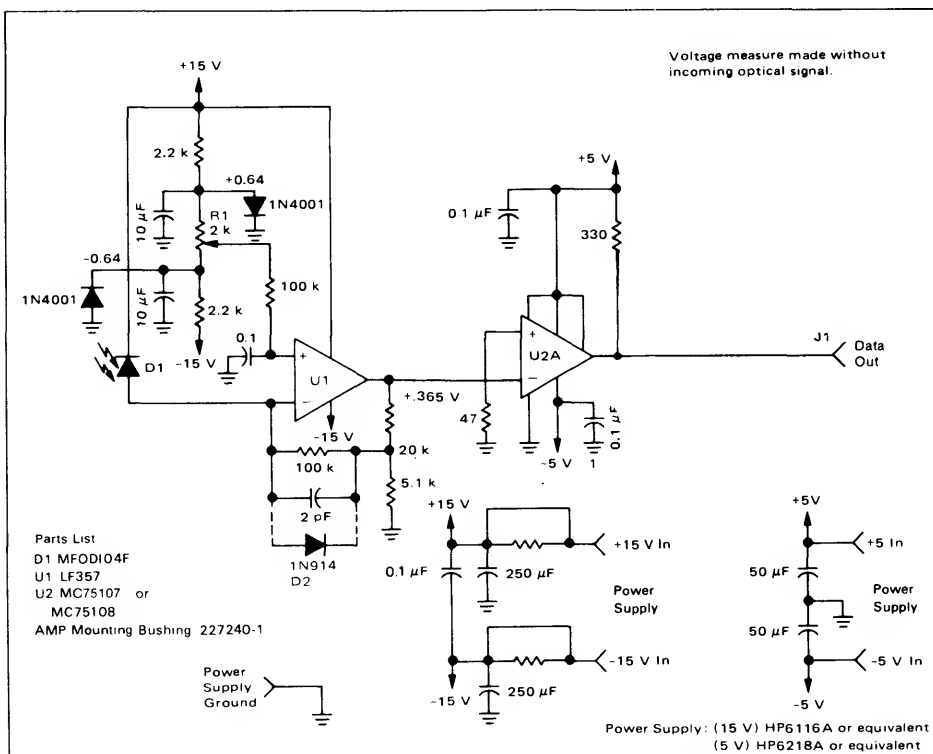
Diode D4 prevents reverse bias breakdown (base-emitter) of transistor Q1 when the integrated circuit U1 output is high. The transmitter requires a power supply voltage of $+5 \pm 0.25V$.

RECEIVERS

The receiver uses an MFOD104F PIN photodiode as an optical detector. The detector diode responds linearly to the optical input over several decades of dynamic range. The PIN detector output current is converted to voltage by integrated circuit U1(Operational amplifier LF357). The minimum photocurrent required to drive U1 is 250 nA. Receiver dynamic range is extended with diode D2 to prevent U1 from saturating at large optical power inputs.

Integrated circuit U2 acts as a voltage comparator. Its worst case sensitivity of 50 mV determines the size of the pulse required out of U1. U2 detects, inverts, and provides standard TTL logic level to the output.

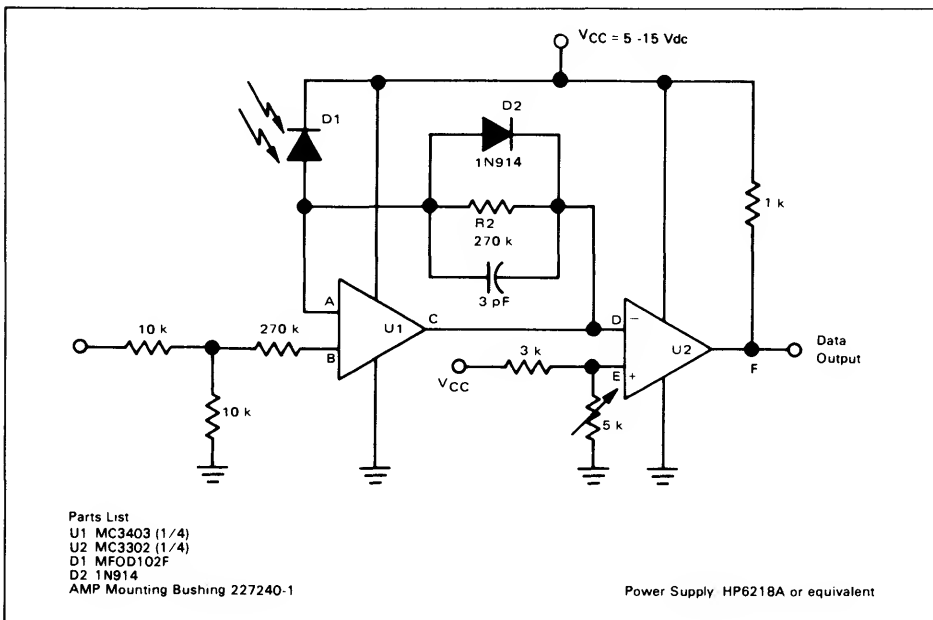
Offset adjustment R1 should be set to accurately reproduce a 1 MHz.50% duty cycle square wave at the receiver output.



FIBER OPTIC CIRCUIT IDEAS

100 KILOBIT RECEIVER

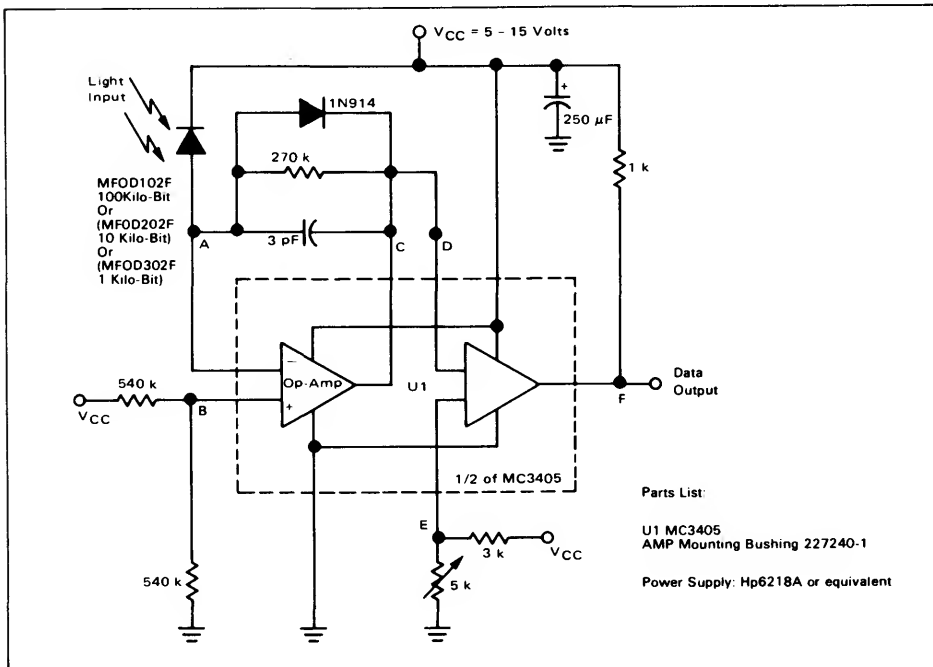
This is a two-IC four-channel receiver. An operational amplifier, U1 (MC3403) translates the PIN detector Photo current into a voltage level. The U1 output voltage is used by open collector comparator U2 (MC3302) to generate TTL or CMOS compatible signal levels at the receiver output. One channel is shown below.



FIBER OPTIC CIRCUIT IDEAS

1/10/100 KILOBIT RECEIVER

This is a single IC two-channel receiver, using an MC3405, which contains two op-amps and two comparators. The receiver is TTL or CMOS compatible and operates up to 100 Kilo-bit data rate.



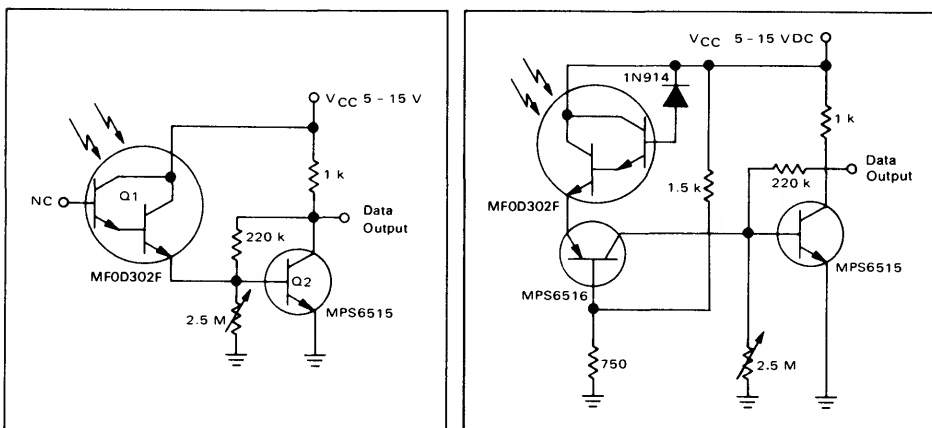
FIBER OPTIC CIRCUIT IDEAS

DARLINGTON RECEIVER

Discrete Low Speed Circuits

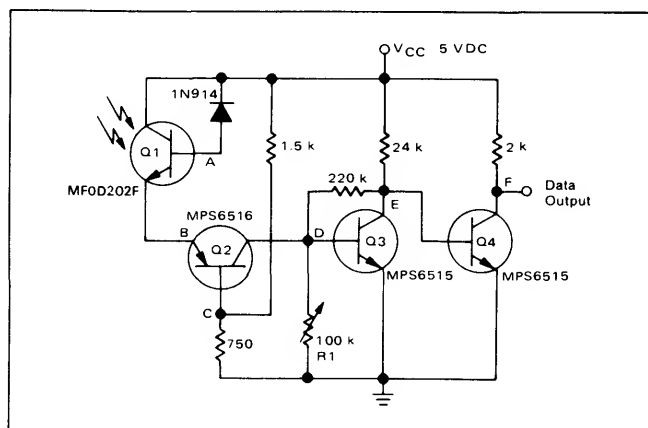
A simple photodarlington receiver may be used in a dc control or low frequency system. The output of the MFOD302F drives a signal (MPS6515) transistor common emitter amplifier. This circuit operates from a +5 to +15 volt power supply, and its output is TTL and CMOS compatible.

By the addition of a second transistor, the circuit described below may be extended in frequency from one Kilo-bit to two Kilo-bit.



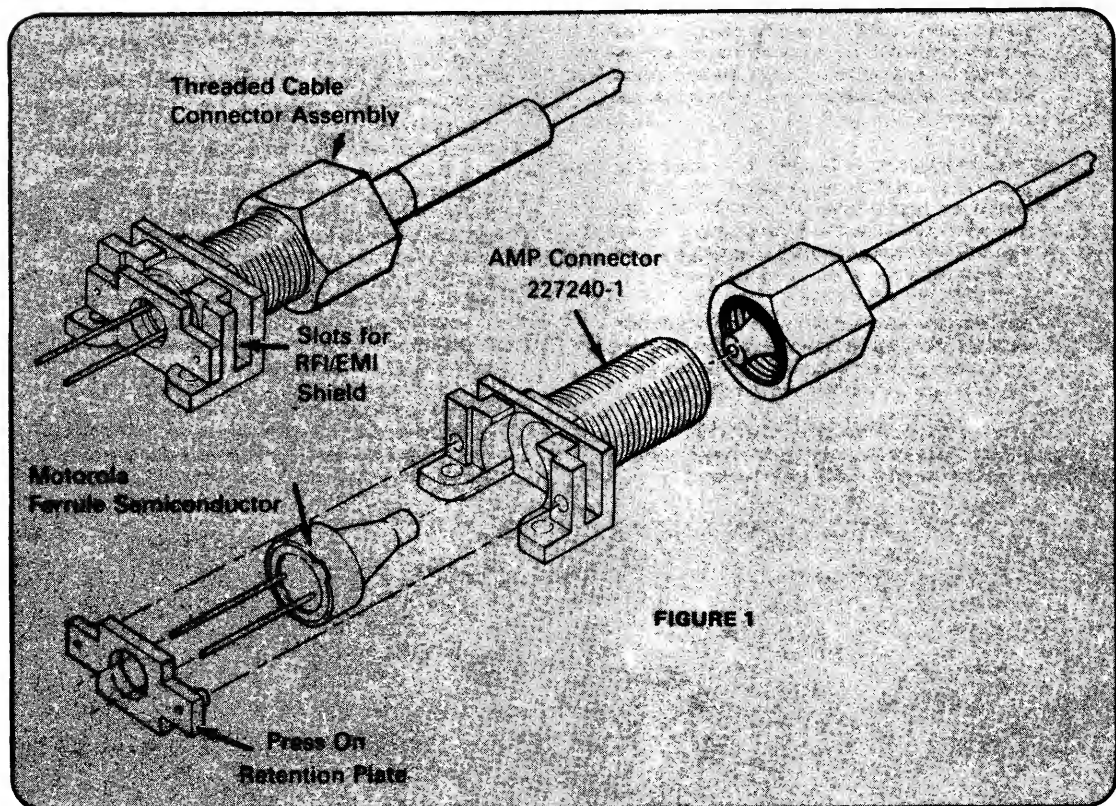
PHOTOTRANSISTOR RECEIVER

The phototransistor receiver circuit shown below may be used for data rates up to 20 kilo-bit. The receiver sensitivity at 10 kilo-bits is 4.7 μW.



A MICROCOMPUTER DATA LINK USING FIBER OPTICS

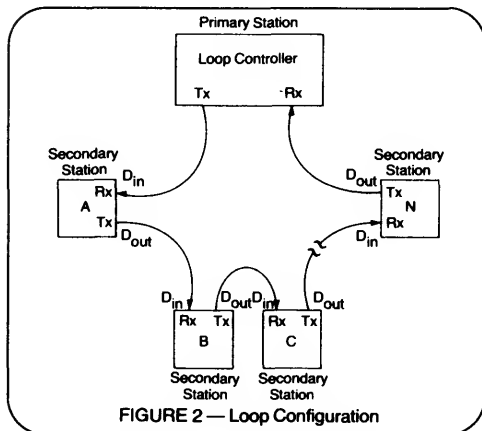
Prepared by:
Scott Evans and
Jim Herman



The performance capability of fiber optics now offers the designer a practical, advantageous alternative to wire for data communications. The advantages of optical fibers over twisted pair or coax wire are easily enumerated:

- 1. Bandwidth.** Standard optical fiber cable on the market today has bandwidth up to several hundred MHz, and a few available cables are good up to several GHz.
- 2. EMI Immunity.** Optical fibers neither radiate nor pick up electromagnetic interference. Thus, crosstalk and RFI-induced errors are eliminated. Optical fibers can be installed alongside high-voltage or high-current-carrying cables or in close proximity to EMI or RFI-intensive systems with no fear of interference. Recently proposed FCC regulations restricting the magnitude of EMI generation in data communication systems create no concern for users of fiber optics.
- 3. Security.** Optical fibers are difficult to tap. Either the fibers must be broken to insert a tap or the cladding stripped to allow another fiber to contact the core and draw off some of the signal. Both methods are difficult to implement and easily detectable, so that optical-fiber-transmitted data is relatively secure.
- 4. Size and Weight.** A one-kilometer reel of optical fiber cable of equal, and often greater data handling ability, weighs about one-tenth that of comparable coax cable. The optical fiber is considerably smaller, also, allowing significantly more signal-handling capability in the same cross-sectional area of a conduit or cable trough.
- 5. Cost.** The price of optical fiber cable continues to drop while that of wire is seen to be facing a future of increasing cost. Even with optical fiber costing more than wire, the overall system cost with fiber optics is often lower.

This article describes a data communication system designed to demonstrate the ability to interconnect a series of microcomputer terminals with a fiber optic link.



System Hardware Requirements

The basic system in this example is illustrated in Figure 1. It uses a cost-effective transmitter and receiver design in a full-duplex, two-terminal arrangement using a pair of fibers for interconnect purposes. The basic system is easily expandable to multiple terminals, however, in a looping configuration shown in Figure 2. Here, the central control, or primary terminal, initiates data flow. The data then passes serially through the secondary terminals and returns back to the primary. Note that this loop arrangement results in any one terminal operating in a half-duplex, one-direction mode. Each secondary serves as a repeater network; that is, the received optical data is fed to the terminal and also retransmitted to the next terminal in the loop. As the data passes around the loop, any secondary recognizing its address in the address field of the Information Frame reads that frame and acts on it. The data continues to pass down the loop whether a terminal has acted on it or not. Secondary stations are given an opportunity to transmit local data when the central terminal transmits a "POLL" command. If a secondary desires loop control, it is granted by the primary by a "GO AHEAD" flag following a "POLL" command. Error detection and recovery are also governed by a full set of rules.

The Motorola EXORterm 220 M6800 development system serves as the basis for the system hardware. The EXORterm 220 is an intelligent CRT display terminal featuring an integral development facility that provides a motherboard and card cage capable of holding up to eight microprocessor modules. Each station is composed of standard M6800 microprocessor modules including an M6800 MPU Module, an MEX6816-22 16K Static RAM Module, an MEX68RR 8K ROM Module, and an MEX6854 ACIA Module interfaced to the CRT terminal. An MEX6854 Advanced Data Link Controller (ADLC) Module with fiber optic transmitter and receiver on-board provides the interface to the fiber optic link. This is shown in Figure 3.

The MC6854 ADLC performs the complex interface function between the MPU data bus and a synchronous communications channel employing a Bit-Oriented-Protocol. It is an NMOS LSI intelligent peripheral device that automatically performs many of the functions required by the communications protocol, thus reducing the amount of software required and increasing the data throughput rate.

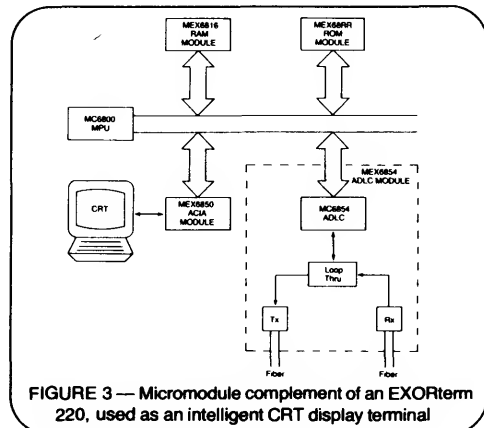


FIGURE 3 — Micromodule complement of an EXORterm 220, used as an intelligent CRT display terminal

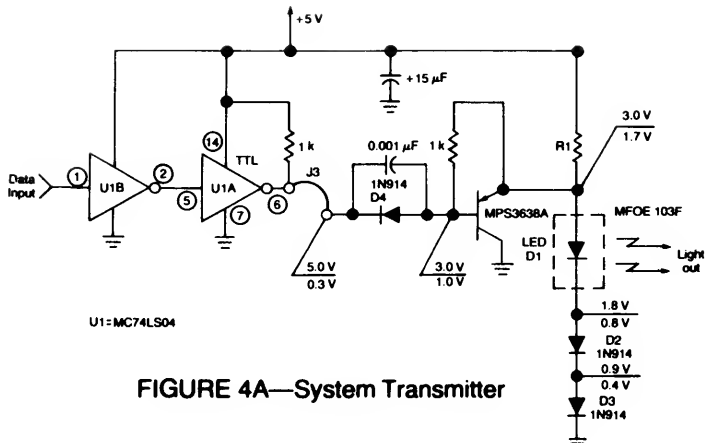


FIGURE 4A—System Transmitter

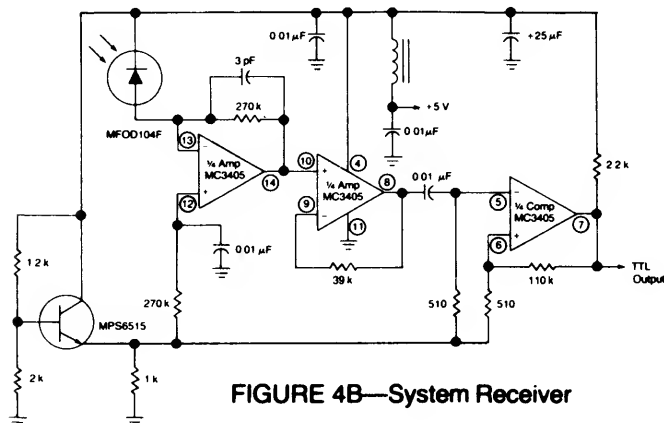


FIGURE 4B—System Receiver

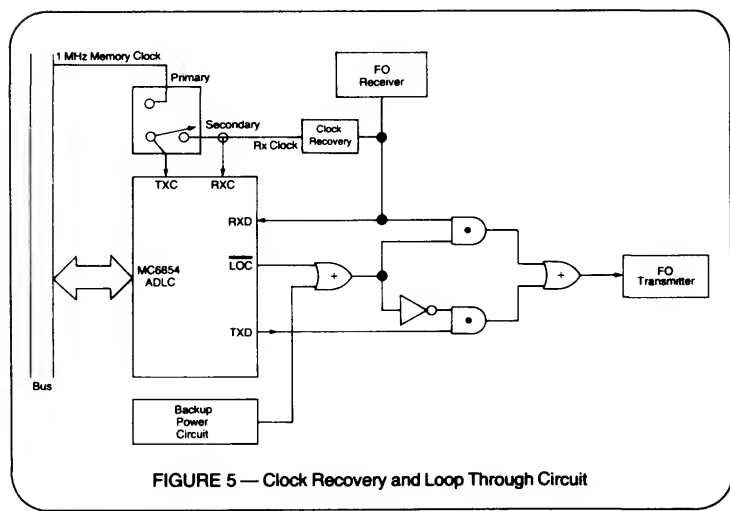


FIGURE 5—Clock Recovery and Loop Through Circuit

Fiber Optic Transmitter and Receiver

The transmitter and receiver modules are built around the Motorola Fiber Optic Active Component (FOAC) products.¹ The transmitter uses an MFOE103F light emitting diode (LED). The receiver component is an MFOD104F PIN diode. The FOAC family and a compatible connector are joint developments of Motorola and AMP Inc. The concept (Figure 1) allows the user to efficiently interface to any of the many types and sizes of optical fibers on the market.

As shown in Figure 4, the transmitter and receiver are mounted directly to the ADLC Module. The driver circuit for the transmitter uses an MC74LS04 inverter and one discrete driver transistor. This circuit is capable of driving the LED at a 1-Mbit/second data rate.

Although the optical fiber is impervious to EMI, the actual receiver circuit is not. It is shielded, therefore, to prevent noise pickup. At 100 kHz, the receiver is capable of reception with a bit-error-rate of 10⁻⁶.

The receiver sensitivity, transmitter power, and system losses (e.g., fiber attenuation) determine the maximum usable distance between terminals. This system was operated with a pair of 70-meter Siecor 155 cables, but was designed to operate up to 120 meters. System length and data rate might be increased with higher receiver sensitivity or increased transmitter power.

Transmitter and receiver are interfaced to the ADLC as shown in the clock recovery and loop-through circuit of Figure 5. The clock recovery circuit synchronizes a 1-MHz oscillator (divided down to the 62.5-kHz data rate) to the incoming data from the receiver. Both the data and the separated clock information are presented to the ADLC. The data rate clock is then also used to route data back to the transmitter so it can be sent to the next downstream station. In the event that power is lost to any terminal on the loop (power failure or maintenance operation), there is a provision for a separate power supply or battery pack to operate the receiver and transmitter circuits. The loop-through control then routes the receiver output directly to the transmitter input line so that repeater performance is maintained during terminal power-down.

System Software

Connecting a series of terminals together requires a well-defined and efficient communications protocol to manage the data link. For this system, a Bit-Oriented-Protocol—known as Synchronous Data Link Control (SDLC)²—was used. This

protocol provides an efficient method for establishing and terminating the conversation between terminals, identifying senders and receivers, acknowledging received information, and error recovery.

A transmit sequence from the primary station to a secondary station starts with the transmission of the Information Frame (I-Frame) containing the address of the intended secondary station in the address field. When a secondary receives an I-Frame with its address, it reads that frame and stores it in a receive buffer. In SDLC, all frames contain a 16-bit error checking code which precedes the closing flag. The receiving station checks this error code to validate transmission accuracy and responds with the appropriate acknowledge or not-acknowledge frame when it sees a "GO AHEAD" flag. A secondary is permitted to suspend the repeater function and go "on loop" and transmit a frame only when it receives the "GO AHEAD" flag from the primary station.

In the two-terminal demonstration system, the M6800 MPU data throughput capability at 1-MHz operation limited the maximum data rate to about 75-kbit/second. By using an MC6844 Direct Memory Access Controller to reduce the amount of processor overhead in data handling, and by incorporating a receiver designed for higher bandwidth, data rates up to 1 Mbaud have been demonstrated. Since the optical fiber possesses such high bandwidth capability, the existing cable easily handles increased data rates or system upgrading. This demonstrates one of the big cost advantages of fiber optic communications.

Conclusion

A practical, cost-effective alternative solution to a specific applications problem has been discussed. As higher power LED's and more sensitive detectors and directional fiber couplers or splitters are introduced, even more flexibility will be in the hands of the system designer.

1. The FOAC line of components is described in Application Note AN-804, "Applications of Ferruled Components to Fiber Optic Systems." The Note is available from your Motorola sales representative or distributor.
2. AMP Bulletin HB5444, "Fundamentals of Fiber Optics."
3. IBM SDLC Document No. GA27-3093-1
4. Motorola Application Note AN-794, "A 20-Mbaud Full Duplex Fiber Optic Data Link Using Fiber Optic Active Components." Available late August from your Motorola sales representative or distributor.

NOTES

NOTES

EUROPEAN MOTOROLA SEMICONDUCTOR SALES OFFICES

DENMARK

Motorola A/S
Gadsaxen 370
2800 Soborg
Tel. (031) 87 44 22

FRANCE

Motorola Semiconductor S.A.
Hausstrasse 15
15-17, avenue de Séguin
75007 Paris
Tel. 551 50 61
Sales Office
42, avenue de la Prairie-Pleine
38240 Meylan (Grenoble)
Tel. (06) 90 22 81

WEST GERMANY

Motorola GmbH,
Geschäftsbereich Heilbronn
Headquarters:
Hausstrasse 18
9043 Unterhaching
Tel. (0911) 92 481

Sales Office
Haus-Böcklin-Straße 30
3012 Leipzigerstrasse — Hannover
Tel. (0511) 78 20 3735

Vinzenz-Bargmannstrasse 43
8500 Nürnberg
Tel. (0911) 57 61

Sträßlumer-Straße 1
7032 Sindelfingen
Tel. (07121) 18 30 7475

Abraham-Lincoln-Straße 26
6900 Wiesbaden
Tel. (0611) 78 19 21

Sales Office
Via Costantino Maes 68
00162 Roma — Tel. 83 47 46

ITALY

Motorola S.p.A.
Headquarters:
Via Città Monferrato 11
20129 Milano
Tel. 738 61 4123

Motorola S.p.A.

Divisione Semiconduttori

Via del Barroccolo 2

40138 Bologna
Tel. (051) 63 34 46

SOUTH AFRICA

Motorola South Africa (Pty) Ltd.
P.O. Box 39580
Bramley 2018
Tel. 786 11 94

SPAIN

Motorola España S.A.

Capitan Hoyos 55

Madrid 20 — Tel. 278 08 02

SWEDEN

Motorola AB.
Vredesweg 19
17140 Solna — Tel. (08) 62 02 95

UNITED KINGDOM

Motorola Ltd.
Headquarters:
York House, Empire Way
Wembley Middlesex
Tel. (01) 902 88 36
Sales Office:
10-12, Mount Street,
London W1
Tel. (01) 533 07 51883-07 37
Sales Office:
Corstorphine Road, Kelvin Estate
East Kilbride, Scotland
Tel. (0355) 31 91 01

**HEADQUARTERS
EUROPEAN OPERATIONS**

SWITZERLAND
Motorola Inc.
Semiconductor Group
15, chemin de la Voie-Créée
P.O. 906 S-1211 Genève 20
Tel. (022) 99 11 11

FRANCHISED MOTOROLA SEMICONDUCTOR DISTRIBUTORS

AUSTRIA

Eibane GmbH
Endressstrasse 56 — 1230 Wien
Tel. (0223) 88 56 11

BELGIUM

Dirkje Belgium
Rue Picard 209-204 — 1020 Bruxelles
Tel. (02) 428 51 05

DENMARK

Distributoren Interalko ApS
Hundsgårdsgade 16 — 4622 Hørveup
Tel. (03) 58 17 57

FINLAND

Faidit Oy
Vesterntorikujantie 18 — 00210 Helsinki 21
Tel. (09) 659 25 77

FRANCE

Bellion Electronique
Zone Industrielle de Keracq/Brest
29219 Le Relais-Keracq — BP 16
Tel. (08) 28 03 03

Cendis S.A.

53-55, rue Sainte-Anne/Frélac — 44260 Gentilly
Tel. (02) 58 06 20

Ets. F. Fournier S.A. (Main Office)

Rue des Trois-Grenouilles

42270 St-Priest-en-Jarez (St-Etienne)

Tel. (07) 74 67 33

Ets. F. Fournier S.A.

Avon 14, Avenue Léopold — Zone industrielle

13120 Cavaillon

Tel. (04) 82 18 41

Fournier fils de France

29, rue Ladurie-Rolin — 92150 Suresnes

Tel. (01) 69 48 48

Ets. Gross S.A. (Main Office)

13, rue Richer-Hugo — B.P. 53

95950 Saint-André-lez-Lille

Tel. (03) 51 21 33

Ets. Gross S.A.

14, avenue Général-Leclerc — 54300 Nancy

Tel. (03) 35 17 36

Ets. Gross S.A.

5, rue Pascal — 84600 Villefranche

Tel. (01) 87 27 21

Ets. Gross S.A.

80, rue d'Arcueil — St-Étienne

94250 Rungis Cedex

Tel. (01) 85 23 13

Sit Commercial Toutelectric (Main Office)

15-17, Boulevard Bonvoisin — 31008 Toulouse

Tel. (05) 61 11 33

Sit Commercial Toutelectric

92, quai des Quétaires — 33100 Bordeaux

Tel. (05) 50 31

GERMANY

Alfred Neys — Eleotechnik GmbH
Schönauerstrasse 14 — D-2085 Quickborn/Hamburg

Tel. (041) 60 5121

Alfred Neys — Eleotechnik GmbH

Bernauerstrasse 2 — D-1000 Berlin 27

Tel. (030) 433 36 32

Alfred Neys — Eleotechnik GmbH

Hildesheimerstrasse 31 — D-3000 Hannover

Tel. (0511) 69 88

Alfred Neys — Eleotechnik GmbH

Stromerstrasse 107 — D-4000 Düsseldorf

Tel. (0211) 66 61 45

Alfred Neys — Eleotechnik GmbH

Rheinstraße 24 — D-1000 Darmstadt

Tel. (0611) 52 44 68

Alfred Neys — Eleotechnik GmbH

Brennweissstrasse 25 — D-7000 Stuttgart 60

Tel. (0711) 67 11 11

Alfred Neys — Eleotechnik GmbH

Maria-Theresia-Strasse 8 — D-8000 München 80

Tel. (089) 47 30 23

Alfred Neys — Eleotechnik GmbH

Gärtnerplatz 3 — D-1000 Berlin 10

Tel. (030) 342 10 4145

Sales Office
Haus-Böcklin-Straße 30
3012 Leipzigerstrasse — Hannover
Tel. (0511) 78 20 3735

Vinzenz-Bargmannstrasse 43
8500 Nürnberg
Tel. (0911) 57 61

Sträßlumer-Straße 1
7032 Sindelfingen
Tel. (07121) 18 30 7475

Abram-H-Lincoln-Straße 26
6900 Wiesbaden
Tel. (0611) 78 19 21

Sales Office
Via Costantino Maes 68
00162 Roma — Tel. 83 47 46

ITALY

Motorola S.p.A.
Headquarters:
Via Città Monferrato 11
20129 Milano
Tel. 738 61 4123

Motorola S.p.A.

Divisione Semiconduttori

Via del Barroccolo 2

40138 Bologna
Tel. (051) 63 34 46

SOUTH AFRICA

Motorola South Africa (Pty) Ltd.
P.O. Box 39580
Bramley 2018
Tel. 786 11 94

SPAIN

Motorola S.A.
Capitan Hoyos 55
Madrid 20 — Tel. 278 08 02

SWEDEN

Motorola AB.
Vredesweg 19
17140 Solna — Tel. (08) 62 02 95

SWITZERLAND

Motorola Inc.
Semiconductor Group
15, chemin de la Voie-Créée
P.O. 906 S-1211 Genève 20
Tel. (022) 99 11 11

UNITED KINGDOM

Motorola Ltd.
Headquarters:
York House, Empire Way
Wembley Middlesex
Tel. (01) 902 88 36
Sales Office:
10-12, Mount Street,
London W1
Tel. (01) 533 07 51883-07 37
Sales Office:
Corstorphine Road, Kelvin Estate
East Kilbride, Scotland
Tel. (0355) 31 91 01

**HEADQUARTERS
EUROPEAN OPERATIONS**

SWITZERLAND
Motorola Inc.
Semiconductor Group
15, chemin de la Voie-Créée
P.O. 906 S-1211 Genève 20
Tel. (022) 99 11 11

SOUTH AFRICA

Motorola Inc.
Headquarters:
15, chemin de la Voie-Créée
P.O. 906 S-1211 Genève 20
Tel. (022) 99 11 11

PORTUGAL

Equipamentos de Laboratório LDA

Rua Pedro Nunes 47 — Lisbon 1

Tel. 97 02 51

SOUTH AFRICA

Motorola Inc.
Headquarters:
15, chemin de la Voie-Créée
P.O. 906 S-1211 Genève 20
Tel. (022) 99 11 11

SPAIN

Motorola Electronics S.A. (Main Office)

Parque Industrial "Última"

Apartado de Correos 48 — Alcorcón (Madrid)

Tel. (01) 619 41 08

Hispano Electronics S.A.

Figueres 27-29

Barcelona 14 — Tel. 256 05 22

SWEDEN

Interpike AB.

Box 32 — 12221 Enskede

Tel. (08) 12 21 60

AB Göteb Blackberg

A-1000megegat 22 — Box 1206

102 30 Stockholm

Tel. (08) 60 98 00

SWITZERLAND

Motorola Inc.

15, chemin de la Voie-Créée

P.O. 906 S-1211 Genève 20 — Tel. (022) 99 11 11

TURKEY

BAA Elektronik Sanayi Ve Ticaret A.S.

Est. Sayyakod Cad. 4/A — Levent

Istanbul

Teknolojik Sanayi Ve Ticaret A.S.

Gazi Mustafa Kemal Bul. 12

Osmangazi 76 — Yenisehir/Antalya

Tel. 75 49 33

UNITED KINGDOM

A.M. Lock & Co. Ltd.

Neville Street, Middleton Road

Oldham, Lancs OL9 6LF

Tel. (055) 652 04 31

Cable Ltd.

37, Newgate Street

Reading, Berks RG1 1ED

Tel. (0734) 585 171

Hawley Electronics Ltd.

Hawley House Green Street

Sunderby on Thames, Middlesex, England

Tel. (0327) 81 55 77

Conrad Electronic Services Ltd.

300, New Road

Slough, Berks SL1 1JE

Tel. (0628) 44 34

RTI Electronic Services

Edinburgh Way

Harrow, Essex CM20 7DF

Tel. (0895) 26 77 77

Jammy Industries

Vestry Estate — Sevenoaks, Kent

Tel. (0732) 5 11 74

Macro Marketing Ltd.

396, Bath Road

Slough, Berks SL1 6JD

Tel. (0628) 4422

YUGOSLAVIA

Elektrotehnika Ljubljana

Export-Import

10100 Ljubljana 24

Tel. (01) 593 07 07

Elektrotehnika Ljubljana

Planinska 10

11000 Beograd

Tel. (01) 59 69 24

UNITED KINGDOM

Motorola Ltd.

Headquarters:

10-12, Mount Street,

London W1

Tel. (01) 533 07 51883-07 37

Sales Office:

Corstorphine Road, Kelvin Estate

East Kilbride, Glasgow (Scotland)

Tel. (0355) 31 91 01

UNITED KINGDOM

Motorola Ltd.

Headquarters:

10-12, Mount Street,

London W1

Tel. (01) 533 07 51883-07 37

Sales Office:

Corstorphine Road, Kelvin Estate

East Kilbride, Glasgow (Scotland)

Tel. (0355) 31 91 01

UNITED KINGDOM

Motorola Ltd.

Headquarters:

10-12, Mount Street,

London W1

Tel. (01) 533 07 51883-07 37

Sales Office:

Corstorphine Road, Kelvin Estate

East Kilbride, Glasgow (Scotland)

Tel. (0355) 31 91 01

UNITED KINGDOM

Motorola Ltd.

Headquarters:

10-12, Mount Street,

London W1

Tel. (01) 533 07 51883-07 37

Sales Office:

Corstorphine Road, Kelvin Estate

East Kilbride, Glasgow (Scotland)

Tel. (0355) 31 91 01

UNITED KINGDOM

Motorola Ltd.

Headquarters:

10-12, Mount Street,